

emc² 20

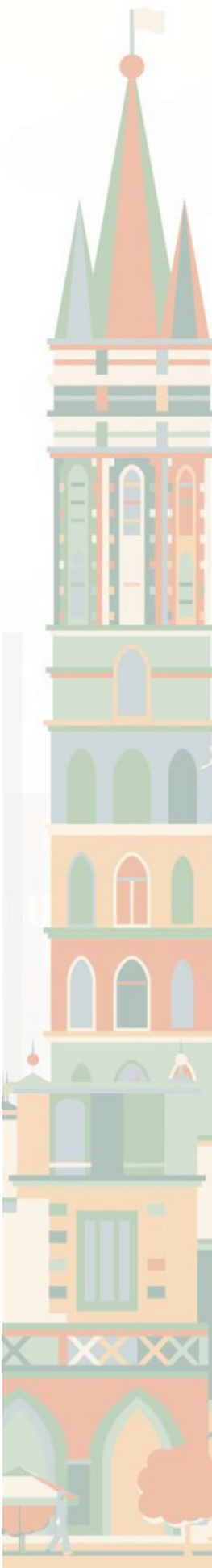
3rd European Mineralogical Conference Cracow Poland

Mineralogy in the modern world

ABSTRACT BOOK

29 August - 2 September 2021





PROGRAMME

oral blocks

| | STAGE 1 (Main Stage) | STAGE 2 | STAGE 3 | STAGE 4 |
|--|-------------------------|--|-----------------------------------|------------------|
| Monday 30th Aug 2021 9:30 – 11:15 11:30 – 13:00 15:00 – 17:15 | T1_S2 | T5_S3+T11_S1 T3_S1 | T2_S1 | T8_S1+T8_S2 |
| Tuesday 31st Aug 2021 9:30 -11:15 11:30 – 13:00 15:00 – 17:15 | T1_S2 T1_S3+ T1_S4 | T10_S2+T10_S3+T10_S4 +T10_S5 T6_S1 | T5_S1+T7_S1 T4_S1 | T10_S1 T12_S1 |
| Wednesday 1st Sept 2021 9:30 -11:15 11:30 – 13:00 15:00 – 17:15 | T1_S5 T1_S1 | T13_S1+T15_S1 T14_S2 | T5_S2 T12_S2+T12_S3 +T12_S4 | T11_S2 |
| Thursday 2nd Sept 2021 9:30 -11:15 11:30 – 13:00 | T9_S1+T9_S2 | T14-S1+T16_S1 | T5_S4 | T11_S3+T11_S4 |

Mineralogy in the modern world

Following the success of the 1st and 2nd European Mineralogical Conference, the emc2020 will be focused on current and future challenges in the Earth, planetary and environmental sciences, and fostering an exchange of new views and research results between scientists from Europe and beyond.

The city of Kraków is a vibrant, academic and tourist city in the heart of Europe. Modern infrastructure, efficient public transportation and famous Polish hospitality make it a safe and friendly place for visitors from all over the world. The city dates back to Middle Ages and has traditionally been one of the leading centers of Polish and European academic, cultural, and artistic life. It was the capital of Poland from 1038 to 1569.

Welcome in Cracow!

Krakau, ክራካው, Cracow, ^{Cracovia}, Кракoв, 克拉科夫, Cracó, Kraká, クラクフ, كراكوف, Cracovie, Krakov, Кракiв, Cra-cóp, Krakovja

Kraków

Scientific Committee

**Tomasz Bajda (Chair, PTMin),
Marc Blanchard (SFMC),
Gerhard Brey (DMG),
Piergiulio Cappelletti (SIMP),
Giuseppe Cruciani (SIMP),
Jose Fernandez-Barrenechea (SEM),
Reinhard Fischer (DMG),
Tapio Halkoaho (MinSocFin),
Heidi Höfer (DMG),
Sergey V. Krivovichev (RMS),
Maciej Manecki (PTMin),
Frank Melcher (ÖMG),
Kevin Murphy (MinSoc),
Ewa Słaby (EMU)**

Organizing Committee

**Tomasz Bajda,
Anna Ingot,
Jakub Kierczak,
Krzysztof Szopa,
Justyna Topolska
Marta Polak**

Editor of the EMC2020 abstract book: Jakub Kierczak

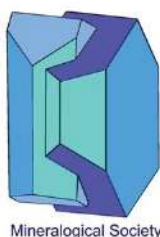


The **EMC2020** is organized by the **PTMin**
(**Mineralogical Society of Poland**) on behalf of other
European mineralogical societies:

DMG – **Deutsche Mineralogische Gesellschaft**
MinSoc – **Mineralogical Society of Great Britain & Ireland**
MinSocFin – **Mineralogical Society of Finland**
ÖMG – **Österreichische Mineralogische Gesellschaft**
RMS – **Russian Mineralogical Society**
SEM – **Sociedad Española de Mineralogía**
SFMC – **Société Française de Minéralogie et de
Cristallographie**
SIMP – **Società Italiana di Mineralogia e Petrologia**
SSMP – **Swiss Society of Mineralogy and Petrology**

with participation of:

EMU – **European Mineralogical Union**
ING PAN – **Institute of Geological Sciences, Polish Academy
of Sciences**
Geo8 – **GFZ German Research Centre for Geosciences**





3rd European Mineralogical Conference Cracow Poland

SPONSORS



Rigaku



**CRYSTAL
IMPACT**



Bureau Veritas
Mineral Laboratories

**BUREAU
VERITAS**

European Journal of
Mineralogy

Open Access



minerals

2020



3rd European Mineralogical Conference Cracow Poland

PLENNARY LECTURES

2020

Plenary Lecture

X-RAY SPECTROSCOPIC, SCATTERING, AND IMAGING STUDIES OF EARTH MATERIALS AND PROCESSES: FROM THE NANOSCALE TO THE GLOBAL SCALE

Brown Jr Gordon E¹, Jew Adam², Noel Vincent², Kumar Naresh³, Bargar John²

¹Geological Sciences, Stanford University, United States, ²Stanford Synchrotron Radiation Lightsource, SLAC National Accelerator Laboratory, United States, ³Environmental Geosciences, University of Vienna, Austria

The development of synchrotron X-ray sources over the past 50 years has resulted in a scientific revolution that has impacted all scientific fields, including mineral and environmental sciences. The extreme brightness and energy tunability of synchrotron X-ray sources made possible spectroscopic, surface scattering, and imaging methods that were not possible with sealed or rotating-anode X-ray sources. We will review applications of these methods to several Earth materials and environmental science problems, including XAFS studies of sorption reactions of environmental contaminants at mineral/aqueous solution interfaces and of environmental transformations of natural and manufactured nanoparticles, crystal truncation rod (CTR) X-ray scattering studies of the structure of hydrated metal oxide surfaces, X-ray photoelectron spectroscopy studies of the reaction of water with mineral surfaces, and micro-X-ray fluorescence imaging of mineral scale formation in oil/gas shales before and after hydraulic fracturing. The field of Molecular Environmental Science can trace its origins back to the mid to late 1980's when the first XAFS studies of sorption reactions of environmental contaminants at mineral/aqueous solution interfaces were carried out. Prior to this development, most of our knowledge of the role that interfacial chemical reactions play in sequestering or releasing inorganic contaminants such as Cr(VI), As(III), Se(IV), Pb(II), Hg(II), and U(VI) came from macroscopic uptake measurements of these and other contaminants at mineral/water interfaces. However, over the past 35 years, there have been hundreds of XAFS studies of these reactions that have provided molecular-level information about the structures, compositions, and modes of attachment of inorganic environmental contaminants to mineral surfaces. Moreover, prior to the first applications of CTR diffraction and X-ray reflectivity to determine the structure of hydrated mineral surfaces, we had little knowledge of their molecular-level structures and assumed that hydrated mineral surfaces were simple terminations of the bulk structure for a specific plane through a given mineral structure. Since the first studies in 2000, there have been approximately 25 CTR diffraction and X-ray reflectivity studies of hydrated mineral surfaces which have shown that the surface structures of minerals in contact with water are significantly different from those of the bulk structure.

Other research areas in the mineral sciences have also benefited from synchrotron X-ray methods. One such area is nanomineralogy where XAFS spectroscopy has been used to study the sulfidation of manufactured silver and ZnO nanoparticles and of natural nanoparticles of ferrihydrite, which partially mitigates their toxic effects. Also, synchrotron-based studies of the chemistry of hydraulic fracturing of unconventional oil/gas shales have shown how the problem of mineral scaling can be addressed. We conclude with a look at the future of these types of studies in areas of societal concern.

Plenary Lecture

THE EFFECT OF PRESSURE ON OPEN-FRAMEWORK SILICATES: ELASTIC BEHAVIOUR AND CRYSTAL-FLUID INTERACTION

Gatta G. Diego¹

¹Dipartimento di Scienze della Terra, Università degli Studi di Milano, Via Botticelli 23, 20133 Milan, Italy

The physical behavior of microporous materials (*i.e.*, materials with structural voids ≤ 2 nm) compressed in a fluid is strongly affected by the potential crystal-fluid interaction, with a penetration of new molecular species through the structural cavities in response to the applied pressure.

Recent experimental findings and computational modeling show that, when no crystal-fluid interaction occurs, the effects of pressure are mainly accommodated by tilting of the (quasi-rigid) tetrahedra, around the bridging oxygen atoms that act as hinges. Tilting of tetrahedra is the dominant mechanism at low-mid *P*-regime, followed by distortion and compression of polyhedra which become dominant at the mid-high *P*-regime. The mechanisms of deformation, accommodating the bulk compression, are governed by the topology of the tetrahedral framework. One of the most common deformation mechanisms in zeolitic frameworks is the increase of channels ellipticity. However, the compressibility of the cavities (in the form of channels or cages) is governed by the ionic and molecular extra-framework content, with different unit-cell volume compressibility in isotopic structures.

Only a few zeolites experience a *P*-induced intrusion of new monoatomic species or molecules from the *P*-transmitting fluids. Natural zeolites, in particular, have well-stuffed channels at room conditions, which tend to hinder the penetration of new species through the structural cavities. A comparative analysis of experimental findings allow us to provide an overview of the intrusion phenomena, which are diverse for monoatomic species (*e.g.*, He, Ar, Kr), small (*e.g.*, H₂O, CO₂) or complex molecules, along with the recently observed *P*-induced polymerization phenomena (*e.g.*, C₂H₂, C₂H₄, C₂H₆O, C₂H₆O₂, BNH₆, electrolytic MgCl₂·21H₂O solution), with potential technological and geological implications. Several variables control the sorption phenomena at high pressure: the “free diameters” of the framework cavities, nature and bonding configuration of the extra-framework population, the kinetic diameter of the potentially penetrating molecules, the partial pressure of the penetrating molecule in the fluid (if mixed with other non-penetrating molecules), the rate of *P*-increase, the surface/volume ratio of the crystallites under investigations, and the temperature at which the experiment is conducted.

Plenary Lecture

AT THE EDGE OF ORDER: STRUCTURAL MINERALOGY IN THE NEW MILLENNIUM

Krivovichev Sergey V.¹

¹St. Petersburg University, St. Petersburg, Russia, Kola Science Centre, Russian Academy of Sciences, Apatity, Russia

Russian mineralogist and geochemist Vladimir Vernadsky once pointed out that ‘geochemistry reveals itself as an atomic chemistry of the Earth’s core, whereas mineralogy can be considered as a molecular chemistry of the Earth’s core’ (Vernadsky, 1923). The recent quest for ‘molecular geology’ (Rustad, 2012) is certainly fulfilled with the recent mineralogical discoveries such as natural polyoxometalates and nanotubules, which position mineralogy as a study of geological matter on the molecular and nano scales, well in agreement with the visionary works of Vernadsky. The aim of the present contribution is to summarize recent findings in the field of natural nanoscale objects in the crystal structures of minerals and to analyze them in the view of the concept of structural complexity of crystals and minerals that we have developed over the last ten years (Krivovichev, 2012, 2013, 2014, 2016, 2017, 2018). The organization of mineral matter into nanoscale-size atomic objects is one of the most important complexity-generating mechanisms in mineral structures (Krivovichev, 2013; Olds *et al.*, 2017). The discoveries of silicate-based nanotubules and polyoxometalates in minerals open up a new area of research in mineralogy that becomes possible due to the methodological advances in crystallography such as introduction of highly-sensitive X-ray detectors and the use of synchrotron radiation and electron diffraction techniques. Application of these technologies to the studies of crystalline mineral matter outlines the path for the future developments of structural mineralogy and nanogeochemistry.

Plenary Lecture

HIGH PRESSURE MINERAL PHYSICS OF THE DEEP MANTLE AND CORE

Ohtani Eiji¹

¹Department of Earth Science, Tohoku University, Japan

Volatiles such as water are the important components which characterize the water planet Earth. The Earth's core has been recognized that it is about 10% less dense compared to iron-nickel alloy which indicates existence of light elements in the core. The light elements may be related to the volatiles in the Earth.

Here we see the transport and circulation of water in the mantle. Water budget and in-gassing/degassing ratio between earth's surface and interior has been debated. The recent estimations of the influx of ocean water are equal to or greater than the outgassing flux, resulting in constant or secular reductions of the ocean mass (e.g., [1]). Water is stored in both hydrous minerals and nominally anhydrous minerals (NAM). Ishii and Ohtani [2] recently studied the water partitioning between hydrous minerals and NAMs and revealed that water is stored in the hydrous phases and the coexisting NAMs, such as olivine, wadsleyite, ringwoodite, and bridgmanite are essentially dry. This solves a paradox of the existence of dry phase transitions which trigger the deep earthquakes [3] and large slab deformation [4] and wet slabs which transport water into the deep mantle.

The main carrier of water into the lower mantle will be phase δ -phase H solid solution of $\text{AlOOH-MgSiO}_2(\text{OH})_2$ since it is stable to the base of the lower mantle [5]. Our recent work showed the CaCl_2 type silica polymorph contain up to 2 wt% of water which is consistent with [6] and carry water into the lower mantle.

It is well known that the density deficit of the core relative to iron or iron-nickel alloy suggests the presence of light elements in the core. Several candidates including O, Si, and H have been proposed for the light elements of the core. We have conducted in situ neutron diffraction study of the Fe-H system at high pressure and temperature [7]. The upper bound of hydrogen content was estimated to be 80 ocean masses assuming the light element in the core is only hydrogen. On the other hand, a recent study of ^{57}Fe isotope fractionation between iron-light element alloy and silicates suggested that hydrogen is not a major light element in the core [8]. Thus, we need to consider the other light elements. Oxygen dissolved in the core crystallizes as SiO_2 and floats upward [9], therefore oxygen is not likely the major light element of the inner core.

Silicon is another important candidate of light elements. We observed that coexistence of hcp and B2 phases in FeNiSi and FeNi alloys at high temperatures below the solidus from 40 GPa to at least 160 GPa suggesting existence of the two-phase mixture in the inner core. This result supports the existence of the two-phase mixture in the inner core suggested by Fisher et al. [10]. Thus, the inner core may be composed of the two phase-mixture of hcp and B2 phases dissolving minor hydrogen.

References:

[1] van Keken, et al. 2011. *J. Geophys. Res.* 116(B1): B01401. [2] Ishii and Ohtani 2021. *Nature Geosci.* <https://www.nature.com/articles/s41561-021-00756-7>. [3] Green et al. 2010, *Nature* 467, 828-831. [4] Mohiuddin et al. 2020. *Nature Geosci.* 13, 170-174. [5] Ohira et al. 2014. *Earth Planet. Sci. Lett.* 401, 12-17. [6] Nisr et al. 2020. *Proc. Natl. Acad. Sci.*, 117, 9747-9754. [7] Ikuta et al. 2019. *Sci. Rep.* 9, 7108. [8] Shahar et al. 2016. *Science* 352, 580-588. [9] Hirose et al. 2017. *Nature*, 543, 99. [10] Fisher et al. 2014. *J. Geophys. Res. Solid Earth*, 119, 2810–2827.

Plenary Lecture

SMECTITES: THE KEY TO THE COST OVERHEADS IN THE CONSTRUCTION OF THE THIRD SET OF LOOKS OF THE PANAMA CANAL

Suárez Mercedes¹, García-Romero Emilia²

¹Department of Geology, University of Salamanca, Spain,²Facultad de Ciencias Geológicas, Universidad Complutense de Madrid, Madrid, Spain

The third set of locks of the Panama Canal, one of the most impressive civil constructions around the world, was inaugurated in 2016. The inauguration was initially scheduled for 2014, just a hundred years after that the first canal started its activity in 1914. The cost overruns in billions and the delay in the construction of the new canal were related in large part to the extraction, storage, and use of the local basalt as the raw material (aggregates and sand) for concrete, and this had wide international media coverage. The construction required an excavation of $\sim 50 \times 10^6$ m³ of rock and over 5×10^6 m³ of concrete for which aggregates and sands derived from the crushing of local basalt were utilized together with $\sim 1.6 \times 10^6$ t of cement. According to the information available to the constructors at the tender stage, the basalt from the excavation was adequate for this purpose. However, when the production of concrete for the first structures began, seven months after the beginning of the excavation, the problems became apparent. The crushing of the materials that had been stored for seven months under the tropical weather at the site resulted in rapid degradation of the basalt, and the generation of a large number of fines. This forced the constructors to modify the crushing plant and to look for a new source of raw materials for the concrete production, which in turn resulted in the delay in the construction and in the important overruns that occurred.

Why did an apparently fresh and sound basalt, ordinarily used for construction, generate much more fines than expected? Why were the rocks coming directly from the quarries able to pass the mechanical test while the stored and processed rocks from the excavation had to be rejected? To answer these questions, an in-depth characterization of the representative rocks from the area was conducted and the results showed the cause of that unexpected problem: smectites, nanominerals with particular swelling properties that are not easy to detect.

The main findings of this study developed with different techniques (optical microscopy, X-Ray diffraction, SEM, HR-TEM, microprobe, VNIR-SWIR spectroscopy, and experimental aging) on representative samples from the quarries, the excavation, and the aggregates are shown. The presence of dioctahedral smectites filling a dense network of micro and nanocracks intensely connected is proposed as the key to explaining the unexpected behavior of the rocks. The results show that not only the presence but also the microstructure of the smectites – nano-minerals with particular swelling properties in contact with water – were responsible for the rapid degradation of the apparently fresh basaltic rock at the stockpile and for the high loss of fines during the industrial process. Although smectites are common products of hydrothermal alteration of basalt and other basic igneous rocks, these rocks are frequently used as construction materials owing to their mechanical properties and durability. However, only a small proportion of smectites can trigger rock deterioration when they are highly interconnected.

Finally, it is pointed that this process of rapid degradation of basic igneous rocks, related to the presence of clay minerals is not frequent, but it is significant enough as for require the development of a new standard for the use of these materials in construction.

Plenary Lecture

ILLITE AND ITS ROLE IN THE GLOBAL CYCLING OF ELEMENTS

Środoń Jan¹

¹ Institute of Geological Sciences, Polish Academy of Sciences, Research Centre in Kraków, PL-31002 Kraków, Poland; ndsrodon@cyf-kr.edu.pl

Illite is one of the clay minerals, i.e. a fine-grained phyllosilicate of the 2:1 layer structure, with a dehydrated interlayer cation, typically K⁺. It was described as a separate mineral, different from mica, from the Pennsylvanian mudstones of Illinois by Grim, Bray, and Bradley in 1937, and a few months later under the name “sarospatakite” by Maegdefrau and Hofmann from hydrothermally altered pyroclastics of the Tokay Mts., Hungary. A few years later, XRD patterns of illitic clays were interpreted as indicative of the mixed-layering phenomenon.

Illite, most often interlayered with smectite, is known from soils, sediments, and rocks altered by diagenetic, metamorphic, and hydrothermal processes, up to temperatures of the epimetamorphic zone (ca. 300°C). Illite (27 wt. %) is the second (after quartz: 35 wt. %) most abundant component of sedimentary rocks. In mudstones, illite-smectite minerals (42 wt. %) surpass quartz (26 wt. %).

Illite occurs as plates, fractions of a micron in diameter, and from two to tens of nanometers thick. The surfaces of these plates are charged and attract hydrated exchangeable cations, thus they have smectitic character. The thinnest plates always occur joined by their smectitic surfaces into parallel aggregates, perceived by XRD as the mixed-layer crystals. Individual smectitic layers or their groups may also be involved in such mixed-layering.

Most of the illite crystallizes during burial diagenesis, above ca. 70°C, at the expense of smectite. First, 2 nm illite crystals nucleate within smectite crystals, then they grow thicker, and finally, 3D growth takes place, producing thick illite crystals at the deep burial diagenetic stage. Also, kaolinite alters into illite during burial diagenesis. During anchimetamorphism, illite growth continues, and 1M_d and 1M illite polytypes recrystallize into 2M₁, which involves resetting their K-Ar ages. During epimetamorphism, illite recrystallizes into coarse mica. During erosion and weathering, a portion of illite dissolves or loses the interlayer cations altering into soil vermiculite, but a significant portion gets recycled into new sediments, as evidenced by the K-Ar dating of sedimentary illites. At least a portion of this detrital illite survives diagenesis and gets recycled if uplift and erosion start before the anchimetamorphic stage has been completed.

Illite, due to its abundance and ca. 4 wt. % OH, is the main component of sedimentary rocks carrying water deep into the epizone, where it is inherited by micas. Illite is also the main carrier of potassium at the diagenetic and anchizonal stages of the potassium geochemical cycle, and it serves as potassium slow-release fertilizer in soils. During diagenesis, illite is the major sink for ammonium (substituting for potassium) and boron (substituting for silica), released during diagenetic maturation of the organic matter, and imports these elements from pore fluids. Thus illite in bentonites (no recycled illite) becomes a tracer of oil- and gas-forming processes in sedimentary basins, and illite inherited from shales or slates is a slow-release nitrogen fertilizer in soils. Illite is also an almost exclusive sink for cesium in sediments, a property important for radioactive contamination removal, and a dominant sink for rubidium.

Plenary Lecture

WASTE MINERALOGY – SPOTLIGHTS ON AN INTERDISCIPLINARY RESEARCH FIELD

Vollprecht Daniel¹

¹Chair of Waste Processing Technology and Waste Management, Montanuniversität Leoben, Austria

At first sight, waste management and mineralogy seem to be completely different disciplines without many intersections. However, a closer look makes clear that mineralogy can contribute significantly to tackle waste management problems, and waste management represents an important working area for mineralogists. According to the EU, “Waste” means any substance or object which the holder discards or intends or is required to discard, whereas the IMA defines a “Mineral” as an element or a chemical compound that is normally crystalline and that has been formed as a result of geological processes. Consequently, a majority of waste is composed of minerals, e.g. excavated soils, tunnel excavation materials, and concrete aggregates. “Waste management” summarizes all activities regarding the prevention, re-use, collection, treatment, recycling, and disposal of wastes, thus not only including economical, but also technical and natural scientific aspects. “Mineralogy” in the modern sense is not only restricted to naturally occurring minerals but also to their synthetic analogues which are formed in technical processes in the production of (glass) ceramics and binders and in the incineration of fossil, renewable, and refuse-derived fuels. Considering all these materials, “mineral wastes” make up 77 % of the Austrian waste production and 95 % of all landfilled waste.

Waste management is characterized by the conflict of objectives between circular economy and contaminant removal. The precautionary principle states that for complex, poorly understood systems preventive actions in the face of the uncertainty shall be taken and was introduced by the UN in 1992. This means that in doubt whether the recycling of waste might harm human health or the environment, landfilling shall be preferred. In waste management practice, the precautionary principle is one important reason why 57 % of mineral wastes are landfilled in Austria which represents a tremendous loss of valuable resources like soil and construction materials. These resources must be obtained from the mining industry which is associated with negative impacts on the environment such as dust, land consumption, groundwater vulnerability and loss of biodiversity.

The EU explained their approach to using the precautionary principle and explained that this principle is “subject to review, in the light of new scientific data”. Mineralogy can contribute to waste management by gaining new scientific data allowing the recycling of wastes that have to be landfilled otherwise due to the precautionary principle. Currently, several European countries including Austria use limit values for total (solid) contents of contaminants to regulate the recycling of wastes. Using concepts and methods from mineralogy for waste management will reveal the mineralogical bonding of these contaminants and determine their behavior at the interface between waste and aqueous solutions under the environmental conditions of possible recycling applications such as road construction.

First studies indicate that the leaching of contaminants from recycled mineral wastes is limited in road construction and suggest that much more mineral waste could be recycled than today by using mineralogical methods and concepts. Finally, waste legislation may abstain from limit values for total (solid) contents of contaminants and focus on leachable contents and mineralogical observations, which may allow increasing the recycling rates for mineral waste.



3rd European Mineralogical Conference Cracow Poland

ABSTRACTS

2020

Mg-(Zn)-CHLORITE NEOFORMATION BY HYDROTHERMAL ALTERATION OF PHLOGOPITE IN A FRAGILE CARBONATE FAULT ZONE (PADUL FAULT, SE SPAIN)

Abad Isabel¹, Nieto Fernando², Jiménez-Millán Juan¹, Reolid Matías³

¹Departamento de Geología y CEACTEMA, Unidad Asociada IACT (CSIC-UGR), Universidad de Jaén, Spain,

²Departamento de Mineralogía y Petrología, Universidad de Granada, Spain, ³Departamento de Geología y CEACTEMA, Universidad de Jaén, Spain

The Neogene and Quaternary faulting activity in the southeastern Iberian Margin (Trans-Alboran Shear Zone), as a consequence of the convergence of the Eurasian and the African plates, includes normal faults with a predominantly NW-SE strike. One of them is the Padul Fault (Internal Zone of the Betic Cordillera), which separates the highest reliefs of Sierra Nevada (footwall block) from the Granada Basin. The rocks affected by this fault are mainly Triassic dolostones but also Palaeozoic calcschists and dark mica schists. This research has focused on the carbonate rocks, which were sampled in a quarry, and includes ultracataclasites and cataclasites formed from Triassic dolostones taken directly from the fault plane and samples from the footwall block including the protolith.

The textural and mineralogical characterization up to the nanoscale and the analysis of the major and trace elements in the samples aim to find out the processes that affected these materials as a consequence of the development of an extensional fault zone from the mineralogical/chemical point of view. A special focus has been paid on clay minerals as it is known that they usually have a crucial role in fault behaviors.

The bulk rock mineralogy determined by X-ray diffraction and the petrographic study with the scanning electron microscope show that the dolostones are composed mainly of dolomite but also by quartz and micas (phlogopite and muscovite). In the fault plane two different types of rocks were sampled: the yellowish ultraclasites, forming discontinuous patches, probably due to fault scarp erosion, up to 8-10 cm thick resting above the underlying grey cataclasites. The ultraclasites (with around 5% of clasts) are composed of carbonates (calcite and dolomite) and a little proportion of fine-grained silicates in the matrix: quartz, chlorite, muscovite, paragonite, and kaolinite. The cataclasites show a much higher presence of dolomite clasts (around 45%) in a matrix composed mainly of dolomite and calcite grains, chlorite, and some Fe and Ti oxides and apatite.

In relation to the geochemical data, the enrichment factors (EF) calculated for trace elements and based on Al normalization, indicate that dolostones in the fault area are enriched in Zn and Pb. Most of the samples show EF > 10, which is considered a moderate to a strong degree of enrichment, relative to their average crustal abundance. The enrichment in Zn was also detected by micro X-ray fluorescence (μ XRF) in the polished sections of some cataclasites. The compositional maps show irregular bands enriched in Si, Al, Fe, and Zn along with the predominantly carbonate matrix of the rocks and surrounding the dolomite clasts. The electron microprobe data showed that the Zn is hosted mainly in chlorites. Nanoscale characterization of them reveals the transformation layer by layer of phlogopites to chlorites that incorporate the Zn. The application of the Lanari and Bourdelle geothermometers gives temperature values for these chlorites around 120°C.

These results point to the presence of fault-controlled hydrothermal fluids that promoted geochemical changes and mineral reactions in the fault rocks as the neof ormation of Mg-chlorite from phlogopite and the kaolinite finely intergrowth with mica crystals. In addition, the presence of other phases in these rocks, as calcite cement, probably was the consequence of precipitation from meteoric fluids during uplift.

SPINODAL DECOMPOSITION OF ALKALI FELDSPAR: AN EXPERIMENTAL AND ATOM PROBE TOMOGRAPHY STUDY

Abart Rainer¹, Petrishcheva Elena¹, Habler Gerlinde¹, Schweinar Kevin², Li Chen³, Gault Baptiste²

¹University of Vienna, Austria, ²Max-Planck Institute for Iron Research, Germany, ³University Antwerpen, Belgium

Atom probe tomography was used to complement electron microscopy for the investigation of experimentally induced spinodal decomposition of alkali feldspar. Gem-quality alkali feldspar with a mole fraction of aK= 0.43 of the K end-member was prepared from Madagascar orthoclase with an original aK= 0.95. To this end, the feldspar was ground and sieved to 100 – 200 µm size fraction and subjected to ion exchange with (NaK)Cl molten salt at 850°C for three weeks. Subsequently, the salt was removed by rinsing with distilled water, and the bare feldspar powder was annealed at 550°C and ambient pressure. These conditions are within the unstable region of the phase diagram, and the feldspar unmixed producing coherently intergrown Na-rich and K-rich lamellae with characteristic lamellar width of about 17 nm approximately parallel to the Murchison plane (-801). Grain mounts were prepared from the powder and EBSD was used to select suitably oriented grains for extracting cone-shaped specimens to be used for analysis by atom probe tomography (APT) with the cone axis perpendicular to the lamellae. APT allows for the chemical analysis of the lamellae at a lateral resolution of better than 5 nm. It was found that the chemical separation of the lamellae was completed and equilibrium Na–K partitioning between the different lamellae was attained within four days. Annealing at 550°C for more than 4 days led to microstructural coarsening producing lamellar width of about 30 nm after 16 days while the lamellar compositions remained unchanged. The observed lamellar compositions of aK= 0.24 and aK= 0.59 are interpreted as the binodal points, which pertain to the Na-rich and K-rich limbs of the coherent solvus at 550°C and ambient pressure. This is in reasonable agreement with an earlier experimental determination of the coherent solvus. A perfect match between the bulk composition by electron probe micro analysis and the integrated composition calculated from lamella compositions and modal proportions obtained from APT testifies to the high accuracy attained with APT analysis of nm-scaled lamellar intergrowth. Based on Cahn–Hilliard's theory and using the initial wavelength of the lamellar microstructure and the lamellar compositions an excess Gibbs energy contribution of $1e-3$ J/m² to $1.7e-3$ J/m² due to the compositional gradients at the lamellar interfaces was determined. This excess energy is by a factor of about 500–1100 smaller than the typical surface energy of a general plane in alkali feldspar. The low excess energy explains the limited efficiency of coarsening in perthites produced from spinodal decomposition, where the gradient energy is the only thermodynamic driving force for coarsening.

ISOTOPIC CHARACTERIZATION OF NO₂⁻ AND N₂O DURING ABIOTIC NO₂⁻ REDUCTION BY FERROUS Fe (II)

Abu Alex Tiewin^{1,2}, Carrey Raúl^{2,3}, Domènech Cristina^{1,2}

¹Grup MAiMA, SGR Mineralogia Aplicada, Geoquímica i Geomicrobiologia, Departament de Mineralogia, Petrologia i Geologia Aplicada, Facultat de Ciències de La Terra, Universitat de Barcelona (UB), 08028, Barcelona, Catalonia, Spain, ² Institut de Recerca de l'Aigua (IdRA), Universitat de Barcelona (UB), 08001, Barcelona, Catalonia, Spain, ³Centres Científics i Tecnològics, Universitat de Barcelona (UB), C/Lluís Solé i Sabarís 1-3, 08028 Barcelona (Spain)

Iron cycling in groundwater is mediated by both biotic and abiotic processes which affect the fate of groundwater contaminants. Biotic Fe(II) oxidation occurs mainly by nitrate-reducing Fe(II) oxidation (NRFO) bacteria in an anoxic condition. There is a concurrence of biotic-abiotic processes during NRFO and the more reactive NO₂⁻ is used as the electron acceptor in the abiotic process (Melton et al., 2014). The abundance of Fe in neutral-anoxic environments plays a significant role in biogeochemical Fe cycling by Fe and NO₂⁻ reaction. NO₂⁻ is chemically highly reactive and is readily reduced abiotically and recent findings have suggested that chemodenitrification largely catalyzed N₂O fluxes (Wankel et al., 2017). Stable isotopes provide a useful tool to study and characterize biogeochemical cycles in water resources. The objectives of this study are (I) to understand the mechanisms on N₂O emission by abiotic nitrite reduction (II) to study the isotopic signatures of δ¹⁵N from NO₂⁻ and N₂O and 15N site preference (SP) during abiotic nitrite reduction by ferrous Fe(II). To get these goals, three series of lab batch experiments were performed at Fe(II)/NO₂⁻ ratios of 5 (S1), 3 (S2), and 1.5 (S3) plus siderite to evaluate the kinetic and isotopic effect of the different Fe/N ratios on the abiotic process. In all series, a mass of FeCl₂·4H₂O was required to attain the Fe(II)/NO₂⁻ ratios. Two control experiments, one with dissolved Fe(II) without siderite and the other with only siderite were tested to characterize the presence of the Fe(II) mineral on the abiotic process. The δ¹⁵N from NO₂⁻ was analyzed following the sodium azide reduction method. SP and 15N-N₂O from the headspace of the vials as well as 15N-NO₂⁻ were analyzed using a Pre-Con (Thermo Scientific) coupled to an IRMS (Finnigan MAT 253, Thermo Scientific). Commercial N₂O used as reference gas was calibrated using the international standard USGS-51. Preliminary results showed that the reaction of S1 was faster than S2 and S3 achieving complete NO₂⁻ removal within 24 hours. Isotopically, 15N-N₂O increased from -26.9 to -12.0 ‰ whereas 15N-NO₂⁻ increased from -51 to -42.1 ‰ in 24 hours. 15N-N₂O increased from -26.5 to -17.3 ‰ whereas 15N-NO₂⁻ increased from -51 to -44.5 ‰ (52 hours) in S2 and S3. 15N-NO₂⁻. Current work is underway to characterize 15N site preference of N₂O and the role of the Fe(II) mineral (siderite) on the abiotic process.

References

- Melton, E.D., Swanner, E.D., Behrens, S., Schmidt, C., Kappler, A., 2014. The interplay of microbially mediated and abiotic reactions in the biogeochemical Fe cycle. *Nat. Rev. Microbiol.* 12, 797–808. <https://doi.org/10.1038/nrmicro3347>
- Wankel, S.D., Ziebis, W., Buchwald, C., Charoenpong, C., De Beer, Di., Dentinger, J., Xu, Z., Zengler, K., 2017. Evidence for fungal and chemodenitrification based N₂O flux from nitrogen impacted coastal sediments. *Nat. Commun.* 8, 1–11. <https://doi.org/10.1038/ncomms15595>

SPATIAL DISTRIBUTION AND SHAPE ORIENTATION ANISOTROPY OF MAGNETITE MICRO-INCLUSIONS IN PLAGIOCLASE FROM OCEANIC GABBRO

Ageeva Olga¹, Bian Ge¹, Habler Gerlinde¹, Abart Rainer¹

¹Department of Lithospheric Research, University of Vienna, Austria

Silicate-hosted magnetite (MT) micro-inclusions endow the grains of the silicate-host with ferromagnetic properties and play an important role in the natural remanent magnetization. The micro-inclusions often form needle-shaped crystals. Considering the shape anisotropy and magnetocrystalline anisotropy of MT, the orientation relationships between the needle-shaped MT micro-inclusions and the silicate host can be important due to their potential influence on the anisotropy of magnetic susceptibility and remanence.

We investigated MT-bearing plagioclases (PL) from samples of oceanic gabbro with different degrees of high- and low-temperature hydrothermal alteration dredged from the Mid Atlantic Ridge. In non-altered gabbro more than 95% of the MT micro-inclusions belong to one of eight orientation classes, seven of which are classified as “plane-normal” due to their elongation direction coinciding with the normal directions to specific low-index lattice planes of plagioclase; these MT crystals are themselves elongated parallel to MT $\langle 111 \rangle$, which is the easy direction of magnetization. The micro-inclusions of the eighth's orientation class are elongated parallel to PL[001] with corresponding elongation direction of the MT parallel to MT $\langle 011 \rangle$. Overall, the MT grains of the different orientation classes show an anisotropic distribution of their shape orientations with respect to the plagioclase host: the micro-inclusions of five out of eight classes are elongated sub-parallel to the PL(010) plane. Moreover, the micro-inclusions are distributed unevenly over the different orientation classes, and about 80% of the MT micro-inclusions belong to three classes oriented close to parallel to the PL(010) plane. The investigated plagioclases show multiple twinning, which increases the dispersion of the needle orientations around the PL(010) plane but does not cause deviation of the micro-inclusions by more than 15° from this plane. As a consequence, the orientation distribution of the MT micro-inclusions with respect to the plagioclase of non-altered gabbros can be described as an oblate ellipsoid with its short axis perpendicular to PL(010). By contrast, in hydrothermally altered and recrystallized plagioclase the MT micro-inclusions elongated parallel to PL[001] are dominant, and their orientation distribution can be represented by a prolate ellipsoid with its long axis parallel to PL[001]. Moreover, the plagioclase grains in gabbro are usually tabular extending parallel to the PL(010) plane. In foliated gabbro plagioclase often shows shape preferred orientation with PL(010) aligned with the foliation plane. Combined with the shape preferred orientation of the MT micro-inclusions, this may lead to a high degree bulk-rock magnetic anisotropy.

We suggest that the shape preferred orientation of the MT micro-inclusions in plagioclase of oceanic gabbro may impart an anisotropy of magnetic susceptibility and remanence to the host plagioclase grains. The anisotropy is expected to be represented by an oblate ellipsoid for unaltered and by a prolate ellipsoid for hydrothermally altered gabbro. In foliated gabbro, the magnetic anisotropy of the plagioclase grains is supposed to lead to bulk-rock magnetic anisotropy.

Funding by RFBR project 18-55-14003 and FWF project I 3998-N29 is acknowledged.

SYNTHESIS AND CHARACTERIZATION OF CHABAZITE-TYPE SILICOALUMINOPHOSPHATE (SAPO-44) WITH DIFFERENT SILICON CONTENTS

Akinbodunse Sileola Joseph¹, Fischer Michael¹, Spieß Iris¹

¹Faculty of Geosciences (Crystallography Research Group), University of Bremen, Germany

Silicoaluminophosphates (SAPOs) are aluminophosphate-based zeolite-like frameworks in which silicon atoms occupy a fraction of the tetrahedral sites. The varying degree of silicon incorporation influences their framework structure, physicochemical properties, and catalytic behavior. SAPO-44 has continued to gain attention in scientific research due to its potential industrial use as a solid acid catalyst and possible applications in wastewater treatment. In this work, we synthesized CHA-type SAPO-44 samples with different silicon contents via a hydrothermal route in the presence of cyclohexylamine as an organic structure-directing agent (OSDA). The samples were characterized with powder X-ray diffraction, X-ray fluorescence (XRF) spectroscopy, thermal analysis, scanning electron microscopy, and N₂ physisorption in order to study the effect of silicon incorporation on various physicochemical properties of SAPO-44, including phase purity, crystallinity, crystal morphology, thermal stability, and porosity. Variation of the silicon content in the synthesis gel within a range of SiO₂/Al₂O₃ molar ratios from 0.5 to 2.0 results in phase-pure SAPO-44, whereas SAPO-44 crystallizes alongside impurities when SiO₂/Al₂O₃ is below 0.5. The incorporation of a large amount of silicon in the framework was confirmed using XRF measurements. For the phase-pure SAPO-44 samples, the varying silicon content does not have a significant influence on thermal stability, pore-volume, and surface area. SAPO-44 has a rhombohedron/cube-like morphology, with twinned crystals of varying particle sizes up to 120 μm. It is thermally stable up to 1000°C but a thermal collapse of the CHA structure occurs between 1000 - 1100°C. The chabazite cages of SAPO-44 contain approximately six OSDA molecules per unit cell, indicating nearly complete filling of the pores. The removal of organic templates from the cages leads to variation in cell parameters, a shrinkage in the overall cell volume, formation of micropores, and the formation of Brønsted acid sites, which are vital for catalytic applications.

THE LOW-TEMPERATURE SINGLE CRYSTAL X-RAY ANALYSIS, IR AND ¹H NMR SPECTROSCOPY OF BERBORITE, Be₂(BO₃)(OH)·H₂O

Aksenov Sergey M.^{1,2}, Chukanov Nikita V.^{3,4}, Tarasov Viktor P.³, Mackley Stephanie A.⁵, Krivovichev Sergey V.^{6,7}, Burns Peter C.^{2,5}

¹Laboratory of Nature-Inspired Technologies and Environmental Safety of the Arctic, Kola Science Centre, RAS, Russia, ²Department of Civil and Environmental Engineering & Earth Sciences, University of Notre Dame, USA, ³Institute of Problems of Chemical Physics, RAS, Russia, ⁴Faculty of Geology, Moscow State University, Russia, ⁵Department of Chemistry and Biochemistry, University of Notre Dame, USA, ⁶Nanomaterials Research Centre, Kola Science Centre, RAS, Russia, ⁷Department of Crystallography, St Petersburg State University, Russia

Beryllium borates and their derivatives [1] are well known classes of inorganic compounds that attract interest due to their applications as deep-ultraviolet nonlinear-optical materials [2]. Most of them are water-free, with the natural mineral berborite, Be₂(BO₃)(OH)·H₂O, being the only exception. A sample of berborite from the Vevja quarry, Tvedalen, Larvik, Norway was studied by a combined approach involving single-crystal X-ray diffraction and ¹H nuclear magnetic resonance (NMR) at different temperatures as well as infrared (IR) spectroscopy. The crystal structure of the studied berborite corresponds to the trigonal 1*T*-polytype with the space group *P*321 [3] and is based on electroneutral [BeO₂(B^AO₃)]-layers formed by BeO₃∅-tetrahedra and B^AO₃-triangles. Adjacent layers are linked *via* hydrogen bonding of hydroxyl groups and H₂O molecules, which statistically occupy the ∅-ligand of the Beφ₄-tetrahedra. The crystal structure of natural berborite is characterized by the negative thermal expansion with the contraction in the temperature range from 90 K to 293 K. This temperature region is characterized by a small rotation of B^AO₃-triangles around the threefold axis with the changes in the geometrical characteristics of the heteropolyhedral layer with further relaxation at 293 K. Due to statistical occupancy of the ∅-ligand by hydroxyl groups (50%) and water molecules (50%), berborite-1*T* and its related polytypes are characterized by complex systems of hydrogen bonds. The analysis of residual electron density maps shows different maxima corresponding to hydrogen atoms disordered about the three-fold axis around ∅-ligands and a saddle-like point between ∅* and ∅' with equal distances to these oxygen atoms of ~1.37 Å is observed. This peak can be explained by the partial proton transfer from the oxygen atom of the ∅'-ligand to the oxygen atom of the ∅*-ligand according to the following scheme: H-∅'-H···∅*-H ↔ H-∅'···H⁺···∅*-H ↔ H-∅'···H-∅*-H. Based on the analysis of the D-H···A distances and taking into account the possible different occupancies and local environments of the ∅-ligands and interactions between them, models of hydrogen bonds in the crystal structure of berborite-1*T* (that are in good agreement with IR and ¹H NMR spectroscopy data) have been proposed. Despite the wide structural diversity of beryllium borates, their crystal structures are classified as simple (20–100 bits per unit cell) or intermediately complex (100–500 bits per unit cell). The complexity of berborite polytypes increases in accordance with the quantity of layers from 29.038 (1*T*) to 78.077 (2*H*), which is in good agreement with the negative contribution of complexity to the configurational entropy.

Acknowledgements: This study was financially supported by Russian Foundation for Basic Research (grant No. 18-29-12005_mk; 18-29-12007_mk), Russian Science Foundation (grant No. 20-77-10065) and the state task, state registration number AAA-A19-119092390076-7. PCB's involvement in this work was funded by the Chemical Sciences, Geosciences and Biosciences Division, Office of Basic Energy Sciences, Office of Science, U.S. Department of Energy, Grant No. DE-FG02- 07ER15880.

[1] F.C. Hawthorne, D.M.C. Huminicki, *The Crystal Chemistry of Beryllium*, *Rev. Mineral. Geochemistry*. 50 (2002) 333–403. [2] Y. Yang, X. Jiang, Z. Lin, Y. Wu, *Borate-based ultraviolet and deep-ultraviolet nonlinear optical crystals*, *Crystals*. 7 (2017) 1–16. [3] G. Giuseppetti, F. Mazzi, C. Tadini, A.O. Larsen, A. Asheim, G.. Raade, *Berborite polytypes*, *Neues Jahrb. Fuer Mineral. Abhandlungen*. 162 (1990) 101–116.

PROCESS MINERALOGY OF THE LLALLAGUA TAILINGS: TOWARDS A SUSTAINABLE ACTIVITY

Alfonso Pura¹, Ruiz Miguel², Sendrós Miquel¹, Garcia-Valles Maite³, Zambrana Rubén⁴, Jiménez-Franco Abigail¹

¹Enginyeria Minera, Industrial i TIC, Universitat Politècnica de Catalunya, Spain, ²Universidad Técnica de Oruro, Bolivia, ³Mineralogía, Petrología i Geología Aplicada, Universitat de Barcelona, Spain, ⁴Tecnología, Universidad Siglo XX, Bolivia

The Siglo XX mine, located close to the city of Llallagua (Bolivia), has been considered one of the richest Sn mines in the world. It is exploited from the beginning of the 1900s. The Llallagua mineralization belongs to the Central Andean Tin Belt and is mainly related to the Salvadora shallow magmatic porphyritic stock. However, a significant amount of the total reserves of Sn in Llallagua occur in dumps and tailings resulted from the mining activity and the processing in the Catavi plant. These wastes represent more than 20.7 million tonnes with an average grade of 0.3 wt.% SnO₂. Nowadays, in this plant, the ore from the mine and the tailings are being processed. The processing is mainly based on gravity concentration and the secondary tailings obtained are still rich in Sn. In this research, a process mineralogy characterization of materials from the Llallagua tailings was carried out to design an optimal processing chart.

The chemical composition of the concentrate obtained in the Catavi plant is 52-60 wt.% of SnO₂ and 0.9-1.3 wt.% of rare earth elements (REE). In the tailings still remains more than 0.2 wt.% SnO₂ and 0.02wt.% of REE. The mineralogy of the primary tailings, concentrate, and secondary tailings was determined by powder X-ray diffraction, scanning electron microscopy, and mineral liberation analysis (MLA). The tailings are mainly constituted of quartz, tourmaline of dravite and schorl types, illite, K-feldspar, plagioclase, cassiterite, rutile, zircon, and monazite. The concentrate contains mainly cassiterite (57.4 wt.%), tourmaline, quartz, hematite, and rutile. In addition, rare earth minerals are relatively abundant, about 1.62 wt.% of monazite and minor amounts of xenotime and florencite.

The MLA indicated that only 57.6 wt.% of cassiterite from the concentrate is liberated. This low liberation is responsible for the low grade of SnO₂ in the concentrate. The mean grain size of monazite is 65 µm, whereas the mean particle size is 100 µm. The non-liberated cassiterite is mainly associated with quartz, tourmaline, and rutile. The mean grain size of monazite is 45 µm and 57.5 wt.% of this is liberated and in the other cases, it occurs in particles associated with tourmaline, quartz, cassiterite, and muscovite.

To make this mining activity more sustainable, the grade of the concentrate and the metal recovery should be improved. Finer particle size of the processed tailings will increase them. In addition, the recovery of the REE present in the concentrate as a by-product should be assessed.

HIGH SPATIAL RESOLUTION MAPPING OF H₂O CONCENTRATION IN SILICATE GLASS

Allabar Anja¹, Nowak Marcus²

¹Department of Mineralogy, Georg-August University Göttingen, Germany, ²Department of Geosciences, Eberhard Karls University Tübingen, Germany

Volatile concentrations in geological glasses are routinely analyzed by several spectroscopic techniques. High spatial resolution techniques are necessary to quantify small-scale concentration gradients. A common method to analyze volatile concentrations in glasses with a high spatial resolution, in e.g. partially degassed silicate melts that are quenched to glasses, is transmission FTIR-spectroscopy using a focal plane array (FPA) detector. This method, however, requires complicated preparation of samples polished on both sides accompanied by a high amount of sample loss, and the spatial resolution is limited by the sample thickness.

Here, we present the novel usage of mid-infrared attenuated total reflection (ATR-) FTIR spectroscopy (instead of transmission) combined with an FPA detector to analyze H₂O concentration gradients in hydrous silicate glasses with high spatial resolution. Single-sided standard sample preparation as applied for electron microprobe or scanning electron microscopy is sufficient for this purpose.

Lowenstern & Pitcher (2013) calibrated total and molecular H₂O concentration in glasses with ATR-FTIR spectroscopy using a single element detector, providing a lateral spatial resolution of ~8 μm and a low sampling depth of <2 μm. The coupling of ATR with a 64x64 pixels FPA improves the lateral spatial resolution significantly, with a minimum pixel size of 0.5 μm that can theoretically be obtained. Using this ATR-FPA setup, total and molecular H₂O concentrations in peralkaline rhyolitic glass were calibrated and then applied to experimentally vesiculated and quenched glasses. The results document the ability of the method to spatially resolve and quantify H₂O gradients in the glass surrounding vesicles on a μm-scale (Allabar & Nowak, 2020) that are caused by H₂O resorption from vesicles back into the melt during isobaric cooling (McIntosh et al. 2014). Schanofski et al., (2019) calibrated ATR-FTIR spectroscopy using a single element detector for CO₂ concentrations in silicate glass. Thus, future studies may apply the high-resolution ATR-FPA method for CO₂ concentration mapping. Although the errors in H₂O concentrations obtained from ATR-FPA measurements are higher than compared to single element detector measurements, we suggest the ATR-FPA method as a useful tool for the spatially resolved analysis of both H₂O and CO₂ in melt inclusions, partly crystallized glasses, or strongly vesiculated samples for which transmission measurements are complicated or impossible. The adaption of spectrometer equipment or the usage of a synchrotron MIR light source may improve the ATR-FPA method for future applications.

Allabar, A. and Nowak, B. (2020): High spatial resolution analysis of H₂O in silicate glass using attenuated total reflection FTIR spectroscopy coupled with a focal plane array detector, *Chem. Geol.*, 556.

Lowenstern, J.B. and Pitcher, B.W. (2013): Analysis of H₂O in silicate glass using attenuated total reflectance (ATR) micro-FTIR spectroscopy. *Am. Min.* 98, 1660–1668.

Schanofski, M., Fanara, S. and Schmidt, B. (2019): CO₂-H₂O solubility in K-rich phonolitic and leucititic melts. *Contrib. Mineral. Petrol.* 174, 52.

McIntosh et al. (2014): Distribution of dissolved water in magmatic glass records growth and resorption of bubbles. *EPSL* 401, 1-11.

DEVELOPMENT OF A NOVEL HYDROPHOBIZATION METHOD FOR SILICA AEROGELS REINFORCED WITH NANO-SCALE POLYSTYRENE FIBERS

Allar Christian¹, Roth Thomas¹, Pöllmann Herbert², Krcmar Wolfgang¹

¹Faculty of Materials Engineering, University of Applied Sciences Nuremberg, Germany, ²Institute of Geosciences and Geography, Mineralogy/Geochemistry, University of Halle, Germany

Since S. Teichner first described the synthesis of silica aerogels using an alkoxy silane-based sol-gel approach, aerogels have increasingly become the focus of numerous research activities. This is because silica aerogels exhibit a number of remarkable properties due to their microstructural makeup. In particular, they are distinguished by extremely high porosities associated with exceptionally low densities and thermal conductivity values. In addition, silica aerogels exhibit good transparency, low refractive index, and high specific surface area. Due to this distinct property spectrum, silica aerogels are suitable for various applications in the field of science as well as in industrial applications. However, aerogels also have characteristics that prevent their widespread use. They exhibit extremely brittle mechanical properties, are very sensitive to moisture if they do not undergo a hydrophobization step, and are expensive to produce despite many efforts to simplify the manufacturing process. In order to improve the mechanical properties of silica aerogels, various approaches have been studied by numerous research groups. Besides direct chemical modifications of the aerogel matrix, the use of fibers as reinforcing structures has been investigated. Although fiber addition typically leads to an improvement in mechanical properties, the thermal insulation performance of the aerogels suffers as a result of fiber modification. This undesirable effect is mitigated in the case of polymer fibers, as they exhibit an acceptable level of mechanical strength while their intrinsic thermal conductivity is comparatively low. However, the use of polymeric reinforcement fibers also introduces new requirements to the aerogel synthesis process. Since fiber incorporation can only take place during the sol-gel process, the process conditions, as well as the chemicals used, must not lead to any chemical or physical damage to the polymer fibers. In addition, gelation must take place as quickly as possible after fiber addition in order to minimize buoyancy and segregation effects and thus ensure homogeneous fiber distribution in the gel. In this presentation, results on different approaches for the synthesis and surface modification of silica aerogels are presented. It was tested whether the chosen synthesis methods were suitable for incorporating nanoscale PS fibers. The hydrophobic and thermal properties of the unreinforced aerogels and their fiber-reinforced counterparts were evaluated using contact angle measurements, thermal analysis, infrared spectroscopy, and transient hot plane analysis. The best results in terms of thermal conductivity and hydrophobic properties were achieved by a new tetraethoxysilane (TEOS) based silica aerogels using methyltriethoxysilane (MTES) as hydrophobic coprecursor and trimethylethoxysilane (TMES) as secondary hydrophobizing agent. With this synthesis route, contact angles of 146° and thermal conductivity values of 0.020 W/mK were achieved. The developed synthesis route proved to be very well suited for the incorporation of nanoscale polystyrene reinforcement fibers into the silica aerogel matrix.

GALLIUM INCORPORATION INTO ALUMINUM GERMANATES WITH MULLITE TYPE STRUCTURE

Altona Karim¹, Spieß Iris¹, Birkenstock Johannes¹, Schneider Hartmut¹, Fischer Reinhard X.¹

¹Departement of Geosciences, University of Bremen, Germany

Mullite is an alumino-silicate crystallizing in the orthorhombic space group Pbam. Its main characteristic are the chains of edge-sharing AlO₆ octahedra parallel [001], interconnected by di-/tri-clusters of AlO₄ and SiO₄ tetrahedra. A variety of thermo-mechanical properties such as low thermal expansion and high fracture toughness and strength makes it an indispensable material for functional ceramics. The solid-solution series between Si-, Ge- mullite with a full miscibility has been described by Schwiete et al. (Archiv Eisenh., 1905, 1958, 513). We have recently claimed according to our preliminary results that Si-, Ge mullite can be described by the extended general formula: $^{VI}Al_2^{IV}Al_{2+2x}^{IV}(Si_y, Ge_{1-y})_{2-2x}O_{10-x}$.

It had been postulated, that the substitution of Si by Ge takes place in the tetrahedral T position. In this study we are investigating the incorporation of gallium into aluminum germanate with mullite type structure (Ge- mullite). We are expecting the substitution of gallium in the octahedral position. The synthesis approach is the sol-gel method followed by sinter-crystallization.

Phase identification and refinement of crystal structures were based on powder diffraction data. Miscibility and phase purity over almost the full range of the solid-solution series is observed, except for compositions close or equal to the Ga- endmember where a second phase with andalusite type structure was formed. The substitution of Al by Ga caused a unit-cell volume expansion of 9.7 %. The lattice parameters of the mullite phase increased as a function of gallium content ranging from: a = 7.6606 Å, b = 7.7657 Å, c = 2.9205 Å for the aluminum endmember to a = 7.8704 Å, b = 8.0327 Å, c = 3.0144 Å for the gallium endmember. Optical microscopy revealed particle sizes in the range of 5 µm to 100 µm with a tendency to agglomerate, whereas the individual crystallite size was not exceeding 30 µm. We present a general crystal-chemical formula for the solid-solution series:

$^{VI}(Al_{1-z}Ga_z)_2^{IV}(Al_{1-w}Ga_w)_{2+2x}^{IV}Ge_{2-2x}O_{10-x}$.

Potential distortions of 6- and 4- fold coordinated Ga-polyhedra are currently under investigation. To determine particle shapes and their chemical compositions, scanning electron microscopy measurements together with energy dispersive X-ray spectroscopy are in progress.

A MULTIDISCIPLINARY APPROACH TO THE STUDY OF GRAPHITE-PAINTED POTTERY FROM THE NEOLITHIC/CHALCOLITHIC BALKANS

Amicone Silvia¹, Berthold Christoph¹

¹Competence Center Archaeometry- Baden-Wuerttemberg , University of Tuebingen, Germany

Graphite decoration on ceramic vessels is a distinctive phenomenon spread over most of the Balkans during the 5th millennium, becoming one of the dominant forms of decoration for Neolithic and Chalcolithic material cultures in the region for over 1000 years. This technique consists of applying a slip containing graphite to vessel surfaces either before or after the firing. Traditionally, archaeologists have closely related graphite decoration with the rise of metallurgy. However, the emergence and development of this decorative technique on pottery remain unclear, mostly due to the lack of systematic technological investigations of this technique.

An interdisciplinary approach employing macro observation and analytical methods including thin section petrography, XRPD, μ -XRD2, μ -Raman, and SEM was applied to a selection of ceramic samples decorated with graphite from different areas of the Balkans, including Serbia, Romania, and Bulgaria. The results give important information about the procurement and processing of raw materials as well as essential insights into the pyrotechnology related to graphite painted pottery. Very importantly, the combination of μ -XRD2 and μ -Raman analysis revealed that both well crystalline natural graphite and the application of pigments containing poorly crystalline carbon were used, pointing to the possible existence of at least two different manufacturing recipes to produce this type of decoration. The initial results of our research illustrate well the advanced pyrotechnology knowledge reached by these populations at that time.

CRYSTAL CHEMISTRY OF ION CONDUCTING Li-GARNETS

Amthauer Georg¹

¹Chemistry and Physics of Materials, University of Salzburg, Austria

Recent research has shown that certain Li-oxide garnets with more than 3 Li atoms per formula unit, such as $\text{Li}_7\text{La}_3\text{Zr}_2\text{O}_{12}$ (LLZO), have high ionic conductivities, as well as good chemical and physical properties for use in solid-state batteries.

“Garnet” is the common name for a large number of natural and synthetic metal-oxide phases. Conventional oxide garnets have the general formula $\text{A}_3\text{B}_2\text{C}_3\text{O}_{12}$ and crystallize in the cubic space group Ia-3d. In LLZO the A-positions are occupied by La^{3+} , the B-positions by Zr^{4+} , and the C-positions by Li^+ . In addition to these cation sites, there are other interstices within the garnet oxygen framework, which are empty in the conventional garnet structure and which are in LLZO filled by “excess” Li^+ ions giving rise to the excellent ionic conductivity. There is a low-temperature tetragonal modification of pure LLZO (SG: I41/acd) and a high-temperature non-quenchable cubic phase of LLZO (SG: Ia-3d). The tetragonal phase has distinctly lower ion conductivity than the cubic phase. Fortunately, the cubic phase can be stabilized at low temperatures by doping with low amounts of Al, Ga, and Fe. In our contribution, the results of single-crystal X-ray diffraction studies will be presented. While Al-doped LLZO garnets always crystallize within the space group Ia-3d, Ga and Fe-doped LLZO garnets crystallize within the space group I43d (Wagner et al., 2016). This symmetry change is combined with an increase in ionic conductivity up to $10^{-3} \text{ S cm}^{-1}$ which is very high for those kinds of solid-state electrolytes used in Li-ion batteries. These results will be discussed on the basis of the slightly different topologies of both space groups, respectively.

CHARACTERIZATION OF THE PIAVITSA CARBONATE-REPLACEMENT SULFIDE MINERALIZATION, GREECE: CONCURRENT XCT/XRF SCANNING AND TRADITIONAL METHODS

Andersson Stefan S.¹, Sandoval Moreno Daniel G.¹, Jonsson Erik², Högdahl Karin¹, Sahlström Fredrik³, Luth Stefan², Bakker Edine², Zack Thomas⁴, Hansson Alexander⁵, Kalampaliki Sofia⁶, Baker Tim⁷, Arvanitidis Nikolaus²

¹Department of Earth Sciences, Uppsala University, Sweden, ²Department of Mineral Resources, Geological Survey of Sweden (SGU), Sweden, ³Department of Geosciences, UiT The Arctic University of Norway, Norway, ⁴Department of Earth Sciences, University of Gothenburg, Sweden, ⁵Orexplore AB, Sweden, ⁶Hellas Gold, Greece, ⁷Eldorado Gold Corp., Canada

The Piavitsa carbonate-replacement sulfide mineralization is part of the larger mineralized system of the Stratonii fault zone within the Kassandra Mining District in northern Greece. As part of the X-MINE Horizon-2020 project (No 730270), drill cores from Piavitsa have been scanned by concurrent X-ray computed tomography and fluorescence (XCT-XRF) imaging using the GeoCore X10. To validate and refine the results from the scanning technology, a detailed characterization of the mineral assemblages and the distribution of base, precious and critical metals have been conducted utilizing optical and electron microscopy and EDS, EMPA-WDS, and LA-ICP-MS in situ microchemical analysis. From the XCT-XRF imaging, mineralized sections of the drill cores can be quickly identified and separated into ore and gangue minerals based on differences in X-ray attenuation. The chemical data (XRF) provide a good indication of the presence and relative concentrations of some major (Cu, Fe, Mn, Pb, and Zn) and minor (As, Sb, Sn) elements within the mineralization.

From the mineralogical studies, three fundamental sulfide assemblage types have been recognized: 1) the main ore zone consisting of sphalerite-pyrite-galena-quartz-(chalcopyrite) ore with late carbonate-quartz infill, 2) sphalerite-alabandite-(pyrite-galena) ore with carbonate-quartz infill and, 3) sphalerite-pyrite-galena-tetrahedrite-(chalcopyrite) ore with carbonate infill. In general, euhedral sphalerite, pyrite, quartz, and minor arsenopyrite are the earliest ore-related phases followed by chalcopyrite-tetrahedrite-galena ore assemblages. Many of the sulfides are partly brecciated and show corroded grain boundaries towards the enclosing and later carbonate infill. Some more uncommon ore assemblages characterized by the presence of tetrahedrite, seligmannite-bourbonite, and kesterite locally cross-cut both the earlier sulfide assemblages and the carbonate infill.

Most of the carbonates in the infill exhibit compositions close to kutnahorite although some approach rhodochrosite compositions. The Mn-rich carbonate compositions are associated with the sphalerite-alabandite ore assemblages, where euhedral rhodochrosite has partly replaced and overgrown sphalerite and alabandite. Ca-Mn-Mg-carbonates occur as open-space fillings and have overgrown the early carbonates. The Mn-rich character of this ore assemblage is also reflected in the composition of sphalerite, which hosts 3 to 7 wt. % Mn, and when intimately associated with alabandite, up to c. 13 wt. % Mn.

Main ore zone sphalerite has Mn concentrations of about 1 wt%, and further contains up to 1000 ppm Cu, 60 ppm Ga, and 600 ppm Sn. Sphalerite from the tetrahedrite-rich ore assemblages exhibits the highest concentrations of these trace elements (600-8000 ppm Cu, 110-230 ppm Ga and 250-6400 ppm Sn). In the tetrahedrite-rich assemblages, tetrahedrite is the preferred host for Au (2-8 ppm) instead of pyrite (< 5 ppm), which overall is the primary Au carrier at the mineralization. The highest concentrations of Au in pyrite are from the sphalerite-alabandite ore assemblages (reaching 75 ppm). The sphalerite-alabandite and tetrahedrite-rich ores in Piavitsa generally host higher concentrations of trace metals compared to the main ore zone (e.g., Ag, Au, Ga, Sb, Sn) and are suggested to represent different, and in part later stages of ore formation in the system.

INTERCALATION OF KAOLINITE. NEW INSIGHTS FROM A COMBINED NEAR-INFRARED AND XRD INVESTIGATION

Andreou Fevronia T.¹, Siranidi Eirini¹, Chryssikos Georgios D.¹, Ciesielska Zuzanna², Szczerba Marek², Derkowski Arkadiusz²

¹Theoretical and Physical Chemistry Institute, National Hellenic Research Foundation, Greece, ²Institute of Geological Sciences, Polish Academy of Sciences, Research Centre in Cracow, Poland

Kaolinite intercalation is a chemical reaction related to the spontaneous penetration and subsequent self-assembly of specific organic compounds in the interlayer space of the mineral. In the present study, FT-near infrared spectroscopy (NIR) and XRD are employed for the first time to study in situ, in real-time, and as a function of temperature the kinetics of kaolinite intercalation with N-methylformamide (NMF). XRD probes the evolution of coherently expanded interlayers along *001*, whereas NIR measures the increasing concentration of the intercalated species under controlled environmental conditions. This combined experimental approach was applied to three different kaolinites differing in stacking order and particle size distribution (KGa-1b, KGa-2 from the Clay Minerals Society, and Hywite Superb from Imerys). With both techniques, the reaction was studied in closed reactors and the presence of excess NMF.

NIR monitoring relied on the increasing intensity of the 2νNH mode of the intercalating NMF molecules. At any given temperature, the position and width of this band, which were identical in all kaolinites, remained stable during intercalation. This implied a common NMF-hosting interlayer environment, independent of reaction progress. This constant configuration can only be attributed to full intercalation because partially intercalated interlayers would exhibit time-dependent environments for NMF. Sigmoidal kinetics were recorded in the 25-80°C range and demonstrated perfect time-temperature superposition collapsing to a single master curve, unique for each kaolinite. All samples exhibited the same activation energy ($E_a=62\pm 3$ kJ/mol, 14.8±0.7 Kcal/mol).

No partially intercalated interlayers and no interstratification of intercalated and pristine kaolinite were detected by XRD, suggesting that the intercalation of large portions of crystallites was instant. Kinetics based on the changing *001* reflection intensities of pristine and intercalated kaolinite resulted in sigmoidal traces matching NIR, despite the different time/length scales.

It was concluded that both NIR and XRD monitored the switching between pristine and fully intercalated kaolinite entities and not the elementary chemical processes leading to the filling of the interlayers. For this reason, it is proposed that the sigmoidals represent the temporal distribution of intercalation events and can be fitted with the log-normal function. The multiplicative standard deviation of the distribution which determines the steepness of the sigmoidal is a sample-specific property of kaolinite.

Work at NHRF was supported by a) project “Advanced Materials and Devices” (MIS 5002409) of TPCI-NHRF, funded by the Operational Program "Competitiveness, Entrepreneurship, and Innovation" and co-financed by Greece and the European Union, and b) the Applied Spectroscopy Lab at TPCI.

FLY ASH-BASED ZEOLITES VS ZEOLITE-CARBON COMPOSITES – PROPERTIES AND POSSIBILITIES OF ABSORPTION OF PESTICIDES

Andrunik Magdalena¹, Skalny Mateusz¹, Bajda Tomasz¹

¹Faculty of Geology, Geophysics and Environmental Protection, AGH University of Science and Technology, Poland

Nowadays, it is difficult to imagine the cultivation of plants without chemicals. Food has to be produced at low cost, on farmlands that are less and less fertile. The solution to this problem through the use of pesticides and artificial fertilizers is only a temporary solution in a large-scale, intensive farming economy. Due to their persistence in the environment, even pesticides banned decades ago are still detected in the environment. In this study, three zeolites with faujasite (NaX-C), LTA (NaA-C), and gismondite (NaP1-C) structures and three composites of active carbon and zeolites were investigated. The zeolites were produced from F-class fly ash, while the composites were synthesized from high carbon fly ash, derived from the combustion of hard coal. The properties of zeolites and zeolite-carbon composites were studied by X-ray diffraction (XRD), Fourier transform infrared spectroscopy (FTIR), and scanning electron microscopy (SEM). The adsorption of 2,4-D (2-(2,4-dichlorophenoxy)acetic acid), MCPA (2-(4-chloro-2-methylphenoxy)acetic acid), carbendazim (methyl N-(1H-benzimidazol-2-yl)carbamate) and simazine (6-chloro-2-N,4-N-diethyl-1,3,5-triazine-2,4-diamine) were tested under static conditions. The concentration of pesticides in the remaining solutions was determined by high-performance liquid chromatography (HPLC) with a diode array detector.

The phase composition of the tested sorbents was obtained during XRD analysis. The diffraction patterns of individual materials show reflection characteristics of NaA, NaX, and NaP1 zeolites. All composites exhibit a characteristic baseline elevation, indicating the presence of an amorphous phase in the range of 20-30 °2θ. FTIR spectra of zeolites and zeolite-carbon composites allow identifying the characteristic bands originating from the secondary building units (SBU) present in the zeolite structures. SEM images of zeolite-carbon composites show that zeolites crystallized in the intermolecular spaces and on the carbon surface. The shape of zeolites depends on the zeolite type. SEM image of NaA zeolite shows well-shaped cube-like crystal, for NaX is an octahedron that is composed of eight equilateral triangles, while for NaP1 lamellar aggregates are formed. In all zeolite samples, residues of unreacted fly ash are visible. Experiments of pesticide adsorption revealed that zeolite-carbon composites exhibit higher adsorption capacity than zeolites. In aqueous solutions, 2,4-D and MCPA occur in anionic form. Since the surface of zeolites is negatively charged, it is not surprising that the adsorption efficiency of zeolites and zeolite-carbon composites is limited. The adsorption properties depend on the zeolite and composite type, however, there are not strict correlations between the adsorption efficiency and the type of zeolite in the analyzed materials.

The zeolite carbon composites are characterized by good sorption ability, especially towards simazine and carbendazim. Adsorption efficiency depends on the type of pesticide, which suggests that the structure of molecules plays an important role in the mechanisms of removal.

This research was financed by the Foundation for Polish Science (FNP), Poland, Grant No. TEAM-NET-POIR.04.04.00-00-14E6/18-00.

HEAT CAPACITY AS A CONSTRAINT ON EQUATION OF STATE PARAMETERS: APPLICATION TO GARNETS

Angel Ross J.¹, Gilio Mattia², Alvaro Matteo²

¹IGG-CNR, Italy, ²Earth & Environmental Sciences, University of Pavia, Italy

The determination of precise Equations of State for minerals is the basis for both thermodynamic calculations for minerals and their elastic properties. Equations of State (EoS) are thus crucial for petrology and geophysics. Unfortunately, even for the most extensively studied minerals such as garnets, the available measurements of the volumes and bulk moduli at high pressures, high temperatures, and simultaneous high P and T, are often not sufficient to allow their EoS parameters to be determined unambiguously. On the other hand, heat capacity measurements (C_p) at room pressure are widely available, but these have not often been used to constrain EoS. Here we present new features that we have introduced into the summer 2021 update of the EoSFit software to calculate heat capacities from EoS.

For thermal-pressure types of EoS, such as Mie-Grüneisen-Debye or that used in Thermocalc, the thermal pressure is expressed in terms of the heat capacity at constant volume, C_v . In EoSFit this is converted into the heat capacity at constant pressure C_p by using the bulk modulus, volume, and thermal Grüneisen parameter calculated from the EoS. For other types of EoS in which the heat capacity is not explicitly given, we use the Grüneisen relationship to calculate the C_p from the bulk modulus and thermal expansion coefficient, which are defined by the EoS parameters, and the thermal Grüneisen parameter which can be specified by the user. If adiabatic elastic moduli are used along with volume data to refine the EoS parameters, the thermal Grüneisen parameter is also defined completely by the EoS.

We will use the example of garnet end-members to show how being able to calculate C_p from EoS can help to identify inconsistent data, thereby yielding more reliable EoS that provide insights into the atomic mechanisms behind the variation of elastic and thermodynamic properties in garnets. In particular, we will show that garnet elasticity and volume variation can be described completely by q-compromise forms of the MGD EoS, and thus behave thermodynamically as quasi-harmonic solids.

The update of the EoSFit software package released in summer 2021 includes the calculation of heat capacities from EoS, and the q-compromise version of the MGD EoS, along with other new features including EoS for mixtures, internally consistent EoS for anisotropic minerals, and host-inclusion calculations for anisotropic minerals. The software can be downloaded for free from www.rossangel.net

This work has been supported by the European Research Council under the European Union's Horizon 2020 research and innovation program through grant 714936 to Matteo Alvaro, and by the SIRMIUR Grant MILE DEEp (no. RBSI140351) to Matteo Alvaro.

CONSTRAINTS ON DIAMOND GROWTH ENVIRONMENTS IN THE MANTLE FROM INCLUSION ORIENTATIONS

Angel Ross J.¹, Nimis Paolo², Alvaro Matteo³, Nestola Fabrizio²

¹IGG-CNR, Italy, ²Geosciences, University of Padova, Italy, ³Earth & Environmental Sciences, University of Pavia, Italy

The mineralogy and chemical compositions of inclusions in diamonds are the primary sources of information about the mantle environment in which diamonds grew. While the idea that orientations can also contribute such information dates back at least to the 1950s, the literature has been confused for 70 years by the conflation of orientation measurements with their analysis and interpretation. Clarity has been brought to the subject by the concepts and terminology of Crystallographic Orientation Relationships (CORs) between a host and its inclusions as developed by the Vienna group. In combination with the analysis tool of the OrientXplot program (www.rossangel.net) and the rapid increase in the number of orientation measurements made in the last decade, this allows statistically robust conclusions to be drawn about the mechanisms of diamond growth in the mantle.

We have shown that olivines and garnets exhibit no specific orientation relationship with respect to their host diamonds; this is termed a random COR and is consistent with the presence of a fluid film found between the inclusions and diamonds. However, inclusions in a single diamond often exhibit similar orientations. This indicates that lithospheric diamonds grew from a C-rich fluid by nucleation on grain boundaries in the mantle and subsequent dissolution of the surrounding mineral grains, with the iso-oriented inclusions representing undissolved surviving fragments of the original mineral grains. Analysis of the spacing of these inclusions indicates the mineral grain size in the mantle. Approximately half of magnesiochromite inclusions in lithospheric diamonds also exhibit a random COR consistent with the observation of a fluid film and diamond growth in the mantle from a fluid. The others approximate a rotational COR with [111]mgchr close to [111]diamond, which indicates mechanical interaction between diamond and spinel octahedra during entrapment.

Preliminary data on relatively Fe-rich ferropicriole inclusions in sub-lithospheric diamonds show a rotational COR, rotated around [111] or [112] that approximates a specific COR in which the crystallographic axes of the cubic inclusions are very close to those of the diamonds. The small distribution of orientations suggests that the ferropicriole inclusions exhibited a specific COR when they grew as a result of interfacial energy minimization, in turn implying that no fluid film separated the inclusions and diamond during growth and that these inclusions are a product of the diamond-forming reaction. This would mean that the compositions of such inclusions are not representative of bulk mantle ferropicriole, but only of the reaction itself. The interpretation is that the specific COR was subsequently transformed into a rotational COR by post-entrapment plastic deformation of the diamonds.

Modern analysis tools with a sound theoretical and statistical basis in the concept of CORs will allow further measurements of large numbers of inclusions in diamond to be used to provide further robust constraints on the growth mechanisms of diamonds and the mineralogy and petrology of the mantle in which they grew.

This work has been supported by the European Research Council under the European Union's Horizon 2020 research and innovation program through grants 307322 to Fabrizio Nestola and 714936 to Matteo Alvaro, and by the SIRMIUR Grant MILE DEEP (no. RBSI140351) to Matteo Alvaro.

Keynote

IRON OXIDE CHEMISTRY – RECENT ADVANCES AND APPLICATIONS IN LOW-TEMPERATURE ORE GENESIS

Angerer Thomas¹, Thorne Warren², Hagemann Steffen G.², Tribus Martina¹

¹Institute of Mineralogy and Petrography, Innsbruck University, Austria, ²CET, University of Western Australia, Australia

Iron oxides are ubiquitous minerals in the earth's crust and their structural and chemical complexity has enticed earth scientists for a long time. In recent years, the trace element content of magnetite and hematite in ore systems has been receiving enormous attention. This contribution reports on recent advances in the use of iron oxides as “archives” of ore-forming processes.

During mineralization, iron oxides can form by contrasting mechanisms, such as monomer precipitation, coalescence of nanoparticles, and oxide transformation (redox and non-redox CDR and dehydration). These processes may have a significant impact on the oxides' chemistry, and thus can potentially be used for deciphering ore genesis and ore type discrimination.

An example, where all of these iron oxide forming mechanisms are preserved and that allows for a wealth of new inferences based on oxide chemistry, are low-temperature, high-grade (60-69 wt.% Fe) iron ore deposits hosted in banded iron formation (BIF). The Mt. Tom Price and Mt. Whaleback deposits in the Western Australian Hamersley Province are amongst the largest and highest-grade iron oxide accumulation in the accessible crust - yet their genesis remains unclear. The deposits consist of nearly monomineralic porous magnetite and microplaty hematite orebodies with locally preserved, variable reduced to oxidized, alteration haloes with an uncertain relationship to ore. In-situ laser ablation reveals that magnetite chemistry in carbonate-silicate-altered BIF are very different from magnetite in unaltered BIF (i.e., relatively enriched in most cations), while hematite in ore shows trace metal patterns similar to magnetite and hematite in altered BIF. This suggests that carbonate alteration “prepared the ground” for hematite. Furthermore, ore-forming hematite chemistry reveals distinct and contrasting gradients of metal abundances across orebody, which are spatially and genetically controlled by extensional faults. Here, characteristic reservoir-controlled fluid chemistries (e.g. from mafic country rocks) and Eh-pH gradient are a parameter that controls oxide chemistry. Hematite petrography down to the nanoscale supports protracted precipitation from fluids by showing complex zones around cores of early BIF-related hematite. Contrasting hematite types, from nano-coalescence and goethite dehydration, are also preserved, on mineral surfaces and in weathering-related zones, thus seemingly unrelated to ore-formation. The multi-stage sequences of early Fe-carbonate-silicate alteration controlling multiple zones of fault-controlled hydrothermal hematite mineralization are supported by Fe and O isotope trends, and compatible with models for various other BIF-hosted hematite orebodies worldwide.

The study shows that combined petrography and mineral chemistry of iron oxides are valuable genetic “archives” that record fluid/rock interaction and potential cryptic alteration stages. Their chemistry records signatures that are inherited from pre-existing (i.e., replaced) mineral phases, from the mineralizing fluid chemistry, and/or are dependent on solubility (i.e., eH-pH variation). To attain more quantitative conclusions, some critical shortcomings need more work: these include the need for data sets of partitioning coefficients for the solid solution and surface sorption, information on the open system behavior of metals, and an increase of analytical accuracy and sensitivity by matrix-matched reference materials.

CRUSTAL MAGMATIC SYSTEMS ENVISIONED AS COMPLEX DYNAMIC NETWORKS

Annen Catherine¹, Lesieur Claire²

¹Institute of Geophysics, Czech Academy of Sciences, Czech Republic, ²Institut Rhônealpin des systèmes complexes, IXXI-ENS-Lyon, France

A series of evidence suggest that magmatic systems are highly dynamic complex networks. Magma chambers are open systems that are regularly replenished with new magma and many plutons show evidence of incremental emplacement and growth by the addition of successive magma batches. Geophysical observations reveal the presence of multiple melt reservoirs in currently active magmatic systems, whereas geochemical and petrological data show that some eruptions are fed by several magma reservoirs that evolved independently and connected shortly before the eruption.

Volcanic activity is characterized by multiscale cycles that are typical of complex systems. Similar forms of scale invariance are recognized in intrusive activity. The relationship between eruption size and eruption frequency follows a power law that indicates a complex system behavior.

If we acknowledge that magmatic systems behave as complex networks, we can use the science of complex systems to better understand their dynamics. In this context, magma reservoirs are the nodes of the network and the links between nodes are dykes, sills, or networks of veins. With magma and mush being networks of crystals, melt, and volatiles, not only are magmatic systems networks of magma reservoirs, but they are networks of networks so that the dynamics of the system is controlled at different spatial scales. The behavior of a complex system cannot be reduced or inferred from the properties of its constituents due to the emergence of a new phenomenon at a global scale. Processes at one scale affect processes at another scale and understanding complex systems requires understanding the connections between the components of the network at all other scales. Therefore, the information acquired on one or even several magma bodies is not sufficient to predict the evolution of the magmatic system as a whole, which limits our ability to forecast eruptions.

For a magmatic event to happen, either intrusive or eruptive, links between nodes must be activated. One fundamental question is how the network is activated and how many nodes are involved. A related question is what controls the size of an eruption. Are the largest eruptions resulting from a feedback effect that leads to the accumulation of magma on one or a few nodes only or, on the contrary, are they due to cascading events involving a large number of nodes and links? A meaningful observation is that the long-term average eruptive flux from stratovolcanoes characterized by frequent small eruptions is not statistically different from the eruptive flux of caldera-forming volcanoes characterized by rare voluminous eruptions. This suggests that different types of eruptions are not due to more magma volume being injected into the system but correspond to different topologies of the magmatic network.

DECAY OF HISTORICAL BUILDING STONES AND THEIR CONSOLIDATION: INFLUENCE OF MINERALOGY AND MICROSTRUCTURES

Aquino Andrea¹, Pagnotta Stefano¹, Lezzerini Marco¹

¹Earth Sciences, University of Pisa, Italy

Through the centuries, different stones have been used throughout Tuscany as building materials. One among them has been widely used in most of the historical buildings of the main cities of Tuscany, like Florence, Pisa, Lucca, and of the main buildings of minor towns and villages. This lithotype is a particular sandstone from the Macigno Formation (Upper Oligocene to Lower Miocene), a flysch-like deposit that crops out extensively in the Northern Apennines, and it is made of sandstones ranging in color from grey to bluish-grey, well-consolidated, with a grain size from fine to medium, poorly to moderately sorted, containing quartz, feldspars, and micas. This stone, characterized by a peculiar, old-time look, gives to the places where it has been employed their typical aspect, displaying a show of colors ranging from bluish-grey to yellowish-grey depending on its weathering grade. Within the framework of a major research program dedicated to understanding the influence of mineralogy and stone microstructures of the natural stones quarried in north-western Tuscany, a thorough study with respect to the mineralogy and also to physical and mechanical properties was performed according to European Standards/Norms indications. Generally speaking, the studied stones can be classified as heavy and compact rocks, characterized by both low values of porosity and water absorptions at atmospheric pressure, unaffected by freeze-thaw cycles, with high strength for compression, flexure, and impact stress. In this work, selected samples have been artificially degraded and subsequently subjected to consolidating treatments. A comparison of their mineralogical features between unweathered and weathered samples and of the effects of the consolidating products is given.

POLYTYPIISM OF $\text{AlPO}_4 \cdot 2\text{H}_2\text{O}$ VARISCITE

Ardit Matteo¹, Phillips Brian², Bish David³

¹Department of Physics and Earth Sciences, University of Ferrara, Italy, ²Department of Geosciences, Stony Brook University, United States, ³Department of Chemistry, Indiana University Molecular Structure Center, United States

Variscite (orthorhombic), a hydrated aluminophosphate with formula $\text{Al}(\text{PO}_4) \cdot 2\text{H}_2\text{O}$, and metavariscite (the monoclinic polymorph) are uncommon secondary minerals that are relevant in environmental applications and particularly in technological applications when synthesized in a dehydrated form. Although two orthorhombic modifications are known (so-called "Lucin-type" and "Messbach-type"), the fine-grained nature of the "Messbach-type" variscite has hampered the determination of its crystal structure.

In this contribution, the crystal structure of the latter (a natural specimen from Tooele County, Utah) has been solved and refined using X-ray powder diffraction data via ab initio charge-flipping methods and the Rietveld method. Our results, structural interpretations, and topological analysis demonstrate that the two orthorhombic structural modifications are polytypes, and we refer to them as variscite1O ("Lucin-type") and as variscite2O ("Messbach-type"), to be consistent with modern polytype terminology. The structure of variscite2O is similar to that of the 1O polymorph, with a doubling of the b unit-cell parameter. The variscite2O crystal structure contains two crystallographically independent Al^{3+} cations coordinated by two H_2O molecules and four oxygen atoms of the PO_4 groups. Two crystallographically independent PO_4 tetrahedra share their corners with four adjacent $\text{AlO}_4(\text{OH})_2$ octahedra. Both orthorhombic polymorphs belong to the family of framework 3D MT structures in which octahedra (M) and tetrahedra (T) are linked by bridging O atoms, and topological analysis suggests that these two structures may be considered polytypes. Similarities between these polytypes, along with observed broadening of diffraction peaks of the Tooele material, suggest that interstratifications of the two forms may exist in nature. Besides the long-range characterization of the crystal structure by X-ray diffraction, information on the short-range structural properties of this mineral has been gained through ³¹P and ²⁷Al MAS/NMR measurements. Results from NMR corroborate the crystal structure determination and they show distinct signals for each of the two independent P and Al positions in variscite2O. In addition, high-temperature XRD, thermal analyses, and NMR measurements clarified the nature of the transformation of variscite2O to the derivative AlPO_4 structure. The crystal structure of this new anhydrous AlPO_4 phase (AlPO_4 -variscite2O in analogy to its parent structure) can be described as a 3D framework of alternating AlO_4 and PO_4 tetrahedra linked by bridging O atoms. Thermogravimetric analyses revealed almost complete dehydration above ~450K, and NMR results were consistent with Al and P atoms located at tetrahedral sites.

CERAMIZATION OF HAZARDOUS ELEMENTS: BENEFITS AND PITFALLS OF THE INERTIZATION PROCESS IN SILICATE CERAMICS

Ardit Matteo¹, Zanelli Chiara², Conte Sonia², Molinari Chiara², Cruciani Giuseppe¹, Dondi Michele²

¹Dept. Physics and Earth Sciences, University of Ferrara, Italy, ²ISTEC, CNR, Italy

The worldwide production of silicate ceramics implies a huge demand for raw materials, which represents an open challenge for turning ceramic manufacturing fully sustainable in the long run. The transition towards a Circular Economy requires to enhance the resource efficiency also by reducing the consumption of strategic raw materials by waste recycling; this could turn into a common practice in the manufacturing of silicate ceramics of particularly high throughput productions, from bricks to whiteware. However, it must be taken into account that the introduction of wastes can considerably expand the compositional spectrum of raw materials with possible inclusion of hazardous components. Therefore, prior to the resorting of any waste as secondary raw material, it is fundamental to assess the degree of inertization of hazardous elements through the ceramization process. The present contribution examines the relevant literature, with a quantitative approach, to unveil whether the benefits of incorporating hazardous elements (HE) in silicate ceramics can hide pitfalls. The mobility of HE (Ba, Zn, Cu, Cr, Mo, As, Pb, Ni, Cd) was parameterized by three descriptors (efficiency of immobilization, mobilized fraction, and hazard quotient) using leaching data. The incorporation of HE can take place both in crystalline and glassy phases, according to the type of ceramic body: largely unreacted, largely recrystallized and largely vitrified. The new formed crystalline phases (i.e., plagioclase, orthoclase, clinopyroxene, melilite, mullite and spinel) may offer a range of structural sites able to host HE, differing for metal-oxygen mean bond distance, polyhedral volume, polyhedral distortion index and effective coordination number. On the other hand, the vitreous phases formed in silicate ceramics can also accommodate HE under different conditions, which include valence state, oxygen coordination, metal-oxygen distance, and possible occurrence of complexes, implying a more or less efficacious incorporation of HE into the glass network. To fulfill the acceptance limit for inert materials, ceramics must have a remarkably high efficiency of immobilization (often >99.9%). This was generally accomplished for Ba, Cd, Ni and Zn. Barium, for instance, is well immobilized in all ceramic product types, firstly, for the presence of plagioclase and K-feldspar where it can be hosted; secondly, for its role of charge compensator for Al³⁺, that implies Ba²⁺ ions connected with the tetrahedral framework of aluminosilicate glass. Conversely, a high hazard quotient was sometimes found for Mo, As, Cr, Pb, Cu. Such behavior is related to the occurrence of oxy-anionic complexes (Mo, As, Cr) forming their own phases or being not linked to the tetrahedral framework of aluminosilicate glass. To improve the stabilization in silicate ceramics, often ineffective for As and particularly Mo, it is necessary to design a specific inertization strategy.

CONSTRAINING TIME SCALES OF THE DECOMPRESSION OF MANTLE ROCKS FROM SECONDARY CHEMICAL ZONING OF GARNET FROM THE GFÖHL UNIT, MOLDANUBIAN ZONE

Asenbaum Rene¹, Racek Martin², Petrishcheva Elena¹, Abart Rainer¹

¹Department of Lithospheric Research, University of Vienna, Austria, ²Institute of Petrology and Structural Geology, Charles University, Czech Republic

Several meters to 100 m sized mafic-ultramafic lenses embedded in felsic rocks of the Gföhl unit, Moldanubian zone, are considered as mantle fragments incorporated into mid-crustal rocks during the Variscan orogeny. We investigated several 100 m sized garnet-pyroxenite occurrences in felsic granulites. The primary mineral assemblage comprises calcium-rich garnet ($X_{\text{Grs}}=0.4$), kyanite, and aluminum-rich clinopyroxene ($X_{\text{CaTs}}=0.23$) which indicate pressures of about 1.9 GPa and temperatures of 1100°C. Towards the margins of the mafic lens, the garnet pyroxenites were increasingly overprinted at lower pressure conditions leading to the destabilization of kyanite, Na-rich clinopyroxene, and garnet. A first decompression phase is represented by garnet-hosted sapphirine-spinel-plagioclase symplectites supposedly replacing kyanite and clinopyroxene. A second stage is evident from partial resorption of garnet by plagioclase and clinopyroxene in the form of “corrosion tubes” penetrating the garnet in a worm-like fashion. Phase relations indicate temperatures of about 1100°C and pressures of 1.0 GPa. Finally, at pressures below about 0.8 GPa and temperatures of about 800°C garnet was partially replaced by plagioclase-orthopyroxene-spinel symplectites. In all cases, garnet shows pronounced secondary compositional zoning towards the decompression products. For the sapphirine-spinel-plagioclase symplectites and the plagioclase-clinopyroxene corrosion tubes, the secondary zoning is characterized by a decrease of the Ca content from $X_{\text{Grs}}=0.4$ in the pristine garnet down to $X_{\text{Grs}}=0.15$ at the interface to the replacement domains and a concomitant increase of the Mg- and Fe-contents from $X_{\text{Pyr}}=0.4$ to $X_{\text{Pyr}}=0.55$ and from $X_{\text{Alm}}=0.2$ to $X_{\text{Alm}}=0.3$, respectively. The secondary zoning towards the plagioclase-orthopyroxene-spinel symplectites is due to an increase of the Fe-content and concomitant decrease of the Mg content at constant Ca-content. In all cases, the compositional changes are gradual suggesting diffusion-mediated re-equilibration of the garnet at decreasing pressures. Time scales for the duration of the decompression history were estimated by fitting a multicomponent diffusion model to the observed compositional patterns. Depending on the choice of the diffusion coefficients, the time scales vary from several hundred to hundred thousands of years, where the earliest decompression features deliver time scales that are five times longer than those obtained from the corrosion tubes and about ten times longer than those obtained from the plagioclase-orthopyroxene-spinel symplectites. These timescales reflect the duration of the decompression process from the start of the respective decompression reaction to the time when the rocks cooled below about 700°C so that the composition patterns of the garnet were effectively frozen. The longest timescales obtained from the early decompression reactions are on the order of 100000 years and the shortest timescales obtained from the late-stage symplectites are on the order of 1000 years. These timescales are remarkably short in the context of the evolution of the Moldanubian zone and suggest rapid transport of the mafic-ultramafic lithologies from mantle depth into an intermediate crustal level and concomitant integration into a dominantly felsic environment accompanied by immediate cooling.

ESTIMATING NON-DESTRUCTIVELY THE CRYSTAL CHEMISTRY OF BIOTITES BY RAMAN SPECTROSCOPY

Aspiotis Stelios¹, Schlüter Jochen², Mihailova Boriana¹

¹Erdsystemwissenschaften, University of Hamburg, Germany, ²CeNak, Mineralogisches Museum, University of Hamburg, Germany

Hydrous layered silicates can be found in a variety of cultural heritage objects such as clay tablets, earth pigments, blotting sand, weathering products on the surface of silicate-based written artifacts, and inscribed gems. Among them, clay tablets are of critical importance as they are one of the oldest examples of inscribed objects. Thus, the determination of their phase composition as well as the crystal chemistry within a single mineral constituent is extremely significant, as it can provide valuable information about clay-tablet provenance. As a first step towards the truly non-destructive characterization of rock-based written artifacts, we have analyzed a series of biotite samples. Biotite represents a group of hydrous layered silicates that is commonly stable in a variety of geological environments and present in several geomaterials, including clays. The general formula of biotite is $A_1M_3T_4O_{10}X_2$, where A = K⁺, Na⁺, □ (vacancy), Ca²⁺ and Ba²⁺; M refers to the octahedrally coordinated cations (Mg²⁺, Fe²⁺, Fe³⁺, Al³⁺, Ti⁴⁺, Mn²⁺, Cr³⁺, Zn²⁺, Li⁺, and □); T refers to the tetrahedrally coordinated cations (Si⁴⁺, Al³⁺, and Fe³⁺), X denotes the anion site occupied by OH⁻, F⁻, Cl⁻ and O²⁻. Traditionally, the crystallochemical characterization of minerals is carried out through wavelength-dispersive electron microprobe analysis (WD-EMPA) and X-ray diffraction. However, such analytical methods require special sample preparation, which is highly undesirable or even prohibitive due to the uniqueness of the examined sample from the viewpoint of cultural heritage. Therefore, alternative non-invasive, preparation-free methods such as Raman spectroscopy are becoming increasingly popular among the scientific community. In this study 18 biotite crystals with various chemical compositions covering the whole biotite solid-solution series between the endmembers phlogopite [KMg₃AlSi₃O₁₀(OH)₂] and annite [KFe²⁺₃AlSi₃O₁₀(OH)₂] have been analyzed by WD-EMPA and Raman spectroscopy. The goal was first to verify whether the Raman scattering arising from the framework vibrations (15-1215 cm⁻¹) and OH-bond stretching (3000-3900 cm⁻¹) can assist in the identification of biotite-group minerals and second to establish the relationship between the Raman signals (peak positions, integrated intensities and full widths at half maximum) and the crystallochemical composition of the biotite-group minerals. We show that the content of major elements in the tetrahedral and octahedral sites can be quantitatively determined with reasonable uncertainty. In addition, the amount of ^MTi as a minor element can also be extracted from the established calibration curves.

Acknowledgments: The research for this study was funded by the Deutsche Forschungsgemeinschaft (DFG, German Research Foundation) under Germany's Excellence Strategy – EXC 2176 “Understanding Written Artefacts: Material, Interaction and Transmission in Manuscript Cultures”, project no. 390893796. The research was conducted within the scope of the Centre for the Study of Manuscript Cultures (CSMC) at Universität Hamburg.

EARLY MEDIEVAL (7TH–9TH CENTURY AD) GLASS BEADS FROM THE CARPATHIAN BASIN: A MICROTTEXTURAL, MICROCHEMICAL AND MINERALOGICAL STUDY

Bajnóczi Bernadett¹, Fülöp Réka², Szenthe Gergely³, Szabó Máté¹

¹Institute for Geological and Geochemical Research, Research Centre for Astronomy and Earth Sciences, Hungary,

²Archaeological Heritage Protection Directorate, Hungarian National Museum, Hungary, ³Department of Archaeology, Hungarian National Museum, Hungary

In the Avar era (6th–early 9th century), a special spectrum of glass bead types was in use in the Carpathian Basin. In the early Avar period, southern (Byzantium) and western (Italy, Merovingian Western Europe?) influences were more noticeable on glass beads. The situation changed for the 'late Avar period', at the end of the 7th century. At around this time, not only a northward shift can be detected in the communication system of the Avar khaganate due to the weakening contacts to Byzantium, but local production structures seem to have developed as well. In the 8th century, most bead types were produced in the Carpathian Basin. Later, in the last phase of the Avar period, new production techniques, new colorations, and new bead types occurred again, indicating the emergence of a new production and redistribution system of beads in the macroregion, coexisting for a certain period with the old structures. Concurrently, external connections of the region seem to be reoriented as well. Among the locally-made bead types, the bead-strings comprise the products of early Islamic centers, arriving into the Carpathian Basin via long-distance trade. The problem of this twofold transformation – once of the inner production and the redistribution structures, and secondly, that of the external trade connections – is connected to one of the most exciting questions of the early medieval transformation processes in the Carpathian Basin, the question of the continuity of production and communication between the 8th and 10th/11th centuries.

Early Avar-period glass beads from the Carpathian Basin were formerly extensively studied archaeometrically. At the same time, the material of the late Avar-period beads received little attention, although, as our sampling reflects, the shape and color of the beads are exceedingly heterogeneous. In our study, microtextural, microchemical, and mineralogical characterization of more than thirty late Avar-period glass beads (late 7th–early 9th century) were performed by SEM-EDX and micro-XRD methods.

Beads are dominantly soda-lime-silica glasses with mineral natron as a flux (LMG). Plant ash soda-lime-silica glasses (HMG) are subordinate. Most of the studied beads are blue, green, and bluish-green with copper and iron as main colorants, accompanied by lead in several cases. These glasses were manufactured using different production technologies: both transparent and translucent beads occur, the latter contain tin-bearing inclusions, calcium antimonate, or rarely lead antimonate particles, respectively. Two opaque yellow beads studied are characterized by different types of opacifiers, one contains lead antimonate, whereas the other one includes lead stannate. Two red beads studied, colored by cuprite and/or metallic copper crystallites, belong to the dull red opaque glasses characterized by low lead and copper contents. Two black beads analyzed in this study were colored by iron, but manufactured differently: one is translucent brown-black, whereas the other one is opaque black soda-lead glass containing iron slag remnants together with copper- or tin-bearing inclusions. All these various technologies indicate that several different methods were used to produce beads, so there was no uniform centralized production. In some cases, we can even assume the recycling of old Roman glasses.

IMPACT OF BENTONITE SOLUBLE PHASES IN HYDRAULIC SANDWICH SEALING SYSTEMS ON ION TRANSPORT AND CATION EXCHANGE AT SEMI-TECHNICAL SCALE (HTV-2 AND HTV-3)

Bakker Eleanor¹, Busqesi-Ahmeti Durime¹, Stefanescu Eduard¹, Königer Franz¹, Gruner Matthias², Hofmann Martin², Schuhmann Rainer¹, Emmerich Katja¹

¹Competence Centre for Material Moisture (IMB-CMM), Karlsruhe Institute of Technology, Germany, ²Institut für Bergbau und Spezialtiefbau, TU Bergakademie Freiberg, Germany

Bentonites are considered for use as barrier materials for the disposal of high-level radioactive waste (HLRW). The Sandwich structure of equipotential segments (ES) with higher conductivity alternating between sealing segments (DS) of bentonite (Königer et al., 2008; Emmerich et al., 2009) was further investigated in two long-term semi-technical scale experiments, HTV-2 and HTV-3, in horizontal alignment to simulate drift sealing. Rock-salt solution (density 1.15 g cm⁻³ NaCl, to replicate natural brines) was forced through the columns for 446 or 525 days respectively and the experiments terminated when the solution reached the final DS. Dismantling of the column provided a detailed view of the bentonite system at a moment during the saturation process.

Salt concentrations within the columns decrease from 9.0 to 0.3 mass% (HTV-2) and 7.3 to 0.2 mass% (HTV-3) as the distance from the fluid inflow increases. Transformation of Ca- Mg-bentonite (Calcigel) into Na-bentonite depends on the extent of the exposure to the rock-salt solution, and is greatest in samples with the longest exposure to the rock-salt solution. A nearly constant decrease in CEC was observed for the bentonite in all DS in HTV-2 while in HTV-3 CEC a more linear decrease through the column was seen, with the largest decrease closest to the fluid inflow. Bohac et al. (2019) demonstrated a reduction in CEC with increasing salt content, however, the magnitude of the decrease observed in HTV-3 is larger than can be accounted for by salt content alone, so further investigation into the mechanism of CEC reduction is required.

Thermal analysis shows that the decomposition of carbonate phases is impacted by proximity to the fluid inflow, and that alteration of sulfate phases also takes place. Despite the changes to soluble phases, the concentration of soluble ions with a segment showed little variation, indicating that the ES were effective at equilibrating the system. Residual Ca²⁺ and Mg²⁺ as interlayer cations of the smectite in the bentonite even after > 400 days exposure to the rock-salt brine indicates soluble phases influence the long-term composition of bentonite pore fluid and thus exchangeable ion composition. Artificial defects introduced in DS had little to no impact on overall ion concentrations with the exception of the bentonite immediately adjacent (within 5 cm), overall demonstrating the efficacy of the multilayer Sandwich sealing system.

FLUIDS IN INCLUSIONS AND FLUIDS IN MINERALS OF GRANULITIC GARNETITES: CONFLICTS AND AGREEMENTS

Bakker Ronald¹, Pushkarev Evgenii²

¹Resource Mineralogy, Montanuniversity Leoben, Austria, ²Geology and Geochemistry, Ural Branch, Russian Academy of Sciences, Russian Federation

Garnetites in Khabarny Complex (Sakmara Zone, Ural) are found in the lens and block-like bodies among two-pyroxene schists within the mafic-ultramafic rock (ophiolite allochthone). The garnetites consist mainly of almandine-pyrope-rich garnets, Mg-cordierite, quartz, and rutile, and abundant solid and fluid inclusions. Fluid components are characterized in fluid inclusions in quartz and garnet, and the large channel sites of the ring structure of cordierite. There is a large contrast in fluid composition between cordierites and fluid inclusions, that apparently belong to the same granulitic metamorphic event. Garnets contain small fluid inclusions (< 3 µm) with a fluid mixture of CH₄ (79 ± 4 mole%) and N₂ (21 ± 4 mole%) in addition to entrapped pyrophyllite and siderite. Quartz nodules (positioned between garnet and cordierite grains) contain CH₄ (>96 mole%), and locally minor amounts of C₂H₆, N₂, and H₂S. The inclusions occur mainly in trails that are restricted within single quartz grains. Locally, inclusions with similar properties occur in clusters. Many inclusions also contain graphite that is deposited in a late-stage on fluid inclusion walls. Raman spectroscopic analyses of cordierite reveal the presence of H₂O, CO₂, and N₂ within the channel structure. Enigmatic observations are defined by the presence of aragonite within fluid inclusion trails, partly enclosed in the inclusions, and the presence of cristobalite inclusions in garnet. Quartz inclusions in garnet are coated with tiny CH₄-rich fluid inclusions. The fluid components detected in cordierite correspond to the relative oxidized fluid environment that is common in granulites (H₂O-CO₂-rich fluids). In contrast, a highly reduced fluid environment is preserved in fluid inclusions in quartz nodules and garnets (CH₄-rich fluid). The initial granulite facies conditions that led to the formation of a cordierite and garnet mineral assemblage must have occurred in a relative oxidized environment (QFM-buffered) with H₂O-CO₂-rich fluids. Abundant intrusions or tectonic emplacement of mafic to ultramafic melts from the upper mantle that were internally buffered at a WI-buffered (wüstite-iron) level must have released abundant hot CH₄-rich fluids that flooded and subsequently dominated the system. The origin of the granulite-facies conditions is similar to peak-metamorphic conditions in the Salda complex (Central Urals) and the Ivrea-Verbano zone (Italian Alps) as a result of magmatic underplating that provided an appearance of positive thermal anomaly, and further joint emplacement (magmatic and metamorphic rocks together) into the upper crustal level as a high-temperature plastic body (diapir). Locally, SiO₂-inclusions in garnet provide evidence of a strong positive temperature anomaly by the preservation of cristobalite and the high titanium content of quartz. The presence of aragonite in CH₄-rich fluid inclusion assemblages in quartz nodules must represent metastable precipitation conditions well below its stability field, or a relict of high-pressure metamorphism.

A CHALLENGE IN THE “CHALLENGE”: NON-INVASIVE MULTIANALYTICAL APPROACH TO CHARACTERIZE THE ALEXANDER MOSAIC

Balassone Giuseppina¹, Cappelletti Piergiulio², De Bonis Alberto², Di Martire Diego², Graziano Sossio Fabio³, Grifa Celestino⁴, Izzo Francesco², Langella Alessio², Mercurio Mariano⁴, Morra Vincenzo², Rispoli Concetta², Verde Maria², De Simone Antonio⁵, Piezzo Amanda⁶, Operetto Maria Teresa⁶

¹ Center for Research on Archaeometry and Conservation Science (CRACS), inter-university center, Federico II University (Naples) and University of Sannio (Benevento), Italy, ²Department of Earth, Environmental and Resources Sciences, Federico II University (Naples), Italy, ³Department of Pharmacy, Federico II University, Italy, ⁴Department of Science and Technology, University of Sannio (Benevento), Italy, ⁵Suor Orsola Benincasa University (Naples), Italy, ⁶Museo Archeologico Nazionale di Napoli (MANN), Naples, Italy

On October 24th, 1831, the Alexander Mosaic (Battle of Issus) was discovered in the House of the Faun in Pompeii; it is the most important mosaic of the Roman era and is now located at the National Archaeological Museum of Naples (MANN). The millions of tesserae that make up the mosaic add up to exceptional dimensions: approximately 582 x 313 cm. The scene, depicted in detail, is that of the battle of Issus, in which Alexander the Great defeated the Persian army led by Darius III.

The Interuniversity Centre “CRACS”, Center for Research on Archaeometry and Conservation Science (University of Naples Federico II, the University of Sannio at Benevento, Italy), contributed to a major restoration project regarding the Alexander Mosaic headed by the MANN.

CRACS analyzed in detail the whole mosaic with modern analytical techniques of non-invasive diagnostics in the field of mineralogy and petrography: Video-microscopy, Endoscopic Video Analysis, portable X-Ray Fluorescence Spectrometry (pXRF), infrared thermography, multispectral imaging, Fourier transform infrared (FTIR), and Raman spectroscopy.

The goal of the study was to determine the nature of the various materials that constitute the mosaic (tesserae, mortar, protective coatings, etc.), their state of conservation, as well as the geological origins of the lithoid materials used as mosaic tesserae. All data from the different analytical methodologies have been combined into a QGIS project. This multi-analytical strategy allowed for the distinction of ten groups of color (white, beige, pink, red, yellow, brown, gray, black, green, light blue), with multiple chromatic nuances. From a mineralogical-petrographic point of view, the tesserae belong to two compositional types: carbonate-calcic and silicate. Synthesis materials, such as green glass pastes, have also been found. Possible geological sources of lithoid materials are both intra-regional (Campania volcanic rocks) and extra-regional (various types of "marbles", oficalci “green stones” etc.). A chromatic variation has also been detected in the jointing mortars of mosaic tesserae, which show a color variable from light yellow, to red, to dark green and with a prevailing calcium carbonate/sulfate composition. Vibrational spectroscopy reports the occurrence of natural waxes and calcium sulfate hydrate (i.e., gypsum), with traces of calcium oxalate (whewellite), onto the surface of the mosaic. Multispectral imaging analyses showed variations of luminescence attributable to organic protections and/or to lithotypes of different nature. Moreover, endoscopic observations allowed for the investigation of the state of conservation of the wooden frame support, while IR thermography detected some areas with thermal anomalies. Finally, a number of mosaic tesserae between 1.890.000 -1.616.000 have been counted. The data set acquired by the CRACS is fundamental for a correct restoration project and it will be part of a new technological device provided by the Italian telecommunications company TIM. Indeed, for the first time TIM - NTT Data Italia is realizing for the Alexander Mosaic special smart glasses (based on the Augmented Reality technology, AR), which will be worn directly by the restorers and will be essential to the constant monitoring of the correspondence between the area of intervention and its non-visible internal layers; these smart glasses will combine the whole available data set acquired so far.

ZEOLITE FROM FLY ASH MODIFIED WITH B-CYCLODEXTRIN – SYNTHESIS, CHARACTERISATION, AND SORPTION PROPERTIES TOWARDS ORGANIC MICROPOLLUTANTS

Bandura Lidia¹, Białoszewska Monika¹, Malinowski Szymon¹, Franus Wojciech¹

¹Lublin University of Technology, Poland

Zeolites belong to the group of crystalline hydrated aluminosilicate minerals. The unique structure gives them a number of properties including, ion exchange and adsorption. Therefore, natural and synthetic zeolites are minerals widely involved in wastewater treatment. Zeolites are hydrophilic in nature. Therefore their surface needs to be modified to improve sorption efficiency towards organic compounds present in waters. Recently, an important worldwide issue is the increasing amount of organic micropollutants (OMs). OMs are a group of compounds that can be divided into several main categories: pharmaceuticals, personal care products, steroid hormones, surfactants, industrial chemicals, and pesticides. So far, the most popular modifications of zeolites are made with the use of surfactants or chitosan. One of an interesting alternative to those organic modifiers are cyclodextrins (CDs) which belong to the group of cyclic oligosaccharides with cone shape of the hydrophilic outer surface and hydrophobic interior. That makes them capable of forming inclusion complexes with organic compounds. The aim of this study was to obtain a novel hybrid organic-inorganic material, consisting of a zeolite mineral matrix modified with β -CD and investigate the sorption properties of the material towards OMs present in water. As a mineral matrix zeolite of NaX type from fly ash was used. To obtain NaX-CD material β -CD was dissolved in DMF with Na using a stirrer. Then, linking agent GLYMO was dosed and the mixture was stirred at 85-90°C for 5 h. Further, NaX zeolite was added and the mixture was stirred overnight at 110-120°C. The obtained material was filtered, washed and dried at 105°C for 24 h.

NaX and NaX-CD were characterized in terms of chemical, mineralogical, and textural properties. Bisphenol A and caffeine (IBU, BPA, and CFN) were used as model representatives of different OMs. The effect of the adsorbent dose, initial concentration, and the contact time was studied.

CHN elemental analysis, thermal analysis (TG/DTA), X-ray diffraction (XRD), infrared spectroscopy (FTIR), scanning electron microscope (SEM), and nitrogen adsorption/desorption confirmed successful modification with β -CD. It was proven that the structure of the mineral remained intact after the modification, while changes in surface morphology were observed. NaX-CD had a smoother surface, made up of elements with softer shapes than NaX, and with less homogeneity and crystallinity.

NaX-CD exhibited different sorption behavior towards OMs. The sorption rate was as follows: CFN>IBU>BPA. Maximum adsorption capacity in mg/g was 31.3 for IBU, 32.7 for BPA, and 11.8 for CFN. A hydrophobic interior of β -CD cup favors BPA and IBU sorption by hydrogen bond formation between the hydroxyl groups in adsorbates and the secondary hydroxyl groups of β -CD. Thus IBU and BPA were sorbed more effectively than CFN. Obtained results indicate that zeolite from fly ash modified by cyclodextrin can be a lower-cost alternative to biochar and activated carbon sorbents.

The „Fly ash as the precursors of functionalized materials for applications in environmental engineering, civil engineering and agriculture” no. POIR.04.04.00-00-14E6/18-00 project is carried out within the TEAM-NET program of the Foundation for Polish Science co-financed by the European Union under the European Regional Development Fund.

A 3D PHOTOGRAMMETRIC PROTOCOL TO DIGITALIZE MINERAL SPECIMENS: STRUCTURE AND STANDARDIZATION

Barengi Fabiana¹, Xiong Miner¹, Mangano Chiara¹, Merlini Marco¹, Fumagalli Patrizia¹, Zucali Michele¹

¹Dipartimento di scienze della terra Ardito Desio, Università degli Studi di Milano, Italy

The 2020 was a striking year marked by the worldwide Covid-19 pandemic. This issue has led to a strong focus on the digitization of cultural and naturalistic heritages in order to make use of them in any situation. In this point of view, work has been structured to make it possible to digitize the mineralogical specimens preserved in the museum of the Mineralogical, Petrographic, Gemological, and Mining geological collections of the Earth's Science Department "Ardito Desio" of the University of Milan "La Statale". This work has led to the structuring of a standardizable procedure that allows the 3D rendering of these materials in a simple and replicable way. The selected specimens are various: specimens from the Baveno area for their historical-cultural value, and the form of their interesting crystal habit; other specimens from the world's mineral collections were picked to test the potential and limits of the software Agisoft Metashape, which was used for the realization of the 3D models. This work also identified the critical points that may be encountered in a photogrammetric acquisition process, and furthermore, to find out the most effective methods to reduce disturbs. Difficulties, in fact, arise because of the transparency and vitreous luster of crystals as well as reflectance due to the metallic luster of the most interesting minerals. In this way, the models once created, could be uploaded to some free platforms, and become useful in the divulgational field, such as a digital substitution of museum visiting; on the other hand, they could also be used in the educational field for their scientific value, for example, in distance learning lessons.

PHYSICAL COMPARISON BETWEEN ASHLARS OF BASALTIC STONE AND ALKALI-ACTIVATED MATERIALS BASED ON PYROCLASTIC DEPOSITS (Mt. ETNA VOLCANO, ITALY)

Barone Germana¹, Belfiore Cristina Maria¹, Finocchiaro Claudio¹, Mazzoleni Paolo¹

¹Department of Biological, Geological, and Environmental Sciences, University of Catania, Italy.

Alkali-activated materials (AAMs) can be regarded as synthetic materials due to their production process itself which foresees the mixing of solid aluminosilicate precursors with alkaline activators [1,2]. Moreover, they are assumed as a “green” alternative to traditional concrete with the high potentiality of use in different application fields (e.g., restoration of built heritage) [3,4]. According to this foreword and the satisfying results of previous studies on AAMs based on volcanic ash from Mt. Etna volcano (Italy) [4–6], in this work, we propose a comparison, at laboratory scale, between natural and synthetic materials, which show a strong chromatic affinity each other. As for natural materials, specimens of massive basaltic stones from Mt. Etna volcano were taken into account. Regarding the synthetic materials, Etnean powdered pyroclastic deposits were used as precursors. Specifically, four different sets of samples were prepared, two of which through the addition of specific quantities (10 and 20 wt.%, respectively) of metakaolin (MK) as a solid additive to the total amount of the volcanic source; for the others, the 30 wt.% of pyroclastic aggregate (< 2 mm) was added to the previous binders and mixed with 2 wt.% of tap water to achieve satisfying workability. All samples, both natural and synthetic, have been shaped with a small cubic size (2x2x2 cm). After that, the four AAMs series have been cured for 28 days before being analyzed to ensure the total hardening. The following analytical techniques were then applied to assess the physical behavior of the tested materials: i) infrared thermography to evaluate the heat release during the natural cooling of samples; ii) the capillary water absorption test to assess their hydric behavior as a function of textural features and pore structure. In addition, tests of uniaxial compressive and drilling strength were also carried out to assess the mechanical performance of the sample set.

The AGMforCuHe project is acknowledged for its financial support (PNR 2015-2020, Area di Specializzazione “Cultural Heritage” CUP E66C18000380005).

[1] J. Davidovits, *J. Therm. Anal.* 1991, 37, 1633. [2] J. L. Provis, J. S. J. Van Deventer, *Geopolymers: structure, processing, properties and industrial applications*, Woodhead, 2009. [3] G. Barone, M. C. Caggiani, A. Coccato, C. Finocchiaro, M. Fugazzotto, G. Lanzafame, R. Occhipinti, A. Stroschio, P. Mazzoleni, in *IOP Conference Series: Materials Science and Engineering*, Institute of Physics Publishing, 2020, vol. 777, p. 012001. [4] G. Barone, C. Finocchiaro, I. Lancellotti, C. Leonelli, P. Mazzoleni, C. Sgarlata, A. Stroschio, *Waste and Biomass Valorization*, DOI:10.1007/s12649-020-01004-6. [5] C. Finocchiaro, G. Barone, P. Mazzoleni, C. Leonelli, A. Gharzouni, S. Rossignol, *Constr. Build. Mater.*, DOI:10.1016/j.conbuildmat.2020.120095. [6] C. Finocchiaro, G. Barone, P. Mazzoleni, M. Sgarlata, Caterina Lancellotti, Isabella Leonelli, Cristina Romagnoli, *J. Mater. Sci.* 2021, 56, 513.

ARCHAEOLOGICAL CAMPAIGN AT MONREALE CATHEDRAL (SICILY): THE DIFFERENT MATERIALS OF THE OPUS SECTILE FRIEZE WITH PALMETTES.

Barone Germana¹, Caggiani Maria Cristina¹, Coccato Alessia¹, Finocchiaro Claudio¹, Fugazzotto Maura¹, Lanzafame Gabriele¹, Mazzoleni Paolo¹, Occhipinti Roberta¹, Starinieri Silvia², Stroschio Antonio¹

¹Department of Biological, Geological and Environmental Sciences, University of Catania, Italy, ²Prato, Piacenti S.p.a., Italy

Monreale Cathedral (Sicily, Italy) was built starting from 1172 for the will of the Norman king William II “The Good”. Thanks to the assimilation ability of the Normans and the unifying force of the culture proposed by William II, the Cathedral manages to show the balance achieved between Western, Byzantine, and Arab-Islamic civilizations. The extensive mosaic decoration manufacture, encompassing both figurative scenes and geometric motifs, was concluded in the 19th century. The geometric motifs separate the figurative scenes from the tall marble dado. This work is focused on a section of the opus sectile frieze with palmettes located on the South aisle wall, including both mosaic and marble, and running all along the perimeter of the Cathedral. The tesserae here employed have different shapes (square, triangle, diamond...) and dimensions (15-30 mm) and seem obtained from various materials: natural stones (whitish), glass and polychrome glass pastes (blue, light and dark green, red and black), including gilded ones. Mosaic tesserae are a well-known archaeometry research topic. Decorative polychrome mosaics are found in Hellenistic, Roman, Paleo Christian, and Byzantine contexts, as well as in Islamic ones.

Archaeometrical studies aim at identifying the raw materials, colorants, and opacifiers as well as the microstructure of the tesserae. All these data convey information on manufacturing technology, which is related to production practices, which in turn can support provenance and chronological interpretations on the mosaics manufacture. As colored glass is a complex material, a multi analytical approach is required in order to achieve these objectives. The archaeometric investigation carried out on these materials was part of an in situ campaign on the pilot conservation-restoration site of the mosaics, within the project Advanced Green Materials for Cultural Heritage (AGM for CuHe) (PNR fund with code: ARS01_00697; CUP E66C18000380005), aimed to the implementation of innovative, alkali-activated materials for conservation and restoration of cultural heritage monuments by exploiting Sicilian raw materials. In this framework, the diagnostic survey was performed in parallel with the experimental application of mortars and replicated tesserae produced in situ with geopolimetric materials. To assess the different chemical and mineralogical composition and chromatic characteristics of the tesserae, both original and replicas realized through geopolymer mortars, non-invasive analyses were carried out. A combination of X-ray Portable Fluorescence (pXRF), vibrational spectroscopies (Diffuse Reflectance Infrared Spectroscopy (DRIFT) and micro-Raman), and colorimetry were performed. The characteristic chromophores were detected by means of pXRF, while the glass recipe was studied by means of vibrational spectroscopies. To the authors' knowledge, DRIFT is sporadically used in the field of cultural heritage, and even more rarely for the investigation of mosaic materials: the preliminary results of this study show how it can constitute a valid complementary technique to Raman spectroscopy, with the additional advantage of portability with respect to FT-IR (-ATR) instrumentations.

RESTORATION FEASIBILITY STUDY BY USING ALKALI ACTIVATED MORTARS BASED ON Mt. ETNA VOLCANIC ASH: THE CASE STUDY OF MONREALE CATHEDRAL (PALERMO, ITALY)

Barone Germana¹, Caggiani Maria Cristina¹, Coccato Alessia¹, Finocchiaro Claudio¹, Fugazzotto Maura², Lanzafame Gabriele¹, Mazzoleni Paolo¹, Occhipinti Roberta¹, Starinieri Silvia³, Stroschio Antonio¹

¹Department of Biological, Geological and Environmental Sciences, University of Catania, Italy, ²Department of Human Sciences, University of Catania, Italy, ³Piacenti SPA, Italy

The Monreale Cathedral, located in the Metropolitan City of Palermo (Sicily), is one of the greatest existent examples of Norman architecture. Since 2015 it is part of the Arab-Norman route of Palermo and it has been recognized as UNESCO Heritage site. The internal facades are decorated with stone and glass mosaics, remaining the spirit of Byzantine culture. The magnificence of this Cultural site is also given by the mosaic's extension (around 6.340 m²), even higher than that of the Basilica of San Marco in Venice (Italy) and second in the world only to the Church of Santa Sofia in Constantinople (Turkey).

Within the project Advanced Green Materials for Cultural Heritage (AGM for CuHe) (PNR fund with code: ARS01_00697; CUP E66C18000380005), aimed to the implementation of innovative, alkali-activated materials for conservation and restoration of monuments by exploiting Sicilian raw materials, the Monreale Cathedral has been chosen as pilot restoration site. Alkali-activated materials (AAMs) are assumed as a "green" alternative to traditional cements with high versatility. They are produced by the mixing of solid aluminosilicate precursors with alkaline activators. Previous studies on AAMs based on volcanic ash from Mt. Etna (Italy) have shown promising results in terms of workability, strength, and durability, opening the possibility to use these innovative materials in the restoration of valuable historical objects. Thus, after a preliminary diagnostic campaign on the mosaic decorations, a small area located on the South aisle, including both mosaics and marbles, was selected for the in situ application and tests of volcanic ash-based AAMs. The restoration project was performed in collaboration with a well-established restoration company (Piacenti S.P.A.) and it has foreseen the application and testing of bedding and finishing mortars for the larger lacunae; the reposition of detached original tesserae and the replica of the mosaic decorations by engraving and painting on the finishing mortar. Furthermore, tesserae of different shapes and colors have been also reproduced directly in situ. This study allowed to evaluate the criticisms related to the preparation and application of this kind of materials in restoration sites.

The AGMforCuHe project is acknowledged for its financial support (PNR 2015-2020, Area di Specializzazione "Cultural Heritage" CUP E66C18000380005).

IN SITU XRF INVESTIGATIONS TO UNRAVEL THE PROVENANCE AREA OF “PROTO-CORINTHIAN AND CORINTHIAN” CERAMICS FROM EXCAVATIONS IN MILAZZO (MYLAI) AND LIPARI (LIPÁRA)

Barone Germana¹, Belfiore Cristina Maria¹, Mastelloni Maria Amalia², Mazzoleni Paolo¹

¹Department of Biological Geological and Environmental Sciences, University of Catania, Italy, ²Polo Regionale delle Isole Eolie, Parco, Museo Archeologico “L. Bernabò Brea”, Lipari, Italy

Between the VIII and VI centuries BC the proto-Corinthian and Corinthian vessels form a class of pottery widespread throughout the Mediterranean which plays the role of indicator of the chronology of the settlements and their belonging to the Greek culture. In this contribution, a non-destructive approach has been used aiming at investigating the chemical composition of 37 ceramic finds belonging to the collections of the Regional Aeolian Museum “Luigi Bernabò Brea” in the Lipari Island (Sicily, Italy). Different vessel types have been selected for analysis, including aryballoi, skyphoi, kotylai, olpai, all belonging to the “pre-Corinthian and Corinthian” ware class. The finds, dating back to the period comprised between the end of the VIII and the beginning of the VI century BC, come from two different archaeological contexts in the province of Messina (Sicily). Specifically, seventeen samples (all entire vessels except for two fragmented aryballoi) have been recovered from the Istmo necropolis of Milazzo, in the northern Sicilian coast, while twenty finds (all fragmentary vases except for one entire aryballos) come from the acropolis and the necropolis of Lipari, in the Aeolian islands.

The chemical characterization of ceramics (in terms of major, minor, and trace elements) was carried out through portable XRF spectrometry, a technique increasingly used for in situ analysis of museum collections that cannot be removed and/or sampled.

The autoptic analysis of the studied ceramics points to Corinthian imports, though the results of analyses seem to suggest a colonial production for some of them. In addition, the comparison with published data on stylistically similar vessels permits us to attribute some specific finds to “local” production (Strait of Messina area).

APS MINERALS IN EARLY-MIDDLE TRIASSIC ROCKS OF THE WESTERN PERI-TETHYS (ALTO ADIGE, ITALY).

Barrenechea Jose F¹, Borrueal-Abadía Violeta², De la Horra Raúl³, López-Gómez José¹, Gianolla Piero⁴

¹IGEO CSIC UCM, Spain, ²Geology, University of Salamanca, Spain, ³Geodynamics, Stratigraphy and Paleontology, Universidad Complutense de Madrid, Spain, ⁴Physics and Earth Sciences, University of Ferrara, Spain

The Early Triassic was marked by the prolonged recovery of life after the devastating End Permian Mass Extinction. The recovery was probably conditioned by pulses of volcanic activity from the Siberian Traps, linked in turn to new extinction events, the most important of which took place at the Smithian-Spathian boundary (SSB). Different studies have recently related the presence of strontium-rich hydrated aluminum phosphate-sulfate (APS) minerals in continental sedimentary rocks to acidic environmental conditions during the SSB biotic crisis on land, at least in equatorial latitudes for Early Triassic times (Iberian Ranges, Catalan-Coastal Range, Minorca, and Sardinia). The regional nature of the presence of APS minerals in these basins is considered as evidence of a large-scale environmental disturbance. The aim of this work is to verify the extension of these acidic conditions in the SSB of continental-marine transitional zones of the near-equator western Tethys domain by searching APS minerals and considering the clay mineralogy of the samples. Special attention is paid to the indicators of organic activity at the levels that may show signs of higher or lower acidity. For that purpose, we have studied the exceptional outcrops of the Alto Adige area, Dolomite Alps, Italy.

The Lower-Middle Triassic in the studied sections of the Alto Adige (Monte Guiza) represents the transition from continental to marine sedimentation. The samples correspond mostly to red siltstones and fine-grained sandstones. The XRD data reveal that the bulk mineralogy of these samples is composed of quartz (25-72 %), feldspar (0-17 %), hematite (<5 %) and it may contain calcite (<10 %) and dolomite. The latter is only present at the top of the section, where it reaches 27 % of the mineral composition. The clay fraction is dominated by illite (6-35 %) and less abundant kaolinite (2-7 %), although one sample near the top of the section contains 55 % smectite. In addition, APS minerals have been identified in samples from the basal and middle parts of this section. They are found as pseudocubic crystals of very small size (<1 µm) between quartz and feldspar grains. The crystals are surrounded by quartz and illite cements that adapt to their regular shapes, occasionally leaving molds. They are frequently associated with detrital micas partially altered to kaolinite, which form stacks of both mineral phases. These features are very similar to those found in neighboring peritethian continental basins. The presence of these APS minerals with similar textural and compositional features suggests widespread acidic conditions on land and on transitional continental-marine environments for the SSB in equatorial latitudes.

THE REDOX ANOXIC SYSTEM, Fe-HIGH SUBCRITICAL WATER, FOR THE PRODUCTION OF FERRIC IRON

Bassez Marie-Paule¹

¹University of Strasbourg, France

It is shown that ferrous iron in strongly alkaline water at temperature and pressure near the supercritical point is oxidized into ferric iron in the absence of oxygen. The representative system is the electric redox system Fe-high subcritical alkaline water. Pourbaix diagrams or potential-pH diagrams are analyzed for the system Fe-water near the supercritical point.

Electrochemical systems, with exchanges of electrons between ionic species, occur everywhere in the universe. The study of such systems starts with the simple definition that one species is said to be oxidized when it loses electrons. The redox potential E of an electrochemical system, also named the potential of the redox couple, expressed in volts (i.e., joules/coulomb), is an electric potential energy per unit charge. It is different from the electrochemical potential, which is expressed in joules/mole. The redox potential is a function of the activities (concentrations) of the oxidized a_{ox} and reduced species a_{red} , and it is given by the Nernst equation: $E_H = E^\circ + (RT/nF) \cdot \ln(a_{ox}/a_{red})$. E° is the standard potential and F is the Faraday constant. An electric potential is always defined with respect to infinity, where it has the value 0. As for the gravitational field, it is the difference in potential energy, which counts since it equals the kinetic energy. Thus, in an electrochemical system in equilibrium, redox potential is usually expressed relative to the standard hydrogen electrode (SHE), with the potential set by choice to 0 volts. The standard reduction potential for the reduction half-reaction $O_{2(g)} + 4H^+_{(aq)} + 4e^- \rightarrow 2H_2O_{(l)}$ is +1.23 volts, and the standard reduction potential $E^\circ(H^+/H_2)$ for the reduction half-reaction $2H^+_{(aq)} + 2e^- \rightarrow H_{2(g)}$ is 0 volt by choice.

A gravitational system evolves spontaneously towards decreasing potential energy, for instance, a marble sliding down a slope. In electricity, positive charges move from high electric potential to low electric potential, and negatives charges, such as electrons, move from low electric potential to high electric potential. By analogy, I propose that an electrochemical system that undergoes chemical reactions evolves spontaneously in the direction of decreasing potentials, with electrons moving towards higher potentials. Since 2013, I apply this spontaneous change to the redox lines $E^\circ(H^+/H_2) = f(pH)$ and $E^\circ(Fe^{3+}/Fe^{2+}) = f(pH)$. I show that the redox couple H^+/H_2 oxidizes the redox couple Fe^{3+}/Fe^{2+} at pH 11.5-14, 300-350°C, 10-25 MPa, water densities 700-600 kg/m³ and without oxygen. The electron released from ferrous iron moves towards higher potential and the following equations can be written: $Fe^{II}(OH)_3^-_{diss} + H_2O_{hsubc} \rightarrow Fe^{III}(OH)_4^-_{diss} + \frac{1}{2} H_{2\,diss}$

The above redox equation, when applied to anoxic geological terrains such as those of Archean times, contributes to explaining the observed ferric minerals, without the intervention of oxygen, nor microorganisms.

THERMAL AND COMPRESSIONAL BEHAVIOUR OF NATURAL BORATES: A POTENTIALLY AGGREGATES IN RADIATION-SHIELDING CONCRETES

Battiston Tommaso¹, Comboni Davide², Pagliaro Francesco¹, Lotti Paolo¹, Gatta G. Diego¹

¹Earth Sciences Department, University of Milan, Italy, ²European Synchrotron Radiation Facility, France

Natural borates represent the first worldwide source of boron. Boron is a key constituent in different industrial sectors, including glass, ceramics, agricultural, metallurgical, electronics, textile, cosmetics, and chemistry. Recent technological developments have further expanded the use of borates, as underlined by the doubling of global production in the last decade. The recent addition (on 2014) of borates to the European Union list of Critical Raw Materials is a further evidence of the large global demand for this commodity. Due to the ability of ¹⁰B (ca. 20% of the natural boron) to absorb thermal neutrons, related to its high cross-section for the ¹⁰B(n,α)⁷Li reaction (~3840 barns), several recent studies investigated the utilization of natural borates as light aggregates in radiation-shielding materials, such as concretes. In this light, the use of natural borates would provide also an economic advantage: synthetic B₄C, for example, proved to be efficiently adopted in this field, but its use is hindered by the high costs of synthesis.

In order to characterize the phase stability field, the thermo-elastic properties, and the mechanisms of thermal-induced dehydration, we have investigated the behavior at non-ambient T and P of some of the most common hydrous borates, i.e. kernite, colemanite, kurnakovite, ulexite, and meyerhofferite, by means of in situ single-crystal synchrotron X-ray diffraction. In situ non-ambient conditions were obtained using diamond anvil cells (for high-P), nitrogen cryostats (low-T), and gas blowers (high-T). High-pressure experiments show that all the analyzed borates remain stable at pressures exceeding those to which radiation-shielding materials may be subjected. Among them, colemanite shows the lowest bulk compressibility ($K_{V0}=67(4)$ GPa and $K_{V0}'=5.5(7)$, where $' = \partial K_{V0} / \partial P$; $\beta_{V0} = 1/K_{V0} = 0.0149(9)$ GPa⁻¹). The refined isothermal bulk moduli for ulexite and kurnakovite are ~ 37 GPa ($\beta_{V0} \sim 0.0270$ GPa⁻¹), which lie between those of other minerals commonly used as aggregates in concretes, while kernite and meyerhofferite are slightly softer ($K_{V0} \sim 30$ GPa; $\beta_{V0} \sim 0.0333$ GPa⁻¹).

The high-temperature experiments on kurnakovite and colemanite show that the presence of structural H₂O leads to dehydration processes that result in a structural collapse. In the light of a potential application as aggregates, this phenomenon is more critical in kurnakovite (~48% H₂O), where the crystal structure is no longer stable above 120 °C, while in colemanite (~22% H₂O) significant dehydration starts at T > 240°C. The structural collapse of kurnakovite at relatively low temperatures implies severe questions on its potential applicability in radiation-shielding concretes, while the thermal-induced dehydration of colemanite should not represent an issue for several applications of radiation-shielding materials.

CRYSTAL-FLUID INTERACTIONS AT HIGH PRESSURE IN NATURAL ERIONITE-K

Battiston Tommaso¹, Comboni Davide², Pagliaro Francesco¹, Lotti Paolo¹, Gatta G. Diego¹

¹Earth Science Department, University of Milan, Italy, ²European Synchrotron Radiation Facility, France

Investigating the P-induced intrusion of molecules and ions, from the P-transmitting fluids, into the structural nano-cavities of microporous compounds, e.g. zeolites, has experienced a boosted interest in the last two decades. Zeolites have a consolidated history of technological and industrial applications, but the understanding of these phenomena may further expand their utilizations, opening new routes for tailoring functional materials. In this study, we have focused on a natural zeolite: erionite. Its behavior has been investigated when compressed in non-penetrating and potentially penetrating fluids, i.e. those fluids made by molecules having a kinetic diameter that may allow their P-mediated adsorption into the zeolite structural cavities.

Erionites represent a series belonging to the zeolites group, with a wide chemical variability expressed as solid solutions among three end-members: erionite-Ca, erionite-Na, and erionite-K. Our sample, classified as erionite-K, has the following average chemical formula:

$K_{2.31}Na_{0.02}Ca_{2.15}Mg_{0.69}Ba_{0.04}Sr_{0.02}Al_{9.00}Si_{27.19}O_{72} \cdot 18.66H_2O$. The erionite-framework is characterized by the presence of large cages (23-hedron, called "erionite-cage"), superposed along the c-axis, hosting most of the extra-framework population.

Experiments by single-crystal X-ray diffraction under in-situ high-pressure conditions, using an ETH-type diamond anvil cell (DAC) and ruby as P-calibrant, were conducted at the Xpress beamline of the Elettra Synchrotron (Trieste, Italy). Two P-ramps were performed using different P-transmitting media: the first one using the non-penetrating silicone oil, up to 2.60(5) GPa, and the second one with the potentially penetrating methanol:ethanol: H₂O = 16:3:1 (hereafter mew) mixture, up to 4.97(5) GPa. A II-order Birch-Murnaghan equation of state was fitted to the P-V data obtained by the silicone oil ramp, yielding the refined isothermal bulk modulus of erionite: $KV_0 = 44(1)$ GPa ($\beta V_0 = KV_0 - 1 = 0.0227(5)$, where βV_0 is the bulk volume compressibility). P-V data from the mew ramp displays markedly lower compressibility, which is unambiguously related to the P-induced intrusion of H₂O (and possibly alcohol) molecules. The adsorption, which appears irreversible in decompression, seems to occur in three different steps, approximately around 0.2, 1.2, and 2 GPa. The magnitude of the intrusion process appears to be comparable with that previously observed for synthetic zeolites (as e.g. SiO₂-ferrierite or AlPO₄₋₅ zeolites), and this is of particular relevance if we consider that it was observed in this study not on a synthetic compound characterized by controlled crystal chemistry, but on a sample of natural erionite, with structural voids largely filled by the extraframework population (i.e., cations and H₂O molecules). Preliminary experiments performed with different classes of potentially penetrating fluids (e.g., 2:2:1 and 1:1:2 mew mixtures), by synchrotron single-crystal X-ray diffraction, seem to corroborate the aforementioned results in terms of compressibility, although apparently continuous adsorption without discontinuities in the P-V trend was detected. Further experiments will allow a full understanding and constraints of the P-induced adsorption phenomena in erionite.

ECONOMIC EVALUATION OF IRON FORMATION USING DUAL AND MULTI ENERGY XRT AND CT ANALYSES

Bauer Christine¹, Wagner Rebecca¹, Orberger Beate², Firsching Markus¹, Ennen Alexander¹, García-Piña Carlos³, Wagner Christiane⁴, Honarmand Maryam⁵, Nabatian Ghasem⁶, Monsef Iman⁵

¹Development Center X-ray Technology EZRT, Fraunhofer Institute for Integrated Circuits IIS, Germany, ²Earth Sciences, Université Paris-Saclay, France, ³DMT GmbH & Co. KG, Germany, ⁴Université Pierre et Marie Curie IStEP, Sorbonne Université, France, ⁵Department of Earth Sciences, Institute for Advanced Studies in Basic Sciences, Iran, Islamic Republic of, ⁶Department of Geology, University of Zanjan, Iran, Islamic Republic of

Iron-ore industries need to optimize exploration, mining, and processing in order to be competitive on the market. Rapid and in-field evaluation of the iron content, its matrix minerals (quartz/ carbonates), and associated heavy metals (e.g. REE phosphates, sulfides, zircon, native gold) which may be extracted as byproducts during beneficiation or metallurgical processing, allows increasing resource efficiency in a holistic approach. Dual and multi-energy X-ray transmission imaging (DE-/ME-XRT) was used on different iron oxide ore types: banded and nodular magnetite-hematite-quartz ore from northern Iran, and jaspilite ore from banded iron formation in South Africa. XRT allowed to quantify the areal density and mass fraction of iron and the quartz matrix, and thus to distinguish waste from valuables. CT allowed quantifying size, distribution, and orientation of internal structures, such as banding, folding, and fractures and the mineral groups hosted in fractures. Comparison of the XRT and CT data with laboratory chemical and mineralogical data shows that the data provided by both methods are reliable. Data processing, such as blob analysis, can be successfully applied for distinguishing iron oxide-rich parts from waste. Heavy minerals such as baryte, uraninite, galena, and monazite can be detected and quantified. XRT can be used as a real-time inline process for continuous monitoring. CT data recording and reconstruction depends strongly on the acquisition parameters and is typically in the range of hours per meter. Therefore, CT should be performed on selected samples in a workshop at the mine site or laboratory. Machine and measurement protocols, X-ray parameters, and resolution can be customized in collaboration with the mining geologist and processing engineers.

Keynote

MINERALOGY OF THE ASTEROID BELT

Beck Pierre¹

¹IPAG, France

The Solar System host a population of small objects that seems to have escaped the major geological process that occurred on terrestrial planets. They are thus of great interest to the cosmochemical community in order to unravel the first steps of formation of our planetary system. I will review what we have learned on the mineralogy of asteroids based a combination of laboratory studies, ground-based observations and space missions. I will also discuss the connection between comets and asteroids.

MAGMATIC VOLATILES RELEASED FROM INTRAOCEANIC ARC MAGMAS: CONSTRAINTS FROM APATITE COMPOSITIONS AND IMPLICATIONS ON MAGMATIC PROCESSES FOR BROTHERS VOLCANO

Beckmann Philipp¹, Holtz Françios¹, Zhang Chao²

¹Institute for Mineralogy, Leibniz University Hannover, Germany, ²Department of Geology, Northwest University, China

The active Brothers volcano of the Kermadec arc is an ideal location to study the magmatic-hydrothermal processes that control the transfer of volatiles and metal elements from Earth's interior to the surface at an intraoceanic subduction zone. Brothers Volcano is characterized by relatively evolved compositions (dacitic bulk rocks, dacitic to rhyolitic melts), high melt chlorine contents but probably low meltwater contents. Three of the five drilling sites consisting of fresh lavas and volcanoclastics were recovered and cored during IODP expedition 376 and are exclusively addressed in this presentation. To clarify the controversy regarding the nature of magmatic source and composition of primitive magmas, a large dataset of compositions of bulk volcanic rocks, minerals, and melt inclusions for various eruptive stages is crucial for exploring the most "primitive" magmas, as well as temporal and spatial relations between "primitive" and evolved magmas. In this presentation, analytical results on the volatile concentrations in apatite are discussed. Cl and F concentrations (1.42 – 2.15 wt.% and 1.25 – 2.81 wt.% respectively) have been measured for both phenocryst apatite and apatite as inclusion in plagioclase and pyroxene. Both types show a similar compositional range in terms of volatiles with distinctively higher Cl contents compared to the majority of apatites observed in volcanic-plutonic systems (Webster and Piccoli, 2015), indicating an uncommon high Cl concentration in magmas from Brothers volcano. The variation of apatite compositions seems to have been largely controlled by fractional crystallization with negligible influence from degassing of hydrosaline fluids (McCubbin et al., 2013). The low OH concentrations in apatite indicate that at least some of the coexisting melts may have contained more Cl than H₂O, which is expected to influence significantly the fractionation trends. The low water content is confirmed by the presence of only anhydrous mafic mineral phases in the volcanic rocks (plagioclase, pyroxenes). Depending on the concentrations of Cl and H₂O present in the melts, fractionation trends (and degassing behavior) may differ significantly, which could explain partly the variety of melt compositions that have been determined so far from quenched glasses and melt inclusions.

RADIATION-DAMAGE IN ZIRCON: MECHANICAL PROPERTIES

Beirau Tobias¹, Huber Norbert², Salje Ekhard³, Oliver Warren⁴, Nix William⁵, Pöllmann Herbert¹, Ewing Rodney⁶

¹Institute of Geosciences and Geography, Martin Luther University Halle-Wittenberg, Germany, ²Institute of Materials Mechanics and Institute of Materials Physics and Technology, Helmholtz-Zentrum Hereon and Hamburg University of Technology (TUHH), Germany, ³Department of Earth Sciences, University of Cambridge, United Kingdom, ⁴KLA-Tencor, United States, ⁵Department of Materials Science and Engineering, Stanford University, United States, ⁶Department of Geological Sciences and Center for International Security and Cooperation, Stanford University, United States

Nanoindentation and mechanical modeling results indicate that the radiation-damage (mainly α -decay) induced crystalline-to-amorphous transition in zircon (end-member composition ZrSiO_4) that can be described as a percolation problem with two percolation points. Young's modulus (E) has been found to be threshold sensitive. Interfaces and underlying hard shells, enclosing the depleted amorphized cores, stabilize the hardness (H). In general, the increasing structural disorder leads to a noticeable decrease in E and H. Nanoindentation high-resolution mapping of a zoned zircon shows how a multi-layered ceramic material accommodates volume expansion and changes in mechanical properties due to radiation damage. The zoning is due to variations in the U and Th concentrations (α -decay event doses $\sim 3.7 \times$ to 7.5×10^{18} α -decays/g). Radiation-damage-related variations in mechanical properties of zircon provide useful additional information for geo- and thermochronological data analysis.

STABLE ISOTOPE COMPOSITIONS AS PROVENANCE SIGNATURES OF ANTIQUE ARTEFACT CORALS

Bente Klaus^{1,2}, Gerdes Axel³, Ende Martin⁴, Beirau Tobias⁵, Hoelzig Hieronymus⁶

¹IMKM University Leipzig, ²CCA-BW University Tübingen, bente46@gmx.de, ³University Frankfurt, gerdes@em.uni-frankfurt.de, ⁴University Vienna, martin.ende@univie.ac.at, ⁵University Halle, tobias.beirau@geo.uni-halle.de, ⁶IMKM University Leipzig, hieronymus.h@gmx.de

In order to differentiate provenances and raw materials, red and white artifact corals from different sites and historical periods are exemplarily studied due to Sr-, B-, C- and O-isotopes. Red coral artifacts from the Hanseatic Age (HA: Greifswald, Lübeck) [1, 2] and Africa ~ 1800 (A: Algeria, Tunisia, Kingdom of Benin) [3] are identical with the original *corallium rubrum*. Iron Age artifact corals from Central Germany (CG: Hänichen, Kleinkorbetha, Gräfenhainichen, Leimbach) [2, 4] are white supposed to result from the decay of red polyene pigments provoked by firing events. These artifact corals from CG show single-crystalline calcites [2] recrystallized from original coral mesocrystals. In contrast to this finding, white artifact corals from Langenau (SG: Southern Germany) and Dürrenberg (AS: Austria) contain polyene pigments [1] and meso-crystalline calcite with high amounts of Mg [4] that are typical for *corallium rubrum* and artefact red corals as from A [1] and HA [2]. The artefact corals ($^{87/86}\text{Sr} = 0.7092$; $\sim 2000 \text{ ppm} < \text{Sr} < \sim 10000 \text{ ppm}$) derive from recent *corallium rubrum* grown in modern days seawater ($20 \text{ ppm} < \text{B} < 50 \text{ ppm}$ and $10 \text{ ‰} < \delta^{11}\text{B} < 30 \text{ ‰}$). Carbon and oxygen isotopic (NBS 19) compositions of Mg-rich and polyene containing red and white artifact corals show $\delta^{13}\text{C} < 0 \text{ ‰}$ and $-1.5 \text{ ‰} < \delta^{18}\text{O} < 0.5 \text{ ‰}$ identical with the original *corallium rubrum* [5]. White Mg- and polyene-free artifact corals showing $\delta^{13}\text{C} < -0.5 \text{ ‰}$ and $\delta^{18}\text{O} < -2.5 \text{ ‰}$ are also suggested to derive from *corallium rubrum*. Thermally treated branches of *corallium rubrum* whitened by the decay of polyenes at $T > 200^\circ\text{C}$ do not show $\delta^{13}\text{C}$ and $\delta^{18}\text{O}$ changes. Reacted with huminates simulating soil depositions *corallium rubrum* branches show significantly lowered $\delta^{13}\text{C}$, but no $\delta^{18}\text{O}$ change. White Mg- and polyene-free artifact corals from Hänichen show typical marine B-isotope composition and very low $\delta^{13}\text{C} = -8.5 \text{ ‰}$ and $\delta^{18}\text{O} = -5.5 \text{ ‰}$ attributed to secondary freshwater influence. Angle skin corals show $\delta^{13}\text{C}$ and $\delta^{18}\text{O}$ typical for *corallium rubrum*. But they are excluded as raw materials because of their microstructure. Fossil corals of different ages [6] with $\delta^{13}\text{C} > 0 \text{ ‰}$ and $\delta^{18}\text{O} < 0 \text{ ‰}$ as well as fresh water bio-calcites cannot be alternative raw materials because of their B- and Sr-isotopy. The artifact corals are suggested to derive from *corallium rubrum* grown in modern days seawater indicating trade routes between the Mediterranean and the Baltic Sea (associated amber). Actually, recent cold water corals and reasons for white artefact corals despite polyene red pigments are studied.

- [1] K. Bente, C. Berthold, M. Keuper, A. Gerdes, J. Ansorge, A. König, Arch. Berichte aus MV, 2017, 69-79
- [2] K. Bente, C. Berthold, R. Wirth, A. Schreiber, A. König, METALLA, 2021 (submitted)
- [3] K. Bente, C. Berthold, S. Dolz, A. Gerdes, METALLA 7, 2015, 24-26
- [4] K. Bente, C. Berthold, R. Wirth, A. Schreiber, H. Hölzig, R. Panneerselvam, S. Keilholz, D. Poppitz, A. König, METALLA 11, 2021, 74-76
- [5] S. Chaabane, M. López Correa, P. Montagna, C. Linares, P. Ziveri, Marine Chemistry, Vol. 186, 2016, 11-23
- [6] G. Auer, W. E. Piller, M. Reuter, M. Harzhauser, Paleoceanography, 2014, DOI 10.1002./2014PA002716

U-Pb DATING OF SULFATES BY LA-ICP MS

Beranoaguirre Aratz¹, Gerdes Axel¹, Vasiliev Iuliana², Leitner Christoph³

¹Goethe University Frankfurt, Germany, ²Senckenberg Biodiversity and Climate Research Centre, Germany,

³University of Salzburg, Austria

Sulfates such as anhydrite or gypsum occur in numerous environments and provide valuable information about different characteristics of sedimentary basins. The sulfates can also play a role in oil and gas formation and several problems in its extraction. Accurate U-Pb dating of sulfates could contribute to a better understanding of their formation and/or transformation (hydration-dehydration) processes along with different geological events. The development of low-U phases geochronology has been successfully applied in carbonate and garnet dating and it is nowadays expanding to other minerals like fluorites. In this contribution, we present the advances carried out in the FIERCE laboratory concerning U-Pb dating of sulfates.

The feasibility of the laser ablation-based method requires reference material of known age that behaves similar to the sulfates in order to correct the laser-induced fractionation and instrumental drift. Analysis performed in the temporally well-established Messinian Salinity Crisis (the Mediterranean Sea, 5.97-5.33 Ma) gypsum samples, suggest that carbonate reference materials are reliable for in-situ U-Pb dating of sulfates. The bias between our U-Pb and cyclostratigraphic ages, if any, is included in the uncertainty (5 %).

On the other hand, sulfates are prone to (de-) hydration reactions. Therefore, it is often difficult to ascertain if a sample is primary or secondary in origin. Direct dating of sulfates would provide the means to distinguish between primary crystallization and subsequent fluid circulation events. Thus, analysis of more than 50 evaporites samples from the Triassic Grabfeld Formation (SW Germany) have disclosed at least 3 clusters of younger ages, at Middle Jurassic, Lower Cretaceous, and Upper Cretaceous. Those results show that tectonic movements and/or fluid activities could also play a crucial role in the meso- and telogenetic crystallization of gypsum and anhydrite.

EFFECT OF CHEMICAL VARIABILITY ON RAMAN SPECTRA OF ENARGITE AND FAHLORE

Berkh Khulan¹, Rammlmair Dieter¹

¹Federal Institute for Geosciences and Natural Resources, Germany

Enargite (Cu₃AsS₄) and tennantite (Cu₁₂As₄S₁₃) are typical As-bearing sulfides in intermediate- and high-sulfidation epithermal deposits. Trace and major element variations in enargite and tennantite (as members of fahlore group) and their substitution mechanisms are widely described. However, Raman spectra of the minerals with correlative quantitative chemical information are relatively rare, especially for enargite. Therefore, comparative electron and μ-Raman microprobe analyses were performed on enargite and fahlore from Ministro Hales, a transitional porphyry copper-high-sulfidation epithermal deposit, in Chile.

According to electron microprobe analyses, enargite hosts trace amounts of Sb, Te, Zn, and Fe. Element distribution maps and spot analyses show an inverse correlation between Sb and As concentrations, indicating a simple substitution of Sb⁵⁺ for As⁵⁺. Te and Zn in turn correlate positively with each other, but negatively with As and Cu. This can be achieved via a coupled substitution of Te⁴⁺ and Zn²⁺ for As⁵⁺ and Cu⁺. Similarly, Sb³⁺ arbitrarily substitutes for As³⁺ in fahlore resulting in a complete solid solution series from tetrahedrite (Sb-rich member) to tennantite (As-rich member), whereas in goldfieldite (Te-rich member) Te occupies the As and Sb sites by the coupled substitution: Te⁴⁺ + Cu⁺ → (As, Sb)³⁺ + (Cu, Fe, Zn)²⁺. The different substitutions mechanism affects Raman spectra of the minerals and is visualized by mapping method using a Raman microprobe.

Lastly, a secondary phase in enargite was observed in a weathered sample. Its chemical composition and Raman spectra have an intermediate position between enargite and tennantite. It has low total contents due to microporosity and the lower the total content, the lower the As and S contents compared to primary enargite and tennantite.

NITROGEN BEHAVIOR IN SILICATE MELT AND N-RICH FLUID UNDER MAGMATIC CONDITION AND REDUCED fO_2

Bernadou Fabien¹, Gaillard Fabrice², Slodczyk Aneta¹, Furi Evenlyn³, Marrocchi Yves³

¹ISTO, CNRS, France, ²CNRS, France, ³CRPG, CNRS, France

Nitrogen is the most abundant element in Earth's atmosphere and a major actor in surficial biogeochemical cycles. However, its involvement in deep geochemical cycles, its mantle abundances, and the timing and magnitude of its degassing from the planetary interior to the atmosphere remain unclear. Here, we investigate magmatic degassing of nitrogen using high-pressure high-temperature experimentation in conjunction with vibrational and mass spectrometry. The aim is to develop a thermodynamic model defining both nitrogen solubility and speciation in silicate melts and fluids.

Most studies emphasize that the nitrogen solubility in silicate melts is very sensitive to the nitrogen and oxygen fugacities (fN_2 , fO_2). Three main nitrogen species have been described in silicate melts: N^{3-} and NH_3 dominant under reduced conditions.

Here we will present results on both silicate melt and N-rich fluid. For the silicate melt, we will present results on the solubility of nitrogen as a function of different parameters such as pressure (from 1 kbar to 10 kbar) or fO_2 (from IW+2 to IW-4). We will then discuss the parametrization of a nitrogen solubility model in silicate melt as a function of P-T- fO_2 . Lastly, this model is used in a magma ocean degassing code to capture the fO_2 dependence of N-outgassing. We show that for $fO_2 < IW-2$, most nitrogen remains dissolved in the magma ocean, whereas for more oxidized conditions, nitrogen is massively outgassed in the atmosphere. The abundance of nitrogen at the Earth's surface may be the consequence of the degassing of the last magma ocean stage.

KINETIC STUDY OF HIGH TEMPERATURE RAMSDELLITE-PYROLUSITE TRANSFORMATION

Bernasconi Davide¹, Curetti Nadia¹, Benna Piera¹, Fiore Gianluca², Pavese Alessandro¹

¹Earth Sciences, University of Turin, Italy, ²Chemistry, University of Turin, Italy

The two most common polymorphs of MnO₂, ramsdellite and pyrolusite, are often found in natural association. Our starting sample is a massif rock coming from the Mistake mine (Arizona) and containing macroscopic crystals of both ramsdellite ($a = 4.5131(6)$, $b = 9.2689(13)$, $c = 2.8610(4)$ Å, $V = 119.69(3)$ Å³; S.G. Pbnm) and pyrolusite ($a = 4.4030(2)$, $c = 2.87392(16)$ Å, $V = 55.715(5)$ Å³; S.G. P42/mnm), along with a smaller amount of “groutellite”. A mixed powder was used to investigate the transformation of the ramsdellite into pyrolusite by in-situ high-temperature X-ray powder diffraction. Our results reveal that this transformation is not a direct transition, but it occurs in two steps, as a function of temperature: ramsdellite transforms into an amorphous phase, which then recrystallizes into pyrolusite. Amorphization of ramsdellite and crystallization of pyrolusite kinetics were studied by the universal equation for solid-solid reactions. The two activation energies are comparable, but the pre-exponential factor of the ramsdellite amorphization is two orders of magnitude larger than pyrolusite crystallization. As a consequence, the transformation of the ramsdellite into pyrolusite implies the formation of a transition glass, due to a mismatch between conversion rates that approach one another upon increasing temperature.

APPLICATIONS OF SULFIDE GEOCHEMISTRY FOR CONSTRAINING ORE-FORMING PROCESSES OF THE SEDIMENT-HOSTED Cu-Co DOLOSTONE ORE FORMATION, NAMIBIA

Bertrandsson Erlandsson Viktor¹, Wallner Daniela¹, Ellmies Rainer², Melcher Frank¹, Raith Johann G.¹

¹Department Applied Geosciences and Geophysics, Montanuniversität Leoben, Austria, ²Gecko Namibia, Namibia

Deducing the metal source of ore deposits is always a challenge but something that is key to fundamentally understand the ore-forming processes. The primary metal source of sediment-hosted Cu deposits is conceptually assumed to be underlying red bed sediments, in a typical transgressional rift succession. Sulfide mineralization would occur early on, during diagenesis to pre-metamorphism. The Dolostone Ore Formation (DOF) is a recently discovered Cu-Co(-Zn) mineralization hosted in Neoproterozoic marls and dolomitic carbonates; situated within the Kaoko Belt, the northern branch of the Damara Orogen, Namibia. Ore sulfides occur in different styles of disseminations within the host rocks and as veins and breccias. Trace element concentrations of sphalerite, chalcopyrite, pyrite, and pyrrhotite were measured by LA-ICP-MS to investigate the geochemistry of the sulfides from the different styles of mineralization. Elements measured were: S, V, Cr, Mn, Fe, Co, Ni, Cu, Zn, Ga, Ge, As, Se, Mo, Ag, Cd, In, Sn, Sb, Te, Au, Hg, Tl, Pb & Bi.

The trace element data show distinct grouping of mineralization styles between the individual sulfides, suggesting a polyphase development of the DOF sulfide mineralization. Trace element grouping and trends point towards at least a four-stage mineralization history of the DOF, which is now supported by microscopic paragenetic investigations. Furthermore, geochemical trends of the individual sulfide phases suggest that, at the least, greenschist facies metamorphism played a major role in the formation or equilibration of the sulfide mineralization. Ga-Ge-In-Mn-Fe in sphalerite geothermometry indicates that sphalerite formed at temperatures above 310 ± 50 °C (the closing temperature of the geothermometer). This is further supported by Raman analyses of carbonaceous matter (STA geothermometer) which indicate that temperatures of 340 ± 32 °C have affected the Neoproterozoic sedimentary package.

Earlier pyrite is hypothesized to be a possible source for the elements resulting in the formation of sphalerite, chalcopyrite, and galena. Trace element liberation (e.g. Cu, Zn & Pb) from preexisting iron-sulfides during greenschist to amphibolite facies metamorphism has been recognized in several other studies. The liberated elements tend to form new separate phases, e.g. sphalerite, chalcopyrite, and galena, rather than remain in the recrystallized iron-sulfides. The presence of sedimentary to diagenetic sulfide mineralization cannot be discredited. The possible role of pre-metamorphic sulfides for the DOF mineralization is still to be investigated.

WALL-ROCK ALTERATION GEOCHEMISTRY AND FLUID EVOLUTION IN DEGANA TUNGSTEN DEPOSIT, INDIA

Bhattacharya Sourabh¹, Roy Jitendra²

¹Indian Institute of Science Education and Research Mohali, India, ²School of Earth Ocean and Climate Sciences, Indian Institute of Technology Bhubaneswar, India

There is substantial ongoing research on the matter of rarity of wolframite [Fe,Mn(WO₄)] deposits and their genetic links with Fe budget and evolution of ore fluid. This study aims to reflect upon these issues through studies on Degana Granite (DG) that hosts the richest wolframite deposit in India. Geochemical and fluid inclusion studies were carried out on DG-hosted ore lode comprising steeply-dipping quartz veins and adjacent granite wall-rock.

The mineral paragenesis and chemistry reveal that the ore fluids affected the pre-ore assemblage of K-feldspar, magmatic topaz, and siderophyllite. This resulted in a concomitant increase in modal contents of lithian siderophyllite, lithian ferroan muscovite, topaz, and quartz. Mass balance calculations infer enrichment of W, Fe, Li, and Sn in the wall-rock lode. Both tri- and di-octahedral micas show Li gain and Fe loss, although with distinct substitution behavior. In trioctahedral mica, heterovalent substitutions play the key role, as defined by the vector: ${}^{\text{VI}}\text{Li}^{+}_{11} {}^{\text{IV}}\text{Si}^{4+}_{2} {}^{\text{VI}}\text{Al}^{3+}_{1} {}^{\text{VI}}\xi_{1} {}^{\text{VI}}\text{Fe}^{2+}_{-3} {}^{\text{IV}}\text{Al}^{3+}_{-2}$ (where ξ = vacancy). In contrast, the ore-stage dioctahedral mica incorporates Li⁺ into vacancies of the dioctahedral sheet; this substitution is defined by ${}^{\text{VI}}\text{Li}^{+}_{14} {}^{\text{IV}}\text{Si}^{4+}_{1} {}^{\text{VI}}\text{Fe}^{2+}_{-1} {}^{\text{IV}}\text{Al}^{3+}_{-1} {}^{\text{VI}}\text{Al}^{3+}_{-1} {}^{\text{VI}}\xi_{-2}$.

Fluid inclusion studies show that the pre-ore fluids entrapped in barren DG typify as (a) magmatic topaz-hosted CO₂-poor (XCO₂: 0.05 to 0.07) H₂O-CO₂-NaCl fluids, and (b) silicification-induced (post-magmatic) matrix quartz-hosted H₂O-CO₂-NaCl fluids with varying XCO₂. Tungsteniferous lodes constituting quartz veins and wall-rock show minor variations in nature of entrapped fluids. The veins show a predominance of CO₂-only and moderate salinity (12.2 to 17.9 wt% NaCl equiv) H₂O-CO₂-NaCl fluids. Contrarily, the wall-rock that hosts the bulk of the ore, contains an assemblage of H₂O-CO₂-NaCl inclusions with somewhat relatively higher salinity (11.0 to 22.2 wt%). The CO₂-only inclusions also co-occur along with or without halite-bearing H₂O-NaCl inclusions. In both the types of hosts (veins and wall-rock), we argue for H₂O-CO₂ immiscibility, as the H₂O-CO₂-NaCl inclusions in individual clusters show – (a) varying H₂O/CO₂ ratios, and (b) total homogenization at comparable temperatures (with a difference of ≤ 25 °C) into opposite modes in accordance with H₂O/CO₂ ratio. In wall-rock, the PT conditions of fluid entrapment are estimated as 1.1-1.7 kbar/330-410 °C, using the isochore intersection method. For this purpose, the end-member fluid inclusions of CO₂-only and halite-bearing H₂O-NaCl nature, hosted in wall-rock are utilized. The deduced PT conditions imply limited variations in pressure regime during ore enrichment; the CO₂-effervescence was perhaps driven by retrograde boiling on a cooling path. The role of fluid-rock interaction involving feldspar and muscovite hydrolysis is also evident, as indicated by a broader and higher range of salinity for H₂O-CO₂-NaCl fluids in the wall-rock zone as against veins.

This study surmises that magmatic ore fluids of moderate salinity H₂O-CO₂-NaCl nature introduced W (\pm Sn) into the wall-rock zone. Such fluids also caused the addition and redistribution of Li and Fe, resulting in the predominance of lithian ferroan muscovite in the ore zone. The K-feldspar and muscovite played a key role in the acid neutralization process, a pre-requisite for wolframite enrichment. Thus, the potassic alteration that precedes the ore fluid activity acted as a pre-conditioning process for ore formation.

MUSEUM HISTORICAL COLLECTIONS TO BE REVISITED: REINSTATEMENT OF THE NAME “BRANCHITE” AFTER TWO CENTURIES.

Biagioni Cristian¹, Farina Simone², Pasero Marco¹, Bonaccorsi Elena¹

¹Earth Sciences, University of Pisa, Italy, ²Natural History Museum, University of Pisa, Italy

During a study of the activity of Paolo Savi (1798 - 1871) as director of the Museum of Natural History of the University of Pisa, a note from 1839 on the description of a new organic mineral, called "branchite", was found. It was possible to examine the samples of "branchite" studied by Paolo Savi in the late 1830s, and a comprehensive investigation was undertaken by single crystal X-ray diffraction. Their isotopic relationship to hartite, C₂₀H₃₄, described in 1841, was demonstrated. The refined parameters of the unit cell were $a = 11.4116(7)$, $b = 20.9688(12)$, $c = 7.4100(4)$ Å, $\alpha = 93.947(2)$, $\beta = 100.734(2)$, $\gamma = 80.524(2)^\circ$, $V = 1716.99(17)$ Å³, $Z = 4$; space group P1. The crystal structure was resolved and refined to $R1 = 0.0423$ for 13512 reflections with $F_o > 4\sigma(F_o)$ and 1266 refined parameters. Since branchite has priority over hartite, reinstatement of the former name and discrediting of the latter was approved by the IMA Commission on New Minerals, Nomenclature, and Classification. Branchite is one of the few mineral species formed by C and H only reported in the official IMA mineral list. Type locality of branchite is Botro di Lavajano, Monte Vaso, Chianni, Pisa, Italy; the neotype material is preserved in the Museum of Natural History of the University of Pisa under catalog number 14426.

PLAGIOCLASE HOSTED MAGNETITE MICRO-INCLUSIONS ORIGIN DETERMINATION

Bian Ge¹, Ageeva Olga¹, Rečnik Aleksander², Habler Gerlinde¹, Abart Rainer¹

¹Department of Lithospheric Research, University of Vienna, Austria, ²Department of Nanostructured Materials, Jožef Stefan Institute, Slovenia

Oriented needle- and lath-shaped magnetite (Mt) micro-inclusions are frequently observed in plagioclase (Pl) from oceanic gabbros dredged at the Mid Atlantic Ridge. Their formation pathways and temperatures are of interest for paleomagnetic reconstructions. Systematic crystallographic and shape orientation relationships (CORs, SORs) of Mt micro-inclusions and Pl host have been rationalized through correlated optical- and scanning electron microscopy (SEM) including electron backscattered diffraction (EBSD) [1]. The preferred orientations can be explained by a good lattice match between the densely packed Mt{222} oxygen planes and various oxygen layers of Pl, including Pl(112), Pl(150), Pl(1-50), Pl(-312), etc. In order to understand the origin of the Pl-hosted Mt inclusions, selected inclusions were studied by transmission electron microscopy (TEM) combined with selected area electron diffraction (SAED), high-resolution imaging (HRTEM), and energy-dispersive X-ray spectroscopy (TEM-EDS).

Two TEM foils containing needle-shaped Pl(112)_n-Mt and Pl(1-50)_n-Mt micro-inclusions were prepared using the focused ion beam (FIB) technique. The nomenclature Pl(112)_n-Mt inclusion designates an inclusion elongated parallel to Mt{222} // Pl(112) plane poles. The FIB foils were extracted so that the needle elongation direction lies in the plane of the foil and the Mt-Pl interfaces are edge on.

SAED confirmed the orientation relationships that ensure alignment of oxygen layers between Mt and Pl. In combination with HRTEM images of Mt-Pl interfaces, this indicates that the Mt micro-inclusions formed in contact with the Pl host crystal. Most of the inclusions terminate at the twin boundaries after the Albite law, which indicates that the Mt micro-inclusions formed coevally with or after Albite twinning. Based on the observations the Mt inclusions most likely formed by precipitation from a supersaturated Fe-bearing Pl. Mass balance considerations show that Mt may precipitate from Fe-bearing Pl without an external supply of Fe but requires out-diffusion of oxygen from Pl to facilitate partial reduction of ferric iron originally contained in Pl. Oxygen loss from the Pl may have been driven by low fO_2 in the environment, and the Albite twin boundaries may have served as passageways for oxygen diffusion. Additional phases, such as ortho- and clinopyroxene may have co-precipitated with the Mt. The Mt micro-inclusions contain oriented lamellae of ilmenite, the abundance, shape, and size of which indicate direct exsolution or oxidation exsolution from a Ti-rich Mt at a temperature in excess of 600°C, which is well above the Curie temperature of Mt. Thus, the most likely formation pathway of the Mt inclusions is precipitation from a Fe-bearing Pl in a solid-state reaction at > 600°C. As a consequence, the magnetic signature of the Mt-bearing Pl grains must be considered as thermoremanent magnetization.

Funding by FWF grant I 3998-N29 and RFBR grant 18-55-14003 is acknowledged.

Reference

[1] Ageeva et al (2020) *Contrib. Mineral. Petrol.* 175(10), 1-16.

SORPTION OF TETRACYCLINE ON THE β -CYCLODEXTRIN-MODIFIED ZEOLITE MATERIALS.

Białoszewska Monika¹, Bandura Lidia¹, Franus Wojciech¹

¹Department of Geotechnical Engineering, Lublin University of Technology, Poland

In recent years, there has been increasing pollution of the environment by organic compounds. They occur in the environment at low concentration levels (in the range of ng/L to μ g/L) but are constantly present in the environment. Their presence even at such low levels can have harmful effects on human and animal health and the environment. Their presence also contributes to the development of antibiotic-resistant bacteria (ARB), which in turn may reduce their therapeutic effectiveness against human and animal pathogens. Therefore, there is a need to develop methods to capture pharmaceuticals and especially antibiotics from water and wastewater. The most popular way of capturing them is adsorption, and special attention should be focused on adsorbents produced in accordance with the principles of sustainable development, e.g. from waste. An example of such materials are zeolites. However, in order to use them as adsorbents of organic compounds, there is a need for their surface modifications, since they are hydrophilic in nature.

The aim of this study was to investigate the sorption process of tetracycline (antibiotic) on β -cyclodextrin modified zeolite materials (NaX-CD, NaA-CD, and NaP1-CD). The effects of adsorbent dose, contact time, and initial concentration on the sorption process were studied. The optimal dose of adsorbent is 0.5 g/L. The optimal contact time for tetracycline adsorption is about 32 h, 32 h, and 4 h for NaX-CD, NaA-CD, and NaP1-CD, respectively. It was found that the adsorption kinetics follows the pseudo-second-order model in the case of NaX-CD ($R^2 = 0.982$) and NaP1-CD ($R^2 = 0.996$), whereas pseudo-first-order model in the case of NaA-CD ($R^2 = 0.958$). The results obtained by measuring the effect of initial concentration were fitted to 4 isotherm models: Langmuir, Freundlich, Temkin, and Dubinin-Radushkevich. The analysis of equilibrium sorption data showed that the sorption process of tetracycline follows the Langmuir model for NaX-CD and NaP1-CD and the Freundlich model for NaA-CD. The highest values of sorption capacities are 45.88 mg/g for NaX-CD, 55.71 mg/g for NaA-CD, and 38.18 mg/g for NaP1-CD. Obtained results indicate the important role of the zeolite type on the efficacy of cyclodextrin modification and its influence on the tetracycline sorption process.

Funding

The „Fly ash as the precursors of functionalized materials for applications in environmental engineering, civil engineering and agriculture” no. POIR.04.04.00-00-14E6/18-00 project is carried out within the TEAM-NET programme of the Foundation for Polish Science co-financed by the European Union under the European Regional Development Fund.

AB INITIO PREDICTION OF EQUILIBRIUM ISOTOPIC FRACTIONATION OF LIQUID SYSTEMS: THE CASE OF S ISOTOPES

Blanchard Marc¹, Vuilleumier Rodolphe², Desmaele Elsa², Pokrovski Gleb¹

¹GET, CNRS - Univ Toulouse 3, France, ²ENS, Chemistry Depart., PSL Research Univ, Sorbonne Univ, France

First-principles (also known as Ab initio) atomistic calculations can be used to determine equilibrium isotopic fractionation factors in fluid-metal systems that are essential parameters for understanding the isotopic variability observed in Nature. In the meantime, this theoretical approach enables to relate directly these macroscopic isotopic properties to the molecular-scale structural properties of species and minerals. In the case of liquid systems, molecular dynamics (MD) simulations run at finite temperatures are required. However, the conventional method consists in deriving the fractionation factors from snapshots sampled along the MD trajectory, where the atomic positions are subsequently optimized at zero temperature. A part of the configurational disorder characterizing the fluid is thus lost. In the present study, we develop an approach based on the atomic kinetic energy, which allows the isotopic fractionation factors to be determined directly from the whole MD trajectory.

This work will present the example of four key sulfur-bearing species in hydrothermal fluids. In particular, we will explore here, for the first time, the isotopic signatures of the two sulfur radical ions recently identified in hydrothermal-magmatic fluids (S^{2-} , S^{3-}), and provide comparisons with those of the common sulfate and sulfide (SO_4^{2-} , H_2S). The results of this study offer improved quantitative predictions of sulfur isotope systematics in high temperature-pressure geological fluids inaccessible to direct observation and analyses.

SAPONITE FORMATION MECHANISM AT AMBIENT PRESSURE IN LABORATORY SYNTHESIS

Blukis Roberts¹, Schindler Maria¹, Couasnon Thaïs¹, Benning Liane G.¹

¹German Centre for Geosciences GFZ Potsdam, Germany

Saponite is a clay mineral occurring in multiple natural settings such as weathering volcanic glass, weathered mafic and ultramafic rocks, and alkaline hydrothermal vents. It also possesses useful catalytic properties for several chemical industrial processes and has also been used in nanocomposites intended for structural and catalytic applications. Readily available saponite of a controlled composition, crystallinity, particle size and morphology, would be highly beneficial, however, synthetic methods to form such saponite are lacking and the understanding of mechanisms and processes controlling some of these parameters, especially crystallinity, particle size, and morphology, are currently rather limited. Understanding the saponite formation mechanism is important for the development of a more highly-tuned synthesis of saponites of specific particle sizes, morphologies, and chemical compositions. Here we report a new chemical reaction mechanism explaining the formation kinetics of saponite under laboratory-controlled conditions. Saponite was synthesized from aluminosilicate gel and magnesium salt solution under pH-controlled conditions at atmospheric pressure and 95-100°C. Our results show that the main factors affecting its formation and growth are the reaction pH, the rate of initial nucleation, and the reactivity of the aluminosilicate gel. This pathway makes our findings applicable to easily scalable industrial processes.

HIGH TEMPERATURE PHASE TRANSITION OF $3(\text{CaTi}_{0.66}\text{Fe}_{0.33}\text{O}_{2.83}) \cdot \text{CaO}$ PEROVSKITE OF THE RUDDLESDEN-POPPER SERIES

Boiadeiro Ayres Negrão Leonardo¹, Reissner Michael², Stöber Stefan¹, Kalil Cortinhas Alves Tiago¹, Pöllmann Herbert¹

¹Mineralogy/Geochemistry, Martin-Luther Halle Wittenberg University, Germany, ²Institute of Solid State Physics, TU Wien, Austria

Layered Ruddlesden-Popper (RP) perovskites have the generic formula $n(\text{ABO}_3) \cdot \text{AO}$, which represents perovskite-like structures with an excess of A cation (i.e. Ca) structurally composed of distorted rock-salt type cubic intergrows within ABO_3 perovskite blocks. The RP-perovskite $3(\text{CaTi}_{0.66}\text{Fe}_{0.33}\text{O}_{2.83}) \cdot \text{CaO}$ ($n=3$), which as far as we know is to date not reported elsewhere, was sintered by solid solution at 1300°C. High-Temperature X-ray Powder Diffraction (HT-XRPD) in transmission geometry was used to investigate possible structure changes of this phase from 293 to 1175 K. The RP-perovskite has an orthorhombic Pbca structure at room temperature (293 K), which changes at approximately 670 K, as a and b cell parameters assumed very close values. HT-XRPD patterns show the Pbca structure remains but assuming a pseudo-tetragonal character as evidenced by a and b. Endothermic peaks in the DSC curve of the sample confirm the pseudo-transition at this temperature, which is accompanied by a discrete mass loss observed in the thermogravimetric curve. The different Mössbauer spectra of the sample at room temperature and at 670 K (water-quenched) suggest that iron (as Fe^{+3} , or even Fe^{+4}) partially changes its coordination. The structure of the phase was refined, and described in a crystallographic information file (.cif), considering iron as Fe^{+3} sharing the Ti^{+4} positions equally in the perovskite-block octahedra.

ECO-CEMENTS BASED ON RESIDUES OF BAUXITE MINING

Boiadeiro Ayres Negrão Leonardo¹, Pöllmann Herbert¹, Lima da Costa Marcondes²

¹Mineralogy/Geochemistry, Martin-Luther Halle Wittenberg University, Germany, ²Institute of Geosciences, Federal University of Para, Brazil

The expressive and increasing global CO₂ emissions of the cement industry, associated with the world-environmental agenda to limit global warming, has triggered the research on less carbon-intensive ECO-cements. Competitive ECO-cements have the challenge not only to be environmental-friendly but also economically viable in order to be competitive to the world-used Ordinary Portland Cements (OPC). In this work, different calcium sulfoaluminate (CSA) cements were produced using clay overburden residues from the bauxite mining in Brazil. This material lies on the surface after bauxite mining, and to date has no other use than landfill. The clays are enriched in Al accommodated in kaolinite and gibbsite, besides Si, Fe in goethite and hematite, and minor Ti in anatase. To produce CSA cements, the high alumina contents are addressed to form ye'elimite, the main hydraulic mineral phase of CSA, whereas additional Si and Fe promote, respectively, the formation of belite and ferrite. Statistical design of experiments was conducted to test different raw-material compositions of the bauxite residue mixed with calcite and gypsum, at different sintering temperatures and times. Mineralogical quantification, using X-ray diffraction Rietveld analysis, was used to shape ideal compositions for the CSA cements produced using as much as possible of the bauxitic clayey residue. The lab-scaled experiments show that belite-rich CSA cements and ternesite-rich CSA cements can be successfully produced using the largely available and low-cost clay residue. The obtained CSA cements can be produced under reduced clinkering temperatures and save expressive amounts of CO₂ (~30%) when compared to OPC, showing similar hydration time and strength development.

AUDIENCE PRELIMINARY STUDY FOR MULTI-SENSORY EXHIBITS ALONG THE MINERAL EXPOSITION OF THE NATURAL HISTORY MUSEUM (UNIVERSITY OF PISA)

Bonaccorsi Elena¹, D'Andretta Marilina², Zannella Alessandra²

¹University of Pisa, Italy, ²Museo di Storia Naturale, University of Pisa, Italy

The described study took place between January and June 2019, in the Natural History Museum of the University of Pisa. The purpose of the study was to investigate the views of the museum visitors, to design multi-sensory exhibits in the Mineral Gallery favoring the accessibility to a visually impaired and blind audience. Sixty-five people participated in this screening activity, including Museum single visitors, organized visiting groups, people of the Museum staff, as well as some people belonging to the local section of the "Italian Union of the Blind and Visually Impaired".

Some workstations containing a series of minerals were set up in a room adjacent to the Mineral Gallery. Each station included the presence of certain specimens of minerals and rocks with certain physical characteristics and specific properties. Participants, except for the blind and visually impaired, were randomly assigned to one of two different experiences. The former should have been done with a blindfold over their eyes, thus involving an approach to the mineral samples based on touch, smell, and hearing; the latter, without a blindfold, including sight, touch, smell and hearing.

During the multisensory experience, the museum operator wrote down in a notebook the participant's behavior, taking also a note of their spontaneous comments. For each station, the operator performed a brief structured interview aimed at understanding what the visitors thought they had touched and what features they perceived. At the end of the test, a further interview was carried out, in semi-structured mode, aimed at collecting both data on the enjoyment of the experience and suggestions for improving the stations.

The subdivision of the experience into two types, with a blindfold and without, allowed to collect data on two different ways of approaching the minerals allowing to understand how the perception of the relevant characteristics of the minerals varied depending on the presence or absence of the sense of sight. Moreover, it was possible to analyze the impressions of the visitors related to the experience and the suggestions related to the future exhibition.

All the results were discussed together with the person in charge of the exhibition in order to integrate the visitors' points of view in the design of the future multisensory stations that will be included in the Mineral Gallery.

TITANITE FROM METACARBONATE: A POWERFUL PETROLOGICAL AND GEOCHRONOLOGICAL TOOL (VALLE STRONA DI OMEGNA; IVREA-VERBANO ZONE, ITALY)

Bonazzi Mattia¹, Langone Antonio², Nazzari Manuela³

¹Department of Earth and Environmental Sciences, University of Pavia, Italy, ²Institute of Geosciences and Earth Resources (IGG), Italy, ³Experimental Volcanology and Geophysics High Pressure High Temperature Laboratory, Istituto Nazionale di Geofisica e Vulcanologia (INGV), Italy

Titanite (CaTiSiO₅) is a common accessory mineral in the calc-silicate and mafic rocks. It contains several important geochemical elements, such as REE, Pb, U, Zr resulting in a useful petrological and geochronological tool (Kohn, 2017).

We performed a geochemical and petrological characterization of titanite from metacarbonate rocks occurring at the different levels of the Variscan continental crust exposed along the Valle Strona di Omezna, Ivrea-Verbano Zone (IVZ). The crustal section consists mainly of middle-high grade metapelites and metabasites, with numerous lenses of metacarbonate rocks. The crustal section is characterized by a progressive increase of temperature conditions, from amphibolite to granulite facies, with increasing crustal depth. Metacarbonate rocks range in composition from impure marble to calc-silicates and contain mostly calcite, with the local occurrence of dolomite. Clinopyroxene, feldspar, amphibole, and epidote are common in amphibolite facies rocks whereas scapolite, garnet, and olivine appear in granulitic samples.

Major and trace elements were determined for titanite from metacarbonates with different mineral assemblages along the crustal profile. The chemistry of titanite shows interesting correlations with lithologies, mineral assemblages, and titanite modal abundance. In order to constrain temperature, we adopted the Zr-in titanite thermometer (Hayden et al., 2008) by considering Pressure estimates from adjacent coexisting rocks. The obtained temperatures are in the range of 700-900 °C and are coherent with the high-temperature conditions recorded by surrounding metapelites/metabasites at the Carboniferous-Permian interval (Kunz and White, 2019; Redler et al., 2012). The titanite U concentration ranges from about 20 to 300 ppm without apparent correlation with metamorphic grade and/or mineral assemblages. U–Pb dating was only performed for titanite grains containing more than 100 ppm of U and preliminary U–Pb dates range from Middle Triassic to Lower Jurassic.

Bibliographic references

- Hayden, L. A., Watson, E. B., Wark, D. A. (2008). A thermobarometer for sphene (titanite). *Contrib. Mineral. Petrol.*, 155(4), 529-540.
- Kohn, M. J. (2017) – Titanite petrochronology. *Rev. Mineral. Geochem.*, 83, 419-441.
- Kunz, BE, White, RW. (2019) – Phase equilibrium modelling of the amphibolite to granulite facies transition in metabasic rocks (Ivrea Zone, NW Italy). *J Metamorph Geol.* 37, 935-950.
- Redler, C., Johnson, T. E., White, R. W., Kunz, B. E. (2012) – Phase equilibrium constraints on a deep crustal metamorphic field gradient: metapelitic rocks from the Ivrea Zone (NW Italy). *J. Metamorph. Geol.*, 30, 235-254.

STABLE ISOTOPE AND TRACE ELEMENT DISCRIMINATION BY MODERN CARBONATE-PRECIPITATING STREAMS IN THE TEMPERATE CLIMATE ZONE: INSIGHTS FROM RÜGEN AND WESTERHOF

Böttcher Michael E.¹, Winde Vera¹, Bünning Jens¹, Dellwig Olaf¹, Müller Katrin¹, Struck Ulrich², Schafmeister Maria-Theresia³, Escher Peter¹, Schmiedinger Iris¹

¹Geochemistry & Isotope Biogeochemistry, Leibniz Institute for Baltic Sea Research (IOW), Germany, ²Berlin, Naturhistorisches Museum, Germany, ³Applied Geology, University of Greifswald, Germany

Processes in the dissolved carbonate system of surface waters may contribute and are sensitive to variations of boundary conditions associated with climate change. Carbon dioxide super- and calcium carbonate-saturated ground waters that emerge from springs lose dissolved carbon dioxide to the atmosphere; this process leads to the development of CaCO₃ supersaturation of the aqueous solution. When exceeding a critical value, solid carbonates precipitate, thereby linking the past marine with the present terrestrial carbon cycles. The associated distribution of trace elements and stable isotopes leads to proxy formations. The magnitude of trace element and isotope fractionations is linked to non-equilibrium processes, impacted by the initial solution composition, hydrodynamics, and possible biological activity in the stream beds.

Two examples of recent sinter formation from streams in the temperate climate zone were investigated: One from the cliff zone of Rügen Island at the southern Baltic Sea coast line (Site R) and another one from Westerhof in the south-western Harz foreland (Site W). It is found at both sites, that two phases of surface water development can be differentiated: An induction period starting at the spring, where only degassing of carbon dioxide takes place and a second stage where calcite formation from the highly supersaturated solution is continuously driven by further degassing. The liberation of CO₂ is associated with an enrichment of the heavy carbon isotope in the remaining dissolved inorganic carbon. By following the isotope and trace element composition of aqueous solutions and recent calcite precipitates along the flow path, distribution coefficients (Li, Na, Mg, Sr, Ba, SO₄, ¹³C, ¹⁸O) between aqueous solution and calcite are derived. The empirical quantitative observations at Site W can be compared with observations dating back to the late 60s of the last century. Those at Site R are compared to results from laboratory experiments using natural water as starting solution. Furthermore, the distribution coefficients are compared to calibrated experimental studies to estimate calcite precipitation rates. Trace-element-based rate estimates for Site W are higher than published direct measurements, which is likely due to hydrodynamic boundary conditions impacting the in-situ growth experiments. Idiomorphic BaSO₄ was observed in the recent carbonate sinter at Site W for the first time, which is in agreement with slight supersaturations modeled for the stream water. At the bottom of the cliff (Site R), the carbonate stream water is finally entering the Baltic Sea where mixing with brackish surface waters occurs. The excess in dissolved CO₂ compared to the atmosphere is enhancing the degassing capacity in the mixed coastal waters.

MINERALOGICAL RECONCILIATION IN ORES USING CHEMICAL ASSAYS, X-RAY DIFFRACTION, AND AUTOMATED MINERALOGY

Bouzahzah Hassan¹, Solomon Betelehem¹, Riegler Thomas², Pirard Eric¹

¹GeMMe, University of Liège, Belgium, ²Ideas, ERAMET, France

Mineral characterization in earth sciences, process mineralogy, and environment is usually achieved through X-ray diffraction, microscopy, and sometimes modal calculation based on chemical assays. The automated mineralogy based on SEM-EDS micro-analysis has strongly developed in the last three decades and also become widely used in mineral characterization offering a wide suite of information (modal mineralogy, textural quantification, chemical assay, etc). The data obtained by each characterization technique, whether chemical, mineralogical, or by microscopy, are often divergent and cannot be used without a cross-interpretation of the results requiring data reconciliation. The objective of this paper is to illustrate how the reconciliation of the data should be performed using chemical assays, X-ray diffraction, and Automated Mineralogy. For this purpose, four samples from an alluvial deposit were analyzed to accurately determine the mineralogy, their stoichiometry, and the elemental department

THE UPPER KAAPVAAL SUBCRATONIC MANTLE: HIGHLY DEPLETED SPINEL HARZBURGITES, WEHRLITES AND WEBSTERITES

Brey Gerhard¹, Shu Qiao², Pearson Graham³, Legros Helene³, Hofer Heidi¹, Heckel Catharina¹, Gerdes Axel¹, Marschall Horst¹

¹Institute of Geosciences, Goethe-Universität Frankfurt, Germany, ²State Key Laboratory of Ore Deposit Geochemistry, Institute of Geochemistry, CAS, Guiyang, State Key Laboratory of Ore Deposit Geochemistry, Institute of Geochemistry, CAS, Guiyang, China, ³Department of Earth and Atmospheric Sciences, University of Alberta, Edmonton, Canada, brey@em.uni-frankfurt.de, shuqiao@mail.gyig.ac.cn; gdpearso@ualberta.ca; hlegros@ualberta.ca; hofer@em.uni-frankfurt.de; checkel@em.uni-frankfurt.de; gerdes@em.uni-frankfurt.de; marschall@em.uni-frankfurt.de

Little work has been done on peridotites from the shallow levels of the Kaapvaal subcratonic mantle (Boyd et al. 1999; Carlson et al. 1999; Gregoire et al. 2005). The results suggest that the spinel harzburgites have several features in common with deeper-seated garnet peridotites: high forsterite contents of olivine (Ol), excess orthopyroxene (Opx) abundances, complex trace element patterns, and overlapping TRD ages. We have collected fifteen spinel harzburgites, three websterites and one composite xenolith (harzburgite+wehrlite) from the Star diamond mine. The tabular, coarse-grained harzburgites consist mainly of Ol and Opx (up to 50 %). Small primary clinopyroxenes (Cpx) are rare or absent (three samples). Spinel occurs in symplectites. One Cpx-bearing harzburgite contains K-feldspar. The websterites of only Opx and Cpx are equal coarse-grained and wehrlite in the composite xenolith consists of Cpx, Opx, Ol and euhedral spinels.

Olivine in all peridotites is homogeneous in major and trace elements with forsterite contents between 92.4 and 93.1. Pyroxenes show ubiquitous exsolutions on the micrometer scale due to cooling from higher temperatures. Pyroxene thermometry, the Fe-Mg_{ol}-cpx partitioning, the Al, Cr, and Ca contents of Ol, and the projection onto the Kaapvaal-craton conductive geothermal gradient of Hasterok and Chapman (2011) yield temperatures between 700–800°C corresponding to depths between 70–90 km. The REE patterns of the pyroxenes are complex and quite diverse. Orthopyroxene from Cpx-free harzburgites has the lowest REE abundances and positive-sloped patterns. A number of coexisting Opx and Cpx have flat V-shaped patterns with somewhat higher overall REE abundances. Pyroxenes from two further harzburgites have negatively sloped REE patterns, the highest overall abundances and in one of the latter negative Eu anomalies because of coexisting K-feldspar. Clinopyroxene and Opx in the three websterites (low Mg-values) have negative- and positive-sloped REE patterns respectively. The pyroxenes in the wehrlite portion of the composite sample have V-shaped patterns like those in their harzburgite part. The PUM-normalized PGE patterns of the harzburgites are in general flat from Os to Ru and increasingly depleted from Pt to Pd. They lie parallel to the 30–40 % partial melting patterns as modeled by Lorand et al. (2008), i.e. the harzburgites are residues of high degrees of partial melting. The TRD ages from nine samples range from 1.73 to 3.18 Ga and are negative for two samples. The ages peak at 2.83 Ga in a frequency diagram. Our new results substantiate earlier findings about the genetic similarities between the upper and the lower part of the Kaapvaal subcratonic mantle. They also show that percolating silicate melts left their traces as websterites and that carbonatitic melts led to the formation of wehrlites.

THE LINK BETWEEN CENTRAL DALMATIAN KARST BAUXITES (CROATIA) AND MIOCENE CLIMATIC OPTIMUM

Brlek Mihovil¹, Gaynor Sean², Mongelli Giovanni³, Bauluz Blanca⁴, Sinisi Rosa³, Brčić Vlatko¹, Peytcheva Irena⁵, Mišur Ivan¹, Tapster Simon⁶, Trinajstić Nina¹, Laita Elisa⁴, Yuste Alfonso⁴, Allard Thierry⁷, Mathian Maximilien⁸, Šuica Sanja⁹, Grizelj Anita¹, Kukoč Duje¹, Schaltegger Urs²

¹Department of Geology, Croatian Geological Survey, Croatia, ²Department of Earth Sciences, University of Geneva, Switzerland, ³Department of Sciences, University of Basilicata, Italy, ⁴IUCA-Departamento de Ciencias de la Tierra, Universidad de Zaragoza, Spain, ⁵Geological Institute, Bulgarian Academy of Sciences, Bulgaria, ⁶Geochronology and Tracers Facility, British Geological Survey, United Kingdom, ⁷IMPMC, Université Pierre et Marie Curie, France, ⁸Institut des Sciences Exactes et Appliquées, Université de la Nouvelle-Calédonie, New Caledonia, ⁹Rock and Fluid Analysis, INA-Industrija nafte, d.d., Croatia

The Miocene Climatic Optimum (MCO) represents a global warm period from approximately 17.0 to 14.7 Ma, which interrupted a period of long-term Cenozoic cooling. Continental paleoclimate records for the MCO vary in quality and global coverage, and due to the unique formation conditions for bauxites, they may serve as an excellent constraint of local climate during this period. In order to elucidate if the MCO promoted the establishment of a wet and warm climate allowing the formation of bauxites in southeastern mid-latitude Europe, we studied a section of previously undated massive karst bauxite (Crveni Klanac, CK) in central Dalmatia, Croatia, hosted in Upper Cretaceous limestones and overlain by Miocene Sinj Basin lacustrine deposits. Integrated mineralogical, morphological, and geochemical analyses indicate the predominant mineral phases of the homogenous bauxite matrix are authigenic, subhedral to euhedral kaolinite, and gibbsite. The in situ mineralization as a consequence of pedogenic processes indicates that the CK bauxites formed autochthonously. In situ U-Pb zircon ages of the lower, middle and upper stratigraphy of the CK bauxite are similar, dominated by Miocene and Oligocene ages, indicating they share similar protolith(s). Subsequent high-precision chemical abrasion-isotope dilution-thermal ionization mass spectrometry analyses indicate a maximum depositional age for bauxite parent material of 16.9576 ± 0.021 Ma. This maximum age of autochthonous bauxitization coincides with the onset of the MCO, and additional stratigraphic geochronological constraints limit the duration of bauxitization to less than approximately 700 ka. In order for in-situ bauxitization to have occurred in southeastern parts of the mid-latitude continental European areas, paleoclimatic and paleoenvironmental conditions must have had mean annual temperature greater than 17–22°C and mean annual precipitation of more than 1100–1200 mm (literature data). Therefore, the CK autochthonous bauxites provide an independent climatic constraint, and serve as a novel example of using bauxite deposits for high precision paleoclimate constraints.

CARBON AND SULPHUR ISOTOPE CHARACTERIZATION OF EAST VARDAR OPHIOLITE OF NORTH MACEDONIA

Brombin Valentina¹, Barbero Edoardo¹, Saccani Emilio¹, Lepitkova Sonja², Milevski Ivica³, Ristovski Igor⁴, Milcov Igor⁴, Bianchini Gianluca¹

¹Department of Physics and Earth Science, University of Ferrara, Italy, ²Department for Petrology, Mineralogy and Geochemistry, Goce Delcev University of Štip, Macedonia, The Former Yugoslav Republic of, ³Department of Geography, Faculty of Natural Sciences and Mathematics, Ss. Cyril and Methodius University in Skopje, Macedonia, The Former Yugoslav Republic of, ⁴GAYA-CER Non-Governmental Organization, Skopje, Macedonia, The Former Yugoslav Republic of

The central Balkans host several ophiolites formed in response to the long-lasting tectono-magmatic evolution of the Mesozoic Tethys and emplaced as a consequence of the convergence between Africa and Europe. The central part of North Macedonia comprises the Eastern Vardar Ophiolitic Units, which are interpreted as the remnants of the Tethyan Vardar Ocean. These ophiolites consist of basic magmatic sequences (pillow basalts, sheeted dykes, and gabbros), associated with intermediate and acid magmatic intrusions showing the subduction-related affinity and locally bearing adakitic signature (Božović et al., 2013). To give new insights on these ophiolites, new samples were collected within the framework of CEI-KEP project (Ref. No. 1206.006-19) titled “Promoting geological, ecological and cultural heritage through sustainable development and creation of geo-parks”. The rocks were sampled in the Lipkovo and Demir Kapija localities, in the northern and southern part of North Macedonia, respectively.

Three groups of rocks are distinguished on the basis of whole-rock major and trace element composition and major element composition of clinopyroxene. Group 1 is characterized by tholeiitic basalts from Demir Kapija that exhibit slight enrichments in light Rare Earth Element (LREE) and slight negative Nb anomaly. These features are comparable with those of backarc basin basalts. Groups 2 and 3 are represented by calc-alkaline rocks, showing typical subduction-related chemical affinity, as exemplified by N-MORB normalized spider diagrams showing typical Nb and Ta and, locally, P and Ti, negative anomalies along with Th-U positive anomalies. Group 2 rocks, which are from Demir Kapija, exhibit a weak adakitic affinity, as they are characterized by high LREE/HREE fractionation, high Sr/Y and La/Yb ratios.

Additional insights were provided by $\delta^{13}\text{C}$ and $\delta^{34}\text{S}$ analyses. Group 2 and 3 rocks show more pronounced negative $\delta^{13}\text{C}$ (-22‰ to -18‰) and positive $\delta^{34}\text{S}$ (+2.3‰ to +4.9‰) values compared to those of Group 1 rocks ($\delta^{13}\text{C}$: -16‰ to -10‰; $\delta^{34}\text{S}$: +0.7‰ to +2.4‰), suggesting that Group 2 and 3 rocks record comparatively higher metasomatic interaction of their mantle sources with slab-derived components. Based on these preliminary data, we proposed that carbon and sulfur isotopes could be used as additional tracers for distinguishing various ophiolite affinities. Further investigations are required for better constraining the meaning of these isotopic signatures.

References

Bozović M. et al. 2013. The Demir Kapja Ophiolite, Macedonia (FYROM): a snapshot of subduction initiation within a back-arc. *J. Pet.*, 54, 1427-1453.

POSSIBILITY OF FAVORING POLLUCITE OVER CAS IN THE THERMAL TRANSFORMATION OF Cs-CLINOPTILOLITE

Brundu Antonio¹, Cerri Guido²

¹Department of Architecture, Design and Urban Planning, Sassari University, Italy, ²Department of Architecture, Design and Urban Planning, Sassari University, Italy

Cs-clinoptilolite transforms by heating to CsAlSi₅O₁₂ (CAS) and subordinate CsAlSi₂O₆ (pollucite). These phases can nucleate, but in lower amounts, also from (Cs,NH₄)-clinoptilolite, however, the high Si/Al ratio of clinoptilolite always favors the formation of CAS over pollucite.

By heating mixtures made with Cs-clinoptilolite and some Al₂O₃-based materials, this research investigated the possibility to modify the solid-state transformation of Cs-clinoptilolite, trying to favor the nucleation of pollucite over CAS.

A powder containing ≈90% of clinoptilolite was obtained by authogenous comminution, dry sieving, and separation in the water of a rock sampled in Sardinia, Italy. Two series of cation exchanges were performed, with NaCl and CsCl solutions, to get Cs-clinoptilolite. Three powders containing Al₂O₃ were considered: corundum, gibbsite, and “L”, an amorphous form of Al(OH)₃. The starting materials were characterized by TG-DTA (TA Instrument SDT Q600) and XRD (Bruker D2 PHASER), then several bi-component mixtures were prepared and heated up to 1300°C using the thermal analyzer. Phases in the fired products were identified by XRD. Some mixtures were prepared by pre-heating one or both components. In some cases, the effect of a second firing was evaluated, as well as that of two different cooling rates.

Corundum did not react with Cs-clinoptilolite, which turned into CAS, amorphous, and traces of pollucite. Mixtures containing gibbsite gave analogous outcomes, as gibbsite turned into boehmite at 350°C, and subsequently underwent a sequence of transformations into Al₂O₃ polymorphs (γ , β , δ , α) that began prior to the amorphization of Cs-clinoptilolite, which then turned following the ordinary path. Conversely, amorphous Al(OH)₃ reacted with the zeolite, giving rise to evident nucleation of pollucite for concentrations of L in the mixture between 20-84%. CAS was detected in all products except for L=84%, with XRD peaks decreasing in intensity with L increase. All fired products contained, besides amorphous, Al₂O₃ polymorphs (mainly α). Sometimes metastable phases (a Cs-silicoaluminate; rarely Cs-aluminates for L≥70%) were observed after a fast cooling but disappeared with a second treatment (even when followed by another rapid cooling).

As a rule, regardless of the Al₂O₃-based material used, preheating of one component (or both) of the mixture did not bring advantages in terms of pollucite crystallization. In particular, pre-amorphization of Cs-clinoptilolite generally seemed to favor the nucleation of CAS.

Unlike corundum and gibbsite, L is amorphous up to 745°C, hence more reactive. Moreover, its dehydroxylation at 745-820°C might have contributed to an early Cs-clinoptilolite breakdown so favoring the reaction between the components, and this led to enhance pollucite nucleation.

Further experiments with the most promising mixtures will be carried out using a muffle furnace, then determining the quantitative composition of the fired products.

SPECTRAL VNIR PROPERTIES OF OXIDE SPINELS: A POSSIBLE TOOL TO REMOTELY CONSTRAIN THE PETROLOGY OF PLANETARY BODIES?

Bruschini Enrico¹, Carli Cristian¹, Borgognone Costanza², Andreozzi Giovanni Battista²

¹IAPS, INAF, Italy, ²Earth Sciences, Sapienza University of Rome, Italy

Spinels are usually found as accessory minerals in a wide variety of terrestrial and extraterrestrial rocks. Very often they are accompanied by other mafic minerals like pyroxenes and olivines crystallized under the same pressure-temperature-oxygen fugacity (P-T-fO₂) conditions. During the last decades, many oxy-thermobarometer equilibria based on the paragenetic assemblages of spinels and olivine/pyroxenes have been developed and tested in many terrestrial rocks and meteorites. The possibility to retrieve the abundance and chemical composition (X) of spinels associated with other mafic minerals from remotely acquired data of planetary bodies would allow a huge step forward in the exploitation of such equilibria and in the comprehension of the formation and evolution of our Solar System. However, to date the systematic investigation of the reflectance spectral features of spinels, especially when associated with silicates, is scarce. Given spinel's low abundance in extraterrestrial rocks, it is commonly assumed that it has a negligible effect on the spectral properties of rocks, but no systematic data support this assumption. Actually, considering that some reflectance absorptions attributable to spinels are around 1 and 2 mm, their presence could affect the spectral indicators used to identify olivine, pyroxene, and their relative abundance. In this work, we analyzed the VNIR reflectance properties of a suite of synthetic spinels to define their spectral features as a function of chemical composition and cation distribution. Our samples encompass a wide range of chemical compositions broadly described with the general formula (Mg, Fe²⁺, Fe³⁺, Al)(Cr³⁺, Al, Fe²⁺, Fe³⁺, Ti)₂O₄. All the investigated samples have been previously characterized in order to assess their exact chemistry and cation distribution. Our systematic work will increase our knowledge of the spectral properties of spinels, which then will allow assessing their influence on the remotely acquired spectra of planetary bodies.

FIRST LOOK ON SUBDUCTION EVENT(S?) RECORD FROM OROGENIC ULTRAMAFICS OF THE SEVE NAPPE COMPLEX IN THE SCANDINAVIAN CALEDONIDES, NORTHERN JÄMTLAND, SWEDEN

Buczko Daniel¹, Matusiak-Małek Magdalena², Majka Jarosław³, Klonowska Iwona⁴, Ziemniak Grzegorz²

¹University of Wrocław, Poland, ²Institute of Geological Sciences, University of Wrocław, Poland, ³Department of Earth Sciences, Uppsala University, Sweden, ⁴Faculty of Geology, Geophysics and Environmental Protection, AGH University of Science and Technology, Poland

The central segment of the Scandinavian Caledonides is abundant in outcrops of orogenic ultramafic bodies. This study focuses on ultramafic rocks from the Seve Nappe Complex (SNC) in the northern part of Swedish Jämtland county, representing the hypothetical outermost margin of Baltica.

The studied bodies of ultramafics range in size from meters to kilometers and consist predominantly of peridotites of spinel and garnet facies. The studied rocks are locally affected by serpentinization and/or recrystallization; degrees of serpentinization recorded in a single ultramafic may vary. Based on textural and chemical observations the ultramafics were divided into two main groups:

Group 1 is represented by Spl-peridotites recording a wide range of serpentinization (subgroup A) to recrystallization processes (subgroup B). Heavily serpentinized peridotites consist of Ol+Opx+Spl+Srp, with relicts of Ol and Opx having Mg# (Fo)=90.6-92 and Mg#=90.5-91.5, respectively. The recrystallized ultramafics consist of Ol+Tr+Chl+Spl±Opx; recrystallized Ol and Opx show higher Mg# ranging from 93.4 to 95.3 and from 93.2 to 94.8, respectively. For this subgroup, 120° triple-point boundaries in Ol and growth of metamorphic Chl close to grain boundaries are common. Similar features of Spl ultramafic rocks within the SNC were also described in [1].

Group 2 consists of Grt and Spl facies ultramafics with metamorphic phases. The Spl peridotites contain Ol+Tr+Chl+Spl+Opx, with Ol and Opx having Mg#=90.0-91.7 and 89.9-90.9, respectively. Locally, 120° triple-point boundaries in Ol appear. The Grt peridotites consist of Ol+Opx+Cpx+Grt+Spl+Prg. Ol Mg# values (90.3-92.0) are similar to Spl ultramafics, while Opx and Cpx show higher Mg# values (90.4-92.5 and 94.7-96.7, respectively). Garnet (Prp69-60, Alm25-16) has Cr#=0.5-4.0 and is often overgrown by Prg. The chemical composition of Ol in both Spl and Grt ultramafics of this group tends to show a correlation between different samples.

Group 1 ultramafic rocks are interpreted to be an effect of deserpentinization process, which took place in a subduction setting. The origin of the serpentinized "protolith" can be either related to ultramafic bodies exhumation due to (hyper-)extension of continental margin during Rodinia breakup, minor collisional event(s) during Caledonian Wilson cycle, or to obduction from serpentinized mantle wedge.

In Group 2, prograde metamorphism within the Spl facies peridotites (triple-point junctions in Ol, occurrence of Chl) also suggests subduction of ultramafic bodies. Thus, the evolution of the rocks may comprise obduction of fragments of non-serpentinized mantle wedge by subducting plate. A similar solution is proposed for the Grt facies peridotites in [2] and [3], where Grt is considered as entirely metamorphic. The chemical continuum between the Spl and Grt facies within Group 2 hints towards the possible common origin of both lithologies. Such observation may imply that obducted Spl-facies fragments of mantle wedge could have been subducted into Grt stability field.

Founded by Polish National Science Centre grant no. 2019/35/N/ST10/00519.

[1] Clos et al. (2014). *Lithos* 192-195, 8-20.

[2] Gilio et al. (2015). *Lithos* 230, 1-16.

[3] Klonowska et al. (2016). *J. Metamorph. Geol.* 34(2), 103-119.

LA-ICPMS, TEM AND RAMAN STUDY OF THE EXPERIMENTALLY ALTERED MONAZITE AT 250-750°C: DISTURBANCE OF U-Pb AND Th-Pb AGES DUE TO FLUID-INDUCED ALTERATION

Budzyń Bartosz¹, Wirth Richard², Sláma Jiří³, Birski Łukasz⁴, Tramm Fabian¹, Kozub-Budzyń Gabriela⁵, Rzepa Grzegorz⁵, Schreiber Anja²

¹Polish Academy of Sciences, Institute of Geological Sciences, Kraków, Poland, ²GeoForschungsZentrum Potsdam (GFZ), Section 3.5 Interface Geochemistry, Potsdam, Germany, ³The Czech Academy of Sciences, Institute of Geology, Prague, Czech Republic, ⁴Polish Academy of Sciences, Institute of Geological Sciences, Warszawa, Poland, ⁵Faculty of Geology, Geophysics and Environmental Protection, AGH University of Science and Technology, Poland

Radiation damage and disturbance of U-Pb and Th-Pb ages were studied in monazite experimentally metasomatized at 250–750°C (experimental products from Budzyń et al., 2015, *Ann. Soc. Geol. Pol.*; Budzyń et al., 2017, *Miner. Petrol.*). Starting materials included Burnet monazite (ca. 1100 Ma), albite, K-feldspar, biotite, muscovite, SiO₂, CaF₂, Na₂Si₂O₅ and H₂O. Monazite from experiments at 250–550°C is partially replaced by secondary fluorcalciobriholite and REE-rich steacyite, and developed patchy zoning. Monazite from runs at 650 and 750°C is partially replaced by fluorcalciobriholite and cheralite, with no signs of compositional alteration (such as patchy zoning) observed in EPMA-BSE imaging. The Raman data show narrowing of the $\nu_1(\text{PO}_4)$ stretching band in unaltered domains, indicating increasing annealing of monazite structure with increasing temperature, and narrow $\nu_1(\text{PO}_4)$ band in altered domains.

Unaltered domains of monazite from experiments at 250–550°C have mottled diffraction contrast in TEM imaging, similar to the starting Burnet monazite, which indicates a low to moderate degree of metamictization. The altered (patchy) domains are crystalline with no signs of structural disorder. Monazite from the experiment at 650 °C shows a low degree of metamictization in TEM imaging; fluid-aided alteration along the cleavage resulted in the development of nanoporosity and partial replacement by fluorcalciobriholite and cheralite. Monazite from the experiment at 750°C is crystalline with no signs of metamictization; however, demonstrates significant nanoporosity and secondary cheralite nanocrystals formed across the monazite grains.

The unaltered domains of monazite from runs at 250–550°C yielded U-Pb and Th-Pb dates similar to the age of the Burnet monazite, whereas altered domains show various degree of Pb-loss (up to 99.4 %) and discordant dates. Lower intercept ages vary from -266 ± 160 Ma (run 350°C, 200 MPa) to -1 ± 48 Ma (450°C, 800 MPa), corresponding to “the age” of experiments. Monazite from experiments at 650 and 750 °C is affected by initial disturbance of U-Th-Pb system with 8.4% Pb-gain to 18.6% Pb-loss and linear regressions with lower intercepts of -53 ± 420 Ma and -55 ± 610 Ma.

To summarize, fluid-induced alteration processes result in various degree of U-Th-Pb age disturbance in monazite, which age, in nature, can be constrained by isotopic microanalysis. The particularly important case is the fluid-induced alteration of monazite in the submicron scale, which occurs at 650–750°C. These can be unnoticed when using standard microanalytical techniques and, consequently, may lead to significant geochronological misinterpretations.

Acknowledgements: This work was supported by the NCN grant no. 2017/27/B/ST10/00813.

IS THE SUB-CONTINENTAL LITHOSPHERIC MANTLE CAPABLE IN FIXING C AND N? NEW EVIDENCE FROM THE FINERO PHLOGOPITE PERIDOTITE (IVREA-VERBANO ZONE, ITALY)

Cannaò Enrico¹, Tiepolo Massimo¹, Fumagalli Patrizia¹, Grieco Giovanni¹

¹Earth Science Department, University of Milan, Italy

Mechanisms ruling the exchanges and partitioning of carbon (C) and nitrogen (N) between the different Earth's reservoirs are still not completely understood and, in particular, how much C-N are transferred and fixed in the mantle in relation to slab recycling is still matter of debate. In this context, the Finero Phlogopite Peridotite (FPP; Ivrea-Verbano Zone), which is interpreted as a portion of the sub-continental lithospheric mantle (SCLM) metasomatized by subduction-related melts, may represent a key natural laboratory.

In this contribution, we present a detailed study on the total C and N concentrations and the total C isotope composition of the FPP. Potential entrapped volatile species in inclusions were investigated with the micro-Raman technique. Together with these analyses, we provide new in-situ LA-ICP-MS trace element data on rock-forming minerals and in-situ B isotope in amphibole, determined with LA-MC-ICP-MS.

The FPP consists of phlogopite-bearing harzburgites locally showing diopside veins and chromitite lenses enveloped in dunitic channels. A key feature for all the investigated samples is the occurrence of primary and/or pseudo-secondary trails of inclusions of both solid and fluid/gaseous infilling. LA-ICP-MS analyses reveal that all metasomatic minerals have relatively high concentrations of fluid mobile elements (FME; e.g., B, As, Sb, Li, Pb, U) and incompatible elements (e.g., LREE, Th). These enrichments are coupled with high C and N concentrations (up to 680 and 40ppm, respectively) that, according to the micro-Raman investigations, are hosted in the inclusions as graphite, carbonates, and gaseous N₂. The $\delta^{13}\text{C}$ signature of olivine and clinopyroxene (determined by OEA-IRMS) is as low as -22.7‰ that contrasts with the less depleted values characterizing amphibole and phlogopite (up to -12.6‰). The $\delta^{11}\text{B}$ signature of amphibole is $-13.2 \pm 2.4\text{‰}$ (2SDmean, n = 11), dissimilar to the mantle value of $\sim -7.1\text{‰}$.

The enrichment in FME, incompatible elements (e.g., LREE 100 times chondrite values and LaN/LuN up to 42), and C-N support the involvement of a crustal-derived metasomatic agent. Phlogopite/amphibole partition coefficients (Amph/PhlDs) for incompatible elements approach the equilibrium conditions whereas the Amph/CpxDs for REE lie at the upper limit for equilibrium conditions. These evidences suggest a continuum metasomatic process leading to the crystallization of clinopyroxene prior to that of amphibole and phlogopite. The $\delta^{13}\text{C}$ as low as -22.7‰ reported for olivine and clinopyroxene reflects an overprinting of the common C mantle signature with a ¹²C-rich reservoir. The ¹³C-enriched isotope composition of amphibole and phlogopite compared with that of olivine and clinopyroxene fit with a single-stage metasomatic process, a scenario supported by trace element evidence. The negative $\delta^{11}\text{B}$ imprint shown by amphibole requires the involvement of an ¹¹B-depleted reservoir, which is compatible with the residual slab materials at 120km depth in agreement with C isotopic data. Our results show that subducted modified metasomatized SCLM is capable to fix, entrapped in inclusions, significant amounts of C and N and is thus a not negligible reservoir that must be considered in mass balance calculations.

RARE EARTH ELEMENTS (REE) EXTRACTION FROM PHOSPHOGYPSUM BASED ON CIRCULAR ECONOMY PRINCIPLES.

Cánovas Carlos R.¹, Basallote Maria Dolores¹, Macías Francisco¹, Pérez-López Rafael¹

¹Earth Sciences, University of Huelva, Spain

Rare Earth Elements (REEs) are a group of chemically similar metallic elements which are becoming increasingly important in the transition to a green and low carbon economy. The absence of primary deposits in many countries encourages the search of alternative secondary sources of REE. One promising source of REE is the phosphogypsum generated by the fertilizer industry. During the manufacturing of phosphoric acid around 70% of REEs originally contained in the phosphate rock are transferred to solid phosphogypsum. Taking into account the worldwide growing production of phosphogypsum to support the increasing levels of farming production, REE could be recovered to satisfy the needs of raw materials. This route has been extensively explored in the last years, being the hydrometallurgical approach the most commonly followed. However, this approach usually involves the use of high amount of chemicals which may be harmful for the environment. This study evaluates the suitability of using pyrite-rich wastes to enhance the dissolution of REE carrier minerals together with different waste waters from the fertilizer and mining industry.

IN-SITU HIGH TEMPERATURE SYNCHROTRON X-RAY POWDER DIFFRACTION (HT-SXRPD) STUDY OF DOPED ORDINARY PORTLAND CEMENT (OPC) CLINKERING

Cantaluppi Marco¹, Marinoni Nicoletta², Pavese Alessandro³, Cantaluppi Marco¹

¹Università degli Studi di Milano, Italy, ²Earth Science, Università degli Studi di Milano, Italy, ³Earth Science, Università degli Studi di Torino, Italy

The role of minor elements on Ordinary Portland Cement (OPC) clinkering is one of the most challenging phenomena at an industrial scale, foremost for their impact on final cement technical performances. A vast literature is available on the effects individually induced by each minor element, whereas only a few studies reported the effects due to the combination of several elements, and even fewer explored the related potentiality by in-situ non-ambient experiments at large scale facilities.

The present research aims to investigate the impact of a complex mixture of minor elements addition on OPC clinker: in particular, CaCl₂ was added on SO₃, MgO, Na₂O-doped industrial OPC clinker kiln feeds and its effects on the OPC clinkering upon heating have been studied. High-Temperature Synchrotron X-Ray Powder Diffraction (HT-SXRPD) data and the Rietveld method are here used to determine accurate phase compositions as a function of temperature, and thereby to investigate the clinkering reactions occurring in the samples doped with the mentioned minor elements. The distribution of dopants in the crystal structures of the main clinker phases, as well as the microstructures occurring in the OPC clinker, were determined by means of an Electron Probe Micro-Analyser.

Upon clinkering, all the doped samples exhibit a lower temperature of first liquid phase appearance and a higher liquid phase content respected to OPC; conversely, large differences in the reactivity and phase composition are detected after quenching. In terms of clinker mineralogical composition, dopants dramatically affect mainly the polymorphism of calcium silicate (C3S and C2S), which change the hydration reactivity; chlorine doping boosts the formation of mayenite and stabilize β-C2S, M1-C3S, and cubic C3A. Moreover, differences are also observed in terms of doped clinker microstructures (grain size of calcium silicates and interstitial phase spatial distribution).

A REDISCOVERED COLLECTION: PRELIMINARY STUDIES OF THE METAL OBJECTS OF THE ASCANIO FILOMARINO COLLECTION (1794)

Cappelletti Piergiulio¹, Pellino Annamaria², Petti Carmela³, Balassone Giuseppina², Langella Alessio², Mercurio Mariano⁴, Rispoli Concetta²

¹Federico II University, Italy, ²DiSTAR, Federico II University, Italy, ³Centro Musei delle Scienze Naturali e Fisiche, Federico II University, Italy, ⁴Dipartimento di Scienze e Tecnologie, Università del Sannio, Italy

This study reports the results of a preliminary investigation on metal objects preserved in the Real Museo Mineralogico of the University of Naples (Italy). In July 1847 Arcangelo Scacchi, Director of the museum (1844-1892), acquired 132 objects from the private collection of the noble Ascanio Filomarino, duke della Torre (1751-1799), a distinguished Neapolitan naturalist, volcanologist, and fine collector. Keen on the Vesuvius, Filomarino set up in his palace a valuable scientific cabinet dedicated to the volcano. During the popular turmoil of the Neapolitan revolution of 1799, he was killed by rioters and his precious collection was destroyed. All the objects were found in Torre del Greco, a small town near Vesuvius volcano (southern Italy), by the English mineralogist William Thomson (1761 -1806). They had been buried by the lava of the 1794 Vesuvius eruption and found, after a few years, during the reconstruction of the city. The collection has a historical value, representing probably the only testimony of the vast collection of Ascanio Filomarino. The collection is composed of everyday metal objects such as pieces of iron bars, a brass bell, a little iron anchor and hook, a piece of a harquebus with a calcinated flint, several different pieces of brass, copper, and iron objects, and a bunch of carbonized grapes. All these artifacts appear partly or entirely mineralized. Scacchi gave a brief macroscopic description of the type of objects and described their mineralization as composed of hematite, limonite, and copper oxide. The preliminary SEM-EDS analysis (Jeol JSM 5310 coupled with EDS Oxford Inca X-act), carried out on twenty samples of the collection, shows great variability in the type of mineralization. Iron objects appear strongly mineralized with the presence mostly of hematite (Fe₂O₃), goethite (α -Fe³⁺O(OH)), pyrite (FeS₂). In several of these samples an iron chloride, molysite (FeCl₃), and a K-Fe sulfate, possibly jarosite [KFe³⁺₃(SO₄)₂(OH)₆] have also been observed and are still under investigation. Most of the copper or copper alloy objects present common Cu oxides (tenorite, CuO, and cuprite, Cu₂O), sulfides (covellite, CuS), halides (atacamite, Cu₂(OH)₃Cl), and sulfates (chalcocyanite, CuSO₄) as crusts and patinas. Analyses of the metals show that some objects have been misinterpreted; several samples that had been classified as brass are constituted by a Cu-Sn alloy (probably bronze). FT-IR, XRD, and XRF analyses are ongoing to determine the composition of the alloys and the alteration patinas, with the final aim of providing a correct exhibition of the findings in the Museum.

CHARACTERIZATION OF AL HUWAYSAH 010 UNGROUPED ACHONDRITE

Carli Cristian¹, Barbaro Anna², Murri Mara³, Domeneghetti Maria Chiara², Langone Antonio⁴, Bruschini Enrico¹, Alvaro Matteo², Stefani Stefania¹, Cuppone Tiberio⁵, Casalini Martina⁵, Moggi Cecchi Vanni⁶, Migliorini Alessandra¹, Roush Ted L.⁷, Pratesi Giovanni⁵

¹IAPS, INAF, Italy, ²Department of Earth and Environmental Sciences, University of Pavia, Italy, ³Department of Earth and Environmental Sciences, University of Milano-Bicocca, Italy, ⁴IGG, CNR, Italy, ⁵Department of Earth Science, University of Florence, Italy, ⁶Natural Historical Museum, University of Florence, Italy, ⁷AMES, NASA, United States

The existence of ungrouped meteorites reflects the complexity in placing these specimens in a correct interpretative framework. The issue is not only a taxonomic problem but also genetic. The problem is even more relevant when it comes to achondrites. These meteorites, in fact, experience a series of very complex processes ranging from partial differentiation to complete fusion. It is therefore very important to focus our attention on ungrouped achondrites. In this work, we have investigated the meteorite Al Huwaysah 010. This meteorite has been studied, using Scanning Electron Microscopy, Electron Probe Microanalysis, Reflectance Spectroscopy, micro-X-ray diffraction, and Laser-Ablation inductively coupled plasma Mass Spectrometry, to obtain new constraints about this ungrouped achondrite and try to associate it with a parent body family.

Al Huwaysah 010 is characterized by high olivine abundance (80 vol%), high-Ca pyroxene (6 vol%), low-Ca orthopyroxene (4 vol%), plagioclase (3 vol%), chromite (3 vol%), and other than weathering products (4 vol%) including iron oxides and oxyhydroxides, Ca-sulphates and Ca-Mg carbonates. It is worth mentioning the presence of a tiny plate of graphite along with a possible occurrence of oldhamite.

Mineral phases show compositionally homogenous olivine with $Fo_{83.3}$ and a low Fe/Mn ratio of 29.3, whereas the high-Ca pyroxene, occurring as subhedral and anhedral crystals, has an augitic composition ($En_{45.5}Fs_{10.8}Wo_{43.7}$) and a Mg# of 80.2. The orthopyroxene occurs only in a fine-intergrowth with a composition of $En_{85.5}Fs_{13.9}Wo_{0.7}$ and a Mg#85.6. Both pyroxenes are homogenous without any compositional zonation. The plagioclase has a homogenous composition of An48. Other phases are spinel, chromite, and accessories like iron grains (Ni-free or Cr-bearing Fe-Ni alloy), troilite, chlorapatite, pentlandite (as inclusion in chromite), and graphite. Moreover, iron oxides, iron oxyhydroxides, calcium sulfate (gypsum), and dolomite are present in the sample, likely resulting from significant terrestrial weathering of the meteorite. Olivine-chromite intercrystalline and pyroxene-based intracrystalline geothermometers yielded temperatures of $864 \pm 42^\circ C$ and $520 \pm 30^\circ C$ respectively.

This work also presents the reflectance spectra obtained on Al Huwaysah 010 ungrouped achondrites in the range of VNIR and Mid-IR. The spectral properties provide evidence of the mafic mineralogy, and the low VNIR spectral reflectance is consistent with the presence of opaque phases like chromite, fine graphite, and metals. Although we can recognize the presence of olivine from VNIR spectra, comparing the spectral parameters to potential parent bodies characterized by olivine-pyroxene mineralogies it falls within the field of the SIII type below the olivine-orthopyroxene line.

The obtained characterization allows us to suggest for this ungrouped achondrite a classification as the most reduced of the brachinites.

Acknowledgments: Authors thank the financial contribution from the agreement ASI-INAF n.2018-16-HH.0 OI-BODIES project.

Keynote

EVIDENCE FOR FLUIDS DURING ANATEXIS OF THE DEEP CRUST: ARE WE LOOKING RIGHT?

Carvalho Bruna B.¹

¹Università degli studi di Padova, Italy

Predominant fluid-absent melting of the lower crust is a widely accepted concept mainly because of the lower porosity of rocks at high depths, the H₂O-undersaturated character of granites, and uncertainties on the origin and mobility of fluids at such deep levels. Yet, recently more and more works with diverse approaches provide strong new evidence that challenges such a view.

The presence of high-density monophase carbonic fluid inclusions in high-grade metamorphic rocks remains as the main advocate of the active role of fluids in the deep crust, though inconsistencies on the timing of entrapment of such inclusions relative to metamorphic peak conditions still hamper the acceptance of volatiles as essential constituents of the lower continental crust.

A study of three world-renowned high- to ultra-high temperature granulite terranes [Carvalho et al., 2020, EPSL 536, 116170] investigated clearly primary fluid inclusions coexisting with former melt inclusions in peritectic garnet to assess the fate of fluid inclusions in these metamorphic terranes. A combination of classical and cutting-edge techniques revealed that those primary fluid inclusions are actually multiphase, composed of fluid and aggregates of solids. In the fluid phase, CO₂ is the most common component and no free H₂O has been detected. Methane and N₂ are also present in some samples. The solids comprise siderite, ferroan magnesite, pyrophyllite, calcite, and in some cases kaolinite, corundum, quartz, dolomite, biotite, and muscovite. Phase equilibria modeling of the system fluid-host garnet after entrapment at peak conditions demonstrates that during cooling the CO₂-bearing fluid and garnet interact to form metastable assemblages, similar to those found in the natural multiphase FI. These results show that unmodified monophase fluid inclusions in garnet previously reported in the literature are likely secondary, retrograde features and that only primary multiphase fluid inclusions in peritectic garnet are reliable witnesses of fluids operating during deep crustal metamorphism.

Careful examination of the literature shows that there are more than twenty-five locations worldwide where multiphase FI have been reported, this means that fluid-present conditions in the lower crust may be a more common scenario than expected during the formation of granitic magmas. Thus, a new reassessment of the evidence and role of fluids is vital for a complete comprehension of processes that rule the deep portions of the continental crust.

DISTRIBUTION OF CO₂ IN THE NORTHERN VICTORIA LAND (ANTARCTICA) SCLM AS REVEALED BY PETROLOGY, FLUID INCLUSIONS CHEMISTRY AND X-RAY MCT IN MANTLE XENOLITHS

Casetta Federico¹, Rizzo Andrea Luca², Faccini Barbara¹, Ntaflos Theodoros³, Lanzafame Gabriele⁴, Faccincani Luca¹, Mancini Lucia⁵, Giacomoni Pier Paolo¹, Coltorti Massimo¹

¹Department of Physics and Earth Sciences, University of Ferrara, Italy, ²Sezione di Palermo, Istituto Nazionale di Geofisica e Vulcanologia, Italy, ³Department of Lithospheric Research, University of Vienna, Austria, ⁴Department of Biological, Geological and Environmental Sciences, University of Catania, Italy, ⁵Elettra-Sincrotrone Trieste S.C.p.A., Italy

Understanding the carbon cycle in the Earth's deepest reservoirs, which may contain >90% of terrestrial C, is crucial for modeling the evolution of our planet. Indeed, large-scale geodynamic processes are intimately related to the storage and mobility of volatiles in the mantle, where C-O-H species act as driving forces of melt extraction, metasomatism, and refertilization processes. In the last few years, the combined application of petrology, fluid inclusions (FI) geochemistry, and high-resolution imaging techniques to mantle xenoliths have become an increasingly effective tool for exploring the carbon cycle in the deep Earth, and especially in the Sub-Continental Lithospheric Mantle (SCLM).

In this work, the extent and modality of C storage into depleted and fertile (or refertilized) SCLM portions was modeled through the investigation of modally and/or chemically heterogeneous ultramafic xenoliths brought to the surface by the Cenozoic rift-related magmatism in northern Victoria Land (Antarctica). This was done by combining measurements of CO₂ released from bulk-rock- and single-phase- (olivine, orthopyroxene, clinopyroxene, and amphibole) hosted FI with mineral chemistry and 3D textural/volumetric characterizations of intra- and inter-granular microstructures performed by X-Ray computed microtomography (μ CT).

Although heterogeneously distributed among the different xenoliths populations, FI are generally numerous in both olivine and pyroxenes, especially in association with inter-granular reaction zones, to which they are sometimes related. In most of the samples, olivine resulted the CO₂-poorest phase, being capable of storing between 0 and 39 μ g(CO₂)/g(sample). The highest CO₂ amounts (up to 187.3 μ g(CO₂)/g(sample)) were released from amphibole- and pyroxene-hosted FI. A comparison between the amounts of CO₂ released from FI hosted in bulk-rock and those retained in mineral-hosted FI was performed to quantify eventual CO₂ unbalances, and in turn, relate them to the volumetric abundance of melt/fluid components identified by X-Ray μ CT. This latter technique enabled us to isolate and quantify the abundance and connectivity density of melt/fluid components, which have tetrahedral to prismatic shape and size comprised between 2 and 50 μ m, as well as to distinguish between them and the network of small-scaled secondary fractures.

Complemented by mineral chemistry data and T-fO₂ estimates, these results were used to i) model the storage and distribution of carbon in intragranular and intergranular zones in peridotite xenoliths; ii) relate the mobility of CO₂ to the partial melting and metasomatic processes that took place in the SCLM beneath Antarctica; and iii) understand the role played by intragranular and intergranular fluids during melt extraction and enrichment events.

Keynote

FIRE AS A TOOL" - THE EARLY STAGE OF PYROTECHNOLOGY IN ARTIFICIAL HEMATITE PRODUCTION

Cavallo Giovanni¹

¹Dept. Environment Construction Design, Institute of Materials and Constructions, University of Applied Sciences and Arts of Southern Switzerland, Switzerland

Pyrotechnology is connected with cognitive capacities of early humans. The intentional use of fire technology for transforming goethite-rich minerals into hematite can be considered an important human achievement. This technological process has been scientifically evidenced in several Prehistoric sites combining mineralogical (X-ray powder diffraction; XRPD) and micro-structural (Transmission electron microscopy; TEM) analysis. The possibility to explore the production of artificial hematite in the temperature range 250-800 °C using XRPD has been confirmed in experimental and archaeological case studies by the evidence of anisotropic peak broadening, crystal size and modification of I_{104}/I_{110} ratio. In addition, TEM provided important insights into the porosity and crystal morphology resulting particularly sensitive for evidencing the temperatures reached during the heating process.

PATTERNS FROM FLUID-MEDIATED ROCK TRANSFORMATIONS IN DIAGENETIC CONDITIONS: A RELATIONSHIP BETWEEN ADVECTION-DRIVEN REACTION, ORE DEPOSIT AND POROSITY VARIATION

Centrella Stephen¹, Beaudoin Nicolas E.¹, Koehn Daniel², Motte Geoffrey¹, Hoareau Guilhem¹, Callot Jean-Paul¹

¹Universite de Pau et Adour, E2S UPPA, CNRS, TOTAL, LFCR, Pau, France, France, ²GeoZentrum Nordbayern, University Erlangen-Nuremberg, Germany

Hydrothermal dolomitization is an important diagenetic process that occurs in tectonic environments worldwide and forms conventional reservoirs associated with ore deposits and hydrocarbon accumulation, while forming efficient reservoirs for carbon sequestration. To better understand this widespread phenomenon, it is essential to recognize the governing and limiting transport mode of the dolomitizing fluid. An extensive analytical study of well-preserved dolomitization interfaces observed at the outcrop scale in the Layens anticline (north-western Pyrenees, France) is presented. By coupling different analytical techniques (SEM, EPMA, EBSD, fs-LA-ICP-MS, X-Ray μ CT), it appears that the replacement of calcite by dolomite led to a mass loss without volume change, through the generation of ca 11 vol.% porosity. Fluid infiltrates the host rock by advection in the grain boundary network causing at the same time the replacement of calcite and the mobilization of ore deposit (Centrella et al., 2020).

Modelization of such fluid allows us to better understand the governing transport mode (advection and diffusion). Using the 'ELLE' modeling toolbox, numerical simulations can be made to test the role of advection/diffusion ratio on the pre-existing structure before fluid infiltration to reproduce natural microstructure such as contact roughness between minerals and/or rocks. This was applied to hydrothermal dolomite breccia (HDB) in the north-western Pyrenees. This process is often associated with ore deposits and usually interpreted as related to hydro-fracturing, considered as univocal markers of fluid overpressure. Detailed study coupling EBSD and surface analyses show that the rough contacts between the dolomite crystals and an initial sedimentary breccia structure along with the different distribution of both clasts and oxide particles, lead us to propose that the HDB results from texturally controlled, hydrothermal fluid-initiated recrystallization of the initial sedimentary breccia. Simulations confirm that the temperature gradient related to fluid advection locally triggers grain boundary migration that replaces the texture of initial breccia while preserving large, impermeable cold fragments. This transferable model raises the question about the usual interpretation of HDB as pinpointing episodes of fluid overpressure in carbonates (Centrella et al. accepted).

References

Centrella, S. et al., 2020. Micro-scale chemical and physical patterns in an interface of hydrothermal dolomitization reveals the governing transport mechanisms in nature: case of the Layens anticline, Pyrenees, France. *Sedimentology*.
Centrella et al., accepted. How fluid-mediated rock transformations create hydrothermal dolomite breccias without fluid overpressure.

SORPTION CAPACITY OF NATURAL ZEOLITE AGAINST DIFFERENT MOLECULES SIZE OF POLYCYCLIC AROMATIC HYDROCARBONS (PAHs)

Chaber Paulina¹, Gworek Barbara¹

¹ Institute of Environmental Protection – National Research Institute, Krucza 5/11D str., 00-548 Warsaw, Poland, paulina.chaber@ios.edu.pl, barbara.gworek@ios.edu.pl.

The U.S. Environmental Protection Agency distinguishes 16 PAHs and classifies them as highly toxic and hazardous to health because of their mutagenic and carcinogenic properties and also being very resistant to degradation, especially compounds with a high number of aromatic rings (4 rings or more) in their molecule. The reduction of polycyclic aromatic hydrocarbons (PAHs) is one of the major problems because they are present in the environment are harmful to humans but also the ecosystem. Natural zeolite can be useful to separate harmful organic substances from water and wastewaters because of its high adsorption capacity and high surface area. It is also easily available and inexpensive adsorbent. The sorption properties of natural zeolites to selectively sorb molecules are well known. This study aims to evaluate the sorption capacity of natural zeolites towards PAHs with different numbers of rings in their molecule.

The series of experiments were performed in glass beakers at room temperature. The water solutions were fortified with a mixture of PAHs from the US EPA priority pollutant list. The PAHs mixture solutions contained the sum of 2 rings PAHs, 3 rings PAHs, 4 rings PAHs, 5 rings PAHs, 6 rings PAHs and Σ 16PAHs. The 50 g natural zeolites (Ca – K ground natural zeolite containing about 60% of clinoptilolite with the size of grain from 0.5 to 1.0 mm) were added to each fortified water solution. After a 1h time, the zeolite was separated from the solution. Both the solution and zeolite were analyzed on the content of PAHs by High Performers Liquid Chromatography (HPLC).

After the experiment, the concentration of Σ 16PAHs in solution significantly decreased by about 70%. The concentration of 4 and 5 rings compounds decrease average by 60% and 3 and 4 rings compounds by 50%. The 2 rings compounds decrease only by 30% - 40%. The highest content of PAHs in zeolite was for 4, 5 and, 6 ring PAHs. The content of 2 and 3 rings PAHs was at least twice lower. Scanning electron microscope (SEM) image of natural zeolite before and after the experiment did not show changes in its structure therefore it can be concluded that PAHs were adsorbed on the surface of the zeolite. Regardless of the number of benzene rings in the molecule of PAHs, the best-adsorbed compound was dibenzo(a,h)anthracene (decreased by an average of 86%) followed by indeno[123-cd]pyrene (70%) and benzo[b]fluoranthene and benzo[k]fluoranthene (65%). This shows that compounds with chain structures were adsorbed much better than compounds with cluster structures..

NON-CONVENTIONAL ELEMENT TRANSPORT IN GARNET SINGLE CRYSTALS

Chakraborty Sumit¹

¹Institut fuer Geologie Mineralogie und Geophysik, Ruhr Universitaet Bochum, Germany

Diffusion couples made of two gem-quality single crystals are typically used for measuring diffusion coefficients. Polished faces of crystals are placed in contact with each other and the couple is annealed at high temperatures and sometimes, high pressures. The resulting concentration gradients are measured and modeled to yield diffusion coefficients. Significantly, the measured concentration distributions conform to those expected from diffusion models (concentration fronts propagate parallel to the interface and the profile shapes are consistent with those expected from solutions to the diffusion equation). Such experiments have been carried out successfully with garnets, for example, with almandine – pyrope (e.g. Ganguly et al., *Contrib. Mineral. Petrol.*, 1998, 131: 171-180) and almandine – spessartine diffusion couples (e.g. Chakraborty and Ganguly, *Contrib. Mineral. Petrol.*, 1992, 111: 74-86). However, when analogous experiments are carried out with pyrope-spessartine or pyrope-grossularite diffusion couples a very different and novel behavior is observed. The single crystals remain intact and unreacted, but the concentration front in the diffusion zone forms irregular wave-like features and the profile shapes have oscillations unlike those expected from solutions of diffusion equations. These concentration distributions also do not correspond to those expected due to uphill diffusion. Tentatively, such behavior may be rationalized as the result of the novel transport mechanism recently found by Beyer and Chakraborty, *Amer. Mineral.*, in press. Further studies are in progress to characterize the transport behavior more fully.

SUPERHYDROUS HEMATITE AND GOETHITE: A POTENTIAL WATER RESERVOIR IN THE RED DUST OF MARS?

Chen Si Athena¹, Heaney Peter¹, Post Jeffrey², Fischer Timothy³, Eng Peter⁴, Stubbs Joanne⁴

¹Geosciences, Pennsylvania State University, United States, ²Department of Mineral Sciences, Smithsonian Institution, United States, ³Chevron, United States, ⁴Center for Advanced Radiation Sources, The University of Chicago, United States

Water can be stored in nominally anhydrous minerals as substitutional hydroxyl, generating vast but often unrecognized H₂O reservoirs in ostensibly dry regimes. Researchers have long known that hematite (α -Fe₂O₃) can accommodate small concentrations of hydroxyl through the substitution of Fe³⁺ by 3H⁺. Our study of natural hematite has demonstrated the occurrence of “hydrohematite” phases that are 10-20 mol% deficient in Fe and accordingly contain 3.6-7.8 mol% structural water. Intergrown with natural hydrohematite samples were superhydrous goethite-like phases exhibiting a Fe deficiency of 10-20 mol% relative to endmember goethite (α -FeOOH). We synthesized hydrohematite in alkaline solutions (pH 9-12) at low temperatures (< 200 °C) using fresh ferrihydrite as the transient precursor, and we observed a nonclassical crystallization pathway involving vacancy inoculation by Fe as nanocrystals evolved. The high level of incorporation of H₂O in iron (hydr)oxides dramatically alters their behaviors as catalysts and pigments, and the presence of hydrohematite in rocks may rule out high-T diagenesis. We propose that hydrohematite is common in low-T occurrences of Fe oxide on Earth, and by extension, it may inventory large quantities of water in apparently arid planetary environments, such as the surface of Mars.

SORPTION OF Co(II) FROM AQUEOUS SOLUTION ONTO HALLOYSITE

Chojnacka Maria¹, Warchoł Jolanta²

¹Polytechnic Faculty, The Calisia University - Kalisz, Poland, ²Department of Advanced Material Technologies, Wrocław University of Science and Technology, Poland

Halloysite is a natural nano-sized clay mineral with a tubular structure and is a member of 1:1 kaolin group of clay minerals. Each layer of halloysite is composed of tetrahedral (Si-O) and octahedral (Al-OH) sheets and one alumina octahedron sheet, identical to those in kaolinite. Halloysite adsorption potential is mainly dictated by mineral structure and properties which can be easily tuned in halloysite through internal or external surface modifications (Anastopoulos et al., 2018). This rare mineral is found in a Polish deposit, located in the Lower Silesia near Legnica town, which is owned by the Intermark Company. Despite being cheap, abundantly available, and having high biocompatibility, this mineral has not found practical application in wastewater treatment. It results from the fact that natural halloysite without modifications has low heavy metal ions loading capacity in comparison to other minerals (Yuan et al., 2015). On the other hand, the raw or biofilm coated halloysite can be used as a component of filtration barrier in the aquifer, for example near a solid domestic waste landfill. Yunsong et al. (2019) identified the high efficiency of halloysite in remediation of heavy metal's contaminated river sediments. Owing to the interest in halloysite application for environmental remediation comprehensive research on the use of this clay for heavy metals adsorption is necessary. The equilibrium study is the priority step since it provides information about the possible interactions of adsorbent and adsorbate and identifies the adsorption capacities. The objective of this study was to investigate Co(II) sorption onto halloysite. We choose cobalt since it is the main component of wastewater coming from industrial production processes such as smelting of steels and alloys. Cobalt is also used as a pigment in glass and ceramics industries as well as a catalyst. Aqueous Co(II) solution was prepared by dissolving $\text{Co}(\text{NO}_3)_2 \cdot 6\text{H}_2\text{O}$ (Chempur, Poland) in deionized water. The sample of halloysite "CSW" mineral with a particles size ≤ 0.05 mm was purchased by Intermark Company. The chemical composition of halloysite was analyzed with an X-ray fluorescence spectrometer (ARL QUANT'X EDXRF ANALYZER). Batch experiments were carried out to determine the adsorption isotherm of Co(II). For this purpose 0.5 g samples of halloysite were mixed with 50 mL of $\text{Co}(\text{NO}_3)_2$ solutions having single metal concentrations ranging from 5 to 300 mg/L. The pH was adjusted to pH_{init} 6. The mixtures were placed in screw-top polyethylene tubes and agitated at room temperature on an end-over-end tumbling shaker at 140 rpm, for 24 h (a period demonstrated to be sufficient to reach adsorption equilibrium). Then the sorbent was separated from the aqueous solution by decantation, and the supernatant was analyzed towards cobalt content using a NANOCOLOR standard test, method 1-51 Cobalt. The amount of metal ion adsorbed was calculated from the mass balance equation. The maximum adsorption capacity obtained was 4,46 mg/g. However, this value could be higher as can be concluded from the concave increase of experimental points.

ZONES OF ENRICHMENT IN METALS IN THE OCEANIC AND CONTINENTAL UPPER MANTLE

Ciażela Jakub¹, Pieterek Bartosz², Marciniak Dariusz¹, Mazurek Hubert³, Słaby Ewa¹

¹Institute of Geological Sciences, Polish Academy of Sciences, Poland, ²Institute of Geology, Adam Mickiewicz University, Poland, ³Institute of Geological Sciences, University of Wrocław, Poland

Cu-rich sulfide deposits of economic importance in ophiolites such as Troodos in Cyprus or Semail in Oman often occur along the crust-mantle transition zones. Although secondary sulfides now prevail, the relics of magmatic sulfides indicate the igneous nature of enrichment in sulfides at the Moho level. In fact, crust-mantle transition zones in situ in the oceans have been recently suggested to be enriched in sulfides and many chalcophile metals via melt-mantle reaction. The enrichment in sulfides seems to be ubiquitous along the crust-mantle transition zone and might be expected even at the continental Moho. This is possible as sulfides precipitate during melt-mantle reaction independently on pressure. The process seems to work at low pressures of the oceanic crust-mantle transition zones (0.1–0.2 GPa) (Marciniak et al., this session), medium pressures of the continental crust-mantle transition zone (~1.0 GPa) (Pieterek et al., this session), and in high pressures related to various melt-metasomatized mantle xenoliths (up to 2.5 GPa) (Mazurek et al., this session). The refertilization of the mantle with metals during melt-mantle reaction at the crust-mantle transition and along melt channels in the upper mantle may affect the local, regional, and even global metal mass balance of the oceanic and continental lithosphere. The distribution of mantle sulfides is heterogeneous and zones of enrichment in metals occur mostly at the crust-mantle transition or in melt-modified mantle rocks along melt channels in the upper mantle. In the oceans, especially along slow-spreading ridges, shallow magmatic sulfide horizons are penetrated by hydrothermal fluids operating along faults to form massive sulfides on the seafloor. On land, the re-mobilization of the mantle sulfides horizons by sulfide-undersaturated melts or by buoyant CO₂ bubbles can contribute to the formation of porphyry and related epithermal mineral deposits.

INFLUENCE OF PALEOFIRE OF COAL SEAM No 505 ON CARBONATES COMPOSITION IN GANGUE ROCKS, UPPER SILESIA COAL BASIN, POLAND

Ciesielczuk Justyna¹, Krzykowski Tomasz¹, Fabiańska Monika¹, Misz-Kennan Magdalena¹, Jura Dominik¹

¹Institute of Earth Sciences, University of Silesia in Katowice, Poland

Coal-bearing sedimentary units in the Upper Silesian Coal Basin are composed mainly of siltstones, claystones, and sandstones with subordinate carbonate rocks, as dolomite or siderite. In the southwestern part of the basin, some coal seams are vanished because of intra-deposit paleofire, which affected surrounding rocks. Fire intensity and oxygen access differ significantly depending on the distance to the coal seam subcrops and their depth. In the northern part of the Jas-Mos coal mine, vanishing coal seam no 505 is located deep, ca 500 m below the sea level. Based on organic geochemistry and palynology, it was subjected to prolonged heating at relatively low temperatures, ca 150°C, without oxygen access. The conditions make weak changes in the mineral composition of gangue rocks. Apart from organic matter, they are composed of quartz, muscovite, illite, kaolinite, Mg>Fe chlorite, Na- and K-feldspars, framboidal pyrite, carbonates such as calcite, dolomite, siderite, accessory zircon, monazite, and xenotime, which are of sedimentary and/or detrital origin. Other minerals, i.e., hematite, goethite, barite, cristobalite-tridymite, halite, anatase, hydroxylapatite, alunite, alunogen, ZnS, and elemental lead, can also reflect low-temperature heating, which did not decompose carbonates, but could have intensified their crystallization and influenced their properties. SEM-EDS, EPMA, XRD, and Raman spectroscopy were used to precisely investigate carbonates of the siderite-magnesite series to check if they recorded the thermal influence in any way. They form thin veins located within the gangue rocks and coal or at the border between them and are scattered within the rock, revealing xenomorphic habits.

The chemical composition analyzed by EPMA-WDS allowed us to determine the diagenetic trend of siderite variability, from pure varieties to varieties that can be classified as pistomesites, with the general formula $\text{Fe}_{0.71}\text{Mg}_{0.17}\text{Ca}_{0.03}\text{Mn}_{0.09}\text{CO}_3$. Siderite in the form of vein started the crystallization in coal and continued in gangue rock. Carbonate crystallization in this trend ends in dolomite, with an average composition of $\text{Ca}_{1.06}\text{Mg}_{0.78}\text{Fe}_{0.16}(\text{CO}_3)_2$. The hydrothermal effect is marked by the appearance of the second siderite generation (xenomorphic siderite in the rock matrix), the composition of which corresponds to pistomesite, with over 30% MgCO_3 in the structure. The average chemical composition of this variety is represented by the formula $\text{Fe}_{0.59}\text{Mg}_{0.36}\text{Ca}_{0.03}\text{Mn}_{0.02}\text{CO}_3$. This series ends with siderite which contains 46.96% MgCO_3 in the structure. The second trend is found in gangue rock influenced by paleofire.

Funds from project 2016/21/B/ST10/02293, National Science Centre, Poland, are acknowledged.

MINERALOGY AND GEOCHEMISTRY OF COAL WASTES DEPOSITED ON DUMPS; A CASE STUDY FROM THE JANINA AND MARCEL COAL MINES, UPPER SILESIAN COAL BASIN, POLAND

Ciesielczuk Justyna¹, Szczerba Marek², Fabiańska Monika¹, Więclaw Dariusz³, Misz-Kennan Magdalena¹, Szram Ewa¹, Ciesielska Zuzanna²

¹Institute of Earth Sciences, University of Silesia in Katowice, Poland, ²Institute of Geological Sciences, Polish Academy of Science, Poland, ³Faculty of Geology, Geophysics and Environmental Protection, AGH University of Science and Technology, Poland

The coal industry in Poland generates a substantial amount of gangue stores in coal-waste dumps, which can undergo self-heating and self-ignition, causing environmental damages. The highest intensity of the process is observed in the western part of the Upper Silesian Coal Basin. The aim was to compare mineralogical and geochemical characteristics of gangue rocks representing two parts of the Upper Silesian Coal Basin, represented by the Janina (the eastern part) and Marcel (the western part) Coal Mines. Additionally, the influence of weathering caused by deposition of the wastes at dumps in the time span 1998-2018 was also investigated. Fourteen samples of coal wastes were collected from the Marcel site. Three (sandstone, siltstone, and coal) were fresh gangues, and others were deposited for 6, 11, 12, and 20 years. Thirteen samples were collected from the Janina site. Three (sandstone, siltstone, and coal) were fresh gangues, and others were deposited for 1, 2, and 10 years. Additionally, two were thermally affected by self-ignition.

Samples in both locations are containing mostly quartz (up to 54 %), kaolinite (up to 48%) muscovite + illite-smectite (up to 28 %), K-feldspar (up to 22 %) and chlorite + serpentine (up to 13 %) mixed with coal in different proportions (from 0 to 58 %). Pyrite with its oxidation products (up to 7 %) and titanium oxides (up to 1 %) were found in both localities. Carbonates in the form of dolomite/ankerite and siderite are more common in samples from the Marcel site (up to 6 %). Analyzed samples from the Marcel site show lower variability in coal, clay minerals, and other phases' contents than the Janina site. The same trends are visible also for major and trace chemical elements. Samples from the Marcel site contain a visibly higher chlorite + serpentinite, kaolinite, and illite-smectite + muscovite relatively to quartz compared to the Janina site. The ratio between particular clay minerals does not show significant differences for both the studied sites. Only the ratio between chlorite + serpentinite and muscovite + illite-smectite is higher for the Marcel site.

The signature of the previous thermal process was found to be a complete loss of clay minerals with lower dehydroxylation temperatures (kaolinite, chlorite, and serpentine), while muscovite and illite-smectite were retained. The amount of coal also decreased close to zero. Parallely to the decomposition of the kaolinite, chlorite, and serpentinite, a new amorphous phase was formed, which has a composition similar to a mixture of kaolinite with Mg-chlorite. No anatase to rutile transformation was observed, as both these minerals were found in samples from fresh and historical dumps and for samples that underwent the thermal process. The average temperatures of dehydroxylation measured in laboratory conditions for kaolinite are 500-550°C, for serpentine: 575-700°C, for Fe-chlorite: c.a. 600°C, for Mg-chlorite: c.a. 800°C, while for mica: 800-1000°C. However, prolonged heating of kaolinite at lower temperatures of 450°C was also shown to lead to significant dehydroxylation of the mineral.

The financial support of the National Science Centre, grant No 2017/27/B/ST10/00680 is gratefully acknowledged.

RECORDS OF NATURAL SILICIFICATION AND CARBONATION IN PARTIALLY SERPENTINIZED PERIDOTITES FROM THE SZKLARY MASSIF: INSIGHT INTO SiO₂ AND CO₂ MINERALIZATION

Cieślak Błażej¹, Kierczak Jakub¹, Pietranik Anna¹

¹Institute of Geological Sciences, University of Wrocław, Poland

Silicification and carbonation are common reactions in peridotites associated with various geological processes. Recent studies of natural systems provide information on the potential capture and storage of anthropogenic CO₂ in ultramafic rocks. In detail, the presence of carbonates and silica as final products of peridotites alteration could prove that these rocks have the potential for carbon dioxide sequestration by mineral carbonation.

The Szklary Massif is an isolated ultramafic massif located within the Niemcza left-lateral shear zone, also it is a fragment of the tectonically dismembered Central Sudetic Ophiolite (SW Poland). The Szklary Massif is mostly composed of partly serpentinitized peridotites with heterogeneous lateritic cover on its surface. Previously published studies have distinguished a few types of weathered ultramafic rocks, including silica-rich birbirite. In this study, new outcrops of silicified serpentinites (SiSp) have been documented during fieldwork. Mineralogical and geochemical study of the rocks has been undertaken to verify previous hypotheses about SiSp origin and to recognize eventual signs of natural ultramafic rocks carbonation in the studied samples.

Silicified serpentinite outcrops have been localized within partly serpentinitized peridotites and their weathering cover. Due to textural, mineralogical, and chemical differences, two types of SiSp have been distinguished. The studied SiSp consist mostly of silica (from 62 to 82 wt.% SiO₂). Petrographic analyses done with an electron microscope (SEM-EDS) combined with a cathodoluminescence microscope (SEM-CL) showed the presence of four varieties of silica. The first type is represented by quartz crystals with euhedral growth zones. This form is a common texture observed in hydrothermal quartz. The second type is represented by so-called microquartz, which could precipitate due to incongruent dissolution of serpentine group minerals under tropical conditions. The third type is represented by amorphous silica (colorless opal) and the last one consists of miscellaneous varieties of cryptocrystalline quartz (mostly chalcedony). Amorphous silica veinlets cut SiSp samples irregularly in many directions, however, unweathered rock-forming silicates are usually cut along their cleavage planes. Moreover, some unidentified Mg-rich amorphous phases were observed which composition and form of occurrence show close association with carbonates. This may suggest a reaction between CO₂ and magnesium silicates in course of hydrothermal or/and weathering events.

Petrographic studies on silicified serpentinites from the Szklary Massif were based on analysis of silica forms. In studied samples, two major types of silica have been distinguished: crystalline and cryptocrystalline. Qualitative observation of quartz crystals combined with analysis of other rock-forming minerals and chemical data, suggest that SiSp from the Szklary Massif probably formed due to two-stage silicification: (1) earlier stage - hydrothermal processes and (2) later stage - chemical weathering processes. Partially serpentinitized peridotites from Szklary Massif seem to be a promising material for the experimental study of anthropogenic CO₂ mineralization.

RESOLVING JIGSAW PATTERNS OF LARGE 2D CRYSTAL STRUCTURES: Pb-Bi-(Sb)-SULFOSALTS AND THEIR INTERGROWTHS

Ciobanu Cristiana¹, Slattery Ashley², Cook Nigel³, Wade Benjamin², Ehrig Kathy⁴

¹School of Chemical Engineering and Advanced Materials, University of Adelaide, Australia, ²Adelaide Microscopy, University of Adelaide, Australia, ³School of Civil, Environmental and Mining Engineering, University of Adelaide, Australia, ⁴BHP Olympic Dam, Australia

Lead-Bi-Sb-sulfosalts are some of the largest 2D structures known from nature that have been explored in terms of their suitability as a new class of semiconductors for photovoltaic applications. Their structures are built by simple PbS- or SnS-derived modules sliced along different crystallographic directions. The modules are combined within blocks of incremental width forming series of homologs with variable periodicity defined by crystallographic operators and/or chessboard structural arrangements. Examples from two types of homologous series are considered here: (i) twinned structures from the lillianite series: $\text{Pb}_{(N-1-2x)}\text{Bi}_{(2+x)}\text{Ag}_x\text{S}_{(N+2)}$ ($N=4-\infty$; $x=0-1$); and (ii) chessboard structures from the Sb-Bi rich members of the kobellite series: $2(\text{Cu,Fe})_2\text{M}_{10N+6}\text{S}_{11N+13}$ ($M=\text{Pb,Sb,Bi}$; $N=\text{homologue number}$).

HAADF STEM imaging, EDS, and EELS analysis are used to directly relate homology to atomic arrangements. Secondly, we show lattice-scale intergrowths and replacement structures which explain compositional variation at the scale of the electron microprobe. Lillianite (Lil) and its corresponding Ag-rich endmember gustavite (Gus) are the $N=4$ endmembers of a series linked by $\text{Bi}^{3+}+\text{Ag}^+=2\text{Pb}^{2+}$ substitution. High-resolution imaging on $[001]_{\text{Lil}}$ reveals the N number as 4 atoms representing BiS_6 octahedra along $(311)_{\text{PbS}}$ directions counted on either side of mirror planes with a larger atom representing Pb in bicapped trigonal prismatic coordination (PbS_6^{+2}). Kink patterns observed on $[100]_{\text{Lil}}$ indicate monoclinic rather than orthorhombic symmetry. The specimen has intermediate composition $\text{Lil}_{45}\text{Gus}_{55}$ and features nanoscale heterogeneity expressed as thin (~ 20 nm-wide), acicular Gus-richer lamellae. Gustavite substitution is also shown by mapping of particle arrays diffusing away from the contact to adjacent phases towards a sulfide inclusion. Such diffusion can be associated with fluid percolation and the formation of μm -scale electrum ($\text{Au}_{70}\text{Ag}_{30}$), discontinuously marking the sulfosalt elsewhere in the sample. Structurally controlled replacement by Cu is imaged and mapped by EELS along bands forming one side of the mirror planes in Lil. Replacement of octahedral Bi by Cu in the crystal structure, rather than as random Cu-bearing phases, is demonstrated.

The second case comprises non-stoichiometric kobellite (Kob) and izoklakeite (Izok) displaying chessboard patterns of alternating structural motifs that are readily imaged on $[001]_{\text{Kob/Izok}}$. These comprise the PbS- and SnS-modules forming blocks with number of atoms counted as: $n_1=18$; $n_2=8$ for Kob, and $n_1=30$; $n_2=16$ for Izok. Knowing that the topology of the PbS- and SnS-modules is $\text{M}_{6(N+1)}\text{S}_{7N+9}$ and $\text{M}_{4N}\text{S}_{4(N+1)}$, respectively, N for Kob (2) and Izok (4) can be calculated using the formulae $N=n_1/6-1$ and $N=n_2/4$. Atomic-scale mapping of Kob reveals that Sb and Bi preferentially concentrate in the SnS and PbS modules, respectively, with Pb framing both modules and Fe located at motif corners. Primary growth features show the two species intricately intergrown with one another forming a jigsaw arrangement with the smallest units just half unit cells of either Kob or Izok. Crosscutting veins, as small as 1-2 nm in width, show a variation of the smallest intergrowths, and in particular, single or double PbS-modules, thus explaining both Pb-depleted Izok and variable Sb/Bi ratios in Kob. Sulfosalts can modulate compositional variation via atomic-scale jigsaw patterning, a natural blueprint for design of smart materials.

THE CROWN JEWELS: UNDERSTANDING ORE-FORMING PROCESSES AT THE WORLD-CLASS PANASQUEIRA AND NEVES CORVO DEPOSITS, PORTUGAL

Codeço Marta S.¹, Weis Philipp¹, Trumbull Robert¹, Relvas Jorge², Veksler Ilya¹, Gleeson Sarah A.¹

¹Geochemistry, GFZ German Research Centre for Geosciences, Germany, ²Department of Geology, University of Lisbon, Portugal

The Panasqueira and Neves Corvo deposits in Portugal are leading producers of tungsten and copper-zinc concentrates in the European Union. Both are situated in the Iberian Massif but formed in very distinct geological and temporal contexts. They have in common that in both cases, the influence of tectonic and magmatic processes, the origin and composition of the mineralizing fluids, and the hydrothermal processes involved in ore deposition are topics of much debate.

The Panasqueira deposit is situated in the Central Iberian Zone and consists of subhorizontal W-Sn-Cu-bearing quartz veins hosted by metasediments. The deposit is genetically and spatially related to a late-Variscan, peraluminous, S-type granite (ca. 300 Ma). Hydrothermal alteration of the wall rocks around the veins produced concentric zones consisting of a proximal tourmaline-quartz-muscovite zone, and a distal muscovite-quartz zone, with minor tourmaline. We addressed the question of fluid source, composition, and evolution from the results of in-situ microprobe, LA-ICP-MS, and SIMS measurements of coexisting tourmaline and white mica. Boron isotopic and trace element compositions of tourmaline, and white mica support a magmatic source for the early hydrothermal fluids. Furthermore, the fractionation of B-isotopes between tourmaline and mica provides an estimate for the temperature of vein formation (ca. 460°C) and of a later fluid pulse recorded in cross-cutting, mineralized fault zones (ca. 260°C). The in-situ LA-ICP-MS data show that Rb, Cs, Ba, Li, Nb, Ta, W, and Sn preferentially partition into white mica over tourmaline while Zn, V, and Sr do the opposite. Thus, white mica better reflects the hydrothermal fluid and its evolution, whereas tourmaline compositions reflect the composition of the host rocks.

The Neves Corvo deposit is located in the Iberian Pyrite Belt and is one of the most important volcanogenic massive sulfides (VMS) provinces globally. The Cu-Zn-(Sn) mineralization is either hosted by black shales or by felsic-volcanic rocks and formed between 366 to 358 Ma. Ongoing work aims to determine the origin and evolution of the ore-forming fluids and mineralization mechanisms by combining melt inclusions in the volcanic host rocks and fluid inclusions in quartz and ore minerals. Preliminary results show that the footwall volcanic rocks have abundant silicate melt inclusions in quartz, which is the only primary mineral that survived the hydrothermal alteration associated with the mineralizing event. The primary and pseudo-secondary melt inclusions vary in shape and size and are typically from a few microns to 100 microns in diameter. They are typically randomly distributed and are predominantly crystalline. In addition, many secondary melt inclusions form along fluid inclusion trails and fractures. Fluid inclusions around melt inclusions and along trails are in general tiny (<10 microns) and display a small bubble suggesting either low temperature or high pressures during entrapment.

HIGH P BEHAVIOR MASCAGNITE [(NH₄)₂SO₄]: A CANDIDATE TO HOST AMMONIA IN PLANETARY BODIES

Comodi Paola¹, Fastelli Maximiliano¹, Criniti Giacomo², Glazyrin Konstantin³, Zucchini Azzurra¹

¹Dipartimento di Fisica e Geologia, Università di Perugia, Italy, ²Universität Bayreuth, Bayerisches Geoinstitut, Germany, ³Hamburg, Deutsches Elektronen-Synchrotron, Germany

Ammonia is expected to be one of the major constituents of giant planets in the Solar System. Neptune is thought to have a layered structure with a hot ice layer (a dense fluid with C-H-O-N composition) localized between a rocky core and a gaseous atmosphere. NASA's New Horizons space mission has found evidence of ammonia on the surface of Pluto and remains an intriguing phenomenon how ammonia can survive long on the surface of Pluto without being destroyed by ultraviolet light, cosmic rays, or other radiation. The hypothesis is that ammonia comes from a subsurface ocean, which spews ammonia-containing water toward the cold surface in a form of cryo-vulcanism. Ammonia, which allows the water to be liquid at cold temperatures (up to 176 K) improves the evidence of the ocean under the cold crust of Pluto. Moreover, ammonium bands in both Nix and Hydra remote sensing spectra were observed by New Horizons LORRI and Ralph, together with H₂O ice in the crystalline phase. Ammonia is an important precursor to prebiotic chemistry, including the formation of amino acids and a cascade of other biologically interesting chemicals, so the knowledge of the stability, as well the structural evolution with P and T of the ammonium minerals, can have a strong interest on the paleontological field. In this study, the high-pressure behavior of mascagnite (NH₄)₂SO₄ are investigated collected X-ray synchrotron single-crystal data at DESY beam line Petra III P2.02 up to ~17.8 GPa using diamond anvil cell, ruby as pressure calibrant, and Neon as pressure transmitting medium. The volume-pressure data were fitted by a third-order Birch-Murnaghan equations of state (BM3-EOS), as suggested by F-f plot, yielding $K_0 = 20.4(7)$ GPa, $K' = 6.1(2)$ and $V_0 = 499(1)$ Å³. The axial compressibility's, calculated with a BM3-EOS, were $K_{0a} = 35(3)$, $K'_a = 7.5(7)$, $K_{0b} = 10(3)$, $K'_b = 6.8(1)$, $K_{0c} = 25(1)$, $K'_c = 4.4(0.2)$. The axial moduli calculated using a BM2-EOS, fixing K' equal to 4, were $K_{0a} = 52(2)$, $K_{0b} = 21(1)$, $K_{0c} = 27(1)$ GPa and the anisotropic ratio of $K_{0a}:K_{0b}:K_{0c} = 1:0.4:0.52$. This mineral is characterized by a phase transition at low temperature, with a change in the electric characteristic from paraelectric at room temperature to ferroelectric at 223 K and of the space group from Pnam to Pna21. The evolution of crystal lattice and geometrical parameters indicate no phase transition up to 17.8 GPa, sulfate and ammonium polyhedra are incompressible, and the high compressibility, which implies an increase of density of about 32% over the pressure range investigate, is due to the reduction of the complex hydrogen bond system. Some of them, directed along [100], are very short at room temperature, below 2 Å and this configuration explains the anisotropic compressional behavior and the lowest compressibility along a axis.

A MULTI-SCALE MINERO-CHEMICAL ANALYSIS OF BIOMASS ASHES TO EVALUATE THEIR EMPLOYMENTS IN CIVIL ENGINEERING

Comodi Paola¹, Cambi Costanza¹, Cotana Franco², Cavalaglio Gianluca³, Vivani Riccardo⁴, Susta Umberto⁵, Zucchini Azzurra¹, Fastelli Maximiliano¹

¹Dipartimento di Fisica e Geologia, Università di Perugia, Italy, ²Dipartimento di Ingegneria, Università di Perugia, Italy, ³Dipartimento di Giurisprudenza, Pegaso Università, Italy, ⁴Dipartimento di Scienze farmaceutiche, Università di Perugia, Italy, ⁵AUSL Umbria 1, UOC PSAL, Italy

The percentage of ashes produced during biomass burning varies according to the biomass type, ranging from a few units to about 10 dry weight percent. In view of the renewable energy growth, as that from biomasses, large amounts of ashes will have to be stored, and their disposal can represent an environmental hazard. On the other hand, civil engineering earthworks are nowadays increasingly performed by means of local materials in order to avoid their transfer impacting on the environment. However, the local raw materials sometimes need to be treated if their geotechnical characteristics are not good enough. Among the different employments suggested to re-use ashes from biomass, beyond in concrete industry and in agricultural as a soil amendment, the employment in clayey soils, to improve geotechnical properties as a substitution of lime, has recently attracted the interest of the scientific community.

The present study presents the results of a multi-methodic analysis performed on five samples of fly ashes coming from different biomasses. The aim of the study was to evaluate their dangerousness to people and the environment and their possible re-use in civil engineering. Optical granulometric analyses indicated that the average diameter of the studied fly ashes was around 20 µm, whereas only ~1 vol% had diameters lower than 2.5 µm. The chemical composition, investigated with electron probe microanalysis, indicated that all the samples had a composition in which Ca was prevalent, followed by Si and Al. Large contents of K and P were observed in some samples, whereas the amount of potentially toxic elements was always below the Italian law thresholds. Polycyclic aromatic hydrocarbons were completely absent in all the samples coming from combustion plants, whereas they were present in the fly ashes from the gasification center. Quantitative mineralogical content, determined by Rietveld analysis of X-ray powder diffraction data, indicated that all the samples had high amorphous content, likely enriched in Ca, and several K and P minerals, such as sylvite and apatite. The data pointed out that biomass fly ashes could be interesting materials for amendments in clayey soils, as a substitution for lime, that might also stimulate pozzolanic reactions and improve their geotechnical properties. That is, the proposed technique allows, on the one hand, to avoid the need of mining raw materials and, on the other hand, the re-cycling of a waste product. The results of experiments devoted to the study of compressibility and shear resistances, by using different types and amounts of ashes added to clayey soils with respect to the classical CaO treatments, will be presented.

The research was founded by Fondazione Cassa di Risparmio, project. #9858, 2018.0508 to Paola Comodi

A PROMISING WAY FOR CERIUM RECOVERY: THE ION EXCHANGE CAPACITY OF LTL ZEOLITE

Confalonieri Giorgia¹, Vezzalini Giovanna², Di Renzo Francesco³, Gozzoli Vittorio², Arletti Rossella²

¹European Synchrotron Radiation Facility - grenoble, France, ²Department of Chemical and Geological Sciences, University of Modena and Reggio Emilia, Italy, ³Institut Charles Gherard - Montpellier, France

Nowadays the interest in technologies to recover Rare Earth Elements (REE) from wastes is increasingly growing. Indeed, on one hand, Europe presents scarcity of natural resources for these elements, and, on the other one, this process would promote the development of circular and green economy good practices. Among the different methods to separate and recover REE from leached liquids obtained by wastes, the ionic exchange is one of the most promising. So far MOFs or ion exchangeable resins have been applied, however, efficient recycling can be achieved using other porous materials such as zeolites. Despite the well-known ion-exchange properties of these materials, just a few preliminary works investigated their application for REE separation and recycle [1, 2, 3, 4]. Thus, their potential use to recover these elements from acid-leached liquors of industrial waste should be better investigated. In this work, we present a double ion-exchange experiment to recover cerium from a very diluted solution ($[Ce^{3+}] = 0.002$ M) using a NH_4 -LTL zeolite. This concentration was chosen to test the zeolite in a very extreme condition representative of the real concentration of leached liquids obtained from spent fluid catalytic cracking (FCC) catalysts. In the first ion exchange experiment, the zeolite was put in contact with the very diluted solution for 72 h at room temperature, testing different liquid/solid ratio (i.e. 30, 60, 90, 180, 270, 750 mL/g). ICP analysis was performed monitoring daily the cerium concentration into the solution and the obtained exchanged zeolite were fully chemically characterized.

The best working conditions for the initial complete exchange of NH_4 -LTL with Ce^{3+} are liquid/solid ratio = 90 mL/g and 24 h of contact at 25°C. The kinetics was proved to be fast and consistent with industrial timing, no energy cost for temperature setting is required and the acid pH of the solutions does not affect the zeolite structure and its exchange performance. At these conditions, all cerium of the solution was first incorporated into the zeolite porosities and then completely recovered.

1. Mosai, A. K.; Chimuka, L.; Cukrowska, E. M.; Kotze, I. A.; Tutu, H., The Recovery of Rare Earth Elements (Rees) from Aqueous Solutions Using Natural Zeolite and Bentonite. *Water Air and Soil Pollution* 2019, 230.
2. Faghihian, H.; Amini, M. K.; Nezamzadeh, A. R., Cerium Uptake by Zeolite a Synthesized from Natural Clinoptilolite Tuffs. *JRNC* 2005, 264, 577-582.
3. Duploux, L. Preliminary Investigation of Rare Earth Elements Ion Exchange on Zeolites. University of Helsinki, Université de Lille, 2016.
4. Barros, O.; Costa, L.; Costa, F.; Lago, A.; Rocha, V.; Vipotnik, Z.; Silva, B.; Tavares, T., Recovery of Rare Earth Elements from Wastewater Towards a Circular Economy. *Molecules* 2019, 24.

IMAGING AND UNRAVELING THE AMAZING ALEKSITE HOMOLOGOUS SERIES

Cook Nigel¹, Ciobanu Cristiana², Slattery Ashley³, Wade Benjamin³, Ehrig Kathy⁴

¹School of Civil, Environmental and Mining Engineering, The University of Adelaide, Australia, ²School of Chemical Engineering and Advanced Materials, The University of Adelaide, Australia, ³Adelaide Microscopy, The University of Adelaide, Australia, ⁴BHP Olympic Dam, Australia

Lead-Bi chalcogenides of the aleksite homologous series occur as trace constituents of many Au-bearing ore deposits and are defined chemically by the formula $Pb_nBi_4Te_4S_{n+2}$. Their synthetic analogs show considerable potential as topological insulators and in thermoelectric energy conversion. These mixed-layer compounds can be built from odd-numbered blocks derived by expansion of the 5-atom tetradymite structure (Bi_2Te_2S , Te-Bi-S-Bi-Te) with incremental addition of Pb and S atoms defining homology. For example, the named minerals aleksite ($PbBi_2Te_2S_2$, $n=2$) and saddlebackite ($Pb_2Bi_2Te_2S_3$, $n=4$) comprise regular repeats of 7- and 9-atom stacks (Bi-Te-Pb-S-Pb-Te-Bi, and Bi-Te-Pb-S-Pb-S-Pb-Te-Bi, respectively), while the third named mineral, hitachiite ($Pb_5Bi_2Te_2S_6$, $n=10$) features regular repeats of a 15-atom stack (Bi-Te-Pb-S-Pb-S-Pb-S-Pb-S-Pb-S-Pb-Te-Bi).

Nanoscale imaging of aleksite homologues by high angle annular dark field scanning transmission electron microscopy has proven an effective method to directly visualise layer sequences, including multiple previously unreported phases with non-integer n . A characteristic feature of the series is the occurrence of distinct polytypes of individual species. For example, $PbBi_4Te_4S_2$ ($n=1$), occurs as packages of [5.7], [5.5.5.9] and [5.5.7.5.5.9] layers within the same specimen, corresponding to 24R, 48R and 72R polytypes, with c dimensions of ~23, 46, and 69 Å, respectively. A further feature is the extensive disordering at the nanoscale, which is particularly evident in specimens that have been exposed to infiltrating fluids and/or thermal gradients after initial crystallization.

The number of named minerals will continue to grow as new structural arrangements are documented at the nanoscale and correlated with chemistry at the scale of the electron microprobe, e.g., our recent imaging of $PbBi_6Te_6S_4$ ($n=0.67$), which is composed of regular packages of two 5-atom and one 7-atom layer [5.5.7]. These new species are found as blocks of variable length (e.g., up to 50 repeats of the 13-layer, $n=8$ homologue, $Pb_4Bi_2Te_2S_5$) separated by single 5-atom layer units, and preferentially hosted within Bi-Sb-Pb-sulphosalts. In contrast, limited range sequences (no more than a dozen sequential repeats) of Pb-S-rich homologues with higher n (17-, 19-, 21- and 23-atom repeats, $n=12, 14, 16$ and 18) occur along $\langle 111 \rangle$ directions within galena. The same specimen contains still longer (50-100 atom) sequences of aleksite homologues. Compositionally, these correspond to blocks of galena (effectively $n=\infty$) albeit with pairs of Bi and Te atoms at their outer margins, thus raising a conundrum for characterisation and naming of phases in the series. These thick layers likely formed via thermal overprinting and recrystallization of Bi-Te-bearing galena. Stability and degree of ordering in aleksite homologues appear highly dependent upon host assemblage. Such responses to buffering conditions are a good premise for the fine-tuning of their physical and thermoelectric properties under experimental conditions.

MAGNETITE (Fe₃O₄) U-Th-He DATING: ANALYTICAL CHALLENGES AND APPLICATIONS

Corre Marianna¹, Schwartz Stéphane¹, Agranier Arnaud², Lanson Martine¹, Brunet Fabrice¹, Gautheron Cécile³, Pinna-Jamme Rosella³

¹ISTerre, France, ²IUEM, France, ³GEOPS, France

The (U-Th)/He dating method is based on the accumulation within the crystal structure of radiogenic ⁴He produced during alpha-decay of the ²³⁸U, ²³⁵U, ²³²Th, and ¹⁴⁷Sm. This method has been already used to date magnetite emplacement (Blackburn and al., 2007), or magnetic exhumation (Cooperdock and Stockli, 2016). The method has important potential but suffers from the challenge due to the low He, U, Th, and Sm content. For example, magnetite of an HP-LT ophiolitic body from the French Alps between 14.8 ± 2.1 My and 20.9 ± 3.0 Ma, containing 5 at 20 ppb of U and 3 to 6 ppb of Th (Schwartz et al., 2020). However, some magnetite grains, in contact with titanite, display older ages ranging from 30.4 ± 4.4 Ma to 32.0 ± 4.6 Ma. This difference in age is accounted for by He contamination through implantation coming from neighboring titanite. Whereas magnetite located apart from any titanite crystal, features (U-Th)/He thermochronometric ages in agreement with fission-track ages on zircon and apatite, coming from the same locality, allowing to determine the thermal history of the ophiolitic body. The geological understanding of the (U-Th)/He ages required thus the determination of the He-U-Th-Sm content with a high precision.

Radiogenic ⁴He content in magnetite is very low as well, especially for magnetite of young age. However, helium contents ranging from 0.1 pmol/g to 20 pmol/g can routinely be measured using noble gas mass spectrometers; therefore, even for father isotope concentrations of 10 – 100 ppb, ages down to 100 Ma are accessible. Moreover, the U-Th-Sm isotopes measurement is technically challenging, and to improve the method, since no certified magnetite standard is yet available, we synthesized our own by precipitating magnetite nanocrystals with controlled concentrations of U and Th (43 ppm to 50 ppb). This allows to developed and tested two ways to determine the U-Th content by isotope dilution mass spectrometry (IDMS) and by Laser Ablation mass spectrometry (LA-ICPMS). Among these two methods, IDMS is the most precise and accurate, nevertheless, it requires a long preparation time in a clean lab (dissolution, purification by ion exchange resin columns, dilution). The first quantitative results obtained by LA-ICP-MS using this synthetic material along with international glass standards, are promising. The laser-ablation technique overcomes the analytical difficulties related to sample dissolution and purification, permitting faster data collection. In this study, results collected with both methods are presented and the potential for dating natural magnetite is discussed accordingly.

Our dating methods open the path to the He magnetite dating to various ultramafic rocks such as serpentinized peridotites in ophiolites coming from the Alps, New Caledonia, and Oman or abyssal peridotites.

Blackburn, T.J., Stockli, D.F., Walker, J.D., 2007. Magnetite (U-Th)/He dating and its application to the geochronology of intermediate to mafic volcanic rocks. *Earth Planet. Sci. Lett.* 259, 360–371.

Cooperdock, E.H., Stockli, D.F., 2016. Unraveling alteration histories in serpentinites and associated ultramafic rocks with magnetite (U-Th)/He geochronology. *Geology* 44, 967–970.

Schwartz S., Gautheron C., Ketcham R.A., Brunet F., Corre M., Agranier A., Pinna-Jamme R., Haurine F., Monvoisin G., Riel N., 2020. Unraveling the exhumation history of high-pressure ophiolites using magnetite (U-Th-Sm)/He thermochronometry. *Earth Planetary Science Letters* 543.

SYNTHESIS AND CHARACTERIZATION OF LAYERED STRUCTURE COMPOUNDS CONTAINING CHROMATE, SELENATE, AND MONOCARBOXYLIC ACIDS ANIONS

Cortinhas Alves Tiago Kalil¹, Boiadeiro Ayres Negrão Leonardo¹, Beirau Tobias¹, Pöllmann Herbert¹

¹Institut für Geowissenschaften Mineralogie Geochemie, Uni Halle, Germany

AFm-phases refer to a family of lamellar calcium aluminum hydroxy salts that are common phases crystallizing during the hydration of Portland-, calcium aluminate-, and calcium sulphoaluminate cements. The OH⁻ in the lamellar structure of AFm-phases can be replaced by different organic (incl. monocarboxylic acids from cement-admixtures), and inorganic anions, as toxic Cr^{+VI}, Se^{+VI}. In this work, stoichiometric proportions of CaAl₂O₄, CaO, and monocarboxylic acids (HCOO⁻, CH₃COO⁻, C₂CH₅COO⁻) were mixed with CaCrO₄ or CaSeO₄·2H₂O at 25°C to investigate the possible formation of different AFm-Phases at different relative humidities. The experiments were conducted in a glove box under the Ar atmosphere to avoid carbonation. The resulted hydrated mixtures regarding the phase relation between C₃A·CaCrO₄·mH₂O - C₃A·CaX₂·nH₂O, and C₃A·CaSeO₄·mH₂O - C₃A·CaX₂·nH₂O (X= formate, acetate, or propionate) were studied using X-ray powder diffraction, SEM-EDS, thermal analysis, Raman, and IR-spectroscopy. The X-ray diffraction patterns of all CrO₄⁻²-containing mixtures show well crystalline AFm-phases with Trigonal or monoclinic structure. The synthesized AFm-phases containing CrO₄⁻² and monocarboxylic acids seem to form neither solid solution nor an intermediary compound. Likewise, the SeO₄⁻²-containing mixtures formed SeO₄⁻²-AFm and X-AFm phases with different water contents, but an intermediary phase with nominal composition C₃A·5/6CaSeO₄·1/6Ca(CH₃COO)₂·nH₂O was identified and described in detail. Scanning electron microscopic analysis shows well-developed pseudo hexagonal crystals. Our XRD measurements indicate that this compound crystallizes with the space group R3/R-3. Lattice parameter was calculated using a Pawley fit: a = 5.47 Å, c = 93.91 Å, R_p = 0.0380, R_w = 0.0519, GOF = 1.30. The results shed light on possible interactions of cement-admixtures and harmful compounds in the hydration products of different types of cements.

TITANITE AS POWERFUL PETROCHRONOMETER FOR UNRAVELLING THE EVOLUTION OF A MAJOR EXTENSIONAL SHEAR ZONE IN THE MIDDLE CRUST (VAL D'OSSOLA, WESTERN ALPS, ITALY)

Corvò Stefania¹, Langone Antonio², Maino Matteo¹, Piazzolo Sandra³, Kylander-Clark Andrew⁴

¹Department of Earth and Environmental Sciences, University of Pavia, Italy, ²Institute of Geosciences and Earth Resources, CNR, Italy, ³School of Earth and Environment, University of Leeds, United Kingdom, ⁴Department of Earth Science, University of California, United States

Titanite is a useful accessory mineral for understanding crustal processes because is considered as a powerful petrochronometer that allows to determine both age (U-Pb isotopes) and pressure-temperature (P-T) conditions (trace-element composition: Zr, rare earth elements (REE)). However, titanite has a propensity to recrystallize during metamorphism, fluid flow, and deformation, which can result in modifications to its isotopic and trace-element compositions. Consequently, how titanite records host rock evolution is still uncertain. We combine microstructural and petrological data with the aim to reconstruct the Pressure-Temperature-timing-Deformation (P-T-t-D) path of mylonites and wall rocks coming from the Anzola shear zone (Val d'Ossola, Ivrea Verbano Zone, Italy). The Ivrea Verbano Zone (IVZ) is an exhumed section of the pre-Alpine middle to lower continental crust mainly made of (ultra-)mafic rocks intruded into high-grade metapelites and metabasites. Following the Variscan orogeny, the IVZ was characterized by post-orogenic extension and subsequently, in the Triassic-Jurassic time interval, by a complex and polyphasic rifting stage, which resulted in mid-lower crustal shear zones (Petri et al., 2019). In particular, the Val d'Ossola exhibits an ideal section of the IVZ that is characterized by the occurrence of main extensional shear zones (i.e., Anzola and Premosello shear zones) showing progressively higher T conditions with increasing crustal depth. While magmatism and amphibolite to granulite metamorphism are constrained between the Carboniferous and Permian times, the timing of extensional shear zones activities is still poorly constrained.

We performed a quantitative orientation analysis of zircon and titanite using SEM-EBSD in order to characterize their internal deformation features from different rock types across the shear zone. Microstructural analyses have been combined with trace element analyses and U-Pb age dating by LA-ICP-MS. Preliminary zircon data obtained from the mylonitic amphibolites revealed a weak or absent intracrystalline deformation and a wide range of U-Pb dates (310-230 Ma), mainly overlapping with the Carboniferous-Permian magmatic and metamorphic events recorded by the crustal section. Titanite is commonly present within amphibolites at different crustal levels as well as within the shear zone. Preliminary petrochronological results on titanite for amphibolites far from the shear zone indicate U-Pb lower intercept ages older (Permian - Upper Triassic) with respect to titanite from mafic granulite and calcsilicate adjacent to the shear zone (Triassic-Jurassic U-Pb lower intercepts). Mylonites are characterized by abundant titanite grains in different textural positions. Grains along the foliation show sigmoidal shapes, intracrystalline deformation, and incipient recrystallization (subgrain formation) with a maximum orientation change within an individual grain up to 20°. The trace element characterization of titanite grains showed a U concentration ranging from 50 to 150 ppm. The petrochronological analyses are in progress. The combination of a multidisciplinary approach and different systematics on multiple geochronometers may allow to better constrain the role of the shear zone in the rifting phase of the IVZ.

Petri B., Duret T., Mohn G., Schmalholz S.M., Karner G.D. and Muntener, O., 2019. Thinning mechanisms of heterogeneous continental lithosphere. *Earth Planet Sc. Lett.*, 512: 147–162.

ORIGIN OF FELSIC MELTS BY ANATEXIS OF ARCLOGITES IN ARC ROOTS: AN EXAMPLE FROM MERCADERES, COLOMBIA

Costa Benedetta¹, Gianola Omar¹, Alvaro Matteo², Gilio Mattia², Ferri Fabio³, Cesare Bernardo¹

¹Department of Geosciences, University of Padova, Italy, ²Department of Earth and Environmental Sciences, University of Pavia, Italy, ³EIT RawMaterials, Italy

The Granatifera Tuff formation in the Mercaderes – Rio Mayo region contains abundant xenoliths which sample the entire lithospheric arc section above the subducting Nazca plate. Among the xenoliths, we studied a garnet pyroxenite (arclogite) showing evidence of partial melting.

The rock consists of garnet, clinopyroxene, and plagioclase, minor amphibole, accessory rutile, and apatite. Quartz is only present in the cores of garnet, often together with glassy inclusions. The bulk rock composition corresponds to a low-alkali basalt. The rock has an average grain size of 1.0 ± 0.5 mm and contains a well-developed foliation defined by 2-3 mm-thick monomineralic garnet layers.

Minerals are virtually unzoned: composition of garnet is $\text{Alm}_{42-43}\text{Pyr}_{38-41}\text{Grs}_{16-20}\text{Sps}_1$; clinopyroxene contains 15-16% Jd and has a XMg of 0.73; amphibole is a pargasite with 0.27 apfu Ti, 0.87 apfu Na and XMg of 0.87; plagioclase composition is $\text{Ab}_{72}\text{An}_{26}\text{Or}_3$.

The garnet frequently contains primary glassy inclusions at the core. Inclusions have a size between 10 and 50 μm , range in shape from irregular to negative crystal, and contain either brown or colorless glass, with one or more shrinkage bubbles. Under SEM inspection the glass shows evidence of local partial crystallization. The composition of the glass in inclusion is rhyolitic and peraluminous ($\text{ASI} = 1.0-1.2$), with an inferred range of H_2O of 0.5-6.0 wt.%. This melt is different from the interstitial glass infiltrated from the host lava of the Granatifera Tuff, which has lower total alkalis.

The presence of primary melt inclusions, along with the occurrence of quartz exclusively as inclusions in garnet, indicate that garnet is a peritectic phase and that the rock contained quartz at the onset of partial melting. Therefore, the studied arclogite is probably the residue after partial melting of a precursor metabasite protolith. In order to produce a rhyolitic melt and a garnet-bearing residue (but not omphacitic pyroxene), the degree of melting must have been low and pressure must have exceeded 1.0 GPa. We have constrained the P-T conditions of equilibration and possible partial melting of the xenolith by intersecting the equilibrium curves provided by the Grt-Cpx geothermobarometer with the isomekes defined by the quartz-in-garnet elastic geothermobarometer. The resulting values – 970-1060 °C, 1.6-1.9 GPa – locate the origin of the studied arclogite xenolith at a minimum depth of about 55 km in the arc root.

This is one of the first and most straightforward examples of the reworking of the sub-arc crust by partial melting, with the production of felsic melts and a highly residual and dense restitite.

GEOTECHNICAL APPLICATIONS OF ALKALI ACTIVATED VOLCANIC ASHES

Costa Letizia Teresa¹, Russo Giacomo¹, Cappelletti Piergiulio¹, Vitale Enza¹, Rispoli Concetta¹, Graziano Sossio Fabio²

¹EARTH SCIENCES, University of Naples Federico II, Italy, ²PHARMACY DEPARTMENT, University of Naples Federico II, Italy

Due to their poor mechanical performances, soft clay-rich soils are considered not suitable as construction materials in civil works, and in most cases, they are placed in disposal as wastes. Soil improvement by the addition of traditional binders (lime and cement) is widely accepted as a sustainable solution for their reuse. Nevertheless, the production of traditional binders is undoubtedly responsible for high rates of CO₂ emissions into the atmosphere, due to the high processing temperatures. An eco-friendlier alternative is the use of alkali-activated materials as sustainable binders with a Zero Impact CO₂ emission process. Alkali-activated binders are cementitious materials formed by the reaction of precursors rich in silica and alumina with a solution of alkaline salts, obtaining a mixture of gels and crystalline compounds that eventually harden in a new strong matrix [Verdolotti et al., 2008]. Several studies show the effectiveness of artificial materials with pozzolanic activity (fly ash, ground granulated blast furnace slags, etc.) as precursors of alkali-activated binders, whereas less attempt has been devoted to the alkali activation of natural pozzolanic materials as green and sustainable binders. A systematic study on this topic has been started at the Department of Earth Sciences, Environment and Resources of University of Napoli Federico II by a multidisciplinary and multiscale approach, in the perspective of developing sustainable, not traditional binders for soil improvement. In this study, the chemo-physical evolution of natural pozzolanic materials during activation has been focused on. The two materials selected are two different volcanic ashes from Mount Etna, sampled respectively in the localities Milo and Acireale, CT, after the recent eruption of February 2021. An extensive mineralogical characterization of raw materials has been performed. Alkali-activation solutions with different molar ratios of fundamental constituents (e.g. SiO₂, Na₂O, Al₂O₃) have been considered in order to investigate their influence on the alkali-activation. In the paper, some results of X-Ray diffraction, Fourier-Transform InfraRed Spectroscopy, Scanning Electron Microscopy with Energy Dispersive Spectroscopy, and Mercury Intrusion Porosimetry performed on treated samples for the analysis of chemo-physical evolution at particle and microstructure levels are presented and interpreted. Further development of the research will be devoted to the link between the microscale evolution and the macroscopic behavior of the treated materials, which will be checked by a specific mechanical testing program.

Verdolotti, L., Iannace, S., Lavorgna, M., Lamanna, R., 2008. Geopolymerization reaction to consolidate incoherent pozzolanic soil. *J. Mater. Sci.* 43, 865–873.

PARTIAL AQUEOUS OXIDATION OF MAGNETITE TO MAGHEMITE - MECHANISTIC ASPECTS

Couasonn Thaïs¹, Desmau Morgane², Blukis Roberts¹, Benning Liane G.¹

¹Interface Geochemistry, GFZ German Research Center for Geosciences, Germany, ²Synchrotron DESY, Deutsches Elektronen-Synchrotron DESY, Germany

Iron oxide nanoparticles such as magnetite ($\text{Fe}^{\text{II}}\text{Fe}^{\text{III}}_2\text{O}_4$) are attractive materials for industrial applications due to their biocompatibility, magnetic and electronic properties, ease of functionalization, and low production costs. Whether in biomedicine, energy storage, environmental remediation, or catalysis such as heterogeneous Fenton oxidation, magnetite nanoparticles are exploited in aqueous solutions. The nanoparticles are immersed for instance in body fluids in biomedicine, surface water in environmental remediation, or aqueous electrolyte amended with hydrogen peroxide H_2O_2 during heterogeneous Fenton oxidation catalysis. However, magnetite nanoparticles are known to be relatively unstable in water, and easily oxidize to a ferric maghemite mineral ($\text{Fe}^{\text{III}}_2\text{O}_3$). As the specific properties for the above-mentioned applications are different for the two minerals, partial oxidation of magnetite in an aqueous solution could hence affect the efficiency of their use in the targeted industrial applications. Thus, it is necessary to develop a robust approach to determine and quantify the phase transformation of magnetite to maghemite in aqueous solutions.

The two iron oxides minerals exhibit a cubic spinel structure and have almost identical unit cell lengths ($a=0.839$ nm and 0.835 nm). Such similarity in structure and composition leads to an overlap of the signals when characterized using conventional mineral characterization techniques such as Raman and infrared spectroscopy, X-ray photoelectron spectroscopy, and X-ray or electron diffraction methods. Here, we present a novel characterization method based on conventional X-ray diffraction (XRD) technique to study the transformation/corrosion of synthetic nanoscale magnetite in aqueous water in presence of various concentrations of molecular O_2 , and in presence of hydrogen peroxide H_2O_2 . The combination of synchrotron-based technique X-ray absorption spectroscopy (XAS) and conventional XRD allowed us to characterize and quantify the corrosion and transformation of our magnetite nanoparticles into maghemite. For each condition, quantification of magnetite/maghemite ratio based on oxidation and valence state of iron in XAS was compared to the ratio estimated from the position of (511) XRD reflection. The novel method for quantification of the phase transformation of magnetite to maghemite in aqueous solutions allowed to unravel the controls of magnetite partial oxidation in various aqueous systems and allow further study on the role of other oxygen-based transient species affecting magnetite surface reactivity.

Keynote

**PLANETARY ZIRCONS: INVESTIGATING SOURCES OF AGE
RESETTING**

Crow Carolyn¹

¹Geological Sciences, University of Colorado Boulder, United States

Accessory phase geochronology has greatly benefited from the improved spatial resolution of analytical techniques such as electron backscatter diffraction, NanoSIMS, and atom probe tomography. These advancements have been particularly useful for investigating zircons that have witnessed the extreme pressure and temperature conditions in impact structures. These grains often host a range of shock microstructures that have a variable, and sometimes unknown, influence on zircon geochronology. In this talk, I will use zircons from the Apollo collection to demonstrate why conventional methods are not always adequate for characterizing these complex grains, and the advantage of high spatial resolution NanoSIMS in identifying sources of age disturbance. I will also highlight some of the challenges of using these higher-spatial resolution techniques, as well as some current work that will give insights into the best practices for coordinated geochronologic, geochemical, isotopic, and structural analyses of accessory phases. As we move forward in the decade of planetary sample return, the insights gained from these studies will help inform our analytical protocols and improve our ability to unravel complex geologic histories on other planets.

GRANITOID ECLOGITE-FACIES GNEISSES IN THE WESTERN GNEISS REGION GIANT (U)HP TERRAIN, NORWAY: THE ROLE OF WATER AND IMPLICATIONS FOR BUOYANCY DURING SUBDUCTION

Cuthbert Simon¹, Włodek Adam¹

¹Faculty of Geology, Geophysics and Environmental Protection, AGH University of Science & Technology, Poland

(U)HP terranes are often dominated by granitoid gneisses whose physical properties must have influenced the tectonic evolution of orogens, yet their (U)HP mineralogy is usually poorly preserved. To gain insights into density evolution, compositions of common granitoid gneisses and metabasic eclogites in the Western Gneiss Region (WGR) giant HP-UHP terrane, Norway, were used to generate isochemical phase diagrams and rock densities across the same P-T space. For examples in the southern WGR, where metagranitoid HP mineral parageneses have survived retrogression sporadically over a wide area the mineral assemblages are well reproduced by the model calculations. The density pattern for all modeled compositions shows a strong gradient between medium- and low-P facies into eclogite facies, while under eclogite facies conditions a wide P-T realm has densities that vary little, except for a sharp step at the quartz-coesite transition. Hence if metamorphic transformations are efficient during subduction most lithologies will undergo a rapid increase in density above about 1.7 GPa. Mafic rocks become negatively buoyant with respect to mantle rocks while common granitoid lithologies achieve densities slightly less than dry mantle even under coesite-stable conditions. Hence felsic compositions would have tended to remain slightly positively buoyant with respect to the mantle unless the latter was serpentized. However, where large eclogite massifs are common as in the WGR they may contribute to a higher average density.

Mafic eclogite in southern WGR gneisses has zoned garnet with amphibole and epidote inclusions in their cores, suggesting that initially, dry gabbro experienced an ingress of water under amphibolite facies conditions prior to their conversion to eclogite. Garnets show a network of healed fractures of identical composition to unfractured rims, interpreted to result from dehydration of an amphibolite (or blueschist?) paragenesis and hydro-fracturing, also supported by macroscopic omphacite fracture-fills in all HP lithologies. The modeling gives insights into the evolution of density during retrogression. Mafic to tonalitic compositions favor low phengite, omphacite-rich parageneses that require ingress of water in order to retrogress to lower density parageneses. Granitic compositions have more phengite at high pressure, which decomposes and dehydrates spontaneously upon decompression, so would have undergone a rapid reduction in density, enhancing uprise through buoyant upthrust. However, where lack of water retarded retrogression in mica-poor lithologies, higher densities may have persisted. Water, then, plays a key role in the density and buoyancy evolution of granitoid-dominated, subducting crust. Thus in the southern WGR transformation of dry, granulite metagranitoids to omphacite-garnet gneiss was associated with a substantial ingress of water, but limits to its availability resulted in survival of unreacted, low-density rock volumes. The metamorphic transformations predicted by the modeling would, if efficient, have increased the density of the predominant mass of felsic rocks in the WGR, but not quite to the extent that it could become negatively buoyant. During exhumation, the sharp density gradient in P-T space associated with feldspar formation and reduction in garnet would have enhanced buoyancy and perhaps acted to accelerate exhumation. Partial melting at this stage would have further enhanced the buoyant upthrust.

Al, Si INTERDIFFUSION UNDER LOWER MANTLE CONDITIONS: ANALYTICAL TEM STUDY OF Al-BEARING BRIDGMANITE

Czekay Laura¹, Miyajima Nobuyoshi¹, McCammon Catherine¹, Frost Daniel¹

¹Bayrisches Geoinstitut, Germany

Earth's lower mantle is considered to consist of 80% MgSiO₃ bridgmanite (Brg) by volume that contains significant amounts of aluminum (Al). Al can be incorporated by substituting for silicon (Si), with charge balance provided through the formation of oxygen vacancies (OV) or by charge-coupled (CC) substitution of magnesium (Mg) and Si by 2Al. Previous theoretical studies on deformational strain rates show that the key mechanism for deformation in Brg is a diffusion-controlled creep of the slowest element, Si. This study aims to investigate Al, Si interdiffusion in Brg experimentally. The Brg diffusion couples for the interdiffusion experiments were synthesized from 0-5 mol.% Al₂O₃-bearing MgSiO₃ enstatite at 24 GPa and 2023 K using conventional multianvil apparatuses. The recovered samples were analyzed by a transmission electron microscope (TEM) equipped with an energy-dispersive X-ray spectrometer (EDS). In TEM-EDS, compositions on the nanometer scale are evaluated and then used to infer Al substitution mechanisms in Al-bearing crystalline bridgmanite diffusion couples. The crystal orientation and lattice defects in the couples are also characterized by TEM.

The interdiffusion coefficients resulting from the diffusion experiments were $D_{\text{Si-Al}} = 5(1) \times 10^{-20} \text{ m}^2/\text{s}$ (3.5 annealing hours), and $D_{\text{Si-Al}} = 3(1) \times 10^{-20} \text{ m}^2/\text{s}$ (7 annealing hours) at 24 GPa and 2023 K. Judging from 2-dimensional element distributions in EDS chemical maps, grain boundary diffusion did not influence the obtained diffusion profile and unaffected interdiffusion could be measured. Compared to the previously reported Si self-diffusion coefficient $1(1) \times 10^{-18} \text{ m}^2/\text{s}$ at 25 GPa and 2073 K (Yamazaki et al. 2000), the current results seem to suggest a slower diffusion rate. For further insight, TEM samples will be thinned further to increase the spatial resolution of the EDS measurements. In addition, strategies such as a reference measurement on a diffusion sample with a brief heating period, i.e., zero-time diffusion experiment, will be carried out for signal deconvolution in the diffusion profiles.

We plan to perform more diffusion experiments on bridgmanite with different temperatures and compositions to obtain the temperature- and OV concentration dependencies of the diffusion-controlled creep rate. The resulting data will be used to place limits on the deformational strain rates of bridgmanite in the lower mantle.

CHEMICAL AND MINERALOGICAL CHARACTERIZATION OF BOTTOM ASHES (BA) FROM MUNICIPAL SOLID WASTE INCINERATION (MSWI)

De Matteis Chiara¹, Mantovani Luciana¹, Funari Valerio², Dinelli Enrico³, Tribaudino Mario¹

¹Dipartimento di Scienze Chimiche, della Vita e della Sostenibilità Ambientale, Università di Parma, Italy, ²ISMAR-CNR Bologna Research Area, Istituto Nazionale delle Ricerche, Istituto di Scienze Marine, Italy, ³Dipartimento di Scienze Biologiche, Geologiche e Ambientali, Università di Bologna, Italy

Although the term “Anthropocene” and its origin is debated and not shared by all the scientific community, the impact that man and his activities have on the environment are evident. The main products of this period can be represented by the huge quantity appearance of new materials as anthropogenic minerals, cement and metallic materials, plastic polymers and spheroidal carbonaceous particles. Deep and critical knowledge of everyday life products and goods, their provenance and their potential reuse can be a good starting point to respect and protect the environment. Although the use of separate waste collection is constantly growing (about 65% on average in Italy in 2016, ISTAT 2017), we still have huge amounts of undifferentiated waste (about 89 kg/inhabitants pro years, ISPRA 2017), with the consequent rise of the related residual outputs. Bottom ashes (BA) are, together with fly ashes, the modification of the undifferentiated waste after an incineration process. BA are currently classified by the European Waste Catalogue (EWC) as industrial non-hazardous waste, but a focal point debated after the European Council Regulation 2017/997 points to the potentially harmful elements bearing phases (both glass and minerals), their identification and characterization as well as their weathering behaviour. For these reasons, the main goal of this work is to measure the composition of this potential raw materials and to assess comprehensively the potential risks for environment and human health but also to evaluate their potential re-use scenarios. In this work, BA from five northern Italy Waste-to-Energy (WtE) plants were sorted by different grain size. For each grain size, X-ray fluorescence (XRF), X-ray powder diffraction (XRD) and Rietveld refinement, thermogravimetric analysis (TGA) and leaching test were performed. XRD analysis showed a similar mineralogical composition between BA of the selected WtE plants and the different grain sizes; the mineralogical phases identified belong mainly to silicates, carbonates, sulfates, and metal oxides. Rietveld refinement showed a prevalence of an amorphous fraction (between 60 and 90 wt. %) in each grain size of BA from different WtE plants. The amount of mineralogical phases analysed varies between the different WtE plants and this is probably due to the different input of waste. Silicates are most present in large grain size while carbonates and Ca-rich hydrated phases in smaller ones. XRF analysis confirms this opposite trend between Si and Ca and grain size: Si increases in the major grain size while Ca decreases and viceversa. Elements like Rb, Zr, K and Na follow the Si behaviour, whereas the Ca trend is followed by Zn, Cl and S. Other elements like Fe and Al show a different trend possibly depending on different incinerators. TGA analysis, conducted between 30°C and 800°C, showed a continuous and more pronounced mass loss in the smaller particle sizes; we also noticed two temperature ranges with higher mass loss, related to de-hydration and de-carbonation processes. Leaching test showed higher extraction in fine-grained fractions and the release of potentially harmful elements such as Pb, Zn and Cr is different in the five WtE plants analysed. In some cases, the concentrations of these elements found in the eluate exceed the regulatory limits, being possibly a detrimental factor for their recycling. In addition, sequential extraction procedures are in progress to obtain an exhaustive mineralogical characterization and understand metal partitioning in crystalline and amorphous phases.

XRF AND XANES ANALYSIS IN BOTTOM ASHES FROM MUNICIPAL SOLID WASTE INCINERATOR (MSWI)

De Matteis Chiara¹, Mantovani Luciana¹, Pollastri Simone², Tribaudino Mario¹

¹Dipartimento di Scienze Chimiche, della Vita e della Sostenibilità Ambientale, Università di Parma, Italy, ²Elettra, Sincrotrone Trieste, Italy

Waste management is one of the major challenges in our society. As an example, each year in Italy about 30 million tons of municipal waste are produced, of which 5.3 million are disposed of in incinerators, and consequently about one million tons of ashes are produced.

Recycling the ashes from municipal solid waste incinerators (MSWI) as a secondary raw material is an actual goal and several processes have been proposed, like inclusion in ceramics or in concrete. However, any form of recycling requires an assessment of the potential pollution for the environment and health risks. This can be achieved through a detailed analysis of the chemical and mineralogical composition of MSWI and how it changes when subjected to aging, leaching, and weathering. In general, BA are made by crystalline phases, i.e. silicate, carbonate, oxides, sulfates, amorphous glass, and metallic inclusions. They are mainly composed of Si, Al, Fe, Ca, Mg, K, Na, S, Cl. However, bottom ashes contain also potentially dangerous elements (PTE) such as Zn, Pb, Cu, Cr, and Ni. Their actual danger depends on the mineralogical environment in which they are found, which controls the potential release in the environment, so for any potential reuse, it is important to determine their speciation. A useful technique to identify element speciation is X-ray absorption spectroscopy (XAS); in our case, we focused the study in the XANES region (X-Ray Absorption Near-Edge Structure) which is sensitive to the oxidation state and local environment of specific chemical elements. On few grains (sized 0.5 - 1 mm) of bottom ashes from a WtE plant, SEM-EDS mapping, XRF mapping, and XANES measurements were performed.

Zn, Cu, Cr, Ni, and Pb were analyzed, finding their presence by SEM-EDS and XRF induced by synchrotron radiation, and detailing the environment by XANES. Preliminary results showed that PTE are present in different oxidation states and structures: in metallic form, amorphous phases, silicates, and carbonates. A preliminary look at the XANES data collected at the Cr K-edge on different clasts permits to exclude the presence of Cr⁶⁺, as all the collected spectra have features resembling that of Chromite (Cr³⁺). Also, all the XANES data collected at Pb L3-edge on various clasts are almost identical, and from the comparison with Pb metal foil and PbO standard compound spectra, we can qualitatively derive that Pb is oxidized in all the clasts. Cu appears to be present both in metal and oxide form. The precise oxidation state and coordination geometry of all the investigated chemical elements will be determined through linear combination fit (LCF) analyses.

Keynote

REDOX RECORD OF THE SERPENTINIZED FOREARC MANTLE WEDGE

Debret Baptiste¹

¹Institut de physique du globe de Paris, France

Subduction zones are active sites of chemical exchange between the Earth's surface and deep interior and play a fundamental role in regulating planet habitability. However, the mechanisms by which redox-sensitive elements (e.g., iron, carbon, and sulfur) are cycled during subduction remains unclear. Here I examine forearc serpentinite clasts recovered during the IODP expedition 366 from deep-sea drilling of mud volcanoes formed above the Mariana subduction zone in the Western Pacific. I show that the recovered ultramafic clasts record different stages of fluid/rock interactions between the slab and the mantle wedge at a temperature ranging from 200°C to 400°C. The serpentinitization of the forearc at high temperature (>350°C) produces dramatic $\delta^{56}\text{Fe}$ variation. Negative correlations between serpentinite bulk $\delta^{56}\text{Fe}$, fluid-mobile element concentrations (e.g., B, As) and $\text{Fe}^{3+}/\Sigma\text{Fe}$ suggest concomitant oxidation of the mantle wedge through the transfer of isotopically light iron by slab derived fluids. This process must reflect the transfer of either carbonate-bearing fluids that preferentially complex isotopically light Fe. The presence of abiotic carbonaceous matter within high-temperature clasts shows that molecular hydrogen production associated with forearc serpentinitization represents an efficient reducing mechanism for the conversion of slab-derived carbonates into abiotic organic compounds. This emphasizes the need to consider the forearc mantle as an important reservoir of abiotic organic carbon in subduction zones.

MINERALOGICAL STUDIES OF THE W-Sn VEIN SKARNS OF MONTE TAMARA (NUXIS, SULCIS DISTRICT): INSIGHTS FOR STRATEGIC MINERALS EXPLORATION IN SW SARDINIA (ITALY).

Deidda Matteo Luca¹, Moroni Marilena², Naitza Stefano¹, De Giudici Giovanni Battista¹, Fancello Dario¹, Idini Alfredo¹

¹Dipartimento di Scienze Chimiche e Geologiche, Università degli Studi di Cagliari, Italy, ²Dipartimento di Scienze della Terra, Università degli Studi di Milano, Italy

Skarn deposits are a relevant source of critical raw materials such as W, Sn, and In. Recent studies conducted in South Sardinia pointed out the relationships between various Sn-W-Mo deposits and the early Permian (289-286 Ma) F-bearing, ilmenite-series ferroan granites (e.g., Sulcis pluton). This new evidence triggered a broad re-examination of granite-related deposits including skarn deposits hosted by Cambrian limestones of the low-grade Variscan basement of the Sulcis district (SW Sardinia). With this purpose, field investigations and OM, SEM-EDS, EMPA, and LA-ICP-MS observations, and analyses have been conducted on the skarn ores of Monte Tamara (Nuxis, northern Sulcis) where scheelite has been reported in the old San Pietro and Sinibidraxiu mines. The San Pietro mine exploited a 1-5 m thick and 70 m deep, steeply dipping skarn orebody located at the tectonized contact between early Cambrian sandstones and limestones. The orebody includes layers of Grt-Cpx-Wo, magnetite, and Zn-Pb-Cu-Fe sulfide bands. Prograde and retrograde stages with oxides and sulfides can be recognized. Clinopyroxene is the foremost mineral of the prograde stage; garnets (andradite-grossular) are usually dark green with typical anomalous birefringence and distinctly zoned (Fe-rich cores and Al-rich rims). Hematite turned to mushketovite, and Mo-rich scheelite, followed by In-bearing cassiterite, occasionally occur in the prograde assemblages. Amphiboles and epidotes mark the retrograde stage, together with abundant Zn-Cu-Fe-Pb sulfides and accessory molybdenite, stannite, bismuthinite, and Bi-Ag-Pb sulfosalts. At San Pietro, dominant sphalerite displays highly variable Fe, Mn, and Cd contents. Relict-looking blebs of Fe-Mn-poor Sp are scattered in high-Fe-Mn Sp where Sn EMPA peaks may correlate with cassiterite-stannite micro-inclusions. Galena composition suggests localized intergrowths with micro-inclusions of bismuthinite, Bi-Se, and Bi-Te sulfosalts. The stannite-sphalerite geothermometer provided a temperature range of 325-200°C for the sulfide stage. The Sinibidraxiu old mine exploited a 1,5 m thick and 60 m deep columnar body, hosted in early Cambrian marbles. It consists of a sphalerite-wollastonite assemblage with late sulfides, quartz, and calcite, hosting cm-sized arsenopyrite and scheelite. Scheelite is Mo-poor; Sn-, other Mo-phases and Bi-phases are absent. High-Fe Sp, rimmed by low-Fe Sp and blebby galena, is finely intergrown with wollastonite cockades. The results from this study suggest that a wide range of skarn-related mineralizing phenomena occurred in the Monte Tamara area. Both orebodies resulted from a structurally controlled migration of metasomatic fluids inside the hosting carbonate formation. Mineral zonation and composition of the San Pietro skarn point towards skarn development under varying fO₂ conditions, oxidizing then rapidly turning to moderately reducing within the prograde W-Sn skarn stage and into the sulfide stage. The features of the Sinibidraxiu orebody (e.g., Mo-poor, As-devoid scheelite) suggest a formation from reducing metasomatic fluids but S-poor compared to San Pietro, probably at more distal environments (e.g. low Sn-Bi contents). From this point of view, the Monte Tamara area still maintains an economic potential, linked to the possible presence of proximal skarn ores at depth; thereby representing a key area for further exploration for granite-related strategic and critical metals in SW Sardinia.

NUMERICAL STUDY OF MECHANICAL PROPERTIES OF Mg_2SiO_4 GLASSES

Delbecq Valentin¹, Carrez Philippe¹, Cordier Patrick¹, Paul Jean-François¹, Pipolo Silvio¹

¹University of Lille, France

$(\text{Mg,Fe})_2\text{SiO}_4$ olivine is the main constituent of the upper mantle of the Earth. A recent experimental study has shown that under low-temperature and high-stresses conditions, olivine deforms by grain boundary sliding (GBS) along amorphized grain boundaries. Thus, the rheology of amorphous olivine (hereafter referred to as a-olivine) appears to be one of the keys missing to a better understanding of the GBS mechanism in olivine polycrystals. However, as it is well known that amorphous olivine is highly difficult to quench, we propose here to study the mechanical properties of a-olivine through molecular dynamics simulations. MD simulations are therefore performed on Mg_2SiO_4 glass in order to compute the elastic properties of glass (i.e. Young's modulus, Poisson's ratio, or shear modulus). Moreover, we show that stress-strain curves of a-olivine show stress drops which highlight the viscoplastic behavior of the glass.

TEXTURAL ANALYSIS OF CANDOGLIA MARBLE

Delledonne Chiara¹, Merlini Marco¹, Zucali Michele¹, Marinoni Nicoletta¹, Poli Stefano¹, Scolari Marco¹, Canali Francesco¹

¹Dipartimento di Scienze della Terra Ardito Desio UNIMI, Italy, chiara.delledonne@studenti.unimi.it, marco.merlini@unimi.it, michele.zucali@unimi.it, nicoletta.marinoni@unimi.it, stefano.poli@unimi.it, marco.scolari@duomomilano.it, dl.cantieri@duomomilano.it

Candoglia marble is a unique natural material, one of the most valuable stones used in Cultural Heritage due to its relevance from a historical, cultural, and architectural point of view. Since the 14th-century Candoglia marble has been used exclusively by the Veneranda Fabbrica del Duomo for construction and maintenance of the Milan Cathedral in Italy (in Italian: Duomo di Milano). Marble was used as cladding, decoration, and building material for the supporting structures, statuary, and sculptures of the Cathedral. In the present study, the marble samples investigated were selected in the Cava Madre close to Candoglia (VCO; Piemonte-NW Italy) in the Val d'Ossola, a few kilometers west of the mouth of the Toce river in Lake Maggiore. The samples represent the several chromatic and composition varieties of Candoglia marble. The prevalent colorations are white, pink, and grey; it is composed of around 80-85% of calcite (CaCO₃) and 15-20% of minor accessory minerals, such as phlogopite (KMg₃[(F,OH)₂AlSi₃O₁₀]) and pyrite (FeS₂), concentrated along with discrete layers. The purpose of this research is to investigate the texture of Candoglia marble as it is characterized by a particular schistosity and there are no previous studies on this matter.

Crystallographic preferred orientation of calcite was determined with the Maud software (Lutterotti et al.; 1997) used to analyze neutron diffraction raw data (experimental setup similar to the one described in Zucali et al. 2019). The results indicate that crystals of calcite are oriented with the c-axis perpendicular to the schistosity plane of the marble. The data correlate with textural analysis performed on other Alpine marbles (Zucali et al., 2019), where preferred orientation is evident. On the contrary, Candoglia marble in terms of crystallographic orientation is different, if compared with other ornamental stones, such as Carrara Marble (Zucali et al., 2019). These features may correlate with long-term durability, especially related to daily and seasonal thermal excursions. Marble is sensitive to temperature variations due to the anisotropy in the coefficient of thermal expansion along with the different crystallographic directions of calcite, this has an expansion along the c-axis and a contraction along the a-axis during heating, while behaves in the opposite way during cooling. Laboratory thermal cycling of different marbles is in progress to correlate the effects of preferred orientation with the long-time stability of these materials.

SILICATE AND METALLIC MINERALOGY THE PYROMETALLURGICAL Cu-SLAGS FROM THE NORTH SUDETIC BASIN, POLAND AND THE IMPLICATIONS FOR ENVIRONMENTAL STABILITY

Derkowska Katarzyna¹, Kierczak Jakub¹

¹Institute of Geological Sciences, University of Wrocław, Poland

In this contribution, we will present the mineralogical and geochemical analyses of the 18th and 19th-century industrial residues originating from copper processing led in the North Sudetic Basin, Poland. We focus on primary silicate and metallic assemblages and their relation in texturally different slags. Four dominant silicate phase assemblages are distinguished and consist of glass and synthetic analogs of natural minerals: 1) amorphous (glassy) type, 2) glassy type with melilites (alumoåkermanite, åkermanite, ironåkermanite), 3) pyroxene type (pigeonite, augite, hedenbergite, diopside) and 4) crystalline type with leucite, clinopyroxenes, anorthite, and wollastonite. Phases present strong variations in the chemical composition, especially in the matter of Ca and Fe content. The mineralogical types are associated with different smelting technological processes and are reflected in sample's bulk chemical composition. Metallic phases (sulfides, metallic compounds, and metals), constitute critical industrial wastes components since they concentrate potentially toxic metal(loid)s. We distinguished 3 dominant types of metallic phases: 1) copper-iron-sulfur with the following subtypes: 1a) bornite-pyrrhotite, 1b) chalcocite, and 1c) chalcopyrite, 2) metallic copper and 3) iron-phosphorous (Fe-P) type, all of which vary in size, and affinity to sample's texture since Fe-P metallic phases tend to appear in amorphous slags and copper-rich phases are more common within crystalline samples. In the presentation, we will also discuss the frequency of the metallic phase's appearance, and the chemical diversity in relation to natural sulfides. Weathering signs are not common but present in the analyzed set of slags. The mineralogical data show that, among the primary phases, Cu-rich assemblage, namely bornite is the most easily weathered, followed by chalcocite and metallic copper. Iron-dominated phases proved to be the most resistant to secondary alterations. Secondary phases are also valuable indicators of supergene alterations and conditions of slags deposition. We recognized a set of sulfates (mainly Cu-sulfates) of varying solubility, including brochantite, devilline, antlerite and gypsum.

This study was funded by the National Science Center, Poland research project number UMO-2019/35/N/ST10/04524 to KD.

NANOPARTICULATE GOLD IN ULTRAMAFIC-HOSTED MASSIVE SULFIDE DEPOSITS FROM WESTERN CUBA

Domínguez-Carretero Diego¹, Proenza Joaquín A.¹, González-Jiménez José María², Torres Harlison³, Aiglsperger Thomas⁴, Jiménez-Franco Abigail¹, García-Casco Antonio²

¹Departament de Mineralogia, Petrologia i Geologia Aplicada, Facultat de Ciències de la Terra, Universitat de Barcelona, Spain, ²Departamento de Mineralogía y Petrología, Facultad de Ciencias, Universidad de Granada/ Instituto Andaluz de Ciencias de la Tierra (CSIC-UGR), Spain, ³Calle 42, 63A-198, Medellín, DataRock Ingeniería SAS, Colombia, ⁴Department of Civil Engineering and Natural Resources, Luleå University of Technology, Sweden

The Habana-Matanzas ophiolites (western Cuba) host several hydrothermal ultramafic-hosted Cu-Au-Co rich massive sulfide deposits (e.g. Loma Majana and Salomón). The ore mineralogy of these deposits consists of pyrrhotite, pyrite, and chalcopyrite, with minor Co-Fe-Ni arsenides/sulfarsenides (mainly safflorite and cobaltite), gold (electrum), and relicts of Cr-spinel grains. Gold abundance correlates with the presence of Co-Fe-Ni arsenides/sulfarsenides.

The processing of a representative sample from the Loma Majana deposit at the Hydroseparation Laboratory of the University of Barcelona (www.hslab-barcelona.com) allowed the separation of heavy mineral concentrates with gold particles up to 30 µm. Single-spot analyses of these gold particles by means of electron probe microanalysis (EPMA) reveal the average composition of 57 at.% Au, 37 at.% Ag and 4 at.% Fe, approaching electrum. Additional analysis by means of Field Emission Scanning Electron Microscopy (FE-SEM) also reveals the presence of several gold particles (nano to micrometer-sized) hosted in Co-Ni-Fe-bearing arsenides and sulfarsenides within pyrrhotite-pyrite. The analyses of these gold grains using High Resolution Transmission Electron Microscope (HRTEM) on a thin-foil (~50 nm, thickness) obtained by means of Helios650 Focused Ion Beam (FIB). The thin foil was cut through the contact pyrrhotite-arsenide-sulfarsenide and showed a systematic association of gold nanoparticles (10 nm – 1 µm) with the arsenides (safflorite-rammelsbergite-löllingite solid solution series). The HRTEM observations indicate that gold nanoparticles are predominantly located at the arsenide-sulfarsenide boundary. The measured (2.5 Å) d-spacing of these particles is close to the 2.35 Å corresponding to the {111} plane of pure gold. However, HRTEM elemental maps also indicate that these gold grains contain significant amounts of Ag, suggesting a certain degree of alloying during the mineralizing process. The High Magnification TEM images show that gold domains have a common lattice orientation to the host arsenide-sulfarsenide. The association of gold with the As-rich minerals in the studied samples clearly attests the role of As in the nanoscale partitioning of gold, such as observed in natural and experimental work applied to magmatic and hydrothermal systems. The nanostructural relationship of the gold particles with their larger host counterparts seems to indicate an exsolution-induced process related to the replacement of pre-existing Co-Fe-Ni arsenides during a sulfurization mechanism. Finally, it is worth noting that the deposits in the Habana-Matanzas region are hosted in the supra-subduction zone (SSZ) peridotites (fore-arc mantle peridotites), as opposed to the most common slow and ultra-slow mid-ocean ridges setting for similar ultramafic-hosted massive sulfide deposits related to oceanic core complexes.

IRON OXIDATION STATE OF FERROPERICLASE COEXISTING WITH CARBONATE AND DIAMOND: IMPLICATIONS FOR THE ORIGIN OF SUPERDEEP DIAMONDS

Dominijanni Serena¹, Stagno Vincenzo², McCammon Catherine¹, Miyajima Nobuyoshi¹, Irifune Tetsuo³, Frost Daniel¹

¹Bayerisches Geoinstitut, University of Bayreuth, Germany, ²Department of Earth Sciences, Sapienza University of Rome, Italy, ³Geodynamics Research Centre, Ehime University, Japan

Carbon is transported into the deep mantle in the form of both carbonates and elemental carbon. Natural evidence of carbon from Earth's interior comes from sub-lithospheric diamonds (SD), which host carbonate phases in equilibrium with mantle minerals, mostly ferropericlasite. Its chemical variability as trapped inclusions has been often explained as resulting from local redox reactions with subducted oxidized fluids. Although several studies have emphasized the role of oxygen fugacity (fO_2) on the fate of subducted carbonates, little is known about the Fe oxidation state in ferropericlasite at redox conditions where both diamond and carbonate (either solid or liquid) coexist.

We investigated the effect of oxygen fugacity, pressure, and temperature on the ferric/ferrous ratio of ferropericlasite. Experiments were performed at pressures of 25 and 45 GPa and temperatures between 1500 and 1700°C using the multi-anvil apparatus. A starting composition made of a mixture of natural magnesite, graphite, synthetic ferropericlasite, iridium powder (to act as a redox sensor), and Ni metal was chosen as representative of a simplified carbonated lower mantle mineral assemblage. Sample characterization was performed firstly using the scanning electron microscope and the electron microprobe for chemical analyses and textural observations, and additionally using Focused Ion Beam and Transmission Electron Microscope to explore possible evidence of redox reactions at the nanoscale. We conducted point source ⁵⁷Fe Mössbauer measurements on recovered run products to determine the $Fe^{3+}/\Sigma Fe$ ratio in ferropericlasite, while the fO_2 was experimentally determined using Ir as a redox sensor.

Our preliminary results provide unique information on the maximum ferric iron content that ferropericlasite can incorporate during redox-driven diamond formation and can be compared with the few data available of natural ferropericlasite inclusions in SDs. These results can be used to quantitatively model the redox state of the lower mantle at conditions where diamond forms through redox freezing of subducted carbonates.

THE IMPORTANCE OF CLAY AS MULLITE PRECURSOR IN THE FIRING OF WHITEWARES

Dondi Michele¹, Zanelli Chiara¹, Conte Sonia¹, Molinari Chiara¹, Ardit Matteo², Cruciani Giuseppe²

¹ISTEC, CNR, Italy, ²Physics and Earth Sciences Dept, University of Ferrara, Italy

Clays have a recognized technological role in whitewares (porcelain, porcelain stoneware, vitreous china, etc.) that is traditionally restricted to the milling, shaping, and drying operations, where clay minerals fulfill their function of slip stabilizer and plasticity provider. Indeed, the action of clay minerals during firing is largely underestimated, being they are considered as mere precursors of new crystalline and amorphous phases, especially mullite after kaolinite (or illite). Although several studies concerned the kinetics of mullite formation and its microstructural aspects, little is known about the quantitative degree of mullitization and its repercussion on the sintering behavior of whitewares. To fill this gap, three samples of porcelain stoneware bodies were designed with the same formulation but a different ratio between two clays containing kaolinite (with a distinct degree of structural order/disorder) and illite (or illite-rich interstratified terms). Every batch underwent a laboratory simulation of the tilemaking process and was characterized from the technological viewpoint, then by XRPD-Rietveld, SEM, and optical thermodilatometry. The degree of mullitization changed according to the clay assemblage and the structural order of kaolinite. This brought about a significant variation in the amount, composition, structure, and physical properties of the liquid phase. Increasing the amount of mullite from 4 wt. % to 12 wt. % affected some features of the melt, such as the alumina saturation index and the degree of depolymerization (ASI decreasing from 2.0 to 1.4 and NBO/T from 0.31 to 0.21) and the shear viscosity estimated at 1200°C (increasing from 4.5 to 5.1 log₁₀ Pa·s). Such differences are mirrored in the firing behavior of whitewares, and particularly sintering kinetics, the efficiency of densification, and dimensional stability at high temperature, which are improved by increasing mullitization. The degree by which clay minerals give rise to mullite (with a given chemical composition) can explain why batches with analogous chemical and mineralogical composition behave in a distinct way during firing.

COMPARING EOARCHEAN RECORDS OF CRUSTAL GROWTH IN THE NORTH ATLANTIC CRATON BETWEEN THE SAGLEK BLOCK OF LABRADOR, CANADA AND THE ITSAQ GNEISS, SW GREENLAND

Dunkley Daniel J.¹, Kusiak Monika A.¹, Whitehouse Martin J.², Wilde Simon A.³, Mieszczyk Marcin J.¹

¹Department of Polar and Marine Research, Institute of Geophysics Polish Academy of Sciences, Poland, ²Department of Geosciences, Swedish Museum of Natural History, Sweden, ³School of Earth and Planetary Sciences, Curtin University, Australia

In high-grade gneiss terranes, much of the interpretation of geological history relies on the microbeam dating of zircon, especially where it is the only mineral that survives metamorphism and deformation. This is especially the case in the Eoarchean, where most rocks of this age have been converted into amphibolite or granulite-facies gneisses. The western edge of the North Atlantic Craton (NAC) possesses large domains of Eoarchean crust. The best known is in the Itsaq Gneiss of SW Greenland, which includes the Isukasia Terrane with the best-preserved Eoarchean field relationships. On the northern Labrador Coast of Canada, the Saglek Block includes the Eoarchean Uivak Gneiss, dominated by tonalite-trondhjemite-granodiorite (TTG). Through careful sub-grain dating of zircon, the Neoarchean metamorphism and deformation that pervades the gneisses of the NAC can be rendered transparent to identify remnant Eoarchean terranes. were possibly assembled during a ca. 3.6 Ga tectonothermal event. New SIMS dating from a ~100 km section of coast between Ramah Bay and Hebron Fjord in Labrador reveals ages between 3.75 and 3.70 Ga, followed by high-grade metamorphism at ca. 3.6 Ga. Thus, the effects of a major tectonothermal event at the end of the Eoarchean, which juxtaposed terranes in SW Greenland, are also evident in the Saglek Block. However, the generations of TTG in the Saglek Block are not the same age as those in the Isukasia Terrane. Specifically, an abundance of ages between 3.75 and 3.70 Ga, and localized remnants of pre-3.85 Ga TTG crust, are found in the Saglek Block but not in the Isukasia Terrane.

Although both the Saglek Block and the Isukasia Terrane have been affected by a 3.6 Ga regional tectonothermal event, the differences between the protolith ages of the Saglek Block and the Isukasia Terrane leads us to propose a new 'Uivak Terrane' that was juxtaposed with Isukasia at the end of the Eoarchean. Similar ages to the 'Uivak Terrane' are also found in the Færingehavn Terrane of the Itsaq Gneiss in SW Greenland, suggesting the latter may include fragments of both the 'Uivak' and Isukasia Terranes, reworked during assembly of the NAC in the Neoarchean.

This research was funded by NCN grant UMO2019/34/H/ST10/00619 to MAK and UMO2016/23/P/ST10/01214 to DJD.

PROTEROZOIC DEEP CARBON - THE GRAPHITE BEARING ROCKS OF THE LOFOTEN-VESTERÅLEN AREA, NORTH NORWAY; CHARACTERISATION, ORIGIN AND THE ROLE OF FLUIDS

Engvik Ane Karine¹, Gautneb Håvard¹, Mørkved Pål-Tore², Knežević Solberg Janja¹, Erambert Muriel³, Austrheim Håkon³

¹Geological Survey of Norway, Norway, ²Department of Earth Science, University of Bergen, Norway, ³Department of Geosciences, University of Oslo, Norway

Graphite formation during granulite facies metamorphism is documented in the Proterozoic gneisses of the Lofoten-Vesterålen Complex, northern Norway. Graphite schist is hosted in sequences of banded gneisses dominated by orthopyroxene-bearing quartzofeldspathic gneiss, interlayered with horizons of marble, calcsilicates, and amphibolite. The schist displays a strong foliation and has a major content of graphite up to a modality of 39%. Quartz and plagioclase (Ab₄₇₋₉₃An₅₋₅₂), pyroxenes, biotite (Mg# = 0.67-0.91; Ti < 0.66 a.p.f.u.), and K-feldspar (Ab₁₋₈Kfs₉₂₋₉₉) or perthite (Ab₃₅₋₆₄An₃Kfs₅₀₋₆₂) are additional major phases. Pyroxene is present either as orthopyroxene (En₆₉₋₇₄Fs₂₆₋₂₉; Mg# = 0.70-0.74), as clinopyroxene (En₃₃₋₅₃Fs₁₋₁₄Wo₄₄₋₅₃; Mg# = 0.70-0.97), or both. High-ordered graphite occurs as euhedral “flakes” (i.e., flake graphite) of fine- to medium grain size, with a strong preferred crystal orientation forming the well-developed foliation contributing to the schistosity of the rock together with the crystal preferred orientation of biotite.

Although graphite usually is described in quartzitic and metapelitic rocks, or as vein deposits in the granulite facies crust, we document graphite in assemblage with metamorphic orthopyroxene. Pseudosection modeling of the plagioclase + orthopyroxene (Mg#-ratio = 0.74) + biotite + quartz + rutile + ilmenite + graphite-assemblage constrains its stability field to pressure-temperature conditions of 810-835°C and 0.73-0.77 GPa. Zr-in-rutile also supports a temperature of formation of 740-870°C.

Stable isotopic $\delta^{13}\text{C}$ in graphite schist shows values from -38 to -17‰ while $\delta^{13}\text{C}$ values of marbles range from +3‰ to +10‰. Mixed graphitic and calcite carbon samples give lighter values for the calcite ($\delta^{13}\text{C}_{\text{calcite}} = -8.65\text{‰}$ to -9.52‰) and heavier values for graphite ($\delta^{13}\text{C}_{\text{grapite}} = -11.50\text{‰}$ to -8.88‰) compared to the “pure” samples. $\delta^{18}\text{O}$ for marble shows relatively light values for calcite ranging from -15.44‰ to -7.53‰. From the stable C-isotopes, we interpret the graphite origin as organic carbon accumulated in sediments contemporaneous with the Early Proterozoic global Lomagundi-Jatuli isotopic excursion.

From petrography and mineral composition, we deduce the reaction equations producing and consuming H₂O- and CO₂-fluids leading to the stabilization of graphite and orthopyroxene. The high Mg#-ratio of biotite and pyroxenes together with a high Cl-content of apatite up to 2 a.p.f.u. indicate the importance of fluids during the high-grade formation of graphite. The results are used to discuss the origin of deep Proterozoic carbon, the petrogenetic processes of graphite deposition in granulite, the role of fluids for its formation, and the rheological weakening and strain localization in the lower continental crust.

AUTOMATED QUANTITATIVE MINERALOGY APPLIED TO ESTIMATION OF RESOURCE POTENTIAL OF NEVES CORVO TAILINGS: AN INTEGRATED APPROACH TOWARDS FUTURE REPROCESSING.

Escobar Alexandra G.¹, Relvas Jorge ¹, Pinto Alvaro MM¹, Oliveira Toscano Mafalda², Blannin Rosie³, Frenzel Max³, Bachmann Kai³

¹Faculdade de Ciências, Instituto Dom Luiz, Faculdade de Ciências, Universidade de Lisboa, Lisboa, Portugal , Portugal, ²Tailings and Waste Management Department, SOMINCOR-Lundin Mining, Neves Corvo mine, Castro Verde, Portugal , Portugal, ³HIF, Helmholtz-Zentrum Dresden-Rossendorf, Helmholtz Institute Freiberg for Resource Technology, Freiberg, Germany , Germany

Mining operations produce large quantities of mine residues disposed of in tailings dams, which are increasingly envisaged by companies as a promising source of secondary mineral resources. The potentially positive impacts of reprocessing of tailings in terms of environmental footprint, waste management, and economic valorization are now widely acknowledged by the various stakeholders along the whole value chain of mineral resources. Geochemical and mineralogical characterization of tailings represents an important component of integrated geometallurgical models, which in turn are crucial to draw accurate scenarios for environmentally responsible policies and the socioeconomic sustainability of future mining.

Neves Corvo is a world-class Cu-(Sn)-Zn VMS deposit of the Iberian Pyrite Belt, being one of the larger active base-metal mining operations in the EU. The Neves Corvo tailings show distinct chemical and mineralogical characteristics that relate to variables such as ore types, orebodies, time of storage, and particle-size distribution. Automated quantitative mineralogy of representative tailings samples from the Neves Corvo copper and zinc processing plants was obtained by Mineral Liberation Analysis (MLA) and Electron Microprobe Analysis (EPMA) used to define liberation and mineral chemistry of target minerals.

The study focuses on the speciation of deleterious elements, such as As, Sb, Hg, Tl, Bi, Co, and Cd, in target minerals of the Neves Corvo Cu-Zn tailings (chalcopyrite, sphalerite, galena). The data were combined with previously acquired physico-chemical characterization of the same group of samples. Preliminary MLA results for tailings samples from the copper and zinc processing plants gave fully liberated pyrite ranging between 67 and 69% in both of them. Conversely, the two processing plants produce significantly different tailings concerning sphalerite: fully liberated sphalerite is around 52% for the tailings of the copper processing plant and only 4% for the tailings of the zinc processing plant. Galena liberation is similar in both beneficiation processes, varying between 31 and 39%. Fully liberated chalcopyrite in the tailings from the zinc processing plant represents 26%, whereas it is ca. 34% for the copper processing plant. The results obtained so far open interesting perspectives for future reprocessing of the Neves Corvo tailings.

This study is part of the work package 1 (WP1) of ETN–SULTAN project (H2020) - European Training Network for the remediation and reprocessing of sulfidic mining waste sites. Publication supported by FCT- Project UID/GEO/50019/2019 - Instituto Dom Luiz.

PROMOTING GEOLOGY THROUGH NEW TECHNOLOGIES IN SCHOOL: CREATION OF A MINERAL CLASSROOM COLLECTION WITH AUGMENTED REALITY

Escobar Pablo¹, Barba-Brioso Cinta¹, Delgado Joaquin²

¹Crystallography, Mineralogy and Agricultural Chemistry, Seville University, Spain, ²Pablo de Olavide University, Spain

This resource was born as an idea to create an educational resource that combines the teaching of Earth Science content, such as rocks and minerals, with one of the most innovative technologies of recent years, Augmented Reality (AR). AR is a type of technology that unites the real and the virtual, allowing the incorporation of virtual elements in a real-world scenario. These virtual elements can be, for example, images, video, or audio, which facilitate a better understanding of any subject. Being a very easy to understand and use technology, it is possible to work any content and subject with AR. Due to the low presence of Geology in recent amendments of Education Laws in Spain (LOMLOE Organic Law 3/2020 from 29 December), several geological associations, colleges and societies have come together to claim the importance of teaching geology at pre-University education, since the number of students in Geology Degrees is falling every year.

The general purpose of this work is to give teachers tools for addressing geology without objection at elementary school, to enhance the interest in geological aspects since basic levels. In this case, an educational resource was created, a virtual collection of minerals for a Primary Education class with a free (or low cost) application available for Android devices in Google Play Store: Qlone®. Through this application, it is possible to scan any object by means of the device's camera, creating a 3D model of the object in question. By creating a folder in a cloud storage service, the files of the models created can be uploaded, so that anyone can access them quickly and easily. Once this is done, through another application designed to work with 3D files and augmented reality, it is possible to use the phone's camera to visualize the models of the minerals that were previously scanned. In this innovative work, the first collection of eight AR minerals has been created which, accompanied by a descriptive file about each mineral property, is presented and provided to elementary school so that the teacher can continue developing a “classroom collection” thus promoting the presence of geology in schoolchildren.

HYDROTHERMAL ALTERATION OF Cr-SPINEL AND MAGNETITE ORE FORMATION IN THE SABZEVAR SERPENTINITE (NE IRAN)

Eslami Alireza¹, Malvoisin Benjamin¹, Brunet Fabrice¹, Kananian Ali², Bach Wolfgang³, Grieco Giovanni⁴, Cavallo Alessandro⁵, Gatta G. Diego⁴

¹University of Grenoble-Alpes, France, ²University of Tehran, Islamic Republic of Iran, ³University of Bremen, Germany, ⁴Universita degli Studi di Milano, Italy, ⁵Università di Milano-Bicocca, Italy

Irregular and intermittent trail of pod-like massive magnetite ore bodies occurred in highly sheared serpentinites of the Late Cretaceous Sabzevar ophiolitic belt, northeastern Iran. Magmatic chromian spinels are preserved as relics in the host serpentinite. They show a porous alteration rim composed of patches of Cr-chlorite, a spinel of composition $(\text{Fe}_{0.6}\text{Mg}_{0.4})(\text{Cr}_{1.4}\text{Al}_{0.4}\text{Fe}^{3+}_{0.2})\text{O}_4$ (Cr-spinel II), magnetite, and ferrichromite (FeCr_2O_4). In the magnetite ore bodies, Cr-spinel II is surrounded by ferrichromite and magnetite. Two generations of magnetite are discernible around the chromian spinel: (i) ~ 20 μm -wide magnetite rim displays a SiO_2 content < 1 wt.%. (ii) larger (40 to 200 μm) magnetite rim and shows a higher SiO_2 content, ranging between 1.21 and 2.35 wt.%. A micrometer ferrichromite rim between Cr-spinel II and magnetite I was recognized with TEM. Orientation mapping at the nanoscale shows epitaxial growth of ferrichromite and magnetite on Cr-spinel II. Thermodynamic modeling indicates that Cr-spinel II and chlorite are first produced after magmatic spinel between 575 and 725 °C. Ferrichromite and magnetite are predicted to form at a lower temperature ($T < 400^\circ\text{C}$) under a high H_2 fugacity, probably associated with serpentinization. The two progressive alteration stages are interpreted as the consequences of seawater/mantle rock interaction during exhumation on the seafloor. Thermodynamic calculations also show that chromium mobility is remarkably low during spinel alteration and magnetite ore formation. Dissolution of nanoscale magnetite grains initially formed in the host serpentinite and olivine breakdown are considered as potential sources for the magnetite ore formation. Mass balance calculations indicate iron transport over distances beyond 10 meters during serpentinization. Early stages of Cr-spinel alteration are sought in other chromitite pods from the Sabzevar ophiolite, which did not reach the magnetite-ore transformation level.

GALLIUM AND GERMANIUM IN METALLURGICAL SLAGS: MINERALOGY AND POTENTIAL RECOVERY

Ettler Vojtěch¹, Mihaljevic Martin¹, Jedlicka Radim², Kribek Bohdan³, Mapani Ben⁴, Kamona Fred⁵

¹Institute of Geochemistry, Mineralogy and Mineral Resources, Charles University, Faculty of Science, Czech Republic, ²Institute of Petrology and Structural Geology, Charles University, Faculty of Science, Czech Republic, ³Czech Geological Survey, Czech Republic, ⁴Namibia University of Science and Technology, Namibia, ⁵University of Namibia, Namibia

Gallium (Ga) and germanium (Ge) are technologically essential critical elements. This study focuses on old metallurgical slags generated by processing non-ferrous metallic ores in Tsumeb, northern Namibia, containing interestingly high concentrations of these elements (up to 156 ppm Ga and 441 ppm Ge). Mineralogical investigation using a combination of XRD, SEM/EDS, and EPMA indicated that the slags were composed of olivine-, melilite- and spinel family phases, metal(loid)-rich glass, and sulfide/metallic inclusions. The EPMA and LA-ICP-MS data confirmed that major carriers of Ga were spinel-family oxides (up to 1890 ppm), and Ge was primarily bound in a glassy phase (up to 465 ppm), especially in the case of granulated slags. The abiotic extraction tests, simulating a hydrometallurgical recovery via agitation leaching, were carried out in sulfuric and nitric acids (pH = 0.2-0.3, 25 °C and 70 °C, pulp density of 1%) to determine the release of Ga and Ge from slags. Their leaching attained a steady state after 6 hours for original granulated slags after 2 hours for finely ground slags. The extractabilities of both Ga and Ge were slightly higher for the high-temperature trials. The overall efficiency of the extractabilities of Ga and Ge from slags attained 86% and 97%, respectively. Our investigation indicates that understanding the specific binding of critical elements is crucial for their potential recovery from slag materials. This study was supported by the Czech Science Foundation project (GAČR 19-18513S).

CALCAREOUS NANNOFOSSILS – A NEW TOOL FOR UNDERSTANDING HISTORIC MORTAR PRODUCTION

Falkenberg Janina¹, Mutterlose Joerg¹, Kaplan Ulrich²

¹Institute of Geology, Mineralogy and Geophysics, Ruhr Universitaet Bochum, Germany, ²Eichenallee 141, Gütersloh, D-33332, Germany, janina.falkenberg@rub.de joerg.mutterlose@rub.de u.k.kaplan@t-online.de

Calcareous nannofossils are < 30 µm large calcitic remains of single-celled marine photoautotrophic algae. Since their appearance in the Late Triassic (about 209 Ma) these algae have been important primary producers in the oceans and are thus present in many marine sediments. These sediments are used as raw material for lime-based mortars and mortar-based materials (plaster, render, color version). To produce lime-based mortars, the raw material (naturally occurring limestone, CaCO₃) is heated up to 900°C. The burning causes the thermal decomposition of CaCO₃ into CaO (=quicklime) and CO₂. The very reactive quicklime is slaked with water, producing Ca(OH)₂ (=lime). In a last step, lime reacts with CO₂ in the atmosphere, forming again solid CaCO₃. In archaeology, calcareous nannofossils have successfully been used for the provenance analysis of various historic materials like building stones, ceramics and statues. The likeliness of finding nannofossils in mortars and mortar-based materials is, however, very low. The high burning temperatures during quicklime production causes the disintegration of calcite, including the decomposition of the microfossils. Unexpectedly, we have encountered remains of these algae in historic mortars and mortar-based materials. Samples from four historic buildings yielded various calcareous nannofossil taxa. In some cases the observed specimens allowed a detailed provenance analysis of the limestone used for producing the mortar. The historic builders exploited carbonate-rich limestones cropping out in the near vicinity of the constructions. To gain a better understanding of the behavior of calcareous nannofossils during the burning procedure, two limestone samples were heated to nine temperature levels (100°C, 300°C, 500°C, 600°C, 700°C, 750°C, 800°C, 850°C, 900°C). Both, original and heated, samples were analyzed with respect to their nannofossil content and preservation by using settling slides. Our results show a decrease of absolute numbers and preservation from 500°C onwards, nannofossils are preserved up to 900°C. Changes in the relative abundance of individual species show that some taxa are more heat resistant than others. This pattern is explained by different crystal sizes and forms. The abundance of calcareous nannofossil, their preservation and the presence / absence of different nannofossil taxa can therefore be used for estimating the burning temperature during the quicklime production. Our study helps to gain a better understanding of historic mortar production. It provides information of a) the provenance of limestones used for producing lime and b) the burning temperatures reached in historic lime kilns. Acknowledgments: We would like to thank the Calcination Lab team from the Lhoist Business Innovation Center (BIC) of Nivelles, Belgium for planning, sample preparation and calcination of the samples.

ARMENITE: A REALLY RARE MINERAL?

Fancello Dario¹, Deidda Matteo Luca¹, Attardi Antonio¹, Cocco Fabrizio¹, Funedda Antonio¹, Naitza Stefano¹

¹Department of Chemical and Geological Sciences, University of Cagliari, Italy

Armenite is a quite uncommon double-ring Ba-Al-Ca silicate hydrate belonging to the milarite-osumilite group and with the general formula $\text{BaCa}_2\text{Al}_6\text{Si}_9\text{O}_{30} \cdot 2\text{H}_2\text{O}$. It generally forms pseudo-hexagonal whitish-pinkish crystals. However, in its structure, Si, Al ordering and H_2O positions produce the deviation from hexagonal symmetry, explaining the belonging to the Pnna or Pnc2 space groups. In thin section, armenite is quite elusive. In fact, it appears colorless, with low relief and low first-order interference color. More complication arises from the tartan-like twinning patterns (resembling that of microcline), patchy-like and/or undulose extinction as well as the monoaxial to strongly biaxial (2V up to 65°) behavior. Its affinity to hexagonal or orthorhombic space groups as well as the reasons for its anomalous optical features have formerly been an object of debate. Up to now, armenite has only been found in a dozen of places worldwide, among which Armen mine (Norway), Quebec (Canada), New South Wales (Australia), Scotland, Switzerland, and Sardinia (Italy). It typically forms veins within the host rocks in different geological environments. These include metasomatic basic to intermediate igneous rocks, mineralized skarn and hornfels, and gneisses indicating that the interaction between fluid phases and a primary Ba source is required for its formation.

Here we report the third occurrence of armenite in Sardinia, from the Rosas mine area (Mitza Sermentus mineworks, south-west Sardinia). Armenite-bearing samples were collected along the contact between a sulfide-mineralized skarn vein and a black phyllite host-rock. The black phyllite matrix consists of muscovite, chamosite and quartz with feldspars, clinozoisite, titanite, and calcite as accessory phases. The skarn is made up of clinopyroxene, amphibole, epidote, chlorite and wollastonite, and calcite; accessory minerals are titanite, apatite, prehnite, and baryte. The ore minerals mainly consist of galena, sphalerite, chalcopyrite, and pyrite. Armenite is usually concentrated in mm-wide white veinlets along the contact between the sulfide mineralization and the host rock or more rarely dispersed in the phyllite matrix. At first, interpreted as an altered feldspar, it was identified by SEM-EDS analyses. Despite being semi-quantitative, the analyses provided compositions very close to stoichiometric armenite, with $\text{SiO}_2 \sim 48$ wt.%, $\text{Al}_2\text{O}_3 \sim 28$ wt.%, $\text{BaO} \sim 13$ wt.% and $\text{CaO} \sim 10$ wt.%. This finding was further confirmed by XRPD analyses on armenite-rich polymineralic samples in which more than 20 peaks were assigned to this phase leading to a good match with an armenite in the PDF database (Ref. code 00-037-0432). Beyond its supposed rarity and its peculiar crystal structure, three reasons make armenite deserving of attention: (i) understanding its genesis could better constrain the P-T-fluid conditions of rocks in which armenite is found and that are often mineralized; (ii) given its difficult recognition by base techniques, it is likely that armenite is more common than previously thought and is usually overlooked; (iii) since its formation requires a primary Ba source, armenite could be used as an indicator of the proximity of Ba-rich deposits.

ZEOLITE-BASED HYBRID UV FILTERS FOR HEALTH AND ENVIRONMENT PROTECTION

Fantini Riccardo¹, Zambon Alfonso¹, Ferrari Erika¹, Fabbiani Marco², Di Renzo Francesco², Mino Lorenzo³, Cavalli Roberta⁴, Argenziano Monica⁴, Baraldi Cecilia⁵, Vezzalini Giovanna¹, Arletti Rossella¹

¹Department of Chemical and Geological Sciences, the University of Modena and Reggio Emilia, Italy, ²ICGM, Univ. Montpellier-CNRS-ENSCM, France, ³Department of Chemistry, NIS Centre of Excellence, University of Turin, Italy, ⁴Department of Drug Science and Technology, University of Turin, Italy, ⁵Department of Life Sciences, University of Modena and Reggio Emilia, Italy

Earth is experiencing quick climatical changes and the interaction between man and the environment is getting more and more complex. Among all, the ozone depletion, which is now slowly restoring, exposed humankind and ecosystems to an enhanced UV exposure with growing concerns for both. Organic and inorganic UV filters are the main defense against solar UV radiation. Nevertheless, some of their physicochemical properties still present unresolved issues. For decades, the environment has been burdened by the spreading of UV filters that are ubiquitous in personal-care products but also in packaging, plastics, and dyes, leading to the rise of new widespread pollutants, which can even pass through present wastewater treatment plants. Inorganic UV filters, e.g. TiO₂ and ZnO, display photocatalytic properties causing H₂O₂ production in coastal waters, in turn affecting phytoplankton. Organic UV filters, on the other side, are photo-unstable under protracted UV exposure and their residues tend to accumulate in the environment, causing endocrine-disrupting effects on the organisms. For the abovementioned reasons, the development of new UV-filtering material, stable and safe both for human health and the environment, is of paramount importance. The encapsulation of UV filters in inorganic or organic matrices has proven to increase the stability of organic UV filters while preventing their percutaneous intake. Unfortunately, the environmental fate of the encapsulated filters was poorly investigated and many matrixes (e.g. mesoporous silica, amorphous silica, and MOFS) were found to be unstable, especially in saltwater. Zeolites, due to their porous nature, easy synthesis, high biocompatibility, and high stability represent a powerful tool to be exploited as a host for the encapsulation of UV organic filters. In this study, we report the synthesis and characterization of zeolite-encapsulated UV filters only marginally investigated by the previous literature. Their UV absorption properties, skin permeation, and behavior in a simulated marine environment will be presented and discussed. These hybrid UV filters overcome the issues of bare filter stability during UV absorption as well as of their spreading in the environment. Different zeolite topologies (MOR, FAU, LTL, MFI) and compositions were investigated revealing an active contribution of the zeolite to the final properties and behavior of the hybrid.

The results are intriguing and, particularly, the systems based on cationic zeolites display improved spectral features compared to those of bare filters, making ZEOfilters a promising and eco-friendly alternative for the future of UV protection.

A NANOSCALE STUDY OF EXTREMELY Ni-RICH OLIVINE IN PERIDOTITIC CLOTS FROM OPHIOLITIC CHROMITITES

Farré-de-Pablo Júlia¹, Proenza Joaquín A.¹, González-Jiménez José María², Llovet Xavier³, García-Casco Antonio⁴

¹Department of Mineralogy, Petrology and Applied Geology, University of Barcelona, Spain, ²Instituto Andaluz de Ciencias de la Tierra, Spain, ³Centres Científics i Tecnològics de la Universitat de Barcelona, Spain, ⁴Department of Mineralogy and Petrology, University of Granada, Spain

Olivine anomalously rich in Ni, such as in highly metasomatized mantle peridotite xenoliths from Avacha volcano in Kamchatka (Russia) and in the Ni–Cu–PGE-mineralized mafic-ultramafic intrusion in Kevitsa (Finland), has been interpreted as a result of Ni diffusion from Ni-rich sulfides or alloys present in the rocks. Here, we report olivine grains extremely rich in Ni within peridotite clots identified in high-Cr chromitites of the Loma Caribe peridotitic belt, Central Cordillera of the Dominican Republic. These clots are generally altered, but some of the biggest ones (up to 4 cm across) preserve pristine olivine at their central part. The composition of the preserved cores mainly consists of orthopyroxene (~70%), olivine (~30%) and accessory chromite (<1%) with a composition similar to that of the hosting chromitite. The olivine grains are up to 3 mm across and are preferentially located at the central part of the clot. They are extensively cross-cut by serpentine veins which are conspicuously filled with awaruite grains (around 1 µm across). Electron microprobe analyses of olivine revealed a composition very rich in Mg and Ni: Fo = 93-94 and 1.79–2.04 wt.% NiO, respectively. The Ni contents of this olivine are much higher than those of olivine from mafic-ultramafic rocks worldwide. The Ni enrichment is also observed to a lesser extent in orthopyroxene (En = 91.92-93.65 with 0.32–0.46 wt.% NiO) and the accessory chromite (0.20–0.52 wt.% NiO) from the clots.

Solid inclusions were identified within the olivine grains by means of field emission scanning electron microscopy (FE-SEM) and electron microprobe mapping. A careful inspection of selected areas of these olivine grains using a combination of focused ion beam technique and transmission electron microscopy (FIB–TEM) revealed that these inclusions are a composite of magnetite (<5 µm and up to 1 µm thick) and Ni-Fe alloys (up to 300 nm across), which are often mantled by a thin nanometric layer (around 100 nm thickness) of serpentine. The Ni-Fe nanoalloys occur both as inclusions within magnetite and as single dispersed grains within olivine. Micro-Raman analyses of the olivine grains also showed the presence of magnetite inclusions which are associated with fluid inclusions consisting in CH₄ and OH. This assemblage of minerals and phases is typical of serpentinization processes.

We suggest that olivine was enriched in Ni previous to the formation of the Ni-rich inclusions observed in the clot. Moreover, we infer that the low-temperature alteration of the Ni-rich olivine gave place to the abundant Ni-Fe-rich alloys observed in the clot and to the awaruite grains in the serpentine veins. The Ni enrichment of olivine is likely the result of magmatic processes, though subsequent general alteration of the clots prevents a definitive explanation.

AMMONIUM SALTS REFLECTANCE SPECTRA AT CRYOGENIC TEMPERATURE AND HOW DISTINGUISH THEM ON THE SURFACE OF ICY PLANETARY BODIES.

Fastelli Maximiliano¹, Comodi Paola¹, Zucchini Azzurra¹, Schmitt Bernard², Beck Pierre², Poch Olivier²

¹Physics and Geology, University of Perugia, Italy, ²Institut de Planétologie et d'Astrophysique de Grenoble (IPAG), Université Grenoble Alpes, CNRS, France

It has been proposed that ammonium minerals are present in varying percentages in icy planetary bodies such as Enceladus, Ceres, Pluto, and its satellites, also a potential occurrence in other celestial bodies. The availability of these compounds is linked to the upwelling of ammonium salts (NH_4^+) from the subsurface of possible oceans resulting from cryovolcanism mixed with ice. The identification of these minerals on the surface can give information about the internal composition/dynamics and potential habitability of icy bodies. We analyzed the temperature evolution of anhydrous [sal-ammoniac NH_4Cl , mascagnite $(\text{NH}_4)_2\text{SO}_4$, ammonium bicarbonate $(\text{NH}_4)\text{HCO}_3$, ammonium nitrate NH_4NO_3 , ammonium carbonate $(\text{NH}_4)_2\text{CO}_3$ and ammonium phosphate monobasic $(\text{NH}_4)\text{H}_2\text{PO}_4$] and hydrated [larderellite $(\text{NH}_4)\text{B}_5\text{O}_7(\text{OH})_2 \cdot \text{H}_2\text{O}$, struvite $(\text{NH}_4)\text{MgPO}_4 \cdot 6\text{H}_2\text{O}$ and tschermigite $(\text{NH}_4)\text{Al}(\text{SO}_4)_2 \cdot 12\text{H}_2\text{O}$] ammonium salts in relation to exchange in anions and water content. Reflectance spectra were collected in the near-infrared (NIR) spectral range (1-5 μm) at a cryogenic temperature range from 293K to 60K using the SHINE spectro-gonio radiometer of the Cold Spectroscopy Facility (<https://cold-spectro.sshade.eu>) at IPAG equipped with a simulation chamber to control the temperature of the minerals. Additionally, we study the effect of sample's grain size between (36-150 μm). Each mineral has been tested before and after the cooling cycles by X-ray powder diffraction. Rietveld refinement was performed to understand possible variation in the mineral composition. Reflectance spectra of anhydrous samples show well define absorption features in the 1-2.5 μm range due to NH_4^+ groups overtones and combinations. The bands located at 1.3 ($2\nu_3 + \nu_4$) and 1.56 ($2\nu_3$) μm could be useful to discriminate these salts. The reflectance spectra of water-rich samples show H_2O fundamental absorption features, overlapped to the NH_4^+ bands, in the area from 1 to 2.8 μm and over 3 μm the spectra became flat. The parameters (area, depth and FWHM) of several absorption bands change in relation to the low temperature and different grain size. In detail, the low-temperature spectra reveal fine structure compared to the room temperature ones displaying more detailed and define absorption bands. The different granulometry affects mainly the bands parameter area and depth. We notice as the grain size becomes larger, the value of an area and FWHM (full width half maximum) increase. Samples mascagnite $(\text{NH}_4)_2\text{SO}_4$, sal-ammoniac NH_4Cl , ammonium phosphate $(\text{NH}_4)\text{H}_2\text{PO}_4$, tschermigite $(\text{NH}_4)\text{Al}(\text{SO}_4)_2 \cdot 12(\text{H}_2\text{O})$ and ammonium nitrate NH_4NO_3 are characterized by phase transition at low temperature and in some cases showed clear and very interesting spectral bands variations during cooling, indicating that a phase transition occurred. These mineral phase transitions, when detected, are characterized by a progressive growth and shift toward a shorter wavelength whit an abrupt change in depth of the sensitive peaks. These collected cryogenic data with a careful analysis of NH_4^+ absorption features could be used to the detection of these salts in the surfaces of planetary bodies. The presence of ammonium minerals in the ice shell could influence the dynamics of icy satellites.

TTG-LIKE INCLUSIONS IN GIANT GARNET MEGACRYSTS: TRONDJEMITIC MELT PRESERVED IN INCLUSIONS AT GORE MOUNTAIN, ADIRONDACKS (US)

Ferrero Silvio¹, Wannhoff Iris², Laurent Oscar³, Yakymchuk Chris⁴, Darling Robert⁵, Wunder Bernd⁶, Borghini Alessia¹, O'Brien Patrick J.¹

¹Universität Potsdam, Germany, ²Freie Universität, Berlin, Germany, ³GET-CNRS, Toulouse, France, ⁴University of Waterloo, Canada, ⁵SUNY College at Cortland, United States, ⁶GFZ, Potsdam, Germany

The garnet megacrysts of Gore Mountain (Adirondacks, US) are world-renown crystals due to their size, up to 1 m in the historical record, which makes them the largest known garnets on the planet. We show here that they are also host to the first primary inclusions of trondhjemitic melt found in natural mafic rocks. The petrological and experimental investigation of the inclusions, coupled with phase equilibrium modeling, shows that this melt is the result of H₂O-fluxed partial melting at T > 900 °C of a lower crustal gabbro.

The compositional similarity between the trondhjemitic melt inclusions and tonalitic–trondhjemitic–granodioritic (TTGs) melts makes these inclusions the first direct natural evidence that melting of mafic rocks generates TTG-like melts, and provide us with the possibility to clarify processes responsible for the formation of the early continental crust. These TTG embryos represent the trondhjemitic end-member of the melts whose emplacement at upper crustal levels, after being modified by mixing and crystallization-related processes, leads to the formation of the TTG terranes.

Our study also shows how the melt from H₂O-fluxed melting of the mafic lower crust has mismatched mineralogical features as well as major and trace element signatures, previously interpreted as evidence of melting at very different pressures. This poses serious limitations to the established use of some chemical features to identify the geodynamic settings (e.g. subduction versus thickened crust) responsible for TTG generation and the growth of early crust.

MODELLING THE ADSORPTION OF PHARMACEUTICALS AND PERSONAL CARE PRODUCTS IN ALL-SILICA ZEOLITES WITH DENSITY FUNCTIONAL THEORY CALCULATIONS

Fischer Michael¹

¹Faculty of Geosciences, University of Bremen, Germany

Pharmaceuticals and personal care products (PPCPs) exhibit considerable environmental hazard potential, especially with regard to water pollution. Due to their hydrophobic properties, all-silica zeolites could play a role in the adsorption-based removal of PPCP pollutants from contaminated water bodies. In a recent computational study (M. Fischer, *Mater. Adv.* 2020, 1, 86–98), molecular mechanics (force field) calculations were employed to investigate the interaction of 21 PPCP pollutants with two all-silica zeolites having mordenite (MOR) and faujasite (FAU) topologies. It was demonstrated that the interaction energies correlated well with removal efficiencies from a previous experimental study (A. Rossner et al., *Water Res.* 2009, 43, 3787–3796), despite numerous simplifications made in the calculations. Electronic structure calculations in the framework of density functional theory (DFT) were also reported for a few PPCPs, however, it was not studied how the choice of exchange-correlation functional and dispersion correction affect the results.

Although the findings from this previous force field study indicate the ability of computational methods to predict promising zeolite adsorbents for PPCP removal, there is an evident need to validate force field parameters against higher-level methods, e.g., DFT calculations, in order to ensure that reliable results are obtained. The present contribution aims to identify a suitable protocol for such higher-level calculations by investigating the influence of the choice of DFT methodology on the computed interaction energies for the 21 PPCPs in MOR- and FAU-type zeolites, taking low-energy adsorption configurations from the force field calculations as starting point. Different exchange-correlation functionals in combination with a pairwise dispersion correction (DFT-D) as well as non-local van der Waals density functionals are considered in these calculations. In addition to comparing interaction energies obtained with different methods, differences in relative trends across the set of PPCPs are also discussed. For selected PPCPs, several adsorption configurations are generated, and their energetic ordering as predicted by different DFT approaches is analyzed. Finally, a preliminary comparison to force field calculations is presented. These results should have important implications for future computational studies of PPCP adsorption in zeolites.

Funding by the Deutsche Forschungsgemeinschaft (DFG grant no. 389577027) is gratefully acknowledged.

NEW DATA ON PRECIOUS METAL MINERALIZATION IN THE POLKOWICE-SIEROSZOWICE DISTRICT, SW POLAND

Foltyn Krzysztof¹, Kozub-Budzyń Gabriela¹, Pieczonka Jadwiga¹, Piestrzyński Adam¹

¹Department of Geology of Mineral Deposits and Mining Geology, AGH University of Science and Technology, Poland

The Kupferschiefer deposit in SW Poland is a classic example of a sediment-hosted stratiform copper deposit. In addition, oxidized rocks below the economic Cu–Ag orebody of the Polkowice- Sieroszowice mine, locally show elevated concentrations of noble metals. Gold, Pt, and Pd occur in red-colored sections of secondary oxidation in the basal Zechstein sedimentary rocks and in the uppermost Weissliegendes sandstone. Reflected light microscopy, scanning electron microscope and electron microprobe were employed to investigate new and archival samples in order to better characterize mineralogy and geochemistry of phases constituting Au-Pt-Pd mineralization.

Ore minerals include a variety of alloys, sulfide, selenide, arsenide, and oxide minerals, namely gold, electrum, clausthalite PbSe, fischerite Ag₃AuSe₂, naumannite Ag₂Se, tiemannite HgSe, Pd arsenides, Pd-As-O phases, Ni-Co arsenides, wittichenite Cu₃BiS₃, bohdanowiczite AgBiSe₂, sobolevskite PdBi, chalcopyrite, pyrite, anilite, yarrowite, hematite, uraninite, and coffinite. Besides sobolevskite, Pd-bearing phases include native gold (up to 1.77 wt% Pd), electrum (up to 0.26 wt. % Pd), Ni-Co diarsenides (up to 7.97 wt% Pd), Pd-As-O phases (up to 67.97 wt. % Pd), fischerite (up to 0.34 wt. % Pd) and tiemannite (up to 0.23 wt. % Pd). The most important Pt-bearing phases are gold (up to 0.33 wt% Pt), Hg-rich electrum (up to 2.95 wt. % Pt) and submicron inclusions of Pt-As phases. Platinum was also measured in sobolevskite (up to 1.7 wt% Pt), bohdanowiczite (up to 0.78 wt. % Pt) clausthalite (up to 0.16 wt. % Pt), fischerite (0.13 wt% Pt), and Pd-As-O phase (up to 0.12 wt. % Pt). Selenide inclusions and symplectites (mainly clausthalite) are commonly observed in chalcopyrite accompanying gold grains. Characteristic intergranular replacement texture, with Au-Ag alloy containing 77-78 wt. % Au replaced by electrum with 35-50 wt. % Au and enriched in Hg (2.2-4.6 wt. % Hg), suggest at least two stages of formation.

Analyzed mineral association show similarities to a group of low temperature, sulfide poor, Au-Pd (±U) deposits such as Coronation Hill (Australia), Serra Pelada (Brazil), Hope's Nose (UK), and Bleida Far West (Morocco) formed by highly oxidizing fluids. The Bohemian Massif nearby is known for abundant occurrences of selenides, mainly in vein and shear-hosted uranium mineralization such as Kletno, Zálesí, and Rožná. Post-Variscan sedimentary basins of Central Europe could constitute a reservoir of highly oxidizing fluids released during periods of tectonic disturbance, particularly at the basin margins (Lubin-Sieroszowice district) or along faults and shear zones penetrating Variscan basement (Bohemian Massif). Interaction with reduced lithologies would result in precipitation of Au-Pd-Pt and U mineralization.

EXPERIMENTAL DIAGENESIS. ARAGONITE INVERSION AND CALCITE RECRYSTALLIZATION DURING THE HYDROTHERMAL ALTERATION OF BIOCARBONATES.

Forjanés Pablo¹, Simonet-Roda María², Greiner Martina², Griesshaber Erika², Astilleros José-Manuel¹, Schmahl Wolfgang W.², Fernández-Díaz Lurdes¹

¹Mineralogy and Petrology, Complutense University of Madrid, Spain, ²Earth and Environmental Sciences, Ludwig Maximilian University of Munich, Germany

Fossil biocarbonates are archives holding valuable geochemical information, which motivates their wide use as proxies in paleoenvironmental reconstruction and past climate studies. Unfortunately, the mineralogical and microstructural changes undergone by biocarbonates during diagenesis can alter this geochemical information. These changes can be difficult to assess when diagenetic changes do not involve transformations between different calcium carbonate polymorphs or when aragonitic biominerals undergo little to no diagenetic transformation into calcite. Recent works have experimentally investigated the kinetics of the biogenic aragonite into abiogenic calcite transformation in different aragonitic biominerals, concluding that it is strongly dependent on the pristine aragonite microstructure.

Aiming to better understand the combined influence of pristine microstructure and calcium carbonate polymorph in the diagenesis of biominerals, we performed hydrothermal alteration experiments (4 to 56 days long at 175°C) using two different skeletons that contain calcite and aragonite layers: The shell of *Patella vulgata*, which consists of a central aragonite layer encapsulated by two layers of crossed lamellar calcite and the shell of *Tegula atra*, which contains calcite prisms and aragonite nacre tablets. The altered skeletons were analyzed with EBSD, SEM, AFM, XRD and TGA.

The features and extent of the hydrothermal alteration strongly vary between not only the two skeletons but also between their different layers. Hence, while the aragonite layer from *Patella vulgata* appears partially transformed to calcite, the aragonitic nacre tablets from *Tegula atra* remain essentially unaltered. Similarly, the calcitic prisms from *Tegula atra* and one of the calcitic layers from *Patella vulgata* appear partially recrystallized, with abiogenic calcite crystals replacing the original microstructure. On the other hand, the other calcite layer from *Patella vulgata* does not display any major signs of alteration.

Our results depict the diagenesis of biocarbonates as a complex process whose progress is strongly affected by the original skeleton microstructure. Knowing the pristine mineralogy and microstructure of the different layers that build up biocarbonate skeletons applying mineral microstructure characterization tools like EBSD can be of great help to identify diagenetic overprint in fossil carbonate biominerals and safely use them as paleoenvironmental proxies.

IRON COMPOUNDS IDENTIFICATION BY MICRO-RAMAN SPECTROSCOPY IN CHRYSOTILE ASBESTOS FROM BALANGERO

Fornasini Laura¹, Bersani Danilo², Raneri Simona¹, Gualtieri Alessandro F.³

¹Institute of Chemistry of Organometallic Compounds, ICCOM CNR, Italy, ²Department of Mathematical, Physical and Computer Sciences, University of Parma, Italy, ³Department of Chemical and Geological Sciences, University of Modena and Reggio Emilia, Italy

Chrysotile, a layered silicate of Si-centred tetrahedral sheets and Mg-centred octahedral sheets with the ideal chemical formula $Mg_3Si_2O_5(OH)_4$, is one of the six regulated asbestos minerals and it is classified as carcinogenic to humans by the International Agency for Research on Cancer (IARC). The Balangero mine (Turin, Italy) was the largest asbestos mine in Europe and chrysotile fibers were extracted until 1990. Chrysotile asbestos from Balangero is currently of great interest in fibers toxicity aimed at understanding the mechanisms which induce lung diseases, mainly mesothelioma. One of the crucial factors in the biochemical reactions is the presence of iron at the surface of the fibers, whose reactivity is responsible for oxidative stress, radicals, and reactive oxygen species (ROS) production.

Here, chrysotile from Balangero has been characterized by micro-Raman spectroscopy in order to identify iron compounds that are associated with asbestos fibers. Micrometric crystals with reddish to black colors have been observed and distinguished. Magnetite (Fe_3O_4) results as the most frequent iron oxide. Other rarer iron oxides and oxyhydroxides have been identified as hematite ($\alpha-Fe_2O_3$), ilmenite ($FeTiO_3$), and lepidocrocite ($\gamma-FeO(OH)$). Black micro-crystals also consist of iron sulfide mackinawite ($Fe(II)S$), in different forms. Nanocrystalline mackinawite is characterized by the main sharp peak at $\sim 280\text{ cm}^{-1}$ and a weak contribution at $\sim 205\text{ cm}^{-1}$. In addition, partially oxidized mackinawite has been distinguished by its Raman signals at $\sim 122, 165, 250, 310, \text{ and } 322\text{ cm}^{-1}$, suggesting the presence of a Fe(III)-containing sulfide.

Hence, the presence of both Fe(II) and Fe(III) species in iron oxides, oxyhydroxides, and sulfides in chrysotile from Balangero should be considered as metals release in the reactivity and dissolution of asbestos fibers in the lungs.

SURFACE PROPERTIES OF URANIUM DIOXIDE (UO₂) IN PRESENCE OF WATER: INSIGHTS FROM FIRST PRINCIPLES MOLECULAR DYNAMICS SIMULATIONS

Foucaud Yann¹, Bertolotto Solène¹, Szenknect Stéphanie¹, Duvail Magali¹, Siboulet Bertrand¹, Dufrêche Jean-François¹, Dacheux Nicolas¹

¹ICSM, Commissariat Energie Atomique, France

After their stay in the reactor, spent nuclear fuels (SNF) are still composed of more than 95 wt.% of uranium dioxide (UO₂) and 1 wt.% plutonium dioxide, which constitute valuable secondary resources. The remaining uranium (and plutonium) can be recovered by reprocessing the SNF. The head-end step of this process deals with the dissolution of the SNF in hot and concentrated nitric acid, followed by the separation and purification of uranium and plutonium oxides. Besides, one of the potential solutions for long-term isolation of the end-of-life SNF is its direct disposal in deep geological repositories, where UO₂ surfaces could be in contact with water with various possible physical-chemical conditions. Acquiring a thorough understanding of the stability of UO₂ in various physical-chemical conditions is therefore of paramount interest to (1) assess the long-term behavior of the end-of-life SNF in geological repository conditions and (2) finely tune the UO₂ dissolution stage in the reprocessing of the SNF. Here, for the first time, we employed ab initio molecular dynamics simulations to thoroughly characterize the hydration mechanisms of the (111) surface -the main cleavage plane- of UO₂, and, particularly, the dynamic equilibrium of this surface in presence of pure water. The surface coverage was gradually increased from a single water molecule to the system where the vacuum above the surface was completely filled with water molecules. For a single water molecule, the molecular adsorption was significantly favored ($\Delta H_{ads} = -47.6 \text{ kJ mol}^{-1}$) over the dissociated adsorption ($\Delta H_{ads} = -13.1 \text{ kJ mol}^{-1}$). However, for two water molecules both introduced in their molecular form, one adsorbed under its molecular form while the second spontaneously dissociated on the surface; the OH⁻ anion adsorbed on a uranium atom of the surface while the H⁺ ion adsorbed on a surface oxygen atom. For higher surface coverages, we systematically observed that a significant part of the water molecules spontaneously dissociated on the surface while ΔH_{ads} tended towards the enthalpy of condensation of water with increasing coverages. When the cell was completely filled with water, about a third of the surface uranium atoms were hydroxylated, which meant that 33% of the water molecules of the monolayer dissociated on the UO₂ (111) surface. A dynamic equilibrium between the bulk of water and the surface was established, with frequent recombination/dissociation of water molecules as well as adsorption/desorption of OH⁻, H⁺, or H₂O. This work will serve as a basis for further studies, particularly about the dissolution mechanisms of UO₂ in presence of nitric acid.

PROCESSING OF A COMPLEX TUNGSTEN SKARN ORE DEPOSIT (TABUAÇO, PORTUGAL): AN INTEGRATED APPROACH

Foucaud Yann¹, Filippova Inna², Filippov Lev²

¹ICSM, Commissariat Energie Atomique, France, ²GeoRessources, Université de Lorraine, France

The Tabuaço Northern-Portuguese tungsten project is composed of two skarn layers, namely “Main” and “Lower” skarns, which display significantly different geochemical and mineralogical features. Although both skarns comprise fine-grained disseminated scheelite, the Lower-skarn gangue is dominated by silicates whereas the Main-skarn gangue contains significant amounts of calcium-bearing minerals including apatite, fluorite, and vesuvianite, in close association with scheelite. During preliminary feasibility studies, the direct separation of scheelite from gangue calcium-bearing minerals, mostly fluorite, by flotation with eco-friendly fatty acids was unsuccessful due to their similar surface properties. Several routes for each skarn type were proposed to produce a marketable scheelite concentrate, with however a strong focus on the Main skarn that displays the most complex mineralogical associations. To attain this objective, high-intensity magnetic separation enhanced gravity separation (Falcon concentrator), and flotation with fatty acids were investigated for the Main Skarn level. Flotation was thoroughly investigated and optimized in terms of depressants, which allowed producing a concentrate assaying 9.2% WO₃ at 87.9% WO₃ recovery from a ~1.1% WO₃ feed, by means of a 1:1 ratio of sodium carbonate and sodium silicate. Fluorite was the most problematic mineral in flotation with fatty acids and, therefore, new fatty-acids-based collector formulations, including saturated fatty acids, were developed to improve the separation contrast between scheelite and fluorite. This allowed producing a concentrate assaying 14.1% WO₃ with 77.1% WO₃ recovery for the fully-optimized conditions (depressants and collectors), with a satisfactory elimination of silicates but still a poor rejection of fluorite. Furthermore, the performance of the Falcon concentrator was investigated by the design of experiments methodology and optimized for gangue minerals rejection. It was used as a desliming and pre-concentrating apparatus: one stage of Falcon SB allowed rejection of 84% of the total amount of fluorite, more than 95% of the slimes, and 85 wt.% of the feed mass. Consequently, it increased significantly the performance of the fully-optimized scheelite flotation: the final concentrate, after one pre-concentrating Falcon SB stage followed by four flotation stages, assayed 62.9% WO₃ with 59.4% WO₃ recovery, which constituted a marketable scheelite concentrate. Both the Falcon SB parameters and the number of fully-optimized flotation stages could be optimized to maximize either the WO₃ grade or the WO₃ recovery, regarding the product specifications. Finally, the high-intensity magnetic separation allowed rejecting around 45 wt.% of the total yield prior to the milling stage with only 6.0% WO₃ losses, which would decrease significantly the energy consumed during the milling stage.

THE EFFECT OF FLUORINE ON REACTION RIM GROWTH DYNAMICS IN THE TERNARY CaO-MgO-SiO₂ SYSTEM

Franke Mees¹, Joachim-Mrosko Bastian¹

¹Institute of Mineralogy and Petrography, University of Innsbruck, Austria

Metamorphic corona and reaction rim structures are examples of a net-transfer reaction, where pre-existing mineral phases react to new phases. The growth of these metamorphic structures indicates a change in physical parameters such as pressure and temperature, a change in the chemical composition of the system, and/or the presence of volatiles. The effect of volatile components on net-transfer reactions remains poorly understood. Volatiles other than water such as N, C, S, and the halogens F, Cl, and Br, in particular, received little attention with regards to component mobility and phase stability, limiting our ability to establish their significance in the upper mantle. In order to accurately model metamorphic and metasomatic processes and test the potential of natural reaction rims to be used as "geofluidometers", a quantification of the effect of volatiles on reaction-rim growth dynamics is necessary.

In this study, we investigate the effect of fluorine on reaction rim growth dynamics in the ternary CaO-MgO-SiO₂ system. A series of piston-cylinder experiments were conducted at P-T conditions of 1000°C and 1.5 GPa. In each experiment, reaction rims were grown for 20 minutes between a natural wollastonite crystal and MgO powder matrix with the addition of 0 to 10 wt. % fluorine. Electron microprobe analyses and Raman spectroscopy were used to analyze the crystal phases present in the reaction rim.

In the fluorine-free system, we produced a monomineralic rim sequence of wo | mer | di | fo | per, complying with phase stabilities at water-saturated conditions. As soon as 0.1 wt. % fluorine was introduced into the system, humite group minerals (HGMs) and monticellite were stabilized resulting in the multilayer rim sequence wo | mer | mtc | fo + HGMs | per. In experiments with fluorine concentrations >1 wt. %, palisades of cuspidine are stable and represent the major fluorine sink. Our data show that the addition of fluorine stabilizes the fluorine-bearing phases cuspidine and HGMs to higher temperatures, which is in agreement with previous studies [e.g. 1]. However, stabilization of the nominally anhydrous mineral (NAM) monticellite at this P-T-condition suggests that the addition of fluorine also affects the stability of nominally fluorine-free minerals. Furthermore, the results of this study reveal a positive correlation between overall rim thickness and fluorine content. Reaction rim widths increased from 12.50 (146) to 105.49 (185) μm in fluorine-free and 10 wt% F experiments respectively.

Our results illustrate the significance of fluorine during net-transfer reactions, where its presence has a strong effect on [I] the overall rim thickness, which increases by 10-fold if 10 wt. % F is added to the dry system, [II] phase stabilities, where fluorine bearing minerals such as humite group minerals and cuspidine are stabilized, [III] the relative mobilities of the individual components and as a consequence [IV] the internal rim microstructure. These findings have important implications for reaction rims to be utilized as a potential "geofluidometer" and may allow us to unravel the chemical composition of metasomatic fluids.

References:

[1] Grützner et al. (2017) *Geology*, 45(5), 443–446

⁴⁰Ar/³⁹Ar IN SITU LASER-ABLATION DATING OF BUDDINGTONITE FROM VOLYN, UKRAINE

Franz Gerhard¹, Sudo Masafumi², Khomenko Vladimir³

¹Applied Geosciences, Technical University Berlin, Germany, ²Geosciences, University Potsdam, Germany, ³Geochemistry, Mineralogy and Ore Formation, Academy of Sciences, Ukraine

Buddingtonite (ammonium feldspar $\text{NH}_4\text{AlSi}_3\text{O}_8$), occurs in two geological settings: igneous hydrothermal environments (e.g. volcanic geyser fields), and organic-rich sediments (e.g. coal seams, oil- and black shales, phosphorites). It frequently occurs together with illite with a high content of NH_4 (tobelite component). It is often characterized as a 'nondescript and amorphous' appearing mineral, mostly fine-grained or in μm -wide rims on K-feldspar, forming a solid solution with K-feldspar, which might be formed either due to partial replacement of igneous/detrital K-feldspar or together with authigenic K-feldspar. The K-content in buddingtonite would allow applying the K-Ar decay system to date its formation, which would give valuable time information for a diagenetic or a hydrothermal event. To our knowledge, no attempts have been made to-date buddingtonite, and here we present results from a sample with a hydrothermal buddingtonite-muscovite association, formed in a Paleoproterozoic pegmatite at Volyn, Ukraine.

Volyn is situated in the north-western part of the Precambrian Ukrainian shield. The pegmatites are associated with rapakivi-type granites of the Paleoproterozoic Korosten plutonic complex with intrusion ages between 1.8 and 1.74 Ga. The rock sample is a hydrothermal breccia that contains fragments of pegmatitic minerals (mainly alkali-feldspar, quartz) and a pseudomorph after beryl, cemented by opal. This pseudomorph consists mainly of the Be-mineral bertrandite, buddingtonite, and muscovite. It also contains organic matter, a degradation product of microbial kerite fossils from the time between intrusion and breccia formation, and which shows oxygenation, accompanied by loss of N. Dissolved N as NH_4^+ transformed K-feldspar into buddingtonite-K-feldspar solid solutions and partly transformed muscovite into tobelite. Buddingtonite occurs as crystals several tens of micrometers large with typical sector zoning. Euhedral appearing crystals consist of μm -sized fibers indicated by slightly different extinction positions in thin sections. In addition, buddingtonite is not only a K- NH_4 -solid solution but contains also significant amounts of $\text{H}_2\text{O}/\text{H}_3\text{O}^+$; the average formula is $\text{Na}_{0.02}\text{K}_{0.20}(\text{NH}_4)_{0.63}\text{H}_3\text{O}_{0.15}[\text{Si}_{3.03}\text{Al}_{1.01}\text{Fe}^{3+}_{0.01}\text{O}_8]$.

The ⁴⁰Ar/³⁹Ar in situ analyses with a Micromass 5400 noble gas mass spectrometer have been performed at the ⁴⁰Ar/³⁹Ar geochronology laboratory in Potsdam University. Samples were prepared as thick sections and in situ analyses with Nd-YAG UV pulse laser were done following back-scattered electron images of the surfaces. Neutron activation was performed at CLICIT (Cadmium-Lined in-Core Irradiation Tube) facility of Oregon State TRIGA Reactor (OSTR), USA. Samples were irradiated for 4 hours together with the neutron flux monitoring mineral, Fish Canyon Tuff sanidine, and K_2SO_4 and CaF_2 for correction of interference.

Eight spot analyses of muscovite yielded an age of 1486 ± 11 Ma (MSWD 0.98), interpreted as the age of the hydrothermal breccia formation. Eleven spot analyses of buddingtonite failed to yield the same age despite close textural association, but give an age range from 386 ± 16 Ma to 561 ± 33 Ma. Apparently, the fine-grained nature and the content of 'water' are responsible for Ar-loss. However, the minimum age obtained for buddingtonite is also valuable geologic information and we would encourage more attempts for dating of buddingtonite.

MAKE IT COUNT. COMPARISON OF THREE EXPERIENCES IN CATALOGUING ITALIAN MUSEUM METEORITE COLLECTIONS USING THE NATIONAL BN-PL STANDARD.

Franza Annarita¹, Morelli Marco², Faggi Daniela², Mancinelli Maria Letizia³, Pratesi Giovanni¹

¹Dipartimento di Scienze della Terra, Università degli Studi di Firenze, Italy, ²Fondazione PARSEC, Italy, ³Istituto Centrale per il Catalogo e la Documentazione, Italy

This contribution deals with the challenges and solutions associated with the implementation of the Italian standard cataloging system for meteorite collections and the increasing awareness regarding this fundamental museum activity. Three case studies, that illustrate the strengths and weakness of indexing diverse meteorite collections using the national BN-PL standard (Beni Naturalistici–Planetologia, Naturalistic Heritage–Planetology), will be presented. The planetological standard followed the other standards promoted by the Central Institute for Cataloguing and Documentation (Istituto Centrale per il Catalogo e la Documentazione, ICCD) for cataloging the Italian mineralogical (BN-M), petrological (BN-P), and planetological (BN-PL) heritage. The resulting General Catalogue of Cultural Properties (Catalogo Generali dei Beni Culturali, CGBC) online database – which gathers information about all the Italian national cultural heritage (historic, artistic, and naturalistic as well) – provides an overview of the geoscientific heritage that has been cataloged through these standards and is now freely accessible. Out of the 2.659.552 items that constitute the CGBC, 55.100 records are devoted to the naturalistic collections. Among these, 41.431 and 429 records describe respectively mineralogical and petrological samples, whereas 370 represent meteorite specimens kept in the National Museum of Antarctica “Filippo Esposito” in Siena, and in the University Museum System in Firenze. To the latter should be added 250 cataloging cards regarding the meteorite collection preserved at the Museum of Planetary Sciences in Prato. The comparison between these three diverse operational settings highlights how the proper use of the BN-PL standard can help in: (1) establishing more precise conservation policies and management strategies of the meteorite collections housed in Italian scientific museums; (2) acquiring social and cultural information useful to prevent bad scientific practice and ethical misconduct in planetary sciences; (3) obtaining unknown scientific and historical data valuable to better characterize previously analyzed samples; (4) providing in-depth information on the most recent recovered specimens; (5) tracing and maintaining over time the data usually collected during in-house museum cataloging campaigns; (6) make these data freely accessible online to anyone interested thus increasing the public understanding of this unique geoscientific heritage .

In conclusion, this presentation shows how standardized and correct cataloging is the prerequisite to an exhaustive and meaningful comprehension of the historical, scientific, social, and cultural, aspects relative to the conservation and valorization of museum meteorite collections.

Acknowledgments

The authors thank the Fondazione Cassa di Risparmio di Firenze for providing the financial support to successfully complete this presentation through the fund “MECSO—Una finestra sul Sistema Solare: progetto per la caratterizzazione spettroscopica dei bolidi.”

ROYAL IMPERIAL MINERALS. THE MINERALOGICAL COLLECTIONS OF THE HOLY ROMAN EMPERORS JOSEPH II AND LEOPOLD II AND BETWEEN MUSEOLOGY, SCIENCE, AND HISTORY.

Franza Annarita¹, Mattes Johannes², Pittarello Lidia³, Pratesi Giovanni¹

¹Dipartimento di Scienze della Terra, Università degli Studi di Firenze, Italy, ²Austrian Academy of Sciences, Austria, ³Naturhistorisches Museum Wien, Austria

After attending this presentation, attendees will gain insights into the scientific, cultural, and social aspects of the mineralogical collection in 18th-century Central Europe. This presentation will impact the mineralogy community by illustrating the different meanings that it had at the Imperial court of the Habsburg-Lorraine family through the investigation of the mineralogical collections that belonged to the Holy Roman Emperors Joseph II (1740–1791) and Leopold II (1747–1792).

As stated by Wilson (1994), Vienna became one of the greatest hotbeds of 18th-century European mineral collecting. Here emerged a very active mineralogical community formed by collectors, mineral dealers, and scholars from all over the Habsburg Monarchy, which were called to build and organize the Royal Imperial mineralogical collections, and to teach in the Imperial mining academies. If Holy Roman Emperor Franz I Stefan of Lorraine's (1708–1765) passion for naturalistic and mineralogical collecting is a well-established topic, few researchers (e.g., Mottana et al. 2012) have addressed the interest in mineralogy, mining science, and mineral collecting showed by his sons, who in turn inherited the Imperial title, Joseph II (1740–1791) and Leopold II (1747–1792). This presentation thus provides the attendees with contextual information about Joseph' and Leopold's general scientific interests, with a special focus on the journey they made, together with Albert Kasimir von Sachsen-Teschen (1738–1822), to visit the mining districts in Lower Hungary in 1764.

Drawing on an extensive range of untapped sources, this presentation then investigates the cores of Joseph's and Leopold's interest in mineralogical collecting. The *Collectio Mineralium* (1765), which was the catalog of Leopold's private mineralogical collection, will be analyzed in detail along with the collection of minerals, which was donated by Joseph II to the Mineralogical Cabinet of the Roman Collegio Nazareno in 1785. The results obtained are compared to highlight the different spatial dimensions these mineral collections embodied, and the relationships they mediated with scholars such as Ignaz Edler von Born (1742–1791) and Giovanni Vincenzo Petrini (1725–1814). The analysis of the mineralogical collections belonging to Joseph II and Leopold II shows not only the scientific development of mineralogy and mining science at the end of the 18th century but also how mineral collections became a source of state knowledge through which to exhibit both the economic and political development of a country (Vogel 2015).

Finally, this presentation includes an overview of the valorization projects that will be launched on Joseph's mineralogical collection that is currently housed at the Istituto Calasanzio in Rome.

References

- Mottana A., Mussino A., Nasti V. 2012. Minerals from the Carpathian Mountains and from Transylvania donated by Joseph II (1785) to the Museum of the Collegio Nazareno, Rome, Italy. *Central European Geology* 55(1): 103–122.
- Vogel J. 2015. Stony realms: mineral collections as markers of social, cultural and political spaces in the 18th and early 19th Century. *Historical Social Research* 40(1): 301–320.
- Wilson W.E. 1994. The history of mineral collecting, 1530-1799: with notes on twelve hundred early mineral collectors. *Mineralogical Record* 25(6): 101–109.

THERMOCHEMICAL MODELING OF ZIRCON CRYSTALLIZATION REVEALS CONTRASTING MAGMA RECHARGE AND STORAGE REGIMES

Friedrichs Bjarne¹, Schmitt Axel Karl¹, Lovera Oscar M.², Atıcı Gokhan³

¹Institute of Earth Sciences, Heidelberg University, Germany, ²Department of Earth, Planetary & Space Sciences, University of California Los Angeles, United States, ³Department of Geology, General Directorate of MTA, Turkey

Mafic recharge into shallow crustal magma chambers thermally enables long-lived volcanic systems and potentially exerts a major control on eruptive style and recurrence. Quantification of recharge rates is possible by reconstructing the thermal history of magma chambers. Zircon in particular is useful as it records magmatic conditions upon its protracted crystallization and can be dated at high temporal resolution.

Mt. Hasan and Mt. Erciyes, the two largest and active stratovolcanic complexes of the Central Anatolian Volcanic Province, Turkey, are characterized by highly regular vs. strongly episodic Late Pleistocene–Holocene eruptive behavior. Notable similarities in the trans-tensional tectonic setting of both volcanoes, their magmatic and volcanic longevity at least since the Middle Pleistocene, and knowledge about their integrated eruptive fluxes identify them as ideal candidates to study their magmatic plumbing systems with the goal to understand the conditions governing their contrasting eruptive recurrence patterns. U–Th–Pb zircon rim and interior crystallization ages for >1000 crystals are combined with trace element analyses on the same spots. Thermochemical modeling of zircon crystallization is then used to quantify magma recharge and to evaluate different regimes of magma storage.

Mt. Hasan shows a Late Pleistocene recurrence of at least one eruptive episode of andesitic lava dome and flow as well as block-and-ash-flow emplacement every ca. 5–15 ka. Zircon from Mt. Hasan displays comparatively narrow ranges of Ti-in-zircon crystallization temperatures as well as differentiation indices like Zr/Hf ratios, Eu anomalies (Eu/Eu*), and U contents over the last ca. 300 ka. Mt. Erciyes, on the contrary, is characterized by episodes of scoria cone and lava dome formation at ca. 105–85 ka followed by a protracted eruptive lull and an eruptive resurgence of four nearly-coeval dacitic to rhyolitic lava domes with associated fall-out and pyroclastic-flow deposits at ca. 9 ka. Thermochemical indices for Mt. Erciyes are variable: comparatively primitive zircon interiors nucleated during the active phases of the volcano, whereas progressively more evolved zircon rims crystallized during the extended Late Pleistocene eruptive lull.

Forward modeling of zircon rim and interior crystallization age spectra indicates integrated upper crustal magma recharge rates of ~1–0.5 km³/ka for Mt. Hasan, but only ~0.1 km³/ka for Mt. Erciyes. The corresponding regime of “warm” magma storage for Mt. Hasan (eruptible magma continuously present) contrasts with the predominantly “cold” magma storage for Mt. Erciyes (magma mostly below the rheological lockup temperature). Because the smaller volume inferred for the Mt. Erciyes plumbing system contrasts with its larger edifice volume, it is suggested that this volcano has reached a waning stage, when only episodically intensified magma recharge can trigger violent eruptions. The early Holocene resurgence of Mt. Erciyes may thus be in response to glacial unloading, whereas the peak-stage Mt. Hasan system may be less responsive to changes in magma recharge because its voluminous magma reservoir acts as a thermal buffer.

CHARACTERIZATION OF Cr-DOPED MELT-GROWN AND FLUX-GROWN Ge-MULLITE

Fuchs Andreas¹, Burianek Manfred¹, Birkenstock Johannes¹, Schneider Hartmut¹, Fischer Reinhard X.¹

¹Fachbereich Geowissenschaften, Universitaet Bremen, Germany, andfuchs@uni-bremen.de, burianek@uni-bremen.de, jbirken@uni-bremen.de, hschnei1@uni-bremen.de, rfischer@uni-bremen.de

The oxide mineral mullite has become an increasingly important constituent for conventional and advanced ceramics. It is a compositional series of orthorhombic aluminosilicates with the chemical formula $Al_2(Al_{2+2x}Si_{2-2x})O_{10-x}$, where the x -value stands for the number of oxygen vacancies per unit cell. In the isostructural germanium-mullites, the silicon atoms are replaced by germanium atoms, which slightly alters the lattice parameters in the same space group *Pbam*. However, the Ge-mullites have an extended compositional stability range including the endmember Al_2GeO_5 (Michel et. al., J. Eur. Ceram. Soc., 16, 1996, 161-168). For the synthesis of these materials the flux-growth method as well as the melt-growth method were used. The doping capabilities of these Ge-mullites were investigated by adding different amounts of Cr_2O_3 to the mixture.

For the flux-growth method, a ground mixture of feed nutrient and flux solvent powders was used in a weight ratio of 1:10. The feed nutrients consisted of Al_2O_3 , GeO_2 , and a small amount of Cr_2O_3 powder, whereas the flux solvents consisted of a fixed 1:1 ratio of MoO_3 and Li_2CO_3 powders. The mixture was put into a platinum crucible, heated up to 1280 °C, kept for 36 hours, cooled down within 24 hours to 500 °C, and quenched to room temperature.

For the melt-growth method, GeO_2 and Cr_2O_3 powder were mixed with millimeter sized Al_2O_3 grains, filled in a welded platinum tube and placed in a tube furnace, where it was immediately heated to a temperature of 1550 °C, which was kept for five days and another day at 1400 °C, gradually cooled down to 400 °C within 4 hours, followed by quenching to room temperature. The desired effect of this method is the growth of Ge-Mullite crystals on the partially molten surface of the Al_2O_3 grains, doped with a Cr-content approximately two to three times higher compared to the flux-grown crystals. For the analysis of the resulting samples, energy-dispersive X-ray spectroscopy (EDX) was used to get an approximate chemical composition, as well as single-crystal X-ray diffraction (SCXRD) for investigation of the crystal structure of the obtained crystals.

Both synthesis methods proved to be successful routes to obtain micrometer sized Ge-mullite crystals, where the x -value of the chemical formula ranges from $x = 0.10$ to $x = 0.35$ and the chromium fraction ranges from ~0.7 to ~5.9 mol% according to EDX-analysis. Typical chemical compositions for a flux-grown Ge-mullite are $Cr_{0.11}Al_{1.89}(Al_{2.60}Ge_{1.40})O_{9.70}$ ($x = 0.30$) with low Cr-content and $Cr_{0.74}Al_{1.26}(Al_{2.28}Ge_{1.72})O_{9.86}$ ($x = 0.14$) for a melt-grown Ge-mullite with high Cr-content.

SCXRD measurements confirmed the formation of Ge-mullite. The lattice parameters of one of the flux-grown single crystals were determined as 7.6683(6) Å, 7.7711(6) Å, and 2.953(2) Å for a , b , and c , respectively, resulting in a unit-cell volume of 174.325(38) Å³ close to the values given for Ge-mullite in the literature.

We thank the DFG for funding this project (FI442/25).

GEOCHEMICAL INVESTIGATION OF EXHAUST CAR CATALYSTS

Funari Valerio¹, Mantovani Luciana², Tribaudino Mario², Dinelli Enrico³, Vassura Ivano⁴

¹ISMAR, CNR, Italy, ²Dipartimento di Scienze Chimiche, della Vita e della Sostenibilità Ambientale, Università di Parma, Italy, ³Dipartimento di Scienze Biologiche Geologiche e Ambientali, Università di Bologna, Italy, ⁴Dipartimento di Chimica Industriale “Toso Montanari”, Università di Bologna, Italy

In the project MATCHER, we develop basic and industrial knowledge for the sustainable treatment of exhaust car catalysts (CEA). The presence of refractory, inert support and a catalytic layer composed of platinum, palladium, and rhodium makes CEA interesting in the context of urban mining.

We aimed to characterize representative samples using XRF and XRD to determine the chemical and mineralogical composition, respectively. Leaching tests (time- and pH-dependent) and three-step sequential extractions (acetic acid: exchangeable fraction; hydroxylammonium chloride: reducible fraction; ammonium acetate + hydrogen peroxide: oxidizable/residual fraction) were performed to evaluate the environmental behavior and leaching potential. Finally, a preliminary hydrometallurgical investigation on precious metals recovery using a non-cyanide acid solution is discussed.

Our results highlighted that CEA are mainly composed of cordierite or moissanite support (verified combining XRD and XRF data) and tend to be acidic in water, showing a pH between 5 and 5.5. Sequential extractions showed relatively high Al, Zn, and Pt concentrations in the exchangeable fraction, Al, Mg, Pd, Rh are preferentially in the reducible fraction, and refractory components, including the most platinum group elements, remain in the residual. The hydrometallurgical process yielded higher Pt in the presence of strong oxidizers, such as H₂O₂, while purification is challenging due to the unwanted presence of Zn, Al, Si, Mg, which are also soluble at low pH. The geochemistry of CEA mineralogical phases and metals therein is thus established to favor future resource recovery and waste management strategies for the circular economy.

THE HALOGEN (Cl-Br-I) RECORD OF METAMORPHIC FLUIDS – SECULAR CHANGES FROM THE ARCHEAN TO THE PHANEROZOIC

Fusswinkel Tobias¹, Niinikoski-Fusswinkel Paula¹, Wagner Thomas¹

¹Institute of Applied Mineralogy and Economic Geology, RWTH Aachen University, Germany

Halogen ratios (Br/Cl and I/Cl) in crustal hydrothermal fluids are exceptional tracers of fluid provenance due to their largely conservative behavior during most fluid-rock interaction processes. The halogen signatures of metamorphic fluids provide crucial insight into crustal-scale element cycles and ore formation in orogenic belts, but they remain poorly studied due to significant analytical challenges. Thanks to recent advances in halogen fluid inclusion microanalysis, we present the first comprehensive triple-halogen fluid inclusion LA-ICP-MS dataset from Alpine and Archean metamorphic systems, and we show that these fluids record fundamental changes in the Earth's halogen cycle through time.

The halogen record of Phanerozoic metamorphic fluids derived from carbonaceous calc-schists is controlled by the halogen composition of pore fluids and organic matter in their shelf sedimentary precursor rocks, which in turn attained their halogen signatures via biogenic halogen sequestration from seawater. This inheritance appears to be largely independent of metamorphic grade and fluid composition, underlining the conservative behavior of halogens in such systems. Depending on the availability and the degree of organic matter interaction, such metamorphic fluids can attain high Br/Cl and very high I/Cl ratios, exceeding seawater values by several orders of magnitude and approaching halogen ratios typical for marine organisms.

By contrast, ore-forming fluids from the Neoproterozoic Pampalo orogenic gold deposit (Finland), display highly anomalous halogen signatures. Ample geological and geochemical evidence points to a metamorphic origin of these fluids, but their I/Cl ratios are orders of magnitude smaller than those found in Phanerozoic metamorphic fluids from similar source rocks and formed at similar metamorphic grades. Their halogen signature is also incompatible with other potential fluid sources in orogenic systems, including magmatic-hydrothermal or mantle-derived fluids, as well as any known halogen fractionation mechanism.

We propose that the Pampalo fluids possess metamorphic halogen signatures that were unique to Archean and Proterozoic times. The present-day marine halogen cycle is controlled by metabolic iodine and bromine uptake and sequestration by eukaryotic organisms and their subsequent accumulation in marine organic matter and pore fluids, and Phanerozoic metamorphic fluids inherit these signatures. However, iodine metabolizing eukaryotic organisms only began to dominate Earth's biosphere ca. 900 Ma ago. Iodine sequestration into marine organic matter and sedimentary rocks thus did not occur to a significant degree before this, leading to iodine-poor metamorphic fluid compositions such as those at Pampalo. The halogen signatures of metamorphic fluids were not constant over time but rather reflect the fundamental secular changes in the Earth's hydrosphere and biosphere since Archean times.

V-ANALOG OF LEVANTITE, $\text{KCa}_3(\text{Si}_3\text{Al}_2)\text{O}_{11}(\text{VO}_4)$ – A POTENTIALLY NEW MINERAL OF THE LATIUMITE GROUP FROM ESSENEITE PARALAVA OF THE HATRURIM COMPLEX, NEGEV, ISRAEL

Galuskin Evgeny¹, Galuskina Irina¹, Vapnik Yevgeny²

¹Institute of Earth Sciences, Faculty of Natural Sciences, University of Silesia, Poland, ²Department of Geological and Environmental Sciences, Ben-Gurion University of the Negev, Israel,

In gehlenite pyrometamorphic rocks of the Hatrurim Complex in the Negev Desert, Israel a new mineral levanite, $\text{KCa}_3(\text{Si}_3\text{Al}_2)\text{O}_{11}(\text{PO}_4)$, forming a solid solution with latiumite, $\text{KCa}_3(\text{Si}_2\text{Al}_3)\text{O}_{11}(\text{SO}_4)$, was recently discovered. In levanite Ba, Fe^{3+} and V^{5+} impurities, the content of which usually lower than 0.1 apfu, are detected. The last investigations have shown that levanite is a rock-forming mineral in unusual esseneite paralava forming thin veins in gehlenite hornfelses. In paralava, besides esseneite and levanite, wollastonite, rankinite, garnet of the schorlomite-andradite series, gehlenite and V-bearing fluorapatite are rock-forming minerals. In paralava between rock-forming mineral crystals a small up to 0.3 mm fine-grained aggregates composed of perovskite, celsian, paqueite, latiumite, vorlanite, minerals of the dorrite-khesinite series, magnesioferrite, gorerite are noted. In the one of such aggregates, in association with paqueite and V-bearing fluorapatite, grains of V-analog of levanite up to 10 μm in size were found. Its composition is described by the empirical formula: $(\text{K}_{0.85}\text{Ba}_{0.15})_{\Sigma 1.00}\text{Ca}_3(\text{Si}_{2.65}\text{Al}_{2.25}\text{Fe}^{3+}_{0.10})_{\Sigma 5.00}\text{O}_{11}[(\text{VO}_4)_{0.5}(\text{PO}_4)_{0.3}(\text{SO}_4)_{0.2}]_{\Sigma 1.00}$, which can be simplified to ideal formula $\text{KCa}_3(\text{Si}_3\text{Al}_2)\text{O}_{11}(\text{VO}_4)$. Raman spectrum of V-analog of levanite significantly differs from the Raman spectra of minerals of the levanite-latiumite solid solution, for which the two strong bands are characteristic at 995 cm^{-1} [$\nu_1(\text{SO}_4)^{2-}$] and 945 cm^{-1} [$\nu_1(\text{PO}_4)^{3-}$]. In V-analog of levanite spectrum there are the four strong bands: 987 cm^{-1} [$\nu_1(\text{SO}_4)^{2-}$], 850 cm^{-1} [$\nu_1(\text{VO}_4)^{3-} + \nu_1(\text{SiO}_4)^{4-}$], 734 cm^{-1} [$\nu_1(\text{AlO}_4)^{5-}$] and 369 cm^{-1} [$\nu_4(\text{VO}_4)^{3-}$]. The band near 942 cm^{-1} responded to vibrations of $\nu_1(\text{PO}_4)^{3-}$ has low intensity. V-analog of levanite is a fourth vanadium mineral discovered in rocks of the Hatrurim Complex. Before, gurimite, aradite and pliniusite were described from high-temperature paralava (~1000-1200°C).

The investigations were supported by the National Science Centre (NCN) of Poland, grant no. 2016/23/B/ST10/00869.

A POTENTIALLY NEW MINERAL, $\text{Ca}_3\text{TiSi}_2(\text{Fe}^{3+}_2\text{Si})\text{O}_{14}$, OF THE LANGASITE-TYPE STRUCTURE FROM PYROMETAMORPHIC ROCKS OF THE HATRURIM COMPLEX, PALESTINE

Galuskina Irina¹, Stachowicz Marcin², Vapnik Yevgeny³, Zieliński Grzegorz⁴, Woźniak Krzysztof⁵

¹Institute of Earth Sciences, Faculty of Natural Sciences, University of Silesia, Poland, ²Institute of Geochemistry, Mineralogy and Petrology, University of Warszawa, Poland, ³Department of Geological and Environmental Sciences, Ben-Gurion University of the Negev, Israel, ⁴Polish Geological Institute - National Research Institute, Poland, ⁵Department of Chemistry, University of Warsaw, Poland

A potentially new mineral with ideal formula $\text{Ca}_3\text{TiSi}_2(\text{Fe}^{3+}_2\text{Si})\text{O}_{14}$, was found in gehlenite-rankinite paralava at Nabi Musa locality situated in the Judean Desert, West Bank, Palestine. This area is a part of the pyrometamorphic Hatrurim Complex. The studied mineral belongs to the langasite structural type ($\text{La}_3\text{Ga}_5\text{SiO}_{14}$) – synthetic family compounds, with the general formula $A_3BC_2D_3O_{14}$, where $A = \text{Ba, Sr, Ca, Pb}$; $B = \text{Sb, Nb, Ta, Te}$; $C = \text{Si, Ge, P, V, As}$; $D = \text{Fe, Co, Mn}$. The studied mineral crystallizes in the trigonal non-centrosymmetric $P321$ space group with $a = 8.0077(5)$, $c = 4.9956(4)$ Å. The potentially new mineral is a Fe^{3+} -analog of paquetteite, $\text{Ca}_3\text{TiSi}_2(\text{Al}_2\text{Si})\text{O}_{14}$, described from Aliende meteorite.

Paralava containing this mineral is composed of rankinite, gehlenite, rarer wollastonite, Ti-bearing andradite, kalsilite. Minerals of khesinite-dorrite series, barioferrite, minerals of magnesioferrite-magnetite-maghemite series, hematite, Si-bearing perovskite, Si-V-bearing fluorapatite, gurimite, hexacelsian are accessory minerals. Baryte, hydrated calcium silicates (tobermorite, afwillite), tacharanite, fabrièsite-like minerals are later, hydrothermal minerals. A Fe^{3+} -analog of paquetteite forms aggregates of flattened crystals up to 40-50 µm in length and lesser than 5 µm in thickness. The mineral shows light-brown color with an insignificant red hue. Lustre is strong vitreous. Mohs's scale hardness is 6. The mineral is brittle and has uneven, conchoidal fracture. The empirical formula calculated on the basis of 14O is $(\text{Ca}_{2.96}\text{Sr}_{0.02}\text{Mn}_{0.01})_{\Sigma 2.99}\text{Ti}^{4+}(\text{Si}_{1.99}\text{P}_{0.01})_{\Sigma 2}(\text{Fe}^{3+}_{1.59}\text{Si}_{0.60}\text{Al}_{0.43}\text{Ti}^{4+}_{0.38}\text{Cr}_{0.01})_{\Sigma 3.02}\text{O}_9$. The simplified formula is $\text{Ca}_3\text{Ti}^{4+}\text{Si}_2(\{\text{Fe}^{3+}, \text{Al}\}_2\{\text{Si}, \text{Ti}^{4+}\})\text{O}_{14}$. The main bands in the Raman spectrum depend on the crystal orientation, so there are listed for the two crystal orientation (cm^{-1} , $\sim \perp Z/\parallel Z$): 166/172, 218/215 related to Ca-O vibrations and/or $\nu_2^B(\text{TiO}_6)^{8-}$; 244/252, 331/ \sim 353 related to vibrations $R(\text{TO}_4)$, $\nu_2^D(\text{FeO}_4)^{5-}$; 437/448 – $\nu_4^B(\text{TiO}_6)^{8-}$, $\nu_4^D(\text{FeO}_4)^{5-}$, $\nu_4^C(\text{SiO}_4)^{4-}$; 611/613 – $\nu_1^B(\text{TiO}_6)^{8-}$, $\nu(B\text{Ti-O}^D\text{Ti})$; 713/718 – $\nu_1^D(\text{FeO}_4)^{5-}$; 766 – $\nu_1^D(\text{TiO}_4)^4$, $\nu_1^D(\text{AlO}_4)^{5-}$; 855 – $\nu_1^C(\text{SiO}_4)^{4-}$; 978/986 – $\nu_3^C(\text{SiO}_4)^4$, $\nu(C\text{Si-O}^D\text{Si})$.

The Fe^{3+} -analog of paquetteite is the first terrestrial mineral of the langasite type compound.

The investigations were supported by the National Science Centre (NCN) of Poland, grant no. 2016/23/B/ST10/00869.

ADVANCED STATISTICAL ANALYSIS OF X-RAY DIFFRACTION DATA: KAOLINITE POLYTYPES

García-Vicente Andrea¹, Lorenzo Adrián¹, Sánchez Migalloón Juan Morales¹, García-Romero Emilia^{2,3}, Suárez Mercedes¹

¹Geology, University of Salamanca, Plaza de la Merced, s/n, 37008 Salamanca Spain, ²Department of Mineralogy and Petrology, Complutense University of Madrid, C/José Antonio Novais, 8 28014 Madrid, ³Geoscience Institute, CSIC-UCM, 28014 Madrid

In order to establish an accurate method of classification, 17 kaolin samples with different purity degrees were studied. The samples come from different locations around the world and have different geological origins. The powder XRD patterns were obtained with a Bruker D8 Advance Eco diffractometer with theta-2theta configuration. The statistical treatment of the X-Ray Diffraction profiles has been carried out, and cluster analysis, as well as Principal Components Analysis (PCA), have been performed prior to the mineralogical identification of the samples. The number of clusters leads to cut the dendrogram into 3 groups, and further analysis reveals that these groups classify the samples according to the kaolinite polytype. From the 17 samples studied, 11 have been identified as kaolinite, 5 as dickite, and 1 as nacrite. The analysis excludes data showing low crystallinity since it uses criteria based on Euclidean distance as an indicator of similarity. The greater the Euclidean distance, the greater the difference in the diffractograms, allowing the classification of polytypes. The software cuts the analysis at a distance of 21.71 by the Euclidean distance method. This method provides an accurate classification of minerals of the kaolinite group and within the kaolinite group, two sub-groups were obtained due to a separation between ordered and disordered kaolinites.

In PCA analysis, Component 1 has been considered on the x-axis, and Component 2 has been considered on the y-axis, since they provide the most reliable PCA. Component 1 explains 43.36% of the variance and Component 2 the 70.96%.

Cluster analysis and PCA analysis of kaolin XRD data represents a rapid method for grouping data into discrete classes based on mineralogical similarities, and thus allows for sets of different polytypes to be defined and investigated in greater detail. This study is viewed as a necessary introduction to the application of cluster analysis and PCA to large datasets of kaolin XRD data, in order to establish a relationship between them, helping to kaolinite polytype distinction. In good agreement with the classical analysis of the XRD results, the statistical analysis, both by cluster analysis and by PCA, allow an unequivocal classification of the samples according to the polytype. The use of the full profile of XRD allows for more samples and accurate identification, even when they have low crystallinity or preferred orientation effects are significant. The software provides an easy-going way of use and contributes to a novel statistical method to rank kaolin samples in order to their similarity, allowing unknown to be quickly identified. So that, from unknown kaolin samples, it is possible to identify groups belonging to kaolin polytypes. The farther up the similarity axis (y-axis) the patterns are joined, the less similar they are. Given the estimated similarity between patterns, it is then possible to classify similar X-ray diffraction profiles belonging to the same cluster.

The Principal Components Analysis (PCA) makes it easier to visualize the relationship between the variables. The eigenvalues plot is one of many methods used for estimating the cut-level of PCA analysis and is based on a correlation matrix.

SORPTION OF Cs-137 ONTO PORTUGUESE BENTONITES: A PRELIMINARY STUDY

García-Rivas Javier^{1,2}, Paiva Isabel¹, Dias Maria Isabel¹, Madruga Maria José¹

¹Center for Nuclear Sciences and Technologies (C2TN), Instituto Superior Técnico, University of Lisbon, 2695-066-ID, C2TN, Portugal,² Department of Geology, University of Salamanca, 37008 Salamanca, Spain, javier.rivas@ctn.tecnico.ulisboa.pt, ipaiva@ctn.tecnico.ulisboa.pt, isadias@ctn.tecnico.ulisboa.pt.

European directive 2011/70/EURATOM obliges all Member States of the European Union to implement National Programs envisaging the implementation of responsible and safe management strategies for radioactive waste developing R&D programs according to a policy of transparency, that accounts for the protection of public, workers, and environment as being fundamental.

In this context, preliminary studies were carried out on the largest known deposit of bentonites in continental Portugal, located in Benavila (in the Alentejo region). Three samples were characterized through X-Ray Diffraction (XRD) in their bulk and < 63 µm fractions, identifying and semi-quantifying the main mineral phases. In addition, their specific surface areas (SSA) and pore diameters were also measured by the BET method, in milled and non-milled samples. The radiocaesium interception potential (RIP) of the samples was measured using the methodology by Madruga et al. (2002), also in milled and non-milled samples.

The XRD characterization of the samples allowed observing that the main mineral component of the samples is dioctahedral smectite, which increases its content in the fraction <63 µm, accompanied by smaller quantities of other minerals such as carbonates, tectosilicates, other phyllosilicates, and amphiboles.

The measurement of the SSA of the samples showed interesting data. The milled fraction of the bulk samples had lower SSA than the fraction <63 µm, as expected due to the higher content in smectites. However, the pore diameters of the fraction <63 µm were substantially smaller than the ones in the bulk sample, due to the textural changes the samples encountered after the wet sieving process performed to separate the fractions. Non-milled samples showed that in both cases the SSA and pore diameters were smaller than in the previous experiments. The differences in the values between milled and non-milled samples are, once again, explained by their different textural properties. The results from the radiocaesium sorption experiments showed that milled bulk samples had higher RIP than the milled fraction <63 µm, clashing with their higher SSA. However, it can be explained by their higher pore diameters, evidencing the importance of the texture of the bentonites. The non-milled samples show smaller RIP values than the milled samples, corroborating the important role the texture plays in the sorption properties of bentonites. These results show that the textural modifications that bentonites suffer in laboratory experiments, where it is typically considered that only the percentage of smectites within the sample and not their textural influence their sorption properties, might negatively influence the results. In addition, thinking in their applicability at real scenarios of radioactive waste disposal sites, it reinforces their possible use, since it is more plausible to mill high volumes of bulk samples on-site rather than separate different granulometric fractions.

VNIR – SWIR ANALYSIS OF POLYMINERALIC SAMPLES: A STATISTICAL APPROACH

García-Rivas Javier¹, Suárez Mercedes¹, García-Romero Emilia^{2,3}

¹Department of Geology, University of Salamanca, Spain, ²Department of Mineralogy and Petrology, Complutense University of Madrid, Spain, ³Geosciences Institute, CSIC – UCM, 28040 Madrid, Spain, javiergr89@usal.es, msuarez@usal.es, mromero@geo.ucm.es.

Visible and near-infrared – short wave infrared (VNIR – SWIR) spectroscopy is a technique gaining more importance in recent times due to the development of field spectroradiometers which allows to rapidly characterize high volumes of samples in situ. In addition, hyperspectral images obtained through remote sensing techniques also allow to perform VNIR – SWIR spectroscopical studies of difficult access locations as well as extraterrestrial bodies. There are spectral libraries with wide information on pure minerals, but the studies on sedimentary materials composed of complex mixtures of different minerals which spectral feature overlap are still scarce.

In this work, 42 samples from the Tajo Basin (Spain) formed by detrital and neofomed minerals, previously characterized by XRD, were studied with the aim of obtaining discriminatory criteria that could enable differentiating these minerals from complex mineralogical natural mixtures by VNIR-SWIR.

The samples are composed of clay minerals mainly, together with variable amounts of quartz, feldspar, calcite, and gypsum. Among the clay minerals, smectites and illite are abundant, while kaolinite and chlorite appear as minor components. The VNIR – SWIR spectra showed absorption features due to the different minerals, so close to each other that are overlapped in some cases, not being able to distinguish to which minerals they correspond. But when the second derivative of the spectra was obtained, it was possible to observe discriminate peaks that allow a deeper study because soft shoulders, which are unperceived in the spectra, are completely separated and identifiable as peaks in the derivative curve, and. In addition, the relative intensities are normalized, which allows to directly compare different samples and relate the peak intensity to the amount of the mineral in the sample.

The correlation of both the position and the intensity of the peaks in the second derivative curve of the spectra and the mineral content semi-quantified by XRD allows the identification of the minerals that originate the peaks. The peaks that correspond to the lowest reflectance of the main absorption features in the spectra are easily identifiable because they are widely referred to in the literature. However, the statistical treatment allowed us to identify minor peaks dues to minority minerals and, from them, determine the spectral signature of each mineralogical association present in the studied area.

The results presented here, which show that the intensities of different absorption features in the second derivative can be correlated with the mineral content, clearly corroborate the potential of this technique. Then, from this preliminary work, the study of the mineralogical composition in a wide zone will be done in a quick way, directly by the VNIR-SWIR field spectroscopy. This works shows the viability of developing mathematical models to semi-quantify the spectra of polymineralic samples.

BOWLESITE, PtSnS, A NEW PLATINUM GROUP MINERAL (PGM) FROM THE MERENSKY REEF OF THE BUSHVELD COMPLEX, SOUTH AFRICA

Garuti Giorgio¹, Vymazalova Anna², Zaccarini Federica³, Laufek František², Mauro Daniela⁴, Stanley Chris⁵, Biagioni Cristian⁴

¹Departement of Applied Geosciences and Geophysics, University of Leoben, Austria, ²Czech Geological Survey, Czech Republic, ³Department of Applied Geosciences and Geophysics, University of Leoben, Austria, ⁴Dipartimento di Scienze della Terra, University of Pisa, Italy, ⁵Department of Earth Sciences, Natural History Museum, United Kingdom

The Merensky Reef is a famed mineralized horizon of igneous rocks in the Bushveld layered complex, South Africa. Although the Merensky Reef contains one of the world's largest concentrations of platinum-group elements (PGE), only 5 platinum-group minerals (PGM), namely atokite, braggite, cooperite, merenskyite, and rustenburgite, have been discovered, for the first time, in this mineralized horizon. In this contribution, we report the discovery of a further PGM found in the Merensky Reef.

During the examination of a sample collected during the third International Platinum Symposium held in Pretoria (South Africa) from 6 to 10 July 1981, having a chemical composition PtSnS was analyzed. This chemistry did not correspond to any accepted mineral specie. Consequently, a formal proposal was submitted and approved by the Commission on New Minerals, Nomenclature, and Classification of the International Mineralogical Association, under the number 2019-079. The studied polished blocks in which the new PGM was discovered comprise a thin layer of cumulitic chromitite, about 0.2 cm thick, in contact with a pegmatoidal feldspathic pyroxenite that contains accessory actinolite, micas, talc, chlorite, and serpentine. The plagioclase shows a composition corresponding to andesine, and the pyroxenes can be classified as augite and enstatite. The new PGM is brittle and has a metallic luster. In plane-polarized light, it appears as light bluish grey and shows no bireflectance and or pleochroism with a weak anisotropism. Internal reflections were not observed. Reflectance values of bowlesite in the air (R1, R2 in %) are: 50.3-51.4 at 470 nm, 48.5-48.9 at 546 nm, 47.9-48.6 at 589 nm, and 47.8-48.7 at 650 nm. Ten analyses of the new PGM give the following average composition: Pt 56.85, Pd 0.02, Sn 34.03 and S 0.15, total 100.05 wt %, corresponding to the empirical formula $(Pt_{1.001}Pd_{0.001})\Sigma_{1.002}Sn_{0.997}S_{1.001}$, based on 3 atoms per formula unit. Therefore, the simplified formula is PtSnS. Due to the small size of the natural bowlesite, the crystal structure was solved and refined from the single-crystal X-ray-diffraction data of synthetic PtSnS. The calculated density is = 10.06 g•cm⁻³. The mineral is orthorhombic, space group: Pca21 with a = 6.12 Å, b = 6.12 Å, c = 6.10 Å and Z = 4. The identity of the natural PGM and the analog synthetic was confirmed by the Raman spectra, The crystallization of the new PGM is related to the formation of an immiscible sulfide melt. Its precipitation is related to the low-T exsolution of Pt-Sn phases from the high-T sulfides crystallized from the sulfide melt, during fluids activity. The name of this newly discovered PGM is bowlesite.

The mineral honors John Bowles, Honorary Visitor at Manchester University, UK, for his contributions to ore mineralogy and mineral deposits related to mafic-ultramafic rocks.

"WATER" IN CALCIUM-SILICATE GARNET: MICRO- AND NANO-SIZE HYDROGARNET CLUSTERS

Geiger Charles A.¹, Rossman George R.²

¹Chemistry and Physics of Materials, University of Salzburg, Austria, ²Geological and Planetary Sciences, California Institute of Technology, United States

The nominally anhydrous calcium-silicate garnets, grossular - $\text{Ca}_3\text{Al}_2\text{Si}_3\text{O}_{12}$, andradite - $\text{Ca}_3\text{Fe}^{3+}_2\text{Si}_3\text{O}_{12}$ and their solid solutions $\text{Ca}_3(\text{Al}_x\text{Fe}^{3+}_{1-x})_2\text{Si}_3\text{O}_{12}$, can incorporate various amounts of structural OH^- . The general term hydrogarnet or the phrase "water-bearing" garnet is often used to describe this class of minerals. A large number of mineralogical, petrological, and geochemical investigations have been made on them for various reasons. However, it was not understood how OH^- was incorporated crystal chemically and this has seriously hampered a full and precise interpretation of the many different research results. The IR single-crystal spectra of a number of calcium silicate garnets, both "end-member" and solid-solution compositions, were recorded at room temperature and 80 K between 3000 and 4000 cm^{-1} . Five synthetic hydrogarnets in the system grossular-andradite-hydrogarnet ($\text{Ca}_3(\text{Al},\text{Fe}^{3+})\text{H}_{12}\text{O}_{12}$) were also measured using IR ATR powder methods. The various spectra are rich in complexity and show a number of different wavenumbers OH^- stretching modes between 3500 and 3700 cm^{-1} . The data, together with published results, were analyzed and the modes assigned by introducing atomic-vibrational and crystal-chemical models to explain the energy of the OH^- dipole and the structural incorporation mechanism of OH^- , respectively. It is argued that OH^- is located in various local microscopic- and nano-size $\text{Ca}_3\text{Al}_2\text{H}_{12}\text{O}_{12}$ - and $\text{Ca}_3\text{Fe}^{3+}_2\text{H}_{12}\text{O}_{12}$ -like clusters with sizes between about 3 and 15 angstroms. The basic substitution mechanism is $(\text{H}_4\text{O}_4)^+ = (\text{SiO}_4)^+$, and various local configurations containing different numbers of $(\text{H}_4\text{O}_4)^+$ groups define the cluster type. Published proposals invoking purely hypothetical defect (e.g., $\text{Al}^{3+} = 3\text{H}^+$, $\text{Ca}^{2+} = 2\text{H}^+$) and coupled-substitution mechanisms (e.g., $\text{H}^+ + \text{Al}^{3+} = \text{Si}^{4+}$, $\text{H}^+ + \text{Na}^+ = \text{Ca}^{2+}$) to account for OH^- in garnet are not needed to interpret the IR and Raman OH^- modes above about 3560 cm^{-1} . Moreover, a new understanding at the atomic level of published dehydration and H-species diffusion studies is now possible for the first time. This also the case for H_2O -concentration and IR absorption-coefficient studies. Similar IR "OH-band patterns" are found among different natural, calcium-silicate garnets possibly indicating that chemical equilibrium operated during their crystallization. Under this assumption, the hydrogarnet-cluster types and their concentrations could potentially be used to decipher petrologic conditions (i.e., P-T-X) under which a garnet crystal, and the rock in which it occurs, formed.

SCANDIUM BEHAVIOR AND MINERAL CHEMISTRY DURING LEACHING OF BAUXITE RESIDUES

Gentzmann Marie¹, Paul Andrea¹, Serrano Juan¹, Adam Christian¹

¹Federal Institute for Materials Research and Testing, Germany

Bauxite residues (BRs) accumulate during the processing of bauxites for alumina production and accrue in large quantities all over the world. The majority is deposited in large disposal areas where risks for the environment and surrounding communities remain. Extensive research is conducted to find strategies for the reuse of this material including the recovery of valuable elements. Scandium (Sc), which was found to be enriched in some BRs, is one of those elements. The beneficial use of Sc in lightweight alloys or solid oxide fuel cells makes it a key enabler for some of the sustainable technologies of the future. The strategies developed for the recovery of Sc from BRs include acid, alkali, and ionic liquid leaching processes. Their efficiency is dependent on physical and chemical parameters e.g. temperature, pressure, liquid/solid ratio, leaching agent, and its concentration. Additionally, the nature and mineralogy of the BR and its precursor bauxite play an important role. In the presented study we aimed to understand how physical and chemical parameters influence the Sc recovery with regard to the changes of the mineral assemblage in the treated BR. Therefore, leaching experiments were performed on BRs of different geological backgrounds. The experiments were planned according to an experimental design that helped to understand parameter interactions and influences and show differences between the treated BRs. Since those residues resulted from the processing of karstic or lateritic bauxites that weathered under oxidizing or partly reducing conditions, the Sc mass fraction and assemblage in the resulting BRs differ. The differences had a strong effect on the recovery which can be better understood by investigating the mineralogy of the leached BRs. In total, three different BRs were studied in detail using sulfuric and citric acid leaching whereas the BR and the acid were considered as categorical factors. Temperature (25°C, 85°C), liquid/solid ratio (10, 20), acid concentration (1N, 3N), and leaching time (2h, 4h) were chosen as continuous factors with two levels. Then, 18 different experimental setups including replicates were randomly performed for three BRs. The leachates and residues were analyzed by ICP-OES and XRD. The BRs of lateritic and karstic bauxites that were formed under predominantly oxidizing conditions, as indicated by the presence of hematite and goethite, showed very similar leaching behavior for Sc. Citric and sulfuric acid leaching yielded Sc recoveries of 40% and XRD analyses showed that hematite and goethite were the main residual phases as they were not dissolved under the chosen leaching conditions. In BR from karstic bauxite formed under partly reducing conditions, sulfuric acid leaching was able to recover 60-80% of Sc with the chlorite group mineral chamosite being dissolved under the strongest leaching conditions. Therefore, the most influential factor for the Sc recovery is the type of the BR, followed by the acid type and temperature. The acid concentration and liquid/solid ratio showed only small influences and the tested time showed no influence. Our study provides insights into the association and behavior of Sc in BR before and during leaching and serves to increase the fundamental knowledge to develop efficient Sc recovery techniques for BRs of different origins.

This research has received funding from the European Community's Horizon 2020 Programme SCALE (H2020/2014-2020) under grant agreement n° 730105.

SOLID SOLUTIONS OF INORGANIC AND ORGANIC HYDROCALUMITE/ KUZELITE-RELATED PHASES WITH SULFATE, CHLORIDE, CARBONATE, AND CARBOXYLATE ANIONS

Gerhardt Sebastian¹, Pöllmann Herbert¹

¹Mineralogy/ Geochemistry, Martin-Luther-Universität Halle-Wittenberg, Germany

Al₂O₃-Fe₂O₃-mono-phases (AFm-phases), similar to some naturally existing minerals like Hydrocalumite and Kuzelite, form a double-layered crystal structure with positively charged main layers and negative charged interlayers. The general structural formula is $[\text{Me}_{(1-x)}^{2+} \text{Me}_{(x)}^{3+} (\text{OH})_2]^{x+} [\text{A}_{(x/y)}^{y-} \cdot m\text{H}_2\text{O}]^{x-}$. These AFm-phases play an important role in the hydration of cementitious materials or in other fields of application like catalysis, medicine and restoration of brownfields. Solid solutions of inorganic and organic AFm-phases will be synthesized in an aqueous environment using calciumsulfate, -chloride and -carbonate, and various calcium carboxylate anions forming the interlayers and calcium and aluminum forming the main layers. The synthesis will be varied according to $\text{CA}_n\text{CaX}+2\text{CaO}+(1-n)\text{CaY}+m\text{H}_2\text{O}$ with X being sulfate, chloride, or carbonate and Y being the carboxylate anion of oxalic, malonic, succinic, acetic, benzoic, phenylacetic, methanesulfonic, ethanesulfonic, propanesulfonic, benzenesulfonic and m-methylbenzenesulfonic acid will be used for synthesis. n will be increased stepwise by 0.1 mole. Since the system only contains aluminum and calcium besides the anions and water, the cation positions of the general formula are fixed. Every synthesis step with the sample containing water will be done using a nitrogen protective atmosphere to decrease the probability of carbon dioxide contamination. New solid solutions will be dried at varying humidity to acquire the different hydration stages. The physical and chemical properties of each new phase will be determined by X-ray diffraction, differential thermal analysis, thermogravimetry, Karl Fischer titration, ion-exchange chromatography, and scattering electron microscopy.

RARE SULFATES IN EFFLORESCENCES AND CRUSTS: STONE-ENVIRONMENT INTERACTION IN THE UNDERGROUND ARCHAEOLOGICAL SITE OF YOSHIMI, JAPAN

Germinario Luigi¹, Oguchi Chiaki T.¹

¹Department of Civil and Environmental Engineering, Saitama University, Japan

Salt weathering is among the most infamous processes of stone decay and has been broadly discussed in previous research for the risk posed to the conservation of cultural heritage. Most studies have focused so far on the built heritage on the surface, while often neglecting underground sites. This contribution will discuss underground stone deterioration by examining the patterns, compositional characteristics, and time-space variability of salt weathering in the archaeological site of Yoshimi Hyaku Ana in Japan. The site includes a cluster of Kofun tombs of the 6th-7th century and galleries of the WWII era excavated into volcanic tuff outcrops. In order to explore the stone-environment interaction, field explorations and the mineralogical analysis of the salts were combined with the petrographic, geochemical, and petrophysical characterization of the tuff, a microclimate monitoring, and the chemical analysis of groundwater and rainwater. The salt weathering in Yoshimi Hyaku Ana involves efflorescences and crusts made of mixed soluble sulfates, mostly hydrated: gypsum, alunogen, alum-(Na), halotrichite, epsomite, polyhalite, tamarugite, thenardite, and mirabilite. Some of these phases have never or rarely been reported in heritage studies. The laboratory and field measurements suggest that the salts derived from the alteration of the rock-forming minerals and components (pyrite, glass, feldspars, etc.); their compositional variability, instead, is affected by both the lithological diversity of the stone substrates and the microclimate changes, especially related to the seasonal fluctuations of relative humidity.

ELASTIC GEOBAROMETRY OF QUARTZ INCLUSIONS IN GARNET FROM GRANULITES

Gilio Mattia¹, Campomenosi Nicola², Musiyachenko Kira³, Angel Ross J.⁴, Cesare Bernardo⁵, Alvaro Matteo¹

¹Department of Earth and Environmental Sciences, University of Pavia, Italy, ²Department of Earth Science, University of Hamburg, Germany, ³Department of Earth, Ocean and Atmospheric Sciences, University of British Columbia, Canada, ⁴Instituto di Geoscienze e Georisorse, Consiglio Nazionale delle Ricerche, Italy, ⁵Department of Geosciences, University of Padova, Italy

Elastic geobarometry is a non-destructive method that allows the determination of the pressure and temperature of entrapment of inclusion still trapped within a host. So far, elastic geobarometry has only been applied to rocks with inclusions that were entrapped at high pressure and low-temperature conditions, such as eclogites. For application to quartz inclusions trapped at high-temperature and low-pressure conditions ($T > 700^{\circ}\text{C}$ and $P < 1.0$ GPa), the significant effects of the α - β transition on the thermal expansion and elastic properties must be allowed for. In this presentation, we will show some preliminary results of quartz-in-garnet elastic geobarometry for inclusions entrapped (or re-equilibrated) within the β -quartz stability field.

The analyzed samples come from three HT terranes: the Athabasca granulite terrane in Canada, the Jubrique Unit in the Beltic Cordillera in Spain, and the Aus granulite terrane from the Namaqua Metamorphic complex in southern Namibia. All of these locations contain crustal rocks such as garnet-bearing gneisses and felsic granulites which equilibrated at, or passed through, low pressures and high temperatures, near or within the β -quartz stability field. Quartz inclusions in garnet show post-entrapment shape change attested by negative crystal shapes and locally by necking. The quartz inclusions display Raman spectra whose peaks are shifted to lower frequencies with respect to unstrained reference quartz crystals. The Raman peak shifts of the inclusions were converted into strains using the software StRainMAN (www.rossangel.com) and have positive volume strains with a tensile strain in the (001) plane ($\epsilon_1 > 0$) and a compressive strain along the c-axis ($\epsilon_3 < 0$). Using a quartz EoS which includes the effects of the α - β quartz transition, it was possible to obtain isomekes crossing the phase transition and to estimate the entrapment pressures and temperatures of quartz inclusions entrapped at HT. The results of elastic geobarometry for the set of samples in question are consistent with the PT conditions estimated by classic geothermobarometry.

This work was supported by ERC-StG TRUE DEPTHS grant (number 714936) to M. Alvaro

ELASTIC GEOBAROMETRY: HOW TO WORK WITH RESIDUAL INCLUSION STRAINS AND PRESSURES

Gilio Mattia¹

¹Department of Earth and Environmental Sciences, University of Pavia, Italy

Elastic geobarometry is a useful tool to estimate the pressure and temperature (PT) of equilibration of rock starting from the residual pressure of crystalline inclusions trapped in a mineral host. Consider a soft inclusion in a stiffer host (e.g., quartz in garnet) entrapped at a certain P_{Trap} condition and exhumed to the surface (P_{Tend}). At P_{Tend} conditions, both host and inclusion have a larger volume than at entrapment, due to pressure being released upon exhumation ($\Delta V > 0$). However, the volume increase of the softer quartz should be greater than that of the stiffer host ($\Delta V_{qz} > \Delta V_{grt}$). Therefore, upon decompression, the host garnet compresses the quartz inclusion into a smaller volume than it would have as a free crystal. Measurement of the inclusion residual pressure (P_{inc} = mean normal stress) at T_{end} (normally room T), combined with knowledge of the elastic properties of host and inclusion, allows one to back-calculate a line in PT space of possible entrapment conditions: the isomeke.

A continuously increasing number of research groups are adopting elastic geobarometry for retrieving pressures and temperatures of entrapment of inclusions into a host from both natural and experimental samples. However, a few misconceptions of some of the general concepts underlying elastic geobarometry are still widespread. One is the difference between various approaches to determine the residual strains and in turn, stresses or pressures from Raman measurements of inclusions. I will discuss in detail the validity of some general assumptions behind these methods, and I will show how to correctly estimate uncertainties. Furthermore, I will provide general guidelines on how to deal with unstrained reference standards, inclusion strain, measurements, inclusion pressure, and their uncertainties.

This work was supported by ERC-StG TRUE DEPTHS grant (number 714936) to M. Alvaro

VOLCANOGENIC MASSIVE SULPHIDE DEPOSITS HOSTED IN ULTRAMAFIC ROCKS (WESTERN CUBA): A SUBDUCTION-INITIATION TYPE OPHIOLITE PRODUCT

Giralt Susqueda Alberto¹

¹Facultat de Ciències de la Terra, Universitat de Barcelona, Spain

Volcanogenic massive sulfide deposits (VMS) hosted in ultramafic rocks represent a rare sub-type within VMS deposits and their nowadays equivalents. These deposits have been described as a new VMS type (Atlantic type) or included within the Chipre-type VMS deposits (Melekestseva et al., 2013).

Ophiolites from western Cuba (Habana-Matanzas region) contain several VMS deposits hosted in ultramafic rocks. These deposits have been exploited for Cu since the 16th century and represent the only example of this kind of VMS sub-type in the Caribbean region. In this contribution, we present new geochemical, textural and mineralogical data from this kind of mineralization. The results of this study are integrated with petrogenetic and geodynamic models produced to understand the ophiolites cropping out throughout the Caribbean region. We propose that the studied deposits might have been formed during the early stages of oceanic lithosphere structuring in a fore-arc region (subduction-initiation type ophiolite).

Geology, geochemistry, and mineralogy of Habana-Matanzas ophiolite is mainly constituted by tectonic blocks of serpentinized peridotites and, to a lesser extent, by gabbros and volcanic rocks characteristic of the crustal levels of an ideal ophiolitic sequence. The studied VMS deposits are located within NE-SW and E-W shear zones (Llanes et al., 2013) that cross-cut ultramafic rocks belonging to the upper part of the mantle (serpentinized harzburgites). The mineralization in these deposits appears as massive lenses, veins, and mineral disseminations. These deposits are enriched in Cu, Co, Ag, Au (up to 4.8 ppm) and Platinum-Group Elements (up to 1.5 ppm). The mineral paragenetic sequence of the studied deposits (Loma Majana, Salomón) is divided in: i) pyrrhotite mineralization with minor amounts of chalcopyrite and pentlandite. Smectite and talc are also formed during this stage as alteration products of the host serpentinite; ii) precipitation of pyrite and a second generation of chalcopyrite; iii) late-stage mineralization of Co-Ni-Fe arsenides and sulfoarsenides, with Au-Ag inclusions. FIB/HRTEM observations have revealed that gold is located as electrum nano-nuggets (410 nm) in the interphase between the arsenides and sulfoarsenides. Electrum's average composition is 60 wt% Au and 40 wt% Ag. VMS deposits hosted by ultramafic rocks have been associated to oceanic core complexes (OCC), which are exhumed by detachment faults in slow and ultra-slow mid ocean ridges (Knight et al., 2018 and references therein). However, the VMS deposits in Habana-Matanzas region are hosted by supra-subduction zone (SSZ) peridotites (U-shaped REE patterns, accessory chromite with Cr# > 0.6, Al- and Ca-poor orthopyroxenes). Relicts of chromite grains within the massive sulfide mineralization also have SSZ signature (Cr# ~ 0.7). This geodynamic setting is also consistent with the volcanic rocks from the upper levels of the Habana-Matanzas ophiolite, which are classified as boninites and island-arc tholeiites (IAT). All these rocks point to a fore-arc setting produced during the first magmatic stages of an extensional regime linked with the subduction initiation and the onset of an intraoceanic island-arc. OCC, similar to the ones described in slow to ultra-slow ocean ridges and that might contain VMS hosted by ultramafic rocks, have been partially preserved in subduction-initiation type ophiolites (Tremblay et al., 2009).

FLUID INDUCED TITANITE CHANGES: INSIGHT FROM CLOSEPET GRANITE (DHARWAR CRATON, INDIA)

Gmochowska Wiktoria¹, Słaby Ewa¹, Ciążela Jakub¹, Bhattacharya Sourabh²

¹Institute of Geological Sciences, Polish Academy of Sciences, Poland, ²School of Earth Ocean and Climate Sciences, Indian Institute of Technology Bhubaneswar, India

Titanite (CaTiSiO₅) is an important tracer of many processes in the Earth's continental crust. Firstly, titanite is reactive with both melts and fluids. Secondly, titanite is suitable for dating, which allows identifying the timing of its crystallization and recrystallization. This way, primary and secondary events can be constrained with time. Here, we use titanites to trace hydrothermal alterations in the late-Archean Closepet batholith, which is located in the central part of the Dharwar craton in southern India (Chardon et al., 2011), and provides an excellent insight into rock–fluid interactions in terms of space and time. The intensive mineral–fluid interaction is well visible in feldspar, apatite, and titanite. There, the origin of the fluid was related to two environments, mantle and lower crust, based on the geochemistry of titanite pristine and altered domains (Słaby et al., 2021). The mineral–fluid interaction process was dated (Słaby et al. 2021). The established timing of late Archean fluids interaction is extended to Palaeoproterozoic, close to the Great Oxidation Event.

The data have been obtained on few samples from the batholith central part only. To extend the previous research, samples from the southern to the northern part of the batholith have been collected and analyzed. On back-scattered electron (BSE) images, the titanites are composed of light and dark domains characterized by irregular shapes with sharp boundaries. In contrast to the dark domains, the light domains usually reflect unchanged zones and represent the composition of pristine titanites. The trends observed for the mineral–fluid interaction in the central part seem to be common for the whole magmatic body. There are, however, significant differences in the intensity of the alteration. The bright, medium and dark domains show common rare earth element (REE) features for all parts of the batholith on spider diagrams. Compared to the bright domains, the darker domains show lower total REE contents, lower fractionation between light REE and heavy REE, and flattening of Eu anomalies. The biggest variations between the dark and bright domains are observed in the northern part, where the Eu anomaly becomes even positive in the dark domains. Especially high positive anomaly and low total REE contents are visible in homogeneous titanites accompanied by oxides, which also occur only in the northern part of the batholith. This is also confirmed on the REE + Y vs Y plots for the northern part, where not only magmatic but also hydrothermal titanite populations can be distinguished. On the southern margin of the batholith, differences between the darker and brighter domains are also pronounced but to a lower extent. Therefore, we think hydrothermal processes were weak in the center of the pluton in contrast to its margins where various fluids penetrated the pluton.

The work was funded by the NCN Project UMO- 2018/31/B/ST10/01060.

References

- Słaby, E., et al. 2021. *Lithos*, 386-387
Chardon, D., et al. 2011. *Geochem. Geophys. Geosyst.* 12, Q02005.

APPLICATION OF NATURAL ZEOLITES TO AMD (ACID MINE DRAINAGE) TREATMENT: A REVIEW AND NEW DATA

Godelitsas Athanasios¹, Kollias Konstantinos², Astilleros José-Manuel³

¹Geology & Geoenvironment, National and Kapodistrian University of Athens, Greece, ²Mining & Metallurgical Engineering, NATIONAL TECHNICAL UNIVERSITY OF ATHENS, Greece, ³Mineralogy and Petrology, Complutense University of Madrid, Spain

The potential of natural zeolites for the treatment and remediation of AMD is well-known. However, most of the existing literature concerns macroscopic experiments with emphasis to pH-stabilization and sorption data mostly for Zn and Cu (Zamzow, 1990; Cui et al., 2006; Li et al., 2007, 2008; Calvo et al., 2009; Motsi et al., 2009, 2010, 2011; Xu et al., 2013; Buenaño et al. 2017; Ciosek & Luk, 2017; Ciosek, 2018; Vaezihir et al. 2018). In recent studies, the combination of macroscopic experiments with microscopic and spectroscopic techniques (in-situ pH measurements, ICP-OES fluid analyses, solid-state ²⁹Si, and ²⁷Al NMR, SEM-EDS, in-situ AFM, and surface analyses by XPS and 12C-RBS) revealed the chemical processes at the zeolite-AMD interface in micro- and nano-scale (Kollias et al. 2021). The investigation of zeolite crystals (HEU-type) interacted with AMD, indicated changes to the microtopography and nanotopography of surfaces, whereas coupled dissolution and sorption (surface precipitation/co-precipitation, nucleation/crystal growth, adsorption, absorption -including ion-exchange and solid-state diffusion-) phenomena occur simultaneously.

References

Buenaño et al., 2017. Zeolitic tuffs for acid mine drainage (AMD) treatment in Ecuador. *Environ. Sci. Pollut. Res. Int.*, 24(7), 6794-6806. Calvo et al., 2009. Continuous elimination of Pb²⁺, Cu²⁺, Zn²⁺, H⁺ and NH₄⁺ from acidic waters by ionic exchange on natural zeolites. *J. Hazard. Mater.* 166, 619–627. Ciosek, 2018. Natural zeolite removal capacity for metallic heavy metal ions. PhD Thesis, Univ. Ryerson, Toronto/CD. Ciosek & Luk, 2017. Kinetic modelling of the removal of multiple heavy metallic ions from mine waste by natural zeolite sorption. *Water* 2017, 9, 482. Cui et al., 2006. Exploration of remediation of acid rock drainage with clinoptilolite as sorbent in a slurry bubble column for both heavy metal capture and regeneration. *Water Res.* 40, 3359–3366. Kollias et al., 2021. Dissolution and sorption mechanisms at the aluminosilicate and carbonate mineral-AMD (Acid Mine Drainage) interface. *Appl. Geochem.* - accepted. Li et al., 2007. Remediation of acid rock drainage by regenerable natural clinoptilolite. *Water, Air, Soil Pollut.* 180, 11–27. Li et al., 2008. Treatment of acid rock drainage by clinoptilolite — Adsorptivity and structural stability for different pH environments. *Appl. Clay Sci.* 39, 1–9. Motsi et al., 2009. Adsorption of heavy metals from acid mine drainage by natural zeolite. *Int. J. Miner. Process.* 92, 42–48. Motsi, 2010. Remediation of AMD using natural zeolite. PhD Thesis, Univ. Birmingham/UK. Motsi et al., 2011. Kinetic studies of the removal of heavy metals from acid mine drainage by natural zeolite. *Int. J. Miner. Process.* 101, 42–49. Xu et al. 2013. Acid rock drainage treatment by clinoptilolite with slurry bubble column: Sustainable zinc removal with regeneration of clinoptilolite. *Appl. Clay Sci.* 80–81, 31–37. Vaezihir et al., 2018. The efficiency of open lime-zeolite Channel system in treatment of Acid Mine Drainage (AMD) released from Sungun copper mine. 11th ICARD/IMWA/MWD Conference (Wolkersdorfer et al. Eds.). Wingenfelder et al. 2005. Removal of heavy metals from mine waters by natural zeolites. *Env. Sci. Technol.*, 39, 4606-4613. Zamzow et al., 1990. Removal of heavy Metals and other cations from wastewater using zeolites. *Sep. Sci. Technol.* Volume 25, Issue 13-15.

ESTIMATION OF STRUCTURAL FEATURES AND ELECTRICAL PROPERTIES OF DISORDERED CARBON OF SHUNGITE BY MICROWAVE PROPERTIES

Golubev Yevgeny¹, Antonets Igor², Shcheglov Vladimir³, Sun Shyong⁴

¹Institute of Geology of Komi SC of UrB of RAS, Russian Federation, ²Syktyvkar State University, Russian Federation, ³Institute of Radio Engineering and Electronics RAS, Moscow, Russian Federation, ⁴Southwest University of Science and Technology, Mianyang, China, yevgenyGolubev74@mail.ru

The widespread use of microwave electronic devices stimulated interest to research in the development of new materials for shielding microwave radiation. The most urgent tasks are to reduce the thickness of shielding materials, to maximize lightness and flexibility, and resistance to corrosion. All these requirements are met by carbon-based materials. Absorbing materials that neutralize the negative effect of re-reflection of electromagnetic radiation in rooms or technical devices are especially interesting. In this work, we propose the results of studying the reflecting and absorbing properties of shielding materials based on karelian shungite microlayers in the frequency ranges of 26–38 GHz. A main task is to assess the influence of the mineral component on the carbon electrical properties based on analysis of the mechanisms of conduction and reflection of disordered carbon and its structure. Shungite is a natural composite material from carbon nanostructures with a variety of mineral inclusions with sizes from one to several tens of micrometers (pyrite, quartz, chlorite). Thin (10–20 µm thick) and flexible plates from pieces of shungite rocks successfully reflect and absorb electromagnetic radiation in the range of carbon contents from 5 to 95 at. %. A significant excess of the dynamic conductivity of shungite plates over the static conductivity at the carbon content of 5–34 at. % was found. The absorption mechanisms in shungite plates cannot be described by the classical electrodynamics equations and are associated with the structure of shungite carbon and the rock microstructure.

The results show that the molecular structure of shungite carbon affects primarily the reflective properties, which are superior to the reflective properties of metals. The microstructure of shungite rock with alternating conductive (carbon) and non-conductive (mineral) regions controls the absorption. For a description of the microwave properties of shungites, the mechanism of intragranular currents was used, which was developed to describe the features of dynamic conductivity in two-phase conductor/dielectric composites. The smaller the size of the carbon regions in shungite, the more the boundary interactions with non-conducting mineral phases affect their structure and properties. In particular, from the analysis of dynamic conductivity, it was found that the conductivity of thin carbon regions in shungite is several orders of magnitude higher than the conductivity of bulk carbon. This is due to the formation of films of an ordered graphite-like structure with thickness tens to hundreds of nm at the contacts with the mineral substrate. It is difficult to obtain such characteristics by methods of measuring static conductivity. Shungite rocks can be considered both as a raw material for the manufacture of shielding materials and as a model for studying the interaction of radiation with disordered matter.

This work was supported by the Russian Science Foundation (RSF, grant 21-47-00019) and the NSFC, grant 42061134018.

ELASTIC GEOTHERMOBAROMETRY FOR FULLY ANISOTROPIC HOST-INCLUSION SYSTEMS

Gonzalez Joseph P.¹, Mazzucchelli Mattia Luca²

¹Department of Earth and Environmental Sciences, University of Pavia, Italy, ²Mainz Institute of Multiscale Modeling and Institute of Geosciences, Johannes Gutenberg of Mainz, Germany

Recent years have seen the rapid development of the theory and analytical methods for elastic thermobarometry, which has led to increased use within the geologic community. Elastic thermobarometry is based on the principle that an isolated and unmodified inclusion contained within a host mineral can retain elastic strains that can be used to calculate the possible entrapment conditions of the inclusion within the host mineral. However, elastic thermobarometry has been limited by uncertainties regarding the anisotropic elastic behavior of inclusions when they are contained within an elastically anisotropic host mineral. Because of this, previous studies of elastic thermobarometry have been limited to inclusions entrapped in nearly elastically isotropic cubic host minerals, such as garnet. When both the host and the inclusion minerals are elastically anisotropic, elastic calculations must account for both the elastic anisotropies of the host and the inclusion and their relative crystallographic orientation (RCO). In this study, we developed an elastic model based on the deformation of the host and inclusion which accounts for the elastic anisotropy and their RCO. This new anisotropic elastic model can be generalized and used for elastic thermobarometry given that the equation of state, elastic properties, and RCO of the host and inclusion minerals are known. The anisotropic elastic model was used to gain insight into the magnitude of the effects of elastic anisotropy, RCO, and varying entrapment conditions by numerically evaluating the fully anisotropic quartz-in-zircon host-inclusion system. These numerical tests demonstrate that anisotropic inclusions are not under isotropic strain or hydrostatic stress when entrapped in an anisotropic host mineral, and therefore, isotropic elastic models cannot be used to determine the complete strain state of an elastically anisotropic inclusion contained in an elastically anisotropic host mineral. Furthermore, results from the evaluation of three different orientations show that the effect of RCO on the volume strain and resulting remnant pressure is relatively small for these investigated sets of entrapment conditions and gives errors of 0.06 GPa. However, this cannot be assumed as a general limit, in particular for non-spherical shapes of the inclusion, and the effects of anisotropy and RCO should be evaluated on a case-by-case basis when applying elastic thermobarometry to fully anisotropic host-inclusion systems.

Acknowledgements:

JPG is supported by a NSF-EAR Postdoctoral Fellowship (No. 1952698) MLM is supported by the Alexander von Humboldt research fellowship and the SIMP PhD Thesis Award.

CRITICAL AND BATTERY RAW MATERIALS IN EU: THE CASE OF NI-LATERITES IN CENTRAL GREECE

Goutzioupa Konstantina¹, Godelitsas Athanasios², Tsakiridis Petros³, Petrelli Maurizio⁴, Sanakis Yiannis⁵, Samouhos Michail⁶, Gasparatos Dionisios⁷, Papadopoulos Argyrios⁸, Maras Serafim⁹, Apostolikas Athanasios¹⁰

¹Department of Geology and Geoenvironment, Zografou Campus, 15784-Athens, e-mail: nadiagoutzioupa@gmail.com, National and Kapodistrian University of Athens, Greece, ²Department of Geology and Geoenvironment, Zografou Campus, 15784-Athens, e-mail: agodel@geol.uoa.gr, National and Kapodistrian University of Athens, Greece, ³School of Mining and Metallurgical Engineering, 15780-Athens, e-mail: ptsakiri@central.ntua.gr, NATIONAL TECHNICAL UNIVERSITY OF ATHENS, Greece, ⁴Department of Physics & Geology, 06100 Piazza Università, Perugia, e-mail: maurizio.petrelli@unipg.it, University of Perugia, Italy, ⁵Institute of Nanoscience and Nanotechnology, 15310-Athens, e-mail: i.sanakis@inn.demokritos.gr, National Centre for Scientific Research 'Demokritos', Greece, ⁶School of Mining and Metallurgical Engineering, 15780-Athens, e-mail: msamouhos@metal.ntua.gr, NATIONAL TECHNICAL UNIVERSITY OF ATHENS, Greece, ⁷Department of Natural Resources Management and Agricultural Engineering, 11855-Athens, e-mail: gasparatos@aua.gr, Agricultural University of Athens, Greece, ⁸57014 Olympias Mine, Chalkidiki, e-mail: 57014argiris.Papadopoulos@eldoradogold.com, Hellas Gold, Greece, ⁹Fragkokklisias Str. Maroussi, 15125-Athens, e-mail: serafim.maras@larco.gr, LARCO GMMSA, Greece, ¹⁰Fragkokklisias Str. Maroussi, 15125-Athens, e-mail: athanasios.apostolikas@larco.gr, LARCO GMMSA, Greece

Ni-laterite ores in central Greece deposits are currently used in the LARCO GMMSA smelting plant (<http://www.larco.gr/nickel.php>) to produce ferronickel -Fe-Ni- alloy. However, new importance arises due to the demand for critical and battery metal resources in the EU and worldwide (such as Co, REE+Y+Sc, Ni [e.g. 1,2]). In the frame of recent research regarding new insights into the mineralogy and geochemistry of the ores, a model laterite profile, together with hanging wall and footwall limestones, at Larymna (central Greece), was studied. PXRD and SEM-EDS confirmed the known crystalline Fe-oxides/oxyhydroxides (hematite and goethite) and Ni-bearing Mg-Fe-phyllsilicates (mainly chlorite-group and serpentine-group minerals). Subsequent new ⁵⁷Fe-Mössbauer measurements indicated that Fe³⁺ is exclusively the Fe component of the Ni-phyllsilicates. Further investigation of a thin green-black layer occurring in the base of the deposit, revealed peculiar phases containing Al-Si-Mn-Ni-Co-Cr-V-Cu-Ca, implying the presence of potential mineral nanoparticles and nanominerals. In accordance, the nanoscopic study by TEM-EDS proved the existence of such micro-areas, consisting most probably of an amorphous/disordered Ni(-Cr)-Co-bearing Mn-(oxy)hydroxide/oxide (hydrated) phase. Bulk analyses by ICP-OES/MS indicated that the ore contains a variety of useful metals (Ni, Co, V, ΣLREE, ΣHREE, Sc -max values: 9212 ppm, 1480 ppm, 379 ppm, 1221 ppm, 253 ppm, 76 ppm, respectively; average values: 3941 ppm, 659 ppm, 317 ppm, 678 ppm, 111 ppm, 71 ppm, respectively-), with remarkable geochemical enrichment with respect to REEs (REE+Y+Sc, max: 2150 ppm; average: 1173 ppm) accompanied by a negative Ce/Ce* anomaly. Cobalt is exceptionally increased (3534 ppm and 7940 ppm, respectively) in the green-black layer at the base of the deposit, as well as in the footwall limestone. Complementary point analyses of Ni-phyllsilicates by LA-ICP-MS confirmed that, despite rather low Ni-content in the ore (average ca. 0.4 wt.%), the metal concentration in these phases is 5.81 wt.%. On the other hand, Co and ΣREE+Y+Sc are remarkably lower (164 ppm and 40 ppm, respectively), meaning that the above critical metals are not consistent with Ni and they are preferentially contained in Fe-oxides/oxyhydroxides and other phases (examined by SEM-EDS) such as REE-fluorocarbonates and -phosphates.

References

1. <https://unctad.org/news/demand-raw-materials-electric-car-batteries-set-rise-further>
2. <https://ec.europa.eu/docsroom/documents/42849>

ULTRAMAFIC-ALKALINE-CARBONATITE TAJNO MASSIF IN NE POLAND – A NEW INSIGHTS INTO ITS ORIGIN

Grabarczyk Anna¹, Gil Grzegorz¹, Kotowski Jakub¹, Jokubauskas Petras¹, Nejbert Krzysztof¹, Wiszniewska Janina²

¹Faculty of Geology, University of Warsaw, Poland, ²Polish Geological Institute – National Research Institute, Poland

The Tajno Intrusion is a small sub-platform ultramafic-alkaline-carbonatite body emplaced within the Paleoproterozoic rocks of the south-western margin of the East European Craton (EEC), ~300 km from the craton edge. Outer parts of the Tajno Massif are composed of alkali clinopyroxenites and syenites, whereas carbonatite, breccia, and pyroclastic material comprise the central part. The Tajno Massif, jointly with the Ełk, Pisz, and Mława intrusions, as well as Olsztynek body and alkali basalts of the Lublin Basin, belongs to coeval, ca. 348-338 Ma, mafic-alkaline intrusions scarce in the marginal part of the Polish segment of the EEC.

Carbonate isotopic compositions of carbonatites and breccias ($\delta^{18}\text{O} = 8.7\text{‰}$ to 10.7‰ ; $\delta^{13}\text{C} = -4.8\text{‰}$ to -0.4‰) spans from primary carbonatites to carbonatites with sedimentary input or affected by a fractionation. In silicate rocks, fluid influx leads to the development of sulfide mineralization-bearing veins, causing elevated bulk-rock contents of Mo (925 ppm), Re (905 ppb), and Pd (29 ppb). The lowest carbonate $\delta^{18}\text{O}$ (9.3‰ to 10.7‰) and $\delta^{13}\text{C}$ (-5.0‰ to -3.8‰) values are reported for veins in alkali clinopyroxenites, whereas the highest $\delta^{18}\text{O}$ (11.2‰) and $\delta^{13}\text{C}$ (-1.2‰ to -1.1‰) values for veins in syenites and trachytes, suggesting hydrothermal overprint of mantle-derived rocks.

The characteristic feature of the Tajno Massif is the presence of fluorocarbonates and fluorite mineralization (F content >10000 ppm). Carbonatites are abundant in LREE, Sr, and Ba-bearing phases, i.e., bastnäsite, burbanikite, parisite-(Ce), synchysite, strontianite, barite, goyazite-(La,Ce) and Sr-rich calcite. High CO_2 , Sr (43895 ppm), Ba (6426 ppm), and total REE (6582 ppm), suggest an involvement of the recycled oceanic lithosphere in carbonatite generation.

Extremely high LREE concentrations indicate the interaction with CO_2 -bearing fluids causing enrichment in the LILE, whereas the presence of fluorite testifies the interaction between the SCLM with F-rich fluids. High Ba content and low Nb/Y ratio (0.01–0.07) for the majority of samples are consistent with fluid-related enrichment. Variable Ba/Th ratios (16-1740) and constant, low ($^{87}\text{Sr}/^{86}\text{Sr}$)_i values (0.7037-0.7038) of carbonatites suggest an influence of the altered oceanic crust (AOC). On the other hand, slightly higher ($^{87}\text{Sr}/^{86}\text{Sr}$)_i values of silicate rocks (0.7043-0.7048), high total REE and variable (La/Sm)_N ratio (2.2-83.0) imply contribution of recycled marine sediments.

The high potassic suite comprising the Tajno Massif, as well as location adjacent to the craton margin, are similar to the geotectonic setting of the carbonatite-associated REE deposits (CARDS). Consequently, an earlier postulated linkage with a distant (~1600 km), rift-related, intracratonic alkaline-carbonatite massifs of the Kola Province (Russia) is unlikely. Carbonatites were probably derived from the SCLM refertilized by F and CO_2 -rich fluids from subducted slab. Tournaisian-Visean age and the distribution of mafic-alkaline intrusions along to the EEC margin, nearly parallel to the Variscan deformation front, point to Variscan subduction beneath the EEC and adjoined Caledonian terranes.

This research was financially supported by the project Excellence initiative – research university (IDUB) at the University of Warsaw grant no. 501-D113-20-0004316 and National Science Centre (NCN) grant no.2019/33/N/ST10/00944.

THERMODYNAMIC DATA OF BELITE POLYMORPHS

Grevel Klaus-Dieter¹, Bellmann Frank², Majzlan Juraj¹, Dachs Edgar³, Benisek Artur³

¹Inst. for Geosciences; Mineralogy, Friedrich Schiller University Jena, Germany, ²F.A. Finger Inst. for Construction Materials, Bauhaus University Weimar, Germany, ³Chemistry and Physics of Materials, Paris Lodron University Salzburg, Austria

One major component of Portland cement clinker is Ca₂SiO₄ (C₂S, belite). Synthetic samples of three polymorphs, β-C₂S (larnite), γ-C₂S (calcio olivine), and x-C₂S were investigated by high-temperature oxide melt solution calorimetry at 700 °C to obtain their enthalpies of formation. A natural sample of wollastonite (CaSiO₃) was measured for comparison. Low-temperature heat capacity data of the C₂S phases were recorded by relaxation calorimetry using a PPMS. Supplementary DSC data of β- and γ-C₂S were obtained to verify their heat capacity evolution to 400 °C. Thermodynamic data from the literature are confirmed for γ-C₂S (calcio olivine) which is the thermodynamically stable Ca₂SiO₄ polymorph at ambient conditions. The enthalpy of the formation of β-C₂S (larnite) obtained in this study is in good agreement to the experimental value obtained by King (1957), the enthalpy data of Ayed et al. (1994) are not confirmed. Our C_p data for the β-phase are systematically lower by about 2.5 J mol⁻¹K⁻¹ than the data from Todd (1951), the resulting S⁰₂₉₈(β-C₂S) = 122.2 ± 0.9 J mol⁻¹K⁻¹ differs by 5.5 J mol⁻¹K⁻¹ from Todd's (1951) value. The recommended values for β-C₂S and γ-C₂S are:

$$\Delta_f H^0_{298}(\gamma\text{-C}_2\text{S}) = -2316.0 \pm 4.5 \text{ kJ mol}^{-1}, S^0_{298}(\gamma\text{-C}_2\text{S}) = 119.7 \pm 0.9 \text{ J mol}^{-1}\text{K}^{-1},$$

$$C_p(\gamma\text{-C}_2\text{S}) = (249.098 - 1949.5T^{-0.5} - 1.60822 \cdot 10^6 T^{-2} + 2.77532 \cdot 10^8 T^{-3}) \text{ J K}^{-1}\text{mol}^{-1}, [T] = \text{K},$$

$$\Delta_f H^0_{298}(\beta\text{-C}_2\text{S}) = -2307.6 \pm 4.5 \text{ kJ mol}^{-1}, S^0_{298}(\beta\text{-C}_2\text{S}) = 122.2 \pm 0.9 \text{ J mol}^{-1}\text{K}^{-1},$$

$$C_p(\beta\text{-C}_2\text{S}) = (259.721 - 2466.09T^{-0.5} + 2.62687 \cdot 10^6 T^{-2} - 4.77891 \cdot 10^8 T^{-3}) \text{ J K}^{-1}\text{mol}^{-1}, [T] = \text{K}.$$

According to XRD, the x-C₂S sample contained 36 % β-C₂S, 6 % γ-C₂S, 57 % x-C₂S, and 1 % amorphous material. The loss of ignition of this sample was 3.1 %. Assuming that this mass loss can solely be attributed to H₂O, the composition of x-C₂S would be approximately Ca₂SiO₄ · 0.5 H₂O.

The resulting thermodynamic data for this phase are:

$$\Delta_f H^0_{298}(\text{Ca}_2\text{SiO}_4 \cdot 0.5\text{H}_2\text{O}) = -2442.1 \pm 4.5 \text{ kJ mol}^{-1},$$

$$S^0_{298}(\text{Ca}_2\text{SiO}_4 \cdot 0.5\text{H}_2\text{O}) = 144.7 \pm 0.9 \text{ J mol}^{-1}\text{K}^{-1}.$$

References

Ayed, F.F., Sorrentino, F., Castanet, R. (1994), Determination par calorimetrie de dissolution des enthalpies de formation de quelques silicates, aluminates et alumino-silicates de calcium, *Therm. Anal.* 41, 755–766.

King, E.G. (1957), Low temperature heat capacities and entropies at 298.15°K of some crystalline silicates containing calcium, *J. Am. Chem. Soc.* 79, 5437–5438.

Todd, S.S. (1951), Low-temperature heat capacities and entropies at 298.16°K of crystalline calcium orthosilicate, zinc orthosilicate and tricalcium silicate, *J. Am. Chem. Soc.* 73, 3277–3278.

Keynote

COMBINING CRYSTALLOGRAPHIC ORIENTATION RELATIONSHIPS AND MICROSTRUCTURES TO DETERMINE MINERAL INCLUSION ORIGINS

Griffiths Thomas¹, Kohn Victoria¹, Alifirova Taisia¹, Abart Rainer¹, Habler Gerlinde¹

¹Department of Lithospheric Research, University of Vienna, Austria

Crystallographic orientation relationships (CORs) provide important insights into the origins of mineral inclusions, as they contain information about how (if at all) the lattices of host and inclusions interacted during inclusion formation. Large datasets have revealed complex orientation relationships in some mineral inclusion–host systems, including the presence of multiple CORs and CORs that are not completely fixed with respect to both lattices. This variety suggests that multiple inclusion-forming processes that generate CORs may exist, requiring new information to differentiate between them.

Electron backscatter diffraction (EBSD) allows hundreds of point measurements of the crystallographic orientation of mineral inclusions to be acquired in a few days. Digital processing allows statistical treatment of data for the comparison of multiple datasets using one set of candidate CORs. Most importantly, EBSD allows in-situ measurements of host-inclusion CORs in polished samples, delivering highly spatially resolved data about CORs that can be combined with microstructural and compositional information to differentiate between multiple hypotheses of inclusion origins. New questions that can be addressed include 1) the relationship between host crystallography and shape-preferred orientations (SPOs) of inclusions, 2) the relationship between the SPO and COR of each inclusion, and 3) potential variations in host-inclusion COR characteristics between different microstructural and compositional domains of host crystals.

EBSD datasets of CORs between rutile inclusions and host metapegmatite garnet from two localities with different geological histories illustrate the new insights that combining COR and microstructural analysis can provide. Inclusion abundance and habit vary in concentric and sector zones of garnet, with concentric zone boundaries parallel to garnet crystal facets. Inner zones bear equant rutile inclusions < 1 μm in diameter, whereas outer zones feature acicular rutile inclusions < 1 μm in diameter and tens of μm in length, following SPOs parallel to garnet crystallographic directions. Multiple CORs coexist in all microstructural domains. The relative frequencies of different CORs vary, both between zones of inclusions exhibiting the same habit and between zones of differing habits. For acicular rutile inclusions, the host-inclusion COR is systematically linked to the inclusion elongation direction. In some zones, the SPO of needles does not follow all crystallographically equivalent garnet directions equally and instead depends on the orientation of the garnet facet.

The correlation of spatial variations of rutile inclusion habit, SPO, and COR frequencies in the metapegmatite garnets with magmatic growth zoning contradicts an exsolution model of inclusion formation. In contrast, the observed heterogeneity can be well explained by heterogeneous nucleation of rutile at the growing garnet-melt interface, followed by intergrowth and finally engulfing of inclusions by garnet. Correlating statistically treated COR characteristics with microstructural and compositional data represents a powerful way to test hypotheses about mineral inclusion origins.

Funded by Austrian Science Fund (FWF): I4285-N37

FLUID IMMISCIBILITY DRIVES CO₂ TRANSPORT AND OUTGASSING DURING COLLISIONAL OROGENY

Gropo Chiara¹, Rolfo Franco¹

¹Dept. Earth Sciences, University of Torino, Italy

Orogenic degassing is emerging as a relevant source of CO₂ from the continental crust, potentially releasing carbon amounts comparable with those emitted by active volcanoes. Understanding the transport dynamics of metamorphic CO₂-rich fluids is crucial for clarifying whether these fluids interact with the host rocks during their ascent toward the surface, eventually causing carbon re-precipitation, or rapidly rise through the crust without interactions with the host rocks. Here we use thermodynamic modeling to investigate the decarbonation of sediments metamorphosed under high geothermal gradients. Our data document that immiscible CO₂-rich fluids and hydrosaline brines are generated at these conditions, with different properties and mobility through the crust. The non-wetting, poorly mobile, CO₂-rich fluid initially accumulates in the deep crust; however, being highly volatile and chemically unreactive, it rapidly rises toward the surface without interacting with the host rocks, as soon as it can carbo-fracture the host rocks, or once that an active fault intersects the reservoir. The hydrosaline brine has a wetting behavior, but it is denser and volumetrically less abundant than the CO₂-rich fluid; therefore, it likely permeates the source rocks, forming well-connected, thin films, adhering to the crystals surfaces. When applied to the currently active Himalayan orogen, our modeling reconciles the CO₂ fluxes actually measured at the surface and the positive conductivity anomalies associated with micro-seismicity at depth. Therefore, we infer that the continental crust represents a relevant reservoir of CO₂ that can be efficiently degassed during hot orogenesis.

ON THE U-Pb GEOCHRONOLOGY OF MAFIC DYKES AND SILLS: FROM ZERO TO HERO

Gumsley Ashley¹, Bleeker Wouter², Chamberlain Kevin³, Chew David⁴, Ernst Richard⁵, Kamo Sandra⁶, Sałacińska Anna⁷, Söderlund Ulf⁸, Schmitt Axel Karl⁹, Szopa Krzysztof¹

¹Institute of Earth Sciences, University of Silesia in Katowice, Poland, ²Geological Survey of Canada, Canada, ³Department of Geology & Geophysics, University of Wyoming, United States, ⁴Department of Geology, Trinity College Dublin, Ireland, ⁵Department of Earth Science, Carleton University, Canada, ⁶Department of Earth Sciences, University of Toronto, Canada, ⁷Institute of Geological Sciences, Polish Academy of Sciences, Poland, ⁸Department of Geology, Lund University, Sweden, ⁹Institute of Earth Sciences, Heidelberg University, Germany

Mafic dyke swarms and sill provinces, as mantle-derived mafic magmatic rocks, have become powerful tools to aid our understanding of large igneous provinces (LIPs), magmatic processes, and their associated environmental consequences, together with paleogeography. Since the first International Dyke Conference in Canada in 1985 organized by Henry Halls, the study of these mafic intrusions has advanced significantly. From a geochronological perspective, these rocks usually contain variable amounts of zircon. However, the work of Heaman and LeCheminant in the '80s and '90s showed that baddeleyite (ZrO₂) is usually the main zirconium mineral in mafic rocks. This mineral can be applied in geochronology using U-Pb ID-TIMS when zircon cannot be found. However, traditional heavy mineral separation techniques (i.e., Franz magnetic separator and heavy liquids) are both less effective, time-consuming, and costly for baddeleyite separation. These problems were overcome by the advent of the so-called water-based method of Söderlund and Johansson, which showed that fair amounts of baddeleyite can be efficiently separated within only a couple of hours. With this new-found ability, the Supercontinent Project (www.supercontinent.org) of Richard Ernst and Wouter Bleeker was launched in 2010, with the ambition to obtain precise ages of dykes, sills, and other components of LIPs. This ambitious project was funded by industrial partners towards 'taking the pulse of the planet Earth'. The project revolutionized the field of LIPs. This was especially evident in terms of paleogeography utilizing the Bleeker and Ernst 'magmatic barcode technique'. This technique uses ages of LIPs to barcode crustal blocks, to identify ancient paleogeographic 'nearest neighbors'.

Today, dyke swarms and sill provinces can be seen to be variably complex temporal and spatial markers. They can provide a wealth of information relating to LIPs, mantle dynamics and mantle plumes, paleogeography, and mass extinctions. However, with greater knowledge, has come greater complexity, with dyke swarms that are composite (i.e., composed of more than one age generation). The ability to date these intrusions has also advanced rapidly, from older K-Ar and Rb-Sr methodologies using whole rocks and minerals to newer U-Pb ID-TIMS dating of baddeleyite, and smaller zircon. In-situ measurement of baddeleyite by SIMS, as well as both ID-TIMS and LA-ICPMS apatite dating have extended the usefulness of mafic dykes and sills relating to chronostratigraphy and thermochronology, especially when combined with paleomagnetic and geochemical studies. Using case studies, we wish to highlight this burgeoning field, looking at the geochronology of a variety of dykes, sills, and lavas from across the globe.

This research was supported by an Sonatina grant awarded to Ashley Gumsley from the National Science Centre in Poland (grant agreement no. UMO-2019/32/C/ST10/00238).

CALCIUM ISOTOPE PARTITIONING UPON SYNTHESIS OF CARBONATE-BEARING APATITE

Gussone Nikolaus¹, Böttcher Michael E.², Conrad Anika C.², Schmiedinger Iris², Fiebig Jens³, Peltz Markus⁴, Grathoff Georg⁴, Schmidt Burkhard⁵

¹Institut für Mineralogie, Westfälische Wilhelms Universität Münster, Germany, ²Geochemistry & Isotope Biogeochemistry, Leibniz Institute for Baltic Sea Research (IOW), Germany, ³Institute of Geosciences, Goethe-University of Frankfurt, Germany, and Senckenberg Biodiversity and Climate Research Center, Frankfurt (Main), Germany, ⁴Economic Geology, University of Greifswald, Germany, ⁵Experimental and Applied Mineralogy, University of Göttingen, Germany

Carbonated hydroxy-apatite (CHAP) was experimentally synthesized in batch-type set-ups by mixing of calcium (Ca)- and phosphate-bearing aqueous solutions and the transformation of calcite powder in an aqueous solution between 11° and 65°C (Gussone et al., 2020). Compositional changes of the experimental solution and solid phase products were followed by elemental analysis, Raman spectroscopy, scanning-electron microscopy, and powder XRD. In the mixing experiments, crystallization of CHAP took place following the precipitation of metastable brushite as a precursor that was then transformed into CHAP. In the transformation experiments using synthetic calcite as a precursor phase, it was found that the reaction at pH values between 7.5 and 7.9 occurs via the direct replacement of calcium carbonate by CHAP.

Calcium isotope fractionation led to an enrichment of the light isotope in the solid CHAP compared to the aqueous solution by about -0.5 to -1.1 ‰, independent from the experimental approach, and the magnitude was essentially independent of temperature. The metastable brushite formed prior to transformation to CHAP showed a reduced fractionation compared to the CHAP. The observed Ca isotope fractionation into the CHAP lattice resembles that of natural phosphorites and lies within the range of the view existing theoretical and experimental studies.

Reference:

Gussone N., Böttcher M.E., Conrad A.C., Fiebig J., Pelz M., Grathoff G., Schmidt B.C. (2020) Calcium isotope fractionation upon experimental apatite formation. *Chem. Geol.*, 551, 119737

The study was supported by German Science Foundation (DFG) to M.E.B and J.F. within the EXCALIBOR project (BO1548/8 and FI 948/7), and to N.G. (GU1035/10), and by Leibniz IOW.

TRANSFORMATION OF AS- AND P-DOPED 2L-FERRIHYDRITE UNDER DIFFERENT T AND PH CONDITIONS AND ITS RELEVANCE FOR NEAR-SURFACE ENVIRONMENTS

Haase Patrick¹, Majzlan Juraj¹

¹Institute of Geosciences, Friedrich-Schiller-University Jena, Germany

Ferrihydrite is an important Fe mineral in soil systems. Its point of zero charge (PZC) close to near neutral conditions and the high specific surface area (SSA) make it suitable for the temporary immobilization of toxic and essential elements like arsenic and phosphorous, respectively. Both elements affect the properties of the metastable ferrihydrite and increase the transformation time to the stable phases goethite and hematite. The successors differ in their properties from ferrihydrite with a much lower SSA. This results in the release of adsorbed elements into the environment and may influence the long-term contamination of mining sites.

In this study, we monitor the transformation of ferrihydrite in acidic, neutral, and alkaline systems for As- and P-doped (cAs/P = 0.45 mmol/L) synthetic ferrihydrite in the temperature range of 40 to 70°C. Sample aliquots were collected in regular intervals and were analyzed by powder X-ray diffraction (PXRD). The phase amounts of ferrihydrite, goethite, and hematite were calculated from the area of selected peaks. The normalized data of the different temperature batches can be used to extrapolate to near-surface conditions and estimate the transformation time of ferrihydrite as well as the release of toxic and essential elements. Reference batches at 70 °C without extraneous elements (As, P) showed a full transformation after 18 days under acidic conditions and 38 days under near-neutral conditions. First extrapolations under the consideration of first-order reactions result in a half-time transformation of undoped ferrihydrite at 10°C within around 4.4 years under acidic conditions and 7.3 years under near-neutral conditions. These values still need to be refined and checked for the As- and P-doped batches. Adsorption of As or P strongly influence the transformation time because of anionic surface-complexation below the PZC of ferrihydrite. Evaluations indicated their full transformation at 70°C after 24 days under acidic conditions and they were completed after 68 days under near-neutral conditions.

MINERALOGICAL AND GEOCHEMICAL CHARACTERIZATION OF THE MINE WASTES STORED UNDER A SHALLOW WATER COVER IN MIRAH, CENTRAL KALIMANTAN, INDONESIA

Hakim Andy Yahya Al¹, Iskandar Irwan¹, Notosiswoyo Sudarto¹, Septianto Cipto Purnandi¹, Fajrin Andi², Febrianto Nugroho Nur², Narang Yerie²

¹Research Group of Earth Resource Exploration, Faculty of Mining and Petroleum Engineering, Institute of Technology Bandung, Indonesia, ²PT Kasongan Bumi Kencana, Indonesia

The formation of acid mine drainage (AMD) in Tailings Storage Facility (TSF) can be prevented by establishing a shallow water cover to prevent the oxidation of sulfides under anaerobic conditions. Using soil profiling, combined mineralogical and geochemical methods allowed description of the weathering process of reactive mineral phases and oxidation mechanism in Mirah gold-silver mine tailings. The Mirah TSF located in Central Kalimantan, Indonesia, contains silicates, carbonates, and sulfides tailings deposited from 2012 to 2015. Mineral processing involved cyanidation from crushed ore at high pH (>10). At the sub-aerial and shallow water cover (<0.5 m) area, the vegetation (*Typha latifolia*) has been growing expansively. Mine tailings, groundwater, and surface water were collected and evaluated to a range of mineralogical and geochemical evaluations. Quartz, chlorite, albite, K-feldspar, chlorite, and calcite are stable over time. Sulfides are dominated by pyrite with less sphalerite and galena, major oxides minerals are magnetite, ilmenite, and goethite. Sulfides alteration index (SAI) parameters indicate that only a few grains of pyrite are weakly altered and capped by a thin (<10 µm) iron oxide (e.g. ferrihydrite) layer. Low SAI measurements (e.g. <2/10) indicate that between 0.30 m and 0.50 m the combined organic and water cover limit the existence of oxygen and pyrite oxidation. Other sulfides, oxides, and silicates remained fresh in submerged environments. Surface water is enriched with calcium, chloride, and sulfate, by contrast, those ligands are low in groundwater. Stable isotope of oxygen and hydrogen, as well as dissolved rare-earth elements data, do not support contamination between surface and groundwater. Geochemical modeling using three scenarios between surface water and minerals within TSF confirmed that the final pH remained neutral (pH>7). The potential of a sulfate reducing bacteria, organic carbon, and shallow water cover provides effective environmental risk, especially acid metalliferous drainage generation due to oxidation and may be an effective strategy for long-term closure of the TSF.

THE KIVINIEMI Sc-Zr-Y MINERALIZATION, EASTERN FINLAND – A POTENTIAL SOURCE OF SCANDIUM IN EUROPE

Halkoaho Tapio¹, Ahven Marjaana², Rämö Osmo Tapani², Hokka Janne¹, Huhma Hannu¹

¹Geological Survey of Finland, Finland, ²Department of Geosciences and Geography, University of Helsinki, Finland

The Kiviniemi mafic intrusion, near the eastern margin of the Paleoproterozoic Central Finland Granitoid Complex is both spatially and temporally associated with post-kinematic Fe-Ti-P-enriched Svecofennian orogenic mafic magmatism. The main rock types in this small (~15 ha) intrusion are garnet-bearing fayalite ferrodiorite, leucoferrodiorite, ferromonzodiorite, and pyroxene diorite. The garnet-bearing fayalite ferrodiorite and leucoferrodiorite contain 50–281 ppm Sc, 275–5600 ppm Zr and 58–189 ppm Y (n=42), delineating a mineralized deposit some 2.5 ha in extent. Overall, these rocks show an evolved (iron-enriched) tholeiitic character, low values of Ni (<20-40 ppm), Cr (<20 ppm) and Cu (<20-80 ppm), and high contents of Zn (213-700 ppm). The rock-forming minerals in the ferrodioritic rocks are (ferro)hedenbergite, plagioclase (~An₄₀), ferropargasite and ferroedenite, almandine garnet and fayalite (Fo₁₋₄). Accessory minerals include zircon, ilmenite, fluorapatite, biotite, pyrite, pyrrhotite, potassium feldspar, grunerite, and clinoferrosilite. Some relict cumulate textures have been preserved, but primary magmatic features have largely been overprinted by strong recrystallization and corona formation. The main carriers of Sc are amphibole, clinopyroxene, and apatite. The remarkably strong enrichment of Sc in ferromagnesian silicates and apatite, rather than in specific Sc-minerals, implies magmatic enrichment. Post-kinematic mafic intrusions in central Finland constitute a bimodal association with co-existing granitoid counterparts. The Kiviniemi mafic intrusion is associated with a coarse megacrystic granite and the two rock types display mingled contacts, indicative of the contemporaneity of the two magmas. This conclusion is in accord with the coincident U-Pb zircon ages for the ferrodiorite, at 1857±2 Ma (multigrain ID-TIMS) and the megacrystic granite, at 1860±7 Ma (single-crystal LA-MC-ICP-MS). The initial εNd value of the ferrodiorite and the granite are +0.1 and -2.5, respectively. These Nd isotope compositions probably reflect a chondritic mantle source for the ferrodiorite and suggest incorporation of some Archaean crustal material into the granite in the course of magmatic evolution. The resource estimation calculated for Kiviniemi intrusion by using 40 g/t Sc cut-off value is 13.4 Mt of rock with an average grade of 162.7 g/t scandium, 1726 g/t zirconium, and 81 g/t yttrium. The concentration of Sc in the Kiviniemi deposit is so high, that it will classify Kiviniemi as a large Sc-deposit.

DATA VALUATION FOR ZIRCON RAMAN DATING: PARTIAL ANNEALING AND BAND ASYMMETRY

Härtel Birk¹, Jonckheere Raymond¹, Ratschbacher Lothar¹

¹Institut für Geologie, TU Bergakademie Freiberg, Germany

Zircon Raman dating is based on the disruption of the crystal lattice by α -disintegration of ²³⁸U, ²³⁵U, ²³²Th incorporated into the crystal lattice, and their daughter nuclides. This radiation damage affects the Raman spectrum by shifting and broadening the major bands. The Raman bandwidths thus provide an estimate for the radiation damage. From this damage estimate, and a measurement of the effective uranium (eU) content in the same spot, a Raman date is calculated. Two issues complicate the interpretation of Raman bandwidths: Partial annealing and band asymmetry. Radiation damage anneals upon heating so that the interpretation of the Raman date depends on the thermal history of the zircon. If the radiation damage has been completely annealed during a heating event, the Raman date is a reset age. In the case of partial annealing, the Raman date is a meaningless mixed age. Band asymmetry usually arises from the mixing of Raman spectra from different zones within a zircon grain. We present an approach to recognize partial annealing and asymmetry, based on the 439, 1008, and 356 cm⁻¹ Raman bands, and discuss the interpretation of such data with respect to zircon Raman dating.

CRYSTAL CHEMISTRY AND NOMENCLATURE OF FILLOWITE-TYPE PHOSPHATES

Hatert Frederic¹

¹Laboratory of Mineralogy, University of Liège, Belgium

Fillowite-type phosphates occur as primary phases in granitic pegmatites, as inclusions in stony and iron meteorites, and in high-grade metamorphic rocks. The fillowite group includes five CNMNC-approved species, namely fillowite, $\text{Na}_2\text{Ca}(\text{Mn,Fe})_7(\text{PO}_4)_6$, johnsomervilleite, $\text{Na}_2\text{Ca}(\text{Fe,Mn,Mg})_7(\text{PO}_4)_6$, chladniite, $\text{Na}_2\text{Ca}(\text{Mg,Fe})_7(\text{PO}_4)_6$, galileiite, $\text{Na}_2\text{Fe}^{2+}_4(\text{PO}_4)_8$, and stornesite-(Y), $(\text{Y,Ca})_{\square_2}\text{Na}_6(\text{Ca,Na})_8(\text{Mg,Fe})_{43}(\text{PO}_4)_{36}$. The fillowite structure was described as a packed derivative of the glaserite structure, $\text{K}_3\text{Na}(\text{SO}_4)_2$, and only a few structure refinements are available in the literature for fillowite-type phosphates: four natural samples of chladniite, one Mg-rich fillowite, as well as four synthetic compounds.

Five new samples of minerals belonging to the fillowite group were structurally investigated: fillowite from the Buranga pegmatite, Rwanda (A), fillowite from the Kabira pegmatite, Uganda (B), johnsomervilleite from Loch Quoich, Scotland (C), johnsomervilleite from the Malpensata pegmatite, Italy (D), and chladniite from the Sapucaia pegmatite, Minas Gerais, Brazil (E). Their crystal structures have been refined in space group R (No. 148), based on single-crystal X-ray diffraction data, to $R_1 = 3.79\%$ (A), 3.52% (B), 4.14% (C), 4.04% (D), and 5.59% (E). Unit-cell parameters are: $a = 15.122(1)$, $c = 43.258(4)$ Å (A); $a = 15.125(1)$, $c = 43.198(3)$ Å (B); $a = 15.036(2)$, $c = 42.972(9)$ Å (C); $a = 15.090(2)$, $c = 43.050(9)$ Å (D); and $a = 15.1416(6)$, $c = 43.123(2)$ Å (E). The asymmetric unit contains 15 cation sites with coordinations ranging from V to IX, as well as 6 P sites. The complex structure can be split into three types of chains running along the c axis. These chains are composed of edge- and face-sharing polyhedra.

Detailed cation distributions were determined for all 5 samples, and their comparison allowed one to establish the general formula $\text{A}_3\text{BC}_{11}(\text{PO}_4)_9$ for fillowite-type phosphates, where A represents the group of sites mainly occupied by Na, B the Ca sites, and C the sites containing the divalent cations Fe^{2+} , Mn and Mg. This formula was accepted by the CNMNC, and the four valid mineral species occurring in the fillowite group are fillowite (C = Mn), johnsomervilleite (C = Fe^{2+}), chladniite (C = Mg), and galileiite (B and C = Fe^{2+}). Stornesite-(Y) is discredited since this mineral corresponds to Y-bearing chladniite. For hypothetical future species, that would contain another dominant cation than Na on the A group of sites, we recommend the addition of a chemical suffix in order to avoid the unnecessary multiplication of root-names.

‘COLD’ SHEARED PERIDOTITES FROM KIMBERLEY (KAAPVAAL CRATON, SA): SHORTLIVED DEFORMATION CONNECTED WITH TRANSIENT HEATING AND METASOMATISM

Heckel Catharina¹, Woodland Alan B.¹, Seitz Hans-Michael¹, Linckens Jolien¹, Gibson Sally Anne²

¹Department of Geosciences, Goethe-University Frankfurt, Germany, ²Department of Earth Sciences, University of Cambridge, United Kingdom, c.heckel@em.uni-frankfurt.de; woodland@em.uni-frankfurt.de; h.m.seitz@em.uni-frankfurt.de; linckens@em.uni-frankfurt.de; sally@esc.cam.ac.uk

Sheared peridotites from the Kaapvaal craton may be divided into i) refertilized, high-T-peridotites and ii) highly-depleted low-T peridotites that equilibrated at conditions above and along the Kaapvaal conductive geotherm, respectively. Here we have studied 13 low P-T sheared peridotites entrained by Late Cretaceous (90Ma) kimberlites in order to constrain the nature and timing of the deformation. The samples are from two localities at Kimberley (Boshof road and Kennelworth dumps) and comprise 10 garnet-peridotites (GP) with various amounts of clinopyroxene (cpx) ± isolated spinel and 3 garnet-free phlogopite-peridotites (PP) with minor amounts of spinel. The peridotites have intensive deformation textures, ranging from porphyroclastic to fluidal mosaic. Olivine (ol) and orthopyroxene (opx) compositions (Mg# = 91 – 94) in the sheared peridotites indicate varying degrees of depletion, like the coarse-grained peridotites from the same localities. Pre-deformation conditions of the GP are preserved in the cores of large (>100 µm – mm diameter) porphyroclasts; these range from temperatures of 930 – 1000 °C at pressures of 4 ± 0.4 GPa, except for one GP recording 840 °C and 3.1 GPa. The PP yield temperatures of 870 – 920 °C at a preset pressure of 4 GPa. A key observation is that T-sensitive minor and trace element contents in ol (Ca, Al, Cr) and opx (Ca) increase in the fine-grained (down to <10µm) neoblasts. Assuming that the deformation took place at the pressure determined for the porphyroclasts, we estimate temperatures up to 1200 °C at the time of neoblast re-crystallization.

Mineral trace element concentrations allow the following metasomatic events to be distinguished in the ‘cold’ sheared peridotites: (i) Garnet (grt) and cpx preserve a pre-deformation event characterized by fluid-metasomatism (Y-Zr in grt). The CI-normalized REE-patterns of these grt are sinusoidal with enriched MREE (Sm ~10x CI) and are depleted in LREE and HREE. This event may also have led to the crystallization of the phlogopite in the PP. (ii) Grt from one sample exhibits a hump at Pr (>30x CI) and strong depletions in HREE probably stem from an older metasomatic event. (iii) A young metasomatic event that led to the crystallization of new cpx and Ti-enrichment of grt (>1x CI) with depleted LREE and enriched and scattered MREE to HREE patterns (Lu = 5 – 25x CI). This last phase of metasomatism may herald the beginning of the event that ultimately led to the strong deformation of the peridotites. Ol- and opx-neoblasts were enriched in Ti by a high-T (1200 °C) metasomatic agent, which also led to the introduction of fine-grained cpx (neoblasts) and Ti-oxides. Deformation textures along with the concurrent chemical enrichment of the neoblast argue for a connection with the intense kimberlite volcanism.

OXYGEN ISOTOPES APPEAR TO RECORD A DRASTIC MESOARCHEAN pCO₂ DROP

Herwartz Daniel¹, Pack Andreas², Nagel Thorsten J.³

¹Institut für Geologie und Mineralogie, Universität zu Köln, Germany, ²Geowissenschaftliches Zentrum, Georg-August-Universität Göttingen, Germany, ³Department of Geoscience, Aarhus University, Denmark

The oxygen isotopic composition of chemical sediments such as cherts and carbonates increases with time over Earth's history. Lower $\delta^{18}\text{O}_{\text{sw}}$ of ancient seawater may explain this trend. Respective modeling of such a low $\delta^{18}\text{O}_{\text{sw}}$ scenario implies elevated triple oxygen isotope $\Delta^{17}\text{O}$ values [1], which is inconsistent with rather low $\Delta^{17}\text{O}$ measured in Archean cherts [2–5]. Therefore, the low $\delta^{18}\text{O}_{\text{chert}}$ has been assigned to diagenesis [2–4] or to ancient seawater temperatures of about 70°C [5]. The later authors argue against a diagenetic overprint of their sample suite. The apparently hot temperatures, however, stand in stark contrast to the faint young sun paradox. Climate modelers struggle to explain why the early Earth was not freezing cold under a 20 to 30% less luminous sun. The elevated $\Delta^{17}\text{O}$ modeled for the low $\delta^{18}\text{O}_{\text{sw}}$ scenario is derived from a steady-state model [1, 6]. In this model, seawater becomes isotopically light when rates of continental weathering or hydrothermal alteration are increased or decreased, respectively. However, this classic model is designed to model the modern Earth, hence the extremely high rates of carbonatization and silicification observed in the Archean rock record, especially before 3 Ga ago, are not accounted for. The Urey reaction ($\text{CaSiO}_3 + \text{CO}_2 \rightarrow \text{CaCO}_3 + \text{SiO}_2$) is ultimately responsible for the observed high degrees of carbonatization and silicification. Upon subduction (or sagduction) the carbonate pyrolyses and the CO_2 is reintroduced into the atmosphere. This CO_2 recycling extracts ^{18}O from the hydrosphere resulting in lower $\delta^{18}\text{O}_{\text{sw}}$ of ocean water. We have expanded the model accordingly and find that seawater $\delta^{18}\text{O}_{\text{sw}}$ decreases while $\Delta^{17}\text{O}$ stays low, which is consistent with Archean chert data (Herwartz et al. in press). This scenario is most plausible for a high CO_2 world. By combining evidence from the literature [7, 8] and via additional modeling we show that 3.2 Ga ago the p CO_2 may have been in the order of 1 bar. Within the Mesoarchean, the p CO_2 then dropped by about one order of magnitude reflecting the redistribution of carbon from the atmosphere, the ocean, and the oceanic crust to long-term storage reservoirs within the continents and the mantle. We suggest that plate tectonics and the emergence of continents provided efficient CO_2 sinks and storage capacities for carbon. Major ice ages on Earth starting at 2.9 Ga probably reflect this overall decreasing CO_2 greenhouse effect. The p CO_2 drop coincides with the increasing oxygen isotopic composition of cherts and carbonates. The later trend implies a moderately low seawater $\delta^{18}\text{O}_{\text{sw}}$ of about -5 per mill before 3 Ga ago. Elevated p CO_2 thus provides plausible explanations both for the apparently hot paleotemperature from pristine cherts and for the faint young sun paradox. Our results suggest that a warm, but not hot early Earth seems to be the most plausible scenario.

[1] Sengupta S., Pack A. (2018) *Chem Geol* 495:18–2; [2] Sengupta S. et al. (2020) *Chem Geol* 554:119789; [3] Zakharov D.O. et al. (2021) *RiMG* 86: 323-365; [4] Liljestränd F.L. et al. (2020) *EPSL* 537:116167; [5] Lowe D.R. et al. (2020) *Am J Sci* 320:790–814; [6] Muehlenbachs K. (1998) *Chem Geol* 145:263–273; [7] Shibuya T. et al. (2017) *PEPS* 4:31; [8] Shibuya T. et al. (2012) *EPSL* 321–322:64–73.

COMPARISON OF CHROMITE GRAIN SIZES AND LIBERATION BY 2D AND 3D MEASUREMENTS

Hicks Matthew¹, Sittner Jonathan², Ricardo da Assuncao Godinho Jose², Renno Axel D.², Cnudde Veerle³, Boone Marijn⁴, De Schryver Thomas⁴, Van Loo Denis⁴, Dewaele Stijn³, Roine Antti¹, Ihanus Jaakko⁵, Liipo Jussi¹

¹Metso Outotec, Finland, ²Helmholtz Institute Freiberg for Resource Technology, Helmholtz-Zentrum Dresden-Rossendorf, Germany, ³Geology Department, Ghent University, PProGRess-UGCT, Belgium, ⁴Ghent, TESCAN XRE, Belgium, ⁵Kemi Mine, Outokumpu Chrome Oy, Finland

The Outokumpu Kemi mine is the only chromium mine in Europe and the biggest underground mine in Finland. Chromite ore is mined from the underground mine and processed in the mills above ground. The annual ore handling capacity is 2.7 million tons producing 0.85 Mt fine concentrate and 0.40 Mt lumpy ore. Concentrates and lumpy ore are delivered to the nearby Tornio ferro chromite- plant and stainless-steel mill.

At the Kemi chromite mine, mineralogical information has been collected and used systematically in production planning for more than 20 years. The grain size of chromite varies in the deposit and this influences processing. Currently, at the Kemi mine, the chromite grain size is visually estimated from unbroken drill core samples and the grain size distribution of chromite is estimated to help with ore processing.

This information is fed into the ore block model. The size distribution of chromite is used to evaluate whether the ore is suitable for fine concentration and to forecast the expected recovery. Estimation is based on findings that the grain size of chromite after grinding follows the grain size of the original chromite in the ore and in the gravity separation. It has been observed that most of the recovery losses are found in the finest particle sizes.

The petrography of most chromitites favors the use of reflected light microscopy for grain size measurements and estimation of chromite liberation and there are several published studies in which the grain size of chromite has been measured from unbroken or crushed ore samples, concentrates, and other process products using reflected light photomicrograph mosaics only or with complementary backscattered electron images from automated scanning electron microscopes or in combination or only by X-ray micro tomography.

In the case of chromitites, reflected light optical microscopy is the most cost-efficient and fastest method for chromite grain size determinations. However, the measured data is in 2D which may have implications for skewed measurement results, as the chromite grains are 3-dimensional. Therefore, the comparison of 2D and 3D is required to evaluate possible errors in 2D measurements.

We present the results of the comparative study on measurements of chromite grain sizes and liberation degree in 2D from unbroken and crushed Kemi chromitite ore samples using reflected light photomicrograph mosaics and back scattered images and in 3D using X-ray micro tomography.

Keynote

INSIGHT INTO THE IMPACT OF MELT/FLUID PERCOLATION ON THE MICROSTRUCTURAL EVOLUTION OF THE LITHOSPHERIC MANTLE

Hidas Károly¹, Padrón-Navarta José Alberto²

¹Departamento de Investigación y Prospectiva Geocientífica, Instituto Geológico y Minero de España, Spain,

²Instituto Andaluz de Ciencias de la Tierra, CSIC & Universidad de Granada, Spain

Despite decades of intense research, processes allowing for ductile deformation of the lithospheric mantle remain poorly understood, yet the role of volatiles has been in the focus of interest since the earliest works. The main pathways to supply these components to the upper mantle are the direct crystallization of hydrous minerals, the incorporation of hydrogen through point defects in the crystal structure of nominally anhydrous minerals (NAMs), and the percolation of aqueous fluids or hydrous melts at mantle depths. The exact role of each of these parameters in controlling the rheology of the deep lithosphere is, however, controversial.

Opposed to common expectation, microstructural data suggests that only the presence of large modal amounts of hydrous minerals in the mantle does not produce significant rheological weakening. By contrast, many laboratory experiments have demonstrated that the strength of NAMs decreases systematically with increasing hydrogen concentration due to easier movement of dislocations in the wet crystalline lattice. Although this weakening effect is commonly accepted, there is an ongoing debate on the extent to which such hydrogen incorporation in NAMs can be responsible for plate tectonic-scale weakening of the upper mantle. Finally, interstitial hydrous melts and aqueous fluids have a pronounced wetting effect at grain boundaries, which facilitate diffusion and promote potential switches in the dominant deformation mechanisms during fluid/melt-assisted reactive percolation in the mantle. Even though important synergetic presence of these agents would be required to have an effect on the overall mantle viscosity, several microstructural studies highlight their strong positive feedback on localization of pervasive deformation in melt/fluid lubricated domains. On the other hand, the speciation of hydrous melts and aqueous fluids primarily depends on the thermal history and phase equilibria along the lithospheric column. This has important consequences on the potential of specific volatiles in contributing to mantle rheology at distinct levels of the lithospheric mantle. Therefore, the prevailing effect of the different volatile species on ductile deformation may be rooted in thermodynamically controlled, physico-chemical processes.

Here we provide recent case studies that shed light on key processes coupled to the different incorporation mechanisms of volatiles at distinct levels of the lithospheric mantle, ranging from the lithosphere-asthenosphere boundary to the shallowest plagioclase lherzolites facies. These results allow for evaluating the relative effect of the different volatile forms on the response of lithospheric mantle to deformation and suggest the influence of either aqueous fluids or hydrous melts outmatches that of the NAMs (or the hydrous phases). We thus propose that, when it comes to mantle rheology, the focus should be shifted on a better understanding of conditions in the lithosphere that control the availability and composition of aqueous fluids and hydrous melts rather than the sole ability of ionic impurities in NAMs in governing the ductile deformation of the upper mantle.

INFLUENCE OF PORE GEOMETRY ON THE THERMAL SHOCK RESISTANCE OF POROUS CORDIERITE HEAT STORAGE MATERIAL INVESTIGATED BY NUMERICAL SIMULATION

Hildebrand Jan Sebastian¹, Seibold Joshua¹, Pöllmann Herbert², Krcmar Wolfgang¹

¹Materials Engineering, Nuremberg Institute of Technology, Germany, ²Institute of Geosciences and Geography, Martin Luther University Halle-Wittenberg, Germany

The optimization of a porous ceramic material for dynamically high-temperature sensible heat storage processes is to be carried out by means of numerical thermal simulation calculations. For this work cordierite ($\text{Mg}_2\text{Al}_4\text{Si}_5\text{O}_{18}$) is considered as a suitable ceramic for use as a sensible heat storage material. In particular, transient quenching processes concerning different pore geometries of the considered porous ceramic material are to be investigated with finite element simulations. For the material properties, a typical set of values, that were previously determined experimentally, for the cordierite ceramic is used, which consists of a density of 2130 kg/m³, a specific heat capacity of 1000 J/(kg·K) and thermal conductivity of 0.708 W/(m·K). These values are considered as not being temperature-dependent for the simulation, while for the thermal expansion coefficient a table of values is used as a function of temperature. The observed pore geometries are modeled in spherical, cylindrical, and cuboid shapes. The volume of each individual pore is 10 mm³. Thermal stresses deriving from the quenching processes are to be simulated. For this purpose, cuboid specimens with a side length of 33.16 mm and an overall porosity of 20 percent by volume are built via computer-aided design (CAD). A simulated case is generated with a finite element-based computational fluid dynamics (CFD), in which the specimens are heated up to a temperature of 720 °C and are afterward abruptly quenched in a volume of 127.35 liters of water at a temperature of 20 °C. The specimens are created with isotropic and non-isotropic aligned pores concerning the directions of the cartesian axes in order to investigate the influence of the directional dependence of the pores on the thermal shock resistance behavior during the quenching process. The simulation results show that the considered cordierite-ceramic specimen containing pores is able to reduce the maximum main stress compared to the zero sample without pores. The non-porous zero sample has a maximum of occurring main thermal stress of 16.4 MPa. The best properties, regarding the application for heat storage, are achieved using the non-isotropic and the isotropic cuboid pore geometry with the lowest maximum main thermal stress of 11.6 MPa and 11.8 MPa. These are followed by the specimen with spherical, isotropic, and non-isotropic cylindrical pores with values of 12.7 MPa, 15.1 MPa, and 15.6 MPa. This means the reduction of the thermal stresses ranges from 4.9 % to 29.3 % just concerning different pore shapes. The impact from the alignment of the cylindrical and cuboid-shaped pores is not particularly high. The thermal stress of the specimen with isotropic cylindrical pores is 3.2 % higher than the thermal stress of the corresponding specimen with non-isotropic cylindrical pores, whereas the thermal stress of the specimen with isotropic cuboid pores is 1.7 % lower than the thermal stress of the specimen containing the non-isotropic cuboid pores.

INFLUENCE OF PORE GEOMETRY ON THE THERMAL INSULATION PROPERTIES OF POROUS BRICK CERAMICS

Hildebrand Jan Sebastian¹, Seibold Joshua¹, Pöllmann Herbert², Krcmar Wolfgang¹

¹Materials Engineering, Nuremberg Institute of Technology, Germany, ²Institute of Geosciences and Geography, Martin Luther University Halle-Wittenberg, Germany

The aim of the work presented here is to investigate the influence of the geometry of macropores on the thermal conductivity of a ceramic brick structure. For this purpose, laboratory bricks are porosified in such a way that the total pore volume of the generated individual pores remains approximately constant for each porosification agent, while only the shape of the pores is varied. Spherical, cuboidal, and cylindrical pores are integrated into the brick structure, which is generated by cauterizing suitable organic polymers. The volume of a single pore should be $9 \text{ mm}^3 \pm 1 \text{ mm}^3$ on the arithmetic average. In the work presented here, 20 % by volume each of spherical, cuboidal, and cylindrical porosification agents are added in monoporosification to a typical clay for the production of lightweight hollow bricks. For porosifying, commercial expanded polystyrene (EPS) in spherical form is used to generate the spherical pores. A sheet of high-impact polystyrene (HIPS) is cut manually to produce the cuboid pores. To create the cylindrical pores, polylactic acid (PLA) granulate is melted down, extruded into a continuous PLA filament and then cut into pieces. During extrusion, 20 % by volume of the porosification agents are incorporated into the clay mixtures, each in monoporosification. After the drying process, the clay blanks are sintered in a laboratory oven heated by electric resistance heating. After firing, the porosants leave pores with the same geometries. The specimen are sawn and ground in a further process. Perpendicular to the extrusion direction, the unporosified brick specimens show a drying shrinkage of 6.71 %, a firing shrinkage of 0.34 % and a total shrinkage of 7.06 %. All porosified bricks exhibit lower drying shrinkage between 4.24 % to 5.39 % across the extrusion direction and firing shrinkage between 0.37 % to 0.41 %. The total shrinkage of the porous bricks perpendicular to the extrusion direction ranges from 4.62 % to 5.78 %. In the extrusion direction, the unporosified brick zero samples exhibit a drying shrinkage of 9.44 %, a firing shrinkage of 0.43 %, and a total shrinkage of 9.87 %. In the extrusion direction, porosity results in a lower drying shrinkage between 7.24 % to 8.39 % and a lower firing shrinkage between 0.36 % to 0.38 %. Thus, the total shrinkage of the porosified bricks in the extrusion direction is reduced to values between 7.60 % and 8.75 %. While the unporosified brick specimens have an average thermal conductivity of $\lambda_{10, \text{dry}} = 0.365 \text{ W}/(\text{m}\cdot\text{K})$, the porosification with cylindrical pores leads to a reduction of the thermal conductivity to $\lambda_{10, \text{dry}} = 0.267 \text{ W}/(\text{m}\cdot\text{K})$, corresponding to 26.97 %. Porosification with spherical pores causes a reduction of the cullet thermal conductivity to $\lambda_{10, \text{dry}} = 0.297 \text{ W}/(\text{m}\cdot\text{K})$, corresponding to 18.69 %, while monoporosification with cuboidal pores reduces the cullet thermal conductivity by 17.66 % to $\lambda_{10, \text{dry}} = 0.301 \text{ W}/(\text{m}\cdot\text{K})$.

PRESERVATION OF A REDUCED PALEOARCHEAN MANTLE PORTION – A CASE STUDY ON KY/COR ECLOGITES FROM THE KAAPVAAL CRATON

Hoefler Heidi¹, Shu Qiao², Brey Gerhard¹, Heckel Catharina¹, Vasilyev Prokopiyy³

¹Institute of Geosciences, Goethe-University Frankfurt, Germany, ²Institute of Geochemistry, State Key Laboratory of Ore Deposit Geochemistry, Chinese Academy of Sciences, Guiyang 550081, China, China, ³Curtin University, Perth, Australia, hoefler@em.uni-frankfurt.de; shuqiao@mail.gyig.ac.cn; brey@em.uni-frankfurt.de; heckel@em.uni-frankfurt.de; prokopiyy.vasilyev@curtin.edu.au

The Earth's mantle was at metal saturation shortly after accretion and core formation ($\Delta FMQ \sim -4.5$; Frost and McCammon, 2004). This supposedly changed very rapidly afterwards to $\Delta FMQ \sim 0$ (= today's MORB mantle) due to the disproportionation of Fe^{2+} in bridgmanite to $Fe^{3+} + Fe^0$. The latter was transferred to the core leaving an oxidized residue behind that mixed with the upper mantle. It is therefore important to determine the oxidation state of the mantle throughout Earth's history. Canil et al. (2002) and Li and Lee (2004) estimated from V abundances and V/Sc ratios of peridotites that the Earth's mantle was at present-day oxidation state since the Archean while Aulbach et al. (2016) demonstrated an increase of the oxidation state around the Proterozoic/Archean boundary from $\Delta FMQ \sim -1.3$ to ~ 0 . The methods in use also comprise the determination of Fe^{3+} in garnet and spinel from eclogites and peridotites and the calculation of fO_2 via experimentally calibrated oxybarometers. It is tacitly assumed that today's oxidation state of Fe reflects that from before metamorphism. This needs to be proven and is attempted here with 3.2 Ga old kyanite and corundum eclogite xenoliths from the Bellsbank diamond mine on the Kaapvaal craton (Shu et al. 2016). They are interpreted as former troctolites i.e. olivine-plagioclase cumulates because of their very low REE abundances, flat C1-normalized REE patterns, and strong positive Eu-anomalies. Initially, such rocks contain only Fe^{2+} . Subsequent seafloor alteration and metamorphism could have lead to partial oxidation of Fe^{2+} that would be reflected in present-day eclogites by Fe^{3+} in the garnets. A measure for oxygen fugacity during accumulation is the V/Cr ratio of the troctolites. It is that of the accumulating olivine and is determined by the prevailing oxygen fugacity. Mallmann and O'Neill (2009) determined $K_V^{ol/l}$ and $K_{Cr}^{ol/l}$ as a function of oxygen fugacity. Modern-day troctolites from the Pacific and the Atlantic form a correlation with a slope corresponding to $\Delta FMQ \sim 0$ applying the above partition coefficients. The calculated bulk compositions (cpx:grt=50:50) of the ky/cor eclogites form a V/Cr correlation with a steeper slope corresponding to $\Delta FMQ \sim -2$. If this oxidation state is preserved until today, the Fe^{3+} contents in the xenoliths should be close to zero. We confirmed this with an accurate determination of $Fe^{3+}/\Sigma Fe$ in garnet with the flank method by electron microprobe analysis (Hoefler and Brey 2007). The analysis of the Bellsbank garnets gave very low $Fe^{3+}/\Sigma Fe$ of < 0.03 that yielded maximum possible ΔFMQ values between -4 and -2 as calculated with the oxybarometer of Vasilyev (2016) for kyanite bearing eclogites. Our results confirm that the oxidation state of Fe can be preserved in eclogites since the Archean. They also indicate a slower increase of the oxygen fugacity in the mantle after the time of core formation over an extended period of time.

UNSPECTACULAR AT FIRST GLANCE – POSSIBLE WEATHERING OF A COLOURED SCOLECITE BEAD FROM LOWER NUBIA

Hoelzig Hieronymus¹, Baehre Oliver², Raue Dietrich³, Mueller Kai², Kloess Gert²

¹Institute of Mineralogy, Crystallography and Materials Science, Leipzig University, Germany, ²Institute of Mineralogy, Crystallography and Materials Science, Leipzig University, Germany, ³Egyptian Museum – Georg Steindorff, Leipzig University, Germany

X-ray diffraction measurements on Nubian crafts provided by the Egyptian Museum – Georg Steindorff – of Leipzig University, revealed the mineral scolecite to have been carved for one visually unsuspecting pendant from Lower Nubia (1900–1600 BCE, excavated in 1914, inv. No. ÄMUL 4483). The collection catalog notes only "white-red pebble" as material. Scolecite is a rather rare monoclinic zeolite mineral ($\text{CaAl}_2\text{Si}_3\text{O}_{10} \cdot 3 \text{H}_2\text{O}$). The "coincidence" of this mineral with an object that, judging by its optical appearance, could just as easily have been made from a more ubiquitous material, requires an explanation. It could come from a Nubian locality with scolecite in significant quantities. In fact, basal alluvial gravel with scolecite at the Nile exists in Sudan. But even if the present scolecite comes from there, it should still be considered that the pendant in question may once have had a more spectacular appearance since, nowadays, scolecite is often traded in the form of characteristically shimmering beads with needle-shaped crystals. The pendant in question is mostly opaque with two red-stained areas and lacks such an optical effect, possibly due to a weathering process. Needle-shaped crystals can barely be recognized but reflex intensities of XRD measurements from different angles prove that the (110) direction runs from the hole to the tip. To simulate daily-use/storage weathering, we stirred a non-archaeological scolecite bead for 7 weeks at room temperature in mixtures of different compositions. In fact, the bead visually fatigued and the shimmering effect decreased. However, the needle-shaped crystals became more visible again after heating at 115 °C for another week. Mere heating of another bead to a maximum of 115 °C over a period of 7 weeks did not lead to any change at all, whereas heating at 200 °C for 2 hours initially led to complete abolition of the shimmering effect and the same treatment again led to an even finer shimmering effect. In addition, the bead was exposed to powders of iron and manganese substances, resulting in a partial red coloration. These phenomena could have been the purpose of a hypothetical scolecite heat treatment in ancient times. However, the bead broke after being exposed to water overnight.

We would like to thank Karl Heinrich von Stülpnagel and Sebastian Blanke for their support.

CHARACTERISATION OF HOST ROCKS AND MINERALISATION AT APLIKI W, CYPRUS: SIMULTANEOUS XRT/XRF ANALYSIS AND CONVENTIONAL METHODS

Högdahl Karin¹, Jonsson Erik², Santana Carlos¹, Andersson Stefan S.¹, Hansson Alexander³, Georgiou Lazaros⁴, Kalageropoulos Georgios⁴, Bakker Edine⁵, Arvanitidis Nikolaos², Arvidsson Ronald²

¹Earth Sciences, Uppsala University, Sweden, ²Department of Mineral Resources, Geological Survey of Sweden, Sweden, ³Orexplore, Sweden, ⁴Hellenic Copper Mines, Cyprus, ⁵Department of Mineral Resources, Geological Survey of Sweden, Sweden

The West Apliki deposit (Apliki W) is a small low-grade resource of disseminated cupriferous mineralization located in northwestern Cyprus. It occurs in the western part of the Solea graben approximately 5.5 km southwest of Skouriotissa, and directly west of the Apliki deposit (Apliki E). The mineralization is hosted by variably altered pillow lavas of the Troodos ophiolite and represents a stringer zone, i.e. the deeper part of the mineralized system. The mineral assemblages of the host rocks and ores have been characterized by means of optical and electron microscopy, EDS and WDS analyses, XRD, LA-ICP-MS, and Raman spectroscopy. Short drill core sections (c. 30 cm) have been collected and scanned by simultaneous XCT/XRF using the GeoCore X10 drillcore scanner, with subsequent data processing utilizing the software Orexplore Insight®. The mineralogical data from the conventional methods of analysis have been utilized to further develop and refine the software and its application, all conducted within the framework of the H2020 project X-MINE (No 730270).

The mineralization at Apliki W is capped by different types of gossan, which are also present in the hanging walls to major faults. The upper and most oxidized gossan is red, porous, and very fine-grained. It comprises quartz and hematite of a low degree of crystallinity. Quartz is present both as round quartz aggregate and in the fine-grained matrix. Yellow silicified gossan is relatively younger and is dominated by quartz with minor amounts of anatase, goethite, and possibly also halite. Below the gossan, the basalt is silicified and exhibits either a purple or green-beige color. Both types are dominated by quartz with regard to crystalline phases. The purple type contains additional hematite, biotite, another phyllosilicate (celadonite-type?), and likely also gypsum, whereas the green-beige variety is made up of goethite, jarosite, and a serpentine-type mineral. The silicified lava is transected by a large number of yellow veins ranging in widths from a few millimeters to more than a decimetre. The dominating phases in these veins are natroalunite-hydronium jarosite solid solution, natrojarosite, and minor amounts of quartz and goethite. The sulfates have grown perpendicular to the vein walls which render them a fibrous impression. A combination of XCT/XRT and petrography shows that goethite-bearing assemblages are typically enriched in V, which suggests that this phase is the main V-carrier. The sulfidic ore minerals are either present as disseminations or as aggregates in veins varying in widths from a few millimeters to several centimeters. Pyrite is the most abundant sulfide and occurs as euhedral to subhedral, occasionally rounded crystals. Covellite and chalcocite are the main Cu-hosts, typically replacing primary chalcopyrite. The latter is preserved as disseminations in a more quartz-rich part of the mineralization. Sphalerite is present both as inclusions in pyrite and as small isolated grains. Malachite and turquoise have formed as superficial crusts and fracture fillings. Microchemical analyses of the pyrite show that it is compositionally zoned. The central or core parts are variably enriched in Ni (up to 1700 ppm), Co (up to 900 ppm), and Se (2000 ppm) and hosts micro-inclusions of Cu, Bi, As, and Pb-bearing phases. The Te content reaches 80 ppm and Au is typically low <0.5 ppm, but micro inclusions may be present. With respect to the high Se contents in general, the mineralization resembles the richer Apliki E and indicates a similar evolution.

TRIASSIC VOLCANO-SEDIMENTARY SUCCESSION – SEKOLJE, Mt. STRAHINJŠČICA, NW CROATIA

Horvat Marija¹, Smirčić Duje², Belak Mirko¹, Baranyi Viktória¹

¹Department of Geology, Croatian Geological Survey, Croatia, ²Department of Mineralogy, Petrology and Mineral Resources, Faculty of Mining, Geology and Petroleum Engineering University of Zagreb, Croatia

The Mt. Strahinjščica in NW Croatia contains volcano-sedimentary successions formed along the NE margin of Adria during the period of arc-related extension in the Middle-Late Triassic. It is built of sedimentary (dolomitic rocks, radiolarites, cherts, clay, siltstones, and sandstones), magmatic rocks (altered andesitic basalts and diabases), and tuffs. The Sekolje section on the southern slope of Strahinjščica Mt. represents a 100-meter thick volcano-sedimentary succession with pyroclastic and siliciclastic lithofacies types. The pyroclastic facies is recorded in the section from the beginning to 38.90 m. It consists of two different lithotypes: vitroclastic and crystalloclastic tuffs. Vitroclastic tuffs are composed of fine ash with glass shards and pumice fragments. Both glass shards and pumice fragments are devitrified into microcrystalline quartz, albite, clay minerals, calcite, and chlorite respectively. Rare crystalloclasts of quartz and K-feldspar/plagioclase are still present. Crystalloclastic tuffs are composed of coarse ash to lapilli-sized pyroclastic material. Dominant crystalloclasts are quartz, plagioclase, and K-feldspars, with less biotite. Quartz crystalloclasts are angular with varied size, show jig-saw fit texture, and occasionally have oval-spherical cavities typical for volatile-rich systems. Plagioclase and K-feldspar crystalloclasts have mainly hypidiomorphic to idiomorphic shapes. Carbonate and silicified tuff lithoclasts and chert are subordinate. Matrix of the crystalloclastic tuffs is made of fine ash devitrified to chlorite, microcrystalline quartz, clay minerals, opaque minerals, with carbonate domains sporadically. The siliciclastic facies between 38.90 and 100.60 m is divided into siltstone and volcanogenic sandstone lithotypes. Dark grey to brown siltstones are homogenous, thin-bedded, or laminated with radiolarian-rich lamina and lenses. Grains of quartz, K-feldspar, and muscovite are recognized in the siltstones, while the matrix is composed of chlorite, clay minerals, sericite, and organic matter. Volcanogenic sandstones are poorly sorted and composed mainly of pyroclastic and volcanogenic particles, with an approximately equal amount of highly altered feldspars and lithoclasts, and some quartz grains. Matrix is composed of chlorite, sericite, fine quartz, and feldspar grains. Described lithofacies types at Sekolje section suggest that the sedimentation of the pyroclastic material occurred simultaneously with active volcanism. The occurrence of two lithotypes in the pyroclastic facies indicates the segregation of the material from the bulk pyroclastic cloud through sedimentation processes. Crystalloclastic coarse pyroclasts were transported and deposited by gravity currents, while fine ash tuffs, consisting mainly of glass shards, settled from suspensions. These processes could have happened after the pyroclastic eruption and syn-eruptive re-sedimentation to the deeper marine environment while the siliciclastic facies was deposited during abating volcanic activity. Siltstones were deposited in distal, probably anoxic environments. The organic matter in these lithofacies consists of charcoaled plant debris, palynomorphs are extremely rare. The coarsening of clastic material in the upper part of the section and transition to the volcanogenic sandstones can be interpreted as shallowing of the basin areas and/or increased proximity to the source area.

This research is supported by Croatian Science Foundation (IP 2019-04-3824).

Keynote

FROM CORE TO ORE: REFLECTIONS ON PGE SOURCE FERTILITY AND ITS CONTROLS ON MINERALIZATION

Hughes Hannah¹

¹Camborne School of Mines, University of Exeter, United Kingdom

As highly siderophile elements (HSE) and chalcophile elements, the PGE have an affinity for sulfur in the Earth's mantle and crust. They are largely hosted by base metal sulfides (BMS) and discrete platinum-group minerals (PGM). The abundance of PGE in the upper mantle is estimated from mantle xenoliths and diamonds, as well as from magma compositions as represented by large igneous province (LIP) and mid-ocean ridge lavas. BMS and PGM contained within different mantle xenoliths indicate that various mantle domains have distinctly different metal budgets. Disparity in the source and extent of partial melting in the mantle (and with possible contributions from the outer core and enriched subcontinental lithosphere in the case of some mantle plumes) can have a significant effect on the PGE geochemistry and mineralogy of a magma and corresponding residues. For example, BMS release a portion of their metal budget into magma during mantle partial melting – if a mantle source region has BMS rich in PGE and other critical metals, magma produced from significant partial melting of this region (mobilizing or even exhausting the BMS) may also be anomalously rich in these metals. However, whilst PGM are regularly observed in mantle xenoliths, their distribution throughout the mantle; their behavior during partial melting and metasomatism; and thus their mobility and contribution to partial melts, remain challenging to quantify. Although volumetrically a tiny component of a mantle source, the high concentration of PGE within PGM means that they are likely to control a significant proportion of the metal basket. In this talk, we seek to highlight recent developments in PGE research conducted by early career researchers in this field: From advances in our understanding of the mantle PGE budget by detailed petrology, mineralogy, and geochemistry; through to machine learning and how this may link magmatic differentiation in the deep Earth to metallogenesis and mineralization in the crust.

OCCURRENCE OF PLATINUM GROUP MINERALS (PGM) IN PODIFORM CHROMITITES FROM SEBUKU ISLAND, SOUTH KALIMANTAN, INDONESIA

Idrus Arifudin¹, Zaccarini Federica², Garuti Giorgio², Wijaya I.G.N.K.¹, Swamidharma Y.C.A.³, Bauer Christoph⁴

¹Department of Geological Engineering, Universitas Gadjah Mada, Indonesia, ²Department of Applied Geosciences and Geophysics, University of Leoben, Austria, ³Geology and Exploration, PT Sebuk Iron Lateritic Ore, Indonesia, ⁴RHI Magnesita, RHI Magnesita, Austria

We report the first occurrence of PGM found in podiform chromitites located in Sebuk Island, South Kalimantan, Indonesia. The studied chromitites consist of small mineralized bodies associated with meta-dunite and meta-harzburgite, Jurassic in age. Microscopically they display a texture variable from massive to disseminated with the modal proportion of the interstitial silicates up to about 50%. The chromite composition plots in the field of podiform chromitite and Cr-rich with Cr/(Cr+Al) higher than 0.7 and Al-rich with Cr/(Cr+Al) lower than 0.6 chromitites have been analyzed. The binary diagrams of TiO₂ versus Al₂O₃ show that the Cr-rich chromitites fall in the field of the Island Arc Basalts (IAB) and Supra Subduction Zone (SSZ). The Al-rich chromitites display compositional similarity with those reported from chromitites in supra-Moho cumulate sequences of the Urals and Sulawesi ophiolite and plot in the overlapping field of SSZ and Middle Oceanic Ridge Basalt (MORB) chromitites. Silicates in the matrix are completely altered to serpentine and chlorite. Serpentine is the predominant silicate in the matrix of the Cr-rich chromitites, and chlorite in the Al-rich. The PGM assemblage of the Cr-rich chromitites consists only of laurite that occurs as polygonal grains (less than 10 µm in size) included in chromite crystals and sometime in contact with silicates. The PGM associated with the Al-rich chromitite of the Sebuk Island display a complex mineralogical assemblage consisting of phases of Os, Ir, Ru, Rh and Pt, and the two groups of PGM, primary and secondary, have been recognized. The primary PGM consist only of laurite that, as in Cr-rich chromitite, forms tiny polygonal grains (up to 20 µm in size) enclosed in fresh chromite or in contact with chlorite. The following secondary PGM have been recognized: alloys of Pt-Fe, garutiite, irarsite, ruthenium inter-grown with magnetite, zaccariniite, and unnamed Ru and Mn oxides. The secondary PGM have an irregular shape and occur exclusively in contact with chlorite and Mn-Ni-Fe hydroxides. Their size varies from 1 up to about 200 µm. The PGM associated in the Cr-rich chromitites crystallized at high temperature and low S fugacity in the mantle. Laurite in the Al-rich chromitite precipitated at higher S-fugacity and the presence of abundant Pt and Rh phases in the altered matrix suggests that sulfur saturation was achieved. Therefore, we can argue that the Al-rich chromitite and associated PGM crystallized in close or above the Moho of the host ophiolite. The strong alteration altered the primary PGM in secondary, forming complex PGM grains and the ruthenium and Pt-Fe alloys by desulfuration of primary PGE-sulfide.

LIZARDITE IN THE SERPENTINIZED ULTRABASIC ROCKS FROM THE ALIMONDE REGION, UPPER ALLOCHTHONOUS TERRANE (UAT) OF BRAGANÇA, NE PORTUGAL

Ínsua-Pereira Guilherme¹, Bobos Iuliu², Pinto de Meireles Carlos³

¹Institute of Earth Sciences - Porto Pole, Rua do Campo Alegre 687, 4169-007 Porto, Portugal, ²Institute of Earth Sciences - Porto Pole, DGAOT, Faculty of Sciences, University of Porto, Rua do Campo Alegre 687, 4169-007 Porto, Portugal, ³National Laboratory of Energy and Geology, Rua da Amieira, Ap. 1089, 4466-901 S. Mamede de Infesta, Portugal

The UAT is comprised of two subunits (lower and upper). The lower subunit of UAT, well exposed at Cabo Ortegale and Bragança Massifs, includes a high-grade metamorphic series and a mafic/ultramafic igneous suite (gabbro, peridotite, dunite, pyroxenite, and hornblendite rocks). Both peridotite and dunite rocks supported a serpentinization process. The serpentinized ultrabasic rocks from the Alimonde region (Bragança) were petrographically and mineralogically (X-ray diffraction, infrared and Raman spectroscopy, and electron microprobe) studied. Several distinct microscopic textures were identified in the altered peridotite and dunite rocks such as olivine-related pseudomorphs, with mesh and hourglass textures, and fracture-filling serpentine veins accompanied by oxide phases (i.e. Cr-spinel, magnetite), or minor sulfide phases. Lizardite is the main species identified by X-ray in serpentinized rocks [$d(hkl) = 7.30 \text{ \AA}, 4.56 \text{ \AA}, 3.66 \text{ \AA}, 2.48 \text{ \AA}, \text{ and } 1.53 \text{ \AA}$], where the 1T polytype is dominant. Infrared spectra show the OH-stretching bands at 3690 cm^{-1} and 3660 cm^{-1} , a strong band at 1090 cm^{-1} corresponding to the Si-O bond and the Al(IV)-OH band at 960 cm^{-1} . A strong vibration band corresponding to Si-O bonds at 690 cm^{-1} was assigned in the Raman spectra. The 1T-lizardite shows the following crystal chemistry composition: $(\text{Mg}_{2.79}\text{Fe}_{0.07}\text{Al}_{0.12})(\text{Si}_{1.94}\text{Al}_{0.06})\text{O}_5(\text{OH})_4$. Lizardite is a low-temperature and pressure species crystallized during the serpentinization of peridotite and dunite rocks.

STABILITY RELATIONS OF REE-BEARING ACCESSORY PHASES IN THE CANCRINITE-BEARING NEPHELINE SYENITE FROM THE ČISTÁ PLUTON (CZECH REPUBLIC)

Jaranowski Maciej¹, Budzyń Bartosz¹, Sláma Jiří², Kozub-Budzyń Gabriela³, Wirth Richard⁴, Klomínský Josef⁵

¹Polish Academy of Sciences, Institute of Geological Sciences, Kraków, Poland, ²The Czech Academy of Sciences, Institute of Geology, Prague, Czech Republic, ³AGH University of Science and Technology, Faculty of Geology, Geophysics and Environmental Protection, Kraków, Poland, ⁴GeoForschungsZentrum Potsdam (GFZ), Section 3.5 Interface Geochemistry, Potsdam, Germany, ⁵Czech Geological Survey, Institute of Geology, Prague, Czech Republic

Post-magmatic processes and stability relations of the REE-bearing accessory phases in the cancrinite-bearing nepheline syenite from the Čistá pluton (the center of the upper-crustal Tepla-Barrandian unit, Bohemian Massif, Czech Republic) were investigated by electron probe microanalysis (EPMA, including compositional X-ray mapping), laser ablation inductively coupled plasma mass spectrometry (LA-ICPMS) and transmission electron microscopy (TEM). The reaction textures include REE-bearing phosphate, silicate, carbonate, and oxide phases intergrown with K-feldspar, albite, biotite, and, occasionally, zircon or iron oxides. Two populations were distinguished within REE-rich accessories. The primary one includes monazite-(Ce), fergusonite, gadolinite-(Ce), and gadolinite-(Y). The second population related to post-magmatic alteration processes includes britholite-(Ce), bastnäsite-(Ce), epidote, aggregates of fine-grained REE-bearing phases (possibly fluorapatite and/or britholite-(Ce)) and, rarely, cerianite and thorianite. Bastnäsite-(Ce) commonly forms symplectite with K-feldspar. Zircon grains demonstrate patchy and convolute zoning related to alteration processes, whereas oscillatory zoned grains are rare. LA-ICPMS U-Pb analysis revealed three individual events at ca. 440–410, 380, and 320 Ma in all textural types. Further trace element measurements are expected to constrain their origin. To summarize, the accessory mineral assemblages and their textural relations are indicative of post-magmatic alteration driven by alkali-rich fluids with high CO₂ activity.

Acknowledgements: This work was supported by the National Science Centre research grant no. 2017/27/B/ST10/00813.

DIVERSITY OF LATE CAMBRIAN FELSIC MAGMAS IN THE SW POLAND: AN INSIGHT FROM U-Pb AND O ZIRCON STUDY

Jastrzębski Mirosław¹, Sláma Jiří², Krzemińska Ewa³, mjast@twarda.pan.pl, slama@gli.cas.cz, ekrz@pgi.gov.pl

¹Institute of Polish Academy PAS, Poland, ²The Czech Academy of Sciences, Institute of Geology, Czech Republic, ³Polish Geological Institute - National Research Institute, Poland

Felsic magmatism that operated at the northern margin of the Gondwana continent in Early Palaeozoic is well represented in SW Poland by the occurrence of various-scale orthogneiss complexes. This study focuses on selected bodies of orthogneisses in the Sudetic area with Late Cambrian protolith ages: the Śnieżnik gneisses from the Sudetes and Doboszowice gneisses and Góry Sowie migmatites from the Fore Sudetic Block. Before the Variscan amalgamation of the Gondwana-derived terranes resulted in the current close adjacency of the studied exposures, the protoliths of Śnieżnik and Doboszowice formed part of the Saxothuringian or Moldanubian terrane, while the Góry Sowie Massif was likely a part of the Teplá-Barrandian terrane. To better understand the duration of the felsic magmatism and to locate possible sources of the parental magmas of the felsic plutons in the Variscan terranes, zircon from these samples have been subjected to U-Pb zircon dating by LA-ICPMS (CAS, Prague) and O isotope analysis by SHRIMP (PGI-Warsaw). The selected samples (1 sample of Śnieżnik gneiss, 2 samples of Doboszowice gneiss, and 1 sample of Góry Sowie gneiss) bear mostly euhedral, prismatic zircons. The calculated ages (concordia ages, upper intercept ages) between c. 494 Ma to c. 500 Ma overlap within errors. They are interpreted as the last igneous crystallization events and reflect coeval magmatism for all studied metagranites. Analysis of oxygen isotopic composition of zircon from the Śnieżnik gneisses revealed relatively low $\delta^{18}\text{O}_{\text{zrn}}$ values ranging from 4.38 to 7.57, including those characteristic for mantle signature. The two samples of Doboszowice gneisses have comparable, consistent oxygen isotope distribution with values in the range 4.58–9.37 and 5.07–9.65, respectively, mostly higher than that of the primitive mantle and interpreted to reflect the Si-rich compositions (e.g. SiO_2 content ~77wt%). Zircons hosted in Góry Sowie migmatite do not have $\delta^{18}\text{O}_{\text{zrn}}$ mantle signature. The $\delta^{18}\text{O}_{\text{zrn}}$ values in a range of 8.14- 11.29‰ are higher than those typical of I-type granitic melt (<8‰). The simplest explanation is that the sources of their protolith had substantial amounts of supracrustal material. The results of this study suggest that the Early Cambrian granitoid massifs were emplaced in the Sudetic parts of the Saxothuringian / Moldanubian and Teplá-Barrandian terranes at the same time. Some differences of $\delta^{18}\text{O}_{\text{zrn}}$ signatures suggest that the c. 500 Ma plutons were composed of variously evolved magmas generated, however, mainly in the crust.

Acknowledgement: LA-ICPMS analyses of zircons were financed through NCN grant no 2014/15/B/ST10/03938. $\delta^{18}\text{O}$ SHRIMP zircon analyses were financed through NCN grant no 2018/29/B/ST10/01120

AFTER THE FLOOD IS BEFORE THE FLOOD: SULFUR AUTHIGENESIS AND ISOTOPE DISCRIMINATION IN A MODERN COASTAL WETLAND

Jenner Anna-Kathrina¹, Boettcher Michael E.¹, Fernández-Fernández Luz Eva², Otto Denise¹, Zeller Mary A.¹, Koebsch Franziska³, Jurasinski Gerald³, Kreuzburg Matthias⁴, Rach Benjamin¹, Winski Lucas¹, Westphal Julia¹, von Ahn Catia M. E.¹, Schmiedinger Iris¹

¹Geochemistry & Isotope Biogeochemistry, Institute for Baltic Sea Research Warnemuende, Germany, ²University of Vigo, Spain, ³AUF, University of Rostock, Germany, ⁴Marine Chemistry, Institute for Baltic Sea Research Warnemuende, Germany

Land-ocean interactions in the coastal zone are of particular interest regarding the exchange of substances, like nutrients, carbon, sulfur, metals, and water. Rising sea levels are and will increase the pressure of salty solutions on previously fresh water ecosystems. We present new results on the isotope biogeochemistry of a modern rewetted wetland, at the southern Baltic Sea, the Huetelmoor, that is under impact by event-type flooding by brackish seawater. Sediment cores on transects within the wetland were investigated for the pore water and soil composition. The fractions in the soils were analyzed for elemental composition, mineral micro-textures, and the stable isotope composition of different fractions to understand the water and biogeochemical carbon-sulfur-metal cycles and the geochemical signatures in authigenic mineral phases. Flooding events with brackish water increase the availability of sulfate as an electron acceptor for microbial carbon transformation. This added sulfur in the peatland impacts the remineralization capacity of organic substrate and creates space for mineral authigenesis and the developing textures. It yields isotope signals that are indicative of ecosystem biogeochemistry and allow for a transfer of proxy information to other modern and past coastal organic-rich peatlands. The soil cores in the peatland reflected the activity of sulfate-reducing bacteria and the associated formation of pyrite with different textures and provided isotopic evidence for a sulfurisation of organic matter. Sedimentary sulfur fractions and their stable isotope signatures are controlled by the availability of dissolved organic matter and/or methane, reactive iron, and in particular dissolved sulfate. In addition, from the relative position with respect to the coast line, they depend on the surface topography and soil characteristics. Further mechanistic investigations consider the role of DOS upon changing sulfur substrate availability.

Acknowledgement for support by BALTIC TRANSCOAST, ERASMUS, DAAD

INFLUENCE OF WATER-ROCK INTERACTION PROCESSES AND CLAY MINERALOGY ON THE SEISMIC BEHAVIOUR OF ACTIVE FAULTS (BETIC CORDILLERA, SE SPAIN)

Jiménez-Espinosa Rosario¹, Hernandez-Puentes Pilar¹, Jiménez-Millán Juan¹

¹Geology, University of Jaen, Spain

The purpose of this study was to carry out a geochemical and mineralogical characterization of the groundwater and the host aquifer rocks in the Tíscar and Larva active fault areas (Betic Cordillera, SE Spain). The main objectives were: a) characterize water-rock interaction and neoformation of clay minerals; b) identify relevant sites with deep-origin waters associated to fault activity; c) contribute to understanding the influence of these processes on the mechanical and seismic behavior of the active faults. Physico-chemical data analysis from 24 different groundwater sites over the fault areas, as well as geochemical modeling, provide a quantitative interpretation for the geochemistry of the fault zones aquifers. The hydrochemical study allowed to differentiate two main groups of water families: a) Ca-Mg-HCO₃ waters with low electrical conductivity and low salinity; and b) Ca-Mg-SO₄-Cl waters with high electrical conductivity (commonly >1000 µS/cm) and higher salinity values. Within the last group, a small family of Na-rich waters with high B-contents (>0.33 ppm) and moderate outlet temperatures (>16.5°C) was found. These waters were found to be the deep-origin fluids in this region. Thermodynamic model calculations indicate that groundwaters with high temperature and abnormal boron content are close to equilibrium with calcite and dolomite and evidence oversaturation with respect to clay minerals (kaolinite, montmorillonite, and illite). XRD and electron microscopy (SEM/TEM) studies of fault-rock samples confirmed the thermodynamically predicted presence of neoformed smectite as slip surface coatings of thin films. These minerals were formed as a result of cataclasis and the interaction of thermal waters with the Tíscar and Larva fault rocks. Smectite could provide lubricating properties to the carbonate rocks, favoring the predominance of creep over seismic stick-slip and reducing the possibility of large seismogenic events. According to this study, a selected sensible warning aquifer site has been proposed including points with indicators of deep-water circulation processes that can be connected to the activity of the Tíscar-Larva active fault zones.

AGGREGATION OF GOLD NANOPARTICLES FROM AGRICULTURAL TREATMENTS IN SEDIMENTS OF THE SALINE WETLAND OF LAGUNA HONDA (SOUTH OF SPAIN)

Jiménez-Millán Juan¹, Medina-Ruiz Antonio¹, Abad Isabel¹, Jiménez-Espinosa Rosario¹

¹Geology, University of Jaen, Spain

Gold nanoparticles (NP-Au) have often been used in agricultural pesticides because of their effectiveness in treatments and their low reactivity in aquatic environments. However, their stability has been shown to be affected in complex media (biologically active, extreme compositions, presence of clays) due to dissolution and aggregation processes that modify their behavior and accumulation. Saline wetlands are complex and dynamic systems in which physical and biogeochemical processes control the chemical evolution of the wetland water table, groundwater, sediments, and communities of organisms in the ecosystem. Many of the saline wetlands at the eastern end of the Guadalquivir Depression are under heavy agricultural pressure from olive cultivation. As a result, their sediments become natural receptors of pollutants. Certain physicochemical alterations in the environmental conditions can affect the behaviour of the sediment, promoting the uptake, degradation, and transformation of pollutants dissolved in the water or, conversely, leading to the release of these pollutants. The present communication reveals the presence of Au nanoparticles and aggregates in the sediments of the Laguna Honda (province of Jaén) and analyses the regulatory role of organic-rich sediments in these environments. Laguna Honda is a karst morphogenetic system formed by the dissolution of evaporites, fed by groundwater and surface water. The mineralization of its waters can reach hypersaline concentrations (100 g/l in low water). The presence of microlaminated sediments with abundant plant remains, are consisting mainly of quartz, calcite, dolomite, illite, and chlorite, significant quantities of gypsum, halite, and feldspars, and smaller quantities of pyrite, barite, haematite, zircon, rutile, and ilmenite. Transmission electron microscopy (HRTEM) images revealed the presence of NP-Au (2 nm size) dispersed in the sediment, mostly adsorbed on the surface of clays or on fragments of plant remains although they usually form small nano-aggregates of 10 nm. In addition, the NP-Au develop elongated or spherical micrometric aggregates (<10 µm) visible in scanning electron microscope (SEM) images. The internal structure of the grains is formed by a mosaic of elongated NP-Au preferentially oriented zones. The surface of the aggregates tends to be rounded with a thin film coating and, occasionally, small perforations, probably associated with dissolution. The small size of the NP-Au observed in HRTEM (10 times smaller than those frequently used in agricultural products) and the evidence of corrosion appearing in the micrometric aggregates suggest that the stability of the NP-Au was affected by dissolution processes that modified their original inert properties and affected in consequence, their behavior. Interaction with the aquatic environment, organic matter, and clay particles must have favored the aggregation of the nanoparticles, leading to the coagulation of heavier and larger particles. Their deposition and accumulation in sediments would prevent the diffusion and spread of contamination through the water. However, the development of films, probably of biological origin, could be indicating Au mobilization processes.

ILLITIZATION PROCESS IN CLAY SMEARING BANDS FROM PLIO- PLEISTOCENE SOFT-ROCKS (BAZA FAULT, S SPAIN)

Jiménez-Millán Juan¹, Abad Isabel¹, García-Tortosa Francisco Juan¹, Jiménez-Espinosa Rosario¹

¹Geology, University of Jaen, Spain

We have studied clay smearing bands developed in faults affecting soft-rocks sequences of interbedded carbonate, marls, sands, silts, gypsum, and clays from an excavated trench in the Baza Fault (SE Spain). This 37-km long structure is an E-dipping active normal fault located in the Guadix-Baza Basin (Betic Cordillera) with a variable strike with N-S and NNW-SSE segments. The fault has associated instrumental and historical seismicity, the most important of which is the 1531 Baza earthquake, with more than 400 fatalities. The trench studied belongs to the central part of the Baza Fault, which occurs in the damage zone of a 1-km wide fault zone including two main NNW–SSE striking strands that concentrate most of the cumulative. The trench is characterized by the presence of marly beds, which are predominant over the carbonate beds, frequently rich in dolomite. Thin beds of clay-rich dark lutites are intercalated with the carbonate and marly beds. Clay smearing appears by deformation of clay-rich sediments producing bands with reorientation, flow, and extrusion of clay minerals. Striations and slip surfaces are also sometimes observed. TEM-EDX data and electron diffraction patterns reveal that clay smearing bands are made of very fine grain-sized fragments of muscovite, paragonite, and beidellitic smectite parallel to the shear foliation. Mineral grain clasts are frequent in the clay smearing bands. They appear as large fragments of calcite, quartz, and feldspar commonly surrounded by foliation. Clay bending close to the borders of the clasts can be seen in the TEM images. The clast fragments develop pressure shadow micropores where crystallize randomly oriented nanometer-sized K and Fe-rich particles of smectite. Bigger pores, especially at the contact between clay bands and carbonate sediments, with evidence of granular flow and local proto-cataclasis of grains, are sealed by precipitation of gypsum and dolomite. Clay smearing bands are mainly characterized by ductile deformation. The dominant deformation mechanism may be controlled by the mineral composition of the shear band and the water content. Incorporation of clays and fluid-rich sediments along shear bands may reduce shear strength. The predominance of beidellitic smectite defining the shear foliation of the bands and bent around the fragile clasts support the reduction of the strength during the seismic deformation. Moreover, the precipitation of gypsum and dolomite crystals, sealing deformation microstructures, suggest that fluids incorporated into the sediments during deformation had high salinity. Our results suggest that the interference of micromechanical processes and the circulation and accumulation of saline fluids in pores generated by pressure shadow processes can be involved in the neoformation of clays. Sedimentary beidellitic smectite interacted with saline lacustrine Mg and Fe-rich fluids in the micropores generated by pressure shadow. The uptake of these elements and the beidellitic substitution produced enough negative charge to facilitate the incorporation of K to start a low-temperature illitization process associated with microenvironments generated in clay smearing bands.

THE ADVANTAGES OF EDS OVER WDS FOR BEAM-SENSITIVE MINERAL ANALYSIS

Jokubauskas Petras¹, Macdonald Ray², Bagiński Bogusław², Harlov Daniel E.³

¹Laboratory of electron microscopy, μ -analysis and x-ray diffraction, University of Warsaw, Faculty of Geology, Poland, ²Department of Geochemistry, Mineralogy and Petrography, University of Warsaw, Faculty of Geology, Poland, ³Section 3.6 Chemistry and Physics of Earth Materials, Deutsches GeoForschungsZentrum – GFZ; Telegrafenberg, D-14473 Potsdam, Germany

Electron microprobe (EMPA) equipped with wavelength-dispersive x-ray spectrometers (WDS) is the most commonly used method for the quantitative non-destructive analysis of minerals at μ or sub- μ scale. Can energy-dispersive spectrometry (EDS) compete with WDS in quantitative analysis?

While trying to analyze experimentally grown gagarinite we found WDS limitations caused by extreme volatile loss (50 % of Na loss in ~ 7.5 nA·s, with an artificial increase in subsequently analyzed elements) from e-beam interaction with the material. We turned to full-sized standard-based EDS on SEM as an alternative, which allowed us to overcome the volatile loss problem. For successful EDS analysis the main forced-restrictions of EPMA need to be strictly followed: use clean and pure standard references coated with the same element and thickness as the unknown; use the same geometry for spot analysis of standard and unknown (identical “working distance”, the analysis only with centrally parked/non-scanning electron beam), the equipment should have the ability to measure the beam current.

The free (public domain) NIST DTSA-II software was used for EDS quantitative recalculations into chemical concentrations. To overcome the volatile loss, 30 EDSes with a dwell time of two seconds and a beam current of 0.605 nA for each were acquired from previously not analyzed gagarinite grains. EDS spectra were summed, forming a single representative 60s EDS, which was further processed with quantification.

EDS-based quantitative results for gagarinite have no Na loss and no increased concentrations of other elements due to Na loss. To insure method correctness as compared with the well-established WDS mineral quantification results, the EDS of albite (interference-free), narsarsukite (few mild interferences), chevkinite, and britholite (strong multiple spectral interferences) were acquired, quantified, and compared. For major and minor elements the results from EDS are on a par with the WDS results (albeit WDS is still the “king” considering the trace quantification or high beam currents). The main advantage of EDS is the same (or better, for beam sensitive samples) precision and accuracy for major elements with lower beam current and shorter analytical time. EDS is generally more available - commonly scanning electron microscopes are equipped with full-size (or large size) single or multiple EDS detectors, with signal processing units (SPU) equipped with the highest spectral resolution options available for low count rates and low beam-currents. For comparison, the EPMA commonly are equipped with only the single and downsized EDS (due to space constraints), where SPU is tailored for much higher beam currents. For beam-sensitive minerals, the SEM-EDS equipment has a clear advantage over EPMA-WDS. It should be mentioned that there are possibilities to combine both (i.e. major and minor element k-ratios measured on SEM-EDS with k-ratios of trace elements on EPMA-WDS), albeit currently, available combination techniques are very cumbersome.

We gratefully acknowledge funding by NCN Harmonia no. 2017/26/M/ST10/00407.

LOW-TEMPERATURE RUTILE-TO-ANATASE PHASE TRANSITION: COUPLED DISSOLUTION-PRECIPITATION REACTIONS AND THE CRYSTAL CHEMICAL ROLE OF Nb IN TiO₂ NATURAL OCCURRENCES

Jorge Pinto Andre¹, Sanchez-Pastor Nuria², Callegari Ivan¹, Pracejus Bernhard³, Scharf Andreas³

¹Applied Geosciences, German University of Technology of Oman, Oman, ²Department of Mineralogy and Petrology, Universidad Complutense de Madrid, Spain, ³Department of Earth Sciences, Sultan Qaboos University, Oman

Rutile, the most commonly occurring TiO₂ polymorph in rocks, is the source of several important crystal chemical discriminant tools for geoscientists, which enable fingerprinting a number of geological processes (magmatic evolution, subduction zone metamorphism, sediment provenance, etc.). The research here presented focuses on TiO₂-bearing volcanoclastic rock samples from Jebel Akhdar, Oman, and relies on Electron Microprobe and Raman spectrometric microanalytical data with the purpose of i) characterizing the different naturally-occurring TiO₂ polymorphs, ii) relate trace element mineral content and hydrothermal alteration, and iii) sorting the reactive pathways behind the observed textural features. The results gathered reveal that Nb plays an important role in stabilizing the structure of anatase at higher temperatures than those expected in a trace element-free environment. Furthermore, our observations recommend evaluating any possible occurrence of TiO₂ polymorphs prior to the application of Zr-in-rutile thermometric methods, especially when hydrothermal alteration mineral paragenesis are present.

USING HYDROSEPARATION TECHNIQUES TO CONCENTRATE PLATINUM-GROUP MINERALS FROM TWEEFONTEIN HILL, BUSHVELD COMPLEX

Junge Malte¹, Rodriguez Marco², Aiglsperger Thomas³, Farré-de-Pablo Júlia⁴, Kaufmann Felix⁵, Kaliwoda Melanie¹, Proenza Joaquín A.⁴

¹Mineralogical State Collection (SNSB-MSM), Germany, ²Institute of earth and environmental sciences, University of Freiburg, Germany, ³Department of Civil Engineering and Natural Resources, University of Lulea, Sweden, ⁴Department of Mineralogy, Petrology and Applied Geology, University of Barcelona, Spain, ⁵Museum für Naturkunde Berlin, Germany

The Bushveld Complex in South Africa hosts gigantic platinum-group element (PGE) resources. In general, the PGE are present as platinum-group minerals (PGM) and hosted within sulfide minerals (Junge et al. 2019). Tweefontein Hill is part of the northern Bushveld Complex and well known for the occurrence of large sperrylite (PtAs₂) grains (Spencer, 1926; Nex 2005). From former mine adits, sample material containing large amounts of visible malachite, secondary Cu-minerals, and goethite/limonite were selected to produce dense mineral concentrates in order to obtain more detailed information about the distribution of PGM in these ores. Heavy mineral concentrates were produced by hydroseparation (HS) techniques at the Hydroseparation Laboratory of the University of Barcelona (<http://www.hslab-barcelona.com/>). Automated mineralogy at the University of Lulea, as well as electron microprobe work, and Raman spectroscopy is used to characterize the mineralogical variation within heavy mineral concentrate and to obtain statistically robust data on PGM at Tweefontein Hill. The results showed the presence of euhedral sperrylites and electrum (Au,Ag) grains as well as Pd-Cu phases showing several textures of chemical modification, composed by Pd-Te-Bi-Cu, Pd-Sb-Se-Cu, and Pd-Ru-Te-Bi-Fe-Cu. Previous investigations into similar occurrences identified elsewhere in the world suggested that this mineralization could be the product of acid, saline late-hydrothermal fluid activity (Cabral et al., 2015).

Cabral, A. R., Ließmann, W., and Lehmann, B. (2015): Gold and palladium minerals (including empirical PdCuBiSe₃) from the former Roter Bär mine, St. Andreasberg, Harz Mountains, Germany: a result of low-temperature, oxidising fluid overprint. *Mineralogy and Petrology*, 109, 649-657.

Junge, M., Oberthür, T., Kraemer, D., Melcher, F., Pina, R., Derrey, I.T., Manyeruke, T., Strauss, H. (2019): Distribution of platinum-group elements in pristine and near-surface oxidized Platreef ore and the variation along strike, northern Bushveld Complex, South Africa. *Mineralium Deposita*, 54, 885-912.

Nex, P. A. (2005): The structural setting of mineralisation on Tweefontein Hill, northern limb of the Bushveld Complex, South Africa. *Applied Earth Sciences*, 114, B243-B251.

Spencer, L.J. (1926): Sperrylite crystals from the Transvaal. *Mineralogical Magazine*, 21, 94-7.

INCLUDING DIGITAL 3D MODELS INTO MUSEUM EDUCATION – AN EDUCATIVE TOOL TO BRING AN EXHIBITION INTO THE LIVING ROOM NOT ONLY DURING CLOSURE OF MUSEUMS

Junge Malte¹, Kaliwoda Melanie¹, Joseph Fabio¹, Schmahl Wolfgang W.¹, Hentschel Felix¹

¹Mineralogical State Collection (SNSB-MSM), Germany

The closure of museums and exhibitions due to the COVID-19 pandemic raised the need to make minerals and rocks accessible digitally. Certainly, a digital model of minerals and rocks will not substitute the visit of a museum, the participation in workshops in the museum or school and university teaching with physical objects, but using 3D models is an additional method to encourage new visitors and make minerals and rocks accessible also during closing times of museums and universities. Not only demonstrating 3D models online on the webpage of the museums is useful, but the integration of 3D models within an exhibition also allows a closer look at exhibits behind the glasses of the museum. Imagine you are standing in front of the showcase in a mineralogical exhibition looking at a mineral or rock. The glass of the showcase is certainly needed to protect the exhibits but in some cases it might be interesting to have a closer look on the mineral. You might want to know what is hidden on the backside of the mineral but turning the mineral or looking on the other side does not always work within the showcase in the exhibition. You also might simply want to have a closer look on the mineral but the glass of the showcase does not allow it. In this case integrating 3D models in an exhibition could bring the mineral or the rock virtually into the hands of the visitors. Scanning for example a QR-code next to the showcase can give the link to the digital 3D model. Therefore, visitors can easily turn the mineral or rock in all directions and zoom into areas of interest. This can be done easily with their own smartphone or tablet or with rental devices of the museum. Including more information with numbers or symbols on the digital model additionally allows providing further information about the specimen. This method therefore also has the opportunity to point the finger on special observations and characteristics of the exhibit, in order to guide the visitors through the exhibitions as you might do it during a guided museums tour. So what is needed to make these 3D models of minerals and rocks? At the Museum Mineralogia Munich, as the public part of the Mineralogical State Collection, we recently assembled a small 3D photogrammetry lab. There generally exist various opportunities for installations depending on needs and budgets. This means that you can already produce 3D models of adequate quality with the camera of your smartphone and low-cost software. In the Museum Mineralogia Munich we installed a computer with 128 GB Ram (recommend at least 16 GB RAM), LED lighting, turning tables, and a digital camera (Sony α6400) with macro and standard objective lenses on a tripod. In order to minimize artifacts and processing time, a green (and other colors to use for different minerals) background is highly recommended. Processing time depends on the resolution, the number of images you took from the mineral or rock, and the computing power. For one mineral with about 150 images with 6000x4000 pixel resolution, with our system at the Museum Mineralogia Munich, we need about 60 minutes of processing time.

P-ANALOGUE OF GURIMITE, A POTENTIALLY NEW MINERAL FROM SILICATE CARBONATE XENOLITHS OF BELLERBERG VOLCANO, GERMANY AND PARALAVA OF THE HATRURIM COMPLEX, ISRAEL

Juroszek Rafał¹, Galuskina Irina¹, Ternes Bernd²

¹Institute of Earth Sciences, Faculty of Natural Sciences, University of Silesia, Poland, ²-, -, Germany

Gurimite, Ba₃(VO₄)₂, approved by the CNMNC-IMA in 2013, was discovered in paralava veins from the gehlenite-flamite hornfels in the Negev Desert, Hatrurim Complex, Israel. Its PO₄-counterpart was identified in two localities: as small single grains up to 15 μm in size, associated with other Ba-minerals like fresnoite, benneshierite, celsian, zadovite, and walstromite in silicate carbonate xenoliths of Bellerberg volcano in Germany, and as plate crystals up to 30 μm in size detected inside small polymineral spherical aggregates composed of gurimite, hexacelsian, fresnoite, walstromite, F-analogue of alforsite, kalsilite and fluorapatite within rankinite-gehlenite paralava of Hatrurim Complex, Israel.

The chemical composition of the P-analogue of gurimite from these two localities shows some differences. The composition of the German specimen is close to the end-member Ba₃(PO₄)₂, and the calculated empirical formula is as follows: (Ba_{2.59}Ca_{0.23}Sr_{0.10}Na_{0.05}K_{0.05})_{Σ3.02} [(P_{1.76}S_{0.10}Si_{0.08}Al_{0.04}Fe_{0.04}V_{0.02})_{Σ2.04}]O₈. For Israeli specimens, the composition varies within the series gurimite – P-analogue of gurimite. Most electron-microprobe analyses correspond to the intermediate members with the following formula - (Ba_{2.62}K_{0.27}Na_{0.07}Ca_{0.04})_{Σ3.00} [(P_{0.82}V_{0.76}S_{0.34}Al_{0.06}Si_{0.05}Fe_{0.01})_{Σ2.04}]O₈, which may be simplified to the Ba₃(PO₄)(VO₄). The calculated formula of the most dominant P-analogue of gurimite from Israel looks as (Ba_{2.72}K_{0.15}Ca_{0.09}Na_{0.04})_{Σ3.00}(P_{1.30}V_{0.43}S_{0.21}Si_{0.05}Al_{0.04})_{Σ2.03}O₈, which is simplified to the Ba₃(PO₄)₂ using the dominant valence rule.

The Raman spectra of the P-analogue of gurimite from Germany and Israel differ and it is connected with the V⁵⁺ content. In the Raman spectrum of the German specimen, the most intense band observed at 928 cm⁻¹ is assigned to the ν₁(PO₄)³⁻ symmetric stretching vibrations. Additional strong bands related to (PO₄)³⁻ group vibrations at 407, 416, and 562 cm⁻¹ are ascribed to the symmetric and asymmetric bending (ν₂+ν₄), while the band at 1043 cm⁻¹ to ν₃ asymmetric stretching modes. The strong Raman bands of Israeli counterpart are mostly related to the vibrations of (VO₄)³⁻ groups and occur at 339 cm⁻¹ (ν₂), 826 cm⁻¹ (ν₃), 840 cm⁻¹ (ν₁ and ν₃), respectively. Bands related to the symmetric stretching vibrations of (PO₄)³⁻ and (SO₄)²⁻ groups have lower intensity and are set at 925 cm⁻¹ and 982 cm⁻¹.

PROJECTS FOR CHILDREN, YOUNG PEOPLE AND STUDENTS AT THE MINERALOGICAL STATE COLLECTION MUNICH (SNSB) - NATIONAL AND INTERNATIONAL PUBLIC RELATIONS FOR GEOSCIENCES

Kaliwoda Melanie¹, Junge Malte¹, Hentschel Felix¹, Schmahl Wolfgang W.¹

¹Mineralogical State Collection Munich, Germany

The Mineralogical State Collection Munich represents a research collection with more than 50,000 minerals, crystals, rocks, and meteorites. In addition to the scientific aspect, the collection also has a public relations mission, namely to bring geosciences closer to a broad community. We succeed in doing this with the Museum Mineralogia Munich, which is located in the university's Department of Geosciences at the Ludwig-Maximilians-University (LMU). The most sensible way to do this is to foster love or interest in the geosciences at a young age. That is why we offer guided tours, children's birthday parties, and project days and weeks for interested young people and children. The children learn about minerals, crystals, and rocks from the earth but also meteorites and material from outer space. Depending on the age group, other so-called MINT (mathematics, computer science, natural sciences) fields are addressed. Therefore, the Mineralogical State Collection Munich is a founding member of MUC-Labs, the Munich School Labs. In addition to us, other student labs, e.g. from the TU Munich, the Max-Planck-Institute or the Fraunhofer Institute, are involved here. Older schoolchildren have the opportunity to book project weeks with us and work together with natural scientists and students. Those children not only accompany our museum work but furthermore, they are allowed to measure with the Raman spectroscope and to accompany other research work in the house. In this way, we have already been able to recruit some teenagers who have later become active in geosciences as bachelor or master's students themselves.

Furthermore, we do not only want to address our program to German students but are moreover open to international students. Thus, we offer the children's programs also in English; therefore, school groups from Oslo (Norway) and Bozan (Italy) already came to us. In addition, we have established a partner museum with Lisbon, Portugal in 2020, i.e. the Centro Ciencia Viva do Lousal. Here we exchange museum and scientific work and give students the opportunity to follow an exchange program. Finally, yet importantly, the new Corona situation has given us the opportunity to offer our programs online. For example, MUC-Labs has already been very successful in offering a student and teacher conference, which in turn has won friends for the individual departments.

PROCESS MINERALOGICAL CHARACTERISTICS OF THE KIVINIEMI SCANDIUM-BEARING FAYALITE FERRODIORITE

Kallio Rita¹, Tanskanen Pekka², Luukkanen Saija¹

¹Oulu Mining School, University of Oulu, Finland, ²Process Metallurgy, University of Oulu, Finland

Scandium is classified as a rare earth element together with yttrium and the fifteen lanthanides. The smaller ionic radius in comparison to the rest of the group makes it a moderately compatible element thus fitting into the lattice of common ferromagnesian rock-forming minerals, such as pyroxene and amphibole. Constrained by the geochemical characteristics, the enrichment of scandium to ore grades by geological processes is scarce with consequently minor global annual Sc production. Scandium deposits can be broadly divided into primary deposits related to igneous and hydrothermal processes, and secondary deposits where Sc has been concentrated by sedimentary processes and weathering, producing laterite and placer deposits. Kiviniemi Sc deposit in Eastern Finland represents an igneous Sc occurrence with estimated total resources of 13.4 Mt and an average Sc grade of 163 g/t. Scandium is mainly incorporated into the lattices of ferrous clinopyroxene and amphibole in the main Sc-bearing unit of the deposit with minor deportment to other ferrous silicates such as fayalite and almandine garnet. This study presents the results of the magnetic separation experiments conducted at a laboratory scale on Sc-bearing composite sample from the main unit. Depending on the separation parameters, rougher concentration with a combination of low intensity and high-gradient magnetic separation resulted in 77-92 % recovery with 211-243 ppm Sc. Process mineralogical characteristics of the feed and the resulting concentrates and tailings are presented with a discussion on implications towards beneficiation possibilities.

ACOUSTIC INSULATION USING ADVANCED GEOMETRY IN CERAMICS – INTRODUCING SOUND STOPPER TECHNOLOGY

Karsdorf Robert¹, Ohlwärter Christian¹, Krcmar Wolfgang¹, Pöllmann Herbert²

¹Materials Engineering, Nuremberg Institute of Technology, Germany, ²Institute of Geosciences and Geography, Martin Luther University Halle-Wittenberg, Germany

Buildings, both in the private and public sector, consume more than 40 % of the provided total energy in Europe. The enormous potential of saving energy, especially on domestic heating with superior heat insulation comes at the cost of less effective acoustic insulation, leading towards the need for innovation. Combining both properties into one product proves difficult since both cases are eventually diametral. Furthermore, the process of inventing and testing new technologies consumes not only time but is also very cost-critical. Operating with advanced FE-methods and 3D-Printing provides the opportunity to enhance both factors simultaneously. The advantage of using sound and heat simulations in an iterative manner delivers quick answers to the question if new technology sustains the introduced properties, whereas the 3D-printed prototypes may verify the results for heat insulation. Two different general approaches have proven to alter the sound insulation behavior without destabilizing the heat insulation, in fact, even improved it marginally in some cases. The first approach is bringing bricks out of tune. Varying some factors as the width of bridges shifts the critical collapse inside the frequency-driven sound insulation towards higher frequencies. The same result can be observed by constructing arch-like bridges inside the hole pattern of heavy-clay bricks. This can be of use by shifting the collapse ultimately out of the critical frequencies width of human speech, leading to an advantage of sound insulation behavior. However this is not reflected by the valued frequency measure, regarded prospect for industrial standards, hence it reduces the complex frequency driven sound to a single, easier to grasp number. Improving the valued frequency measure is achieved by the second approach; impeding the ability of bridges inside the brick to swing. The ability of the individual bridges to oscillate affects the sound transfer inside the brick as a whole. Applying the Sound Stopper Technology attains this. The amplitude of oscillation is restricted, which can be observed in the frequency-driven sound insulation by dampening the critical collapse, resulting in an improved rating of the valued frequency measure by up to 40 % of absorbed sound power. Besides expanding the surface area of the bricks, neither the heat transfer via conduction nor radiation is affected, for the minimal cross-section is not altered and the visual factors barely changed. Convection remains mostly the same, though it is hindered scarcely, resulting in slightly improved properties.

ANTIMONY ISOTOPE FRACTIONATION PATTERNS IN OROGENIC Sb-Au DEPOSITS: A CASE STUDY IN THE NÍZKE TATRY MTS (SLOVAKIA)

Kaufmann Andreas Benjamin¹, Lazarov Marina², Weyer Stefan², Kiefer Stefan¹, Vlasáč Jozef³, Majzlan Juraj¹

¹Institut für Geowissenschaften, Friedrich-Schiller-Universität Jena, Germany, ²Institut für Mineralogie, Leibniz Universität Hannover, Germany, ³Slovak Academy of Sciences, Banská Bystrica, Slovakia

Antimony (Sb) is a redox-active metalloid that occurs in nature predominantly as Sb(III) and Sb(V). The Sb isotopes, among other isotopic systems, have the potential to provide information for metal migration and redox-controlled processes during hydrothermal ore formation as shown recently by [1] for the mineral stibnite (Sb₂S₃). Although stibnite is the most common Sb mineral, other minerals (sulfides, sulfates or oxides) contain Sb, in combination with Cu, Pb, Fe, or other elements. The Sb isotopic composition of selected primary Sb minerals was determined in-situ by a deep UV-fs laser ablation system coupled with MC-ICP-MS. Values were determined against an in-house stibnite standard (SC) and recalculated relative to NIST 3102a, with a precision of 0.1 ‰ [2]. Sulfur isotopes were measured on selected sulfides by combustion of the samples in O₂ and measurement of SO₂ gas by mass spectrometry, reported as δ³⁴S (relative to CDT) with the precision of 0.2 ‰.

All samples come from the Nízke Tatry Mts, a Variscan fragment embedded in the Alpine structures of the Western Carpathians (Slovakia) [3]. The deposits Dve Vody, Magurka and Dúbrava were extensively mined for their hydrothermal Sb ores and belong to orogenic Sb-Au deposits. Mineralogical observations in combination with a limited range of δ³⁴S values (≈+4 to +6 ‰) indicate that all sulfides (except for chalcostibite) formed from one evolving parental fluid and that the formation of stibnite and zinkenite are coeval. The investigated minerals are all primary and their δ¹²³Sb values varied substantially from -0.5 to +1.0 ‰. The dominant sulfides, stibnite and zinkenite (Pb₉Sb₂₂S₄₂) of each individual deposit are characterized by limited δ¹²³Sb range (Dve Vody: +0.43 to +0.97 ‰; Dúbrava: -0.39 to -0.04 ‰; Magurka: +0.06 to +0.41 ‰). The isotopic difference (δ¹²³Sb) between coeval stibnite and zinkenite is ≈0.2 ‰, stibnite being isotopically heavier than zinkenite. The associated less abundant tetrahedrite (Cu₁₀(Fe,Zn)₂Sb₄S₁₃) is isotopically lighter (δ¹²³Sb: -0.44 to -0.51 ‰). The latest but rare antimony mineral is senarmontite (Sb₂O₃) with the heaviest δ¹²³Sb of all measured minerals in that deposit.

Chalcostibite (CuSbS₂) from the Dúbrava deposit is distinctly different in terms of its δ³⁴S composition (≈15 ‰). The difference can be related to the input of heavier sulfur stored in Permian evaporites, probably mobilized during the Alpine orogenesis. However, chalcostibite δ¹²³Sb values are intermediate between-, and thus very similar to those observed for stibnite and zinkenite. Hence, the isotopic composition of sulfur in the Alpine mineralizations is strongly influenced by the country rocks, while the Sb isotope composition is not. Antimony for the formation of the Alpine-aged sulfides could have been simply inherited from the pre-existing, voluminous stibnite and zinkenite.

[1] Zhai et al. (2021), *Geochim. Cosmochim.* <https://doi.org/10.1016/j.gca.2021.05.031>

[2] Kaufmann et al. (2021), *JAAS*, DOI: 10.1039/D1JA00089F

[3] Majzlan et al. (2020), *Geol. Carpath.* 71, 85-112.

APPLICATION OF Ag, Cu AND Pb ISOTOPES IN DETERMINING THE ORIGIN OF THE ORE FOR METALS FROM CASTILLO DE HUARMHEY (PERU).

Kańska Maciej¹, Mathur Ryan², Kamenov George³, Chyla Julia⁴, Prządka-Giersz Patrycja⁵, Giersz Miłosz⁴

¹Department of Geochemistry, Mineralogy and Petrology, University of Warsaw, Faculty of Geology, Poland, ²Department of Geology, Juniata College, United States, ³Department of Geological Sciences, University of Florida, United States, ⁴University of Warsaw, Faculty of Archaeology, Poland, ⁵Faculty of “Artes Liberales”, University of Warsaw, Poland

Discovered in 2012 in Castillo de Huarmey (Peru), the unplanned tomb of the Wari culture elite and the artifacts contained in it allow learning about many aspects of the life of the Wari people. Analyses of Ag, Cu and Pb isotopes of small fragments of metal monuments from this tomb were performed (5 samples of silver alloys and 10 samples of copper alloys). Ag (for silver alloys) and Cu (for copper alloys) isotopes were used to determine the type of ore. The obtained result for both isotope systems indicates the use of primary ore - hypogenic ore. The origin of the ore was determined using the lead isotope. The obtained results indicate that one sample has an isotope signature that matches Bolivian deposits (Potosi, Pulacayo) and Tiwanaku artifacts. This suggests an import from Bolivia. Two samples have a similar signature to the Castillo de Huarmey rock samples and match the Province I ranges. This may indicate a local product. Unfortunately, there is a visible similarity to the isotope signature of the ore samples from Peru, which may indicate an exchange from this region. The lead isotope signature of one of the samples is that of Province IV, indicating imports from southern Peru. The results for the remaining samples are the same as the results of the Conchopata artifacts. This indicates the origin of the ore from the Julcani mine. However, the linear nature of the results obtained for these samples may also indicate the mixing of ores from different mines (eg Cero de Pasco) or the smelting of metals. To be able to more accurately determine the origin of individual artifacts, more analyses of Cu, Ag, and Pb isotopes would be needed for many metal deposits used in ancient times. This would provide a better picture of the correlation or absence of Cu or Ag isotopes with Pb isotopes for different types of deposits and ores.

GEOCHRONOLOGICAL INSIGHTS ON HYDROTHERMAL CARBONATE-SULFARSENIDE VEINS IN DOBŠINÁ, SLOVAKIA

Kiefer Stefan¹, Števkó Martin², Vojtko Rastislav³, Ozdín Daniel⁴, Gerdes Axel⁵, Creaser Robert⁶, Szczerba Marek⁷, Majzlan Juraj¹

¹Institute of Geosciences, Friedrich-Schiller-University Jena, Germany, ²Earth Science Institute, Slovak Academy of Sciences, Slovakia, ³Department of Geology and Palaeontology, Comenius University, Slovakia, ⁴Department of Mineralogy and Petrology, Comenius University, Slovakia, ⁵Department of Geosciences, Goethe University Frankfurt, Germany, ⁶Department of Earth and Atmospheric Sciences, University of Alberta, Canada, ⁷Institute of Geological Sciences, Polish Academy of Sciences, Poland

The ore mineralization near Dobšiná in eastern Slovakia includes many hydrothermal veins that contain siderite, quartz, and Ni, Fe, Co, Cu, Sb-rich ore minerals [1]. The Ni–Fe–Co mineralization in Dobšiná is hosted by the Gemic Unit, one of the major thick-skinned tectonic units of the Central Western Carpathians. Beside the ores in Dobšiná, the Gemic Unit hosts more than 1200 ore bodies [2]. They can roughly be divided into siderite-quartz-sulfide and quartz-stibnite assemblages. Currently, there are two competing models that address the origin and timing of the ore mineralizations in the Gemic Unit. To address this dichotomy, we directly dated major minerals of the ore veins. The hydrothermal ore veins consist of Ni–Fe–Co sulfarsenides in siderite-ankerite and are locally accompanied by alteration zones of fuchsite-quartz-carbonate rocks. Frequent chalcopyrite and tetrahedrite postdate the Ni–Fe–Co sulfarsenides. The aim of our investigation was to determine the age of these mineralizations utilizing U/Pb, Re/Os, and K/Ar dating of selected minerals.

U/Pb dating of hydrothermal siderite and ankerite gave ages from 145 ± 5 Ma to 114 ± 24 Ma. These ages are roughly related to the metamorphic peak in the Gemic Unit and the formation of the Gemic cleavage fan during partial exhumation of this unit. The Re/Os dating of the hydrothermal gersdorffite gave an age of 93.6 ± 0.9 Ma, the time of exhumation of the Gemic Unit. Unfortunately, no data were extracted for the younger Cu sulfides. By correlation with other units in the Western Carpathians, the Cu sulfides could be assigned Late Cretaceous age, corresponding to welding of the Gemic and Veporic units and the formation of the Trans-Gemic shear zone. The fuchsite rocks were dated (K/Ar) to 110 Ma. However, this datum conflicts with textural evidence, which shows that these rocks are older than the hydrothermal carbonates. The age of 110 Ma is therefore considered to be the cooling age after the reset of the geochronometer by the Alpine metamorphism, in agreement with earlier data. The geochronological results are supported by structural measurements and field observations.

[1] Kiefer S, Majzlan J, Chovan M, Števkó M (2017) Mineral compositions and phase relations of the complex sulfarsenides and arsenides from Dobšiná (Western Carpathians, Slovakia). *Ore Geol Rev* 89: 894–908

[2] Grečula P, Abonyi A, Abonyiová M, Antaš J, Bartalský B, Bartalský J, Dianiška I, Drnžík E, Ďud'a R, Gargulák M, Gazdačko L, Hudáček J, Kobulský J, Lörincz L, Macko J, Návesňák D, Németh Z, Novotný L, Radvanec M, Rojkovič I, Rozložník L, Rozložník O, Varček C, Zlocha J (1995) Mineral deposits of the Slovak Ore Mountains. *Geocomplex*, Bratislava, pp 1–829

FOR YOU ARE MICA AND TO MICA YOU SHALL RETURN - INTERACTION OF DIOCTAHEDRAL VERMICULITE WITH SEA-WATERS

Kisiel Marta¹, Skiba Michał¹, Kuligiewicz Artur², Makiel Magdalena ¹, Dragańska-Deja Katarzyna³, Maj-Szeliga Katarzyna¹

¹Institute of Geological Science, Jagiellonian University, Poland, ²Institute of Geological Sciences, Polish Academy of Sciences, Poland, ³Institute of Oceanology, Polish Academy of Sciences, Poland

The aim of the study was to investigate the interaction of dioctahedral vermiculite (divermiculite) with sea-waters. Because no divermiculite standard material was available, divermiculite-rich clay fraction from a soil sample (1E) collected in the Tatra Mt. was used. Aliquots of the sample were treated with two different sea waters using the following protocols: aliquots 1E+OW_C and 1E+GB_C were kept for one year in 1 dm³ of artificial oceanic water or in natural sea water from the Gdańsk Bay, respectively. Two aliquots 1E+GB_O and 1E+GB_O+d were packed into dialysis tubing and immersed in a 5 dm³ beaker filled with the Gdańsk Bay water where they were kept for 6 months. The water in the beakers was changed every three days. After the experiments samples 1E+OW_C, 1E+GB_C, and 1E+GB_O were dried whereas sample 1E+GB_O+d was dialyzed and then dried. All the samples were characterized using X-ray diffractometry (XRD). The elemental analyses were carried out using ICP-OES, and the layer charges were measured with the O-D method.

All products of the experiments performed showed an increase in the mica-like 10 Å interlayers relative to the starting 1E sample. Layer charges of the wettable interlayers (0.72-0.65 per formula unit (p.f.u.)) were smaller than the layer charge (0.79 p.f.u.) of 1E sample. K₂O content (up to 3.66%) was also higher in all products of performed experiments relative to the content in 1E sample (2.65%). Sample 1E_GB_O+d showed lower K₂O content (3.12%) and higher layer charge (0.72 p.f.u.) than 1E_GB_O sample (3.64% and 0.67 p.f.u.) that was dried immediately after the experiment

Obtained results indicated that contraction of divermiculite structure due to selective adsorption of K⁺ from sea-waters and the fixation took place in studied samples. The fixation occurred irrespectively of the chemistry of sea-waters used. The high-charge interlayers were likely to collapse first, which explains the apparent layer charge decrease down to 0.65 p.f.u. Potassium fixation within the interlayers having higher layer charges occurred without dehydration (i.e. drying), whereas drying was necessary to fix K⁺ within interlayers having lower layer charges.

Acknowledgments:

This study was financed by National Science Centre, Poland [grant number: UMO-2016/23/N/ST10/01388].

FROM OXALID TO GLOBALID: A SUBSTANTIAL UPGRADE OF A WELL-KNOWN DATA POOL OF LEAD ISOTOPES FOR METAL PROVENANCING USING R AND SHINY APP.

Klein Sabine¹, Rose Thomas², Westner Katrin J.³, Hsu Yiu-Kang⁴

¹Archaeometallurgy, Deutsches Bergbau-Museum Bochum, Bochum, sabine.klein@bergbaumuseum.de, Germany,

²Dipartimento di Scienze dell'Antichità, Sapienza – Università di Roma, Rome, roseth@post.bgu.ac.il, Italy, ³Ecole Normale Supérieure de Lyon, CNRS, Université de Lyon, Lyon, katrin.westner@ens-lyon.fr, France,

⁴Archaeometallurgy, Deutsches Bergbau-Museum Bochum, Bochum, yiu-kang.hsu@bergbaumuseum.de, Germany

Lead (Pb) isotope geochemistry is an approved key method in archaeological sciences to reconstruct the resource provenance of metals. The method of comparing the Pb isotopic “fingerprints” of objects with the isotope geochemistry of ores has allowed us to reconstruct the trade networks of the past civilizations, enabling insights into economic, societal, and cultural developments of the ancient world. Successful application and interpretation of Pb isotope signatures of metal artifacts rely crucially on the published ore data, which are partly only available from pre- or re-digitalized publications. Most Pb isotope reference data collections were compiled by individual working groups, usually focussing on their projects and regions of interest. A great step towards a large-scale collection of Pb isotope data came with the release of the OXALID database in the early 2000s, which has benefited the scholars in the natural science discipline as well as the more untrained users from the archaeological community. Still up today, OXALID is the most used and cited source for reference data, despite the accumulation of many additional data sets since then. The limitation of OXALID and other currently available Pb isotope data sets is that they are set up as a static data collection that cannot be easily edited, modified, and verified in accordance with the rapid increase in newly published Pb isotope results. Additionally, the majority of data sets are focussed on Europe and particularly the Mediterranean, and therefore of little use to researchers from other parts of the world. Riding the wave of open science and new data infrastructures promoted by the national (German) NFDI4Earth and 4Objects initiatives, the authors are endeavoring to digitalize and construct a global Pb isotope database using the statistical environment R and Shiny App. The presentation will demonstrate this highly promising application for the modernization of archaeometry as an applied geoscience discipline.

References:

Stos-Gale, Z.A., Gale, N.H., 2009. Metal provenancing using isotopes and the Oxford archaeological lead isotope database (OXALID). *Archaeol Anthropol Sci* 1, 195–213. <https://doi.org/10.1007/s12520-009-0011-6>
OXALID database website: <https://oxalid.arch.ox.ac.uk/>

USING TRIPLE OXYGEN AND SULFUR ISOTOPES TO IDENTIFY SULFATE SOURCES AND WATER AVAILABILITY IN THE ATACAMA DESERT

Klipsch Swea¹, Voigt Claudia², Herwartz Daniel¹, Böttcher Michael E.³, Staubwasser Michael¹

¹Institute for Geology and Mineralogy, University of Cologne, Germany, ²Aix Marseille Univ, CNRS, IRD, INRAE, Coll France, CEREGE, France, ³Leibniz Institute for Baltic Sea Research, University of Greifswald, Germany

Calcium sulfates are the dominating salts in soils of the hyper-arid Atacama Desert (N-Chile), one of the driest locations on Earth. Atmospheric and marine sulfate sources have been identified along with transformation and redistribution processes, like biologic sulfate cycling, erosion, and redeposition. To systematically quantify the relative contribution and spatial distribution of primary sulfate sources and secondary processes, the isotopic composition ($\Delta^{17}\text{O}$, $\delta^{18}\text{O}$, and $\delta^{34}\text{S}$) of sulfates from Atacama Desert soils was determined. Soil surface and subsurface samples were taken along four W-E transects between 19.5°S and 25°S, ranging from the Pacific coast across the Coastal Cordillera, the Central Depression, and up the alluvial fans protruding from the Pre-Andean Cordillera. In addition, lacustrine gypsum, sodium sulfates, and a groundwater sample from the Salar de Llamará (Central Depression) and the Salar del Huasco (Altiplano) were analyzed. Previous studies have shown that atmospheric oxidation of reduced sulfur gases via ozone or hydrogen peroxide results in sulfate aerosols with positive $\Delta^{17}\text{O}$ (secondary atmospheric sulfate = SAS). Positive $\Delta^{17}\text{O}$ values throughout all analyzed Atacama Desert soils (0.1‰ to 1.1‰) suggest a significant contribution from SAS. Highest $\Delta^{17}\text{O}$ values are observed in the southernmost transect within the Coastal Cordillera, above the present maximum altitude of fog advection of 1200 m. Lowest $\Delta^{17}\text{O}$ values are observed in sulfates from salars and soils from alluvial fans. In general, low $\Delta^{17}\text{O}$ values can be a result of 1) dilution of the positive $\Delta^{17}\text{O}$ from SAS by marine and/or terrestrial sulfate with $\Delta^{17}\text{O} \approx 0\text{‰}$, and 2) resetting of $\Delta^{17}\text{O}$ due to biological sulfate reduction and reoxidation. During biological sulfate cycling, sulfuroxy intermediates in the sulfate reduction pathway readily exchange oxygen and thereby overprint the oxygen isotope signature of sulfate with the oxygen isotope composition of the ambient water. Thus, biological sulfate reduction and reoxidation lead to higher $\delta^{18}\text{O}$ and lower $\Delta^{17}\text{O}$ values, resulting in an inverse relationship between $\Delta^{17}\text{O}$ and $\delta^{18}\text{O}$. The marine sulfur contribution to the total sulfate sample was estimated using the distinct $\delta^{34}\text{S}$ value of marine sulfur ($=21.15 \pm 0.15\text{‰}$). Generally, $\delta^{34}\text{S}$ decreases with distance from the coast reflecting the decreasing sulfur contribution from the ocean (sea spray and DMS), principally confirming previously published results. Combined $\Delta^{17}\text{O}$ and $\delta^{34}\text{S}$ analyses allow to identify of sulfate originating from oxidized DMS and may help to quantify its relative contribution to the total sulfate depository. The combination of $\Delta^{17}\text{O}$, $\delta^{18}\text{O}$, and $\delta^{34}\text{S}$ may serve as a tool to distinguish primary sources and secondary alteration processes. A nearly linear inverse correlation between $\Delta^{17}\text{O}$ and $\delta^{18}\text{O}$ suggests SAS as the dominant sulfate source affected by variable biological sulfate cycling. Large $\Delta^{17}\text{O}$ anomalies ($\approx 1\text{‰}$) indicate the relative absence of biological sulfate cycling and thus, low water availability.

BIOMINERALIZATION, IDENTIFICATION AND CRYSTAL GROWTH OF BACTERIA ISOLATED FROM POPCORN AND SODA STRAW SPELEOTHEMS OF THE IRON CURTAIN CAVE IN CHILLIWACK, CANADA

Koning Keegan¹, Lawrence Sara¹, Carr Lynnea¹, McFarlane Richenda², Taiwo Aramide³, Hill Patrick², Donkor Kingley³, van Wagoner Nancy³, Boddy Christopher², Cheeptham Naowarat (Ann)¹

¹Biological Sciences, Thompson Rivers University, Canada, ²Chemistry and Biomolecular Sciences, University of Ottawa, Canada, ³Physical Sciences, Thompson Rivers University, Canada

Caves are extreme, often oligotrophic, environments that house diverse groups of microorganisms. Many of these microbes are able to perform microbiologically-induced carbonate precipitation (MICP) to form crystalline secondary cave structures known as speleothems. The urease family is a group of enzymes involved in MICP that catalyze the breakdown of urea, which is a source of energy, into ammonia and carbonate. Carbonate anions are effluxed to the extracellular surface of the bacterium where it then binds to extracellular calcium to form calcium carbonate which then continues to grow in crystal form. Here, we studied bacterial communities from the Iron Curtain Cave (ICC) in Chilliwack, B.C., Canada to determine whether urease-positive (U +ve) bacteria were present in the cave, the species present, and the degree to which they contribute to speleothem growth. The ICC is a carbonate cave located on the northside of Chipmunk Ridge. The cave has a unique environment with high iron content sediment and limestone structures throughout. With six pools of water present from the entrance and throughout the cave, the environment within the cave is highly humid. The temperature inside the cave ranges between 4–12 °C depending on the time of year. Ninety-nine bacterial strains were isolated from popcorn (PCS) and soda straw (SSS) speleothems. These isolates were screened for urease enzyme activity and eleven isolates were found to be U +ve. The selected U +ve isolates were then grown for 62 days on a modified B4 agar medium under high humidity and low temperature ($\phi = \geq 90\%$; 7-9 °C), to mimic the conditions of the ICC. U +ve candidates were also cultured for 84 days into liquid B4 medium to further study the minerals involved and the potential metabolic pathways. After the incubation, species specific crystal morphologies were observed. The U +ve candidates were all identified to the genus level by 16S rRNA analysis. The two best U+ve candidates are identified as *Pseudoarthrobacter* sp. PCS056 and *Psychrobacter* sp. SSS035. The PSC056 and SSS035 were further studied and found to consistently produce crystals as previously observed in both agar and broth media. The results from this study are consistent with the involvement of the U +ve bacteria isolated from the ICC in the formation of the cave's speleothems. Further work will involve additional whole genome sequencing and more specific mineralogical analysis.

SHOCKED NEOBLASTIC ZIRCON: EVIDENCE FOR COMPLETE MELTING FROM NANOSCALE INVESTIGATIONS

Kovaleva Elizaveta¹, Wirth Richard², Schreiber Anja², Kusiak Monika A.³, Habler Gerlinde⁴, Whitehouse Martin J.⁵, Kenny Gavin G.⁵

¹Earth Sciences, University of the Western Cape, South Africa, ²3.5 Interface Geochemistry, Helmholtz Centre Potsdam, Germany, ³Institute of Geophysics, Polish Academy of Sciences, Poland, ⁴Department of Lithospheric Research, University of Vienna, Austria, ⁵Department of Geosciences, Swedish Museum of Natural History, Sweden

Investigation of shock deformation features on Earth at various scales yielded similarities with other terrestrial planets and rocky satellites. Various types of neoblastic granular zircon have been recognized from terrestrial impactites [1,2,3,4], suggesting different mechanisms and conditions for zircon recrystallization during impact events [5,6]. Utilizing transmission electron microscopy (TEM) [7], we have studied shock-induced granular zircon from the Vredefort impact structure, South Africa [8]. To better understand the recrystallization mechanisms, we have also applied electron backscattered diffraction (EBSD) and scanning ion imaging (SII) by secondary ion mass spectrometry (SIMS).

Recrystallized zircon grains from Vredefort are composed of multiple granules with (i) radially fractured rims, (ii) pores, and (iii) characteristic triple junctions. Granules have either random crystallographic orientations or systematic orientations characteristic of so-called “former reidite in granular neoblastic” (FRIGN) zircon, where three mutually orthogonal clusters of [001] directions are observed [9]. Each granule is a mosaic crystal, consisting of slightly misoriented nanocrystals, with the latter also extending from zircon surfaces into the surrounding silicate melt glass. Zircon granules contain round melt inclusions that differ in composition (Al-Ca-Ti-Mn-Fe) from the surrounding glass (K-feldspar in composition), as well as SiO₂, ZrO₂, and Al-rich SiO₂ glass inclusions. The ZrO₂ phase occurs as monoclinic inclusions (> 50µm), and tetragonal and cubic inclusions (< 50µm). Around one of the grains, a 2 µm-thick Y-oxide rim is observed to be composed of granules with similar orientations to neighboring zircon granules. Our nano-scale observations point to the complete disequilibrium decomposition of zircon into SiO₂ and ZrO₂ (and locally YO₂) during the shock event, formation of unmixed melt droplets of oxide and silicate melt, and subsequent crystallization of zircon crystals (granules). All the radiogenic Pb isotopes accumulated in the zircon lattice by the time of the impact were excluded from the newly grown granules, as indicated by ²⁰⁷Pb/²⁰⁶Pb ages obtained by SII. The acquired ages (2062 ±64 Ma) are consistent with the Vredefort impact event (2020 ±3 Ma [10]).

We suggest that characteristic impact-related granular neoblastic zircon forms as a result of melting and crystallization [7] and not necessarily via the solid-state phase transition, as was suggested previously [6,7,9].

References: [1] Bohor et al. (1993) *Earth Planet Sci Lett* 119, 419–424. [2] Cavosie et al. (2016) *Geology* 44, 703–706. [3] Kenny et al. (2019) *Geochim Cosmochim Acta* 245, 479–494. [4] Hauser et al. (2019) *Meteorit Planet Sci* 54, 2286–2311. [5] Erickson et al. (2017) *Cotrib Mineral Petrol* 172:6. [6] Timms et al. (2017) *Earth-Sci Rev* 165, 185–202. [7] Kovaleva et al. (2021) *Earth Planet Sci Lett* 565, 116948. [8] Kovaleva et al. (2019) *Geology* 47, 691–694. [9] Cavosie et al. (2018) *Geology* 46, 891-894. [10] Moser (1997) *Geology* 25, 7–10.

Tb-DOPING IN MULLITE: CZOCHRALSKI CRYSTAL GROWTH AND SOL-GEL SYNTHESIS

Krämer Konrad¹, Burianek Manfred¹, Spieß Iris¹, Schneider Hartmut¹, Fischer Reinhard X.¹

¹Faculty of Geosciences (Crystallography Research Group), University of Bremen, Germany

Mullite is a material best known for its outstanding high-temperature mechanical properties. In recent years it also became popular as a host for luminescent elements. Wet chemical synthesis pathways have successfully been applied for doping experiments, but commonly produce samples with crystals in the nano- to microscale. By using the Czochralski method, this work investigates the feasibility of Tb³⁺ doping in cm-sized single crystals of 2/1 mullite Al_{4.8}Si_{1.2}O_{9.6}. For comparison, the incorporation of terbium was also examined in 3/2 mullite Al_{4.5}Si_{1.5}O_{9.75}, prepared by sol-gel synthesis. Tb-concentrations in the crystals were 0.215-0.5 wt.% Tb³⁺. Grains of Al₂O₃ and SiO₂ were used as feed material for melt growth. Tb₄O₇ powder was added for the growth of doped crystals. Gels were prepared from tetraethoxysilane and Al(NO₃)₃ · 9H₂O dissolved in deionized water. In the sol-gel synthesis, Tb₄O₇ was dissolved in concentrated HCl, using a rapid hydrolysis approach for gel formation and a maximum sintering temperature of 1300°C. The phase composition and lattice parameters were examined by powder X-ray diffraction (PXRD). Chemical analyses were done with energy-dispersive X-ray spectroscopy (EDX). Terbium concentrations were determined through laser ablation with inductively coupled plasma mass spectrometry (LA-ICP-MS). X-ray microtomography was used to determine the macroscopic inner structure in a large doped single crystal of Al_{4.776}Si_{1.224}O_{9.612}. Crystal structure analyses based on single-crystal X-ray diffraction data of melt-grown crystals included the determination of atomic coordinates as well as possible site occupancies of Tb on tetrahedral, octahedral, and oxygen vacancy sites.

Single crystals with a size of some cm were grown from the melt. The average Tb-concentrations in the doped crystal varied between 8 and 30 ppm, with local maxima of more than 2000 ppm. Refined atomic coordinates of Si, Al, and O agree with published values. Changes in the atomic coordinates in the doped sample were caused by an Al₂O₃ deficiency. Through the simultaneous growth of the amorphous phase, a network of oriented cracks formed in the doped crystal. This network was interrupted by a 500 µm thick sheet in the crystal, where the inclusion density dropped sharply, indicating its origin to be related to the growth procedure and not to the foreign ion concentration. Powders synthesized through the sol-gel method contained mullite, corundum, cristobalite, and θ-alumina with varying mass fractions. The grain size of the produced crystals is below 3 µm. Terbium concentrations were close to the weighed fraction but varied depending on the ablation location on the samples, as a result of the local phase composition. Changes in the chemical composition of the educts were noticeable in the products but did not conform to the same stoichiometry. The high eutectic temperature of terbium oxides in the Al₂O₃-SiO₂ melt hindered an even distribution within the used mixing times and required exceptionally high temperatures. Dissolution of Tb₄O₇ for wet chemical synthesis did not occur within reasonable timespans in concentrated acids, even when heated.

We thank the DFG for funding this project under grant FI442/25.

MINERALOGICAL COLLECTIONS AND WORKING WITH THE YOUNGEST - IS THAT THE RIGHT APPROACH?

Kreher-Hartmann Birgit¹

¹Institute for Geosciences, Mineralogical Collection, Friedrich-Schiller-University Jena, Germany

Mineralogical museums face a particular challenge in dealing with their visitors. The objects in the collections are important informants in the current questions and discussions about georesources, technical applications, biomaterials, climate change. To name but a few. So the visitors should be scientists only? Of course not - as we all know. Geoscience thematics should be transferred to everybody from the very youngest to the elderly. And across all educational levels.

So curators and museum education officers have some possibilities to impart knowledge about minerals to the visitors. In the last decades, a lot of technical, digital media had been built up in museums. Curators and their colleagues from the corresponding institute go since years to schools to work with pupils mainly from the upper classes. They communicate interesting facts about vulcanism, origin and changing of our earth, about minerals in our environment, about gemstones, and so on. Now in the last two, three years we started up with explanations in the museum and on homepages in simple language. It seems like waves going through the society to reach hopefully another, a new group of people interested in geoscience. And what we are doing in times of closed museums as we had to experience in the many months of lockdown? You have two chances. Ignore the situation and use it for working in the magazine or on the database. Or try something new. Online tours through the museum, virtual objects of the month, starting with Instagram, digital lectures, and so on. Plenty of creativity is visible now. What will remain from all of this if museums are open again? Some observations have already been made in the summer last year. In the mineralogical collection of the University of Jena/Germany in the last twenty years, there were regular visits of children from nursery schools. They learned a lot of minerals from determination, their occurrence in nature to their use in daily life. Normally these young children come one or two times with their nursery school, later on often with their grandparents. In last summer a lot of them came for the first time with their parents. The parents often obtained first information about the existence of the collection through their children.

The talk will show in an exemplary way what a follow-up reaction the continuous occupation and work with young children can mean for museums. Especially in university museums, this work is often critically observed.

THE ARCHEAN NAPIER COMPLEX — A POSSIBLE MOSAIC OF DOMAINS WITH INDEPENDENT GEOLOGICAL HISTORIES

Król Piotr¹, Kusiak Monika A.¹, Dunkley Daniel J.¹, Wilde Simon A.², Yi Keewook³, Whitehouse Martin J.⁴

¹Department of Polar and Marine Research, Institute of Geophysics, Polish Academy of Sciences, Poland, ²School of Earth and Planetary Sciences, Curtin University, Australia, ³Korea Basic Science Institute (KBSI), Korea, Republic of, ⁴Department of Geosciences, Swedish Museum of Natural History, Sweden

The Napier Complex of east Antarctica is one of several cratons where Eoarchean (>3.6 Ga) crust is preserved. It is a product of crustal evolution throughout the Archean, including at least two metamorphic events: at ~2.8 Ga and ~2.5 Ga. The latter event is characterized by some of the highest metamorphic temperatures known, exceeding 1000°C in places. This event obfuscated much of the earlier geological record. Presently, it is unknown whether the Napier Complex constituted a single crustal unit throughout its evolution or represents a mosaic of crustal domains with independent histories. If the latter is true, the question remains when juxtaposition of the various domains occurred. To shed new light on this problem, we undertook Sensitive High-Resolution Ion Microprobe (SHRIMP) sub-grain analysis of zircon on key samples across the complex to test for evidence of multiple stages of mineral growth and/or modification. To characterize the nature and origin of the magmatic protoliths, whole-rock geochemical analyses were also undertaken.

Orthogneisses from Tula Mountains in the central part of the complex, and the Scott and Raggatt Mountains in the southeastern part, reveal episodic magmatism from 3.8 to 2.5 Ga. In the Tula Mountains, the protoliths to granitic (Budd Peak) and trondhjemitic (Mt. Jewell) gneisses crystallized at ca. 3.75 Ga, followed by diorite at ca. 3.56 Ga. Granitic gneisses from nearby Mt. King record younger protolith crystallization at ≥ 2.8 Ga. In contrast, tonalitic and trondhjemitic gneisses from the Scott and Raggatt Mountains record two magmatic events: at 2.72 Ga and at 2.53 Ga. The former were generated after the ca. 2.8 Ga metamorphic event recorded in the Tula Mountains, whereas the latter occurred just before or at the beginning of the younger high-T metamorphic event that continued until at least 2.44 Ga. Geochemically, the gneisses fall into either low or high Y-HREE-Nb-Ta groups. This variation can be accounted for by differences in the conditions of melting in the crustal sources through the presence or absence of minerals in the restite that sequester Y-HREE (mainly garnet) and Nb-Ta (mainly rutile). As the stability of these minerals is dependent on pressure, the groups represent melts derived at high (at least 1.5 kbar) or low (ca. 1 kbar) pressures.

Integration with existing geochronological and geochemical data from orthogneisses leads to the hypothesis that the Napier Complex is likely composed of three crustal domains with different histories: 1) >3.5 Ga crust without clear evidence of 2.8 Ga metamorphism; 2) 3.3–2.9 Ga crust affected by the ca. 2.8 Ga event; and 3) 2.75–2.65 Ga Ma crust present in the southwestern Napier Complex. Magmatism and high-temperature metamorphism after 2.65 Ga likely represent the cumulation of tectonothermal processes that juxtaposed the various crustal domains.

This research was funded by NCN grant UMO2019/34/H/ST10/00619.

(META)MANGANOLITES IN POLAND: A NEW LIGHT ON AN OLD PROBLEM

Kruszewski Łukasz¹, Siuda Rafał², Jastrzębski Mirosław¹, Ciążela Jakub¹, Białek Dawid³, Wojtulek Piotr M.⁴, Lis Grzegorz⁴

¹Institute of Geological Sciences, Polish Academy of Sciences, Poland, ²Institute of Geochemistry, Mineralogy and Petrology, Faculty of Geology, University of Warsaw, Poland, ³Department of Physical Geology, Institute of Geological Sciences, University of Wrocław, Poland, ⁴Department of Economic Geology, Institute of Geological Sciences, University of Wrocław, Poland

Manganese-rich rocks, known as manganolites, are either related to siliceous sediments deposited in the vicinity of submarine hydrothermal vents or submarine weathering. So is true for their metamorphic counterparts – metamanganolites. Their occurrence is a good marker of the coexistence of metal (e.g., Au, Co, Ni, Sn, W, and others) ore deposits. They are suggested as potential lithostratigraphic markers that may be helpful, e.g., in the case of lacking precise isotopic-dating data for the particular area (e.g., Kennan, 2004). Many of their occurrences mark important oceanic-anoxic events, too (e.g., Hârtopan & Hârtopan, 1996). Surprisingly, the literature on the occurrences, petrology, mineralogy, and genesis of (meta)manganolites in Poland is scarce. A prominent exception concerns once exploited Mn-Fe ores in the Western Tatra Mts. (e.g., Jach & Dudek, 2005), with their full mineralogical composition still within exploration. To begin filling this gap we have studied few sites within the Fore Sudetic Block and Sudetes Mts., Lower Silesia. The most interesting Mn mineralization was detected at Pustków Wilczkowski in the Central Sudetic Ophiolite. The local phyllites/radiolarites were known to bear some Mn oxides (Lis & Sylwestrzak, 2004) but their true, polycomponent mineralogy and unique – at least for Poland – geochemistry was unknown. According to Kennan (2004), the Pustków rocks may represent the same horizon of oceanic sediments that spreads from Irish Caledonides. Indeed classical coticule occurrences in the Ardennes (Belgium) and German occurrences, e.g., in the Harz Mountains, strongly resemble the Pustków ones. Of the Mn minerals, lithiophorite (subsite 1) or a chalcophanite group (subsite 2, with goethite as the main mineral) dominates, with birnessite/bementite, carpholite (first record in Poland), and jacobsonite also confirmed. Other minerals include abundant crandallite, alunite and hydronium jarosite, and plumbogummite. Abundant “illite” is strongly vanadiferous (mean 0.11 apfu V). Goethite bears V, As, Cr, and P impurities. REEs are found in monazite-(Ce), monazite-(La), and minor scandian xenotime (with up to 1.39 wt.% Sc) and florencite-(La). Portable XRF shows the rocks to be also enriched in Ni, Zn, Ga, and Se. A metamanganolite from Szklary bears birnessite, lithiophorite, and trace kutnahorite. The so-called pegmatoids that accompany mica schists of the Orlica-Śnieżnik Dome in Marcinków can be correlated with metamanganolites known from the Moldanubian zone. They represent a likely feldspar-rich metamanganolite, with similar Mn-oxide mineralogy (birnessite and likely lithiophorite). It also bears slightly manganiferous epidote, ilmenite, and titanite, and almandinitic garnet with up to 29 mol.% spessartine molecule.

References

- Hârtopan, P., Hârtopan, I., 1996. New data on the Mn-Fe Delinești deposit, Semenic Mountains. *Rom. J. Mineral Deposits*, 77, 35–47.
- Jach, R., Dudek, T., 2005. Origin of a Toarcian manganese carbonate/silicate deposit from the Krížna unit, Tatra Mountains, Poland. *Chem. Geol.*, 224, 136–152.
- Kennan, P., 2004. The Niemcza Zone and the Kamieniec Żąbkowicki-Strzelin Belt, Western Sudetes: one perspective. *Min. Soc. Pol. Spec. Pap.*, 24, 36–44.
- Lis, J., Sylwestrzak, H., 1996. *Minerały Dolnego Śląska*. Wydawnictwa Geologiczne, Instytut Geologiczny, Warszawa, Poland, 791 pp. [in Polish].

BARIUM MOLYBDATE, Ba(MoO₄) – A POTENTIALLY NEW MINERAL FROM PARALAVA OF HATRURIM COMPLEX, ISRAEL.

Krzyształa Arkadiusz¹, Galuskina Irina¹, Vapnik Yevgeny², Galuskin Evgeny¹

¹Faculty of Natural Sciences Institute of Earth Sciences, University of Silesia in Katowice, Poland, ²Department of Geological and Environmental Sciences, Ben-Gurion University of the Negev, Israel

A potentially new mineral, Ba(MoO₄) – a barium analog of powellite, Ca(MoO₄) (*I*4₁/*a*; *a*, *b* ≈ 5.22 Å, *c* ≈ 11.43 Å) or wulfenite, Pb(MoO₄) (*I*4₁/*a*; *a*, *b* ≈ 5.43 Å, *c* ≈ 12.11 Å), was found as inclusions up to 5 μm in size inside baryte crystals. They occur in the hydrothermally altered rankinite paralava from Gurim Anticline, Hatrurim Basin, Negev Desert, Israel. Ba(MoO₄) associates with Ca-zeolites, ettringite, and minerals of the tobermorite group formed after the primary minerals of rankinite paralavas. The main mineral association of not altered paralava is represented by garnets of the andradite-schorlomite series, melilites of the gehlenite-alumoåkermanite series, rankinite, cuspidine, kalsilite, and minerals of the fluorapatite-fluorellestadite series.

A potentially new mineral contains insignificant Sr, Ca and S impurities and its composition is close to the end-member BaMoO₄. The main bands observed in the Raman spectra of BaMoO₄ are related to vibrations of the MoO₄ tetrahedral groups. The obtained Raman spectrum of the natural BaMoO₄ from Negev Desert is similar to the spectrum of the synthetic BaMoO₄ (*I*4₁/*a*; *a*, *b* ≈ 5.703 Å, *c* ≈ 13.078 Å). Similarly to the synthetic counterpart, the main bands in the Raman spectrum of the natural barium molybdate can be assigned to the following vibrations (natural/synthetic, cm⁻¹): 325/326 ν₂(MoO₄)²⁻, 358/360 ν₄(MoO₄)²⁻, 792/793 ν₃(MoO₄)²⁻, 838/839 ν₃(MoO₄)²⁻ and 891/892 ν₁(MoO₄)²⁻.

Mo-bearing minerals are scarce in all rocks of the Hatrurim Complex and, as a rule, are related to the not-abundant diopside paralava. However, there are recently discovered phosphides – nickolayite, FeMoP, and polekhovskiyite, MoNiP₂, and associating with them molybdenite, MoS₂, and powellite, Ca(MoO₄).

The natural Ba(MoO₄) is the first barium member of the scheelite group, which besides wulfenite and powellite, combines isostructural wolframates of Ca (scheelite) and Pb (stolzite).

SUITABILITY OF CONSTRUCTION AND DEMOLITION RESIDUALS FOR THE PRODUCTION OF NOVEL GEOPOLYMER BUILDING MATERIALS

Kugler Felix¹, Karsdorf Robert¹, Fehn Thomas², Teipel Ulrich², Krcmar Wolfgang¹

¹Materials Engineering, Nuremberg Institute of Technology, Germany, ²Process Engineering, Nuremberg Institute of Technology, Germany

222.678 new construction projects have been authorized in Germany in 2019. In order to construct new buildings on such a scale, large quantities of suitable building materials are demanded in accordance with the requirements, such as concrete, aerated concrete, sand-lime bricks, or bricks. What all building materials have in common is that significant raw material and energy resources have to be used for their production in thermoprocessing plants. In the process, decarbonation of the mineral input materials takes place through thermal treatment at high temperatures with corresponding CO₂ emissions. At the same time, the combustion of the required primary fuels also leads to a release of CO₂. As to achieve the climate protection targets, building materials of the future should already be characterized by lower energy consumption with reduced CO₂ emissions during their production. Future building materials should also contain a feasible proportion of processed recycled material and be able to be reintegrated into the recycling process at the end of their service life. In Germany alone, more than 228 million tons of construction and demolition waste were generated in 2018. Viable recycling of recyclable materials has already been taking place for many years, with the metallic components such as iron, steel as well as copper pipes, wood, and plastics being separated from the inorganic building materials, plasters, and mortars and are returned to the materials cycle. However, a large proportion of the inorganic demolition materials is still sent to construction waste landfills, where it blocks valuable landfill space. The work presented here deals with a new class of building materials, the so-called geopolymers. These are cold-hardening binding building materials that require comparatively significantly lower primary energy consumption in their production, with correspondingly lower CO₂ emissions. It is known from literature data that geopolymers have been synthesized on the basis of metakaolin, fly ash, and blast furnace slags, thereby also saving primary energy and costs. The spherical shape of the fly ash particles offers the advantage that resulting geopolymer glues are easier to process and require less activator solution. The fly ash-based geopolymers prove to be particularly environmentally friendly compared with metakaolin- and slag-based systems. This is mainly attributed to the fact that combustion or drying processes are no longer necessary. To further address this environmental concern, geopolymers based on crushed brick and concrete residues have also been produced. In the work presented here, various typical demolition materials and residual materials from the construction sector, such as brick scrap, brick sanding dust, mixed rubble, and concrete rubble, are being investigated with regard to their suitability as recycling raw materials for the production of novel geopolymer building materials. In particular, it will be investigated whether the residual materials mentioned are already suitable in their "pure form" as singular solid components for geopolymer production. In order to be able to evaluate the suitability of the residue-based geopolymer bricks as building materials, they will be examined with regard to their material parameters, compressive strength, density, and thermal conductivity.

CHEMICAL AND PHASE REACTIONS ON THE CONTACT BETWEEN REFRACTORY MATERIALS AND SLAGS, A CASE FROM THE 19TH CENTURY Zn-Pb SMELTER IN RUDA ŚLĄSKA, POLAND

Kupczak Krzysztof¹, Warchulski Rafał¹, Dulski Mateusz², Środek Dorota¹

¹Institute of Earth Sciences, Faculty of Natural Sciences, University of Silesia, Będzińska 60, 41-200 Sosnowiec, Poland; krzysztof.kupczak@us.edu.pl (K.K.); rafal.warchulski@us.edu.pl (R.W.); dorota.srodek@us.edu.pl (D.Ś.)

² Institute of Materials Engineering, and Silesian Center for Education and Interdisciplinary Research, University of Silesia in Katowice, 75 Pułku Piechoty 1A, 41-500 Chorzow, Poland; mateusz.dulski@smcebi.edu.pl

Slags from the historic metallurgy of Zn-Pb ores are known for unique chemical and phase compositions. The oxides, silicates, aluminosilicates, and amorphous phases present therein often contain in their structure elements rare in natural conditions, such as Zn, Pb, As. The study focuses on processes occurring on the contact of the melted batch and the refractory materials of the furnace, which lead to the formation of these phases. In the study, chemical (X-ray fluorescence, inductively coupled plasma-mass spectrometry) and petrological (X-ray diffraction, electron probe micro-analyses, Raman spectroscopy) analyzes were used. They were performed on refractory material, slag, and contact zone of both.

Two main types of reactions have been distinguished: gas/fluid-refractories and liquid-refractories. The first of them enrich the refractories with elements that migrate with the gas. In the metallurgical furnaces, during the production of zinc, the temperature was about 1000-1300°C. Some of the components present in the melt had a sufficiently low boiling point, and they could be present in the form of a gas. As a result of gas/fluid migration and heating, the refractory materials were partially melted, forming glasses enriched in PbO, K, Na₂O, and to a lesser extent in As and Zn. Moreover, the FeO/Fe₂O₃, MgO, and CaO, which were present in the refractory material, migrated towards the inside of the muffle, creating a layer enriched with them. Several processes have influenced the reaction between the refractory material and the melt. The first is gravitational differentiation. Components of the charge with the low melting point (PbO₂, As₂O₃) were melted at relatively low temperatures (about 300°C). In liquid form, they migrated towards the bottom of the muffle. Then, after reaching the liquidus temperature of the entire system, they were accompanied by the components with high melting points and densities (e.g., Fe oxides). Another type of reaction in the furnace was the contamination of the melt with the refractory materials components. The local change in thermodynamic conditions caused the liquidus temperature to drop, which allowed the outer parts of the lining to melt, causing enrichments in Al₂O₃ and SiO₂. Later, during crystallization in these zones, phases characteristic of slags but enriched in high-density and refractory material-related elements were formed (K-feldspar enriched in Pb, aluminohematites, pyroxenes enriched in Fe, and depleted in Ca). Due to the relatively low solidus of the zones enriched in PbO and As₂O₃, PbO-As₂O₃-SiO₂ glasses were formed in the final stages of crystallization. Incompatible elements, such as K, were also concentrated in these glasses.

Acknowledgments

This study was supported NCN grant no. 2016/21/N/ST10/00838 (awarded to RW) and NCN grant No. 2019/35/O/ST10/00313 (awarded to KK).

CHARACTERIZATION OF SURFICIAL WEATHERING ON CALCARENITE ROCKS IN THE RUPESTRIAN SYSTEM OF "SAN MICHELE DELLE GROTTI" IN GRAVINA IN PUGLIA (BARI, APULIA)

Lacalamita Maria¹, D'Angeli Ilenia Maria¹, Sasso Corrado¹, Schingaro Emanuela¹, Parise Mario¹

¹Earth and Environmental Sciences, University of Bari, Italy

San Michele delle Grotte is a rupestrian cave excavated into the "Calcarenite di Gravina" formation, resting over the Cretaceous formation of the "Calcarenite di Altamura". The artificial cavity develops exactly at the contact between the two lithologies, with the first making the walls and vault, and the second being the pavement. Both formations are characterized by discontinuities and show evident instability features and surficial rock weathering. In particular, patinas and crusts extensively cover the walls, ceilings, and fractures inside the cavity. In the present study, a complete mineralogical and morphologic characterization of selected rock samples was carried out in order to assess the link between petrographic and mineralogical features of calcarenite and the weathering mechanisms and, specifically, to define the intensity of both the biotic and abiotic processes. Unaltered and weathered samples of Calcarenite di Gravina were analyzed through optical microscopy, scanning electron microscopy (SEM), and X-ray powder diffraction (XRPD). In thin section, we observed bioclastic packstone to grainstone fabrics, the samples containing microfossils as foraminifera, bivalve shells fragments, and bryozoans. Overall, the unaltered rock is composed of calcite, aragonite, ankerite, and subordinate quartz. In its surficial portion it is possible to find different types of alterations which can be divided into two main groups: group 1 encompasses rock samples with black to green biological coatings; group 2 includes salt-weathered rocks. Group 1 is dominated by algae constructive and destructive features, and from the mineralogical standpoint it contains calcite and minor quartz and gypsum; group 2 evidences efflorescence crusts (crusty white mineral salts) which are dominated by sulfates such as syngenite ($K_2Ca(SO_4)_2 \cdot 2H_2O$), gypsum ($CaSO_4 \cdot 2H_2O$) and arcanite (K_2SO_4), and other salts including niter (KNO_3) and sylvine (KCl).

Scanning electron microscope images allowed to observe a distinctive enhance of microporosity on the rock surface immediately at the contact with the biological structures and efflorescence crusts. The results of our investigation highlight a higher abundance of biological coating where the host rock is well exposed to light, as well as the occurrence of efflorescence crusts which can originate from both anthropogenic air pollution (wet and dry airborne deposition that provides sulfate and nitrate anions) and circulation of soil water whose composition can be modified, for instance, by fertilizing.

HIGH-TEMPERATURE BEHAVIOR OF FEDORITE, A RARE ALKALINE CALCIUM PHYLLOSILICATE

Lacalamita Maria¹, Mesto Ernesto¹, Kaneva Ekaterina², Radomskaya Tatiana², Shendrik Roman², Schingaro Emanuela¹

¹Earth and Environmental Sciences, University of Bari, Italy, ²Vinogradov Institute of Geochemistry, Siberian Branch of the Russian Academy of Sciences, Irkutsk, Russian Federation

Fedorite is a rare phyllosilicate with an interlayer site occupied by H₂O molecules that coordinate interlayer K⁺ and Na⁺ cations [1]. Fedorite from brookite-quartz-feldspar rocks of the Gavrilovskaya zone (Irkutsk, Russia) underwent petrographic analysis, electron microprobe analysis (EMPA), thermal analysis (TG/DTA), in situ high-temperature single crystal and powder X-ray diffraction (HT-SCXRD and -PXRD) and ex situ high-temperature Fourier transform infrared spectroscopy (HT-FTIR). In the thin section, fedorite (92 vol.%) is associated with quartz (5 vol.%) with several minor phases (all < 1 vol.%). The morphogenetic features of minerals and their paragenetic associations in the thin section allowed us to determine the sequence of mineral crystallization from early to late ones: aegirine, apatite, amphibole, fedorite, microcline, rutile, quartz, pectolite, and calcite. The crystal-chemical formula of fedorite is: $(\text{Na}_{1.56}\text{K}_{0.72}\text{Sr}_{0.12})_{\Sigma=2.40}(\text{Ca}_{4.42}\text{Na}_{2.54}\text{Mn}_{0.02}\text{Fe}_{0.01}\text{Mg}_{0.01})_{\Sigma=7.00}(\text{Si}_{15.98}\text{Al}_{0.02})_{\Sigma=16.00}(\text{F}_{1.92}\text{Cl}_{0.09})_{\Sigma=2.01}(\text{O}_{37.93}\text{OH}_{0.07})_{\Sigma=38} \cdot 2.7\text{H}_2\text{O}$. The TG curve provides a total mass decrease of ~6%, associated with the release of H₂O, H, and F. The DTA curve indicates a continuous reaction from 25 to 800 °C and shows an endothermic peak at 934 °C. HT-PXRD data were collected in the air in the range 25-800 °C. Significant changes in the XRD patterns were observed at T = 200 and 300 °C with the appearance of new additional peaks, and at T ≥ 700 °C. Fedorite crystallizes in the P-1 space group and has: a = 9.6458(2), b = 9.6521(2), c = 12.6202(4) Å, α = 102.458(2), β = 96.225(1), γ = 119.902(1)° and cell volume, V = 961.69(5) Å³. The HT-SCXRD was carried out in the air from 25 to 700°C. On heating, a continuous expansion of the unit cell volume was observed, with two exceptions: at T = 200 °C a reduction of the cell volume occurs due to the contraction of the b and c axes; at T = 700 °C the cell volume reduction is due to the decrease of a and c lattice constants. Structure refinements indicated that the mineral undergoes a dehydration process with the loss of most of the interlayer H₂O molecules from 25 to 300°C. The FTIR analysis showed, in the OH stretching region, a very broad and convoluted absorption consisting of several overlapping components, in agreement with the presence of different H₂O environments in the structure. The HT-FTIR spectra confirmed that fedorite undergoes progressive dehydration in the 25-700 °C T range. The peaks can be clustered into three groups: 1) peaks from 3588 to 3656 cm⁻¹ which decrease in intensity and disappear at T > 325 °C; 2) new growing peaks at 3576 and 3650 cm⁻¹ which reach the maximum intensity at T = 350 °C and decrease at higher temperature; 3) the remaining peaks (at 3177, 3429, 3549, and 3635 cm⁻¹) which gradually decrease in intensity up to 700 °C. Group 3 peaks may be ascribed to stretching vibration of H₂O molecules with a strong hydrogen bond; group 1 and 2 may be attributed to vibrations of OH groups in disordered positions and to hydrogen bonds of medium strengths, respectively. These preliminary results contribute to gain insights into the modifications occurring in the fedorite structure over different T conditions.

[1] Kaneva E.V., Shendrik R.Yu., Radomskaya T.A., Suvorova L.F. (2020) Fedorite from Murun alkaline complex (Russia): spectroscopy and crystal chemical features. *Minerals*, 10, 702.

A CHANGE IN THE CLIMATIC CONDITIONS RECORDED IN LOWER BARREMIAN CLAY-DOMINATED CONTINENTAL SUCCESIONS FROM THE IBERIAN BASIN (NE SPAIN)

Laita Elisa¹, Bauluz Blanca¹, Yuste Alfonso¹, Aurell Marcos¹, Bádenas Beatriz¹

¹Ciencias de la Tierra, IUCA-Universidad de Zaragoza, Spain

The combined facies and clay mineralogy analysis, using X-ray diffraction and optical and electron microscopy, of lower Barremian continental successions within the Torrelapaja and Blesa formations (Iberian Basin, NE Spain) has allowed deciphering the palaeoclimatic and palaeoenvironmental conditions under which they were deposited. These successions developed in two separated subbasins (Torrelapaja and Oliete subbasins, respectively) but both are characterized by grey and ochre to red marls/clays with local root traces and ferruginous pisoids (1 to >5mm in diameter), suggesting lateritic soil development [1,2]. The lower Barremian successions of the Blesa Fm (lower Blesa sequence) studied here are up to 36 m in thickness and include 0.5 to 20 m-thick ochre to violet clays with abundant ferruginous pisoids and intercalated lacustrine limestones (0.4 to 2 m in thickness) some of the containing pisoids. The lower Barremian successions of Torrelapaja Fm are near 70 m-thick of grey and ochre to violet clays and intercalate 0.2 to 5 m-thick lacustrine limestones, distal alluvial conglomerates, and sandstones. Some of the latest contain pisoids. Clay mineralogy analysis of 78 samples (clays and ferruginous pisoids) indicates that the clay matrix is mainly formed of kaolinite, illitic phases, smectite, quartz, and calcite microsparitic cements. Most of the samples also contain goethite, hematite, and minor proportions of K-feldspar, ilmenite, rutile, anatase, and diaspore. Kaolinite presents platy morphologies showing pseudo-hexagonal outlines and it is also forming booklets. Smectite exhibits flake-type morphologies. By contrast, the illitic phases show irregular shapes, and their sheets are frequently separated. Illitic phases/kaolinite intergrowths are also observed. The textural features of kaolinite and smectite are indicative of an authigenic origin, whereas the illitic phases may be detrital. Analysis of pisoids (13) reveals that they are formed by a nucleus and a cortex with several concentric layers, both mainly formed by kaolinite and/or illitic phases, quartz, hematite, and goethite. Therefore, their texture and mineralogy point out an in-situ growth. The mineral association along with the presence of ferruginous pisoids and root traces allows classifying the clayed levels as palaeosols. The microsparitic carbonate cement presents textural features indicative of a diagenetic origin. The lowermost parts of the studied successions in both formations show the highest kaolinite content. By contrast, an upward decrease in kaolinite content is observed in the middle and upper parts coinciding with an increase of quartz and illitic phases and the presence of smectite. These data are interpreted as reflecting a change from warm and humid conditions, to drier and colder conditions during the early Barremian in the two > 100 km apart subbasins of the Iberian Basin.

[1] Aurell, M., Soria, A.R., Bádenas, B., Liesa, C.L. Canudo, J.I., Gasca, J.M., Moreno-Azanza, M., Medrano-Aguado, E., Meléndez, A. (2018). *Journal of Iberian Geology*, 44, 285-308.

[2] Laita, E., Bauluz, B., Aurell, M., Bádenas, B., Canudo, J.I., Yuste, A. (2020). *Sedimentary Geology*, 403, 105673.

EVALUATION OF THE REFRACTORY POTENTIAL OF BAUXITE AND ILLITE- AND KAOLINITE-RICH CLAYS FROM THE NE OF IBERIAN PENINSULA (SPAIN)

Laita Elisa¹, Bauluz Blanca¹, Yuste Alfonso¹, Mayayo María José¹

¹Ciencias de la Tierra, IUCA-Universidad de Zaragoza, Spain

Bauxites and illite- and kaolinite rich-clays are the most important raw materials to manufacture refractory ceramics. The present work analyses a set of cylinders manufactured by pressing and fired at 1000-1270°C, which are composed of pure bauxite and mixtures of bauxite and illite- and kaolinite-rich clay in 75/25 and 50/50 proportions. The aim of the study is to determine the mineralogical and textural transformations with firing and their relation with the physical properties of the final products in order to evaluate their refractory potential by comparing them with various fired commercial bauxites. The pure bauxite and the illite- and kaolinite-rich clay were obtained from the southern Pyrenees and the Iberian Range, respectively (NE Spain). Raw and fired samples were analyzed by X-ray diffraction and optical and field emission scanning electron microscopy and significant physical properties were measured in the fired cylinders. The bauxite was mainly formed by boehmite, kaolinite, and hematite, whereas illite- and kaolinite-rich clay was formed by quartz, illite, and kaolinite. At 1000°C, kaolinite, illite, anatase, and boehmite are not detected indicating that they are the least stable phases during firing. Mullite, corundum, γ -Al₂O₃, ilmenite, and cristobalite are formed from 1000°C and an amorphous phase is also detected. Mullite and corundum contents increase with temperature, although that of corundum increases until 1100°C and then decreases. At 1270°C, the main phases are mullite and corundum, being mullite content higher in the mixtures, whereas corundum content is higher in pure bauxite. At 1000°C, kaolinite-type morphologies are observed and, since kaolinite was not detected by XRD at this temperature, these morphologies could correspond to metakaolinites. Hematite, rutile, and ilmenite crystals are scattered or forming irregular aggregates (>10 μ m) and they occasionally present compositional zonation. At 1200°-1270°C, the texture of the ceramics is much more homogeneous than at lower temperatures, possibly due to the vitrification process. Acicular and prismatic nanometer-sized mullite crystals and acicular nanometer-sized corundum crystals are immersed in the vitreous phase and, in the case of corundum, it also replaces hematite crystals. Their sizes increase with the firing temperature. There is an increase in density and linear shrinkage of the cylinders, which is related to the formation of vitreous phase and mullite and correlates with a decrease in the porosity, water absorption, and thermal conductivity. The changes in the color are related to the decrease in hematite content, whereas the point load resistance depends on the vitreous phase and corundum content. The density values of the pure bauxite fired at 1270°C (3.43 g/cm³) approach to those of the fired commercial bauxites (3.15-3.25 g/cm³). By contrast, the total porosity at 1200°C of the mixtures (9-14.5%) is the closest to those of the fired commercial bauxites (7-14%). Some mixtures fired at 1200-1270°C also show similar water absorption values to those of the fired commercial bauxites and lower thermal conductivity at 1200°C than pure bauxite. This indicates that the mixture of bauxite with illite- and kaolinite-rich clays allow obtaining refractory materials with suitable properties at lower firing temperature.

SOLUBILITIES OF CARBONATE MINERALS IN AQUEOUS FLUIDS UNDER SUBDUCTION ZONE CONDITIONS: CONSTRAINTS FROM HIGH-PRESSURE EXPERIMENTS AND THERMODYNAMIC MODELS

Lan Chunyuan¹, Tao Renbiao², Huang Fang³, Jiang Runze², Zhang Lifei¹

¹Peking University, School of Earth and Space Sciences, China, ²Center for High Pressure Science and Technology Advanced Research (HPSTAR), China, ³CSIRO Mineral Resources, Australia

Subduction processes link the long-term carbon cycle between Earth's surface and interior, which has a profound impact on the Earth's surface ecosystem through geological time. Despite years of studies on the carbon fluxes during subduction, the disagreements of estimated carbon fluxes of different processes still exist, especially for the dissolution of carbonates. In the subduction slabs, carbon recycled into Earth's mantle is mainly in the forms of carbonates (e.g. CaCO₃, MgCO₃). Therefore, in this study, we constrained the solubilities of calcite, dolomite, and magnesite at high-pressure and high-temperature conditions relevant to subduction zones by combining diamond anvil cell (DAC) experiments and Deep Earth Water model (DEW) thermodynamic modeling. Furthermore, a four-apertures gasket technique for DAC is developed and applied to experimentally compare the solubility of calcite, dolomite, and magnesite at the same P and T conditions in our DAC experiments. The results show dissolution of dolomite is an incongruent process, which is different from the congruent dissolution process of calcite and magnesite. Then we used the thermodynamic models calibrated by these experiments to estimate the solubilities of calcite, dolomite, and magnesite at various P-T conditions covering cold to hot subduction paths. By combining these experimental and modeling results as well as the estimated amounts of carbonates and water in subduction zones, we can provide a more accurate constraint on the carbon fluxes from dissolution processes and have a better understanding of the deep carbon cycle.

MINERALOGICAL CHARACTERIZATION OF OLD BOR COPPER MINE TAILINGS FOR POTENTIAL REPROCESSING

Lang Aleksandra¹, Özdemir Erdem¹, Pantović Radoje², Ristović Ivica², Šajn Robert³, Vrhovnik Petra⁴, Saari Juha¹, Liipo Jussi¹

¹Research Center, Metso Outotec, Finland, ²Technical Faculty in Bor, University of Belgrade, Serbia, ³Geological Survey of Slovenia, Slovenia, ⁴Slovenian National Building and Civil Engineering Institute, Slovenia

Efficient processing of tailings, i.e. mine waste, is crucial to eliminate environmental risks often connected with tailings ponds. Tailings also represent a valuable source of secondary raw materials, which has been neglected as an opportunity. Since the mineralogy of the tailings dictates the possibilities of reprocessing and sets the limits for achievable metallurgical responses, the detailed mineralogical and chemical characterization of tailings material is a prerequisite for successful beneficiation of these kind of complex materials.

Serbia has copper deposits that have been exploited since ancient times, and date back to 4500 B.C. These operations have generated large amounts of mineral processing tailings. The Bor copper mine located in the eastern part of Serbia started exploiting the high grade, 17% Cu, copper ores in 1903, the open-pit mining started in 1912 and continued until 1986 with decreasing copper grades. During these mining operations, approximately 27 Mt of tailings with an average copper and gold contents in the range of 0.2- 0.3% Cu and 0.3- 0.6ppm Au, correspondingly, were disposed in the Bor Valley. The old Bor tailings disposal covers an area of approximately 1.6 km². The dumped tailings are extremely acid, with pH values ranging between 2.48 and 4.25 mainly due to the decomposition of abundant pyrite, which has led to acid generation. These acid conditions facilitate the mobility and bioavailability of toxic heavy metals. Overall, a century of mining has left its mark on the Bor area landscapes being one of the most polluted places in Serbia. The mineralogy of the old Bor tailings is complex due to the subsequent alteration of main primary sulfides and the occurrence of water and acid-soluble copper phases. Detailed and versatile mineralogical and chemical characterization, using sequential copper phase assays, X-ray diffraction, optical and scanning electron microscopy, and element to mineral conversions, allowed selecting the accurate methods and conditions for beneficiation of copper and gold. The most abundant copper mineral in the studied sample, which carries approximately half of the tailings total copper content, is secondary, water-soluble chalcantite, CuSO₄•5(H₂O) that forms in arid climates or in rapidly oxidizing copper deposits. In addition, trace amounts of primary chalcopyrite, enargite, and covellite were encountered. However, pyrite is the most abundant sulfide mineral in the tailings. We present results from the detailed mineralogical and chemical characterization of old Bor tailings and show how old tailings can be reprocessed and copper and gold can be recovered effectively into a pyrite flotation concentrate. Reprocessing of old mine tailings can be both an economic and environmentally friendly solution by recovering a substantial amount of copper, gold, and sulfur into concentrate, and at the same time reducing the environmental impact caused by acid mine drainage.

DISLOCATION CHANNELS AT THE CLINOPYROXENE-AMPHIBOLE BOUNDARY, PERȘANI MOUNTAINS VOLCANIC FIELD (TRANSYLVANIA, ROMANIA)

Lange Thomas Pieter¹, Pálos Zsófia², Berkesi Márta³, Molnár Gábor⁴, Pósfai Mihály⁵, Pekker Péter⁵, Szabó Csaba³, Kovács István János⁶

¹Lithosphere Fluid Research Lab (LRG); Pannon LitH2Oscope Lendület Group, Eotvos Lorand University, Hungary, ²Mineral Resources and Geofluids Group, Department of Earth Sciences, University of Geneva, Hungary, ³Lithosphere Fluid Research Lab (LRG); Pannon LitH2Oscope Lendület Group, Eotvos Lorand University, Hungary, ⁴Alba Regia Technical Faculty, Institute of Geoinformatics; Pannon LitH2Oscope Lendület Group, Óbuda University, Hungary, ⁵Nanolab, University of Pannonia, Hungary, ⁶Pannon LitH2Oscope Lendület Group, Institute of Earth Physics and Space Science, Hungary

In the upper mantle beneath the Perșani Mountains Volcanic Field (Transylvania, Romania), there is evidence for interaction between fluid, occurring in fluid inclusion, and host clinopyroxene, resulting in amphibole lamella formation. The fluid inclusions are secondary, isometric, CO₂-rich, with minor H₂O, H₂S, and N₂. Solid phases, dolomite, and anatase, are also found in the fluid inclusions. We propose a composition gradient of CO₂/H₂O increasing with distance from the fluid-solid boundary into the center of the fluid inclusion. Enrichment in H₂O with additional dissolved elements (e.g., Na, Si, Al), at the boundary, should have enhanced amphibole formation. As the studied mantle rock has a slightly deformed porphyroclastic texture, a dislocation-induced precipitation mechanism is considered. The newly formed amphibole lamella results in a new three-phase boundary, from which a 'wet' clinopyroxene-amphibole boundary starts that enhances fluid loss, supporting further amphibole growth. The misfit between clinopyroxene and amphibole results in the formation of asymmetric misfit dislocations that are associated with boundaries between clinopyroxene, amphibole, and wide-chain pyroxene. These misfit dislocations form channels parallel to the [001] direction, as a result, the [001] direction yields the fastest diffusion. A misfit-dislocation migration, in the direction of [100] is modeled and is supported by STEM observations. During the dislocation migration, a translation and rotation of the surrounding structures occurs that is accompanied by the breakup and re-bonding of octahedral chains. Misfit-dislocation channels can store escaped fluid components that will interact with clinopyroxene and pyroxene during the misfit dislocation migration (i.e., amphibole growth). Preliminary calculations of misfit-dislocation channel cross sections suggest the possibility of the diffusion of 'non-wetting' fluid components (e.g., CO₂) from the fluid inclusion that, when the amphibole lamellae reach the host mineral boundary, escape to the open grain boundary system. Our results provide a better understanding of nanoscale mantle CO₂ degassing and suggest that part of the emanating CO₂ originates from fluid inclusions.

RELICT BUT NOT INERT: THE GEOCHEMICAL VARIATIONS OF GARNET PORPHYROCLASTS DURING DEFORMATION

Langone Antonio¹, Corvò Stefania², Maino Matteo², Piazzolo Sandra³

¹Institute of Geosciences and Earth Resources (IGG), National Research Council of Italy, Italy, ²Dipartimento di Scienze della Terra e dell'Ambiente, University of Pavia, Italy, ³School of Earth and Environment, University of Leeds, United Kingdom

Garnet is a useful main mineral phase for understanding crustal processes since it is robust and ubiquitous during metamorphism. It should form in rocks that are sufficiently rich in Al (or Fe³⁺ or Cr) and in different metamorphic contexts (i.e., contact, regional, and subduction-related metamorphism) usually at temperatures above ~400 °C and pressures above ~0.4 GPa, but it can persist up to UHT and UHP conditions (e.g., >1000 °C; Baxter et al., 2013). Garnet may also form as a consequence of anatexis (i.e., partial melting at high metamorphic temperatures) and occurs as an igneous phase in some peraluminous granites. Garnet intracrystalline zonation of both major and trace elements is increasingly used to constrain the timing, duration, and kinetics of tectono-metamorphic processes (Baxter and Scherer 2013). In many cases, element zoning can be disturbed by cracking, retrogression, fluid processes, or thermally activated diffusion, but it still retains records of those specific processes (Baxter et al., 2013). In this study, we combine microstructural and petrological data of garnet-bearing metamorphic rocks across a near-complete continental crustal section exposed in the Ivrea-Verbano Zone (IVZ, Western Alps, Italy). The IVZ is an exhumed section of the Variscan middle to lower continental crust mainly made of (ultra-)mafic rocks intruded into high-grade metapelites and metabasites. The crustal section escaped the Alpine subduction but was affected by several post Variscan extensional shear zones showing progressively higher T conditions with increasing crustal depth. (Rutter et al., 2007). Garnet occurs from upper amphibolite to granulite facies conditions and survived, as porphyroblast, to the ductile deformation. A geochemical study (major and trace elements) of garnet was performed in order to characterize its geochemical features in different rock types (i.e. mafic vs pelitic protoliths), at the different metamorphic degree (i.e., amphibolite vs granulite facies) and different textural features (i.e., porphyroblasts vs porphyroclasts). Microstructural analyses (SEM-EBSD) of garnet from mylonites/ultramylonites have been combined with geochemical analyses. Preliminary major element data reveal that garnet composition is mainly controlled by the metamorphic degree (MgO increases with increasing the metamorphic grade) and protolith (i.e. garnet from mafic rocks is Ca-rich) without significant changes due to deformation. Instead, trace elements of garnet from ultramylonites are completely different (e.g., Y and REE up to 2.5 times higher) from those analyzed in garnet from other rock types. The preliminary results suggest that the trace element composition of garnet porphyroclasts can be severely modified due to the combined effect of intracrystalline deformation and fluid-mineral interaction.

References:

- Baxter, E. F., & Scherer, E. E. (2013). Garnet geochronology: timekeeper of tectonometamorphic processes. *Elements*, 9(6), 433-438.
- Baxter, E. F., M. J. Caddick e J. J. Ague (2013). "Garnet". In: *Elements: An International Magazine of Mineralogy, Geochemistry and Petrology* 9.6.
- Rutter, E., Brodie, K., James, T., & Burlini, L. (2007). Large-scale folding in the upper part of the Ivrea-Verbano zone, NW Italy. *Journal of Structural Geology*, 29(1), 1-17.

ACCESSORY MINERALS FROM MID-LOWER CRUSTAL SHEAR ZONE: A UNIQUE OPPORTUNITY TO DATE DEFORMATION (VAL STRONA DI OMEGNA, IVREA-VERBANO ZONE, ITALY)

Langone Antonio¹, Simonetti Matteo¹, Corvò Stefania², Maino Matteo², Bonazzi Mattia²

¹Institute of Geosciences and Earth Resources (IGG), National Research Council of Italy, Italy, ²Department of Earth and Environmental Sciences, University of Pavia, Italy

Several shear zones have been recognized in the lower crustal section exposed in the Ivrea-Verbano Zone (Rutter et al., 1993) and some of those structures are interpreted as related to different stages of Mesozoic rifting (e.g., Petri et al., 2019). Several geochronological and thermochronological data are available in the literature for this crustal section but the timing of shearing is still poorly constrained. Here we describe the case of the Forno-Rosarolo Shear Zone (Siegesmund et al., 2008), a sub-vertical high-strain zone located at the transition from amphibolite- to granulite-facies metamorphic rocks. Mylonites developed mainly at the expense of paragneisses, felsic granulites, mafic rocks, and calc-silicates. Amphibolite-facies conditions of deformation were estimated in the paragneiss by garnet-biotite geothermometer and GASP geobarometer. We obtained a temperature range between 630 °C and 660 °C and pressure of ~0.55 GPa, which are in good agreement with the observed microstructures and the syn-tectonic mineral assemblage. Metapelites were selected for in-situ monazite U-Th-Pb geochronology. They consist of garnet, sillimanite, feldspar, and biotite with accessory zircon, monazite, and rutile. Monazite occurs in different microstructural positions (included in porphyroclasts or along the mylonitic foliation) and commonly presents complex chemical zoning of Th and Y. We recognize three main Y compositional domains: (1) high to medium-Y cores; (2) low-Y cores; (3) high-Y rims. The latter developed as a consequence of garnet breakdown during deformation and are potentially useful for dating shearing. Mylonitic calc-silicates are made of fine-grained calcite surrounding clinopyroxene, feldspar, and garnet porphyroclasts. Large titanite grains (up to 1mm) occur both along the foliation and as inclusions within porphyroclasts and are potentially useful for in-situ U-Pb dating. The application of two independent geochronometers may allow to shed light on the age of the deformation. Such approach should always be used when dealing with large-scale shear zones involving different types of rocks.

Petri, B., Duretz, T., Mohn, G., Schmalholz, S.M., Karner, G.D., Müntener, O., 2019. Thinning mechanisms of heterogeneous continental lithosphere. *Earth and Planetary Science Letters* 512, 147–162. <https://doi.org/10.1016/j.epsl.2019.02.007>

Rutter, E.H., Brodie, K.H., Evans, P.J., 1993. Structural geometry, lower crustal magmatic underplating and lithospheric stretching in the Ivrea-Verbano zone, northern Italy. *Journal of Structural Geology* 15, 647–662. [https://doi.org/10.1016/0191-8141\(93\)90153-2](https://doi.org/10.1016/0191-8141(93)90153-2)

Siegesmund, S., Layer, P., Dunkl, I., Vollbrecht, A., Steenken, A., Wemmer, K., Ahrendt, H., 2008. Exhumation and deformation history of the lower crustal section of the Valstrona di Omezna in the Ivrea Zone, southern Alps. *Geological Society, London, Special Publications* 298, 45–68. <https://doi.org/10.1144/SP298.3>

NON-INVASIVE PETROGRAPHIC AND MINERALOGICAL INVESTIGATION OF THE DECORATIVE STONES FROM TOMMASO BELLI'S COLLECTION SAPIENZA UNIVERSITY IN ROME

Lazaroiu Andreea¹, Stagno Vincenzo¹, Lupi Stefano², Macis Salvatore², Macri Michele¹, Sardella Raffaele¹

¹Earth Sciences, Sapienza University of Rome, Italy, ²Physics, Sapienza University of Rome, Italy

Along with unique collections of minerals (more than 34,000) and paleontological (about 100,000) samples, the Earth Sciences Museum (MUST) of the Sapienza University (Rome) also hosts important historic collections of ancient marbles, including the 19th-century collections from Tommaso Belli. This consists of 636 small squared and polished decorative stones considered among the most extensive collections worldwide mostly coming from excavations of Ancient Roman sites in Italy and the Roman Empire. The petrographic description and classification of stone materials belonging to a private historical collection are known to be limited by the inaccessibility of these specimens to invasive common techniques that would result to severe damages.

In this ongoing study, we performed a non-invasive petrographic and mineralogical investigation of eight stone materials known with the historical names of Marmo Greco Venato, Giallo Antico, Marmo Cipollino, Lavagna punteggiata con il Giallo, Granito Nero con Feldspati Rossi, Granito del Foro, Granito Bianco e Nero and Marmo Giallo e Nero. Such selection spans from igneous to metamorphic and sedimentary rocks and appears well reproduced by a further historical collection of ancient stones represented by the Corsi's Collection hosted by Oxford University and the F. Belli's Collection in Bari.

For each specimen, we performed a macroscopic study aimed to identify the main textural features such as type, number, and volume fraction of minerals, presence of fractures, dislocations, and altered glazes. The chemical and mineralogical composition was investigated using micro-reflectance infrared spectroscopy. The analyses were carried out in the mid-infrared region of 500-8000 cm⁻¹ with a resolution of 4 cm⁻¹ with respect to a gold mirror using the same aperture of 80 μm. An average of 3 acquisitions of 128 scans each were performed on the selected area. The collected spectra were, then, compared with those of available databases for precise identification of the minerals and constrain their chemical composition.

Our preliminary results are discussed in terms of available petrographic classification schemes and compared with the same ancient stones reported from similar collections (e.g., the F. Belli and the T. Corsi collections) as well as their documented excavation sites.

Keynote

SUPER-HYDRATION FROM ZEOLITES TO LAYERED MINERALS

Lee Yongjae¹

¹Earth System Sciences, Yonsei University, Korea, Republic of

Super-hydration is defined as a special case of pressure-induced insertion whereby water molecules are loaded into the pore space expanding its crystalline matrix. Since its first report in natural zeolite natrolite, super-hydration has been established to be a systematic property of this class of small-pore zeolites. Depending on the type of extra framework cations, the degree of volume expansion and its onset pressure are controlled by up to 21% and in the pressure range of 0.4 – 3.0 GPa, respectively. Such unique high-pressure chemistry occurring in zeolites has intrigued its possible occurrence in nature under higher pressure-temperature conditions such as subduction zones. Recently, we have discovered that super-hydration occurs in a clay mineral kaolinite at conditions corresponding to a depth of about 75 km along a cold subducting slab (ca. 2.7 GPa and 200 °C). This super-hydrated kaolinite has a unit cell volume that is about 31% larger, a density that is about 8.4% lower than the original kaolinite, and, with 29 wt% H₂O, the highest water content of any known aluminosilicate mineral. Yet another class of super-hydration has been found in a well-known manganese oxide mineral, birnessite, at shallower depth environments. The spacing between the edge-sharing MnO₆ octahedral layers expands from ~7 Å to ~10 Å upon super-hydration below ca. 0.2 GPa, increasing the water content to ca. 34.5 wt. % to rival the most hydrous mineral on the Earth. Subjecting these super-hydrated minerals to deeper depth conditions leads to the release of water and sequential chemical breakdowns that may affect global seismicity and geochemistry.

In this talk, I will summarize our evolving efforts in the discovery of super-hydration and its implications for global water cycling.

COULD DEHYDROGENATION DIMINISH THE ROLE OF OXYGEN FUGACITY DURING FE²⁺ OXIDATION IN PHYLLOSILICATES/SILICATES?

Lempart-Drozd Małgorzata¹, Derkowski Arkadiusz¹, Błachowski Artur², Luberd-Durnaś Katarzyna¹, Strączek Tomasz³, Kapusta Czesław³

¹Institute of Geological Sciences Polish Academy of Sciences, Poland, ²Institute of Physics, Pedagogical University, Poland, ³Faculty of Physics and Applied Computer Science, AGH University of Science and Technology, Poland

Phyllosilicates are the most widespread group of minerals on Earth, due to abundant Fe²⁺-bearing constituents they contribute significantly to redox processes. Under high-temperature conditions, Fe²⁺-bearing phyllosilicates undergo two reactions, involving decomposition of OH groups: dehydroxylation and dehydrogenation. While dehydroxylation leads to H₂O release ((OH)₂n → nH₂O + nOr), dehydrogenation produces H₂ gas and oxidizes structural Fe²⁺ (Fe²⁺ + OH⁻ → Fe³⁺ + Or²⁻ + ½ H₂↑). Despite that, no external oxygen is required to oxidize structural Fe²⁺, or other transition metals in phyllosilicates, there is still limited awareness and knowledge of this field in terms of modeling the high-temperature processes shaping Earth.

To study and explain the mechanism of oxidative dehydrogenation, a Mg-Fe²⁺ series of chlorites, biotite, and minnesotaite were thermogravimetrically heated in dynamic and static conditions between 25–1050 °C under nitrogen and synthetic air gas flow, at atmospheric pressure. To trace the volatiles that evolved during heating, especially H₂ and H₂O, a thermogravimetric analyzer (TG) was coupled with a quadrupole mass spectrometer (MS). Selected alteration products collected after TG-MS experiments were analyzed ex-situ by Mössbauer spectroscopy, X-ray diffraction, and Infrared spectroscopy. Under inert gas conditions and dynamic heating, all the Fe³⁺-containing minerals tested revealed simultaneous liberation of H₂O and H₂ as products of dehydroxylation and dehydrogenation, respectively. H₂ release was accompanied by Fe²⁺ oxidation. The tested minerals show a wide temperature range of dehydrogenation, from 400 to 900 °C, but under the geologic timescale of reaction, the temperature can be much lower. Isothermal heating favored dehydrogenation by decreasing its temperature and leading to almost complete oxidation of Fe²⁺ by removing almost all available H₂. Under oxidizing gas conditions, despite a high oxygen fugacity, oxidation of Fe²⁺ was proceeding also through dehydrogenation. Hence, oxygen served as a sink for hydrogen radicals at the sample surface only and, as a consequence, an excess of H₂O was produced in the carrier gas. Dehydrogenation led to the formation of an “oxy” – phase without a breakdown of the structure during thermal decomposition. After the structural breakdown, enhanced dehydrogenation resulted in maghemite and hematite crystallization, while minor dehydrogenation resulted in ferric pyroxene or ferric spinels formation. This work comprises relevant studies regarding dehydrogenation and summarizes the thermal decomposition of Fe²⁺-bearing phyllosilicates. To investigate dehydrogenation by TG-QMS analysis, new methodological approaches were designed. If dehydrogenation proceeds with such ease in laboratory conditions, it raises several as to its consequences in geological environments, e.g. on crystallization conditions of rocks and minerals, abiotic methane production, the sources of ferric iron in BIFs, and the application of Fe³⁺-minerals as environmental indicators etc.

VALORIZATION OF MINE WATERS: SECONDARY SOURCE OF RARE EARTH ELEMENTS IN THE IBERIAN PYRITE BELT.

León Rafael¹, Macías Francisco¹, Cánovas Carlos R.¹, Pérez-López Rafael¹, Ayora Carlos², Nieto José Miguel¹, Olías Manuel¹

¹Department of Earth Sciences and Research Center on Natural Resources, Health and the Environment (RENSMA), University of Huelva, Spain, ²Institute of Environmental Assessment and Water Research, CSIC Barcelona, Spain

Exposure of sulfides to atmospheric conditions produces Acid Mine Drainage (AMD), which is one of the most prevalent and damaging environmental problems worldwide due to their contribution of metal(loid)s to water resources during hundreds and even thousands of years after the cessation of mining activity if control measures are not implemented. Therefore, AMD treatment is an environmental necessity, but could also be considered a strategic alternative as a secondary source of rare earth elements (REE), due to the high concentration of these elements and their preferential enrichment in middle REE (MREE), which have a higher economic potential. The knowledge of the hydrogeochemistry of REE in AMDs and their distribution using normalized patterns would help to discriminate the most potentially marketable AMD sources. Focusing on this fact, and on the analysis of the economic potential and the possibilities of valorization of mine waters, samples have been collected from different AMD sources in the Iberian Pyrite Belt (IPB), where about 1 m³/s of AMD is annually generated as a result of poor mining management that has historically occurred in the region. Due to high annual loads of elements such as Al (6600 ton), Zn (1600 ton), Cu (600 ton), Co (26 ton), Ni (10 ton), LREE (10.7 ton/yr), MREE (2.1 ton/yr), HREE (1 ton/yr), Y (3.7 ton) or Sc (0.7 ton), AMDs of the IPB would have an economic potential of 24.1 M\$/yr (being REE 22.6% of this potential). Nevertheless, the technical and economic limitations would impose a more realistic value of 4.2-10.3 M\$/yr. The magnitude of this economic potential cannot be compared with active mines, however, the longevity of the AMD generation processes and the need to achieve an environmental improvement make valorization of these leachates an interesting option to recover metals, which would help offset the construction and operation costs of treatment plants, improving notably the quality of the receiving water bodies in abandoned mining sites.

CRYSTAL STRUCTURE AND SHORT-RANGE ORDERING IN JANCHEVITE, A LAYERED V-PB OXYCHLORIDE

Lepore Giovanni Orazio¹, Bonazzi Paola¹, Bindi Luca¹, D'Acapito Francesco²

¹Earth Science Department - University of Florence, Italy, ²IOM-OGG, CNR, France

Janchevite, the V-analogue of parkinsonite, is one of the recently described layered lead oxychlorides. From a structural point of view, these minerals are characterized by litharge blocks, made of layers of edge-sharing OPb₄ tetrahedra, alternated with sheets of Cl⁻ ions. Electroneutrality is attained in several ways: substitution of OH⁻ for O²⁻ in the PbO layer; insertion of Pb atoms in the chloride sheet (in form of square planar PbCl₄ groups); substitution of Pb²⁺ by Mo⁶⁺, I³⁺, I⁵⁺, W⁶⁺; removal of some OPb₄ tetrahedra and possible insertion of groups such as SO₄²⁻, SiO₄⁴⁻, AsO₄³⁻, BO₃²⁻. These balancing defects may be ordered (as in the case of *e.g.* vladkrivovichevite, erikjonssonite, sahlinite, and kombatite) or disordered (as in *e.g.* asisite, schwartzembergite, and parkinsonite). Analogously to parkinsonite, janchevite has been previously described as disordered (tetragonal *I4/mmm* substructure); however, due to the low diffraction quality of crystals, no structural determination has been reported to date. To further improve our knowledge on layered lead oxychlorides, we performed a multi-technique investigation on janchevite from the type locality (Kombat mine, Namibia) by means of single-crystal X-ray diffraction (SC-XRD), electron probe micro-analysis (EPMA), and X-ray absorption spectroscopy (XAS). Preliminary EPMA data yielded an average chemical composition of PbO 91.82, V₂O₅ 1.08, As₂O₅ 0.95, MoO₃ 2.13, SiO₂ 0.50, Cl 4.09 total 100.57 wt% indicating that the studied crystals bear significant amounts of As, other than V, Mo and Si. The average empirical formula based on (Pb+V+Mo+Si+As)=8 apfu is Pb_{7.24}V_{0.21}As_{0.15}Mo_{0.26}Si_{0.15}Cl_{2.03}O_{8.18} with 5+ cations prevailing as Pb substituents.

Several, unsuccessful attempts to observe superstructure reflections with long exposure times were made on a single crystal diffractometer equipped with a CCD detector. The crystal quality was however good enough to refine the average structure of janchevite (space group *I4/mmm*). Similarly to schwartzembergite and parkinsonite, we found a residual electron density peak at ~0.3 Å from the Pb(2) atom which can be assigned to the substituent cations. The lack of long-range ordering determination concerning the cationic substitutions prevents to obtain meaningful information on the coordination of V, Mo, As, and Si. To understand the local coordination of these cations, XAS data were collected at the K-edges of V, As, and Mo. XANES (X-ray absorption near-edge structure) data at V K-edge confirm that V is present as V⁵⁺ and show that V local environment in janchevite is extremely close to that of vanadinite, thus as VO₄³⁻ groups as in kombatite. As atoms in janchevite are also in 4-fold coordination as confirmed by the close similarity of the XANES region with that of adamite and by the EXAFS (extended X-ray absorption fine structure) fit, which leads to an As-O mean bond length of 1.69 Å and an estimated coordination number of 4. EXAFS data at Mo K-edge indicate an average Mo-O distance of 1.86 Å, typical of Mo in 5-fold coordination. The XANES region supports this possibility as testified by the increased intensity of the pre-edge peak, compared to that of octahedrally coordinated Mo, associated with the loss of the center of symmetry.

PREBIOTIC SYNTHESIS BY ELEMENTAL SULFUR (α -S₀) IN TERRESTRIAL HOT SPRINGS

Li Yan¹, Li Yanzhang¹, Lu Anhuai¹, Ding Hongrui¹, Wang Changqiu¹

¹School of Earth and Space Sciences, Peking University, China

The prebiotic synthesis of simple organic molecules from inorganic carbon sources has sustainably supplied base materials for further inoculation of complex life substances, which ultimately developed into primitive life forms. However, the pathways and environments that could have given rise to primitive organic molecules have been always in dispute. Although there is geological fossil evidence to support the theory of the possible origin of life in terrestrial hydrothermal systems, there has been a lack of reliable experimental and theoretical models to reveal the possible conditions and pathways for the formation of primitive small biomolecules. We demonstrated that elemental sulfur (α -S₀), as the dominant mineral in terrestrial hot springs, can reduce carbon dioxide (CO₂) into formic acid (HCOOH) under ultraviolet (UV) light below 280 nm. The semiconducting S₀ is indicated to have a direct bandgap of 4.4 eV. The UV-excited S₀ produces photoelectrons with a highly negative potential of -2.34 V (versus NHE, pH 7), which could reduce CO₂ after accepting electrons from electron donors such as reducing sulfur species. Simultaneously, UV light breaks sulfur bonds, giving rise to the surface-active sulfur radicals and promote the chemical adsorption and electron transfer of CO₂ on the mineral surface. Assuming that terrestrial hot springs covered 1% of primitive Earth's surface, S₀ at 10 μ M could have produced maximal 10⁹ kg/year HCOOH within 10-cm-thick photic zones, underlying its remarkable contributions to the accumulation of prebiotic biomolecules.

ENRICHMENT AND DISTRIBUTION OF HAZARDOUS TRACE ELEMENTS (HTES) IN FLY ASH FROM A COAL POWER PLANT IN SHANXI, CHINA

Liu Yunxia¹, Tajcmanova Lucie¹, Sun Beilei², Zeng Fangui², Jia Peng²

¹Earth Sciences, Heidelberg University, Germany, ²Earth Science and Engineering, Taiyuan University of Technolog, China

During the utilization and disposal of fly ash, HTEs in it can bring risks for human health and contaminate the surrounding environment. Swaine (2000) pointed out that 26 trace elements in coal could raise environmental concerns, including As, B, Ba, Be, Cd, Cl, Co, Cr, Cu, F, Hg, Mn, Mo, Ni, P, Pb, Sb, Se, Sn, Th, Tl, U, V, I, Ra, and Zn. According to their partitioning behavior, the elements in Group 1 don't vaporize and be equally distributed in fly ash and bottom ash, such as Cr, Co and Mn, etc. The elements in Group 2 are volatile and can be prone to absorb or deposit on the surface of small particles with the decrease in flue gas temperature, such as As, Pb, Cd, Cu, and Zn, etc. The elements in Group 3 have high volatility and are mainly emitted in a gaseous state, such as Hg, Br, Cl. There are many elements that show intermediate partitioning behavior between Group 1 and Group 2 (Clarke, 1992). Thus Co, Cr, Cu, Mo, Ni, U, V (intermediate elements), As, Pb, Cd, Cu, Zn (in Group 2), and Mn (in Group 1) are chosen in this study. In order to comprehensively understand their enrichment and distribution characteristics in fly ash, a common pulverized coal fly ash collected from the Gujiao power plant (GJFA) was investigated. GJFA was separated into eight size fractions (0.05, 0.10, 0.15, 0.20, 0.25, 0.30, 0.40 mm), five fractions (1.60, 1.90, 2.2, 2.50 g/cm³), and three-phase fractions (magnetic particles, glass phases and mullite+quartz (MQ)). The relative enrichment factor (RE) index was introduced to compare the enrichment characteristics of HTEs in size, density, and phase fractions. Results show that almost all HTEs obtain maximum RE in fine particles. But RE of Mn, Co, and Fe increase with particle size, which is related to their closed atomic radius and the exist of Fe-Al-Si glass in coarse particles. The Fe-bearing glasses have also been detected by Scanning Electron Microscope. HTEs are enriched in particles with large density, and RE of Mn, Co, Ni, and Fe sharply rise when the density above 2.20 g/cm³. Because of the large mass fraction of glass, most of HTEs are distributed in it. The distribution fractions of Co, Ni, As in magnetic particles are much higher than V, Cr, Cu, Zn, U, Mo, Cd. The concentrations of all elements in MQ are lower than the original fly ash. And Cr, Ni, V are relatively enriched in MQ compared to other elements.

IS THERE A MISCIBILITY GAP BETWEEN FLUORAPATITE AND FLUORBRITHOLITE-(Ce)?

Lorenz Melanie¹, Harlov Daniel E.²

¹Institute of Geoscience, University of Potsdam, Germany, ²Chemistry and Physics of Earth Materials, GFZ Geman Research Centre for Geoscience, Germany

Over the past decade, evidence for a miscibility gap between fluorapatite (FAP) and fluorbritholite-(Ce) (FBri) has been documented in a series of natural occurrences. Miscibility gaps were inferred by reports of significant compositional gaps between Ca + P (FAP) and REE + Si (FBri) chemical components in mainly late-magmatic mineral assemblages. The observation of a 4 apfu wide compositional gap between FAP-FBri coupled with exsolution textures of FAP in FBri and vice versa at the Rodeo de los Molles REE Prospect provide the latest and strongest indication that a solvus exists between the two mineral end members. In this study we explore the existence of a miscibility gap as a function of temperature between FAP and FBri via a series of simple experiments performed at 500°, 600°, 700°, and 1100 °C and 200 MPa, utilizing a series of combinations involving synthetic CePO₄ or FAP and CeF₃ plus H₂O and SiO₂ and a series of reactants, i.e. Na₂Si₂O₅, NaOH, NaF, CaF, KOH, and Ca(OH)₂. Reaction products were evaluated using BSE imaging and analysis on the electron microprobe. Experiments involving CePO₄ and Na₂Si₂O₅ were the most reactive with a pervasive replacement of CePO₄ by FBri. Use of NaOH resulted in the formation of moderate amounts of FBri. Experiments containing CeF₃ and synthetic FAP resulted in minor incorporation of FBri in fluorapatite. Experiments involving either CePO₄ or FAP and CeF₃ with KOH and Ca(OH)₂ produced neither FBri nor FAP, suggesting that Na might play a major role in the formation of FBri. On a T vs FAP-FBri composition plot, the miscibility gap of natural samples is situated between FAP₉₂FBri₈ and FAP₃₀FBri₇₀ at T below 350 °C. At T above 350 °C the gap narrows down to FAP₈₀FBri₂₀ and FAP₆₈FBri₃₂. In the experiments, FBri-(Ce) shows a continuous compositional range from FAP₇₈FBri₂₂ to FAP₂₈FBri₇₂ for T = 500 °C, FAP₇₆FBri₂₄ to FAP₅₂FBri₄₈ for T = 600 °C and FAP₈₀FBri₂₀ to FAP₆₀FBri₄₀ for T = 700 °C. This indicates that there is no miscibility gap ≥ 500 °C between fluorapatite and fluorbritholite-(Ce). Data from Budzyn et al. (2015) experiments furthermore show a continuous compositional range for FBri-(Ce) of FAP₈₅FBri₁₅ to FAP₅₇FBri₄₃ at T = 350 °C. This would imply that any miscibility between FAP and FBri in nature occurs only at T below 350 °C.

CHARACTERIZATION OF CIS- AND TRANS-VACANT CONFIGURATION IN THE OCTAHEDRAL SHEET OF HIGH PURITY SMECTITES

Lorenzo Adrián¹, García-Vicente Andrea¹, Morales Juan¹, García-Romero Emilia^{2,3}, Suárez Mercedes¹

¹Department of Geology, University of Salamanca, Plaza de la Merced, s/n, 37008 Salamanca, Spain, ²Department of Mineralogy and Petrology. Complutense University of Madrid. C/José Antonio Novais, 8 28014 Madrid, ³Geoscience Institute, CSIC-UCM, 28014 Madrid

Smectites are phyllosilicates characterized by a 2:1 type structure composed of two tetrahedral sheets and one octahedral sheet in between. Furthermore, they have a layer charge between 0.6 and 1.2 per unit cell (p.u.c.) compensated by hydrated cations in the interlayer. The occupancy in the octahedral sheet determines the trioctahedral or octahedral character of the smectite: if the 3 octahedral positions per half unit cell are occupied, the smectite is trioctahedral, however, if only 2 octahedral positions are occupied and one octahedral position remains vacant, the smectite is dioctahedral. When the vacant sites transversely to the hydroxyl groups, the smectite has a trans-vacant (tv) configuration, but when the vacant sites are adjacent to one of the octahedrons, the smectite has cis-vacant (cv) configuration. The most important difference between cv and tv configurations is the dehydroxylation temperature (TDHX). In smectites with cv configuration, the dehydroxylation occurs within the range of temperatures between 650-700°C, while the dehydroxylation in the smectites with tv occurs at temperatures of 500-550°C. Knowing the vacant configuration, that is, the configuration of the octahedral sheet, helps us predict the properties of smectites. In this work we study 8 smectite samples: APA, COU(V), MILNa, Nau1, Nau2, PUT, SAN, and SUD. A mineralogical characterization by X-ray diffraction (XRD) and a crystallochemical characterization by analytical electron microscopy (AEM) with transmission electron microscopy (TEM) were done. The samples were also analyzed by thermogravimetric and differential thermal studies to know the cv and tv configurations. The XRD characterization showed that all samples are high purity bentonites mainly composed of smectite group minerals and only a small amount of quartz and feldspars as impurities. Moreover, the AEM-TEM analyses showed that the samples are dioctahedral smectites within the montmorillonite-beidellite series, with a variable layer charge between -0.89 and -0.42 p.u.c.

The proportion of cv and tv configurations of the samples were calculated by fitting the derivative thermogravimetry curves between 300-900°C using the Fityk program. The peak that represents the first weight loss in the DTGs of all samples is related to the interlayer water dehydration and its position depends on the exchangeable cations. Afterward, in the temperature range between 500-700°C, another weight loss peak was present, and it is related to the dihydroxylation, so it depends on the cv and tv configuration. Only 5 samples have a low-temperature weight loss peak (tv), while the rest of the samples have their peak with low and high-temperature influences (tv/cv or cv/tv) indicating a mixture of vacants. According to the Emmerich's (2013) classification, the samples have been divided in 3 groups depending on the proportion of cv and tv positions: a) 100% tv: COU(V), NAU1, NAU2, PUT, and SAN; b) tv/cv: APA and SUD; and c) cv/tv: MILNa.

Keynote

IN-SITU DAC EXPERIMENTS: WINDOWS INTO THE COMPOSITION AND PROPERTIES OF SLAB-DERIVED FLUIDS AND MELTS

Louvel Marion¹, Sanchez-Valle Carmen¹, Farsang Stefan², Rosa Angelika³, Anzellini Simone⁴

¹Institute for Mineralogy, WWU Muenster, Germany, ²Dpt. of Earth Sciences, University of Geneva, Switzerland, ³European Synchrotron Radiation Facility, France, ⁴Diamond Light Source, United Kingdom

Slab-derived fluids and melts are key to the geochemical transfer ongoing at subduction zones. While petrological and fluid/melt inclusion studies provide some qualitative constraints about their composition and potential effects on mantle wedge fO₂ or arc magma composition [1,2,3], their actual physico-chemical properties at typical slab dehydration and melting depth remain poorly constrained. This is mostly due to the difficulty in preserving their high P-T chemistry when returning natural samples to the surface, and in quenching and analyzing experimental run products with conventional technics. In-situ spectroscopy in diamond-anvil cells enables us to overcome issues associated with quenching and probe the chemical and structural properties of slab-like fluids and melts directly at the P-T conditions relevant to subduction zones (300-800°C and 1-7 GPa). Especially, in-situ Raman and synchrotron X-ray absorption (XAS) may provide information about the speciation of volatiles (C, S, N) and trace elements in fluids and melts, and thus enable describing the mechanisms that control geochemical fluxes from the slab to the mantle wedge [4,5]. Additionally, Raman and synchrotron X-ray fluorescence (SXRF) may be used to quantify mineral solubilities or the preference of trace elements for fluids or melts [6,7]. In this contribution, we will review in-situ SXRF and XAS experiments we conducted over the last ten years to constrain the fate of trace elements (Zr, REE, Zn) upon slab dehydration and melting [5,7,8] and the subduction zone cycle of volatiles (C and halogens)[9,10]. Then, we will discuss new options available to develop the study of mineral solubility and trace elements speciation to P-T conditions relevant to the deeper subduction cycle (600-1000°C, 4-10 GPa). Altogether, these experiments provide the empirical constraints necessary to develop and test numerical models of high P-T fluid- or melt-induced processes [11,12] and thus bring us closer to quantitative modeling of volatiles and trace elements fluxes from the slab to the mantle wedge and ultimately the volcanic arc.

References: [1] Frezzotti and Ferrando, 2015. *Am. Min.* 100, 352-377. [2] Schwarzenbach et al., 2018. *Scientific Reports* 8, 15517. [3] Spandler and Rirard, 2013. *Lithos* 170-171, 208-223. [4] Facq et al., 2014. *GCA* 132, 375-390. [5] Louvel et al., 2013. *GCA* 104, 281-299. [6] Borchert et al., 2010. *Chem. Geol.* 276, 225-240. [7] Louvel et al., 2014; *Am. Min.* [8] Farsang et al., 2021. *Chem. Geol.* 578, 120320. [9] Louvel et al., 2020. *Solid Earth* 11, 1145-1161. [10] Farsang et al., under review. [11] Huang and Sverjensky, 2019. *GCA* 254, 192-230. [12] Zhong et al., 2020. *G3* 21.

Keynote

THE ROLE OF FLUID AND DEFORMATION IN THE GENERATION OF OUTCROP-SCALE METAMORPHIC PRESSURE VARIATIONS

Luisier Cindy¹, Ballèvre Michel¹, Vaughan-Hammon Joshua², Baumgartner Lukas², Duretz Thibault¹, Schmalholz Stefan²

¹Géosciences Rennes, University of Rennes 1, France, ²ISTE, University of Lausanne, Switzerland

Heterogeneous metamorphic pressure (P) estimates are frequently reported in juxtaposed rocks from coherent tectonic units in orogens. The interpretation of metamorphic P variations is currently one of the hottest debates in the metamorphic petrology community because it is challenging a long-established paradigm. The lithostatic P paradigm enables converting the metamorphic P directly into the rock's burial depth and, hence, quantifying the rock's burial and exhumation history.

The Internal Crystalline Massifs of the European Alps belong to the southernmost tip of the former Briançonnais microcontinent and represent a part of the continental crust that underwent eclogite facies metamorphism during the Alpine orogeny. The Monte Rosa nappe and the Gran Paradiso unit consist of Variscan and older polymetamorphic paragneisses, which were intruded by Permian-age granitoids. The granites locally underwent hydrothermal alteration, leading to the formation of whiteschists during Alpine orogeny. The strain intensity and metamorphic record are heterogeneous in both units, with Alpine peak metamorphic pressure variations up to 0.8 GPa recorded at the outcrop scale. In the Monte Rosa nappe, phase equilibrium modeling indicates that the metasomatic whiteschist recorded a peak P of 2.2 GPa, whereas microtextural, as well as silica in phengite barometry in metagranites, indicate a max. P of 1.6 GPa. In the Gran Paradiso unit, paragneisses from a shear zone recorded a peak P of 1.9 GPa, deduced from phase equilibrium modeling, whereas the paragneiss not affected by Alpine deformation records a max. P of 1.4 GPa. Based on the confrontation between geological data, which includes field observations, petrography, and geochemistry with numerical thermo-mechanical models, we discuss the potential causes of such large discrepancies in recorded peak pressure. We explore the role of the following factors on the development and preservation of high-pressure mineral assemblages: i) H₂O (under-)saturation conditions of the protolith and ii) strength heterogeneities. Based on thermodynamic modeling, we discuss the evolution of prograde reactions in rocks with limited H₂O availability. Alternatively, we use thermo-mechanical numerical models to discuss the deviation from the lithostatic P due to stress heterogeneities developing in rocks with contrasting mechanical properties during deformation.

HP-UHP FLUID INCLUSION POST-ENTRAPMENT EVOLUTION PREDICTED BY MOLECULAR AND ELECTROLYTIC FLUID THERMODYNAMIC MODELS

Maffeis Andrea¹, Ferrando Simona¹, Connolly James Alexander Denis², Groppo Chiara¹, Castelli Daniele¹, Frezzotti Maria Luce³

¹Earth Science, University of Turin, Italy, ²Earth Science, ETH Zurich, Switzerland, ³Environment and Earth Sciences, University of Milan-Bicocca, Italy

A reliable characterization of the fluids released from a subducting plate is of primary importance to understand the processes that regulate the long-term chemical cycles. Ultrahigh-pressure (UHP) fluids are composed of solvent COHNS molecular volatiles and by solute non-volatile elements bounded to inorganic and organic species. Both direct (fluid inclusion, FI) and indirect (thermodynamic modeling, TM) approaches to study UHP fluids have reliability issues: i) post-trapping processes can affect the chemical composition of the FI, ii) the relatively few applications make the electrolytic-fluid TM still a poorly tested method to reconstruct subduction fluid compositions. In this work, we evaluated compositional data from primary FI trapped within UHP diopside from a chemically simple (CMFS-COHS) marble showing evidence for multiple events of mineral dissolution-precipitation (Brossasco-Isasca Unit, Dora-Maira Massif, Italian Western Alps). These FI are tri-phase multisolid aqueous inclusions (5-25 μm in diameter) consisting of $\text{H}_2\text{O}_{\text{Liq}}$ (with traces of dissolved chlorides) + different kinds of solids ($\text{Cc}/\text{Mg-Cc} \pm \text{Tlc} \pm \text{Dol} \pm \text{Serp} \pm \text{Tr} \pm \text{Py} \pm \text{Gr}$) + bubble ($\text{H}_2\text{OV} \pm \text{N}_2 \pm \text{CH}_4$). Classical molecular-fluid TM allowed to model post-trapping reactions between FI and host diopside (i.e., discrimination among daughter, step-daughter, and incidentally trapped minerals). Electrolytic-fluid TM allowed modeling the chemical composition of the peak solute-bearing aqueous fluid (H_2O : 88.5 wt%; solutes: 11.34 wt%; $\text{CO}_2 + \text{H}_2\text{S} + \text{CH}_4$: 0.17 wt%) generated by progressive rock dissolution. The comparison between the modeled fluid composition with that reconstructed from FI allows to recognize the kind and extent of post-trapping chemical re-equilibration that occurred within UHP FI. Applying this multidisciplinary approach, we demonstrate i) that the most impacting post-trapping process in UHP FI is the H_2O loss, with consequent preservation of the geochemical information in those FI lacking relevant post-trapping host-diopside chemical contamination; ii) that the electrolytic-fluid TM is highly supportive of the classical FI study to retrieve geochemical information on deep subduction fluids.

ELECTROLYTIC THERMODYNAMIC MODELLING OF FLUID SPECIATION IN UHP MARBLE (CFMS-COHS) AS A FUNCTION OF fO_2 : IMPLICATION FOR C AND S TRANSFER IN SUBDUCTION FLUIDS

Maffei Andrea¹, Ferrando Simona¹, Connolly James Alexander Denis², Groppo Chiara¹, Castelli Daniele¹, Frezzotti Maria Luce³

¹Earth Science, University of Turin, Italy, ²Earth Science, ETH Zurich, Switzerland, ³Environment and Earth Sciences, University of Milan-Bicocca, Italy

Element speciation in subduction fluids controls the transport efficiency of elements from the down-going slab to the overlying mantle wedge. Elemental speciation is controlled, in rock-buffered systems, by P-T- fO_2 and bulk-rock composition. Elements like C and S are characterized by a wide range of possible valence states (8), so they are crucial in regulating the redox state of the mantle wedge and, consequently, of the upper-plate volcanism. Carbonate successions and carbonate-rich sediments (with up to 20% vol of organic C) represent ~ 70% of the total subducted carbon, with the rest occurring in the thicker altered oceanic crust and, only limitedly, by the underlying serpentinitized peridotite. However, dominant carbonate sediments are only marginally considered in the modeled subduction processes, mostly because of the lack of relevant decarbonation reactions at high to ultra-high pressure (HP-UHP) conditions. Similarly, because S is considered to be primarily subducted at UHP conditions as sulfides or sulfates (depending on the redox state of the rock) within the altered oceanic crust, the S input from dominant carbonate sediments has been rarely considered.

To address the role of dominant carbonate sediments on the C and S long-term cycles, we conducted electrolytic-fluid thermodynamic modeling of the fluid phase in equilibrium with a UHP impure marble (simple CFMS-COHS chemical system) from the Brossasco-Isasca Unit (Dora-Maira Massif, Western Alps). This marble experienced multiple carbonated dissolution-precipitation events during active subduction at HP-UHP conditions. The study of this natural sample allows to link the thermodynamically modeled HP-UHP evolution, of both rock and fluid, to the HP-UHP mineral assemblages and related fluid inclusions. Using the bulk composition of the studied marble, we modeled the chemical evolution of the fluid along the prograde P-T path (from ~490°C-1.5 GPa to ~730°C-4.3 GPa) and of at different fO_2 (between +2 and -2 from the FMQ buffer). At changing P, T, and fO_2 conditions, C and S speciation and concentration in the fluid are different. At oxidized conditions, C and S are speciated as HCO_3^- (with minor CO_3^{2-}) and SO_4^{2-} , respectively. At reduced conditions, C is speciated not only as HCO_3^- , but also as carboxylic acids and hydrocarbons, while S is predominantly speciated as H_2S and HS^- . The dissolution of carbonate-dominated sediments is an effective process for the mobilization of both C and S, with C being more easily released at reduced conditions and S at oxidized conditions instead. Thus, dissolution is a more effective process than decarbonation and desulfurization reactions in releasing C and S during subduction at sub-arc depths.

LOW P PARTIAL MELTING OF METAPELITES DURING CONTACT METAMORPHISM IN THE FORCEL ROSSO-MOUNT IGNAGA ZONE OF THE ADAMELLO MASSIF (NORTHERN ITALY)

Magnani Lorenzo¹, Farina Federico¹, Pezzotta Federico², Dini Andrea³, Mayne Matthew⁴, Bartoli Omar⁵

¹Earth Sciences, Università degli Studi di Milano, Italy, ²Museo di Storia Naturale di Milano, Italy, ³Istituto di Geoscienze e Georisorse, CNR, Italy, ⁴Earth Sciences, Stellenbosch University, South Africa, ⁵Geosciences, Università degli studi di Padova, Italy

Partial melting of metapelitic lithologies in thermal aureoles around shallow felsic intrusions is localized to the first hundreds of meters from the magmatic body and its diagnostic features are often cryptic. The contact aureole of the post-collisional metaluminous tonalitic to granodioritic Adamello pluton (Eocene sup.) at Forcel Rosso-Mount Ignaga imprinted an unmetamorphosed continental to the marine sedimentary succession of Permian to Triassic age. Disorganized melt patches and aplitic-pegmatitic dykes and veinlets in the pelitic-psammitic sequence of the thermometamorphosed Permian Verrucano Lombardo formation indicate that diffuse partial melting occurred up to 500m from the contact. In the study area, metamorphic grade increases from phyllites and schists at sub-greenschist and greenschist facies on the top of mount Foppa and in the Fumo valley, to upper amphibolite facies migmatites near the Western Adamello Tonalite (WAT) intrusion (Adamè Valley). Petrological and geochemical variations together with phase equilibria modeling are used to investigate the metamorphic conditions that determined the formation of migmatites. Peak mineral assemblages are composed of Crd+Sil+Bt+Kfs+Pl+Qz+Tur+Mag indicating a pressure of ca. 300 MPa, obtained through phase equilibria modeling, and a peak metamorphic temperature of 700°C, on which phase equilibria modeling and the Na-in-cordierite geothermometer are concordant. Fluid fluxed, fluid assisted and fluid absent partial melting conditions were modeled using R crust for different unmetamorphosed and low-grade metamorphosed pelitic lithotypes. The obtained data suggest that the migmatites are the result of open-system processes in which fluid assisted melting played a major role as only the fluid present models are concordant with mass balance estimations while fluid absent models produce very low melt fractions in the expected P-T field. Geochemical evidence suggests that primary compositional variations characterizing the Verrucano Lombardo pelitic layers control both the amount of melt that was formed and its composition. Metatexites containing abundant deformed paleosome and cordierite have melt-depleted compositions (up to 20vol.% of produced and extracted melt). Diatexites are mainly composed of melanocratic residuum of high An₈₆₋₉₆ plagioclase, high aspect ratio biotite schlieren, fibrolitic sillimanite, back-reacted cordierite, and euhedral schorl-dravitic tourmaline alternated to Kfs+Qz leucocratic levels. These rocks represent layered cumulate products with syn-anatectic flow structures that were formed after 26vol.% of melt was efficiently segregated from the protolith. The B and H₂O-rich anatectic melts were locally lithium enriched and they collected in dilating fractures forming a limited pegmatitic field of similarly oriented barren to Li-rich pegmatites in the Verrucano Lombardo metapelites of the Forcel Rosso-Mount Ignaga zone.

CONFIGURATIONAL ENTROPY AND VISCOSITY OF MAGNESIUM SILICATE GLASSES

Majzlan Juraj¹, Dachs Edgar², Tangeman Jean³

¹Institute of Geosciences, University of Jena, Germany, ²Chemie und Physik der Materialien, University of Salzburg, Austria, ³Corporate Research Materials Laboratory, 3M Company, United States

A series of magnesium silicate glasses was synthesized by aerodynamic levitation with laser melting. The Mg/Si ratios of the glasses correspond roughly to the compositional variation between enstatite (MgSiO₃) and forsterite (Mg₂SiO₄). The glass spherules were examined by optical microscopy, powder X-ray diffraction, and electron microprobe analyses, to ensure their glassy state and to determine their precise chemical composition. Relaxation calorimetry was used to measure low-temperature heat capacity (C_p) of all glasses. Integration of (C_p/T)dT gave entropy of the glasses at T = 298.15 K. Interestingly, C_p of the glasses is higher than the C_p of the corresponding crystals (or crystal mixtures) at T < 200 K but drops below the C_p of crystals at higher temperatures. High-temperature C_p was measured by differential scanning calorimetry. The glasses are fragile and crystallize rapidly upon entering the region near the glass transition. The glass-transition temperatures were therefore taken from estimates from earlier literature. Heat capacity data for the crystals were taken from literature; enthalpies of fusion were used to calculate entropies of fusion at the fusion temperature. There is notable scatter for the enthalpies of fusion for both enstatitic and forsteritic compositions. Adding all data together, we calculated the configurational entropies of the glasses at their glass-transition temperature: S_{conf}(enstatitic glass) = 16.8 J/mol·K, S_{conf}(forsteritic glass) = 1.9 J/mol·K. The low value of S_{conf}(forsteritic glass) agrees with previous predictions that such entropy should be very close to 0 J/mol·K. We used the expression $\log \eta = A + B/[TS_{\text{conf}}(T)]$, the available experimental viscosities (η) and the temperature-dependent configurational entropy from this work to describe viscosity of forsteritic liquids and glasses. The parameters for this equation are A = -2.3389 and B = 76459, with $S_{\text{conf}}(T) = 1.8971 + (83.739 \ln(T/1040))$. These data can be used to support geological and geophysical models of deep crust and mantle of the Earth.

IANUS BIFRONS: THERMOCHRONOLOGY OR PETROCHRONOLOGY?

Malusà Marco Giovanni¹, Danišík Martin², Villa Igor Maria¹

¹DISAT, Università di Milano Bicocca, Italy, ²Institute for Geoscience Research, Curtin University, Perth, Australia

Thermochronology is based on the assumption that age measurements can be uniquely inverted to give a time-temperature history, which in turn is based on the assumption that the only process occurring in rocks is Fick's Law diffusion. Historically, the first application of this approach exploited the ability of fission tracks to be annealed at a much lower temperature than the stability field of the chronometer mineral (e.g. apatite). This ensures that temperature is the only cause of age resetting. Thus the observed apatite age can be uniquely inverted to model a time-temperature history [1]. Apatite only rarely precipitates from hydrothermal fluids below 100 °C [2]. The diffusion of radiogenic helium, derived from the alpha decay of eU (uranium + thorium + samarium) out of apatite occurs at even lower temperature than the annealing of fission tracks, as the atomic radius of He is so small that it does not require the movement of structure-forming cations, which track annealing does. A necessary property of any system recording true diffusion, such as a bona fide thermochronometer, is the development of a bell-shaped concentration profile. When helium concentration profiles depart from simple assumptions it is still possible to recover time-temperature histories [3], but at an enormously increased analytical and computational effort. Blanket assumptions on "closure temperature" lose meaning even in the simple case of eU-He ages. Other radiogenic daughters (Pb, Ar, Sr) are all quite resistant to thermal resetting [2]. In fact, they are less mobile in a mineral lattice than are the structure-forming cations due to their higher charge and/or larger radius; the failure to document in sufficient detail a bell-shaped concentration profile leads to contradictory results and unsubstantiated models [4]. Therefore all three of these daughters retain a petrochronological information since the petrological constraints (by PTAX calculations) are based on the major elements, which are all at least as mobile as the radiogenic isotopes. An essential parameter of PTAX calculations is A, the activity of aqueous fluids. Whenever fluids interact with a mineral, retrogression occurs with a reaction rate several orders of magnitude higher than diffusion. Its products can be routinely detected by cathodoluminescence (zircon, K-feldspar), electron microprobe (monazite, muscovite), and PTAX disequilibrium associated with the microtextural and microchemical analysis of replacement phases. These are often <5 µm small and thus escape cursory optical screening. Indeed, the fact that diffusion in micas is much slower than retrograde reaction rates has been independently documented [5, 6, and dozens of references therein]. In conclusion, the forward-looking face of Ianus focuses on turning the petrologic, microstructural, and microchemical observations into a better understanding of the real meaning of isotopic ages.

- [1] Malusà & Fitzgerald (2019) *Fission-Track Thermochronology and its Application to Geology*. Springer.
- [2] Balogh & Dunkl (2005) *Mineralogy Petrology* 83, 191-218.
- [3] Danišík et al (2017) *Science Advances* 2017;3:e1601121.
- [4] Villa (2016) *Chemical Geology* 420, 1-20.
- [5] Malusà & Fitzgerald (2020) *Earth-Science Reviews* 201, 103074.
- [6] Bosse & Villa (2019) *Gondwana Research* 71, 76-90.

SYNTHESIS AND CHARACTERIZATION OF REE- AND Th-RICH MIMETITE $Pb_5(AsO_4)_3Cl$

Maneck Maciej¹, Wudarska Alicja², Sordyl Julia¹

¹Department of Mineralogy, Petrography and Geochemistry, AGH University of Science and Technology, Poland,

²Institute of Geological Sciences, Polish Academy of Sciences, Poland

Minerals of the lead apatite group have been shown to be efficient filters for heavy metals from supergene solutions circulating in the vicinity of ore deposits. Mimetite $Pb_5(AsO_4)_3Cl$, belonging to that group, and its synthetic analogs have been extensively studied in terms of their stability, crystal structures, and major element compositions. However, little has been known about the mineral characteristics of trace element-substituted mimetite. Therefore, we undertook this study in which we characterized synthetic mimetite with substitution of rare earth elements (REE), Sc, Y and Th.

Synthetic analogs of REE-substituted mimetite and pure mimetite (for comparison purposes) were precipitated at ambient conditions by dropwise mixing of the aqueous solutions of $Pb(NO_3)_2$, $NaH_2AsO_4 \cdot 7H_2O$, NaCl, and a standard solution of 14 lanthanide-group elements, Sc, Y, and Th in HNO_3 . The experiments were conducted at pH = 3 that was adjusted using NaOH. Both synthetic products were subsequently characterized using scanning electron microscope equipped with an energy-dispersive analyzer (SEM-EDS), powder X-ray diffraction (XRD) as well as Raman and infrared (IR) spectroscopy. The syntheses yielded white, very fine-grained precipitates of mimetite mostly consisting of nano-size crystals with morphology typical for mimetite precipitated at these conditions. SEM-EDS analyses revealed also the presence of some REE-arsenate aggregates. These impurities, however, could not be identified in an X-ray diffraction pattern due to their small amounts and/or amorphous nature. XRD data collected in the range between 2 and $100^\circ 2\theta$ at a resolution of $0.02^\circ 2\theta$ showed systematic shift (by $0.01-0.27^\circ 2\theta$) of most of the peaks in REE-substituted mimetite pattern as compared to peak positions recorded for pure mimetite. Unit cell parameters of REE-mimetite refined in hexagonal system ($a = 10.2564 \text{ \AA}$, $c = 7.3975 \text{ \AA}$, $V = 673.92 \text{ \AA}^3$) are smaller than these determined for pure mimetite control sample ($a = 10.2516 \text{ \AA}$, $c = 7.4310 \text{ \AA}$, $V = 676.33 \text{ \AA}^3$). This probably results from smaller ionic radii of trace elements and sodium cations substituting Pb^{2+} according to the reaction of heterovalent substitution: $2Pb^{2+} = REE^{3+} + Na^+$. Raman and IR analyses showed no substantial differences between the spectra collected for both synthetic phases. However, the interpretation of the Raman spectrum recorded for REE-mimetite was inconclusive due to strong fluorescence. The dataset collected within this preliminary study is ambiguous mostly due to a foreign phase observed in SEM, and therefore, it should be seen as the first step towards the detailed characterization of the extent of trace element (REE and Th) substitutions in mimetite. Further study will include modified synthesis protocols as well as wet chemical analyses of the synthetic products.

This research was funded by Polish NCN research grant no. 2019/33/B/ST10/03379.

80 YEARS OF MINERALOGICAL AND CRYSTALLOGRAPHIC HISTORY IN THE COLLECTIONS OF GIUSEPPE SCHIAVINATO AT THE UNIVERSITY OF MILAN

Mangano Chiara¹, Barenghi Fabiana¹, Xiong Miner¹, Milani Sula¹, Merlini Marco¹, Fumagalli Patrizia¹

¹Scienze della Terra, Università degli Studi di Milano, Italy

Giuseppe Schiavinato was an important geologist and mineralogist who contributed to the development of Earth Sciences considerably in Italy. He studied at the University of Padua, then began his academic career at the University of Bari, and finally became professor of mineralogy at the University of Milan, where he was also Rector.

His first scientific work, dating back to the 1940s, focused on the study of the wollastonite deposit of Alpe Bazena (southern Adamello). He investigated the structure of this mineral using the common crystallographic techniques at the time. Thanks to the materials left by him in the archives of the Department of Earth Sciences - 'Ardito Desio', it has been possible to reconstruct the first steps of diffractometric analysis applied to mineralogy, started by the former Institute of Mineralogy, using the first chambers for single crystal roentgenographic experiments.

The wollastonite samples collected by Prof. Schiavinato are still providing materials for studies of current scientific interest on the high-pressure polymorphism CaSiO_3 compound, with important implications for better comprehension in deep geological processes of our planet. The use of the latest generation of micro-source diffractometers, as well as synchrotron radiation, makes it possible to carry out analyses on the same wollastonite samples of smaller sizes inside the Diamond anvil cell (DACs) simulating the mantle conditions.

The wollastonite samples that deposit in the museum's archives have therefore acquired significant values. Not only being systematic examples of mineral collections for educational purposes, but also the witnesses to petrological processes such as contact metamorphism at the Adamello pluton margin. On the other hand, they could also narrate the history of the development of analytical techniques that relate to the scientific discoveries over the last century. For this purpose, it was decided to make an informative video documentary that narrates the scientific activities performed by Professor Schiavinato, not merely to maintain the historical identity of wollastonite, also to build up, for instance, himself, as a symbol of these significant works. In addition, to reveal the development of crystallographic techniques over time, with the mineral wollastonite as "protagonist".

The scheme adopted is suitable as an example for further dissemination activities.

SULFUR PROFILE AND ORE MINERALS ACROSS THE CRUST-MANTLE TRANSITION ZONE (OMANDP ICDP HOLE CM1A)

Marciniak Dariusz¹, Ciałzela Jakub¹, Jesus Ana², Koepke Jürgen³, Pieterek Bartosz⁴, Strauss Harald⁵, Słaby Ewa¹, Prell Marta⁶, Jokubauskas Petras⁷

¹Institute of Geological Sciences Polish Academy of Sciences, Poland, ²Instituto Dom Luiz, LA Faculdade de Ciências Universidade de Lisboa (FCUL), Portugal, ³Intitut für Mineralogie, Leibniz Universität Hannover, Germany, ⁴Institute of Geology, Adam Mickiewicz University, Poland, ⁵Institut für Geologie und Paläontologie, University of Münster, Germany, ⁶Institute of Geological Sciences, University of Wrocław, Poland, ⁷Faculty of Geology; Laboratory of Electron Microscopy μ -analysis and XRD, University of Warsaw, Poland

Hole CM1A of the International Continental Scientific Drilling Program (ICDP) Oman Drilling Project (OmanDP, <https://www.omandrilling.ac.uk/>) drilled through the Crust/Mantle Transition Zone (CMTZ) composed of layered gabbro (0–160 meters below surface, mbs), dunite (160–310 mbs), and harzburgites (310–405 mbs). This drillhole provided an unprecedented opportunity to study the behavior of metals in the CMTZ, where arriving primitive MORB melts extensively react with the mantle. Here, melts, typically enriched with sulfur and chalcophile elements, are supposed to enrich the mantle and lower crust with sulfides.

Sulfide content increases downwards the gabbro sequence from ~0.004 vol.% to ~1.0 vol.% but decreases again from 0.8 vol.% to 0.01 vol.% below the Moho. Sulfur concentrations data measured with an ELTRA CS800 carbon-sulfur analyzer confirm these results with S concentrations increasing from 341 ± 17 ppm, 2sd (standard deviation) to 832 ± 37 ppm, 2sd, in the gabbro section towards Moho decreasing downwards from the Moho towards harzburgites from 475 ± 21 , 2sd ppm to 63 ± 3 ppm, 2sd.

The sulfides in gabbros are mostly pyrrhotites-chalcopyrite-pentlandite assemblages indicating the magmatic origin (56–87%), whereas those in dunite and harzburgite are exclusively hydrothermal. The hydrothermal sulfides are in the order of their abundance chalcopyrite, pentlandite, bornite, chalcocite, digenite, heazlewoodite, millerite, pyrite, sphalerite, and siegenite. We also observed associated native Cu, awaruite, and oxides including ilmenite, magnetite, Cr-magnetite, and Fe-chromite.

Based on electron probe microanalyzer (EPMA) data (4 samples), pyrrhotite (Fe_{1-x}S) shows a metal/sulfur ratio of 0.90–1.02 so part of those may represent low-temperature exsolutions of troilite (FeS). Chalcopyrite exhibits 0.98–1.04 metal/sulfur ratio. Magmatic pentlandite contains <20 wt %, and shows variable Ni/(Fe+Ni) (0.28–0.56) and metal/sulfur (1.03–1.15) ratios. Scanning electron microscope (SEM) equipped with an energy-dispersive X-ray system (EDX) performed on 16 samples provided additional data for secondary pentlandite, which contains 3–62 wt% Co and exhibits a Ni/(Ni+Fe) of 0.40–0.66 and a metal/sulfur ratio of 1.03–1.14. The enrichment in S and sulfides towards the MTZ might result from the melt-mantle reaction as we proposed previously for the Kane Megamullion Ocean Core Complex (Ciałzela et al., 2018). However, most sulfides, especially in ultramafic rocks are secondary. In the next steps, we need to verify whether these sulfides replaced the primary magmatic sulfides or were brought from late-stage seawater-derived fluids. For this purpose, we plan to measure sulfur isotopes in whole rocks and in situ.

The work was funded by the NCN Project no. 2019/33/ST10/03016 to J. Ciałzela.

CHARACTERIZATION OF CERAMIC MATERIALS RESULTING FROM TREATMENT AND RECYCLING PROCESS OF INORGANIC SPECIAL WASTES

Marian Narcisa Mihaela¹, Giorgetti Giovanna¹, Magrini Claudia¹, Salvini Riccardo^{1,3}, Vergani Fabrizio², Capitani Giancarlo², Galimberti Lucia², Zampini Marco², Viti Cecilia¹

¹Department of Physical Science, Earth and Environment DSFTA (UniSi) V. Laterina 8, I-53100, Siena, Italy, ²Department of Earth and Environmental Sciences DISAT, University of Milano-Bicocca, Italy, ³Department of Environment, Earth and Physical Sciences and Centre for GeoTechnologies CGT (UniSi) Via Vetri Vecchi 34, 52027, San Giovanni Valdarno (Arezzo) Italy, ⁴Grinn Solutions s.r.l., via Wanda Osiris 11, 00139, Roma, Italy

Waste production and accumulation are increasing more and more every day all over the world and the current rate of growth is no longer sustainable. In this context, waste valorization and circular economy are among the most impellent themes of debate in politics and science. The Waste Framework Directive with the associated strategies and priorities as Circular economy action plan and the European Green Deal are just few examples of current actions to support the development of new technologies for the solution of the waste problem. In this research, we collaborate with an innovative startup, GRINN s.r.l., owner of patent n. 0001369219 (“Procedimento per realizzare manufatti termoformati, specialmente utilizzando materiali riciclati o di recupero”), released by the Italian Patent and Trademark Office, 11/01/2010), based on which different kinds of inorganic wastes are successfully recycled to realize a ceramic-like material, named Florentite. The patent is based on thermal processing of industrial special wastes, in very high percentages (from 60% to 90%), mixed to suitable additives as amorphous silica and silico-aluminoferrite. Based on the waste nature and the interaction among wastes, additives and the processing temperatures (950-1050°C) that can be slightly changed to produce different Florentite outputs. In this study, we report on the special wastes from Tuscany territory (Italy), particularly gypsum-bearing red muds, deriving from the deactivation of industrial sulphuric acid and Carrara marble powders, and metallurgic slags from the jewelry manufacturing. The characterization of both wastes and Florentite products has been carried out by mineralogical investigations as well as by physical and mechanical tests on the different outputs. Chemical, mineralogical and microstructural characteristics have been determined by X-ray powder diffraction (XRPD), X-ray fluorescence spectroscopy (XRF), thermal analyses (TA), and scanning electron microscopy coupled with energy dispersive spectrometry (SEM/EDS). Physical and mechanical tests (among which tensile and compressive strength resistance, durability/freezing resistance, "Los Angeles" abrasion resistance and "MicroDeval" wear resistance) on the two different Florentite products, respectively deriving from red muds and slags processing, aim to confirm their high technical performance, comparable to traditional ceramics.

REDOX STATE OF HYBLEAN MANTLE XENOLITHS INVESTIGATED BY CRYSTAL CHEMISTRY, NOBLE GASES AND FLUID INCLUSIONS

Marras Giulia¹, Stagno Vincenzo¹, Caracausi Antonio², Frezzotti Maria Luce³, Andreozzi Giovanni Battista¹, Cerantola Valerio⁴, Perinelli Cristina¹

¹Department of Earth Sciences, Sapienza University of Rome, Italy, ²National Institute of Geophysics and Volcanology (INGV, Palermo), Italy, ³Department of Earth and Environmental Sciences, University of Milano-Bicocca, Italy, ⁴European X-Ray Free-Electron Laser Facility GmbH, Germany

The knowledge of the redox state (i.e., the oxygen fugacity, fO_2) of mantle-derived rocks allows modeling the deep volatiles cycle (e.g. C, H, O, N) in the Earth's interior, which, in turn, plays a key role in magma genesis, diamond formation, metasomatism and volcanic degassing. Mantle xenoliths represented by spinel-harzburgite and lherzolite are worldwide distributed and record fO_2 varying between -2 and 0.5 log units with respect to the fayalite-magnetite-quartz (FMQ) buffer. At these conditions, stable fluids might be oxidized (e.g., CO_2 , H_2O) and either exsolve or lower the melting temperature of the surrounding minerals. Fluid inclusions trapped in silicate minerals like olivine represent a snapshot of this volatile circulation in depth, while noble gases (He, Ar, Ne) are useful to infer their mantle source.

We investigated spinel-peridotite xenoliths from the Hyblean Plateau (Sicily) to determine their fO_2 and to characterize their noble gases signature and fluid inclusions. The obtained results are integrated with the thermodynamic reconstruction of the volatile speciation. Two harzburgites and five lherzolites sampled from the Miocene Hyblean tuff-breccia pipe of Valle Guffari (Sicily) were selected in this study. Textural features of the xenoliths and fluid inclusions trapped in olivine were characterized using backscattered electron (BSE) images and petrographic microscope, respectively. Chemical analyses were conducted by electron microprobe, while the oxidation state of iron in spinels was determined by ^{57}Fe Mössbauer spectroscopy, using both in situ synchrotron (ESRF, Grenoble) and conventional (Sapienza University, Rome) devices. Noble gases isotopes were analyzed on about 1 g of olivine grains by single-step in-vacuo crushing coupled with mass spectrometry (INGV, Palermo). Our preliminary results show that, at the equilibrium pressure and temperature (0.9-1.2 GPa and 950-1050 °C), the measured $Fe^{3+}/\Sigma Fe$ ratio in spinel ranges between 0.27 and 0.31 which is higher than values reported in the literature. This finding makes the Hyblean mantle more oxidized than expected, with fO_2 ranging from 0.7 to 1.8 log units with respect to FMQ. At these conditions, on the basis of thermodynamic calculations, the oxidized fluids CO_2 and H_2O are the main components of coexisting fluids. On the other hand, optical observations reveal at least two different generations of fluid (gases) inclusions along with both melt and minerals, often localized along fractures and serpentinized rims. Noble gases data, in particular $^3He/^4He$ (R/Ra), $^4He/^40Ar^*$, and $^4He/^20Ne$ confirm a deep mantle contribution and highlight a possible intriguing relationship between the R/Ra values and the estimated fO_2 . Further analyses are in progress with the aim to shed light on the high fO_2 of the Hyblean spinel-peridotites due to multiple oxidative events.

ARCHAEOLOGICAL ANALYSIS OF THE OBJECTS FROM THE SCALA SANTA (HOLY STAIRS) IN THE CRYPT UNDER THE PIARIST CHURCH IN CRACOW (POLAND)

Marszałek Mariola¹, Gawęł Adam¹, Pachuta Karolina², Buszko Eliza²

¹Department of Mineralogy, Petrography and Geochemistry, AGH University of Science and Technology, Poland,

²Conservation and Renovation Firm Piotr Białko Ltd., Poland

The study presents findings discovered in the Scala Santa (Holy Stairs), located in the crypt under the 18th-century Piarist Church in Cracow (Poland). The crypt was originally designed as a chapel of the Holy Stairs. A metal-framed, transparent reliquary cross containing a particle of the True Cross, and two opaque beads – a decorated, blue bead, and a black one with hole – were analyzed. Non-invasive and non-destructive methods (scanning electron microscopy with energy dispersive spectrometry, Raman microspectroscopy, and X-ray diffractometry) were used to study the chemical composition and structure of these artifacts. The transparent reliquary cross was found to be made of rock crystal and framed with gold-plated silver or an alloy of gold, silver, and copper. The beads are made of glass. Considering the source of the flux, the glass represents forest plant-ashes potash-lime glass – the blue bead, and plant-ashes soda-lime glass – the black bead. Cobalt, probably along with copper, was used to produce the blue hue of the ornamented glass bead; manganese and iron ions were used to produce that of the black bead. Lead was present in both beads as one of the minor components and also as a component of corrosion products (lead silicates and lead chloride hydroxide) on their surfaces. It may have been introduced to improve the properties of the glass, or it could be a component of the raw materials, e.g. ores used as pigments. The concentration of lead compounds in the blue bead engraving may be related to the accumulation of corrosion product in the carving, although it cannot be excluded that the lead compounds were introduced intentionally to emphasize the decoration. Considering the popularity of reliquary crosses made from rock crystal at the turn of the 17th and 18th centuries, the Piarist object may be dated to the beginnings of the use of the Holy Stairs chapel, consecrated in 1733. Different compositions of ash used to make glass (potash and soda, respectively), suggest that beads could be produced in different geographical regions. Throughout the Middle Ages the production of potash-lime glass developed in northern and central European manufacturing centers. However, even though the Venetian glass-making industry traditionally used soda plant ash, potash plant ashes were occasionally applied as well. Thus, this site cannot be ruled out as the site of manufacture of the blue bead. The black bead representing plant-ashes soda-lime glass might have been associated with the Venetian glass-making industry. The beads were produced after the 8th century (introduction of plant ash as a source of alkaline flux), and, at the latest, around 1733 (consecration the chapel of Holy Stairs). However, some artifacts may have been added after this date, so the beads could have been made even later. Lack of official documents confirming the status of non-significant relics (objects in direct contact with a saint or blessed person) or that they were brought to Cracow as souvenirs from the Holy Land hinders the dating of the beads and connection to a specific saint person.

Keynote

DYNAMIC CRYSTALLIZATION IN BASALTIC SYSTEMS: FROM LABORATORY SCALE TO NATURAL PROCESSES

Masotta Matteo¹

¹Department of Earth Sciences, University of Pisa, Italy

Basaltic magmatism is extremely important to investigate the evolution of the Earth's crust and, from a petrologic point of view, is the most intriguing because of the textural and mineralogical variability that basaltic products acquire during solidification. For these reasons, basaltic systems have been an object of experimental investigations, ranging from simple melting and recrystallization studies to technically challenging in-situ observations of crystal nucleation and growth. In the last decades, the interest in the physico-chemical behavior of basaltic melts during solidification is largely increased, ignited by a growing petrological interest for persistently active, open conduit volcanic systems. From a microscopic perspective, the solidification of a basaltic melt into a solid rock is controlled by two concurring processes that are crystal nucleation and crystal growth. The interplay between these two processes is modulated by the rates at which temperature, pressure, and melt-water content change during the ascent of basaltic magmas from crustal depths towards the surface. Yet, there is much to learn about the mechanisms by which textures and phase compositions evolve under the mutual cooperation of these variables or, in a more general sense, as a function of the degree of undercooling. This parameter represents the thermodynamic force controlling the crystal growth and the delay of a crystallizing melt with respect to the textural and chemical features expected at given equilibrium conditions. By investigating the effect of undercooling it is thus possible to model the crystallization of basaltic melts under dynamic conditions that are characteristic of open conduit volcanoes.

In this contribution, the textural and chemical effects of undercooling on the dynamic crystallization of basaltic melts are discussed in light of recent experimental investigations on natural and synthetic systems. Experimental evidences reveal how the textural and compositional features of mafic minerals, such as titanomagnetite and clinopyroxene, are controlled by the rate at which the temperature of the basaltic melt crosses the liquidus temperature and by the varying degree of undercooling during melt solidification. Collectively, the physico-chemical constraints provided by dynamic crystallization experiments conducted on basaltic melts represent a valuable tool to interpret the crystallization conditions of open conduit volcanic systems. In this perspective, some experimentally derived models for estimating the degree of undercooling of crystallizing magmas are tested on natural products erupted at Mt. Etna and Stromboli volcanoes (south Italy), thus demonstrating the reliability of laboratory-based calibrations to reconstruct the dynamic crystallization of natural basaltic systems.

TIME-RESOLVED SYNCHROTRON RADIATION MICROTOMOGRAPHY TO REVEAL THE MICROSTRUCTURAL VARIATIONS INDUCED BY DAP CONSERVATION TREATMENTS ON NOTO LIMESTONE

Massinelli Giulia¹, Marinoni Nicoletta², Colombo Chiara³, Gatta G. Diego², Mancini Lucia⁴, Merlini Marco², Realini Marco³, Possenti Elena³

¹Università degli Studi di Milano, Italy, ²Earth Science, Università degli Studi di Milano, Italy, ³ISPC-CNR, Italy, ⁴Elettra - Sincrotrone Trieste S.C.p.A, Italy

Inorganic-mineral treatments are commonly used in stone conservation to restore the mechanical and microstructural features of decayed stone materials. These treatments act in a water-based solution and partially transform the original minerals of the carbonatic substrate in newly-formed crystalline phases by a dissolution and recrystallization reaction. The reaction products nucleate on calcite grains of the substrate and form a crystal network that reconnects detached stone grains. At the same time, the crystallization of new phases on calcite induces a micrometric variation of pore walls, which in turn determines a change in porosity. Therefore, new advanced insights are needed in order to understand the nature and the extent of the possible microstructural variations induced by inorganic-mineral treatments to treated lithotypes.

Here, synchrotron X-ray radiation micro-computed tomography (SR- μ CT) was applied to monitor the effects induced by the reaction of dissolution and recrystallization of new phases occurring during a conservation treatment based on diammonium hydrogenphosphate (DAP, $(\text{NH}_4)_2\text{HPO}_4$).

This study has been carried out on specimens of Noto limestone, a porous carbonatic lithotype used in historical monuments (Val di Noto, Siracusa, UNESCO's World Heritage List), treated by DAP water-based solutions. Time-resolved (4D) high-resolution SR- μ CT measurements have been carried out at the SYRMEP beamline of the Elettra synchrotron (Basovizza, Italy).

The total porosity of the samples has been investigated in the 4D SR- μ CT datasets and the connected porosity has been separated by the isolated one. The image analysis of volumes of interest (VOIs) showed that the DAP treatments induce morphological variations to the microstructural features of the lithotype. The kinetics of the reaction is ruled by several variables (i.e., free ions availability, specific surface area, microstructural characteristics of the lithotype) and the induced effects are well visible in the features of pore walls. Selected variations were observed on specific classes of pores, depending on their original size and morphology. This may be attributed to the different conditions of crystallization occurring in different pores having specific morphology, size, and connectivity. The quantitative analysis of different VOIs pointed out changes in the porosity (both the total porosity and its components) after the treatment, as well as in the pores connectivity (Euler Characteristics) and their volume size distribution. The particular experimental setup developed in our study allowed us to critically consider the intrinsic microstructural heterogeneity of the Noto fine-grained limestone, due to the presence of fossils. At the same time, it was possible to observe specific microstructural variations during the treatment and to unambiguously attribute them to the peculiar effect of the DAP treatment to the porous substrate of the Noto limestone.

Above all, this study supplies crucial indications for restoration, supporting the application of inorganic-mineral treatments in conservation worksites on the basis of advanced knowledge on microstructural variations induced by DAP conservation treatments.

SAMPLING OF MAFIC MAGMA EVOLUTION THROUGH MEGACRYSTS OF CLINOPYROXENE – AN EXAMPLE FROM EASTERN PART OF CENOZOIC CENTRAL EUROPEAN VOLCANIC PROVINCE

Matusiak-Małek Magdalena¹, Puziewicz Jacek¹, Ntaflos Theodoros², Woodland Alan B.³, Uenver-Thiele Laura³, Büchner Jörg⁴, Grégoire Michel⁵, Aulbach Sonja⁶

¹Institute of Geological Sciences, University of Wrocław, Poland, ²Department of Lithospheric Research, University of Vienna, Austria, ³Institute of Geoscience, Goethe-University, Frankfurt, Germany, ⁴Senckenberg Museum für Naturkunde Görlitz, Germany, ⁵Géosciences Environnement Toulouse, CNRS-CNES-IRD Université Toulouse III, France, ⁶Frankfurt Isotope and Element Research Center (FIERCE), Goethe-University Frankfurt, Germany

Megacrysts of clinopyroxene carried by mafic melts constitute an indispensable source of information on the evolution of magmatic systems, but also on the nature of the underlying mantle. Clinopyroxene megacrysts occurring in Cenozoic mafic alkaline volcanic rocks from the northern margin of the Bohemian Massif (SW Poland, SE Germany) form three groups differing by Mg# and color: 1) the high Mg# (HMg#) megacryst has Mg# = 90.0–91.5 and is transparent, 2) the medium Mg# (MMg#) megacrysts have Mg#=76.8–83.4 and are transparent to greyish, and the 3) low Mg# (LMg#) megacrysts have Mg#=62.2–74.6 and are typically bottle-green.

The HMg# megacryst (only one sample identified) is characterized by a high content of Cr (0.68-0.72 atoms per formula unit) and strong depletion in LREE. The pressure (~1GPa) and temperature (1280 °C) of its formation together with chemical characteristics point to its mantle origin and strong relation to the MORB-like source. This is the first megacryst of this type described in the European lavas and possibly worldwide. The MMg# megacrysts are LREE-enriched, Cr-poor (0.00-0.54 atoms per formula unit), and record fractionation of mafic melts related isotopically to Cenozoic lavas from the study area. Fractionation of the melts responsible for MMg# formation took place at variable pressures and temperatures – from those corresponding to mantle depths (>1 GPa, 1230–1350 °C) to lower/middle crustal values (0.5–0.9 GPa, 1120–1150 °C). The LMg# megacrysts enclose numerous grains of apatite, oxides, and locally pseudomorphs after amphibole. Their strong LREE-enrichment and lack of Cr (0.00-0.05 atom per formula unit) together with positive anomalies in primitive-mantle-normalized Zr-Hf contents suggest their formation from strongly alkaline magmas at lower to middle crust depths (0.4-1.0 GPa). Those melts, despite having chemical characteristics which are extraordinary for Cenozoic magmatism from the northern margin of Bohemian Massif, are isotopically related to this magmatic event.

Our study evidences, that megacrysts of clinopyroxene record valuable information on the evolution of the magmatic system and lithosphere, which is inaccessible neither from magmas nor from xenoliths.

This study was possible thanks to the project no. UMO-2014/15/B/ST10/00095 of Polish National Centre for Science, and to the bilateral Austrian-Polish projects (WTZ PL 08/2018, WTZ PL16). FIERCE is financially supported by the Wilhelm and Else Heraeus Foundation and by the Deutsche Forschungsgemeinschaft (DFG, INST 161/921-1 FUGG and INST 161/923-1 FUGG), this is FIERCE contribution No. 53

METAL ENRICHMENT AS A RESULT OF SUBCONTINENTAL LITHOSPHERIC MANTLE REFERTILIZATION? THE BEFANG XENOLITHS (OKU VOLCANIC GROUP, CAMEROON) CASE STUDY

Mazurek Hubert¹, Matusiak-Małek Magdalena¹, Ciążela Jakub², Pieterek Bartosz³, Puziewicz Jacek¹, Tedonkenfack Sylvain⁴

¹Institute of Geological Sciences, University of Wrocław, Poland, ²Institute of Geological Sciences, Polish Academy of Sciences, Poland, ³Institute of Geology, Adam Mickiewicz University, Poland, ⁴Department of Earth Sciences, Université de Dschang, Cameroon

Sulfides in mantle xenoliths may provide information about the migration of strategic metals, such as Au, Ag, or Cu through subcontinental lithospheric mantle (SCLM). In this study, we discuss a suite of peridotitic xenolith from Befang in the Oku Volcanic Group (OVG), which constitute the northern part of the Cameroon Volcanic Line (west Africa). The sulfides occur in xenoliths of lherzolitic composition, which are divided into two groups based on their crystallographic preferred orientation and rare earth element (REE) contents in clinopyroxene: 1) group I with LREE-depleted clinopyroxenes, which are supposed to crystallize (or recrystallize) due to percolation of MORB-derived melt and 2) group II with LREE-enriched clinopyroxenes deformed with other silicates before melt percolation (Puziewicz et al., 2021, *Contrib. Mineral. Petrol.*).

The sulfides are globular to subglobular magmatic pyrrhotite-pentlandite-chalcopyrite (Po-Pn-Ccp) assemblages enclosed in pyroxenes. Pentlandite occurs as massive crystals separating pyrrhotite from chalcopyrite or forming thin lamellae dispersed in the entire grain. Chalcopyrite occurs typically on the rim of the sulfide grain. The sulfides from group I xenoliths are hosted mainly by orthopyroxenes (84%), whereas the proportion of pyroxenes hosting sulfides in group II are almost equal (49% of Opx, 51% of Cpx). Group I xenoliths are characterized by higher sulfide abundances (up to 0.031 vol.%) with grain sizes ranging between 2 and 250 μm (avg. 21 μm). On the contrary, the group II xenoliths are sulfide-poor (< 0.002 vol.%) and the grains of sulfides are smaller ranging between 4 and 45 μm (avg. 14 μm). No significant differences in mineral composition of sulfides are observed between the xenolithic groups ($\text{Po}_{27-100}\text{Pn}_{0-28}\text{Ccp}_{0-45}$ in group I, $\text{Po}_{35-81}\text{Pn}_{9-24}\text{Ccp}_{10-42}$ in group II).

Higher sulfide contents and larger size of sulfide grains in group I xenoliths suggest that reactive melt percolation (i.e. melt metasomatism), plays a significant role in transporting Fe-Cu-S melts. Hence, mantle refertilization by DMM-derived melts is supposed to be associated with metal enrichment of SCLM.

This study was supported by the Diamond Grant project 093/DIA/2020/49.

HOW SULFIDES HOSTED BY MANTLE PERIDOTITES RECORD METASOMATIC PROCESSES? INSIGHT FROM THE LOWER SILESIA XENOLITHS (N BOHEMIAN MASSIF)

Mazurek Hubert¹, Ciężela Jakub², Matusiak-Małek Magdalena¹, Pieterek Bartosz³, Puziewicz Jacek¹, Lazarov Marina⁴, Horn Ingo⁴, Ntaflos Theodoros⁵

¹Institute of Geological Sciences, University of Wrocław, Poland, ²Institute of Geological Sciences, Polish Academy of Sciences, Poland, ³Institute of Geology, Adam Mickiewicz University in Poznań, Poland, ⁴Institut für Mineralogie, Leibniz Universität Hannover, Germany, ⁵Department of Lithospheric Research, University of Vienna, Austria

The processes affecting the composition of mantle peridotites, such as partial melting or melt-metasomatism, can be tracked by the composition of silicate phases forming mantle rocks. Sulfides hosted by mantle peridotites are accessory phases but being sensitive to partial melting and metasomatic processes they are useful in studying the transport of chalcophile metals in the upper mantle. To provide more constraints on the influence of metasomatic processes on the budget of chalcophile metals in the lithospheric mantle, we studied sulfides in a set of ultramafic mantle xenoliths from the SubContinental Lithosphere Mantle underlying SW Poland (N Bohemian Massif). We studied xenoliths from four localities (Wilcza Góra, Grodziec, Krzeniów and Księginki) which were carried by Cenozoic mafic magmas.

The mantle peridotites record multi-stage evolution which is reflected in the division of xenoliths into groups. The history of peridotites comprises: 1) strong depletion (group A0), and either 2) weak calico-silicate metasomatism (group A1), or 3) strong melt-related metasomatism (group B). The modal content of sulfide grains (pentlandite, pyrrhotite, and chalcopyrite) increases from group A to B and is followed by their Ni-depletion and Fe-Cu-enrichment. The variations in major element composition of bulk sulfides are accompanied by variations in chalcophile elements and PGE contents. The Mo contents in sulfides from group A are characterized by slightly narrower ranges (28–460 ppm) than group B (1–546 ppm), whereas S/Se ratios in group A are significantly higher (13273–65616) than those in group B (2136–19277). The PPGE/IPGE ratios in group A (2.6–11.3) are elevated compared to those in group B xenoliths (2.5–10.3).

Despite the high variability in ranges of Mo content, Se/Se, and PPGE/IPGE ratios in both groups, they always exceed the primitive mantle values (or chondritic ratio in case of PGEs), pointing to the metasomatic origin of sulfides. This interpretation is in line with a high degree of partial melting significantly exceeding 20% (in some samples reaching 35%), which is the marginal value at which all primary sulfides are removed from the peridotitic system. Therefore, all the studied sulfides must have been reintroduced into peridotites during metasomatism.

Metasomatic processes recorded in silicates in groups A1 and B, despite genetic relations, show well-defined differences. A constant increase in S/Se ratio positively correlated with enrichment in Ni and depletion in Fe from group B to group A1 peridotites may point to similar fractionation of the metasomatic melt responsible for sulfides introduction. Nevertheless, in ~50% of the studied grains the trace element contents were below detection limits while others were significantly depleted in incompatible elements such as Pt and Pd. These data suggest that the metasomatic medium which introduced the sulfides was metal-poor or, alternatively, sizes of analyzed grains were insufficient for in-situ analyses.

The only group of xenoliths where the general trend in sulfides composition is not followed are some of the strongly depleted A0 xenoliths from Krzeniów, which are characterized by extraordinarily high sulfide abundances and enrichment in Fe-Cu-S phases. We suggest that in this group some other type of metasomatism, possibly related to syn-volcanic processes, was operating.

Funded by the NCN projects no. UMO-2014/15/B/ST10/00095 and 2016/23/N/ST10/00288 and the Polish-Austrian project WTZ PL 08/2018.

THE MARBLES OF LASA: PETROGRAPHIC, ISOTOPIC AND EPR CHARACTERISATION OF THE EASTERN ALPS WHITE MARBLE USED IN ANTIQUITY

Mazzoli Claudio¹, Maritan Lara¹, Cavazzini Giancarlo², Sassi Raffaele¹, Piovesan Rebecca³, Zoleo Alfonso⁴, Iacumin Paola⁵, Zorzi Federico¹

¹Geosciences, University of Padova, Italy, ²Institute of Geosciences and Georesources, CNR, Italy, ³LAMA, University of Venice IUAV, Italy, ⁴Chemical Sciences, University of Padova, Italy, ⁵Physics and Earth Sciences, University of Parma, Italy

The marble of Lasa (the eastern Alps, northern Italy) is a white marble used since Roman times, especially to realize milestones. After being abandoned for a long period, the marble quarries have been mined again in the modern age and used especially outside Italy to realise important monuments.

In the present study, we present the results of a multidisciplinary approach to the analysis of a large set of specimens sampled from various quarries of the marble of Lasa. Petrographic analysis was addressed to the definition of the microstructure, crystal boundaries, maximum grain size (MGS), and occurrence of accessory mineral phases. Mineralogical analysis by X-ray powder diffraction (XRPD), were coupled with bulk chemical analysis by X-ray fluorescence (XRF) as well as microchemical analysis by electron microprobe (EMPA) on accessory minerals occurring in the marbles. Moreover, isotope analysis of C, O, and Sr, and EPR spectroscopy were also carried out to fully characterize the Lasa marbles. Results were compared with the literature data on white marbles of the eastern Mediterranean region used in antiquity, including those of the Italian peninsula (Carrara and Campiglia), and the numerous marbles from Greek and Turkish quarries. Petrographic features, mineralogical and isotopic composition, and spectroscopy markers were statistically treated using a multivariate approach (cluster analysis and principal component analysis) to define possible overlapping and identify the combination of variables that maximize the differences with other white marbles used in antiquity. This will allow recognizing the marble of Lasa when used in classical and modern lithic works (especially in central Europe), for which the provenance of the stone material is unknown.

ENTRAPT: AN ONLINE PLATFORM FOR ELASTIC GEOTHERMOBAROMETRY

Mazzucchelli Mattia Luca¹, Angel Ross J.², Alvaro Matteo³

¹Mainz Institute of Multiscale Modeling & Institute of Geosciences, Johannes Gutenberg University of Mainz, Germany, ²IGG-CNR Padova, CNR, Italy, ³Department of Earth and Environmental Sciences, University of Pavia, Italy

Remnant strains in an inclusion trapped inside a host mineral are developed because the inclusion and the host have different thermoelastic properties, and the inclusion does not expand in response to P and T as would a free crystal. When (ultra)high-pressure metamorphic rocks are exhumed to the surface of the Earth, residual strains may be still preserved in mineral inclusions and can be quantified with micro-Raman spectroscopy and/or X-ray diffraction while the inclusion is still contained in its host. If measured and interpreted correctly through elastic geobarometry, they give us invaluable information on the pressures and temperatures of metamorphism during geodynamical processes such as subduction.

EntraPT is an online platform that provides an easy-to-use tool to calculate the entrapment conditions of inclusions, with error propagation, from the residual strain measured in mineral inclusions. EntraPT establishes a method and a workflow to import and analyze the measured residual strains, calculates the mean stress in the inclusions, computes the entrapment isomekes with uncertainty estimation, and visualizes all the results in relevant graphs. It enables the user to avoid the many possible errors that can arise from manual handling of the data and from the numerous steps required in geobarometry calculations. The elastic calculations are based on a consistent dataset of validated Equations of State (EoS) and elastic stiffness tensors that allow barometric calculations to be performed on both quasi-isotropic and anisotropic minerals. For all the calculations involving EoS, EntraPT relies on Eosfit7, a stable and efficient Fortran code that has been validated over many years. All of the data, parameters, and settings are stored in a consistent format and can be exported as project files and spreadsheets, and imported back to EntraPT for further analysis. This allows researchers to store and/or share their data easily, making the checking and the comparison of data and results reliable. We will show how EntraPT can be used to carry out detailed analyses of the residual strains measured in inclusions and to calculate the entrapment isomekes with their uncertainties.

EntraPT is accessible at <http://www.mineralogylab.com/software/>. This work was supported by ERC-StG TRUE DEPTHS (grant number 714936) to MA. MLM is supported by the Alexander von Humboldt research fellowship and the SIMP PhD Thesis Award.

PRELIMINARY STUDIES ON BIOPRECIPITATION PROCESSES MEDIATED BY SULFATE REDUCING BACTERIA (SRB) AND METAL IMMOBILIZATION IN MINE IMPACTED ENVIRONMENTS.

Medas Daniela¹, Dore Elisabetta¹, Fancello Dario¹, Marras Pier Andrea¹, Rigonat Nicola¹, Vacca Salvatore¹, Alisi Chiara², Paganin Patrizia², Sprocati Anna Rosa², Tasso Flavia², De Giudici Giovanni Battista¹

¹Department of Chemical and Geological Sciences, University of Cagliari, Italy, ²Territorial and Production Systems Sustainability Department, ENEA, Italy

Mining activity often leaves a critical legacy represented by huge volumes of mine wastes and residues, usually made up of highly reactive materials, which lead to the mobilization and dispersion of harmful elements in soils and waters. Although these extreme environments are adverse to the development of living organisms, it has been observed that some microorganisms are able to adapt, playing a role in metal mobility, and becoming part of the resilience of the system itself.

The Iglesias and Arburese (SW Sardinia, Italy) mine districts, now abandoned, have been exploited for centuries by mining activities aimed at Pb-Zn extraction from sulfides and non-sulfides (calamine) deposits. Here, biogeochemical barriers naturally occur as an adaptation of the ecosystem to environmental stresses. Studies, from macroscale to microscale, showed that sulfate-reducing bacteria (SRB) may influence metal mobility by mediating the precipitation of secondary authigenic metal sulfides under reducing conditions. Specifically, framboids of Zn sulfides and Fe sulfides have been observed in the sections of stream sediments core characterized by the presence of abundant organic matter, especially residues of vegetal tissues (e.g. roots and stems of *Juncus acutus* and *Phragmites australis*).

Laboratory-scale experiments were performed to better understand the bioprecipitation processes. For this purpose, anaerobic batch tests were carried out using high polluted mining waters (Zn and sulfate concentrations up to 102 and 103 mg/l, respectively) inoculated with native selected sulfate-reducing bacteria from stream sediments collected in the investigated areas. Dramatic decrease (up to 100%) in Zn and sulfate was observed in solutions. Moreover, scanning electron microscopy - energy dispersive spectroscopy (SEM-EDS) analysis, performed on solids recovered at the end of the experiments, showed the presence of precipitates characterized by a tubular morphology and made up by S and Zn. SRB inocula were studied by next-generation sequencing (NGS) approach, with the aim to compare the microbial diversity of the different SRB communities and to search for indigenous novel metal-tolerant sulfidogenic microorganisms.

These findings represent a valuable step forward to plan effective bioremediation strategies for reducing metal mobility and dispersion. Also, bioprecipitation mediated by SRB can have great potentialities for metal recovery and our results can help to develop biomining techniques.

The authors acknowledge CESA (E58C16000080003) from RAS and RAS/FBS (F72F16003080002) grants, and the CeSAR (Centro Servizi d'Ateneo per la Ricerca) of the University of Cagliari, Italy, for SEM analysis.

AUTHIGENIC SULPHIDES AS SINKS FOR Cu AND Hg IN SEDIMENTS FROM HYPERSALINE WETLANDS CONTAMINATED BY AGRICULTURAL ACTIVITIES (LAGUNA HONDA, S SPAIN)

Medina-Ruiz Antonio¹, Jiménez-Millán Juan¹, Abad Isabel¹, Jiménez-Espinosa Rosario¹

¹Geology, University of Jaen, Spain

Hypersaline wetlands are complex and dynamic systems in which physical and biogeochemical processes regulate the chemical evolution of the sediment, the water table, the groundwater, and the organisms that inhabit these ecosystems. The saline wetlands at the eastern end of the Guadalquivir Depression (S Spain) are natural receptors of metal pollutants as a consequence of agricultural treatments of olive trees crop. The uptake, degradation, and transformation of pollutants can promote physical and chemical alterations of the environmental conditions modifying the behavior of the systems.

Laguna Honda is one of these saline lakes (Jaén, Spain). It is a karst morphogenetic system by the dissolution of evaporites. The water supply is mixed, with groundwater and surface water. It has a semi-permanent hydroperiod. The main lithologies are Triassic clays, marls, and gypsum, with isolated nuclei of carbonate materials. The deepest zone of the lake is located at its southern end (1.5 m). The degree of mineralization of its waters can reach hypersaline concentrations, with a salinity that can reach 100 g/l in periods of low water level.

The sediments of Laguna Honda are microlaminated and rich in plant remains. The mineralogy determined by X-ray diffraction and scanning electron microscopy (SEM) shows that the sediments are mainly made of quartz, calcite, dolomite, illite, and chlorite, with significant amounts of gypsum, halite, and feldspars and minor amounts of pyrite, barite, hematite, zircon, rutile, and ilmenite. Field data indicate a pH of 7.8, and an Eh of -31 mV of the sediment. Total organic carbon analysis revealed a percentage ranging between 1.5% and 2.5% at the surface, decreasing to values around 0.8% at 10 cm depth.

The study of Laguna Honda sediments by SEM and EDX analyses revealed the presence of sulfide microcrystals and framboids dispersed in the sediment. Most commonly they are in the form of pyrite, although in some cases with variable amounts of Cu or Mn. In addition, transmission electron microscopy (TEM) revealed the presence of dispersed nanoparticles of mercury sulfides (HgS) on the surface of clays or on fragments of organic matter. The smallest particles (≈ 5 nm) develop irregular dendritic aggregates of up to 80 nm. The redox conditions of sediments in continental environments, often conditioned by the accumulation of organic matter, play a determining role in the mobility of metal nanoparticles. Under suboxic and anoxic conditions, the high affinity for S of many of the metals used in agricultural treatments (Cu, Zn, Pb, Cd, Hg...) means that the behavior of metals in contaminated sediments rich in organic matter is controlled by sulfide precipitation processes, usually of nanometer size, which become real sinks for contaminating materials. Therefore, the sediments of Laguna Honda behave as a reservoir for these metal pollutants, preventing their diffusion and extension through the water sheet and, thus, preventing them from becoming part of the organisms that inhabit the lake. However, due to the different seasonal cycles that occur in the wetland, the transformation of insoluble sulfides into different mineral species could occur, increasing its bioavailability.

MINERAL CHARACTERIZATION OF HYPERASALINE WETLAND, LAGUNA HONDA (S SPAIN)

Medina-Ruiz Antonio¹, Jiménez-Millán Juan¹, Abad Isabel¹, Jiménez-Espinosa Rosario¹

¹Geology, University of Jaen, Spain

The hypersaline lakes are complex and dynamic systems in which physical and biogeochemical processes control the chemical evolution of the wetland water, groundwater, its sediments, and the communities of organisms in the ecosystem. In this context, the mineral and chemical composition of lake sediments is usually the result of a balance between a set of detrital and authigenic processes occurring in the depositional basin. The conditions of salinity, Eh, pH, and microbiological activity determine the neof ormation and transformation of minerals essential in the regulation of biogeochemical cycles. A detailed mineralogical study of the Laguna Honda (S Spain) was done as a starting point to determine how these parameters influence the mineral processes. It is a lake formed by karstic processes produced by the dissolution of evaporitic materials, which gives it its hypersaline character, increasing its salinity in the low water season, with conductivity values reaching 100 ms/l and decreasing to 25 ms/l in winter. X-ray diffraction analysis of powders, oriented aggregates of the total fraction and fractions < 2 µm gave evidence of the main minerals composing sediments. In addition, the study of polished thin sections by scanning electron microscopy (SEM) with EDX microanalysis allowed to detect minerals present in low quantities and to determine the textural features.

Sediments from Laguna Honda are mainly composed of silicates, carbonates (calcite, 18 % average, and dolomite in smaller proportions, 3% average), and sulfates (gypsum, 14 % average, and sporadic anhydrite). With respect to the silicates, as well as quartz (23% average) and sporadic feldspars, there are clay minerals: illite (37 % average), chlorite (6 % average), and sporadic kaolinite. Depending on the area of the lake, different proportions of gypsum, aragonite, and illite were found. Specifically, gypsum is the main mineral in some samples in the center of the lake reaching averages of 30%, while in the nearshore areas the proportions of illite are higher, reaching 48%. Aragonite is mainly found in the surface samples and absent at depth. The presence of the clay minerals is more evident in the <2 µm fraction where were also detected Mg-sulphates such as epsomite and hexahydrite, and chloride salts such as carnallite.

Accessory minerals detected in the SEM are oxides (ilmenite, rutile, and hematite), sulfates (barite, celestine), REE phosphates (monazite), zirconium, and native sulfur. In areas rich in organic matter is very common the presence of pyrite, as idiomorphic crystals or forming framboids, isolated or grouped. The framboids can reach sizes of up to 20 µm and sometimes they appear oxidized. In some cases, the analysis of these sulfides reveals variable amounts of Cu and Mn. Aragonite was also detected in rich-organic samples, inside voids.

Laguna Honda shows a broad variety of minerals with different origins. According to the materials found in the recharge basin where the main lithologies are Triassic materials (gypsum, clays, marls, and carbonate materials), some of them are detrital. However, other phases are probably neof ormed due to their nature, size, and textural appearance as a consequence of the physico-chemical features of the wetland. This is the case of pyrite, aragonite, monazite, epsomite, hexahydrite and carnallite. The oxidized framboids or the presence of native sulfur are also indicative of alteration and/or transformation processes of minerals, which may be due to changes in the dynamics of the lake.

STRUCTURAL AND CHEMICAL DEPENDENCE OF (Ca, Si) ISOTOPES FRACTIONATION AT EQUILIBRIUM: LESSONS FROM ATOMISTIC SIMULATIONS

Meheut Merlin¹, Stamm Franziska², Schauble Edwin³

¹GET, University Paul Sabatier, France, ²Geology, Lund University, Sweden, ³Earth Sciences, University of California at Los Angeles, United States

Isotope compositions are nowadays routinely measured for the reconstruction of geochemical history, or for the assessment of contemporary geochemical processes. To properly interpret these records, accurate estimates of the isotope fractionation associated with specific processes are priceless to the Earth Sciences community. The fractionation of isotopes at equilibrium can be predicted from vibrational properties. Ab initio electronic structure calculations have emerged as a powerful tool to efficiently explore these properties for exhaustive collections of materials. In this work, we realized systematic studies on large sets of materials, in order to emphasize the relationships existing between fractionation properties and other chemical or structural properties, such as redox, cationic coordination, or bond distances. For Si isotopes, many of those parameters have been estimated independently, through various examples relevant to Earth Sciences problematics. Coordination effects might explain the large fractionations observed during biochemical processes (Stamm et al 2020, EPSL V141 p116287), whereas, during magmatic processes inside the Earth's crust, other controls prevail, such as the nature of second atomic neighbors of Si (Meheut and Schauble 2014, GCA V134 p137). Also, in the systems where Si is bonded to O, there is a significant correlation between Si-O distance and fractionation properties, in a large variety of situations.

On another hand, the Ca isotopes system is emblematic of the weak cationic elements such as alkali and alkaline earth elements, which motivate a lot of interest in the Earth Sciences community (Ca, Sr, Li, Ba in particular). Its mobility in the critical zone gives it great potential to characterize processes such as alteration or soil-plant interaction. In the plant, Ca is present as solid (oxalate), dissolved (mainly Ca²⁺), and bonded to organic ligands, and its isotopes fractionate by 0.6‰ between those reservoirs (Schmitt et al 2018, Biogeochem. 137(1), 197-217). To better understand what controls the fractionation of Ca isotopes in those environments, we calculated its equilibrium fractionation properties between simple, well-characterized solids (calcite, dolomite, aragonite, CaO lime, diopside, grossular). Their behavior shows very different than Si isotopes. Si is covalently bonded, whereas Ca is weakly bonded, with bonds characterized by very low vibrational frequencies, difficult to characterize experimentally except in very simple cases. Its fractionation properties appear still somehow controlled by coordination (which changes easily for Ca in Nature), but much weakly, opening the path to the exploration of the controls of other parameters, such as distortion or local valence. In this presentation, we will discuss those controls and their relative importance.

HIGH-VALUE TECHNOLOGICAL APPLICATIONS OF CAMPANIAN IGNIMBRITE

Mercurio Mariano¹, Izzo Francesco¹, Germinario Chiara¹, Grifa Celestino¹, Langella Alessio²

¹Department of Science and Technology, University of Sannio, Italy, ²DiSTAR, University of Naples Federico II, Italy

The Campanian Ignimbrite (CI) is the product of one of the most powerful eruptions of the Campi Flegrei volcanic area, consisting of a stratified, plinian pumice deposit overlain by a grey welded pyroclastic current deposit that grades upwards into a yellow color (Langella et al., 2013).

Different secondary mineralization processes provided it a distinctive mineralogical composition: highest emplacement temperatures determined the welding of the grey, basal portion of the deposit, feldspathized by authigenic mineralization processes; on the contrary, the circulation of meteoric water and the lower-temperature of the overlying, incoherent portion promoted the zeolitization processes, giving rise to a deposit with a zeolite content that often reaches or exceeds 60% (Cappelletti et al., 2003).

Thanks to the occurrence of natural zeolites such as chabazite and phillipsite, the yellow facies of CI displays a peculiar predisposition to the high-value technological applications devoted to environmental and health, generally based on its excellent cation exchange capacity (~3.5 meq/g) and selective removal of cationic pollutants. Recently, particular attention was paid to the characterization and evaluation of the technological performance of a chabazite-rich-tuff belonging to the Campanian Ignimbrite formation and outcropping in the nearby of San Mango sul Calore (southern Italy) (Cappelletti et al., 2017; Izzo 2019 and references therein). This deposit displays interesting technological features such as high zeolite content (i.e., chabazite ~70% wt., phillipsite ~5% wt.), Si/Al ratio ~ 2.6, and external cation exchange capacity ~0.23 mEq/g. The absence of potentially dangerous phases as cytotoxic or carcinogenic fibrous minerals, as well as the low concentration of noxious elements (i.e. As, Cd, Hg, and Pb), never exceeding the legal limits imposed by European legislation, encouraged some investigations regarding the use of this geomaterial as a carrier in the drug delivery and removal of the contaminant of emerging concern in the waste waters. In the light of these findings, the limits posed on the exploitation of CI could be redefined according to the new intended uses and mining procedures.

References

- A Langella et al. (2013), *Applied Clay Science*, Volume 72, Pages 55–73, <http://dx.doi.org/10.1016/j.clay.2013.01.008>
P. Cappelletti et al. (2003), *Mineralogy and Petrology*, Volume 79, Pages 79–97, DOI 10.1007/s00710-003-0003-7
P. Cappelletti et al. (2017), *Microporous and Mesoporous Materials*, Volume 250, 15 September 2017, Pages 232–244, <https://doi.org/10.1016/j.micromeso.2015.05.048>
F. Izzo (2019), *Plinius*, Volume n. 45, Pages 40–46, DOI: 10.19276/plinius.2019.01006

COUPLED PHONON-ELECTRON EXCITATIONS IN HYDROUS Fe-BEARING SILICATES: A KEY TO UNDERSTANDING THE LITHOSPHERIC CONDUCTIVITY

Mihailova Boriana¹, Della Ventura Giancarlo², Waesermann Naemi¹, Xu Wei³, Schlüter Jochen⁴, Galdenzi Federico², Marcelli Augusto⁵, Redhammer Günther⁶, Boiocchi Massimo⁷, Oberti Roberta⁸

¹Erdsystemwissenschaften, Universität Hamburg, Germany, ²Dipartimento di Scienze, Università di Roma Tre, Italy, ³Institute of High Energy Physics, Chinese Academy of Sciences, China, ⁴Centrum für Naturkunde, Universität Hamburg, Germany, ⁵INFN Laboratori Nazionali di Frascati, Italy, ⁶Department of Chemistry and Physics of Materials, University of Salzburg, Austria, ⁷Centro Grandi Strumenti, Università di Pavia, Italy, ⁸Sede Secondaria di Pavia, CNR-Istituto di Geoscienze e Georisorse, Italy

The anomalous high conductivity in subduction zones is a feature known for a long time but still poorly understood. The phenomenon is usually associated with the ionic conductivity of grain-boundary fluids, resulting from dehydration of hydrous silicates at high temperatures. Hopping of electrons between adjacent Fe²⁺ and Fe³⁺ cations as well as diffusion of H⁺ in the bulk of mineral grains have been also proposed as possible mechanisms to explain the anisotropy of lithospheric conductivity in wedge regions. The properties of rocks depend on the physical properties of minerals composing the rock, which in turn ultimately depend on the crystal phonon modes and electron density of states. Amphiboles are among the major hydrous-silicate constituents of subducted slabs and they can incorporate various amounts of iron in their structure. Thus, to elucidate the atomistic origin of the rock conductivity observed in peculiar geological settings, we have studied single crystals of Fe-rich amphiboles by in situ temperature-dependent Raman spectroscopy, a method sensitive to both phonon and electron states. The experiments have been done either in the air or in the N₂ atmosphere. Our experimental results directly evidence the formation of mobile polarons at temperatures typical of the lithosphere, having dipole moments aligned parallel to the strips of linked MO₆ and TO₄ polyhedra within the amphibole structure. These polarons arise from the coupling between polar phonons and electron transitions within Fe²⁺O₆ octahedra and contrary to what is commonly assumed, their occurrence does not require the presence of external oxygen, nor the co-existence of tri- and divalent iron cations in the mineral structure. The experimental observations are fully supported by the results from density-functional-theory modeling of the electron density of states and band structure. Furthermore, Raman scattering data show the formation of mobile H⁺ inside the mineral bulk at high temperatures, which can also contribute to the overall lithospheric conductivity. The similarity in the atomic building blocks between amphiboles and layered silicates suggests that the direction-dependent formation of mobile polarons, as well as the occurrence of delocalized H⁺ at elevated temperatures, is a universal feature of both structure types.

Financial support by the Deutsche Forschungsgemeinschaft (MI 1127/7-2) is gratefully acknowledged.

MINERALOGY, GEOCHEMISTRY AND NATURAL ISOTOPE CONTENT OF BIOMASS BOTTOM ASHES - FIRST INSIGHT FOR FURTHER UTILIZATION POTENTIAL

Mikoda Bartosz¹, Ciapała Bartłomiej¹, Pełka Grzegorz¹, Kozak Krzysztof²

¹AGH University of Science and Technology, Poland, ²Institute of Nuclear Physics PAN, Poland

Combustion of biomass has become more attractive in recent years due to the fact that the energy derived from biomass is considered renewable and close to carbon-neutral. The ashes produced from biomass burning can be potentially valuable for many utilization methods. The aim of this study was to perform a characterization of two exemplary bottom ash samples (laboratory boiler – MA; home boiler – HA) in terms of chemical and phase composition, as well as natural isotope content for preliminary assessment of potential use for these wastes. The methods used comprised of standard characterization methods, such as X-Ray diffraction, X-Ray fluorescence, and scanning electron microscopy. The content of natural isotopes (⁴⁰K, ²²⁶Ra, and ²²⁸Th, as well as ¹³⁷Cs) were determined using the gamma radiation spectroscopy method in a certified laboratory. The chemical composition of the two ashes differs significantly, but both ashes are most abundant in CaO (78% in MA, 39% in HA). The HA sample is also rich in K₂O (22%), P₂O₅ (12%), MgO (11%), MnO (5.3%), SiO₂ (4%) and SO₃ (3.5%), whereas the same constituents occur in MA in much smaller concentrations (6% K₂O, 4.6% MgO, 4.6% SiO₂, 2.8% P₂O₅, 1.6% MnO and 0.5% SO₃). Both HA are also abundant in metals such as Al, Cu, Fe, Ni, and Zn. The phase composition of both samples reflects the chemical composition. The MA sample is composed mostly of CaO and CaCO₃ with small peaks of MgO and SiO₂. Similarly, CaO and CaCO₃ are abundant in HA sample, but also phases such as hydroxyapatite or manganese oxide can be distinguished on the XRD pattern. Also, HA sample is more amorphous than MA, which is reflected by higher background on the XRD pattern. SEM examination revealed that apart from the most abundant phases, metallic grains composed mainly of Pb (but also Cu, Zn, and Sb) occur in both wastes. The natural radionuclide content is significantly higher in HA sample, where ⁴⁰K and ²²⁶Ra concentrations are 3027±97 Bq/kg and 48.3±35 Bq/kg, respectively, whereas in MA the concentration of ⁴⁰K is as high as 334±32 Bq/kg (²²⁶Ra below detection limit); concentration of ²²⁸Th in both samples is below detection limits. The concentration of ¹³⁷Cs is also significantly higher in HA (661±23 Bq/kg) than in MA (99±39 Bq/kg), which may be caused by some ingredients in pellet that were still impacted by Chernobyl nuclear accident. The calculation of I indicator (radioactive isotope concentration indicator) was performed according to Polish law regulation and the values are equal to 0.27 for MA and 1.01 for HA, which means that HA sample has lower potential for utilization in construction, since I indicator value bigger than 1 excludes materials from use in construction. Nonetheless, both samples exhibit high CaO content, and should be more thoroughly examined in terms of potential utilization, especially in the view of circular economy.

OCEAN MAGMATIC ACTIVITY RECORDED BY GABBROS AND PYROXENITES IN MOR AND SSZ PERIDOTITES OF MIRDITA OPHIOLITE (ALBANIA) – PRELIMINARY RESULTS

Mikrut Jakub¹, Matusiak-Małek Magdalena¹, Puziewicz Jacek¹

¹Institute of Geological Sciences, University of Wrocław, Poland

Mirdita ophiolite forms a ~40 km wide and 240 km long zone in northern Albania. It is a part of Dinaridic-Hellenic belt and marks suture after the closure of Neo-Tethyan Ocean. Based mostly on characteristics of crustal rocks, the eastern limb of the ophiolite was interpreted to have Supra-Subduction Zone (SSZ) origin, while the eastern one has a Mid-Ocean Ridge (MOR) affinity.

In this study, we focus on two ultramafic massifs, Kukesi and Puke, of SSZ of MOR affinities, respectively. The Kukesi Massif represents harzburgitic ophiolite, with an increasing amount of dunites towards the top of the sequence. The Puke Massif is a mantle dome, interpreted as a former oceanic core complex (OCC), composed of primary harzburgites and subsequent mylonitic plagioclase/amphibole lherzolites.

Both massifs are pervasively penetrated by magmatic veins and dykes of gabbroic and pyroxenitic composition. Moreover, massive pyroxenites intercalated with peridotites are present at a top of ultramafic sequence in the Kukesi Massif and define crust/mantle transition zone. In both massifs distribution of veins and dykes is uneven and varies in terms of width (from single to few hundreds of cm) and lateral dimension. The veins are usually undeformed, but in mylonitic ultramafics of Puke gabbros are deformed accordingly to peridotites.

Massive pyroxenites have composition of hornblende-clinopyroxenites and websterites, whereas the mantle (vein) pyroxenites are clinopyroxenites, orthopyroxenites, and olivine websterites. Some veins exhibit internal zonation and are composed of clinopyroxenite and orthopyroxenite parts.

Chemical composition of minerals from pyroxenites from Kukesi Massif was studied so far Clinopyroxene occurring in vein websterites and clinopyroxenites is rather homogeneous with Mg#=84-87 and Al=0.05-0.1 apfu, that from massive websterite from transition zone has Mg#=87-88 and Al=0.13-0.16 apfu Clinopyroxene composition in internally zoned veins varies significantly as Mg# is from 85 to 94 and Al from 0.02 to 0.08 apfu Orthopyroxene from two samples of vein olivine websterites have either Mg#=83 and Al~0.07 apfu or Mg#=87 and Al~0.04 apfu Composition of orthopyroxene in zoned veins may vary within a sample (Mg#=83-89; Al=0.04-0.08 apfu) or be homogeneous (Mg#=90-91, Al=0.02-0.03 apfu). In massive websterite the orthopyroxene has Mg#=82-84 and Al=0.12-0.14 apfu, while amphibole has the composition of tremolite-actinolite with Mg#= 85-94. Spinel, where present, is highly chromian (Cr#=0.59-0.80).

Clinopyroxene is LREE-depleted in most of the samples, but those from massive pyroxenites show stronger depletion ((La/Lu)_N=0.03-0.22) than those in veins ((La/Lu)_N=0.33-1.65). Clinopyroxene in all the rocks has positive Th-U, Pb, and Sr and negative Ta and Zr anomalies, but primitive-mantle normalized concentrations of trace elements are significantly higher in veins.

Low LREE contents in clinopyroxene and orthopyroxene suggest their crystallization from tholeiitic melt. However, strong variation in the chemical composition of silicates points to silicate crystallization from different generations/fractionates of melt. However, further research is needed to precisely define the nature of the parent melts and spatial and time relations between different magmatic events. Presence of amphibole points to a retrogressive imprint on the examined rocks.

This study was financed from scientific funds for years 2018-2022 as a project within program “Diamond Grant” (DI 024748).

ELASTIC PROPERTIES AND STABILITY OF ALKALI-CARBONATES AND THEIR ROLE IN REE FRACTIONATION AT EARTH'S UPPER MANTLE CONDITIONS

Milani Sula¹, Spartà Deborah¹, Maurice Juliette¹, Fumagalli Patrizia¹, Baratelli Lisa¹, Comboni Davide², Lotti Paolo¹, Joseph Boby³, Plaisier Jasper R.³, Glazyrin Konstantin⁴, Hanfland Michael², Merlini Marco¹

¹Dipartimento di Scienze della Terra 'A. Desio', University of Milan, Italy, ²ESRF, France, ³Elettra - Sincrotrone Trieste, Italy, ⁴DESY III, Germany

Carbonatites constitute important ore concentrations of strategic metals, such as Nb and rare-earth elements (REE; Simandl and Paradis 2018). Alkali-carbonates are an important fraction of minerals that concentrate REE elements in these ore deposits (Wall et al. 2001; Edahbi et al. 2018). Alkali-carbonates form as primary crystallizing minerals in magmatic environments (Zaitsev et al. 2002; Smith et al. 2018) and their presence in the Earth's mantle is suggested by their occurrence as diamond inclusions (Kaminsky et al., 2009). We, therefore, expect that alkali-carbonates may play a significant role in carbon-related processes (volcanism, mantle metasomatism, diamond formation...) at Earth's upper mantle and transition zone conditions. High-pressure and high-temperature experiments have recently revealed the possible occurrence of a new class of Ca-alkali carbonates above 4 GPa (Shatskiy et al. 2013, 2105). Indeed, in this study, we report the crystal structure and the thermoelastic behavior of Na₂Ca₃(CO₃)₄, K₂Ca₃(CO₃)₄ and two intermediate solid solutions, all synthesized at 4 GPa and 800°C in a multi-anvil press. Textural evidence suggests that the synthesized alkali-carbonates phases were in equilibrium with a liquid phase (crystallized during quenching). The structures of synthetic single crystals have a similar topology to the reported Na₂Ca₃(CO₃)₄ high-pressure phase (Gavryushkin et al., 2014) but a different unit cell and symmetry. Irregular coordination sites for Ca, K, and Na cations and a partially disordered CO₃ group arrangement reveal an anomalous elastic behavior for the different cation sites, suggesting an interesting capability for trace element incorporation in the structure. In-situ single-crystal HP and HT measurements have been performed by synchrotron X-ray diffraction with resistive heated DAC (ESRF, Grenoble, ID15b beamline; Petra, Hamburg, P02.2 beamline; Elettra, Italy, Xpress) and HT synchrotron X-ray diffraction experiments have been done by loading powder of synthetic samples in a quartz-glass capillary. The results are used to model their density evolution at upper mantle conditions and observe if it might be possible for these phases to gravitationally separate from the liquids. Lastly, to observe the possibility of these carbonates to fractionate trace elements we performed a synthesis of alkali-carbonates doped with La³⁺ and we observed that La³⁺ at 4 GPa can be incorporated up to ca. 2wt% in the alkali-carbonates structure.

Gavryushkin P.N., Bakakin V.V., Bolotina N.B., Shatskiy A.F., Seryotkin Y.V. & Litasov K.D. (2014) - Synthesis and crystal structure of new carbonate Ca₃Na₂(CO₃)₄ homeotypic with orthoborates M₃Ln₂(BO₃)₄ (M= Ca, Sr, and Ba). *Crystal Growth & Design*, 14(9), 4610-4616.

RARE EARTH ELEMENTS (REE) USED AS ENVIRONMENTAL TRACERS TO ELUCIDATE THE WEATHERING MODEL OF A PHOSPHOGYPSUM DISPOSAL AREA

Millan-Becerro Ricardo¹, Pérez-López Rafael¹, Cánovas Carlos R.¹, Macías Francisco¹

¹Department of Earth Sciences and Research Center on Natural Resources, Health and the Environment (RENSMA), University of Huelva, Spain

This study proposes the use of rare earth elements (REE) and their North American Shale Composite (NASC)-normalized patterns as a geochemical tracer to elucidate the weathering model of a phosphogypsum stack. The study area is a singular phosphogypsum stack (around 100 Mt of wastes accumulated on 1200 ha of the surface) located directly above naked marsh soils of the Estuary of Huelva (SW Spain). The phosphogypsum stack is a continuous source of pollution to the estuarine environment due to the existence of contaminated residual acid waters, which continually emerge at the edge of the stack, forming leakages known as edge outflows. The stack is divided into four disposal modules; two partially restored and two unrestored, the latter have stored process waters in surface ponds. However, all disposal areas show edge outflows in their perimeters. This fact calls into question the previous weathering model, which pointed to the infiltration of process water stored on the pile through the porous medium as the origin of the edge outflows. In order to clarify the origin of these edge leachates, different water samples were taken in the study area, such as estuarine water and phosphogypsum-related acidic leachates (i.e. process water and edge outflows). The study of the geochemical tracers in these samples showed that the estuarine water has REE patterns with an enrichment of middle-REE (MREE) with respect to light-REE (LREE) and heavy-REE (HREE). On the other hand, the process water shows REE patterns with an enrichment of HREE relative to MREE and LREE. Regarding the edge outflows, they mostly show REE patterns similar to estuarine water. Therefore, the use of this geochemical tool allows us to suggest that there is a clear chemical connection between the stack and the estuary. The results achieved in this study demonstrate the ineffectiveness of the restoration measures carried out in the past and highlight the need to develop new restoration plans.

DATING METAMORPHIC GARNET: Sm–Nd Vs. LA-ICP-MS U–Pb AGES

Millonig Leo J.¹, Beranoaguirre Aratz², Albert Richard¹, Marschall Horst¹, Baxter Ethan³, Gerdes Axel¹

¹Geosciences, Goethe University Frankfurt, Germany, ²Geosciences, University of the Basque Country UPV/EHU, Spain, ³Earth Sciences, Boston University, United States

Orogenic belts are the most spectacular topographic manifestations of collisional tectonics and bear witness to ancient and recent tectonic processes that form and shape the continents. Regional metamorphic rocks are of particular importance for deciphering the complex geodynamic evolution of orogenic belts and for extracting information about the tectonic processes that formed them. They preserve unique pressure-temperature (P–T) and temporal (t) information. In this context, garnet is the ultimate petrochronometer that allows us to characterize the P–T–t evolution of regional metamorphic rocks in much greater detail than would be possible with any other mineral. Currently, the Lu–Hf and Sm–Nd isotope systems are most commonly employed to date regional metamorphic garnet, but both procedures require time- and labor-intensive isotope dilution (ID) techniques. Recent studies, however, demonstrate that U–Pb dating of low-U (~1–100 ng/g) garnet by LA-ICP-MS represents a feasible addition to our geochronology toolbox with a much higher sample throughput compared to conventional solution-based methods.

This contribution compares the Sm–Nd (ID) and U–Pb (LA-ICP-MS) dating methods to assess the accuracy of the latter. For this, a 2.5 cm-diameter garnet crystal from the Austrian Alps was analyzed. Published garnet from this locality had yielded Sm–Nd ages of 27.52 ± 0.54 Ma for the garnet core and 19.97 ± 0.43 Ma for the garnet rim. Our preliminary U–Pb ages for this sample are 30.18 ± 2.53 Ma (MSWD = 1.18) for the garnet core and 20.99 ± 0.66 Ma (MSWD = 1.16) for the rim. In this case, both isotope systems yield consistent garnet core and rim ages (within uncertainty) and indistinguishable garnet growth durations of 7.6 ± 0.7 million years (Sm–Nd) vs. 9.2 ± 2.6 million years (U–Pb).

The results obtained in this study show that the U–Pb ages are in agreement with the Sm–Nd ages and thus demonstrate that the U–Pb LA-ICP-MS technique can be sufficiently precise and accurate to produce meaningful dates from metamorphic garnet.

AN UPDATE ON SOME REMARKABLE NEW TELLURIUM CRYSTAL STRUCTURES

Mills Stuart¹, Missen Owen¹, Rumsey Mike², Kampf Anthony³

¹Geosciences, Museums Victoria, Australia, ²Earth Sciences, Natural History Museum London, United Kingdom, ³Mineral Sciences, Natural History Museum of Los Angeles County, United States

Secondary tellurium mineralogy has been expanding over the past 20 years thanks to several remarkable deposits mostly in western USA and further studies at Moctezuma, Mexico. These deposits continue to produce new minerals with new crystal-structure types and help us to understand the weathering history of this critical metal. The new mineral tomiolloite, $\text{Al}_{12}(\text{Te}^{4+}\text{O}_3)_5[(\text{SO}_3)_{0.5}(\text{SO}_4)_{0.5}](\text{OH})_{24}$, was found on old specimens including privately collected material along with the type specimen of mroseite (described in 1975) collected from the Bambolla mine (Moctezuma mine), Moctezuma, Sonora, Mexico. Tomiolloite has a unique chemical composition amongst natural compounds and is just the third Te oxysalt mineral to also contain Al, after burckhardtite and backite. Chemically, the presence of both SO_3^{2-} and SO_4^{2-} anions is rare; only two other minerals contain SO_3^{2-} and SO_4^{2-} : orschallite and hielscherite. The crystal structure of tomiolloite is a microporous framework built from edge-sharing $\text{M}\phi_6$ octahedra ($\text{M} = \text{Al}^{3+}$ and Te^{6+}), Te^{4+}O_3 trigonal pyramids and Te^{4+}O_4 disphenoids, and SO_3 and SO_4 groups in the channels. The $\text{M}\phi_6$ octahedra each edge-share with two adjacent octahedra to form crankshaft-like infinite chains along c.

The new mineral (pending approval), $(\text{Ca}_{0.5}\text{Pb}_{0.5})\text{Pb}_3\text{Cu}^{2+}_6\text{Te}^{6+}_2\text{O}_6(\text{Te}^{4+}\text{O}_3)_6(\text{Se}^{4+}\text{O}_3)_2(\text{SO}_4)_2 \cdot 3\text{H}_2\text{O}$, occurs at the Grand Central mine in the Tombstone district, Cochise County, Arizona, USA. It has a remarkably thick heteropolyhedral layer containing one Te^{6+}O_6 tellurate octahedron, one Jahn-Teller distorted Cu^{2+}O_5 tetragonal pyramid, one SO_4 sulfate tetrahedron, one Te^{4+}O_3 tellurite trigonal pyramid, one Se^{4+}O_3 selenite trigonal pyramid. Two Cu^{2+}O_5 pyramids link to one another by sharing an Oeq-Oap edge to form a $\text{Cu}^{2+}_2\text{O}_8$ dimer. The Te^{6+}O_6 octahedron and the Te^{4+}O_3 pyramids linked to it form a finite $\text{Te}^{6+}\text{O}_3(\text{Te}^{4+}\text{O}_3)_3$ cluster with a pinwheel-like configuration. This is the first known finite complex including both Te^{4+} and Te^{6+} polyhedra in any natural or synthetic structure.

These two examples showcase the continuing extraordinary chemical and structural diversity of secondary Te minerals. Many more Te oxysalts remain undescribed and undiscovered to further catalog the supergene chemistry of versatile Te.

ELASTIC THERMOBAROMETRY ON ZIRCON-IN-GARNET (ZIG) FROM THE BROSSASCO-ISASCA UNIT (DORA-MAIRA MASSIF, WESTERN ALPS)

Mingardi Giulia¹, Campomenosi Nicola², Mazzucchelli Mattia Luca³, Chopin Christian⁴, Scambelluri Marco⁵, Alvaro Matteo¹

¹Department of Earth and Environmental Sciences, University of Pavia, Italy, ²Department of Earth Science, University of Hamburg, Germany, ³Mainz Institute of Multiscale Modeling and Institute of Geosciences, University of Mainz, Germany, ⁴Laboratoire de Géologie, ENS-CNRS, France, ⁵Department of Earth Science, Environment & Life, University of Genoa, Italy

Here we combine zircon-in-garnet elastic thermobarometry and phase equilibria modeling to metapelites coming from the well-known ultrahigh-pressure (UHP) Brossasco-Isasca unit (Dora-Maira Massif, Western Alps). We determined the residual strain and pressure of zircon inclusions via micro-Raman spectroscopy and the dedicated software available online such as stRAinMAN and EntraPT. The entrapment isomekes obtained for 35 zircon inclusions in garnet from metapelites (Alm₆₈₋₇₆-Py₁₂₋₂₆) have been combined with thermodynamic modeling to constrain the P-T range of garnet growth, assuming purely elastic behaviour.

The presence of chloritoid and/or staurolite inclusions at the garnet core-mantle and the presence of coesite inclusions only at the garnet rim suggests that most of the garnet volume formed during an early prograde path and only a small portion under UHP conditions. Most of the selected inclusions, however, come from the rim of the garnet. Since the rim is limpid, we could localize those inclusions that are spaced enough to be used reliably for elastic thermobarometry without corrections. The entrapment pressures obtained for most zircon inclusions do not match the previously published results obtained from conventional petrologic methods only. For example, combining our results with the available retrograde P-T paths of the UHP unit, the apparent entrapment conditions decrease from the coesite stability field to 0.5 GPa and 600-650 °C. The same discrepancy between the elastic and chemical barometric methods has been documented for the pyrope-bearing whiteschists from the same metamorphic unit. The observed misfit has been tentatively attributed to the post-entrapment viscous relaxation of the garnet-zircon inclusion system, which cannot be accounted for by purely elastic models. These results provide further evidence of a general post-entrapment elastic reset of the zircon-in-garnet pairs along the retrograde path at temperatures near 600-650°C.

This work was supported by ERC-StG TRUE DEPTHS (grant number 714936) to Matteo Alvaro. Nicola Campomenosi and Mattia L. Mazzucchelli are supported by the SIMP PhD Thesis Award and by the Alexander von Humboldt research fellowship.

TELLURIUM BIOGEOCHEMICAL DISPERSION FROM THE NANO TO MACRO SCALE: STUDYING THE WORLD-FAMOUS MOCTEZUMA MINE, MEXICO

Missen Owen¹, Mills Stuart², Brugger Joël³, Etschmann Barbara³

¹School of Earth, Atmosphere and Environment & Department of Geosciences, Monash University and Museums Victoria, Australia, ²Department of Geosciences, Museums Victoria, Australia, ³School of Earth, Atmosphere and Environment, Monash University, Australia

Tellurium (Te) is often classed as a critical metal due to its utility in new technologies such as solar panels, coupled with potential future supply shortages as its present production is tied to aging methods of refining copper (Cu). Humans are coming into contact with larger amounts of Te as a result of its increased usage along with mining greater quantities of telluride-rich ores of elements like gold (Au) and Cu. Despite this, the environmental behavior of Te remains chronically understudied. Tellurium biogeochemistry research is mostly interpreted from laboratory-based studies rather than direct field observations. As a chalcogen with multiple oxidation states and varying solubilities, we expect to see complex and metal-resistant microbiomes in regions of Te-enrichment, as observed for other rare metals (Au and Pt) and metalloids (Se). To examine the in situ weathering behavior of Te and its effects on the regolith, a systematic study of geochemistry, mineralogy, and microbial diversity was carried out in the highly Te-enriched mines around Moctezuma, Sonora, Mexico. Ores at Bambolla mine, the richest Te hotspot in the region, contain dominant native tellurium with minor sulfides such as pyrite (FeS₂), selenides such as naumannite (Ag₂Te), and tellurides such as calaverite (AuTe₂). Surrounding the deposit, Te concentrations in soils exceed 0.1 wt%, indicating extreme levels of Te enrichment. Weathering occurring proximal to ore produces soluble Te oxyanions (namely tellurite, Te⁴⁺O₃²⁻ and tellurate, Te⁶⁺O₆⁶⁻), sometimes precipitated to minerals like tellurite (Te⁴⁺O₂), emmonsite [Fe₂(Te⁴⁺O₃)₂·2H₂O]. Analysis of the microbial communities in regolith samples (Illumina MiSeq DNA sequencing) reveals the presence of microbes from the Bacillus genus, known to reduce toxic soluble Te oxyanions to more benign nanoparticles of native tellurium in some of the Te-rich samples. The presence of Bacillus species shows that microbes mediate the weathering process, especially in their transformations of soluble Te species to more benign forms. Further from the main ore, Te may also undergo structural incorporation into iron oxides such as goethite and may be sorbed onto clay minerals such as illite. Structural incorporation especially provides a longer-term sink for Te in the environment. Tellurium cycling is complex, but following this study we can better predict Te mobility in the environment, especially trending away from Te-rich sources, whether natural or anthropogenic. In particular, we now understand how the most toxic forms of Te are made biogenically inactive by incorporation into soil minerals through microbial mediation and precipitation. Our study provides the first evidence that Te undergoes dynamic cycling in the environment, with nanoscale changes governing the behavior of Te on the macroscale.

SILL INTRUSIONS IN LOWER OCEANIC CRUST: IMPLICATIONS FROM DRILL CORE GT1 OF THE OMAN DRILLING PROJECT

Mock Dominik¹, Neave David Axford², Müller Samuel³, Garbe-Schönberg Dieter³, Ildefonse Benoit⁴, Koepke Jürgen¹, Oman Drilling Project Science Team⁵

¹Institute of Mineralogy, Leibniz University of Hannover, Germany, ²Department of Earth and Environmental Sciences, University of Manchester, United Kingdom, ³Institut für Geowissenschaften, Christian-Albrechts-Universität zu Kiel, Germany, ⁴Géosciences Montpellier CNRS, Université de Montpellier, France, ⁵Worldwide, Geoscience Institutions, United Kingdom

As the largest and best-preserved fragment of the oceanic lithosphere on land, the Samail ophiolite in the Sultanate of Oman provides an ideal field laboratory for studying fast-spread lower oceanic crust. The Oman Drilling Project aims to constrain magmatic processes and crustal accretion mechanisms beneath fast-spreading mid-ocean ridges and obtained several drill cores from different stratigraphic heights between the upper mantle and the dyke/gabbro transition. Drill core GT1 spans about 400 m from the layered gabbros between ~1200 and 800 m above the crust-mantle boundary (maM). The drilled samples are mostly gabbros or olivine gabbros, with a few cm-scale layers of anorthosite, troctolite, and wehrlite. We applied petrological, geochemical, and microstructural methods in order to determine the magmatic environment of lower crustal accretion. Mg#s ($\text{Mg}/(\text{Mg}+\text{Fe}) \times 100$; molar basis) in olivine and clinopyroxene and the Ca# ($\text{Ca}/(\text{Ca}+\text{Na}) \times 100$; molar basis) in plagioclase show parallel fractionation trends from 800 to 1070 maM which can be subdivided into five smaller trends, each between 25 and 80 m thick. Above 1070 maM, phase compositions change towards more primitive compositions over a 15 m thin horizon, revealing decameter-scale fractionation over the uppermost 80 m of the core. These trends are confirmed by trends in bulk rock Mg# and Cr/Zr ratios. The observed decameter-scale trends indicate the presence of in-situ crystallizing stacked magma reservoirs beneath the paleo-spreading center. Rim-to-core ratios of Mg# and TiO₂ content in clinopyroxene reveal significant zoning within the uppermost 80 m of the core, significantly contrasting with the absence of zoning below. Plagioclase and clinopyroxene fabrics evolve from both foliated and lineated at the base of the core towards almost purely foliated at 1070 maM. Above, it shifts back to significantly lineated fabrics along the uppermost 80 m of the core. This trend correlates with the overall mineral fractionation trend suggesting a link between magma composition and rock fabric. Decreasing lineation intensity up to 1070 maM may have resulted from either a higher viscosity or a lower liquid/solid ratio of the fractionated magma, or both, hampering the development of crystal orientation. In contrast, the abrupt increase in lineation intensity and strength of clinopyroxene zoning above 1070 maM are indicative of melt-rock interaction and more developed mineral orientation, both implying increased volumes of interstitial melt. Our results suggest that both magma replenishment and fractional crystallization occurred in the lower oceanic crust and significantly contributed to the accretion of the layered gabbro section of the Samail ophiolite in Oman.

REMEDICATION OF HEAVY METALS POLLUTED GROUNDWATER THROUGH COLLOIDAL SUPERPARAMAGNETIC MAGHEMITE NANOPARTICLES: NEW HINTS ON UNEXPECTED SURFACE PROPERTIES.

Molinari Simone¹, Salviulo Gabriella¹, Magro Massimiliano², Vianello Fabio²

¹Geosciences, University of Padova, Italy, ²Department of Comparative Biomedicine and Food Science, University of Padova, Italy

The increasing presence of heavy metals in groundwater of natural and/or anthropogenic origin represents the main threat to human health and the environment.

Conventional treatments including chemical precipitation, coagulation/flocculation, electrochemical processes, ion exchange, and biosorption suffer from high operational costs and production of a huge amount of sludge. For these reasons, the development of alternative low-cost remediation methods is of primary concern. The present work investigates on the application of a colloidal maghemite nanoparticle, called SAMN (Surface Active Maghemite Nanoparticle) for the selective removal of both arsenic (As) and chromium (CrVI) from water. These nanoparticles are superparamagnetic, displayed unique colloidal stability without any coating or superficial modification. Besides substantiating the efficiency of SAMNs as a competitive and sustainable option for heavy metals removal, even in highly impacted industrial sites, the surface properties of nanoparticles were deeply investigated using heavy metals used as molecular probes and studied by x-ray photoelectron spectroscopy coupled with circular dichroism. The dichroic signal of nanoparticles is directly influenced by the coordination of ligands, thus giving information on crystalline vacancies on the SAMNs surface, identified as the chiral centers and responsible for the selectivity toward ligands. The latter was correlated with the ability to restructure the nanomaterial at the crystal truncation. Moreover, the application was moved on real and complex industrial groundwater with the aim to confirm the possible upscaling of the nanotechnological remediation approach. Metal sequestration as high as 80% was reached, indicating SAMNs as an attractive and economically sustainable option for moving magnetic nanoparticles to large-scale applications. Furthermore, tests aiming at the identification of possible interfering anionic species, possibly affecting the performance of the magnetic separation system and the binding selectivity towards the target metal unveiled an unexpected competition between sulfate and chromate for maghemite, never reported before. In particular, this result highlighted that SAMNs surface binding sites emerged for bearing labile coordination water in analogy with iron oxyhydroxides thus providing an interesting contribution to the continually evolving iron oxide chemistry at a nano-sized scale.

EXPERIMENTAL DETERMINATION OF THE OXYGEN FUGACITY AT THE SULFATE-SULFIDE SATURATION IN SILICIC MELTS

Mollé Valentin¹, Gaillard Fabrice², Iacono Marziano Giada³

¹ISTO, University of Orléans, France, ²CNRS, France, ³ISTO, CNRS, France

Sulfur has multiple oxidation states in magma (-II, 0, +IV, +VI). This diversity is critical for both magma degassing and differentiation and for the genesis of magmatic ore deposits. The relationships between sulfur speciation and oxygen fugacity are however poorly defined. Much work has been conducted under reduced conditions on the solubility of S²⁻ in silicate melt at sulfide saturation; and recently, some efforts have been conducted to define the solubility of S⁶⁺ at sulfate saturation under strongly oxidized conditions. However, most magma displays intermediate redox conditions where both sulfide and sulfate are likely to coexist. This is particularly true for arc magmas. Here, we present a new experimental protocol and the preliminary results on the calibration of the fO₂ at the sulfide-sulfate transition. These experimental data constitute robust anchor points for calibrating the numerous model on sulfur solubility in magma.

We conducted experiments in piston-cylinder (950-1050°C, 1-3 GPa) using a double capsule strategy. This assemblage is composed of an outer capsule containing a silicic melt that is saturated in both sulfide and sulfate and an inner capsule with a redox sensor recording the fO₂. The outer capsule is fO₂-buffered by the following reaction: FeOmelt + CaSO₄anh = CaOmelt + FeSpyr + 2 O₂gas.

In dacitic melts, as the pressure increases, the fO₂ at pyrrhotite-anhydrite saturation is shifted toward more oxidizing conditions (from ca. NNO+1.7 to ca. NNO+2.4) and the sulfur solubility decreases from ca. 2400 to ca. 800 ppm. Such results have important implications for sulfur speciation during magma ascent, as decompression could shift sulfur speciation from the S²⁻ domain to the S⁶⁺ domain for most natural compositions. This speciation shift may act as a fO₂ buffer until all S²⁻ is converted to S⁶⁺ during magma ascent. Some natural lavas, like the 1991 Pinatubo dacite, show a pyrrhotite-anhydrite saturation and display pre-eruptive fO₂ at NNO+1.5. We suggest the pyrrhotite-anhydrite equilibria as defined above may buffer fO₂ in silicic arc magmas.

SYNCHROTRON RADIATION MICRO X-RAY DIFFRACTION: AN ADVANCED APPROACH IN HERITAGE SCIENCE FOR THE INVESTIGATION OF POLYCHROME STRATIGRAPHIES

Morabito Giulia¹, Marinoni Nicoletta¹, Bais Giorgio², Botteon Alessandra³, Cantaluppi Marco¹, Colombo Chiara³, Gatta G. Diego¹, Merlini Marco¹, Polentarutti Maurizio², Realini Marco³, Possenti Elena³

¹Scienze della Terra, Università degli Studi di Milano, Italy, ²Elettra - Sincrotrone Trieste S.C.p.A., Italy, ³Istituto di Scienze del Patrimonio Culturale, Consiglio Nazionale delle Ricerche, ISPC-CNR, Italy

One of the main challenges encountered in Conservation Science concerns the possibility of acquiring more and more qualitative and quantitative information from the study of Cultural Heritage (CH) materials and, for this reason, new more comprehensive analytical protocols are gaining a growing attention nowadays.

Here, a synchrotron radiation micro X-ray powder diffraction in transmission geometry (SR- μ TXRD) approach has been implemented to qualitatively and quantitatively characterize the composition of crystalline phases within multilayered systems.

In particular, the high potential of SR- μ TXRD has been applied to complex polychrome stratigraphies in order to investigate the mineralogical composition of micro-meter size paint layers and to quantify the occurrence of selected crystalline phases present in the complex mixture. The research involved both the optimization of the SR- μ TXRD experimental setup as well as the development of an ad hoc protocol for the advanced analysis of SR- μ TXRD datasets.

The SR- μ TXRD measurements were carried out with a micro-meter size X-ray beam on thin cross-sections at the XRD1 beamline of the Elettra synchrotron (Basovizza, Italy). The analyses were carried out on complex stratigraphies prepared in the lab, that is samples composed of 4-to-6 paint layers. Each layer consisted of at least 4 different crystalline phases in a complex mixture. Different carbonates, silicates, oxides, clay minerals, and other compounds were used as target crystalline phases for specific paint layers. Crystalline phases having a different grain size (coarse grains, powder-like grains) were used in mixture as well.

The pre-processing of SR- μ TXRD data was optimized and critically evaluated. The main XRD diffraction peaks of pigments, paint fillers, or aggregates in the complex mixture within each paint layer were clearly observed. The structural refinement performed by the Rietveld method was carried out on the XRD patterns. The quantitative analysis considered the particular experimental setup, the nature of selected crystalline phases (i.e., highly crystalline natural pigments, less crystalline synthetic phases) and their different grain size.

As the main outcome, our implemented SR- μ TXRD approach permits to discriminate paint layers having a similar mineralogical composition but a different ratio among the amount of crystalline phases and/or a different grain size. Therefore, our research opens novel opportunities to extract new information on the manufacturing of polychrome stratigraphies and other multi-layered systems, combining a spatially resolved investigation with a high-quality mineralogical characterization and quantification.

NANOMECHANICAL PROPERTIES OF DIFFERENT SMECTITE-CLAY MINERALS

Morales Juan¹, Lorenzo Adrián¹, García-Vicente Andrea¹, García-Rivas Javier¹, García-Romero Emilia², Suárez Mercedes¹

¹Department of Geology, University of Salamanca, Plaza de la Merced, s/n, 37008 Salamanca, Spain, ²Department of Mineralogy and Petrology. Complutense University of MAdrid. C/José Antonio Novais, 8 28014 Madrid, ³Geoscience Institute, CSIC-UCM , 28014 Madrid.

Smectites are phyllosilicates with a 2:1 structure in which an octahedral sheet is between two tetrahedral sheets forming a layer. Both, tetrahedral and octahedral sheets can have isomorphic substitutions that generate a negative layer charge (between 0.4 and 1.2 per unit cell) which may be balanced by hydrated cations located at the interlayer space. In addition, regarding to the occupation of the octahedral positions, smectites can be both trioctahedral (all positions are occupied) or dioctahedral minerals (2/3 are occupied). Amount and location of the layer charge, number of octahedral cations, and distribution of the OH⁻ groups are needed parameters for classifying smectites and all of them have an influence on the physicochemical properties of those minerals. Due to the properties of smectite minerals, mainly related to their structure, they have been considered as “special clays” with many industrial and agricultural applications. Moreover, since these minerals are present almost everywhere it is important to fully understand their physical properties and more specifically, the nanomechanical properties.

Nanomechanical properties of ten (air-dried) natural samples of different highly-pure smectite minerals were studied through the Force Spectroscopy method by using an Atomic Force Microscope (AFM; Nanotec-Dulcinea). AFM probes were PPP-NCH (NanosensorsTM; Force Constant 10-130 N/m; nom. Val. 42 N/m). Within this experimental method, a sharp tip (<10nm) fixed beneath a cantilever is moved towards the sample until it is in contact with the surface of the sample and pushed into the sample in a controlled displacement, and then, it is retracted again to reach the initial stage. The force interactions between the tip and the sample are measured while tip movement as electric potentials, and calibrated later (following different methods) to give a numerical value of each mechanical property (e.g. Young's modulus, stiffness, hardness, adhesion). The determination of mechanical properties by the Force Spectroscopy method is based on the mechanics of elastic contact. An important elastic parameter, the so-called “reduced modulus”, is proportional to the contact stiffness, which can be easily obtained from the slope of the initial unloading curve.

AFM-Force curves obtained from natural smectite minerals showed very different behaviors, pointing to different nanomechanical properties. As this should be linked to structural differences like layer charge, surface charge distribution, dioctahedral or trioctahedral character, and octahedral vacant distributions a detailed crystal-chemical characterization by AEM (Analytical Electron Microscopy) has also been done.

Statistical analysis of nanomechanical properties and crystal-chemical information has been conducted in order to study the relationship between those aspects within the smectite group, in which the crystal-chemical variability is extraordinarily great.

AFM has been revealed as a powerful tool in the study of nanomechanical properties of smectites, and clay minerals in general, not only to study the topographic aspect at the nanoscale but also for surface properties analyses.

EXPLORING THE THERMOELASTIC BEHAVIOR OF MINERAL INCLUSIONS BY IN-SITU HIGH TEMPERATURE RAMAN SPECTROSCOPY

Morana Marta¹, Mihailova Boriana², Angel Ross J.³, Alvaro Matteo⁴

¹Department of Chemistry, University of Pavia, Italy, ²Department of Earth Sciences, University of Hamburg, Germany, ³Istituto di Geoscienze e Georisorse, CNR, Italy, ⁴Department of Earth and Environmental Sciences, University of Pavia, Italy

Mineral inclusions, systems constituted by a mineral entrapped inside another mineral, are an interesting playground for mineralogy, geology, and material science. In fact, such host-inclusion systems can be exploited to derive the growth environment, identify growth mechanisms and the pressure and temperature of the formation through their stress state. This last information is also of interest for elasticity studies, since mineral inclusions allow to study the effect of nonhydrostatic stress without the need of recreating it in the laboratory, a task that is extremely difficult to perform in a controlled way. Considering their importance, mineral inclusions have been extensively characterized in recent years, focusing on the first fundamental information that acts as a starting point for any further studies: the determination of the residual pressure on the inclusion. In principle, this information can be obtained both from X-ray diffraction and Raman spectroscopy. However, it is not trivial to apply these two techniques in a proper and reproducible way due to both experimental and theoretical challenges. In the case of Raman spectroscopy, the use of the Grueneisen tensor has been proposed to calculate the strains from the Raman shift and then derive the stress on the inclusion. The Grueneisen tensor has been calculated *ab initio*, then an experimental validation is needed. Furthermore, host-inclusion systems are complex systems that need proper reference datasets on the free minerals to be evaluated correctly. For these reasons, we focused on the characterization of a common host-inclusion system, quartz in garnet, and started our study from a thorough re-examination of the response to compression of the Raman scattering of quartz and used this dataset to test the Grueneisen tensor approach. Then, we further explored the thermoelastic properties of the host-inclusion system by performing an in-situ high-temperature experiment, guided by the characterization of the high-temperature Raman spectrum of quartz. Our data show that the confinement of inclusion in the host deeply affects the response of quartz to heating. In fact, because of the interaction between the quartz inclusion and the garnet host, the quartz does not undergo the alpha-beta transition, but we observe that at a certain temperature there is a thermosalient effect.

HIGH Ba-Sr MAGMATISM IN THE EARLIEST STAGE OF THE ALPINE OROGENY: THE CORNO ALTO UNIT (ADAMELLO BATHOLITH)

Mosconi Angelica¹, Tiepolo Massimo¹, Farina Federico¹, Cannaò Enrico¹

¹Dipartimento di Scienze della Terra , Università degli Studi di Milano,

The nature and composition of crustal granitoids significantly changed at the Archean-Proterozoic boundary highlighting major changes in the mechanisms of continental crust formation/differentiation through the Earth's history. In this context, modern analogs of the Archean granitoids provide valuable clues for investigating continental crust formation/differentiation and its secular evolution.

In the Adamello batholith (Southern Alps, Italy), new and detailed fieldwork on the Corno Alto unit revealed the occurrence of granitoid rocks having peculiar features compared to the typical I-type and S-type granites and also displaying distinctive features if compared to the rest of the Adamello batholith. They possess the highest SiO₂ contents ($61.0 \leq \text{SiO}_2 \leq 71.5$ wt%), K₂O+Na₂O up to 7.2%, and a strong enrichment in Sr and Ba (Sr + Ba \approx 1100-1900). Other geochemical features include relatively high LREE/HREE ratios ($[\text{La}/\text{Yb}]_N > 20$) and Nb negative anomaly. The geochemical signature of the Corno Alto rocks resembles that of a peculiar group of Phanerozoic rocks known as high Ba-Sr granites which are considered as modern analogs of the Archean sanukitoids. The Corno Alto granitoids possess several petrographic microstructures suggesting an origin under conditions of chemical disequilibrium such as oscillatory zoning in plagioclase. Major and trace elements together with Sr isotopic compositional traverses across plagioclase grains of the studied rocks reveal abrupt chemical variations associated with enrichment in radiogenic Sr. Parallel to this, zircon crystals show inner and outer domains of similar age but significantly different $\epsilon\text{Hf}(t)$ isotopic compositions (from +1 to +13). The above evidence contrasts with the origin of the studied rocks either in a closed system or from simple assimilation and fractional crystallization process.

Mixing of melts with different geochemical signature and origin is suggested.

This contribution shed new light on the petrogenesis of the high Ba-Sr granitoids showing that multiple components are required: i.e. a juvenile component similar to the depleted mantle and a component with a significant crustal signature likely responsible for the typical enrichment in LILE elements.

COMPOSITION AND RAW MATERIAL PROVENANCE OF COPPER ALLOYS FROM THE LATE AVAR CARPATHIAN BASIN

Mozgai Viktória¹, Szenthe Gergely², Villa Igor Maria³, Bajnóczi Bernadett¹

¹Institute for Geological and Geochemical Research, RCAES, ELKH, Hungary, ²Hungarian National Museum, Hungary, ³Institute of Geology, Bern University, Switzerland

The Avars traditionally interpreted as a nomadic people arrived in the Carpathian Basin in the 6th century AD. In the first half of the Avar era, their power was sustained primarily at the expense of the neighbors, war booty and gifts played a decisive role in operating Avar society. For this period, we know next to nothing about raw material resources, most probably, the vast majority of processed metals was recycled. Fresh metal – most probably only iron – played a minor role. However, after the mid-7th century AD, rapid changes led to the emergence of a radically new cultural and economic model, characterized by the setback of external communications, or, otherwise, these were restricted on the mediation of some exotic and luxury goods. The emergence of the “late-Avar culture” can be contextualized by the early medieval transformation of the surrounding European and Mediterranean world after the collapse of the late antique world. However, we have still only a little data about the production, distribution, and use of non-ferrous metals during the Early Middle Ages (8th century AD). During the late Avar period, there was a drastic change in the use of metals in the Carpathian Basin, which is primarily reflected by the drastic growth of copper alloys in circulation. The study of the copper alloys distributed en masse in the entire Carpathian Basin contributes not only to our knowledge about the technological traditions in this region but through the combined use of lead isotope and chemical analyses we expect results on the sources of the copper as well. More than a hundred copper alloy objects from the late Avar period were analyzed by using handheld XRF to determine their elemental composition. According to the first results, the mostly cast objects were manufactured from lead-tin bronzes. However, the alloy compositions underwent some changes between the first and second half of the late Avar period. The difference is detectable in the more heterogeneous alloy compositions of the later part of the period, and in the presence of higher zinc content as well. According to material analyses, the remelting of copper alloys was common, we had looked for such objects in case of which the use of fresh metal was predominant. The cast copper alloy ornaments of the late Avar period, surviving in large quantities, were mounted to the strap by rivets. As pure copper is malleable and suitable for wire drawing and hammering, rivets were made from this material. Although in small quantity, copper rivets prove the availability of unalloyed copper from the beginning of the late Avar period. The composition of the rivets has also changed. While the first half of the late Avar period is represented by rather homogeneous unalloyed copper, in the course of time the size of the rivets became smaller and their composition more heterogeneous with higher amounts of lead, tin, and zinc. The lead isotope composition of the unalloyed copper rivets was compared to the lead isotope database of copper ores, and a northern source can be assumed.

LITHIUM QUANTIFICATION IN SPODUMENE PEGMATITE DRILL CORES FROM FINLAND USING LIBS AND OTHER CORE SCANNING TECHNOLOGIES

Mueller Simon¹, Meima Jeannot¹, Havisto Jari², Lindström Hannu², Uusitalo Sanna², Heilala Bryan³, García-Piña Carlos⁴, Bernabé Pierre⁵, Grönholm Pentti⁶

¹B1.2, Federal Institute for Geosciences and Natural Resources BGR, Germany, ²VTT Technical Research Centre of Finland Ltd, Finland, ³Timegate Instruments Oy, Finland, ⁴DMT GmbH & Co. KG, Germany, ⁵University of Liège, Belgium, ⁶Keliber Technology Oy, Finland

Exploration activities and active mining of established mineral deposits rely on extensive drilling campaigns that produce large numbers of drill cores. Geological expertise is needed for their analysis, which benefits from the application of additional methods for fast and reliable classification and quantification. Different drill core scanner technologies exist that allow 1D profile measurements or spatially detailed surface analysis of drill cores in a short amount of time. Combining hyperspectral analysis, Laser-Induced Breakdown Spectroscopy (LIBS), and time-gated Raman spectroscopy bundles their distinct advantages and offers important information on mineral abundances and elemental distribution at high resolution. This enables classification, quantification as well as the detection of economically interesting minerals for ore exploration. LIBS allows the detection of light elements like Li, which we used to quantify Li concentrations in profile measurements of drill cores from Keliber's Rapasaari Li-deposit in Finland, covering three distinct lithologies: Spodumene pegmatite, muscovite pegmatite, and metagreywacke. The spodumene pegmatite contains average estimated Li₂O contents of about 1.0 wt.%, whereas muscovite pegmatite and greywacke are economically uninteresting waste rocks. Li plays an important role in recent advances to reduce greenhouse gas emissions since it is used for battery production in many different fields. Due to the increasing demand, new and innovative methods are needed to enable easy and detailed Li quantification on large scales. LIBS measurements can be performed in-situ on a sample surface under atmospheric conditions. Since nearly no sample preparation is needed, the technology is perfectly suited for spatially-resolved measurements of large samples such as drill cores. Nevertheless, various physical and chemical matrix effects do not allow a straightforward analysis of heterogeneous material, which makes the interpretation of LIBS data a challenging task. Especially quantification remains problematic and therefore, the simultaneous application of hyperspectral imaging and time-gated Raman spectroscopy supports LIBS data processing and validation greatly.

We used a LIBS drill core scanner prototype with a Nd:YAG Q-switched 20Hz 1064nm laser and a high-resolution 285-964nm Echelle spectrometer for 1D profile measurements of ten consecutive drill core meters. Five large samples from Li-bearing spodumene ore and muscovite pegmatite were measured with high resolution in 2D, as well. The measurements were cross-validated with hyperspectral data and time-gated Raman spectroscopy of selected areas of the core. Reference samples were carefully prepared and chemometric models were applied to quantify Li-concentrations in the measured samples.

THE COLORING AND ALTERING ROLE OF IRON AND MANGANESE IN HISTORICAL STAINED-GLASS WINDOWS

Muller Camille¹, Rossano Stéphanie¹, Bedidi Ali¹, Fourdrin Chloé¹, Perez Anne¹, Khomenko Volodymir², Dinh Hoang Duong¹, Day Axelle¹, Loisel Claudine³

¹Laboratoire Géomatériaux et Environnement, Université Gustave Eiffel, France, ²Mineralogy and Ore formation, M.P. Semenenko Institute of Geochemistry, Ukraine, ³Centre de Recherche sur la Conservation - Laboratoire de Recherche des des Monuments Historiques, Museum National d'Histoire Naturelle, France

Medieval glasses represent an impressive artwork that combines ancestral technological skills and complex esthetical criteria. The stained glass windows require the expertise of two trades, the glassmakers who manufacture the glass and the glass painter who created the stained-glass windows. However, the glassmaker recipes have most of the time been lost through centuries. An important challenge is to obtain the intended color or even harder, a colorless piece of glass. Indeed, the natural raw materials most of the time contain iron oxides as impurities that might induce undesired colorations. Colorless glasses can be obtained by introducing manganese oxide in the starting composition to counterbalance the coloration due to iron. Manganese is however also a strong coloring agent that leads to colorations ranging from pink to purple. The simultaneous presence of both iron and manganese oxides thus leads to a large range of colorations due to the variable proportions of both Fe and Mn oxidation states (Fe²⁺, Fe³⁺, Mn²⁺, Mn³⁺, and Mn⁴⁺). Moreover, Mn-bearing glasses are subject to alteration due to weathering conditions, sometimes leading to the appearance of spots on the surface and in the subsurface (browning phenomenon).

The aim of this work is to better understand the chemical speciation and structural environment of iron and manganese within the glass matrix, in order to get information about (1) the medieval glass-making techniques and (2) the alteration process of ancient glasses through time.

Series of model glasses with medieval-like compositions have been synthesized under different conditions. Temperature (1200°C, 1350°C, and 1500°C) and iron to manganese concentration ratio effects have been investigated. The model composition has been chosen on the basis of average composition of calco-potassic historical glasses. The MnO (resp. FeO) content has been varied between 1.5-x wt% (resp. x wt%), with x ranging from 0 to 1.5. Glass compositions have been characterized by microprobe analysis. UV-Vis-NIR spectra of glass thin sections have been recorded in the range of 300 to 1800 cm⁻¹. Helmholtz chromatic coordinates have been calculated in order to characterize glass coloration within the CIE 1931 system in order to determine the oxidation states in presence. In parallel, alteration experiments in aqueous conditions (near neutral pH) have been conducted on 3 glass compositions (with Fe only, with Mn only, and without any of them) to better understand the structural role of iron and manganese within the glass matrix.

Analysis of optical spectra showed that the necessary amount of MnO₂ to counterbalance the iron coloration varies according to the temperature used during glass processing. The quantity of Mn necessary to decolorize a glass made at 1200°C is much lower than those at 1500°C, suggesting that composition, in regard to coloration, might be used to get information on the technical recipes. First alteration experiments results showed that the Fe-bearing glass presents a dissolution rate lower than glass without iron nor manganese. On the contrary, Mn-bearing glass tends to destabilize the matrix and increase the dissolution rate.

THE ROLE OF SYMMETRY BREAKING STRAINS IN ANISOTROPIC HOST-INCLUSION SYSTEMS: AN AB INITIO STUDY ON ALPHA QUARTZ

Murri Mara¹, Gonzalez Joseph P.², Mazzucchelli Mattia Luca³, Prencipe Mauro⁴, Mihailova Boriana⁵, Angel Ross J.⁶, Alvaro Matteo²

¹University of Milano-Bicocca, Italy, ²University of Pavia, Italy, ³ Johannes Gutenberg University of Mainz , Germany, ⁴University of Torino, Italy, ⁵University of Hamburg, Germany, ⁶IGG-CNR Padova, Italy

The study and measurement of elastic strains in natural and synthetic samples are under continuous development due to wide interest in the determination of material's elastic properties and their characterization in the framework of industrial applications. The strain and stress fields in a crystal are a function of the surrounding environment and the elastic properties of the crystal itself. For example, when a crystal is immersed in a liquid medium it will be under hydrostatic pressure, but if it is entrapped within another solid material it will be subjected to strains imposed upon it arising from the elastic properties of the host material. A simple case to consider is when an anisotropic crystal is contained within a quasi-isotropic host, such as when a quartz inclusion is contained within a garnet host. When this host-inclusion system is subjected to changes in pressure (P) and temperature (T) the host crystal will impose a uniform strain on the inclusion, which will in turn develop deviatoric stresses. In this scenario, the symmetry of the inclusion mineral is preserved and the strains in the inclusion can be measured via Raman spectroscopy using the phonon-mode Grüneisen tensor approach. However, a more complex situation arises when the host-inclusion system is fully anisotropic (e.g., when a quartz inclusion is entrapped within a zircon host) because symmetry breaking of the inclusion occurs as P and T change. In this case, the effect of symmetry breaking on the frequencies of phonon modes is not known and may be different from the structural phase transitions involving soft modes. Therefore, we calculated the expected deformations for a quartz inclusion entrapped in a zircon host in multiple orientations and at various geologically relevant P-T conditions. We then performed ab initio Hartree-Fock/Density Functional Theory simulations on alpha quartz in the selected range of deformations to (i) determine the role of the symmetry breaking strains in a completely anisotropic host-inclusion system and (ii) evaluate the possible application of the phonon-mode Grüneisen tensor when the symmetry is broken. A systematic investigation has been performed considering the effects of symmetry breaking on the Raman frequencies and intensities as a function of each applied deformation. Our results show that for the Raman active modes coming from the total symmetric ones in trigonal (i.e., A₁) the new calculated Grüneisen components differ by less than 10% with respect to the trigonal ones implying that the effects of the symmetry breaking are negligible. Therefore, the Grüneisen components for trigonal alpha quartz can be used for Raman elastic geothermobarometry in anisotropic host-inclusion systems without introducing significant errors.

Acknowledgements: MM and MLM are supported by the SIMP PhD Thesis Award. MLM is also supported by the A. von Humboldt research fellowship. JPG is supported by the NSF-EAR Postdoctoral Fellowship (No. 1952698). MA has been funded by the ERC-StG TRUE DEPTHS under the European Union's Horizon 2020 Research and Innovation Programme (n.714936) to M. Alvaro.

Keynote

THE WHAT AND WHY OF GLAUCONITES

Nieto Fernando^{1,2}, López-Quirós Adrián^{2,3}, Abad Isabel⁴, Sánchez-Navas Antonio^{1,2}, Escutia Carlota², Bauluz Blanca⁵, Reolid Matías⁴

¹Departamento de Mineralogía y Petrología, Universidad de Granada, Avda. Fuentenueva s/n 18002, Granada, Spain. nieto@ugr.es, ²Instituto Andaluz de Ciencias de la Tierra, CSIC- Universidad de Granada, ³Department of Geoscience, Aarhus University, Høegh-Guldbergs Gade 2, 8000, Aarhus C, Denmark, ⁴Departamento de Geología y CEACTEMA, Unidad Asociada IACT (CSIC-UGR), Universidad de Jaén, ⁵IUCA-Facultad de Ciencias, Universidad de Zaragoza.

Glaucónites are green micas, usually of marine sedimentary origin, which play a significant role as indicators of paleoenvironment (e.g. López-Quirós et al. 2019). Their composition is peculiar, as they are dioctahedral, but the main octahedral cations are Fe and Mg, and they are interlayer deficient. In spite of having been studied for years, particularly in relation to their genetic significance, their real nature and crystal-chemical relations with other micas had remained dubious.

With increasing maturation, which is not related with temperature, but with reducing conditions, the K content increases and Fe³⁺ reduces to Fe²⁺. In overall, the layer charge increases and changes from the tetrahedral to the octahedral sheet. As celadonite is not interlayer-deficient and its charge comes from the octahedral layer, these changes point to it as a possible end-member of the glauconitic compositional series, but these two micas seldom share geological environments.

All the glauconites described in the literature show medium to minor changes in X-ray diffraction after ethylene glycol treatment and display in high resolution electron microscopy small 10Å packets separated by smectitic areas. Hence, they are mica-smectite mixed-layers, reaching with their maximum maturation, R3 order and >90% of mica layers. Nevertheless, the curve relating K content with % mica layers is asymptotic to near 0.8 atoms per formula unit, that is, the interlayer deficient character is intrinsic of the mica layers and not only the consequence of smectite mixed-layering (Baldermann et al. 2013 and López-Quirós et al. 2020).

A rare occurrence of coexisting celadonite and glauconite linked to Jurassic basalt pillow lavas, with their origin related with bacterial activity, allows the determination of their mutual textural and chemical relations at the nanoscale. In the transition zone between both minerals, they appear as a chaotic mixture of well-separated crystals of the two micas, recognizable by their different compositions and crystallinity. They define a compositional gap; therefore, celadonite cannot be considered as the end-member of the glauconitic series (Nieto et al., 2021). In detail, the two kinds of micas have structural differences responsible of the compositional gap, with celadonite having M1 and M2 octahedral positions very similar in size, in spite of their dioctahedral character (Zvyagin, 1957). By contrast, glauconite has more distorted octahedra to accommodate the bigger size of the tetrahedral sheet, due to the ^{IV}Al by Si substitution.

The identification of mature glauconite, in the late Eocene sediments from the northwestern Weddell Sea (Antarctica), for the first time, is an example which illustrates the value of glauconites as paleoenvironmental indicator (López-Quirós et al. 2019). It allows inferring continuous sea-level rise conditions that predated the onset of Antarctic glaciation during the Eocene-Oligocene transition, linked with the separation between Antarctica and South-America, by the Drake Passage.

IS ACID MINE DRAINAGE A RELIABLE SOURCE OF REES? INSIGHTS FROM AMD PASSIVE TREATMENT SYSTEMS IN THE IBERIAN PYRITE BELT

Nieto José Miguel¹, Macías Francisco¹, León Rafael¹, Ayora Carlos², Cánovas Carlos R.¹, Basallote Maria Dolores¹, Pérez-López Rafael¹, Olías Manuel¹

¹Earth Sciences, Universidad de Huelva, Spain, ²IDAEA - Groundwater and Hydrogeochemistry, CSIC, Spain

The Iberian Pyrite Belt (IPB), located in the SW of the Iberian Peninsula, is one of the larger polymetallic massive sulfide provinces in the world, with original reserves exceeding 1900 Mt. Historical mining activity in the area has left an enormous legacy of mine residues, including 90 abandoned mines and more than 1.000 ha of waste rock dumps and tailings. Therefore, large amounts of Acid Mine Drainage (AMD) are produced due to the oxidation of pyrite-rich residues exposed in the surface that end up in the Tinto and Odiel rivers, the two rivers draining the Spanish part of the IPB. Conventional passive treatment systems of AMD were tested, showing serious problems of clogging and loss of reactivity because of the extremely acid and metal-rich nature of the AMD originated in this region. These drawbacks have recently been overcome using a new passive treatment system known as Dispersed Alkaline Substrate (DAS). Two full-scale DAS treatment plants have been installed in the IPB, located at Mina Esperanza and Mina Concepción, in the upper part of the Odiel watershed. Both plants consist of several DAS reactive tanks based on limestone dissolution and are serially connected with decantation ponds. In both cases, AMD with a mean water flow of 1 L/s (with peaks up to 3 L/s in the rainy season), mean pH values around 2.7, and high metal contents have been successfully treated, resulting in a net alkaline outflow discharge with a mean pH higher than 6.5 and metal contents below detection limits but Fe, with retention ranging 90-97%. Two layers of metal precipitation within the reactive DAS tanks are formed with increasing pH of the treated water: an iron-rich layer in the upper part followed by an aluminum-rich layer. The iron-rich layer (pH > 3.5) is formed by schwertmannite with minor amounts of As, Cr, Sb, and Mo. The aluminum-rich layer (pH > 4.5) is basaluminite and includes the co-precipitation of other metals in solution such as Cu, Zn, Cd, Co, Ni ... and REEs. In fact, most if not all the REEs in the AMD are retained in the basaluminite layer, allowing their easy recovery in DAS treatment plants. A rough estimation of the REE potential of these AMD sources, based on 40 DAS plants operating in the Odiel basin with variable content of REE, will be the production of 11 kton/year of basaluminite containing 21 ton/year of REE₂O₃ and with a REE₂O₃ grade of 0.19%. Given the longevity of AMD production (from 100's to 1000's years), REE from AMD can be considered almost a Renewable Resource of REE for the future.

ARCHAEOLOGICAL ANALYSES OF ANCIENT METAL OBJECTS FROM MESI GLYFADA SEA, NORTH AEGEAN, GREECE: PRELIMINARY DATA

Nikolopoulou Athina¹, Filippaki Eleni²

¹History and Archaeology, National and Kapodistrian University of Athens, Greece, ²Laboratory of Archaeometry, Institute of Nanoscience and Nanotechnology, National Center for Scientific Research, N.C.S.R. "Demokritos", Greece

An archaeological treasure of metal objects was discovered in the sea area between the contemporary settlements of Mesi and Glyfada of North Aegean, Rhodope Prefecture in 2008. The assemblage is consisted of 136 finds and came to light by the Ephorate of Underwater Antiquities. More specifically, 115 objects belong to the category of tools, while interesting are the 19 ingots, which are considered as the raw material of the tools. In addition, two bases of handmade vessels were found, which are dated back to the Early Helladic (EBA) period.

Of the total 134 metal finds, analyses were carried out on 64 of them by the non-destructive XRF method. The measurements took place at the Ephorate of Underwater Antiquities where the portable XRF device of the Laboratory of Palaeoenvironmental and Ancient Metal Structures of the Institute of Nanoscience and Nanotechnology of the N.C.S.R. "Demokritos" was transferred. The results of the XRF analysis showed that all the objects are made of arsenical copper. Moreover, the presence of arsenic within the ingots is also interesting. We sampled 32 objects in order to draw more conclusions about the proportion of their components as well as their manufacturing technology. The purpose of this paper is to briefly present the first analytical results that have been obtained so far. Our research aims at reconstructing the early metallurgical techniques practiced in the above region and northern Greece in general.

THE SECOND OCCURRENCE OF THE ZEOLITE FLÖRKEITE, THE HATRURIM COMPLEX, ISRAEL

Nowak Katarzyna¹, Cametti Georgia², Galuskina Irina¹, Vapnik Yevgeny³, Galuskin Evgeny¹

¹Faculty of Natural Sciences, University of Silesia, Poland, ²Institute of Geological Sciences, University of Bern, Switzerland, ³Department of Geological and Environmental Sciences, Ben-Gurion University of the Negev, Israel, katarzyna.k.nowak@us.edu.pl; irina.galuskina@us.edu.pl; evgeny.galuskin@us.edu.pl; vapnik@bgu.ac.il

Zeolite mineralization in the pyrometamorphic rocks of the Hatrurim Complex in Israel was recognized in gehlenite hornfels and paralava. Numerous voids filled with zeolites and other low-temperature minerals were found in both types of rocks. In paralavas, vesicles are predominantly filled with thomsonite-Ca or flörkeite in the association with vertumnite.

In partly melted hornfels, low-temperature mineralization is more diverse and represented by vertumnite, tobermorite, hydrogarnet, barite, and the following zeolites: flörkeite, thomsonite-Ca, high sodium fibrous zeolites, gismondine, analcime, and rarer willhendersonite. Additionally, potentially new strontium zeolite with the gismondine type structure was found in the association.

Flörkeite is a rare zeolite, which overgrows on the thomsonite-Ca, gismondine and Sr-zeolite in gehlenite rocks of the Hatrurim Complex. This is the second reported occurrence of flörkeite, which was previously found in a Ca-rich xenolith from a quarry at the Bellerberg volcano near Ettringen, East Eifel volcanic area, Germany.

Flörkeite has phillipsite framework type (**PHI**) with ordering arrangement of the extraframework cations and completely ordered Si and Al at *T-sites*. Crystals from Israel has unit cell parameters ($a = 8.694$, $b = 14.252$, $c = 16.545$, $\alpha = 91.36$, $\beta = 99.64$, $\gamma = 91.75$, $V = 2019.187$, $P-1$) close to the holotype from Germany ($a = 8.704$, $b = 14.274$, $c = 16.572$, $\alpha = 91.37$, $\beta = 99.62$, $\gamma = 91.63$, $V = 2028.3$, $P-1$). The empirical crystal chemical formula of flörkeite can be written as follows: $K_{2.91}Ca_{1.99}Na_{0.94}Si_{8.01}Al_{7.99}O_{31.92} \cdot 12H_2O$. The topology of the framework was confirmed by Raman spectroscopy. The following bands are featured in the Raman spectrum (cm^{-1}): 415, 473, 704, 833, 981, 1613 and 3369, 3486. The characteristic ordered structure of flörkeite and its occurrence indicate typical low-temperature conditions of crystallization.

The investigations were supported by NCN of Poland, grant no. 2019/35/O/ST10/01015.

PRELIMINARY RESULTS OF DETAILED STUDIES OF THE INTERACTIONS BETWEEN HOST-ROCK AND THE PERIDOTITE XENOLITHS FROM CENOZOIC VOLCANIC ROCKS OF SW POLAND.

Nowak Monika¹

¹Institute of Geology, Adam Mickiewicz University, Poland

During previous studies interactions between host-rock and peridotite xenoliths were observed in several outcrops from Cenozoic volcanic rock from SW Poland (both Lower Silesia and Opolian Silesia)(Nowak, 2012; Nowak, Kowal-Linka 2018). Interactions may be grouped into four types: a) a reaction rim around a xenolith (with additional Cpx crystallization), b) diffusion Mg-Fe rims in olivine crystals, c) melt pockets showing the presence of magnetite, and d) veins with host-rock rock material inside a xenolith. The main aim of the present study is to answer the question of whether it is possible that as a result of interaction with magma, rock-forming minerals from xenoliths of smaller sizes (less than 4 cm in diameter) could show a completely changed chemical composition. Two research paths were chosen during the study: (1) recognizing whether the content of main and trace elements in rock-forming minerals found inside a xenolith may be reduced or increased, (2) determining the degree of changes in the chemical composition of minerals inside the xenolith. Preliminary results consist of thirteen profiles of main chemical elements from seven peridotite xenoliths from two different outcrops (Wilcza Góra, Sichów). According to the new data from Wilcza Góra strong interactions are limited mostly in close proximity to the surrounding volcanic rock (as it was observed before). The predominant homogeneity inside xenolith is observed regardless of the direction of the profile. Variations in chemical content are small and are limited to a few measuring points. Xenoliths from Sichów show strong internal heterogeneity and significant differences in chemical composition. The preliminary hypothesis is that interactions involving the entire xenolith can only occur in exposures where specific conditions occurred during ascent to the surface. However, these are only very preliminary studies and research is in progress.

The study was funded by National Science Centre, Poland, Miniatura 4, no. 2020/04/X/ST10/00542.

References:

- Nowak, M. 2012. Genesis of the Cenozoic volcanic rocks based on study of the chosen xenoliths from the Lower Silesia. PhD thesis, Adam Mickiewicz University, Poznań. Unpublished PhD thesis. [In Polish].
Nowak, M., Kowal-Linka, M., Pécskay, Z., 2018. Brunovistulian lithospheric mantle xenoliths from a newly recognized nephelinite dyke at the Folwark quarry, Opolian Silesia (SW Poland). XXVth Meeting of the Petrology Group of the Mineralogical Society of Poland, Mineralogia – Special Papers 48 pp.71

SCALES OF PRESERVATION OF CHEMICAL HETEROGENEITIES IN THE MANTLE PORTION OF THE LEKA OPHIOLITE COMPLEX, NORWAY

O Driscoll Brian¹

¹University of Manchester, United Kingdom

Ophiolites facilitate assessment of the causes and length scales of mantle compositional heterogeneity because field-based observations can be coupled with geochemical investigations of upper mantle lithologies, resolved relative to the petrological Moho. The ~497 Ma Leka Ophiolite Complex (LOC; Norway [1]) comprises a section of early-Palaeozoic (Iapetus) oceanic lithosphere with well-exposed mantle and lower crustal sections and relatively low degrees of serpentinization ($\geq 20\%$). The LOC mantle section is heterogeneous at the cm-to-m scales, manifested by abundant dunite lenses and sheets in harzburgitic host-rock [2]. Abundant chromitite (≥ 60 vol.% Cr-spinel) and pyroxenite lenses and layers also occur in the uppermost 200-300 m of the mantle section.

Much of the array of mantle lithologies on Leka developed during fluid-assisted melt extraction in a supra-subduction zone setting (SSZ; [3]), offering an opportunity to interrogate the nature of Os isotope and HSE abundance heterogeneities developed in such rocks. At ~497 Ma, the Os isotopic compositions of Leka harzburgites averaged ~2% more radiogenic than the projected average for abyssal peridotites at that time. Several of the harzburgites are characterized by low initial $^{187}\text{Os}/^{188}\text{Os}$ (~0.120), interpreted as reflecting Proterozoic melt depletion, a characteristic that has also been reported from other Iapetan ophiolite mantle harzburgites [4]. Dunites, pyroxenites and chromitites show much more variable initial $^{187}\text{Os}/^{188}\text{Os}$ and HSE abundances; some pyroxenites have extreme Pt abundances (up to 1-2 ppm), supra-chondritic Pt/Os, and $^{187}\text{Os}/^{188}\text{Os}$, yet some of the dunites are also characterized by $^{187}\text{Os}/^{188}\text{Os}$ well within the range of the harzburgites.

Mantle peridotites from 3 x 3 m grids sampled at kilometer distances from one another reveal that HSE and Os isotopic heterogeneities present at the cm- to m-scale are greater than those preserved at the km-scale, suggesting that the drivers for the development of these heterogeneities are a consequence of relatively localized processes. Indeed, mineral scale observations and analyses suggest that the formation of HSE-rich phases during SSZ-related channelized melt-rock interactions may be an important trigger for fractionation of the HSE and modifications of $^{187}\text{Os}/^{188}\text{Os}$ in ophiolite peridotites and pyroxenites. Some of the implications of these findings for the development of $^{186}\text{Os}/^{188}\text{Os}$ mantle heterogeneities, as well as the relative inefficiency of convection in re-homogenizing the oceanic mantle at local scales, will be discussed.

[1] Dunning GR, Pedersen RB. (1988). U/Pb ages of ophiolites and arc-related plutons of the Norwegian Caledonides. Implications for the development of Iapetus. *Contributions to Mineralogy and Petrology*, 98: 12–23.

[2] Maaløe S. (2005). The dunite bodies, websterite and orthopyroxenite dikes of the Leka ophiolite complex, Norway. *Mineralogy and Petrology*, 85: 163-204.

[3] Furnes H, Pedersen RB, Hertogen J, Albrektsen BA. (1992). Magma development of the Leka ophiolite complex, central Norwegian Caledonides. *Lithos* 27: 259–277.

[4] O'Driscoll B, Day JMD, Walker RJ, Daly JS, McDonough WF, Piccoli PM. (2012). Chemical heterogeneity in the upper mantle recorded by peridotites and chromitites from the Shetland Ophiolite Complex, Scotland. *Earth and Planetary Science Letters*, 333-334: 226-237.

INFLUENCE OF IN SITU HYDROGEN POROSIFICATION OF PORTLAND CEMENT PRODUCTS WITH ALUMINIUM AND ZINC POWDER ON THERMAL CONDUCTIVITY AND MECHANICAL PARAMETERS

Oeder Klaus¹, Pöllmann Herbert², Krcmar Wolfgang¹

¹Faculty of Materials Engineering, Technische Hochschule Nuernberg, Germany, ²Institute of Geosciences and Geography, University of Halle, Germany

Thanks to their outstanding mechanical properties, OPC-based building materials play a dominant role in the construction sector. Unfortunately, the production of portland cement leads to the release of a great amount of CO₂. Moreover, the specific thermal conductivity of portland cement-based structures is higher than for competing construction materials, which undermines the implementation of the increasingly stringent legal requirements for energy savings in residential buildings.

A proven process to increase insulation properties is the incorporation of pores into a building material. Concrete foams are currently the subject of scientific research. Foams can be generated by entraining air into the concrete paste. Another concept is the production of the gas used for foaming by means of chemical reactions. Besides oxygen that is released from peroxides, hydrogen gas is generated by the chemical reaction of aluminum or zinc powder with the calcium hydroxide solution that arises, when the cement powder is brought in contact with water. By the use of finely ground metal powders, a network of pores with a diameter in the sub-millimeter range can be formed. First results and a detailed overview of the planned activities and strategies of the ongoing research will be presented. For example, the addition of 0,1 Ma.-% aluminum to a CEM II-A/LL 42,5 R leads to a reduction of the specific thermal conductivity of 59 % and to a reduction of the apparent density of the hardened concrete of 40 %, compared to reference samples that were produced with the same water-to-cement ratio. Combinations of different metals with different grain size distributions and different OPC qualities will be compared regarding density, thermal conductivity, compressive strength, and possible changes in the structure of the hydrate phases.

MULTILEVEL MAGMA STORAGE BENEATH FOGO, CAPE VERDE RECORDED BY BORDEIRA DIKES

Ofierska Weronika¹, Witcher Taylor², Barker Abigail², Burchardt Steffi², Ollie Risby², Tollan Peter¹

¹D-ERDW, ETH Zurich, Switzerland, ²Earth Sciences, Uppsala University, Sweden

Intrusive systems beneath ocean islands transport the magma through the plumbing system, which is transported from storage zones at depth to erupt at the surface. Magma storage zones are connected by dikes which therefore represent the conduits in the magma plumbing system. We focus on dikes exposed in the Bordeira cliffs of Fogo in the Cape Verde archipelago. We applied a multidisciplinary approach including mineral thermobarometry, diffusion chronometry, and 3D modeling of dikes to understand the intrusive magma storage beneath Fogo in space and time. The samples collected from the Bordeira dikes are basanite and nephelinite in composition and intersect at 1.25 to 1.85 km depth. All samples have abundant pyroxene in three different size ranges; megacrysts (>0.5 mm), phenocrysts (0.1 up to 0.5mm), and microcrysts (<0.1 mm). Clinopyroxene exhibits strong and complex zonation patterns. The width of the diffusion boundary varies from 2 µm for microcrysts up to 8 µm in phenocrysts and diffusion chronometry ranges from days to almost 1.5 years. Clinopyroxene-melt thermobarometry suggests that the magma storage beneath Fogo extends from 20 to 890 MPa.

We compared our thermobarometry data from the dikes with the records for historical eruptions in 1951, 1991, and 2014-2015 and discovered that the intrusive and extrusive system is connected at depths of 12 to 23 km, in a deep magma storage zone. Moreover, residence timescales for this level are up to two months, which are in agreement with pre-eruptive zonation recorded by the volcanic rocks (few days to weeks). Another important stagnation level lays between 10-14 km, pooling around the Moho (12km), which was recorded by the microcrysts from the dikes, and overlaps with the record for fluid inclusions from 2014-2015 and 19951 tephrites. Even though this “Moho zone” yields similar thermobarometric data for both, volcanic and intrusive systems, the timescales for these datasets vary significantly. The intrusive system recorded an average timescale of 80 days whereas the data from the fluid inclusions indicate very short periods of equilibration of up to one day. As we approach the surface, the difference between intrusive and extrusive systems becomes more notable. The modeled intersections are in agreement with the earthquake data from the 2014-2015 eruption; thus indicating that magma could be stalling between 1-2 km below sea level during its passage to the surface. The clinopyroxene phenocrysts record prolonged stagnation of up to 1.5 years at depths of 5 to 10 km, whereas the extrusive system made its final ascent to the surface in less than 12 hours for eruption in 2014-2015.

References:

- Hildner, E., Klügel, A., & Hauff, F. (2011). Magma storage and ascent during the 1995 eruption of Fogo, Cape Verde Archipelago. *Contributions to Mineralogy and Petrology*, 162(4), 751–772. <https://doi.org/10.1007/s00410-011-0623-6>
- Hildner, E., Klügel, A., & Hansteen, T. H. (2012). Barometry of lavas from the 1951 eruption of Fogo, Cape Verde Islands: Implications for historic and prehistoric magma plumbing systems. *Journal of Volcanology and Geothermal Research*, 217–218, 73–90. <https://doi.org/10.1016/j.jvolgeores.2011.12.014>
- Klügel, A., Day, S., Schmid, M., Faria, B. (2020). Magma Plumbing During the 2014–2015 Eruption of Fogo (Cape Verde Islands). *Frontiers in Earth Science*, 8, 157. <https://doi.org/10.3389/feart.2020.00157>
- Mata, J., Martins, S., Mattielli, N., Madeira, J., Faria, B., Ramalho, R.S., Silva, P., Moreira, M., Caldeira, R., Moreira, M., Rodrigues, J., Martins, L. (2017). The 2014–15 eruption and the short-term geochemical evolution of the Fogo volcano (Cape Verde): Evidence for small-scale mantle heterogeneity. *Lithos*, 288-289, 91-107. DOI:10.1016/j.lithos.2017.07.001

INCONGRUENT MELTING OF THE MANTLE: PERITECTIC MINERAL ENTRAINMENT PRODUCES SILICATE LAYERING AND CHROMITE SEAMS IN MAGMA CHAMBERS.

Otto Tahnee¹, Stevens Gary¹, Mayne Matthew¹, Moyen Jean-François²

¹Earth Science, Stellenbosch University, South Africa, ²Universite de Lyon, France

The mechanisms responsible for the formation of mineral deposits and layering within cratonic Layered Mafic Intrusions (LMIs) have remained elusive. Similarly, the mantle melting processes that generate the parental magmas to these LMIs are poorly understood. The layered rocks of the Bushveld Complex (BC) in the Kaapvaal Craton (KC), which host the majority of the world's viable chromium (Cr) reserves in the form of chromite seams of variable thickness, are a good example of this. If the solubility of Cr in the broadly basaltic andesitic melts hypothesized to have formed the BC is considered to control chromite accumulation, the volume of magma required in the BC formation is at least an order of magnitude larger than the volume of rocks currently considered to constitute the complex. The formation of the complicated, often repetitive silicate rock layering in the lower portions of the BC that host the chromite layering is similarly difficult to explain, particularly given the details of the Mg# and Sr isotopic stratigraphy of these rocks, indicating magma contributions from many different source rocks and a lack of systematic crystal fractionation from a single magma reservoir. To investigate possible source mechanisms that might produce magmas capable of forming these BC features, this study used a phase equilibrium approach to analyze the nature of the partial melting processes in both an eclogite and garnet peridotite source, similar in composition to those of KC mantle nodules. We studied isobaric sections at 15, 20, 25 & 30 kbar and assumed the rocks to be H₂O & CO₂ free. Fertility for melt production in both sources is strongly controlled by the abundance of clinopyroxene (Cpx), garnet (Gt), and orthopyroxene (Opx), as the Al-, Ca- and Si-rich phases. In the peridotite, the dominant peritectic phase produced by partial melting is spinel (Sp), with Sp production being triggered by the consumption of Cr-rich Opx after Gt and Cpx have reacted out. The amount of Sp produced is positively correlated with pressure. Peritectic Sp is considered to nucleate at the sites of melt production and to be entrainable to the magma, as a moderate degree of partial melting precedes its production. Such magmas extracted from the peridotite source during the interval of peritectic Sp production have a massively higher capability for producing chromite layers by density separation in crustal magma chambers than do magmas leaving the source as pure melts. During incongruent partial melting of the eclogite, peritectic Gt forms from the solidus, and dependent on pressure, the melt proportion increases to 10-30 vol.% before peritectic Gt formation ceases and Gt becomes a reactant mineral. At higher melt proportions of >10 vol.% peritectic Gt is considered likely to be entrained. This substantially enhances the capacity of such magmas to produce layering in upper crustal magma chambers, as during magma ascent Gt reacts to form assemblages of anorthite + pyroxene, segregating by either density or flow dynamics to form anorthosite and pyroxenite layering on entry to the magma chamber. Thus, we propose the formation of Cr and silicate layering in the BC due to the entrainment of undissolved peritectic crystals to the magma in the source.

PRESSURE-DRIVEN METHANOL INTRUSION IN MFI-ZEOLITES AND ITS EFFECTS ON THE STRUCTURAL DEFORMATION IN SILICALITE-1

Pagliaro Francesco¹, Battiston Tommaso¹, Sartbaeva Asel², Wells Stephen², Comboni Davide³, Gatta G. Diego¹, Lotti Paolo¹

¹University of Milan, Italy, ²University of Bath, United Kingdom, ³European Synchrotron Radiation Facility, France

MFI-zeolites are nowadays used in methanol-to-olefins (MTO) production processes as catalysts, representing an alternative to the high-energy demanding Steam Cracking process, which accounts for 95% of the worldwide olefins production. At ambient conditions, only the grain surfaces of the zeolite are supposed to be active in the MTO process. Applying hydrostatic pressure, the methanol molecules may be injected into the structural channels of the zeolites. The structure of MFI-zeolites is characterized by SiO₄ interconnected tetrahedra, which define two major structural channels systems, confined by 10-members rings (10mR) of tetrahedra running along [010] and sinusoidal cavities along the [100] direction; minor rings, constituted by 6mR and 5mR units are also present. Comboni et al. (2020 *Catalysis Today*, 345, 88-96) studied, through in situ synchrotron X-ray powder diffraction, the capability of pressure to improve the methanol absorption process. In order to evaluate the magnitude of the methanol HP-driven injection process, also the intrinsic compressional behavior of silicalite-1 has been studied, using a non-penetrating pressure-transmitting fluid (i.e. silicone oil). A different compressional behavior characterizes the methanol and the silicone-oil ramps (hereafter, Sil-meth and Sil-soil), as a consequence of the intrusion of methanol within the silicalite-1 structural channels. Since no structural refinement was possible based on XRD data, we aim to define the framework deformation and methanol intrusion of silicalite-1 at varying pressure, through template-based geometric modeling, conducted on both Sil-meth and Sil-soil. This modeling identifies the flexibility intrinsic to the geometry and topology of the crystal structure, considered as a mechanical framework. Concerning the compression along the three principal crystallographic axes in Sil-meth, it has been observed that along the a- and the b-axis the structure behaves similarly, whereas along the c-axis, which does not correspond to any of the channel development directions, the structure shows a higher compression. Conversely, the Sil-soil ramp presents a more isotropic compression. As expected, the 10mR's are clearly more compressible in Sil-soil, whereas in the Sil-meth ramp the intrusion of methanol leads to the phenomenon known as "pillar effect". As pointed out by Comboni et al. (2020) for both the P-ramps, a phase transition from monoclinic to orthorhombic (MOPT) occurs at about 0.5 GPa. Although the phase transition does not largely affect the unit-cell volume of silicalite-1, in both the Sil-soil and the Sil-meth, it strongly influences the behavior of the channels under HP, changing their compressional trend at 0.5 GPa. Lastly, the behavior of the Sil-soil is characterized by a "distributed" compression, which results in a rather equal magnitude of the compression of the 10mR, 6mR, and 5mR units. Conversely, in the Sil-meth, the compression of the 10mR is significantly modest, whereas takes place a clear distortion of the 5mR units, which small diameter does not allow any methanol intrusion process.

HIGH-PRESSURE BEHAVIOR OF REE-BEARING ARSENATES AND PHOSPHATES FROM THE HYDROTHERMAL FISSURES OF Mt. CERVANDONE, WESTERN ALPS, ITALY

Pagliaro Francesco¹, Lotti Paolo¹, Comboni Davide², Battiston Tommaso¹, Guastoni Alessandro³, Gatta G. Diego¹, Rotiroti Nicola¹

¹University of Milan, Italy, ²European Synchrotron Radiation Facility, France, ³University of Padova, Italy

ATO4 minerals, where A= Sc, Y, REE, U, and Th, whereas T stands for tetrahedrally-coordinated cations (i.e., As, P, Si), represent a large group of common accessory minerals in hydrothermal alteration of granitoid rocks. These include the REE-bearing arsenates chernovite-(Y) (YAsO₄) and gasparite-(Ce) (CeAsO₄), as well as the more common REE-bearing phosphates, xenotime-(Y) (YPO₄) and monazite-(Ce) (CePO₄). Chernovite-(Y) and xenotime-(Y) share the same zircon-type structure with tetragonal symmetry (I41/amd), whereas gasparite-(Ce) and monazite-(Ce) are characterized by the so-called monazite-type structure and monoclinic unit-cell (P21/n). Although fairly rare, in the last decade, the REE-bearing arsenates have been detected in several sites and their role in REE partitioning might be important. The Mt. Cervandone (Piedmont, Italy) mineral deposit is one of the most renowned within the Alps. In this study, we report the results on the crystal chemistry and high-P behavior of the four above-mentioned mineral species, obtained by EPM-WDS chemical analysis and in situ synchrotron XRD at high-pressure exceeding 20 GPa, using a diamond anvil cell. The chemical analysis reveals a nearly complete solid solution between chernovite-(Y) and xenotime-(Y), whereas a miscibility gap apparently occurs between gasparite-(Ce) and monazite-(Ce). Moreover, the presence of a complex solid solution between the isostructural chernovite-(Y), xenotime-(Y) and thorite, up to ~13 mol % of ThSiO₄ has been observed. The high-pressure behavior of chernovite-(Y), xenotime-(Y), gasparite-(Ce), monazite-(Ce) and Th-rich chernovite-(Y) has been studied. For the zircon-type structure minerals, a P-induced phase transition has been detected, whereas the monazite-type compounds are stable within the whole pressure-range investigated. Based on the P-V data, the isothermal bulk moduli of the five selected minerals (two samples of chernovite-(Y)) have been refined, using a 2-order Birch-Murnaghan EoS: K_{P0,T0}=125(3) GPa (β_{V0}=0.0080(2) GPa⁻¹) for chernovite-(Y); K_{P0,T0}=145(2) GPa (β_{V0}=0.0069(1) GPa⁻¹) for xenotime-(Y); K_{P0,T0}=105(1) GPa (β_{V0}=0.0095(1) GPa⁻¹) for gasparite-(Ce), K_{P0,T0}=121(2) GPa (β_{V0}=0.0083(1) GPa⁻¹) for monazite-(Ce) and K_{P0,T0}=123.8(9) GPa (β_{V0}=0.00808(6) GPa⁻¹) for Th-rich chernovite-(Y). The monazite-type structures are found to be always more compressible with respect to the zircon-type structures. Moreover, within each structure-type, the arsenates are always more compressible than the isostructural phosphates. Although the REE-coordination polyhedron accommodates most of the bulk compression, the tetra-coordinated cation (As or P) controls the different compressibility of arsenates and phosphates: PO₄ tetrahedra acts as rigid bodies under pressure, whereas AsO₄ is characterized by a significant compression, especially in the low-P regime. No significant differences have been observed among the high-pressure behaviors of Th-poor and Th-rich chernovite-(Y).

AN UNSUPERVISED METHOD FOR SEGMENTATION OF ORE MINERALS IN OPTICAL MICROSCOPY

Pagnotta Stefano¹, Aquino Andrea¹, Lezzerini Marco¹

¹Earth Science Department, University of Pisa, Italy

Optical microscopy analysis is one of the main methods in the study of ore minerals and ore beneficiations. In recent years, methods that provide for unsupervised classification of minerals constituting the rocks under consideration are becoming increasingly successful. This happened thanks, above all, to the luck obtained from the QEMSCAN analysis, which however requires very complex and expensive preparations of the sample. In the field of optical microscopy, supervised methods for modal analysis are still used, with some exceptions in which multispectral methods and image analysis methods are used that exploit segmentation based on image thresholding such as grey threshold, triangle method, method of k-means, or statistical methods for example Principal Component Analysis (PCA). The increase in the use of artificial intelligence, driven by the technological development of mobile devices, has led to the spread of unsupervised methods, capable of recognizing and classifying features within images. If we carry this type of algorithms in the field of optical microscopy, without disturbing the complex convolutional networks, but using the Self Organized Maps (SOM) coupled with a careful choice of the images to be used for the training of the algorithm, we immediately realize of the enormous potential offered in the segmentation of features hours and the possibility of modal analysis, at the scale of the images produced. Although these algorithms behave like black boxes, from which it is impossible to extract information on the physics that leads to the result, an attentive operator with the right amount of knowledge can reconstruct afterward the physical reasons for which a certain feature is segmented into some way rather than another. The purpose of this short communication is to instil curiosity in the listener, towards the potential use of SOM algorithm in the analysis of images obtained by an optical microscope.

MONITORING AS A PREVENTIVE MAINTENANCE CONCEPT FOR WALL PAINTINGS

Pallas Leander¹, Bellendorf Paul¹, Holl Kristina¹

¹Building Preservation Sciences, University of Bamberg, Germany

The former Dominican Church of St. Christopher in Bamberg is a large mendicant church from the 14th and 15th centuries, which contains a large and complex program of wall painting fragments, that have been uncovered in the course of the 20th century. Extensively renovated between 1999 and 2015, a combined heating system consisting of underfloor and circulating air heating was installed for using the former church as an event venue for the university. During an inspection in 2019, fragments of the wall paintings were found flaked off on the floor. Measurements of the indoor climate show extremely low relative humidities especially during the winter months as well as high fluctuations of the relative humidity.

The objective of the investigations was to examine the state of preservation of the wall paintings and the prevailing indoor and microclimate to assess the damage potential and to develop a concept for a long-term, non-destructive monitoring. By using the method of structured light scanning a concept to inspect the state of preservation of the wall paintings at periodic intervals was developed. For this purpose, the generated 3D data from different points in time are virtually superimposed. Movements or changes in the surfaces are visualized in a false-color representation. This makes it possible to compare the exact surface at different times to show even the smallest changes. Thus, it is possible to intervene at an early stage even in the case of minor damage and avoid the need for extensive restorations, which always also mean an intervention in the historic surfaces.

Initially, 10 significant surfaces of the wall paintings were selected and recorded twice, in July and September 2020. For the examination, a high-resolution Structured Light Scanner (L3D, Carl Zeiss Optotechnik GmbH) was used, which scanned the surfaces in a submillimetre range with two different resolutions at a point distance of 0.03 - 0.1 mm. In this way, the surface could be examined contactless and non-destructive. For the interpretation of the measured movements, the results of the scans were then combined with temperature and humidity measurements to interpret any surface movements for climatic changes. By repeating the recordings two months later, the differences can be visualized directly. Using this technique an enlargement of cracks or even flaking off of entire paint layer packages can be shown. The aim was to record areas with little as well as major surface movements. The analysis of the indoor climate of the church shows high fluctuations especially in relative humidity ranging from 60 to 30 % rh. As the former church is continuously heated to 20 – 21 °C every day, dry periods of less than 20 % rh occur, especially in the winter months. Particularly the short-term fluctuations are significant: strong changes up to 30 % rh within a few hours take place several times a week. The severe dryness, as well as the high short-term fluctuations, pose an enormous potential threat for the wall paintings. The effects of these humidity fluctuations were adequately visualized with the 3D-comparisons. Surface movements were visible on almost all of the 10 surfaces especially at cracks and edges of painting layer fragments. Changes of the surfaces within a few days were also detected.

Carried out by Building Preservation Sciences of the University of Bamberg, the monitoring is now to take place every one to two years and will be repeated for the first time in summer 2021.

THERMODYNAMIC MODELLING ON THE PEAK METAMORPHISM AND FLUID EVENTS DURING EXHUMATION OF THE TSO MORARI COESITE-BEARING ECLOGITE, NW HIMALAYA

Pan Ruiguang¹, Macris Catherine¹, Menold Carrie²

¹Department of Earth Sciences, Indiana University–Purdue University Indianapolis, United States, ²Department of Geology, Albion College, United States

The advancement of computational petrology and the availability of relevant thermodynamic databases provide the mechanism to more precisely quantify metamorphic and metasomatic processes. In this study, we model peak metamorphic pressure-temperature (P-T) conditions of the Tso Morari ultra-high pressure (UHP) eclogite as well as multiple metasomatic events during exhumation. Modeling protocols use the Theriak-Domino program with dataset ds 62 and major metabasic mineral (garnet, omphacite, clinoamphibole, phengite, chlorite, lawsonite, talc, plagioclase, biotite, and quartz) activity-composition relations. The effect of garnet fractionation on the rock's effective bulk composition was considered when simulating prograde garnet growth. A “fishhook” shaped clockwise P-T path was obtained with a peak pressure of ~28.5 kbar at ~563 °C, followed by a peak temperature of ~613 °C at ~24.5 kbar.

Thermodynamic modeling using P-M(H₂O) pseudosections on Tso Morari eclogite matrix indicates three distinct phases of fluid events during exhumation. Fluid I occurs at ~610 °C and ~23.5 kbar with ~3.1 mol % fluid infiltration based on modeling of lawsonite break-down and epidote formation in the eclogite matrix. Fluid II occurs at ~19.0 kbar and ~610 °C with a limited abundance of fluid infiltration due to talc break-down through modeling the formation of amphibole in the eclogite matrix. Fluid III occurs at ~610 °C and ~8.7 kbar with a limited abundance of fluid infiltration due to phengite break-down, based on modeling of symplectitic association (amphibole, plagioclase, biotite, and quartz) formation surrounding omphacite and phengite in the eclogite matrix. This study demonstrates the need of using careful petrographic observations in parallel with thermodynamic modeling to achieve realistic results.

SCALING-UP THE ULTRAPURE Na-X AND Na-A ZEOLITE SYNTHESIS USING A WASTE SOLUTION FROM FLY ASH-DERIVED ZEOLITES PRODUCTION PROCESS

Panek Rafał¹, Madej Jarosław¹, Bandura Lidia¹, Słowik Grzegorz², Skupiński Sebastian¹

¹ Department of Geotechnical Engineering, Lublin University of Technology, Poland, ²Department of Chemical Technology, Institute of Chemical Sciences, Maria Curie-Skłodowska University in Lublin, Poland

Nowadays, using wastes like fly ash for porous materials production is one of the ways to act in accordance to sustainable development principle. A lot of waste solution is generated during zeolite synthesis in a hydrothermal conversion of fly ash. In this work, such solution was used as a substrate for Na-X and Na-A zeolites synthesis at laboratory and technical scale. Zeolites were characterized using among others: X-ray diffraction (XRD), X-ray fluorescence spectroscopy (XRF), transmission electron microscopy (TEM), Fourier transform infrared spectroscopy (FTIR), and nitrogen adsorption/desorption isotherm. Monomineral zeolitic phase composition and very high purity (>98%) were observed. Textural parameters like specific surface area (SBET) showed that Na-X zeolite pores were almost identical to commercial 13X. Other methods confirmed similarity of two zeolites produced in two scales which showed good replicability of the laboratory process in the larger scale. Research work has proven that the waste solution can be successfully treated as a raw material, not a waste. In addition, the successful scale-up of the entire process allows to think about implementing the technology in the industry in accordance with the principles of the circular economy.

Funding

This research was financed within the National Centre for Research and Development project no. LIDER/19/0072/L-9/17/NCBR/2018.

NON-CONVENTIONAL CO₂ MINERALIZATION INTO Ca-OXALATES FOR CARBON CAPTURE, SEQUESTRATION AND REUSE

Pastero Linda¹, Barella Vittorio², Allais Enrico³, Marengo Alessandra⁴, Bernasconi Davide¹, Curetti Nadia⁵, Destefanis Enrico¹, Pavese Alessandro¹

¹Earth Sciences, University of Turin, Italy, ²Earth Sciences, ISO4 c/o University of Turin, Italy, ³Earth and Environmental Sciences, ISO4 c/o University of Pavia, Italy, ⁴Earth Sciences, SpectraLab c/o University of Turin, Italy, ⁵Earth Science, University of Turin, Italy

To control the amount of CO₂ in the atmosphere, many synergic capture methods coupled with the reduction of emissions have been proposed. Mineral trapping and accelerated weathering of silicate rocks have been suggested as the most suitable hosts for mineralized carbon (Zevenhoven and Fagerlund, 2010). Natural weathering can remove some CO₂ from the atmosphere, estimated at 300Mt/yr (Beaulieu et al., 2012). Still, the weathering rate is slow, although the natural process can be accelerated for industrial purposes (Destefanis et al., 2020). Within this framework, we proposed the reduction of carbon from C(IV) to C(III) using ascorbic acid (vitamin C) as a green CO₂ sacrificial reductant (Pastero et al., 2019, 2021). The red-ox reaction was validated and clarified thoroughly. The oxalic acid can be precipitated as calcium oxalate, almost insoluble, which doubles the capture efficiency compared to carbonation. The reaction's effectiveness was evaluated under variable conditions and reached very high values, up to 80% of CO₂ removed from the atmosphere, depending mainly on the total surface exposed to the reaction, but on the CO₂/vitamin C mixing mode, the presence of oxygen in the reaction vessel and the pH of the solution as well.

The reaction products are limited to calcium oxalate dihydrate (weddellite), while occasionally, the monohydrate crystal phase (whewellite) was detected. The system was intentionally kept out from the stability field of the carbonates to avoid competition between the two phases of the carbon capture process. The thermal degradation of the crystalline product was evaluated in situ by XRPD. The dissolution of calcium oxalates does not directly produce CO₂, avoiding its straight release in the environment. The ascorbic acid degradation products have no or just feeble interference with the production of calcium oxalate from CO₂, and are generally considered not harmful.

References

- Beaulieu, E., Goddëris, Y., Donnadiou, Y., Labat, D. and Roelandt, C.: High sensitivity of the continental-weathering carbon dioxide sink to future climate change, *Nat. Clim. Chang.*, 2(5), 346–349, doi:10.1038/nclimate1419, 2012.
- Destefanis, E., Caviglia, C., Bernasconi, D., Bicchi, E., Boero, R., Bonadiman, C., Confalonieri, G., Corazzari, I., Mandrone, G., Pastero, L., Pavese, A., Turci, F. and Wehrung, Q.: Valorization of mswi bottom ash as a function of particle size distribution, using steam washing, *Sustain.*, 12(22), 1–17, doi:10.3390/su12229461, 2020.
- Pastero, L., Curetti, N., Ortenzi, M. A., Schiavoni, M., Destefanis, E. and Pavese, A.: CO₂ capture and sequestration in stable Ca-oxalate, via Ca-ascorbate promoted green reaction, *Sci. Total Environ.*, 666, 1232–1244, doi:10.1016/J.SCITOTENV.2019.02.114, 2019.
- Pastero, L., Marengo, A., Boero, R. and Pavese, A.: Non-conventional CO₂ sequestration via Vitamin C promoted green reaction: Yield evaluation, *J. CO₂ Util.*, 44, 101420, doi:10.1016/j.jcou.2020.101420, 2021.
- Zevenhoven, R. and Fagerlund, J.: Mineralisation of carbon dioxide (CO₂), in *Developments and Innovation in Carbon Dioxide (Co, vol. 2, pp. 433–462, Elsevier Ltd., 2010.*

TOLBACHIK VOLCANO AT KAMCHATKA – THE PRESENT WORLD RECORD-HOLDER IN NEW MINERALS

Pekov Igor¹, Zubkova Natalia¹, Koshlyakova Natalia¹, Shchipalkina Nadezhda¹, Sandalov Fedor¹, Bulakh Maria¹, Turchkova Anna¹, Agakhanov Atali², Sidorov Evgeny³

¹Faculty of Geology, Lomonosov Moscow State University, Russian Federation, ²Fersman Mineralogical Museum RAS, Russian Federation, ³Institute of Volcanology and Seismology FEB RAS, Russian Federation

In 2020, the Tolbachik volcano at the Kamchatka Peninsula, Russia became the world record-holder in a number of new minerals first discovered for one geological object, when passed the former leader, Khibiny alkaline complex, Kola Peninsula, Russia. Today the three leaders in this field are as follows: Tolbachik – 133 IMA-approved new mineral species, Khibiny – 127, and Lovozero alkaline complex (Kola Peninsula) – 114. Tolbachik also demonstrates the world-highest dynamics in discoveries of new minerals for one locality: since 2011, i.e. during the last decade 103 minerals were first described there, including 77 species characterized by our research team. All 133 new minerals were found in deposits of active oxidizing-type fumaroles born by Great Tolbachik Fissure Eruption 1975–1976 (mainly) and the Tolbachik eruption of 2012–2013. Only 14 of them are H₂O-bearing species that formed under temperatures below 100–150°C involving atmospheric agents while others are products of high-temperature fumarolic activity (200–800°C). A very bright geochemical feature of Tolbachik fumaroles is the distinct "ore" specialization reflected, in particular, in the chemistry of new minerals: the majority of them are oxygen compounds or chlorides with species-defining chalcophile elements: Cu, Pb, Zn, As, Se, Te, Tl, Cd, Bi, Sn. Strongly oxidizing conditions of mineral crystallization are illustrated by high oxidation states of indicator elements: minerals with only S⁶⁺, Fe³⁺, As⁵⁺, Mo⁶⁺, W⁶⁺ are known there; some new minerals contain V⁵⁺, V⁴⁺, Se⁴⁺, Te⁴⁺ or Tl³⁺. The distribution of Tolbachik new minerals between chemical classes is as follows: arsenates – 42, sulfates – 41, chlorides – 13, vanadates – 12, selenites – 10, borates – 5, molybdates – 2, silicates – 2, oxides – 2, phosphates – 2, fluoride – 1, and carbonate – 1. All these arsenates, vanadates, selenites, borates, molybdates, silicates, oxides, and phosphates are H-free and known only in high-temperature (> 200–300°C) parageneses. In whole, in deposits of Tolbachik fumaroles about 330 minerals are reliably known now (including products of the supergene alteration of sublimates), i.e. 133 new species consist 40% of their mineral diversity. So high share of new minerals clearly demonstrates the uniqueness of Tolbachik fumarole fields. They can be considered as the world-brightest example of an on-land oxidizing-type fumarolic mineral-forming system, an etalon object for the studies of this genetic type in both mineralogical and geochemical aspects. Such originality is caused by unique for natural systems physical and chemical conditions and mechanisms of mineral formation, namely a combination of high temperatures, atmospheric pressure, very high oxygen fugacity (due to mixing of hot volcanic gas with air), gas transport of the majority of chemical elements and direct deposition of minerals from volcanic gases which have here specific geochemical features including strong enrichment by alkali metals and chalcophile ("ore") elements.

The study was supported by the Russian Science Foundation, grant 19-17-00050.

ZEOLITE-BASED COMPOSITE FOR CHROMIUM (VI) REMOVAL

Peluso Antonio¹, Aprea Paolo¹, Caputo Domenico¹, De Gennaro Bruno¹, Galzerano Barbara¹

¹DICMAPI, Università degli Studi di Napoli Federico II, Italy

Abstract

The fast development of many industries, nowadays, leads to a production of a huge quantity of wastewater with the consequent environmental release of many pollutants, which have toxic effects on living beings and ecosystems. Currently, adsorption seems to be an effective technique for wastewater treatment, its success depends on the efficiency of the adsorbent. Different kinds of low costs adsorbents have been used, such as: activated carbons [1], clays [2], diatomite [3], zeolites [4], etc. Among the others, natural zeolites are still promising materials for wastewater purification. The adsorption capacity of zeolites depends on chemical and structural factors, which can be tuned by several chemical treatments to improve their separation efficiency. The aim of the present research is to verify the possible use of surface-modified natural zeolites (SMNZs), as alternative adsorbents for removing Cr(VI) from wastewater. Samples were obtained by sorption of cetyltrimethylammonium chloride (CTAC) onto phillipsite-rich tuff (PHI) or clinoptilolite-rich tuff (CLI) under dynamic conditions to attain an anionic exchanger. The anion exchange properties of the so obtained SMNZs were studied both in batch and dynamic condition, by performing kinetics and equilibrium runs, with a suitable Cr(VI) amount and an appropriate solid/liquid ratio, and by eluting fixed-bed columns containing the selected SMNZs with Cr(VI) solutions, determining the breakthrough curves on a fixed bed apparatus. Collected data showed fast kinetics and a good affinity of both SMNZs towards Cr(VI). Moreover, CLI-Cl showed a higher uptake (11.39 mg/g) than PHI-Cl (9.22 mg/g), likely due to several parameters such as the zeolite content in the tuffs, Si/Al ratio ECEC and AEC, etc. The column tests, although preliminary, show a good removal of Cr (VI) in dynamic conditions too, as well as a greater treated volume for CLI-Cl.

Lastly, chromate reduction could be enhanced by pelletized SMNZ-Zero Valent Iron (ZVI). The tests that are being developed aim specifically at setting up a combined SMNZ-ZVI system in order to repeat dynamic column tests, comparing them with those previously set up with SMNZs.

References

1. Kadirvelu, K., Kavipriya, M., Karthika, C., Radhika, M., Vennilamani, N., & Pattabhi, S. (2003). Utilization of various agricultural wastes for activated carbon preparation and application for the removal of dyes and metal ions from aqueous solutions. *Bioresource technology*, 87(1), 129-132.
2. Szabó, E., Vajda, K., Veréb, G., Dombi, A., Mogyorósi, K., Ábrahám, I., & Májer, M. (2011). Removal of organic pollutants in model water and thermal wastewater using clay minerals. *Journal of Environmental Science and Health, Part A*, 46(12), 1346-1356.
3. Galzerano, B., Aprea, P., Liguori, B., & Verdolotti, L. (2018, July). Removal of Cd (II) from wastewater by sustainable absorber: Composite diatomite-based foams. In *AIP Conference Proceedings* (Vol. 1981, No. 1, p. 020120). AIP Publishing LLC.
4. Halimoon, N., & Yin, R. G. S. (2010). Removal of heavy metals from textile wastewater using zeolite. *Environment Asia*, 3, 124-130.

ANCIENT BRICK MANUFACTURING TECHNOLOGIES TO CERAMIC INDUSTRY: PHYSICAL BEHAVIOUR AND DURABILITY ENHANCEMENT BY H-T PHASES AND SECONDARY CALCITE

Pérez-Monserrat Elena Mercedes¹, Maritan Lara¹, Garbin Enrico², Cultrone Giuseppe³

¹Department of Geosciences, University of Padova, Italy, ²CIRCe, University of Padova, Italy, ³Department of Mineralogy and Petrology, Faculty of Sciences, University of Granada, Spain

The production technologies of yellow and beige bricks with uniform and heterogeneous textures and a rather good conservation state that shape ancient constructions of the city of Padua (north-eastern Italy) have been addressed through a multi-analytical approach based on spectrophotometry, XRF, XRPD, MOP, and FESEM-EDS analysis. The influence of the production processes on the physical behavior and durability of bricks, defined by means of ultrasounds, uniaxial compressive strength hydric tests, and salt crystallization and freeze-thaw tests, were also stated. Abundant high-temperature phases formed during the firing process: chiefly, Mg-silicates -with a melilite composition rims- and a Ca-aluminosilicate matrix where pyroxene-type crystals developed. Such data reveal that calcium- and magnesium-rich illitic clays were used and that firing temperatures exceeded 900 °C. Secondary calcite, precipitated throughout the groundmass, filling partially or totally the porosity. This calcite most likely comes from the binding lime mortars, although the own carbonate-rich clays might entail another source of the lime required for the secondary calcite precipitation.

An early sintering stage was achieved, since the melting process was blocked by the formation of the high-temperature phases, yielding rather porous ceramic bodies. In the heterogeneous textured bodies, such early sintering yielded bricks rather prone to decay. However, the bricks display an overall quite good physical performance and durability, mainly fostered by the high-density phases formed during firing and by the precipitation of secondary calcite. The amount of both types of mineral phases significantly influence the mechanical behavior of bricks, while the absorption and drying capacity, as well as the resistance to salt crystallization and frost action, are mainly controlled by the porosity. The high-temperature phases have provided strength to the bodies, enhanced in turn by the calcium and magnesium contents of the raw clays. Equally positive were the changes induced by the formation of secondary calcite, increasing the cementation of the ceramic bodies.

The data obtained builds the ground for future comprehensive studies on ancient bricks towards the understanding of their physical behavior and resistance over time from the manufacturing process. In that, the high-temperature phases and the precipitation of secondary calcite have enhanced the physical performance and durability of bricks with early vitrification, the knowledge achieved may provide green solutions to the current ceramic industry. Therefore, the use of Ca- and Mg-rich clays may allow the production of quality and endured bricks by means of a low sintering achievement, hence the consumption of energy and CO₂ would be decreased. The study performed aims to highlight the important role of ancient bricks in Padua and to be part of the collective awareness for the enhancement of the built heritage of the city.

A NEW QUANTITATIVE APPROACH TO DEFINE THE FIBROUS MORPHOLOGY FOR ASBESTOS-LIKE MINERAL FIBRES

Petriglieri Jasmine Rita¹, Barale Luca², Botta Serena¹, Tomatis Maura¹, Pacella Alessandro³, Piana Fabrizio², Turci Francesco¹

¹Department of Chemistry, University of Torino, Italy, ²CNR-IGG, Italy, ³Department of Earth Sciences, Sapienza University of Roma, Italy

The Natural Occurrences of Asbestos (NOA) and potentially hazardous elongated mineral particles (EMPs) pose a risk to the environment and human health when fiber mobilization occurs following natural and human activities. The evaluation of the hazard posed by these fibrous minerals requires that key physico-chemical properties, including morphology, are evaluated. Indeed, the correlation between the fibrous habit of asbestos and its carcinogenic potency is universally accepted (IARC, 2012), an elongated morphology is not an indication of toxicity per se, and a quantitative parameter to express the asbestos-like morphology of a mineral fiber is required. This work introduces the “fibrosity parameter” to quantitatively evaluate the fibrous, asbestos-like morphology of a suspected fibrous mineral. Asbestos is characterized by crystalline planes that easily split along the growth c-axis, resulting in long and thin fibers even after strong mechanical stress, such as milling. A protocol was therefore designed to verify whether a mineral that is suspected to have asbestos-like properties preserved its fibrous morphology after standardized mechanical stress. The mineral morphology and the fiber size distribution were estimated by means of light microscopy coupled with automated image analysis (FPIA) and Scanning Electron Microscopy (SEM). This multi-technique approach allows thousands of particles to be measured with respect to SEM investigation alone, providing a reliable statistical analysis to be used comparatively with asbestos minerals. The fibrosity parameter was evaluated on a set of antigorite samples showing a fibrous to lamellar habit at the macroscopic scale. Data on investigated minerals were compared with data obtained with asbestos, i.e., UICC crocidolite and tremolite asbestos from Val Susa, and a quantitative assessment of the asbestos-like morphology of the samples was proposed.

Fibrous antigorite preserved its fibrous morphology, indicating that this antigorite sample fractures easily along the c-axis and exhibits an asbestos-like morphology. Standardized grinding generated from 65% to 80% of EMPs (% of particles with Length/Diameter >3 of the total particles; NIOSH, 2011) most of which have the dimensions of respirable fibers (L>5 µm, D<3 µm, L/D>3; WHO, 1997). Fibrous antigorite is in the range of fibrosity of asbestos (% EMPs 83%, and from 80 to 69% for UICC crocidolite and tremolite VS, respectively), exhibiting a trend similar to tremolite asbestos, defined by a little but negligible decrease in fibrosity with increasing the time of grinding. As expected, the lamellar antigorite preserved its lamellar habit, indicating that lamellar antigorite does not fracture preferentially along the crystal growth direction. The % EMPs generated after grinding is about 35%. Application of the fibrosity parameter to suspected asbestos-like minerals will be promising for quantifying the asbestos-like morphology of natural mineral fibers from the perspective of their toxicological profiling.

EPIDOTE U–Pb GEOCHRONOLOGY BY LA-ICP-MS SHEDDING LIGHT ON HYDROTHERMAL ACTIVITY IN THE AAR MASSIF (CENTRAL SWISS ALPS)

Peverelli Veronica¹, Berger Alfons¹, Wille Martin¹, Piccoli Francesca¹, Pettke Thomas¹, Herwegh Marco¹

¹Institute of Geological Sciences, University of Bern, Switzerland

Unraveling the timing and dynamics of fluid circulation in the crust relies on geochronology and isotopic analyses of suitable vein-filling minerals. Minerals of the epidote–clinozoisite solid solution (hereafter simply epidote) are common both as vein-filling minerals and rock-forming ones in greenschist- to blueschist-facies metamorphic rocks. The incorporation of Sr, Pb, and U renders epidote an appealing target to investigate fluid circulation and vein formation. In particular, in the Alpine setting epidote ± quartz veins are widespread in granitic rocks. On the assumption that each vein crystallized from one fluid in one opening event, the Tera–Wasserburg approach can be used to calculate U–Pb ages and initial ²⁰⁷Pb/²⁰⁶Pb ratios in epidote without assumptions on the initial Pb isotopic composition (see Peverelli et al., 2021).

We performed U–Pb geochronology of epidote by LA-ICP-MS in hydrothermal veins from the Aar Massif, with different microstructures and relations to well-investigated shear zones (Wehrens et al., 2017; Herwegh et al., 2020). The obtained epidote ages define two clusters: 1) ca. 20–17 Ma and 2) ca. 14–12 Ma. These age clusters overlap with known deformation phases (Herwegh et al., 2020). Two epidote samples yield ages of 51 ± 15 and 26.3 ± 3.7 Ma respectively, which cannot be correlated with known tectonic events in the area. Initial ²⁰⁷Pb/²⁰⁶Pb ratios of all studied samples (0.7818–0.8109) are lower than those predicted for their host rocks at the time of vein formation, indicating that the vein-forming fluids equilibrated with more radiogenic components along their pathways. The samples overlapping in ages also overlap in initial ²⁰⁷Pb/²⁰⁶Pb ratios, hinting at a common fluid pathway for each vein family. The ⁸⁷Sr/⁸⁶Sr ratio of 0.716145 and of 0.726552 measured by TIMS respectively in the 51 ± 15 Ma sample and in a 19.2 ± 4.3 Ma one indicate that the vein-forming fluid of the younger sample equilibrated with a more radiogenic component. Since the oldest shear zones in the area are 22 Ma, it is possible that the difference in ⁸⁷Sr/⁸⁶Sr ratios is due to the biotite-rich shear zones acting as fluid pathways at 20–17 Ma.

Epidote is demonstrated to be a powerful geochronological and isotopic tool to reconstruct the timing of fluid circulation and to gain a better insight into the fluid pathways. The combination of U–Pb geochronology and isotope geochemistry to minerals of the epidote–clinozoisite series might prove crucial in samples with no datable minerals other than epidote in a broad range of geological contexts.

RHEOLOGICAL WEAKENING BY MELT MIGRATION AND REPLACEMENT REACTIONS: SIGNATURES AND CONSEQUENCES

Piazolo Sandra¹, Daczko Nathan², Gardner Robyn², Ghatak Hindol², Silva David²

¹School of Earth and Environment, University of Leeds, United Kingdom, ²Australian Research Council Centre of Excellence for Core to Crust fluid systems, Macquarie University, Australia

High strain zones, shear zones, and faults are Earth's primary crustal-scale conduits of fluid (*sensu lato*) migration and mass transfer. At the same time, these zones localize deformation from millimeter to lithospheric scale, consequently playing a major role in the deformation of the continental and the oceanic crust. While the role of aqueous fluid in the hydration and rheological weakening of the crust has been extensively studied, the role, signature, and consequence of silicate melt migration in localized zones of deformation have seen less attention. We present detailed field, microstructural and chemical studies of melt present high strain zones from two different geotectonic and lithological environments, namely intracontinental orogeny and oceanic core complex formation. The Alice Spring Orogeny (450–300 Ma) is an intracontinental orogen exposed in Central Australia. It is characterized by several km thick schistose belts which facilitated orogeny in the relatively low-stress environment of Central Australia. Similarly, the drill core from the Atlantis Bank oceanic core complex, South West Indian Ridge, preserves signatures of several stages of melt present deformation which is thought to have played a major role in core complex formation. Sample scale chemical signatures of melt present deformation in both sites include replacement reactions resulting in local and pervasive host hydration, depletion of silica of host, and changes in rare earth elements. Microstructurally, former melt presence is documented by, for example, interstitial oxides (ilmenite and magnetite) with low dihedral angles, pseudomorphed melt films along grain boundaries, and the three-dimensional connectivity of grains grown after melt. Field evidence of large displacements seems, at first sight, at odds with microstructural, igneous or “annealed” microstructural character. Mineral alignment without significant intragrain deformation but relatively coarse-grained, low angle triple junctions, 3D connectivity of interstitial grains suggest melt-assisted grain boundary sliding with relatively minor dislocation creep signatures are typical. Rheologically, melt flux does not only result in reaction weakening through mineral replacement of rheologically “hard” minerals by rheologically “soft” minerals but also in rheological weakening caused by syntectonic melt presence at grain boundaries.

Our combined microstructural and microchemical study highlights that the recognition of melt-related deformation is critical for understanding and therefore modeling progressive strain localization, melt flux, and the rheological evolution of hot deformation zones.

DATING METAMORPHISM AND METASOMATISM OF THE ULTRAMAFIC OCEANIC LITHOSPHERE USING PEROVSKITE AND TITANITE

Piccoli Francesca¹, Rubatto Daniela¹, Hermann Jörg¹, Vitale Brovarone Alberto²

¹Institut für Geologie, Universität Bern, Switzerland, ²Dipartimento di Scienze Biologiche, Geologiche e Ambientali (BiGeA), Alma Mater Studiorum Università di Bologna, Italy

Dating metamorphic events in ultramafic rocks such as serpentinites is notoriously difficult because of the lack of suitable minerals for geochronology. Perovskite (CaTiO_3) and titanite (CaTiSiO_5) can form during hydration of rodingite dykes within the serpentinitized mantle during subduction-related metamorphism. Therefore, dating these minerals may open new avenues to investigate the timing of fluid-rock interaction and deformation during oceanic alteration and metamorphism. We present preliminary results of in situ U-Pb dating and trace element analysis by LA-ICP-MS on perovskite and titanite in rodingite blackwalls and perovskite in ophicarbonates from different metamorphic terranes. Titanite U-Pb dating in samples from the Zermatt-Saas unit (Switzerland) returned an age of 45.0 ± 0.8 Ma, consistent with dehydration of the serpentinite and formation of the blackwall at high-pressure conditions. Perovskite in blackwalls have very low U content (\sim ppb) and could not be dated. However, perovskite in ophicarbonates have higher U, ranging from tens to few hundreds of ppm, and are a potential candidate for geochronology of ultramafic lithologies. Perovskite in the two investigated localities Sasso Moro (Malenco unit, Italy) and Balangero (Lanzo Massif, Italy) yield an age of 46.9 ± 1.8 Ma and 49.6 ± 3.8 Ma, respectively. These ages are in line with other constraints on the age of metamorphism in each locality. Moreover, perovskite in blackwalls and in ophicarbonates have different trace element composition suggesting important inheritance from the protolith. The results have implications for U mobility in metamorphic fluids and dating of metamorphic mafic-ultramafic rocks.

METAL ENRICHMENT ACROSS CRUST-MANTLE TRANSITION ZONE: INSIGHT FROM THE IVREA-VERBANO ZONE, ITALY

Pieterek Bartosz¹, Ciałęła Jakub², Tribuzio Riccardo³, Kuhn Thomas⁴, Matusiak-Małek Magdalena⁵, Nowak Izabella⁶

¹Faculty of Geographic and Geological Sciences, Adam Mickiewicz University in Poznan, Poland, ²Institute of Geological Sciences, Polish Academy of Science, Poland, ³Department of Earth and Environmental Sciences, University of Pavia, Italy, ⁴Federal Institute for Geosciences and Natural Resources, Germany, ⁵Institute of Geological Science, University of Wrocław, Poland, ⁶KGHM Cuprum - Research and Development Centre, Poland

Copper deposits or sulfide enrichment have been found along the crust-mantle transition zones in numerous ophiolites and along the oceanic Moho. However, scarcity of suitable exposures limits the knowledge on the migration of chalcophile metals across the subcontinental crust-mantle boundary. This study aims at providing new constraints on the distribution of sulfides and on understanding the migration of sulfide-associated chalcophile metals at the transition between the subcontinental mantle and lower crust. For this purpose, we have investigated rocks exposed along the contact between the mantle peridotites of the Balmuccia massif and adjacent gabbro-norites of the Mafic Complex (NW Italy).

An ~80-m-thick zone composed of interlayered pyroxenites and gabbro-norites (Contact Series) showing igneous contact with the mantle peridotites was sampled along the Val Sesia river, close to Isola village. We focus on sulfides and distribution of chalcophile metals along a transect from mantle peridotites, through the Contact Series, to the lower crustal gabbro-norites of the Mafic Complex. In general, the mantle peridotites are sulfide poor (0.08 vol.%), in contrast to gabbro-norite vein (~2.0 vol.%) and Contact Series rocks (up to 7.8 vol.%). We observed enhanced sulfide modes together with higher Cu, Ag, and Cd contents in three sampling sites across the Contact Series. This sulfide- and chalcophile-rich metal zone ends ~70 m away from the margin of mantle peridotites implying a probable thickness of the enrichment zone. In addition, we found that margins of pyroxenite and gabbro-norite layers within the Contact Series contain on average ~5 times more sulfides (5.0 vol.%) than the internal parts of the layers (0.9 vol.%). Most sulfides are pyrrhotite-(troilite)-chalcopyrite-(cubanite)-pentlandite assemblages of magmatic origin. In two sampling sites along the Contact Series, pyrrhotite is mostly replaced by pyrite but we observed relics of former pyrrhotite. We found that sulfides sampled close to the crust-mantle boundary contain more Ni (abundant pentlandite) compared to the Fe-dominated sulfides (abundant pyrrhotite or pyrite) towards the Mafic Complex. The stagnant melts at the crust-mantle boundary extensively react with the mantle yielding enrichment in sulfides and chalcophile elements, which is known to yield enrichment in sulfides (Ciałęła et al., 2018 – GCA, Patkó et al., 2021 – Lithos). However, the contact between the Balmuccia mantle peridotites and the lower continental crust of the Mafic Complex is highly heterogeneous with the alternating layers of the pyroxenites and gabbro-norites. These layers may have formed from distinct magma batches as suggested by the along-transect Mg# variations (Mg# of 71–57). Therefore, the mechanism of observed sulfide-enrichment is probably more complex and may involve several stages of melt-peridotite and melt-pyroxenite reactions. These might explain the exceptionally large ~70-m-thick sulfide-rich horizon observed at the Contact Series.

Our results indicate that substantial chalcophile metal inventory may be trapped at the Moho level never reaching the continental crust. This may explain the relative deficit of these elements in the continental crust when compared its bulk composition to the composition of primitive mantle melts.

This research was funded by the grant of the National Science Center Poland (2018/31/N/ST10/02146).

ZIRCON REVEALS DIVERSE TRENDS OF MAGMA CRYSTALLIZATION FROM TWO TYPES OF POST-COLLISIONAL DIORITES (VARISCAN OROGENY, NE BOHEMIAN MASSIF)

Pietranik Anna¹

¹Institute of Geological Sciences, University of Wrocław, Poland

Magmatism related to post-collisional settings could be derived from multiple sources including heterogeneous mantle and lower crust. In this study, zircon from different types of monzodiorite, the most mafic rocks in the suite, is used to determine possible sources and conditions of crystallization during a widespread magmatic episode dated at ca. 340 Ma, in the NE Bohemian Massif. Zircon provides a wealth of information on the magmatic history including age, temperature, and chemical as well as the isotopic composition of the magma. However, zircon may be a late crystallizing phase in dioritic magmas. Two major types of diorite are recognized, containing magmatic clinopyroxene or amphibole, consistent with different water contents during crystallization. CA-ID-TIMS zircon ages for amphibole- and clinopyroxene-bearing diorites are similar suggesting that the emplacement of such diverse magmas was closely spaced in time. Trace elements in zircon are distinct between clinopyroxene and amphibole types, whereas ϵHf and $\delta^{18}\text{O}$ in zircon are more diverse between samples of the same diorite type than between clinopyroxene and amphibole types. The sources that contributed to dioritic magmas include an enriched mantle or a lower crust formed during subduction, ophiolite, and older continental crust. The diversity in trace elements in zircon is complex and is consistent with different conditions during magma evolution such as different water content, temperature, and oxidation level. However, interestingly, only phases from the clinopyroxene diorite (zircon, plagioclase, apatite) are in equilibrium with the whole rock composition and record crystallization conditions well reproduced by MELTS modeling. On the contrary, amphibole diorite contains zircon and other phases in disequilibrium with the whole rock composition and this is explained by fluid-induced re-melting and remobilization of clinopyroxene - plagioclase crystal mush culminating in full replacement of clinopyroxene by amphibole, formation of plagioclase-rich melt, and oxidation. The whole process may be envisioned as metasomatism at magmatic temperatures and is linked to major re-distribution of ore-forming metals (Cu, Au, Sb, Pb) with fluid-induced remobilization taking place less than 400ky after crystallization of dry magmas.

Acknowledgements: The research was funded by the National Science Centre (Poland) the OPUS project UMO-2013/09/B/ST10/00032.

INCLUSIONS IN DETRITAL GARNETS FROM ČESKÉ STŘEDOHOŘÍ MTS.

Pisova Barbora^{1,2}, Skala Roman^{1,2}

¹Institute of Geochemistry, Mineralogy and Mineral Resources, Faculty of Science, Charles University, Prague
²Department of Analytical Methods, Institute of Geology of the Czech Academy of Sciences, Czech Republic

Mineral inclusions in detrital garnets from selected localities of the České středohoří Mts. were identified by optical microscope and SEM/EDS. However, their size was too small to allow reliable chemical analysis by either SEM/EDS or EPMA. Consequently, the minerals constituting the inclusions were determined by Raman microspectroscopy. Loose host garnet grains were imaged by SEM/EDS and their major and trace element compositions were determined by EPMA and LA-ICP-MS, respectively.

The Erzgebirge Mts., located in the Saxonian unit are known for the occurrence of several regions, which underwent UHP metamorphism. Diamond- and coesite-bearing garnets in mafic granulite provide unequivocal evidence of the UHP process (Kotková et al., 2011). Denudation of the Erzgebirge Mts. basement in Carboniferous and Permian resulted in the transport of garnets and their deposition into sediments in the area. For the purpose of this study, garnets hosted by Carboniferous feldspathic sandstones from the borehole Tř-1 drilled on the eastern edge of the village Třtěno (50.42028° N, 13.87778° E) were selected. These garnets are about 200 – 700 μm in diameter, light-orange-colored or clear, and chemically slightly heterogeneous. Their composition (in mol.%) varies between 36 – 38 of pyrope, 28 – 33 of almandine, and 27 – 30 of grossular components; other end-members are present only marginally.

Two multiphase inclusions representing nanogranite inclusion sensu, e.g., Cesare et al. (2009) were selected for the detailed Raman study presented in this abstract. The association consisting of kumdykolite, kokchetavite, apatite, calcite, rutile, paragonite, quartz, and relicts of melts containing OH⁻, CH₂⁻ and CH₃ groups is found in the round inclusion of 8×8 μm size. Another inclusion of short prismatic shape (8×10×7 μm) is composed of quartz, orthoclase, albite, apatite, calcite, and mica. Major bands observed in Raman spectra of kokchetavite are located at 108 cm⁻¹, 390 cm⁻¹, and 834 cm⁻¹. This agrees satisfactorily with published data for synthesized kokchetavite (Romanenko et al., 2021). Major bands observed in Raman spectra of kumdykolite are located at 155 cm⁻¹, 219 cm⁻¹, 407 cm⁻¹, 461 cm⁻¹, 491 cm⁻¹, minor bands are located in 608 cm⁻¹ and 856 cm⁻¹. These results are identical within experimental errors with data (Hwang et al., 2009). Kokchetavite is assumed to represent a high-pressure polymorph of K-feldspar which precipitates from K-cymrite by dehydration (Romanenko et al., 2021). Kumdykolite corresponds to a high-pressure polymorph of albite (Hwang et al., 2009). Both kumdykolite and kokchetavite indicate HP conditions (Hwang et al., 2009; Kotková et al., 2014; Schönig et al., 2020), however, the UHP origin of the studied inclusions is not supported since the absence of coesite in the association.

References

- Cesare B et al. (2009) *Geology* 37:627
Hwang SL et al. (2009) *Eur J Mineral* 21:1325
Kotková J et al. (2011) *Geology* 39:667
Kotková J et al. (2014) *Amer Mineral* 99:1798
Romanenko AV et al. (2021) *Amer Mineral* 106:404
Schönig J et al. (2020) *Gondwana Res* 87:320

INTER-MINERAL FE ISOTOPE FRACTIONATION IN ECLOGITES OF THE MÜNCHBERG MASSIF (GERMANY) AS A FUNCTION OF OXIDATION STATE

Pohlner Johannes¹, El Korh Afifé¹, Chiaradia Massimo², McCammon Catherine³, Grobéty Bernard¹, Klemd Reiner⁴

¹Department of Geosciences, University of Fribourg, Switzerland, ²Department of Earth Sciences, University of Geneva, Switzerland, ³Bayerisches Geoinstitut, University of Bayreuth, Germany, ⁴GeoZentrum Nordbayern, University of Erlangen-Nürnberg, Germany

Stable Fe isotope fractionation ($\delta^{56}\text{Fe} = [({}^{56}\text{Fe}/{}^{54}\text{Fe})_{\text{sample}}/({}^{56}\text{Fe}/{}^{54}\text{Fe})_{\text{IRMM-524a standard}} - 1] \times 1000$) is sensitive to redox processes. Under equilibrium conditions, the heavy Fe isotopes tend to partition into more oxidized phases as Fe^{3+} , but the bonding environment can also play a substantial role. We investigate Fe isotope fractionation between eclogitic minerals as a function of their oxidation state. Mineral separates are analyzed for $\delta^{56}\text{Fe}$ by multi-collector ICP-MS and for their oxidation state by Mössbauer spectroscopy.

In the eclogite samples from the Variscan Münchberg Massif (bulk atomic $\text{Fe}^{3+}/\Sigma\text{Fe} = 0.06\text{-}0.27$), the Fe budget is essentially controlled by garnet (65-85%), omphacite (10-27%), high-pressure amphibole (1-8%), and pyrrhotite (0-5%). Garnet ($\text{Fe}^{3+}/\Sigma\text{Fe} \leq 0.03$) is generally more reduced than omphacite ($\text{Fe}^{3+}/\Sigma\text{Fe} = 0.07\text{-}0.56$), amphibole ($\text{Fe}^{3+}/\Sigma\text{Fe} = 0.07\text{-}0.28$), and pyrrhotite ($\text{Fe}^{3+}/\Sigma\text{Fe} = 0.29$ as Fe_7S_8). $\delta^{56}\text{Fe}$ values of omphacite and amphibole (up to 0.3‰ heavier than the whole rocks) are consistently higher than those of garnet and pyrrhotite (up to 0.3‰ lighter than the whole rocks). These systematic differences are especially large for samples with strongly oxidized omphacite, but still notable in the samples with the most reduced omphacite. Garnet, the only mineral with major element zonation, reveals to be zoned in Fe isotopes as well, with $\delta^{56}\text{Fe}$ values increasing rimwards by up to 0.3‰. Fe isotope fractionation between omphacite/amphibole and garnet seems to result from a combination of both differences in redox conditions and different coordination of Fe in these minerals. Garnet acts as a sink for isotopically light Fe and drives the matrix towards heavy Fe isotope compositions, especially due to its isotopic zonation which we ascribe to Rayleigh fractionation. Reduced and growth-zoned garnet within a matrix of more oxidized minerals is a widespread feature of high-pressure metabasites. We thus expect that any potential Fe mobilization from subducted metabasites by fluids or melts would involve rather isotopically heavy Fe from matrix minerals, while isotopically light Fe is effectively stored in garnet and transported into the deep mantle.

AMINO ACIDS ADSORPTION IN MORDENITE ZEOLITE: THE EFFECTS OF SPATIAL CONFINEMENT AND PRESSURE

Polisi Michelangelo¹, Fabbiani Marco², Vezzalini Giovanna¹, Arletti Rossella³

¹Department of Chemical and Geological Sciences, University of Modena and Reggio Emilia, Italy, ²Department of Chemistry, University of Torino, Italy, ³Department of Chemical and Geological Sciences, University of Modena and Reggio Emilia, Italy

In this study the absorption of glycine, α -alanine, and β -alanine amino acids within the pores of a synthetic Na-mordenite was investigated with the aim of: i) evaluating the effectiveness of MOR framework type in amino acid adsorption (via vapor and aqueous loading); ii) understanding the host-guest and guest-guest interactions to possibly design a tailor-made material and a loading procedure able to maximize the amino acid adsorption; iii) study the effect on the adsorbed amino acids when applying pressure.

The structural characterization, carried out with the combination of diffractometric and infrared spectroscopy analyses, shows that MOR can adsorb amino acids, which are present both in protonated/deprotonated (possibly also generating zwitterions) form. Vapor loading is ineffective for α -alanine, while it is effective in β -alanine and glycine adsorption, even if the loading degree results different. The shape and size of MOR channels is suitable to accommodate a peptide. In the Glycine loaded sample some molecules condensate to form cyclic dimers, while linear oligomers are present only in β -alanine loaded samples. The sample loaded with α -L-Alanine from aqueous solution did not show the presence of amide bond signals, indicating that the molecules are mostly hosted in zwitterionic form in Na-MOR channels. The application of external baric stimuli did not induce substantial modifications in the structure of the loaded sample: this may be explained by the low number of molecules hosted in the channels. the amino acid amount within the zeolite is the most important reactivity parameter and an increased loading could induce chemical modifications.

THE USE OF MXRF FOR THE CHARACTERIZATION OF POZZOLANIC ROCKS FROM KAMTSCHATKA

Pöllmann Herbert¹, Kilian Ruediger¹

¹mineralogy/geochemistry, University of Halle, Germany

Nowadays, due to the increased demand of finding new materials which do produce less amounts of CO₂ in the production of cementitious materials, it is important to characterize these materials. Therefore the mineralogical parameters of potential pozzolanic materials must be determined. This is mainly done by XRD and microscopic methods, including the overall chemistry. Additionally, some tests for the pozzolanic activity and other technical characterizations are necessary for describing these materials. The exploration for pozzolanic materials worldwide is therefore an important step for finding supplementary cementitious materials usable in large quantities to reduce the overall CO₂ output of building materials. Besides different industrial residues, also natural materials are under investigation. Mainly temperature-induced clays and volcanic ashes can be interesting substitutes because they are available in large quantities.

μRFA is a method to perform spatially resolved chemical analysis using a focused X-ray source. Sample surfaces up to 300 cm² are scanned down to a 20 μm resolution yielding chemical composition at each point. The data is used to segment phase maps and derive microstructural information such as the grain size distribution, modal proportion of phases, matrix-clast ratios or spatial relation of phases. Area-integrated μXRF spectra are comparable to conventional XRF with the advantage that no physical separation of e.g. clasts and matrix is required.

In this study selected solid volcanic rocks from the Kamchatka area were investigated in detail, in particular, pozzolanic materials originating from the Shiveluch, Halaktyrsky, Tolbachinsky, Ksudach, Mutnovsky and Gorely areas were studied by means of μXRF. A comparison of the results acquainted by different methods will be given as well as the various crystalline and amorphous parts of the rock samples. Here, μXRF is a helpful additional tool in understanding pozzolanic activity in relation to the microstructure and bulk properties of the material.

XRD INVESTIGATIONS AND EVALUATIONS USED FOR QUANTITATIVE LITHIUM DETERMINATIONS OF LITHIUM MINERALS

Pöllmann Herbert¹, Koenig Uwe²

¹mineralogy/geochemistry, University of Halle, Germany, ²Malvern Panalytical, Netherlands

The demand for lithium has increased in the past years dramatically as it is increasingly needed in batteries. Besides the large occurrences in large salt lakes in dry areas also various lithium mineral ores from mining are of interest. As lithium is normally identified by time-consuming wet chemical analysis other techniques for the more rapid determination are of interest. This paper describes the analytical technique of indirect lithium determination by quantifying the lithium mineral content in a lithium ore and the recalculation of the lithium oxide content in the mineral. It is shown, that in some ores, coming from different places from around the world the minerals spodumene, petalite, triphylite, amblygonite, zinnwaldite and lepidolite can be determined and the calculation of the lithium content can be made. Depending on the mineral assemblage, which can be rather simple in these ores, as mainly quartz or sometimes feldspar is additionally present. For these ores the determination was based on Rietveld analysis and for direct application also some statistical treatment methods of the XRD results were performed. Using PLSR (partial least squares regression analysis) and PCA (principal component analysis) or cluster analysis a fast and reliable determination method is proposed, when many XRD results must be interpreted in a short time. The detection limits for lithium mineral determinations in these ores were determined to ca. 1-2 %. Based on the detection of these lithium minerals by XRD the determination of lithium oxide in these mineral assemblages is around 0.1% Li₂O. For different applications it also is possible to calculate some clusters covering contents over an enhanced concentration range depending on the available data and time consumed. It will be shown, that in these different ores the XRD data can be used to encounter reliable lithium values based on XRD measurements.

DOES BACTERIUM PSEUDOMONAS FLUORESCENS AFFECT STABILITY OF SILICON AND IRON BEARING MINERALS IN SANDSTONES?

Potysz Anna¹, Bartz Wojciech¹

¹Department of Experimental Petrology, University of Wrocław, Poland

The discovery of the role of microorganisms in minerals dissolution provides a basis for a term of bioweathering, known to involve biotic and physico-chemical factors affecting stability of various solid surfaces. Today, bioweathering process is one of the main study chains being pursued towards better understanding of minerals dissolution.

Sandstones are common rocks composed of framework grains, generally silicates and aluminosilicates, with interstitial pore space occupied by fine grained matrix and cement minerals. Framework minerals are generally recognized as relatively weathering-resistant minerals, whereas matrix and cement minerals, notably diversified in mineralogy, in general are less resistant. This entails concerns about stability of these materials in natural and anthropogenic environments.

This study investigated the contribution of heterotrophic bacteria *Pseudomonas fluorescens* to dissolution of Fe-poor and Fe-rich sandstones (quartz arenites). In particular, this study aimed to determine, whether Fe content and the form of its occurrence in sandstone determine activity of microorganism and whether degree of sandstone dissolution can consequently be affected. Combined experimental approach applying petrological and geochemical analytical tools was implemented to decipher sandstones (bio)dissolution. Deteriorative effect of bacteria was quantified by means of (bio)leaching, whereas direct surface alteration was observed using scanning electron microscope. The result of this study generally demonstrated that sandstones with variable chemical and mineralogical composition stimulated activity of bacteria to a different extent. In turns, bacterially mediated dissolution of individual sandstones took place to a different degree. Generally, bacteria accelerated dissolution of sandstones as compared to abiotic weathering rates. We found that the presence of siderophore in the solution improved the dissolution rate of the sandstones promoting the release of Fe and Al from matrix and cement minerals. In the studied bioweathering system, goethite was more susceptible to dissolution than hematite. This work is a novel contribution regarding dissolution of sandstones exposed to biotic and abiotic factors.

Acknowledgements: This work was financially supported by the National Science Centre (NCN) in Poland in the frame of SONATA program under grant agreement UMO-2018/31/D/ST10/00738 to AP.

WEATHERING OF METALLURGICAL WASTE IN SOIL: INSIGHT INTO REDOX CONDITIONS AND METAL(LOID)S MOBILITY

Potysz Anna¹, Grybos Malgorzata²

¹Department of Experimental Petrology, University of Wrocław, Poland, ²Université de Limoges, France

Large volumetric quantities of metallurgical wastes combined with the relatively high residual metal content necessitates a full understanding of the geochemical stability of the waste in the environment. In many soils, redox conditions are highly dynamic due to seasonal water table fluctuations or due to the presence of snow cover. Changing redox conditions in turns can strongly influence the pH and microbial activity and thus, impact the release and behavior of metals from metallurgical wastes. This work deals with the evaluation of Cr, Co, Ni, Cu, Zn, As, Cd, Sb and Pb mobility in soil naturally exposed to oscillating redox conditions. The dynamic of released metal(loid)s was monitored during 30 day long soils incubations with or without metallurgical waste supplementation and under oxic and anoxic conditions. This study demonstrated that the presence of wastes under oxic conditions in soils results in a higher release of some potentially toxic elements (e.g. Cu, Zn and Ni) as compared to soil alone. This proved that metallurgical waste was not inert under studied oxic conditions even if field weathering would undoubtedly proceed at lower rates as compared to the executed laboratory tests. In addition, the presence of metallurgical waste in soil environment causes slight local acidification, however the release of some elements was decreased (e.g. Pb) after 30 days proving that precipitating mechanisms also occurred in the studied system. Under anoxic conditions, it was observed that contribution of metallurgical waste to metal release was negligible.

Acknowledgements: This work was financially supported by the National Science Centre (NCN) in Poland in the frame of SONATA program under grant agreement UMO-2018/31/D/ST10/00738 to AP. Mobility of Anna Potysz at PEIRENE laboratory was supported by French Government and French Embassy in Poland Scholarship, project 927219D.

F/OH RATIO IN A RARE FLUORINE-POOR BLUE TOPAZ FROM PADRE PARAÍSO (MINAS GERAIS, BRAZIL) TO UNRAVEL TOPAZ'S AMBIENT OF FORMATION.

Precisvalle Nicola¹, Martucci Annalisa¹, Gigli Lara², Plaisier Jasper R.², Hansen Thomas C.³, Nobre Augusto Gonçalves⁴, Bonadiman Costanza¹

¹Physics and Earth Sciences, University of Ferrara, Italy, ²Elettra Sincrotrone Trieste, Italy, ³Institut Laue-Langevin, France, ⁴Geosciences Institute, University of São Paulo, Brazil

Topaz is one of the principal fluorine-bearing silicates that occurs as an accessory mineral in fluorine-rich silicate rocks (rhyolites and granites) associated with pneumatolytic/hydrothermal events, and in ultrahigh-pressure rocks. Its composition ranges from a nearly OH-free end member, $\text{Al}_2\text{SiO}_4\text{F}_2$, in acid igneous rocks, to $\text{Al}_2\text{SiO}_4\text{F}_{1.4}(\text{OH})_{0.6}$, with $\text{XOH} = \text{OH}/(\text{OH}+\text{F}) = 0.30$, in hydrothermal deposits. Higher OH content was reported for topaz found in ultrahigh-pressure (UHP) -rich topaz-kyanite quartzites from Hushan (west of Dongai), ($\text{XOH}=0.35$), and southern Sulu ($\text{XOH} = 0.40-0.55$), eastern China. A series of hydroxyl-rich topaz (OHtopaz) from $\text{XOH} = 0.22$ up to the pure end-member $\text{Al}_2\text{SiO}_4(\text{OH})_2$, were synthesized at high-pressure/high temperature conditions (pressure from 5.5-10 GPa, temperature up to 1000°C) in the Al_2O_3 - SiO_2 - H_2O system. For this reason, the study of the OH/F ratio plays a key role to understand the topaz's formation ambient. In this work, we fully characterized blue topaz from Padre Paraíso (Minas Gerais, Brazil) by means of in situ synchrotron X-Ray and neutron powder diffraction measurements (temperature range 298-1273 K) combined with EDS microanalyses. The fluorine content estimated from neutron diffraction data is ~ 1.03 a.f.u (10.34 wt%), in agreement with the chemical data (on average 10.0 wt%). The $\text{XOH} [\text{OH}/(\text{OH}+\text{F})]$ (0.484) is close to the maximum XOH value (0.5), and represents the OH- richest topaz composition so far analyzed in the Minas Gerais district. Up to 1010K there is a general increase of the unit cell parameters, stating that the samples acts according to the typical mechanism of thermal expansion. Then, after reaching this temperature, it is possible to notice a sudden change in the trend underlying structural modifications induced by the defluorinization. At 1170K the main diffraction peaks associated with the topaz phase declined fairly rapidly with continued heating, indicating a rapid decomposition of the sample. A second phase appeared to grow at the same rate as the peak from the previous phase declined thus revealing the formation of mullite $\text{Al}_{4+2x}\text{Si}_{12-2x}\text{O}_{10-x}$. On the basis of this behavior, it is possible to interfere that this temperature may represent the potential initial topaz's crystallization temperature from supercritical fluids in a pegmatite system. The $\log(\text{fH}_2\text{O}/\text{fHF})_{\text{fluid}}$ (1.27 (0.06)) is coherent with the fluorine activity calculated for hydrothermal fluids (pegmatitic stage) in equilibrium with the forming mineral ($\log(\text{fH}_2\text{O}/\text{fHF})_{\text{fluid}} = 1.2-6.5$) and clearly different from pure magmatic (granitic) residual melts [$\log(\text{fH}_2\text{O}/\text{fHF})_{\text{fluid}} = <1$]. The modelled H_2O saturated fluids with the F content not exceeding 1 wt% may represent an anomalous water-dominant / fluorine-poor pegmatite lens of the Padre Paraíso Pegmatite Field.

NEW OCCURRENCE OF DEMANTOID GARNETS IN SA SPINARBEDDA MINE (SARDINIA – ITALY): CHEMICAL AND STRUCTURAL CHARACTERIZATION

Precisvalle Nicola¹, Martucci Annalisa¹, Pollastri Simone², Stani Chiara Maria², Angeli Celestino³, Bonadiman Costanza¹

¹Physics and Earth Sciences Dept, University of Ferrara, Italy, ²Elettra Sincrotrone Trieste, Italy, ³Department of Chemical, Pharmaceutical and Agricultural Sciences, University of Ferrara, Italy

In this work, we present new geochemical and structural data in order to document a new occurrence of andradite garnet ($\text{Ca}_3\text{Fe}_2(\text{SiO}_4)_3$) “demantoid variety” in Sardinia, Italy. This yellowish-green to intense green variety of andradite is a precious and greatly appreciated gemstone. It is mined mainly in Russia, Namibia, Madagascar and Italy (Valmalenco, Lombardy). The studied samples come from a new site from Domus de Maria municipality, nearby “Sa Spinarbedda” mine, Sardinia. This finding is important, because, although the beauty of these samples, it has not been previously reported. In this work we investigated the structural and chemical features of new Sardinian dermatoid by combining electron microprobe analyses (EMPA), laser ablation-inductively coupled mass spectrometry (LA-ICP-MS), single-crystal X-ray diffraction (XRSD), IR and X-ray absorption (XAS) spectroscopies. Sardinian demantoids are chemically close to the andradite endmember (97-99%) with minor Mn contents ($\text{MnO} = 0.55\text{-}1.32$ Wt%), but with very low contents of Cr and Ti (~ 8 and 60 ppm respectively). Fe and Mn K-edge XAS data were collected to better understand the coordination number of both ions. The position of the absorption edge together with the analysis of the pre-edge peak, point to the presence of only Fe^{3+} in octahedral coordination. For Mn pre-edge peaks analysis indicate that it should be mainly in the form of Mn^{2+} and 8-fold coordination, occupying the X crystallographic site, beside a small amount of Mn^{3+} is probably present in octahedral Y site. The infrared spectra of andradite show a prominent absorption band at about 3560 cm^{-1} , suggesting the well-known hydrogarnet substitution of $(\text{SiO}_4)_4$ with $(\text{O}_4\text{H}_4)_4$. These absorption features are related to hydroxide. X-ray single-crystal diffraction experiments refinement ($\text{Ia}\bar{3}\text{d}$ space group) highlighted a unit cell volume ($1757.15(2)\text{ \AA}^3$) larger than that reported usually in the literature thus confirming the presence of a slight water content. It has been noticed that a small Ca-Mn and Fe-Al substitution occurred. Then, according to Adamo et al. (2011) the potential partial occupation of tetrahedral site has been checked. In fact, the site resulted occupied only for ~98%, the other 2% has been refined for O (same position and same thermal factor), suggesting the presence of structural water. Refining the site occupancy factor (s.o.f.) at the Si-site, a s.o.f. value of ~98% has been obtained, which barely confirmed potential hydrogarnet substitution [i.e., $(\text{SiO}_4)_4$ with $(\text{O}_4\text{H}_4)_4$].

DICIANOAURATE AS THREE SITE TECTON TOWARD SILVER IN GOLD-SILVER BIMETALLIC SUPRAMOLECULAR NETWORKS

Priola Emanuele¹, Diana Eliano¹, Giordana Alessia¹, Andrea Luca¹

¹Department of Chemistry, University of Turin, Italy

Dicyanoaurate demonstrates in literature to be a good tecton to build up supramolecular networks with very peculiar properties like Non Linear Optical properties, abnormal behavior to temperature and pressure and vapochromism. These properties are usually linked to the presence of Au(I)...Au(I) aurophilic interactions. However, interactions of Au(I) to other d10 metals (called in general metallophilic interactions) have been studied and are good driving forces to obtain desired crystal structures in engineering optics. In this case, we analyze the behavior of dicyanoaurate anion in the presence of differing silver cationic complexes. In the 8 new structures that we obtained, we discover that the metallophilic interaction between Au(I) and Ag(I) can compete to a more classical covalent Ag-N attach of cyanide. This peculiar counterintuitive behavior makes in these cases the dicyanoaurate anion a three-site connecting unit, and made possible to construct very peculiar crystal structures. To fully characterize these compounds, they have been studied also with ab-initio calculations and electronic and vibrational spectroscopies. This study will be useful to comprehend the energies and driving forces of this new class of materials, building a new approach to crystal engineering of gold materials

CA-ID-TIMS DATING OF ORGANY WIELISŁAWSKIE RHYOLITES— INSIGHT INTO AGES OF THE CARBONIFEROUS TO PERMIAN VOLCANIC ACTIVITY IN CENTRAL EUROPE

Przybyło Arkadiusz¹, Pietranik Anna¹, Kierczak Jakub¹

¹Institute of Geological Sciences, University of Wrocław, Poland

Zircon in silicic systems may record prolonged history of crystallization in interconnected magma reservoirs or compositionally distinct melt pockets resulting in complex chemical composition-age relationships. The time-scales of crystallization of a silicic magma chamber leading to the eruption and caldera collapse could be up to 1 Ma as seen from recent eruptions, but antecrysts preserving the records of longer magmatic history could be several My older. Taking this into account it is difficult to pinpoint the real eruption ages if age measurements are done on complex zircon populations. Recognition of zircon antecrysts could be based on their chemical or isotopic composition, but these interpretations are also affected by the complex evolution of large silicic magma reservoirs. Ideally ages of zircon should give clear distinction between antecrystic and autocrystic components, but the age difference is usually too low to be measured by in-situ techniques. CA-ID-TIMS zircon dating may provide precise ages with the resolution below 0.5 Ma and the spread of ages obtained using this method is interpreted to represent antecrystic component. However, despite chemical abrasion used in this approach that is designed to remove parts of zircon affected by lead loss, the lead loss can still affect abraded zircons and give younger ages. Specifically, if lead loss occurred within several My after eruption, e.g. due to prolonged hydrothermal activity common in areas of voluminous volcanic activity, the ages of zircon population may be reset to postmagmatic ones. One approach is to define “the age plateau” with several zircon having similar ages. The problem evident for rhyolitic rocks is that such a plateau may comprise either the oldest or the youngest grains or sometimes two plateaus of different ages can be defined due to high resolution of CA-ID-TIMS techniques (Lützner et al. 2020). Therefore, to fully recognize the potential of CA-ID-TIMS dating we have applied different techniques to characterize zircon before chemical abrasion to see if correlations between structural position of zircon in the rock or structure of individual zircons can be correlated with variations in CA-ID-TIMS ages. This approach is interesting for rhyolite from Organy Wielisławskie (Bohemian Massif), which showed typical zircon-in-biotite occurrence in thin section, therefore relatively simple structural position of zircon, contrary to other rhyolitic rocks (Przybyło et al. 2020). Despite that, the age distribution showed two plateaus at 298.24 and 296.59 Ma, and two grains yielded older ages of 299.6-300.4 Ma. Tentatively, we interpret the distribution as the record of ca. 298 Ma crystallization of the system followed by its resetting due to hydrothermal activity, probably related to agate formation or gold mineralization in the area at 296 Ma.

Acknowledgements: The research was funded by the National Science Centre (Poland) the project UMO-2017/25/B/ST10/00180 to APietranik

Lützner H., Tichomirowa M., Käbner A., Gaupp R. (2020). Latest Carboniferous to early Permian volcano-stratigraphic evolution in Central Europe—U-Pb CA-ID-TIMS ages of volcanic rocks in the Thuringian Forest Basin (Germany). *Int. J. Earth Sci.*, 110, 377–398.

Przybyło A, Pietranik A, Schulz B, Breitzkreuz C. Towards Identification of Zircon Populations in Permo-Carboniferous Rhyolites of Central Europe: Insight from Automated SEM-Mineral Liberation Analyses. *Minerals*. 2020; 10(4):308.

NANODIAMOND IN LOW-PRESSURE FLUID INCLUSIONS IN MAFIC AND ULTRAMAFIC ROCKS

Pujol-Solà Núria¹, García-Casco Antonio^{2,3}, Proenza Joaquín A.¹, González-Jiménez José María^{2,3}, Del Campo Adolfo⁴, Colás Vanessa⁵, Canals Angels¹, Sánchez-Navas Antonio², Roqué-Rosell Josep¹

¹Mineralogía, Petrología i Geologia Aplicada, Universitat de Barcelona, Spain, ²Mineralogía y Petrología, Universidad de Granada, Spain, ³Instituto Andaluz de Ciencias de la Tierra, CSIC, Spain, ⁴Instituto de Cerámica y Vidrio, CSIC, Spain, ⁵Instituto de Geología, Universidad Nacional Autónoma de México, México

Methane- and hydrogen-rich secondary fluid inclusions mainly in olivine, but also in orthopyroxene and clinopyroxene, have been increasingly reported in ultramafic and mafic rocks from a wide range of geodynamic settings, including spreading mid-ocean ridges, subduction zones, and subcontinental lithospheric mantle. These inclusions typically contain, besides the gas/fluid phase, serpentine, magnetite and brucite, and are interpreted to be formed during serpentinization under super-reduced conditions. We have studied CH₄-rich inclusions in olivine from low-pressure oceanic gabbros and chromitites from the Moa-Baracoa ophiolitic massif (eastern Cuba). To analyze these inclusions, we applied an approach that used optical and electron microscopy, confocal Raman spectroscopy, and transmission electron microscopy (TEM) on thin foils extracted by focused ion beam (FIB). The inclusions have sizes between <1 and 14 μm and they are encapsulated well below the polished olivine's surface, confirming their natural origin. Some of the CH₄-rich inclusions host nanodiamond (200–300 nm) associated with the typical serpentinization assemblage (serpentine and magnetite), and locally other super-reduced phases such as metallic Si and graphite-like amorphous carbon in addition to calcite, diopside, and chlorite. However, brucite was not identified in any of the studied inclusions. TEM studies show that the nanodiamond is surrounded by serpentine with a tubular texture, corresponding to polygonal serpentine. The selected area electron diffraction (SAED) pattern of the nanodiamond confirms a diamond structure with a measured d111-spacing of 2 Å. We interpret that H₂O-CO₂ fluid mixtures derived from ocean water infiltrated during episodic fracturing were encapsulated forming the fluid inclusions. The fluids subsequently reacted with the host olivine producing secondary serpentine and brucite (later dissolved). This process consumed H₂O and triggered the oxidation of the fayalite component in olivine, producing magnetite and H₂ that reacted with CO₂ to form CH₄. Ultimately, carbon saturation was reached and the precipitation of graphite or metastable nanodiamond took place. Furthermore, the thermodynamic modeling suggests that metastable nanodiamond in the fluid inclusions were formed upon extreme reduction of the fluid (logfO₂ (MPa) = -45.3; ΔlogfO₂[Iron-Magnetite] = -6.5) at a reference P-T conditions typical for serpentinization (i.e., 350 °C and 100 MPa). These findings demonstrate that metastable nanodiamond in olivine-hosted CH₄-rich inclusions is formed after a serpentinization process at low pressure. Therefore, the presence of nanodiamond could be widespread in ultramafic and mafic rocks on Earth.

EFFECT OF ROCK COMPOSITION AND MINERAL ASSEMBLAGES ON THE DIVERSITY OF INTERNAL MICROSTRUCTURES IN GARNET PORPHYROBLASTS: A CASE OF THE ISUA SUPRACRUSTAL BELT

Ramírez-Salazar Anthony¹, Müller Thomas², Piazzolo Sandra¹, Sorger Dominik², Zuo Jiawei³, Webb A. Alexander G.³, Dey Joyjit¹, Haproff Peter J.⁴, Harvey Jason¹

¹School of Earth and Environment, University of Leeds, United Kingdom, ²Department of Mineralogy, Georg-August-Universität Göttingen, Germany, ³Division of Earth and Planetary Science and Laboratory for Space Research, University of Hong Kong, Hong Kong, ⁴Department of Earth and Ocean Sciences, University of North Carolina Wilmington, United States

The microstructural evolution of porphyroblasts during crystallization is controlled by different parameters such as changes in pressure and temperature, deformation, and bulk composition. Inclusions are commonly enclosed by porphyroblasts during growth, creating internal microstructures with valuable information. While inclusions are often used to interpret the sequence of tectonometamorphic events, their characteristics are rarely used to explain the crystallization processes.

To explore the effect of rock chemistry and local variations in mineral assemblages on the nature of garnet porphyroblast growth, we studied 20 samples of different mineralogical-compositional groups (i.e., meta-mafic rocks, meta-felsic rocks, and (Ca-rich) metapelites) from the Isua supracrustal belt that experienced comparable amphibolite-facies metamorphism and show quasiuniform strain intensities. Syntectonic porphyroblasts exhibit a wide range of microstructures mainly differing in the proportion of inclusions which varies from almost inclusion-free porphyroblasts to “skeletal” porphyroblasts with around 60% of inclusions.

Skeletal porphyroblasts are formed by a singular garnet interpreted to be interconnected in 3D due to the common crystallographic orientation. These grains seem to preferentially grow on pre-existing mica-quartz-felspar microstructures, resulting in elongated garnet crystals. They generally show patchy or no clear chemical zoning. Electron Backscatter Diffraction (EBSD) analysis of some garnets reveals subtle, but significant orientation changes within the syntectonic porphyroblasts, where the degree of orientation change coincides with compositional changes, and for post-tectonic overgrowths. The morphology of the less skeletal syntectonic porphyroblasts resembles single garnets enclosing other minerals, and chemical zoning is generally concentric. The EBSD data show changes in orientation for post-tectonic overgrowth. Snowball garnets exhibit significant changes in orientation that match changes in composition and inclusion orientation.

In mafic and felsic rocks with higher abundance of reactant phases, garnet porphyroblasts are less skeletal. Moreover, the availability of Fe, Mg, and Mn appears to play an important role for metapelites, and mafic and felsic rocks, the latter showing less skeletal porphyroblasts at higher contents of Fe-Mg-Mn. We propose that sluggish element mobility and lowered nucleation rates are controlling the formation of the skeletal garnets in the different lithologies, in agreement with the patchy zoning and the preferential growth following pre-existing microstructures. Our findings highlight that tectonometamorphic interpretations could improve with a better understanding of the individual crystallization process, since porphyroblasts with a similar evolution show significantly different microstructural and chemical patterns controlled by spatial variations in chemistry and pre-existing textures

CARBON ISOTOPE FRACTIONATION AT REDOX FREEZING

Reutsky Vadim¹

¹V.S.Sobolev Institute of geology and mineralogy SB RAS, Russian Federation

Crystallization of carbides via carbonate reduction is accompanying by a significant depletion of ¹³C in the carbide comparing to the initial carbonate. Diamonds also can crystallize in this process in both metal and carbonate matrix. Our experiments show extremely diverse carbon isotope composition of the diamonds because of kinetic isotope fractionation.

POTENTIALLY TOXIC ELEMENTS (PTES) IN TREMOLITE ASBESTOS AS A CONCERN FOR HUMAN HEALTH.

Ricchiuti Claudia¹, Pereira Dolores², Punturo Rosalda¹, Giorno Eugenia³, Pinizzotto Maria Rita⁴, Cantaro Carmelo⁴, Bloise Andrea⁵

¹Department of Biological, Geological and Environmental Sciences, University of Catania, Italy, ²Department of Geology, University of Salamanca, Spain, ³Department of Chemistry and Chemical Technologies, University of Calabria, Italy, ⁴Laboratory L1, Regional Environmental Agency of Sicily, Italy, ⁵Department of Biology, Ecology and Earth Sciences, University of Calabria, Italy

Now a day, the toxicity of asbestos mineral fibers is undeniable and well known. The toxicity degree of these hazardous minerals can be further increased by the presence of trace elements, especially heavy metals hosted in the fiber structure. With the aim of determining the concentration levels of potentially toxic elements (PTEs), a chemical characterization of two tremolite asbestos samples from Episcopia and San Severino Lucano villages (Basilicata region, Southern Italy) has been conducted, and results are here presented.

Micro X-ray fluorescence (μ -XRF) and Inductively Coupled Plasma spectroscopy with Optical Emission Spectrometry (ICP-OES) techniques have been used to quantify the concentration of major, minor (Si, Mg, Ca, Al, Fe, Mn) and trace elements (Ag, As, Ba, Be, Cd, Co, Cr, Cu, Li, Mo, Ni, Pb, Sb, Sn Sr, Ti, Te, V, W, Zn, Zr), with the aim of providing a contribution related to the asbestos toxicity knowledge up to now. Specifically, among minor elements, high amounts of Fe and Mn were found in the studied samples, with Fe values of 3.33 wt% and 5.20 wt% and Mn values of 0.23 wt% and 0.11 wt% in tremolite from Episcopia and San Severino Lucano respectively. As far as trace elements are concerned, results revealed high concentrations of Cr and Ni in both the studied samples, thus suggesting high toxicity character of the fibres.

Taking into account the pseudo-total PTEs concentrations in the tremolite asbestos samples, it is possible to speculate that one of the samples (3572 ppm) is more toxic than the other one (1384 ppm), since PTEs transported through asbestos in the air, water and soils come in contact with the human body and therefore can represent a source of risk to human health.

TRANSFORMATION OF REE- ENRICHED PYROMORPHITE (Pb,REE)(PO₄)₃Cl INTO OXALATES AND SULFATES

Rogala Patrycja¹, Stępień Ewa¹, Sordyl Julia¹, Manecki Maciej¹

¹Faculty of Geology, Geophysics and Environmental Protection, AGH University of Science and Technology, Poland, lissaxina@gmail.com, estepien12@interia.pl, sordyl@agh.edu.pl, gpmmanec@cyf-kr.edu.pl

Nowadays, rare earth elements (REE) play a very important role in society, as they are crucial in many branches of industry and modern technologies. As described in the literature, pyromorphite (Pb₅(PO₄)₃Cl), which belongs to the apatite-group, may contain trace amounts of REE. However, there is no information on attempts to recover REE from this mineral source. Usually, efficient extraction of REE from mineral phases is done by leaching and selective precipitation of REE in pure forms. In the present study, a first attempt was made to convert REE-enriched pyromorphite into oxalate or sulfate for efficient separation of REE from Pb. A series of experiments was performed using 0.5 g of the synthetic REE-enriched pyromorphite (containing nearly 10 wt. % of REE combined) reacted with aqueous solutions of 0.5 M and 1 M oxalic acid or 1.25 M, 2.5 M, and 5 M sulphuric acid. After 24 hours the reaction products were centrifuged, washed, dried, and analyzed using scanning electron microscopy with energy dispersive spectroscopy (SEM-EDS) and powder X-Ray diffraction (XRD). The solutions were analyzed using inductively coupled plasma mass spectrometry (ICP-MS).

Reaction of REE-enriched pyromorphite with sulphuric acid resulted in complete transformation into lead sulfate PbSO₄, as indicated by XRD. The precipitate formed aggregates of thin, rhomboidal, tabular crystals, up to 5 μm in size. The volume of the unit cell, refined in the orthorhombic system, was larger by 2.72 Å³ than the unit cell of pure lead sulfate. This is caused by the REE incorporation into the structure of lead sulfate. Analysis of the solution in which the transformation experiment was performed showed that 85% of the REE initially present in pyromorphite was coprecipitated with Pb in the form of PbSO₄ while 15 % went into solution. In the experiments with oxalic acid, complete dissolution of REE-enriched pyromorphite resulted in formation of two distinct, crystalline phases: lead (II) oxalate and REE oxalate. SEM images showed thin, needle-like crystals of PbC₂O₄, 10-20 μm in size, and tabular crystals of REE₂(C₂O₄)₃ measuring up to 30 μm. Unit cell volume of precipitated lead oxalate, calculated in the triclinic system, was 185.37 Å³, which is identical to pure lead oxalate. This indicated that REE did not incorporate into the lead oxalate structure. This remains to be confirmed by chemical microanalysis. Kinetics of transformation of REE-enriched pyromorphite in both, sulphuric and oxalic acid is very rapid, while the mechanisms of REE precipitation are different. Therefore, the right combination of both processes can be in future perspective for efficient separation of REE from Pb.

This research was funded by NCN research grant no. 2019/35/B/ST10/03379

OPTIMIZATION OF SPODUMENE IDENTIFICATION BY STATISTICAL APPROACH FOR LASER-INDUCED BREAKDOWN SPECTROSCOPY DATA OF LITHIUM-PEGMATITES

Romppanen Sari¹, Pölonen Ilkka², Häkkänen Heikki³, Kaski Saara¹

¹Department of Chemistry, University of Jyväskylä, Finland, ²Faculty of Information Technology, University of Jyväskylä, Finland, ³Department of Biological and Environmental Science, University of Jyväskylä, Finland

Interest towards lithium has increased intensively in recent years, especially due to the development of rechargeable battery technology and electric cars. In 2020, lithium was also identified as critical raw material by the EU. Laser-induced breakdown spectroscopy (LIBS) measures rapidly an emission spectrum directly from the solid sample surface. LIBS reveals all chemical elements and it is also suitable for the detection of light elements, e.g. lithium. Thus, LIBS can be beneficial for analyzing lithium-bearing minerals in different steps of exploration and mining activities.

In presented research, the focus was to develop a procedure for the detection of spodumene contents of Li-pegmatites from the Kaustinen lithium pegmatite province in Finland. The LIBS measurements were done side by side from the sample surface in 2d area, which enabled the estimation of mineral percentage levels and textural information about the samples. Mineral identification was tested with three statistical approaches: K-means, DBSCAN, and vertex component analysis (VCA). These methods classify chemically similar LIBS spectra into groups and no knowledge about the investigated sample is needed before the analysis. The main minerals were identified from the mean spectra of each group based on the emission lines of characteristic elements. All three methods were able to distinguish the locations of the main Li-mineral spodumene in the sampled areas.

In the second step of this study, the analyzed spectral range was optimized to spodumene detection keeping in mind that for in situ and online measurement purposes, both the data handling time and storage requirements should be minimized. For these reasons, it can be practical to decrease the size of LIBS data set. The three statistical approaches developed in this study were used in data of limited LIBS spectral information measured from Li-pegmatites of various grain-sizes. As a result, VCA worked efficiently with all samples, but K-means and DBSCAN were functional only with coarse- and medium-grained samples.

Finally, a way to investigate the accessory minerals of the Kaustinen Li-pegmatites was developed during the research. The strongly differing spectra of the data, i.e., the global outliers, could be detected with the combination of PCA and DBSCAN, e.g., spectra recognized as Nb-Ta oxide were observed.

STRUCTURAL CHANGES AND THERMAL BEHAVIOR OF Pb²⁺-MODIFIED STELLERITE

Roos Diana¹, Churakov Sergey¹, Cametti Georgia¹

¹Institute of Geological Sciences, University of Bern, Switzerland

Pb-exchanged zeolites are used for environmental remediation and in industrial processes (Thanos et al., 2017; Sökmen and Sevin, 2003; Chibani et al., 2017; Ju et al., 2001; Misaelides, 2011). Thermal pre-treatment is often applied on zeolites and it is therefore important to examine their stability range under non-ambient conditions. In this study, the structural modifications of a fully Pb²⁺-exchanged zeolite stellerite (STI framework type) and its behavior upon heating have been investigated between room temperature and 450 °C by in situ single-crystal X-ray diffraction, molecular dynamics (MD) simulations and infrared spectroscopy.

Chemical analyses indicated that Pb-stellerite is approximately 50% Pb²⁺-overexchanged. The surplus of Pb²⁺ cations is charge-balanced by hydroxyl groups, the presence of which was corroborated by infrared spectroscopy. At room temperature, the orthorhombic space group Fmmm of the original natural stellerite is maintained. The extraframework content (Pb²⁺, OH- and H₂O) is highly disordered in the zeolitic cavities. MD simulations showed that Pb²⁺ cations are coordinated by approximately 2.5 H₂O at distances between 2.3 and 3.0 Å and by 1.1 OH- between 2.1 and 2.6 Å at room temperature. Pb-O bonding interactions between Pb and the oxygen of the framework are less significant (0.5 oxygen at 2.8 Å).

With the increase of temperature, the orthorhombic structure with Fmmm space group transforms to the monoclinic one with space group A2/m at 50 °C. This transformation is accompanied by a negative thermal expansion and elliptical shaping of the ten-membered ring channels. The maximum unit cell volume contraction is observed at 75 °C and corresponds to -3.5%, with respect to the volume at room temperature. Between 100 and 150 °C, the unit cell volume surprisingly expands by +1.9% and the shape of the channels gets roundish. At 125 °C, the monoclinic structure transforms to the orthorhombic space group Fmmm. This structure remains stable at least up to 450 °C. The observed peculiar positive thermal expansion of Pb-exchanged stellerite is in contrast with the typical negative thermal expansion (throughout the whole temperature range) reported for other zeolites with STI framework type. This contraction of the unit cell volume usually involves the statistical breaking of T-O-T bonds and subsequent occlusion of the channels (Cruciani et al., 1997; Arletti et al., 2006; Ori et al., 2009; Cametti et al., 2017; Cametti et al., 2019). In contrast, these structural modifications are not observed in Pb-stellerite. Thermal analyses suggested that Pb-stellerite dehydration is a continuous process. The structure is expected to be H₂O free approximately above 400 °C, resulting in increased interactions between Pb²⁺ cations and framework oxygens. After the thermal treatment, Pb-stellerite crystals were exposed to high humidity conditions. Rehydration was observed, pointing out that the re-/dehydration processes are reversible.

PSEUDOMORPHIC REPLACEMENT OF ANHYDRITE BY CALCIUM PHOSPHATE: KINETICS, REACTION PATHWAY, AND TEXTURAL FEATURES.

Roza-Llera Ana¹, Jiménez Amalia¹, Fernández-Díaz Lurdes²

¹Department of Geology, University of Oviedo, Spain, ²Department of Mineralogy and Petrology, Complutense University of Madrid, Spain

Mineral replacement phenomena occur in a wide range of geological settings as a result of fluid-solid re-equilibration processes. Most mineral replacements that affect minerals in sedimentary rocks involve the development of interface-coupled dissolution-precipitation (ICDP) reactions and result in the formation of mineral pseudomorphs. The progress of ICPD reactions is commonly associated to the formation of a transient network of porosity that facilitates a continuous communication between the fluid phase and the reaction front located at the primary mineral-secondary mineral interface. Anhydrite (CaSO₄) is a most common mineral sulfate that is involved in a variety of mineral replacement processes both during diagenesis and in hydrothermal environments. Previous works have reported on the pseudomorphic replacement of anhydrite by calcite and celestite after interaction with aqueous solutions bearing carbonate and strontium, respectively. Here we study the pseudomorphic replacement of anhydrite by calcium phosphate phases upon interaction with hydrothermal phosphate-bearing aqueous solutions in the temperature regime between 120 and 200°C. Phosphorus (P) is a pollutant that causes water eutrophication and endangers aquatic wildlife. The formation of phosphate minerals through the interaction with the surface of moderately soluble minerals like anhydrite can help to remove phosphate from natural waters and reduce bioavailability of this contaminant.

X-ray diffraction (XRD), Scanning Electron Microscopy (SEM), Micro-CT scanning, Infrared spectroscopy and Raman spectroscopy analyses of anhydrite samples reacted during 1 to 96 hours evidence that: (i) Calcium phosphate pseudomorphs after anhydrite consist of varying weight percentages (wt%) of both, rhombohedron-shaped β -tricalcium phosphate (β TC) and elongated hydroxyapatite (HA) crystals, with the latter phase wt% rapidly increasing with interaction time. (ii) Calcium phosphate pseudomorphs after anhydrite contain a volume of porosity above 26%. (iii) In partially replaced samples, a transformed rim encapsulates an unreacted anhydrite core, defining a sharp reaction front. (iv) In this rim, HA crystals are arranged highly co-oriented, with their length perpendicular to the rim-anhydrite core interface. This arrangement favors the connectivity between pores in the porosity network, making the replaced rim permeable to mass transfer from the fluid to the reaction front. (v) The pseudomorphic replacement of anhydrite by a calcium phosphate is a temperature-dependent process limited by the dissolution of anhydrite. (vi) Both, the time to a given fraction and the rate constant methods yield empirical activation energy (E_a) values around 40 kJ/mol for the anhydrite by calcium phosphate replacement reaction. We discuss these results taking into consideration the solubility and molar volume changes involved in the replacement.

STABILITY OF NATROJAROSITE AND PRECIPITATION OF ANGLESITE UNDER ACIDIC CONDITIONS.

Roza-Llera Ana¹, Marban Gregorio², Jiménez Amalia¹

¹Department of Geology, University of Oviedo, Spain, ²Instituto Nacional del Carbono, CSIC, Spain

The crystallization behavior of jarosite and schwertmannite has been studied by precipitation-aging experiments performed using different parent-solution concentrations as well as in the presence and absence of dissolved lead under extreme conditions similar to those found in acid mine drainages. Schwertmannite ($\text{Fe}_8\text{O}_8(\text{OH})_{8-2x}(\text{SO}_4)_x \cdot n\text{H}_2\text{O}$) is a poorly crystalline phase that precipitates initially under atmospheric conditions in all experiments. However, a relatively rapid Ostwald ripening process leads to the transformation of schwertmannite into a Na-rich member of the $(\text{Na},\text{H}_3\text{O})\text{Fe}_3(\text{SO}_4)(\text{OH})_6$ solid solution after aging at 20°C (1 day) or 70°C (3 hours). SEM images show that the presence of sodium modifies the morphology of the obtained phases and TEM studies reveal that schwertmannite particles consist of disoriented nanodomains (~6nm) spread in an amorphous bulk whereas natrojarosite particles exhibit a single-domain, highly-crystalline core, the crystallinity decreasing from core to rim. TG and DTG analyses show that the dehydration of schwertmannite favors the transformation into natrojarosite. The transformation mechanism is followed by an internal structural reorganization within the individual nanoparticles in which Fe(III) is transported from the solid to the liquid and the other ions (SO_4^{2-} and Na^+) in the opposite direction as confirmed by spectroscopic analyses. Interestingly, the presence of Pb in acidic sulfate-rich aqueous solutions results in the precipitation of anglesite (PbSO_4), which is the only responsible for the removal of lead (98.7-99.2%) in short periods of time of 3h and 7 days at 70 and 20°C, respectively. The present results highlight the role of the ripening processes in epigenetic conditions and could be crucial in interpreting the formation of jarosite in Earth and Martian surface environments. Finally, these results provide useful insights to understand the geochemical behavior of Pb and open new sceneries for the recovery of Pb from acidic mine wastes.

Fe³⁺ PARTITIONING BETWEEN PYROXENE AND MELT AT HIGH P AND T WITH IMPLICATIONS FOR OXYGEN FUGACITY OF THE EARTH'S UPPER MANTLE

Rudra Avishek¹, Hirschmann Marc¹

¹Department of Earth and Environmental Sciences, University of Minnesota, United States

To understand the variation in Fe³⁺/Fe^T observed in basalts and their mantle source regions, it is important to constrain the fractionation of Fe³⁺ in the light of basalt petrogenesis. However, models with constant DFe³⁺ peridotite/melt, either applying batch or fractional melting conditions, from a source Fe₂O₃ of 0.3 wt.% fail to produce the range of Fe³⁺/Fe^T observed in global MORBs and OIBs. In addition, current thermodynamic and empirical models suggest that the fO₂ of spinel and garnet peridotite is ~1.5-2 log units lower than that of most primitive partial melts. This is at odds with the notion that chemical equilibrium exists between peridotite and basalt at the final pressure of melting and reflects a lack of understanding of Fe³⁺ fractionation during partial melting of peridotite. Since cpx and opx together host roughly 75% of the Fe³⁺ reserve in fertile peridotite, both pyroxenes play crucial roles in controlling Fe³⁺ concentration in the equilibrium partial melt throughout the melting interval. To this end, we have performed high P, T, fO₂ monitored piston-cylinder experiments to understand Fe³⁺ partitioning behavior between cpx, opx and mafic melt. Experiments were dynamically cooled to grow large, homogeneous pyroxene crystals and the fO₂ was monitored by using Fe-Pt alloy capsules with variable initial enrichment of Fe. Fe³⁺/Fe^T of the pyroxenes and glass were measured by Fe K-edge X-ray absorption near edge structure (XANES) spectroscopy using the newly developed Mössbauer-based calibration of Rudra et al. (submitted) and Zhang et al. (2018), respectively. Our experimental results show that DFe³⁺ cpx/melt is not constant and increases with increasing P and fO₂. DFe³⁺ cpx/melt correlates strongly with the Al³⁺ and moderately with the Fe³⁺ content of cpx suggesting the non-ideal nature of Fe³⁺ substitution in crystal structure. Compared to the thermodynamic models embedded in pMELTS and perple_X, the experimentally derived DFe³⁺ pyroxene/melt are systematically lower at all fO₂ and P. Our results highlight a variable DFe³⁺ pyroxene/melt and consequently a variable DFe³⁺ peridotite/melt across the melting interval of fertile source peridotite, which is required to explain the global variation in Fe³⁺/Fe^T observed in MORBs and OIBs.

CLINOPYROXENE MEGACRYSTS REVEAL A COMPLEX MAGMATIC HISTORY AT NEROTHER KOPF, WEST-EIFEL, GERMANY

Ruppel Anna¹, Woodland Alan B.¹, Heckel Catharina¹, Seitz Hans-Michael¹

¹Institut für Geowissenschaften, Goethe-Universität Frankfurt, Germany, s9555083@stud.uni-frankfurt.de; woodland@em.uni-frankfurt.de, c.heckel@em.uni-frankfurt.de; h.m.seitz@em.uni-frankfurt.de

Clinopyroxene megacrysts crystallizing in alkaline basaltic magmas have the potential to provide important petrological information about the nature of the magmatic plumbing system at depth. In addition to gaining estimates of crystallization depths, zoning in such crystals can also reveal episodes of magma mixing. We have investigated a suite of 10 megacrysts (up to 4 cm) from the small west Eifel volcano “Nerother Kopf”. To understand the underlying mechanisms of their formation, as well as thermodynamic and kinetic controls and the magmatic history, different methods were applied, including electron microprobe analysis and element mapping (EPMA) to document major and minor element variations within the megacrysts, laser ablation-ICP-MS to observe variations in trace element concentrations, and Mössbauer spectroscopy to determine the $\text{Fe}^{3+}/\Sigma\text{Fe}$ in larger domains that can be reasonably separated.

Most samples reveal complex compositional structures, indicating crystallization occurred at several different stages: (i) The megacrysts commonly have a core region with alternating compositional zones several mm across. (ii) The cores are mostly enclosed by a resorption surface. (iii) After the resorption event, tooth-shaped crystal growth occurred, which has a preferential crystallographic orientation. These crystals also exhibit fine zoning. (iv) In some cases, heterogeneous darker-colored sectors follow the resorption event and suggest a growth stage from a modified melt composition. These domains are patchy with wavy boundaries and are once again terminated by a resorption surface. (v) The outermost parts of the megacrysts reveal renewed finely zoned crystal growth. One sample has been fractured and recemented by new dark-colored Cpx.

The compositional data is spatially resolved and shows the enrichment of Al and Ti in darker zones of the crystals, and an enrichment of Mg in lighter appearing zones. Thermobarometric calculations have been performed applying calibrations based upon clinopyroxene composition. Calculated formation T and P show deviating formation conditions for the zones appearing in the pyroxenes. Dark and light-colored cores record temperatures averaging 1150°C and pressures of ~4.5 and 3 kbar, respectively. Suspected diffusion zones (stage iv) are enriched in Al, Ti and Fe and apparently formed under even higher pressures of 5 to 6 kbar. The zoned outer rims are enriched also in Al and Ti and depleted in Mg corresponding to the broader zones found in the cores. Further, zoning is also apparent in the distribution of trace elements with Ni, Ba, Sc, V and Sr enriched in Al-Ti-rich zones. The megacrysts generally have high Fe^{3+} contents ($\text{Fe}^{3+}/\Sigma\text{Fe} = 0.30-0.47$). The diverse and complex structures of the megacrysts, as well as their estimated T and P of crystallization suggest magma mixing and the influence of transport under chemical and thermal gradients.

NUCLEATION DELAY OF FELDSPAR IN WATER-SATURATED METALUMINOUS RHYOLITE DURING DECOMPRESSION – EXPERIMENTAL AND THEORETICAL APPROACH

Rusiecka Monika¹, Martel Caroline¹

¹Institut des Sciences de la Terre d Orleans, France

Volcanic eruptions constitute a major risk for regions in the proximity of the volcano and can also affect the weather patterns in areas located far away from the volcano (e.g., eruption of Tambora in 1815). Large felsic, volcanic systems (e.g., Long Valley Caldera) are source of the biggest and most violent eruptions. Nucleation of crystals during ascent of the magma can lead to changes in the network formed by the gas bubbles and change the permeability of the magma. As a result, the eruption style can change from calm, effusive one, when the gas is able to escape, to dangerous, explosive one, in which the gas remains trapped in the magma.

We developed a model to predict nucleation delay of feldspar in water-saturated metaluminous rhyolite during decompression. The model is based on the Classical Nucleation Theory and a model developed previously by Rusiecka et al. (2020) for nucleation delay of quartz and feldspar in metaluminous rhyolitic melt with 4 wt. % water under isobaric conditions. The theoretical calculations were compared to a series of decompression experiments conducted in an Internally Heated Pressure Vessel at 825 °C and pressures of 200 to 50 MPa. The experimental charges were first brought to 200 MPa and 825 °C for 24 h to homogenize the melt with water and then decompressed at a rate of 10 MPa/min to the crystallization pressure for duration ranging from 4 to 120 h. Moreover, a series of continuous decompression experiments were conducted to compare to the theoretical model and the single step decompression experiments.

The theoretical model agrees well with the experimental results which creates an opportunity to quantitatively predict the nucleation delay of the major mineral phase in an ascending rhyolitic magma. Better understanding of this process can potentially help to constrain the time between the intrusion of magma and the onset of crystallization leading to fluid saturation and consequently an eruption.

Rusiecka, M.K., Bilodeau, M., Baker, D.R. (2020). Quantification of nucleation delay in magmatic systems: experimental and theoretical approach. *Contributions to Mineralogy and Petrology*, 175, 1-16.

GRANITE EMPLACEMENT AND REGIONAL TECTONICS: INSIGHTS FROM MICROSTRUCTURAL AND AMS INVESTIGATIONS OF UPPER CRUSTAL LATE-VARISCAN GRANITOIDS

Russo Damiano¹, Fiannacca Patrizia¹, Fazio Eugenio¹, Cirrincione Rosolino¹, Mamtani Manish A.²

¹Dipartimento di Scienze Biologiche, Geologiche ed Ambientali, Università degli Studi di Catania, Italy,

²Department of Geology & Geophysics, Indian Institute of Technology, Kharagpur, India

The relationships between regional tectonics and emplacement of granitoid bodies are often challenging because even syn-tectonic granites may exhibit an apparent isotropic texture, with weakly-developed, if any, meso- or microstructural fabric. In light of this, an integrated microstructural and Anisotropy of Magnetic Susceptibility (AMS) study was carried out to detect any possible deformation microstructures and mineral preferred orientations in the granitoids that make up the upper levels of the Serre Batholith, in central Calabria. The studied rocks are two-mica granodiorites and granites (BMG; c. 295 Ma) passing upwards to weakly peraluminous biotite ± amphibole granodiorites (BAG; c. 292 Ma), although no intrusive contact has been observed in the studied areas. Microstructural investigations document that deformation was prevalent during all the cooling phases of both granitoids, starting from submagmatic conditions ($T > 650^{\circ}\text{C}$), as revealed by chessboard patterns in quartz and local submagmatic fractures. High-T solid state deformation (T about 550°C) is attested by evidence of feldspars and quartz grain boundary migration recrystallization, while subsolidus low-temperature deformation microstructures (T about 450°C) are represented by bulging quartz grain boundaries, quartz core-and-mantle structures, deformation twins in feldspar and kinked micas. Non-coaxial deformation is documented by sigmoidal porphyroclasts, grain boundaries orientation of polymineral aggregates and mica fish. From the comparison between BAG and BMG rocks, our investigations show no direct relationships between emplacement depth, age or composition and the type of deformation microstructures developed in the rocks. Preliminary AMS data highlighted mineral preferred orientations in both granitoids, not revealed by field and thin-section analyses. AMS measurements on oriented samples reveal an oblate shape of the AMS ellipsoid. Lower hemisphere equal area projections bring out similarities between BAG and BMG suggesting a similar, though not identical, control on the magnetic fabric orientations. Finally, magnetic foliations and lineations array might reveal the existence of a possible post-emplacement tectonic structure or, alternatively, reflect the geometry of the batholith roof levels. This research provides new information on the granitoids that make up the Serre upper crustal levels and underline the importance of AMS in studying apparently isotropic rocks.

NON-SILICATE AUTHIGENIC MINERALS REFLECTING OXYGEN DEFICIENCY AND SALINITY OF A CONTINENTAL SHELF SEA SEDIMENTS

Rzepa Grzegorz¹, Łukawska-Matuszewska Katarzyna², Manecki Maciej¹, Brodecka-Goluch Aleksandra², Broclawik Olga², Gawel Adam¹, Bolalek Jerzy²

¹Department of Mineralogy, Petrography and Geochemistry, AGH University of Science and Technology, Poland,
²Division of Marine Chemistry and Environmental Protection, University of Gdańsk, Poland

Because of their relatively shallow depths and high nutrient and organic matter input, shelf seas are areas of increased productivity compared to the open ocean and play a key role in biogeochemical cycling of various major and trace elements. In the present study, we focused on the processes involving iron, sulfur, and phosphorus cycling in sediments of the Baltic sea. Biogeochemical cycles of these elements depend on redox conditions and salinity and are linked with one another by organic matter mineralization and the formation of authigenic phases in the sediments. The aim of the study was to assess the impact of catchment area characteristics, oxygen conditions, and salinity on iron, sulfur, and phosphorus mineralogy and cycling in marine sediments. For this purpose, sediment cores, pore water and near-bottom water were collected from three stations representing different environments within the continental shelf. The sampling of the Gdansk Deep was carried out from r/v Baltica, and the sampling of the Gotland Deep and the Bothnian Sea from s/y Oceania. Mineralogical analysis of the sediment samples and sequential chemical extractions of iron, sulfur and phosphorus were carried out, coupled with chemical analysis of the water samples and hydrogeochemical modeling. Mineralogy of the sediments was evaluated using powder X-ray diffractometry (PXRD), scanning electron microscopy (SEM/EDS), Raman microspectroscopy, and simultaneous thermal analysis (STA-QMS).

Sediments from all three stations were fine-grained and consisted of allo- and authigenic minerals. They were dominated by (alumino)silicates: allogenic and authigenic phyllosilicates (mica, illite, chlorite, kaolinite) accompanied by quartz and alkali feldspars. The sediment composition varied markedly in the type and proportion of authigenic non-silicate minerals. These included iron sulfides (mainly framboidal pyrite), iron phosphates (vivianite), iron carbonates (siderite), and Ca-Mn carbonate, apatite, opal, and barite. The presence of iron (oxyhydr)oxides was also possible: these have only been demonstrated by sequential chemical extractions, the results of which show high agreement with the results of the mineralogical analysis of the sediments. Mineralogy of the non-silicate authigenic components of sediments reflects different solution-sediment interactions (influenced by changes in water chemistry, salinity, and oxygen conditions) as a result of different catchments. Variation in water chemistry and sediment mineral composition also mirrors, on a broader scale, the impact of human activities and climate change (the increase in riverine input and changes in the salinity regime, among others).

The study was financed by the National Science Centre, Poland (Projects no. UMO-2013/11/B/ST10/00322 and UMO-2016/21/B/ST10/02369) and AGH-UST (grant no. 16.16.140.315).

MINERALOGICAL CLASSIFICATION OF ORE TYPES OCCURRING IN THE WINGELLINA Ni (Co)- LATERITE PROJECT (WESTERN AUSTRALIA): THE XRPD-RIETVELD AND SEM-AUTOMATED MINERAL

Santoro Licia¹, Putzolu Francesco², Mondillo Nicola², Herrington Richard³, Boni Maria², Dosbaba Marek⁴

¹Earth Science, Università degli Studi di Torino, UNITO, Italy, ²Dipartimento di Scienze della Terra, dell'Ambiente e delle Risorse, Università degli Studi di Napoli, Federico II, Italy, ³Earth Science, Natural History Museum, United Kingdom, ⁴Tescan Ltd, Czech Republic

Ni(Co)-laterites account for over 60% of global nickel supply. Ni(Co)-laterite deposits derive from the weathering of mafic-ultramafic rocks under humid tropical conditions. Due to their mineral complexity, the accuracy of the mineralogical and geochemical characterization of these ores is often challenging, thus affecting both the reliability of resources estimation and the evaluation of the best processing strategy.

Although largely used, routine analytical techniques alone (XRPD, SEM-EDS, etc.) are often time-consuming and not always fully effective for the identification and quantification of poorly crystalline phases commonly occurring in Ni(Co)-laterites (i.e. amorphous, Fe- and Mn-oxy-hydroxides, smectite clays). In this frame, the use of integrated approaches by means of SEM-based Automated mineralogy techniques would be beneficial to the overall comprehension and, most importantly, to the quantification of the complex ore-bearing minerals and to the definition of the metals department.

Therefore, in this work, we present quantitative mineralogical data obtained by SEM-Automated mineralogy (TIMA-X, Tescan) analyses combined with XRPD-QPA (Rietveld method) of several samples from the Wingellina Ni(Co)-laterite deposit (Western Australia). The two methods were used in parallel in order to validate the results and taking advantages of the two different analytical techniques during data acquisition. The samples were collected from the "oxide" and "saprolite" horizons of the laterite profile. The main aim was i) to determine the mineralogy and the role of the poorly crystalline phases in the ore distribution and ii) to reach a deeper understanding of the relationship between the modal mineralogy and the department of both Ni and Co.

The combination of the two methods allowed to define the nature of poorly to non-crystalline MnO/OH (mainly lithiophorite – asbolane intermediates), resolving the complex textural relationships between economic and gangue phases and to assess the modal mineralogy of the oxide and saprolite ores. The former consists of goethite and MnO/OH (up to ~76 wt % and ~49 wt %, respectively), whereas the saprolite ore is dominated by serpentine, Fe/Mg-smectite and montmorillonite (up to ~42 wt% and ~19 wt%, up to 57 wt% respectively). The gangue consist of carbonates, kaolinite, gibbsite, primary oxides and quartz. Nickel and Co department was also accurately evaluated; Ni in oxide ore samples being hosted mainly within lithiophorite - asbolane (up to 91%) and goethite (up to 55%) while in the saprolite Ni is mainly concentrated in montmorillonite (up to 71%), serpentine (up to 36%) and smectite (up to 18%). As regards Co, it is mainly bounded within lithiophorite - asbolane and goethite (up to 96% and to 25%, respectively) in oxide zone, whereas in saprolitic lithologies, where a relative paucity of oxy-hydroxides has been observed, the Co department is still dominated by lithiophorite - asbolane and goethite (up to 81% and 23% respectively).

Controversial results and limitations were met during the discrimination of clay species by Automated mineralogy as for i) their high variable chemistry and ii) fine-grained size, resulting in the detection of mixed compounds and misleading phases. In this case, the accuracy of the results benefited from quality control of Automated SEM data through geochemical reconciliation based on whole-rock geochemistry- and XRPD-QPA-related whole-rock compositions.

IMPROVEMENT OF THE THERMAL INSULATION PROPERTIES OF THIN-BED MORTAR BY USING OF DIATOMACEOUS EARTH AS AN ADDITIVE

Sappa Daniela¹, Glenk Mischa¹, Pöllmann Herbert², Krcmar Wolfgang¹

¹Faculty of Materials Engineering, University of Applied Sciences Nuremberg, Germany, ²Institute of Geosciences and Geography, Martin Luther University of Halle-Wittenberg, Germany

In its new climate protection plan, the German government has further tightened its climate policy targets for the period up to 2050. The national goal is to reduce the primary energy demand of buildings by 80 % by 2050 compared to 2008, with a "roadmap for a nearly climate-neutral building stock" anchored in the buildings sector. This states that by 2030 the reduction in greenhouse gases in the building sector should be between 66 and 67 % compared to 1990.

In order to improve the thermal insulation properties of monolithic wall structures with highly insulating plane bricks, cement-based thin-bed mortars are used in the construction of energy-efficient buildings. The physical requirements are specified in DIN 1053, DIN EN 998-2, the German application standard DIN V 20000-412, and DIN EN 1015-11. In this context, a value of $\beta D \geq 10.00$ MPa must be maintained for the thin-bed mortar of compressive strength class M10 after a curing time of 28 days. While highly thermally insulating plane bricks now have equivalent thermal conductivities of only $\lambda_{equiv.} = 0.07$ W/(m·K), the thermal conductivity of $\lambda_{10, dry} = 0.21$ W/(m·K) for this type of mortar was not further thermally optimized. Thus, the bed joint of the thin-bed mortar, despite the low layer thickness, represents a cold bridge within the masonry.

The present poster deals with the improvement of the thermal insulation properties of a mineral thin-bed mortar, while maintaining the compressive strength class M10. For this purpose, the sieve fractions of the thin-bed mortar powder with a particle size ≥ 125 μ m were to be proportionally substituted by the additives "calcined diatomaceous earth" and "dried diatomaceous earth". The calculations of these formulations were carried out by means of the concrete volume method with adjusted water-mortar ratio, whereby the "capping" property of the thin-bed mortar was always maintained. The thin-bed mortar zero samples were produced in accordance with the manufacturer's specifications with a water-mortar ratio of 0.58. After a hydration time of 28 days, the material properties of compressive strength and thermal conductivity were determined. The starting material used was a thin-bed mortar from a well-known manufacturer with a thermal conductivity of 0.21 W/(m·K) and a compressive strength of 10 MPa. In almost all test series with the addition of diatomaceous earth, the thermal conductivity of the thin-bed mortar was reduced while the compressive strength was maintained or improved.

For example, by substituting 20 % by volume of the mortar powder coarse fraction with dried diatomaceous earth at a water-mortar ratio of 0.88, an average 28-day compressive strength of $\beta D = 10.60$ MPa was obtained. This value corresponds to the compressive strength class of the zero sample, which has a compressive strength of $\beta D = 10.4$ MPa after 28 days of hydration. At the same time, the coefficient of thermal conductivity was reduced from $\lambda_{10, dry} = 0.21$ to $\lambda_{10, dry} = 0.17$ W/(m·K) which approx. 19 %.

The thin-bed mortar sample modified with 20 % by volume of calcined diatomaceous earth, with a water-mortar ratio of 0.78, achieved a compressive strength of $\beta D = 15.00$ MPa after 28 days of hydration. This is an increase of 50 % compared to the zero sample while the thermal conductivity was reduced from $\lambda_{10, dry} = 0.21$ W/(m·K) to $\lambda_{10, dry} = 0.17$ W/(m·K). This corresponds to an improvement in thermal insulation by approx. 19 %.

Keynote

ENGINEERED CLAY COMPOSITE MATERIALS FOR WATER CONTAMINANTS CLEAN-UP

Sarkar Binoy¹

¹Lancaster Environment Centre, Lancaster University, Lancaster, United Kingdom

Widespread contamination of the aquatic and terrestrial environment with various natural and anthropogenic pollutants is obstructing the global sustainability because almost all countries and societies are impacted by the pressing issue of environmental pollution. Emerging contaminants such as pharmaceutical and personal care products, poly- and perfluoroalkyl substances, agrochemical cocktails and microplastics are found in household and industrial wastewater, surface water or even groundwater because wastewater treatment plants or industrial processes cannot completely remove these toxic chemicals. Due to high chemical stability and resistance to biodegradation, some of the emerging contaminant chemicals have been reported to contaminate drinking water sources of world's big cities, and detected in environmental matrices of even the remotest parts of the world, including the Arctic. The United Nations, therefore, included 'Clean Water and Sanitation' Sustainable Development Goals (SDGs) which aims to provide safe water to citizens of all countries. Removal of emerging contaminants from water is an urgent need for the global community, but largely technologically constrained because of the highly persistent chemical nature of most of the emerging contaminants. Some existing contaminant removal methods and materials have not seen widespread industrial acceptance mainly due to the poor contaminant removal performance and/or high energy and cost requirements for the cleaning process. Natural materials such as clay minerals are inexpensive, highly reactive and available abundantly throughout the world. They hold great potential for water contaminants removal, both with and without surface modification. Owing to high cation exchange capacity, surface area and intrinsic surface charge, natural clay minerals show considerable affinity to some emerging contaminants. The affinity of clay minerals towards contaminant chemicals can be enhanced many folds by modifying the clay mineral surface and/or via preparing clay-composite materials. For example, incorporation of surfactant molecules, deposition of reactive nanoparticles or loading microorganisms on clays have shown remarkable contaminant adsorption or degradation properties, helping to clean up contaminated water. Prominent groups of such engineered clays and composite materials include organoclays, nanoscale zero valent iron (nZVI) deposited clays, clay-polymer nanocomposites, clay-carbon composites and bio-reactive clays. Recent studies reported that clay-carbon composite materials, specially the inexpensive and energy-saving clay-biochar composites showed outstanding performances for removing emerging contaminants including PPCP and PFAS from water. This talk aims to highlight some recent advances in interdisciplinary research where clay-based surface-modified and composite materials have been applied for emerging contaminants removal from water. The talk will first give a brief outline of the source, fate and transformation behaviors of some key emerging contaminants in the environment, and then present successful research examples for the removal of emerging contaminants using clay-based materials. The talk will also identify key challenges for the use of clay-composite materials for water treatment, and suggest some future research directions for developing a cost-effective and green clay technology to solve the ever-increasing water contamination problem throughout the world.

NEW AGES FOR LATE CARBONIFEROUS TO TRIASSIC FELSIC MAGMATISM IN THE STRANDJA ZONE OF BULGARIA AND TURKEY

Sałacińska Anna¹, Gerdjikov Ianko², Gumsley Ashley¹, Szopa Krzysztof¹, Chew David³, Kocjan Izabela⁴

¹Wydział Nauk Przyrodniczych Uniwersytet Śląski w Katowicach, Poland, ²Faculty of Geology and Geography, Sofia University "St. Kliment Ohridski", Bulgaria, ³Department of Geology, School of Natural Sciences, Trinity College Dublin, Ireland, ⁴Institute of Geological Sciences Polish Academy of Science, Poland

Variscan terranes have been documented from the Balkans to the Caucasus. However, the southeastern portion of the Variscan Belt is not well understood. The Strandja Zone along the border between Bulgaria and Turkey encompasses one such terrane linking the Balkanides and the Pontides. However, the evolution of this terrane, and the Late Carboniferous to Triassic granitoids within it, is poorly resolved. Here we present LA-ICP-MS U-Pb zircon ages, coupled with petrography and geochemistry from the Sakar Batholith, as well as the Levka and Izvorovo plutons within the Sakar Unit (Strandja Zone). The ages obtained from granitoids from Sakar Batholith (ca. 301-306 Ma), are consistent with previously published data. The age of the Levka pluton (ca. 319 Ma) confirms that this magmatic body was emplaced before the intrusion of Sakar Batholith, as was proposed based on structural field data. The Izvorovo pluton yields crystallisation ages of ca. 251-256 Ma. These ages are older than the previously suggested age constraints of the Izvorovo pluton based on an assumed genetic relationship between the Izvorovo pluton and Late Jurassic to Early Cretaceous metamorphism. A better understanding of units across the Strandja Zone can now be achieved, revealing two age groups of plutons within it. An extensive magmatic episode occurred at ca. 305-295 Ma. It is predated by a more minor pulse at ca. 319 Ma, and a more long-lived episode at ca. 275-230 Ma. All of the granitoids were previously assigned as a product of long-lived subduction. Intrusions associated with both magmatic events were emplaced into pre-Late Carboniferous basement, and were overprinted by Early Alpine metamorphism and deformation. The two stages of Late Carboniferous to Triassic felsic magmatism of the Strandja Zone are not identified solely using geochronology – they also vary in the characteristics of their zircon populations (degree of inheritance), and differences in magma generation temperatures calculated based on zircon saturation temperature (TZr). The geochemical signatures, however, do not show any direct evidence for two groupings. The differences in the zircon populations and temperatures of magma generation of these two groups show that the conditions of melting were different, with lower temperatures and a likely fluid influx during the Late Carboniferous and higher temperatures and the absence of a fluid during the Permian-Triassic. These two stages of magmatism are likely attributed to changes in tectonic setting in the Strandja Zone. Such a change in tectonic setting is likely related to the collision between Gondwana-derived terranes and Laurussia, followed by either subduction of the Paleo-Tethys Ocean beneath Laurussia or rifting on the southern margin of Laurussia, with the granitoids forming in different tectonic environments.

Acknowledgements

This research was supported by a Preludium Grant awarded to AS from the National Science Centre (Narodowe Centrum Nauki), NCN, in Poland (grant agreement no. UMO-2018/29/N/ST10/00368).

MAGMATIC HSE-RICH NANOPARTICLES CONTROL THE METAL INVENTORY OF THE SUBCONTINENTAL LITHOSPHERIC MANTLE BENEATH SOUTHEAST IBERIAN MARGIN

Schettino Erwin¹, González-Jiménez José María¹, Marchesi Claudio¹, Saunders Edward², Hidas Károly³, Gervilla Fernando⁴, Garrido Carlos Jesus⁵

¹Instituto Andaluz de Ciencias de la Tierra, Universidad de Granada, Spain, ²Division of Earth Sciences - School of Environmental and Rural Science, University of New England, Australia, ³Departamento de Investigación y Prospectiva Geocientífica, Instituto Geológico y Minero de España, Spain, ⁴Departamento de Mineralogía y Petrología, Universidad de Granada, Spain, ⁵Instituto Andaluz de Ciencias de la Tierra, Consejo Superior de Investigaciones Científicas, Spain

The metal inventory of the subcontinental lithospheric mantle (SCLM) has been commonly regarded as controlled only by base-metal sulfides (BMS), whereas the role of nano-sized metal particles and minerals remains poorly constrained. In this contribution, we have selected a suite of metasomatized peridotite xenoliths from Tallante volcanic center (SE Spain) containing metal-rich nanoparticles. These xenoliths sampled the SCLM underlying the ore-productive Neogene Volcanic Province of the southeast Iberian margin. The metal-rich nanoparticles mainly consist of highly siderophile elements (HSE), sometimes bounded to semi-metals, such as Pt-(Pd)-Sn and/or Au-Pt. They are associated with sulfide droplets (pentlandite ± chalcopyrite ± bornite) enclosed in metasomatic clino- and orthopyroxene crystallized during the percolation of silicate melts in the shallow lithospheric mantle. Careful analysis of the nano-sized metal-rich particles using field-emission scanning electron-microscopy (FE-SEM) and a combination of the focused ion beam (FIB) and transmission electron microscopy (FIB-TEM) reveal the presence of euhedral grains of tatyrite (ideally Pt₉Cu₃Sn₄) as well as Au crystals with no crystallographic continuity with the host BMS. This new observation suggests the crystallization of nano-sized metal particles and minerals occurred prior to BMS rather than by low-temperature exsolution upon cooling. The mechanical incorporation by sulfide melts of these metal-rich nanoparticles imparted a wide variability of chondrite-normalized platinum-group elements systematics in their host sulfides, which is ultimately controlled by the presence or not of these Pt-rich and Au-rich particles and minerals. Remarkably high Au concentrations in Tallante BMS suggest that the precipitation of metal-rich nanoparticles provided an efficient mechanism for generating a gold-rich mantle source beneath the ore-productive volcanic province of southeast Spain.

THE REFRACTIVE INDEX OF MgO AND FERROPERICLASE AT THE PRESSURE CONDITIONS OF THE EARTH'S MANTLE

Schifferle Lukas¹, Lobanov Sergey S.¹

¹Chemistry and Physics of Earth Materials, German Research Centre for Geosciences, Germany

Here we present the evolution of the optical refractive index of MgO and (Mg_{0.87}Fe_{0.13})O with pressure as inferred from direct measurements in diamond anvil cell up to 138 GPa. In MgO, the refractive index is almost pressure-independent and is only slightly decreasing with pressure. The refractive index is proportional to both density and electronic polarizability, that is, the light-induced electron cloud distortion. We assign the slight lowering in the refractive index with pressure in MgO to the decreasing polarizability, counter-balancing the increase in density. In contrast, in ferropericlase (Mg,Fe)O up to ~40 GPa the refractive index raises with pressure. At P > ~40 GPa, the pressure-dependent increase in the refractive index is continuously reduced and at P > ~70 GPa the index is almost insensitive to pressure. We assign this drastic change in the refractive index pressure-derivative to the iron spin crossover. At the conference, we will discuss these results in full detail as well as their geophysical implications.

DETRITAL ZIRCON IN MODERN RIVER SEDIMENT FROM THE EAST EIFEL VOLCANIC FIELD

Schmitt Axel Karl¹, Schmitt Fabian¹

¹Institute of Earth Sciences, Heidelberg University, Germany

Evolved (trachytic-phonolitic) magma is an important end-member in the compositional spectrum of many intracontinental volcanic fields, and the East Eifel (Germany) hosts three such evolved centers (Rieden, Wehr, Laacher See) which have been volumetrically dominating the volcanic output of the field since ca. 440 to 13 ka. These evolved systems contain zircon, although erupted magmas are often zircon undersaturated, and thus zircon is commonly sourced from cogenetic crystal-rich intrusions that are represented by plutonic ejecta. Similarly, zircon megacrysts in mafic (basanitic-tephritic) lavas from the East Eifel volcanic field originate from such evolved intrusives. Zircon is thus a potential indicator for the accumulation of magma in crustal reservoirs where it cooled and differentiated. Earlier studies for the East Eifel have selectively analyzed zircon from such plutonic enclaves mainly from pyroclastic deposits from Rieden, Wehr, and Laacher See, as well as rare zircon megacrysts found isolated in lavas. To test if these zircon ages are representative for the entire field, and to obtain a clearer picture on the duration of zircon crystallization in evolved intrusions underlying the East Eifel volcanic field, we have sampled modern river sediment from the two main regional catchments drained by the Nette and Brohlbach streams. Magnetite-rich black sand in the size fraction <2 mm was high-graded on site using gold pans, and further processed in the laboratory via magnetic and density (heavy liquid) separation. Zircon abundances in individual black sand samples range between 0.01 and 0.2 %, with other tentatively identified heavy minerals comprising clinopyroxene, corundum, garnet, hornblende, olivine, rutile, sulfides, and titanite. Reconnaissance U-series zircon dating using SIMS indicates rapid crystallization of individual crystals within the uncertainty of the ²³⁰Th-²³⁸U method, and crystallization ages between the eruption age of Laacher See (ca. 13 ka) and 45 ka were obtained for a preliminary subsample (n = 10) with further analyses underway. Upon completion, this study would be the first to assess the potential of detrital accessory mineral studies for Quaternary volcanic fields, a currently underutilized method to constrain the magmatic prehistory of such distributed magmatic systems.

SUBMARINE HIGH-GRADE HEMATITE ORE (LAHN-DILL-TYPE) FORMATION AND ITS IMPLICATIONS ON FE PATHWAYS

Schmitt Leanne¹, Kirnbauer Thomas¹, Angerer Thomas², Kraemer Dennis³, Volkmann Rebecca⁴, Klein Sabine⁵

¹Geo-Resources and Process Engineering, Technische Hochschule Georg Agricola, Germany, ²Institute of Mineralogy and Petrography, University of Innsbruck, Austria, ³Department of Physics and Earth Sciences, Jacobs University Bremen, Germany, ⁴Interface Geochemistry section, Helmholtz Centre Potsdam, Germany, ⁵German Mining Museum Bochum, Germany

Sedimentary iron ore systems provide excellent opportunities to study Fe pathways in paleo-environmental settings. Lahn-Dill-type iron ores are submarine chemical sediments with high Fe content of up to 60 wt.%, providing unique insights into Fe mobilization, metal scavenging during precipitation, and (post-)depositional processes. During the Middle to Upper Devonian, Lahn-Dill-type iron ores formed associated with intraplate alkali basaltic volcanism within the Rhenohercynian back-arc basin. They precipitated on top of volcanoclastic successions proximal to centres of volcanic activity. The Fortuna mine (Lahn syncline, Germany) hosts one of the largest Lahn-Dill-type ore deposits. There, we sampled a sub-vertical ore profile composed of a lower three m hematite-quartz and an upper two m siderite-hematite-quartz ore, as well as ~120 m of underlying volcanoclastic rocks. We conducted a petrographic study, as well as whole rock and in situ laser ablation geochemistry with the aim to decipher ore forming processes and Fe pathways from source to sink.

Based on our studies, submarine ore forming processes can be subdivided into (1) mobilization in the volcanoclastic substrate, (2) iron-rich particle precipitation and their metal scavenging in seawater and (3) deposition on the seafloor. (1) Primary mineralogy in footwall volcanoclastic rocks is completely replaced by calcite, chamosite, muscovite, quartz, albite and leucosene during seawater alteration (i.e., spilitization). Proximal to the ore, rocks show a lower modal chamosite but higher modal calcite abundance which is geochemically reflected by Fe-depletion and Ca-enrichment. Overlying ores display positive correlations between Fe and traces of HFSE. We suggest that acidic CO₂-rich fluids induced continuous carbonatization of footwall rocks, which led to an increase of pH. These alkaline fluids subsequently mobilized Fe and also HFSE. (2) Ores depict positive correlations between Fe and both, compatible and incompatible transition metals including Zr, W, Mo, Pb, V and Zn suggesting contrasting sources, i.e. the mafic rock substrate and seawater. We thus interpret that upon venting into the shallow, oxidized Devonian basin at the flanks of volcanoes, plumes of colloidal Fe-oxyhydroxides immediately formed and scavenged metal ions and complexes from the hydrothermal plume as well as the ambient seawater. (3) Mineral assemblages within the ore range from fused hematite “mats”, nanocrystalline hematite dispersed in quartz and/or siderite, to almost pure quartz. Crescent-shaped shrinking cracks within hematite- and quartz-hematite assemblages indicate formation from a Si-Fe-rich gel, whereas siderite dominating over SiO₂ in the top two meters may suggest biotic or abiotic reduction of Fe during or after deposition.

HYDRAULIC REACTIVITY OF ALITE RICH MATERIAL FROM POST-TREATED BASIC OXYGEN FURNACE SLAGS

Schraut Katharina¹, Adamczyk Burkart¹, Adam Christian¹, Stephan Dietmar², Simon Sebastian³, von Werder Julia⁴, Meng Birgit⁴

¹4.4 Thermochemical Residues Treatment and Resource Recovery, Bundesanstalt fuer Materialforschung und pruefung, Germany, ²Institut für Bauingenieurwesen, Technische Universität Berlin, Germany, ³7.4 Technology of Construction Materials, Bundesanstalt fuer Materialforschung und pruefung, Germany, ⁴7.1 Building Materials, Bundesanstalt fuer Materialforschung und pruefung, Germany

Basic oxygen furnace slags (BOFS) are a by-product of steel production. In 2016, 10.4 Mt of BOFS were produced in the European Union (EU). The main part of BOFS is used in road construction, earthwork and hydraulic engineering. A smaller part is returned to the metallurgical circle, used as fertilizer or landfilled. However, it is also possible to produce higher value products from BOFS. For example, many researchers have investigated the possibility of producing Portland cement clinker and crude iron from BOFS by a carbothermal post-treatment (Kubodera et al. 1979, Piret and Dralants, 1984, Dziarmagowski et al. 1992, 2003, 2005, 2007, Reddy et al. 2006 and Wulfert et al. 2013).

In this study, German BOFS was reduced in a small-scale electric arc furnace using petrol coke as a reducing agent. The carbothermal treatment reduces the iron oxides in the BOFS to metallic iron, which accumulates at the bottom of the furnace by density separation. In addition to metallic iron, the process generates a mineral product rich in the tricalcium silicate solid solution alite. As the main constituent of Portland cement clinker, the hydraulic reactive mineral alite is of high economic importance.

In previous studies, the hydraulic reactivity of the mineral product was investigated by testing the compressive strength of blends with 70 wt.% ordinary Portland cement (OPC) (Wulfert et al, 2013). Recent investigations focused on the hydraulic properties of the pure mineral product from the reduced BOFS. The heat of hydration of the mineral product was measured by isothermal calorimetry and compared with the heat of hydration of a synthetic low-iron slag and OPC. In addition, the formation of hydration products was investigated with differential scanning calorimetry (DSC) and x-ray diffraction analysis (XRD) on freeze-dried samples after defined curing times. The results of the calorimetric measurements indicate that the mineral product produced less heat of hydration and its reaction was delayed compared to the synthetic low-iron slag and OPC. Hydration products such as portlandite and calcium silicate hydrates (C-S-H) formed later and in lower amounts. The production of a hydraulic material from BOFS by reductive treatment is of great interest to both the cement and steel industries. The substitution of cement clinker in OPC with a hydraulic material such as reduced BOFS leads to a reduction in greenhouse gas emissions from cement production. The steel industry benefits from an application for its by-products that avoids cost expensive landfilling and may even bring economic advantages. Furthermore, it may be possible to return the recovered crude iron to production.

STRUCTURAL TRANSITION IN SUPERCRITICAL WATER AND ASSOCIATED CONSEQUENCES FOR ION HYDRATION

Schulze Maximilian¹, Jahn Sandro¹

¹Institute of Geology and Mineralogy, University of Cologne, Germany

Structural and physical properties of supercritical fluids change smoothly as a function of temperature (T), pressure (P) or density (ρ). Until a few years ago the picture of a physically homogeneous single-phase fluid at conditions above the critical point was the predominant view. More recent work in the field of physics and physical chemistry has led to a more differentiated conception. For example, the Frenkel line was proposed to subdivide the supercritical state into a gas-like and a liquid-like region. Both, experiments and molecular dynamics (MD) simulations provide evidence of distinct structural changes between these two regions. Independent of these works from adjacent disciplines, there is indirect evidence of structural discontinuities in supercritical water (SCW) from research within the geoscientific community. It is known from experiments on 1 m NaCl solutions that the partial molar volume of the solute in SCW can change from large negative values at low densities to positive values at higher densities during isothermal compression. This behavior was interpreted as a consequence of the increasing contribution of the P-T-independent intrinsic volume of the respective ions in SCW towards higher densities.

In this work we carry out classical MD simulations with two particular problems in mind:

(1) We investigate how the sign change of the partial molar volume of a solute is related to changes of the solvent structure.

(2) We elaborate on the question how the solvation properties of ions change at the same conditions.

We perform MD simulations of pure H₂O and the NaCl-H₂O system in the dilute limit range under supercritical conditions. Structural information is obtained from radial distribution functions. In addition, we derive volumetric information about hydration shell water from Voronoi tessellations. To study the partial molar volume of NaCl, we determine the Krichevskii parameter along isotherms at different densities. Our preliminary data show that the sign change conditions of the partial molar volume mark a transition point between areas with different compression behavior in SCW. This is indicated by distinct changes in the intermolecular distances within the bulk water and by a change in the compressibilities of solvation shell molecules.

This work was funded within EU2020 project GEOPRO, grant agreement ID 851816. Computing time was provided through the John von Neumann Institute for Computing (NIC) on the JUWELS supercomputer at Jülich Supercomputing Centre (JSC) under project ID CHPO15.

INFLUENCE OF THE REACTION INTERFACE ORIENTATION ON THE MICROSTRUCTURE AND TEXTURE OF SPINEL FORMED BY TOPOTACTIC GROWTH ON CORUNDUM

Schuster Roman¹, Habler Gerlinde², Tiede Lisa², Ageeva Olga², Abart Rainer²

¹Christian Doppler Laboratory for Interfaces and Precipitation Engineering CDL-IPE, Institute of Materials Science and Technology, TU Wien, Austria, ²Dept. of Lithospheric Research, University of Vienna, Austria

A natural about 150 µm thick spinel corona that formed around a centimeter-sized corundum single crystal through chemical reaction between the corundum xenocrystal and the hosting basaltic melt was investigated by EBSD and µ-CT analysis. The interface between corundum and spinel consists of straight segments of several 100 µm lateral extension. A combination of EBSD and µ-CT was used to identify the full 3D orientation of the interface segments with respect to the corundum lattice and to characterize the spinel microstructure and texture for different reaction interface orientations. Our investigation revealed microstructural and textural features differing between segments with different interface orientations, whereas other features are independent of the latter.

The common topotactic orientation relationship between corundum and spinel, where one of the $\langle 111 \rangle$ directions of spinel is parallel to the c-axis of corundum and three $\langle 110 \rangle$ directions of spinel are parallel to the $\langle 10-10 \rangle$ directions of corundum is roughly adhered to in all corona segments. This topotaxy results in a pronounced texture, where the two spinel orientations compatible with the crystallographic orientation relationship dominate over other orientations, regardless of the orientation of the corundum-spinel interface relative to the corundum lattice. However, the relative prevalence of the two preferred texture components varies between corona segments and is controlled by the orientation of the corundum-spinel interface relative to the crystallographic orientation of the two texture components of spinel. Furthermore, the spinel grains exhibit small (up to about 7°) but systematic deviations from the ideal topotactic orientations. These deviations result from rotations about the c- and a-axes of corundum, where the activation of these rotations is controlled by the orientation of the corundum-spinel interface with respect to the lattice of corundum. For rim segments associated with roughly prismatic corundum facets, the spinel rotation about the corundum c-axis is always active, while rotation about a specific corundum a-axis only occurs for corona segments corresponding to corundum facets that are oriented close to normal to that a-axis. The latter rotation shows a preferred sense depending on the sign of direction of the a-axis with respect to the growth direction. Furthermore, the grain shapes and grain boundary orientations in the spinel corona are controlled by both, the crystallographic orientation of the corundum crystal and by the reaction interface orientation relative to the corundum lattice. Spinel twin boundaries strictly follow the spinel $\{111\}$ plane that is subparallel to the corundum basal plane, whereas the general grain boundaries are preferentially oriented parallel to the spinel growth direction. Our findings have substantial implications for the petrogenetic interpretation of reaction microstructures, as they show that particular reaction interface orientations and the crystallographic orientations of the involved phases are critical for the development of reaction microstructures.

THE ROLE OF PHYLLOSILICATES FABRIC IN THE MECHANICAL RESPONSE OF DEEP-SEATED LANDSLIDES. THE CASE OF EL FORN LANDSLIDE (ANDORRA).

Segui Carolina¹, Veveakis Manolis², Tauler Esperança³

¹Institute of Geomechanics and Underground Technology, RWTH Aachen., Germany, ²Civil and Environmental Engineering Department, Duke University, United States, ³Departament de Mineralogia, Petrologia i Geologia Aplicada, University of Barcelona, Spain

Deep-seated landslides are among the most devastating natural hazards on earth, usually involving a rigid rock mass sliding over a weak, clayey shear band rich in phyllosilicates. The mechanical response of this shear band to the loading of the overburden is, therefore, critical for the stability and the evolution of a landslide. We hereby show that this mechanical response is strongly associated with mineralogy and microstructure of clay minerals forming the shear band, and vice versa. By presenting a detailed mineralogical, textural, and mechanical characterization of a shear band of an active deep-seated landslide, we attempt to shed light on processes determining the failure mechanism of a large deep-seated landslide. The case study chosen is the Cal Ponet – Cal Borronet lobe with a sliding mass of 1Mm³, inside the large El Forn landslide located in Andorra Principality (Eastern Pyrenees) with a sliding mass of approximately 300Mm³. Its shear band is formed of black shales of the Silurian period. Using core samples of this landslide, we have performed mineralogical and microstructural analyses such as X-Ray diffraction (XRPD), Scanning Electron Microscope (SEM-EDS), and MicroCT scan, combined with mechanical tests (liquid limit, plastic limit) to study the interplay between the internal texture of the material of the shear band and its mechanical response. Our results show that the highest mechanical alteration of the material occurs at the center of the shear band, where the phyllosilicates are perfectly aligned parallel to the shearing direction. The alignment of the crystals and their face-to-face contact increases the plasticity index of the material and reduces its porosity, which is concentrated along a band of interconnected pores. Hence, the shearing movement rearranges the contacts of the phyllosilicate grains inside the shear band, reducing the resistance of the material and promoting the slip of the overburden. Outside the shear band, the phyllosilicates are randomly oriented by forming aleatory and very sinusoidal folds, presented as the common fabric of shales. This fabric shows lower values of plasticity index of the material as the phyllosilicates contacts are face-edge or edge-edge, and lower values of porosity, with not interconnected pores. At the edges of the shear band, the phyllosilicates are aligned forming smoother folds, this structure decreases sharply the porosity and plasticity of the material as the compacted rearrangement in these areas. Thus, where the phyllosilicates are randomly oriented and/or forming folds, the resistance of the material is higher than at the center of the shear band where the minerals are completely aligned. With the results obtained in this study, we present the evolution of the mineralogy, fabric, porosity, and plasticity of the Silurian shales along the shear band of an active deep-seated landslide, by correlating them with the shearing movement and the mechanical response of the landslide.

THE ROLE OF MgO IN THE SO₂ SORPTION UNDER FLUIDIZED COMBUSTION CONDITIONS

Sęk Magdalena¹, Hycnar Elżbieta¹

¹Faculty of Geology, Geophysics and Environmental Protection, AGH University of Science and Technology, Poland

In the power industry, high-quality limestones are commonly used as SO₂ sorbents. Dolomites or magnesites and even dolomitic limestones are not used. The literature data and laboratory experiments indicate that Mg-rich carbonates can show an even better ability to bind sulfur dioxide compared to calcium carbonate (e.g. Kaljuvee 2005, Anthony 1995). Two different types of rocks were studied: Triassic dolomite from the Chruszczobród II deposit (Upper Silesia, Poland) and magnesite mineral waste from the Wiry mine (Lower Silesia, Poland). The sorption efficiency towards SO₂ was determined by following the Ahlstrom Pyropower Development Laboratory test (1995) at bench-scale installation. The tests included two steps: (1) calcination of raw samples and (2) sulfation of calcined samples. The sulfate experiment was carried out on a laboratory stand constructed based on a gas-tight retort furnace acting as a fixed bed. Samples (natural, calcined, sulfated) were examined by physicochemical and mineralogical methods, including XRD, DTA, TG, SEM/EDX, ICP-MS, mercury porosimetry.

Dolomite samples were characterized by nearly monomineral phase composition, except CaMg(CO₃)₂ only traces of SiO₂ were found. The content of non-carbonate components in magnesite waste reaches a value of 21,6 wt.%. Apart from magnesite, the presence of dolomite and quartz was noticed. The reactivity with SO₂ indicates excellent sorption properties of both, dolomite (ca. 235 gS/kg of sorbent) and magnesite (126 gS/kg of sorbent). In order to determine the active participation of magnesium in the process of SO₂ binding under fluidized furnaces conditions, XRD analyses of products of reactions were carried out. In the case of dolomite-based sorbent, apart from the synthetic analog of anhydrite (CaSO₄), the presence of calcium and magnesium double sulfate (CaMg₃(SO₄)₄) was noticed. In the case of magnesite-based sorbent, the predominant component was magnesium sulfate (MgSO₄) with a smaller contribution of CaMg₃(SO₄)₄. Both magnesium sulfates are stable in the temperature characteristic for fluidized combustion conditions. The decomposition begins after exceeding 950°C.

Magnesium sulfates synthesized in experiments had an extremely developed porous texture confirmed by mercury porosimetry analyses. That kind of porosity is significant in the sorption capacity increasing, due to extending the reaction time between CaO and MgO with SO₂ (Hycnar 2018). It was also shown by the observation of the sorbent grain cross-sections using the SEM/EDS and elemental mapping.

The research was funded on 11.11.140.158 and carried out with the support of the infrastructure of the AGH Center of Energy.

Ahlstrom Pyropower Reactivity index, 1995. Ahlstrom Pyropower.

Anthony, E.J. (1995). Fluidized bed combustion of alternative solid fuels, status, successes and problems of the technology. *Progress in Energy and Combustion Science*, 2, 239-268.

Hycnar E., 2018. The structural and textural characteristics of limestones and effectiveness of SO₂ sorption in fluidized bed conditions. *Economy of Mineral Resources*, 34 (1), 5-24.

Kaljuvee, T., Trikkel, A., Kuusik, R., & Bender, V. (2005). The role of MgO in the binding of SO₂ by lime-containing materials. *Journal of Thermal Analysis and Calorimetry*, 80(3), 591-597.

OCCURRENCE OF OPHIOLITIC CHROMITITE AND ASSOCIATED PGM IN SULAWESI AND KABAENA ISLANDS, INDONESIA

Septiana Sara¹, Idrus Arifudin¹, Zaccarini Federica², Garuti Giorgio²

¹Departement of Geological Engineering, Gadjah Mada University, Indonesia, ²Departement of Applied Geosciences and Geophysics, University of Leoben, Austria

The present study reports on the mineral chemistry of chromite and associated platinum-group minerals (PGM) of Indonesian ophiolitic chromitites. The investigated samples were collected in remote areas of the South and Southeast Arms of Sulawesi and Kabaena Islands. According to the variation of the Cr#, intermediate and Cr-rich chromitites occur in all the localities, whereas Al-rich chromitites have been analyzed only in the South Arm of Sulawesi. TiO₂ is generally lower than 0.4 wt % in all the analyzed samples, as is typical for podiform chromitite. In the diagram Al₂O₃ versus TiO₂ all the analyzed samples plot in the field of the supra-subduction zone (SSZ) chromitite, with the exception of the Al-rich chromitites that fall in the overlapping field of SSZ and MORB (mid-oceanic ridge basalt). The same diagram shows that in all the studied localities two types of chromitite were identified. Type I chromitite plots in the field IAB (island arc basalt) and type II displays affinity for the chromitite that formed in the supra-Moho sequence of ophiolites. Several PGM have been found in all the studied chromitites. They form tiny grains, less than 10 µm in size, and consist of laurite (RuS₂) and less abundant irarsite (IrAsS). Laurite is polygonal and occurs enclosed either in fresh chromite or in contact with fractures filled with chlorite and serpentine. Few grains of laurite occur associated with Ni-sulfides and apatite. Irarsite was found as small irregular blebs in contact with laurite, awaruite, pentlandite that occur in the altered silicate matrix. The composition of chromitites suggests a vertical zonation due to the fractionation of a single batch magma with an initial boninitic composition, with the accumulation of Cr-rich chromitites at deep mantle and the formation of more Al-rich chromitites close or above the Moho. All of the laurites formed were entrapped as solid phases during the crystallization of chromite at temperature of around 1200 °C and a sulfur fugacity below the sulfur saturation. Irarsite crystallized at low temperature, less than 400 °C, as an exsolution product. The data presented in this work indicate the possible existence of a wide ophiolite belt in Indonesia that hosts potential economic chromium deposits.

EFFECTS OF TEMPERATURE ON REACTIVITY AND GEOPOLYMERIZATION PROCESS OF MINING BY-PRODUCT UNTREATED CLAY.

Sgarlata Caterina¹, Formia Alessandra², Ferrari Francesco³, Leonelli Cristina¹

¹Department of Engineering “Enzo Ferrari”, University of Modena and Reggio Emilia, Italy, ²Sibelco Ankerpoort NV, 6223 EP Maastricht, The Netherlands, Netherlands, ³Sibelco Italia S.p.A., 41053 Maranello (MO), Italy

The heart of this research is the study of the possibility of reusing waste materials from industrial processes to obtain more sustainable high-performance materials. Halloysitic clay classified as a mining by-product has been used in this work for producing dense alkali-activated solid materials. Attention was focused on the influence of temperature on the geopolymerization process, as the effects on microstructure of the samples obtained. The challenge is to alkali activate the clay as received without any firing pre-treatment. The fresh paste of untreated clay was cured in 50% relative humidity (RH%) at temperatures just above room temperature ($\leq 80^{\circ}\text{C}$). Halloysitic clay has been then mixed with a sand, also classified as by-products of mining industry, to achieve greater chemical stability. The results showed a clear difference in chemical stability for samples containing sand compared to those without sand. Low percentages of metakaolin (5-15%) were also added in same formulations to observe improvements in terms of chemical and physical properties of samples and reducing the curing time. For mixtures consisting of untreated clay and sand only NaOH was added as alkaline activator. The effect of curing temperature and microstructure of geopolymers, were analyzed by different techniques: measure of pH and ionic conductivity of the eluate of the chemical stability test in water, X-ray diffraction (XRD), scanning electron microscopy (SEM), bulk density, and mechanical test.

REPEATED UHT GRANULITE METAMORPHISM DURING TERRAIN ASSEMBLY, CRATONIZATION AND STABILISATION OF THE KAAPVAAL CRUST AND MANTLE

Shu Qiao¹, Marschall Horst², Gerdes Axel², Beranoaguirre Aratz², Hofer Heidi², Hezel Dominik², Heckel Catharina², Walters Jess², Brey Gerhard²

¹State Key Laboratory of Ore Deposit Geochemistry, Institute of Geochemistry, Chinese Academy of Sciences, Guiyang 550081, China, ²Goethe-Universität Frankfurt, Germany

The determination of the age and duration of metamorphism generally relies on accessory minerals, such as zircon and monazite. Yet, age determination on main metamorphic minerals would be highly desirable, as it would enable us to directly connect P–T estimates to time information. Recently, Millonig et al. (2020) determined U–Pb ages by LA-ICP-MS on pyrope-almandine garnet from regional metamorphic schists. Here, we apply a similar method to prp-alm garnet from ultra-high temperature (UHT) granulite xenoliths from the Star diamond mine on the Kaapvaal craton. The Star kimberlite and three further kimberlites along the NNE trending axis of the Witwatersrand basin transported petrologically identical UHT granulite xenoliths to the Earth's surface. Dawson et al. (1997) studied the petrology of 18 xenoliths from the Lace Mine and Schmitz and Bowring (2003) analyzed U–Pb isotopes in zircon and monazite from all four localities. From the paragenesis garnet, sillimanite, quartz and sapphirine Dawson et al. (1997) estimated peak-metamorphic temperatures exceeding 1050°C and pressures of 0.9–1.2 GPa. We obtained U–Pb ages by LA-ICP-MS from eight garnet samples from the Star mine. The method relies on a large number of garnet analyses in each sample that form a linear array in a Tera-Wasserburg diagram. The lower intercept yields the age with a typical 2 σ uncertainty of ≥ 2 %. One sample yielded the youngest age of 2.72 Ga, five ages between 2.93 and 3.0 Ga and two ages around 3.09 Ga. The latter overlap with the time of the final assembly of the Kaapvaal East Block at 3.1 Ga, of voluminous granitoid intrusions and of the eruption of mafic and felsic volcanics of the Dominion Group. The main garnet age overlaps with the time of the infilling of the Witwatersrand basin between 2.99 and 2.78 Ga and with the collision of the Kaapvaal East and West Blocks at 2.88 Ga. The youngest garnet age coincides with the outpouring of the Ventersdorp flood basalts at 2.73–2.71 Ga. The zircon and monazite ages determined by Schmitz and Bowring (2003) lie at around 2.72 Ga. These authors estimated 5–10 million years for the duration of UHT metamorphism and named the Ventersdoorp volcanism as its cause. This contrasts with most of the much older garnet ages of this study. The complete age range of the garnets could indicate an exceptionally long duration of UHT metamorphism, twice as long as the previously suggested limit of 150 million years. An extended duration of UHT metamorphism could be caused by a thickened crust, high internal crustal heating from high contents of radioactive elements and high thermal advection from the mantle in the Archean (Harley, 2016). At present, however, we prefer the interpretation of episodic metamorphism with a first phase of metamorphism lasting from 3.09 to 2.93 Ga and a second, short episode at 2.72 Ga related to the Ventersdorp volcanism.

FLUID-CONTROLLED APATITE-CALCITE EQUILIBRIUM IN CALC-SILICATE ROCKS FROM ZAVALLYA, PODILLYA DOMAIN OF THE UKRAINIAN SHIELD (UKRAINE)

Shumlansky Leonid¹, Gawęda Aleksandra², Chew David³, Szopa Krzysztof², Bekker Andrey⁴, Dunkley Daniel J.⁵

¹Faculty of Science and Engineering, Curtin University, Australia, ²Faculty of Natural Sciences, University of Silesia in Katowice, Poland, ³Faculty of Natural Sciences, Trinity College Dublin, Ireland, ⁴college of Natural and Agricultural Sciences, University of California, Riverside, United States, ⁵Institute of Physics, Polish Academy of Sciences, Poland

Apatite in metamorphic rocks is a carrier of trace elements and is often used as a tool for constraining the cooling history and chemical evolution of metamorphic rocks. The Bouh Series (Podillya Domain of the Ukrainian Shield) is composed of metapelitic rocks with thick layers of calc-silicate rocks and quartzite, exposed in the Zavallya open pit. The maximum depositional age of the sequence, obtained from detrital zircons, is 2.5-2.7 Ga, whereas granulite-facies metamorphism took place at ca. 2.05 Ga. The calc-silicate rocks are composed of calcite, dolomite, Mg-rich orthopyroxene, diopside and olivine (locally replaced by Mg-serpentine), blue (Cl, F)-apatite and 2H graphite. Secondary magnetite and hematite fill the fractures. Carbonate minerals have $\delta^{13}\text{C}$ values ranging between -0.5 and -1.8 ‰ V-PDB and negative $\delta^{18}\text{O}$ values ranging from -8.2 to -10.8 ‰ V-PDB. Patchy distribution of Cl and F substitutions in apatite are observed.

All the analyzed apatite (41 analyses) and calcite (28 analyses) crystals are nearly concordant and yield a Tera-Wasserburg lower intercept age of 1390.2 ± 5.4 Ma (MSWD = 2.0). Uranium, Th, Pb in apatite and calcite are equilibrated, while Sr, Mn, Y and the REE show the non-consistent behavior. REE are strongly fractionated in apatite ($\text{LaN/YbN} = 94-225$), with slightly negative Eu/Eu* anomaly (mean value 0.88), while in calcite the REEs are moderately fractionated ($\text{LaN/YbN} = 13-18$; mean Eu/Eu* = 0.81). Two trends on the diagram showing Sr versus total REE and Th versus Sr in apatite may have resulted from recrystallization of apatite and re-equilibration with calcite associated with hydrothermal fluid flow. This is probably due to the interaction of the metasedimentary rock (with very low REE and Sr contents and low oxygen fugacity) with hydrothermal fluid. Fluid influx related to the thermal episode probably caused the sudden change in oxygen fugacity, responsible for the co-existence of graphite and Fe-oxides. The thermal event with ca. 1.4 Ga age has not previously been recognized in the Ukrainian Shield and might provide important information bearing on paleogeographic reconstructions involving the Ukrainian Shield in the Mesoproterozoic.

CHROMITITES FROM VAVDOS OPHIOLITE - PGE MINERALOGY AND GEOCHEMISTRY (CHALKIDIKI, GREECE)

Sideridis Alkiviadis¹, Zaccarini Federica², Koutsovitis Petros¹, Grammatikopoulos Tassos³, Tsikouras Basilios⁴, Garuti Giorgio², Hatzipanagiotou Konstantinos¹, Karali Marina¹

¹Department of Geology, Section of Earth Materials, University of Patras, Greece, ²Department of Applied Geological Sciences and Geophysics, University of Leoben, Austria, ³SGS Canada Inc., Canada, ⁴Faculty of Science, Physical and Geological Sciences, Universiti Brunei Darussalam, Brunei Darussalam.

Chromitites from the Vavdos ophiolite are associated with dunite bodies, which are hosted within a highly depleted harzburgitic mantle section. These chromitites seem to have been formed in deep parts of the mantle, from interaction of boninitic parental melts with the harzburgite. The chemistry of the PGE and consequently PGM hosted within the chromitites, are characterized by high IPGE/PPGE ratios, a trait typical of most Tethyan ophiolites. PGE liberation in the parental melts of the chromitites was induced after high partial melting degrees in SSZ settings and more specifically within a fore-arc. All the presented PGM phases were encountered as inclusions in magnesiochromite hosted within texturally various chromitites, ranging from massive to disseminated. The PGM are euhedral to subhedral and are less than 7 µm in size. The most common phase identified was laurite, demonstrating an extensive solid solution series, attributed to the cooling of the magmatic system. The presence of Os-Ir alloys set the initial PGM-entrapment temperature at ~1200°C with low sulfur fugacity. The absence of secondary PGM and the low alteration degrees of the chromitites suggests that post-magmatic events did not significantly alter their primary mineralogical and chemical features.

MELTING RELATIONS OF Ca-Mg-CARBONATES IN THE EARTH'S UPPER MANTLE

Sieber Melanie J.¹, Wilke Franziska D.H.², Appelt Oona³, Oelze Marcus², Koch-Müller Monika³

¹GFZ German Research Centre for Geosciences, Germany, ²3.1, GFZ German Research Centre for Geosciences, Germany, ³3.6, GFZ German Research Centre for Geosciences, Germany

We here present experimentally derived, supra-solidus phase relations of Ca Mg carbonates up to 9 GPa and partition coefficients for Li, Na, K, Sr, Ba, Pb, Nb, Y, and rare earth elements (REEs) between carbonates (magnesite and Mg-calcite) and dolomitic melt. We performed quenched multi-anvil experiments at 6 and 9 GPa in a rotating multi-anvil press, overcoming quenching problems as observed in previous studies and promoting equilibrium between solid carbonates and carbonate liquid. The experiments were designed to (a) examine the phase relations of the nominally anhydrous CaCO₃-MgCO₃-system and to (b) establish partition coefficients for Li, Na, K, Sr, Ba, Pb, Nb, Y, and REEs between carbonates and dolomitic melt.

Establishing the melting relations of carbonates is essential to better understand their stability in the upper mantle playing a critical role in the Earth's long-term and deep carbon cycle. Further, the first melt produced by the melting of carbonate-bearing peridotites is (partially) controlled by the melting relations of carbonates. This makes knowledge of the melting relations of the pure carbonate system a first step to better understand and model melting of a carbonated mantle. In addition to affecting the melting relations, the presence of carbonates also promotes melting of peridotites at lower temperatures compared to CO₂-free peridotites. Thus, the onset of melting depends on the presence of carbonates and melting of carbonate-bearing peridotites may generate the parental magma of some carbonate-rich igneous rocks, such as kimberlites and carbonatites indicating a significant role for CO₂ during melting in the source region.

Moreover, carbonate melts are suggested to transport significant amounts of incompatible trace and minor elements and thus are considered to be highly effective metasomatic agents. Also, carbonate melts are of economic importance as sources of critical metals (e.g. Nb, REEs). As carbonates (partially) control the composition of the incipient melt of carbonated peridotite, the trace element signature of such a carbonate-rich melt might also be affected by the trace element distribution between carbonates and CO₂-rich melts. Therefore, we here establish the partition coefficients of minor and trace elements in the melting of Ca-Mg-carbonates.

GEOCHEMICAL ANALYZES OF THE SPEISS/MATTE FROM THE PRE-HISPANIC SITE OF CASTILLO DE HUARMEY (PERU)

Sierpień Paula¹, Warchulski Rafał², Kałaska Maciej³, Pisarek Marcin⁴, Kaproń Grzegorz³, Marciniak-Maliszewska Beata³, Jokubauskas Petras³, Kotowski Jakub³, Prządka-Giersz Patrycja⁵, Giersz Miłosz⁵

¹Institute of Geological Sciences, Polish Academy of Sciences, Poland, ²Faculty of Natural Sciences, University of Silesia, Poland, ³Faculty of Geology, University of Warsaw, Poland, ⁴Polish Academy of Sciences, Institute of Physical Chemistry, Poland, ⁵Faculty of Archaeology, University of Warsaw, Poland

Pre-Hispanic metallurgy of the Wari or Huari civilization (650-1050 AD), the largest empire in the Andes before the Incas, is relatively little-studied due to the small number of metal relics found in secured archaeological contexts. In 2018, a Polish-Peruvian team of archaeologists, directed by Miłosz Giersz of the University of Warsaw, Poland, discovered the Metallurgist's Burial at the Wari site of Castillo de Huarney, north-western Peru. The burial contained the preserved remains of a young male individual with a unique set of copper alloy objects and metallurgical byproducts. One of them, placed in the hand of Wari 'metallurgist', was a speiss/matte that macroscopically resembles metallurgical slag. The sample consists of an outer layer with weathering phases, and an inner part composed of non-oxidized phases and primary oxide phases and glass. To fully characterize the speiss/matte, a series of mineralogical and geochemical analyzes were performed, like XRD, XPS, FE-SEM-EDS, EMPA, and Raman spectroscopy. The XRD analysis showed the main crystalline phases: arsenic ion, arsenates of iron and copper, iron hydroxides and copper sulfides and copper and iron sulfides. The EMPA analysis made it possible to determine that the main phase that builds the non-oxidized part of the studied object are iron arsenides with an admixture of copper (Cu = 4.831 - 6.293 wt%). The iron content is in the range of 50.081 - 56.805 in wt%, while the arsenic content in the range of 37.312 - 42.824 in wt%. There is also an increased content of cobalt (0.435 - 0.993 wt%) and sulfur (0.134 - 0.460 wt%). As an additional mineral phase in the unoxidized part of the studied object, there are copper sulfides with an admixture of iron (the range of 3.187 - 30.324 in wt%) as well as copper (the range of 33.736 - 81.225 wt%) and sulfur in the range of 16.347 - 32.980 wt%. Using Raman spectroscopy, there were distinguished five different phases: Fe-As (not weathered part); Fe-As (from altered part); As-Fe-O; Cu-S; Cu-Fe-S. The XPS analysis produced additional supporting data results. Occurrence of residual glass was determined in between other phases within sample. Chemical composition of it is dominated by Fe, As, and O. On the basis of phase and chemical composition and textural dependencies of the analyzed sample, it is possible to approximate the ore composition, temperature, and oxidation-reduction conditions during the smelting process, as well as the order of crystallization of the material. The temperature results calculated on the basis of the chemical and phase composition of the studied sample indicate reaching temperatures above 1200°C. Described phase composition corresponds well to the factual Cu, Fe and As bearing minerals occurring in this region e.g. chalcopyrite (CuFeS₂), bornite (Cu₅FeS₄), chalcocite (Cu₂S), digenite (Cu₉S₅), tennantite ((Cu,Fe)₁₂As₄S₁₃), enargite (FeS₂), arsenopyrite (FeAsS). The discovery of speiss/matte smelting waste in one of the Metallurgist's Burial at the Castillo de Huarney archaeological site may indicate the existence of an arsenic copper smelting center in the Huarney Valley. Such an activity has never been confirmed before in this region. The results also lend evidence to the hypothesis that the individual interred in the burial may have been associated with metallurgical activities at or in connection with the Wari Empire provincial center at Castillo de Huarney.

"FORUM DER GEOWISSENSCHAFTEN" – A NEW EXHIBITION SITE IN CENTRAL MUNICH

Simon Gilla¹, Kölbl-Ebert Martina²

¹Forum der Geowissenschaften, Staatliche Naturwissenschaftliche Sammlungen Bayerns, Germany, ²Forum der Geowissenschaften, Ludwig-Maximilians-Universität München, Germany

A new campus is being built in central Munich that will also house an innovative exhibition on geosciences, the "Forum der Geowissenschaften". This exhibition site will be a joint venture being operated by the Department of Earth and Environmental Sciences at the Ludwig-Maximilians-Universität München (LMU) and the geoscientific collections of the Bavarian Natural History Collections (Staatliche Naturwissenschaftliche Sammlungen Bayerns - SNSB).

The teaching and research facilities are set up in three different locations so far. In the new building, these institutions will be merged and presented to a wide audience. The "Forum der Geowissenschaften" will be an open and innovative place for meeting and dialogue where the public will have a view behind the scenes of modern scientific procedures and research methods.

The offer of the forum ranges from a free accessible exhibition in the foyer of the building over special exhibitions in an adequate room, an informative website, lectures, events and workshops to excursions for groups which have a particular interest thereon. Last, but not least, the forum should contribute to raise public awareness especially for the geosciences, and make it possible to experience their important role in society.

Although the realisation of the "Forum der Geowissenschaften" is expected by the end of 2029 at the earliest, a team of scientists, curators and museum educators has recently started to plan the exhibition. Currently, a catalogue of topics for the forthcoming permanent exhibition is being prepared and potential visitors were involved in the planning process based on an online survey. A cooperation with exhibition designers is planned to start in 2022.

ARCHEAN MAGMATISM AND CRUSTAL GROWTH IN THE BUNDELKHAND CRATON, INDIA: INSIGHTS FROM ZIRCON U–Pb–Hf ISOTOPES AND GEOCHEMISTRY OF TTG GNEISSES AND GRANITOIDS

Singh Pradip K.¹, Verma Sanjeet K.², Singh Vinod K.³, Moreno Juan A.⁴, Oliveira Elson P., Li Xian-Hua⁶, Malviyag Vivek P.⁷, Prakash Divya¹

¹Geology, Banaras Hindu University (BHU), India, ²División de Geociencias Aplicadas, Instituto Potosino de Investigación Científica y tecnológica (IPICYT), San Luis Potosí, Mexico, ³Geology, Bundelkhand University, Jhansi, India, ⁴Departamento de Mineralogía y Petrología, Universidad Complutense (UCM), Madrid, Spain, ⁵Institute of Geosciences, University of Campinas (UNICAMP), Brazil, ⁶State Key Laboratory of Lithospheric Evolution, Institute of Geology and Geophysics, Chinese Academy of Sciences (IGG-CAS), Beijing, China, ⁷24E Mayur Residency Ext, Indra Nagar, Lucknow, India

The Bundelkhand Craton is one of the oldest cratonic nuclei of the Indian shield, comprising the Paleoproterozoic to Neoproterozoic crust that preserves the record of protracted crustal-mantle evolution and plays a crucial role in understanding the early Earth's history. The present study reports on the field, the petrographic, zircon U–Pb–Hf isotopes, bulk-rock Sm–Nd isotopes and the geochemistry of the tonalite-trondhjemite-granodiorite (TTG) gneiss, sanukitoid and anatectic granites from the Central Bundelkhand granite-greenstone terrane (CBGGT). This study reports the first evidence for two distinct episodes of Neoproterozoic TTG magmatism at ~ 2.71 and ~ 2.68 Ga in the Bundelkhand Craton, and a Paleoproterozoic ~3.34 Ga TTG pluton documented in the eastern part of the craton. In addition, Neoproterozoic 2.58–2.50 Ga synchronous magmatism of the sanukitoids and anatectic granites are also reported. This synchronous magmatism shows peak continental growth during in the craton. Geochemistry, In-situ $\epsilon\text{Hf}(t)$ and bulk-rock $\epsilon\text{Nd}(t)$ values suggest Proterozoic to Neoproterozoic crustal reworking in the Bundelkhand Craton. Neoproterozoic TTGs produced in arc creation/collision to the Paleoproterozoic nucleus of the Bundelkhand Craton. The fusion of various micro-blocks happened by the arc-continent collision and plausible breakoff of the descending slab between crustal blocks of the craton during Neoproterozoic. This incident caused anatectic granites by concentrated partial melting of the existing crust, which led to as a subduction closure and marked as final stabilization and cratonization of the Bundelkhand Craton.

THE EFFECT OF DEUTERATION AND DEHYDRATION ON THE VIBRATIONAL SPECTRUM OF EXPANDED HALLOYSITES

Siranidi Eirini¹, Chryssikos Georgios D.¹, Hillier Stephen^{2,3}

¹Theoretical and Physical Chemistry Institute, National Hellenic Research Foundation, Greece, ²The James Hutton Institute, United Kingdom, ³Department of Soil and Environment, SLU, Sweden

Halloysite is a polytype of kaolinite ($\text{Al}_4[\text{Si}_4\text{O}_{10}](\text{OH})_8$) formed most commonly with a hollow nanotubular structure and with many potential industrial or environmental applications. Opposite to the other members of the kaolin subgroup, natural halloysite is formed with a ~ 10 Å basal spacing owing to a monolayer of interlayer H_2O . Upon drying to ambient relative humidity, most of this interlayer H_2O is irreversibly lost and the basal spacing collapses to ~ 7 Å. Some residual H_2O in halloysite-(7 Å), sometimes termed "hole water", is observed at 3550 and 1650 cm^{-1} in the infrared spectra. A similar H_2O spectrum is reported for the nanoroll structures formed by the exfoliation of intercalated kaolinite.

Infrared studies of the various types of halloysite are usually performed on stable halloysite-(7 Å) samples. Due to experimental difficulties, the infrared spectra of halloysite-(10 Å) and their transition to those of the -(7 Å) structure upon drying were not reported. A detailed vibrational comparison of two cylindrical and two polygonal halloysites is presented. These samples were available and studied for the first time in their original 10Å form, saturated with either H_2O or D_2O , and as a function of in situ drying in the 70-2% RH (RD) range. Attenuated Total Reflectance (ATR) spectra were acquired in the mid infrared (4000 – 550 cm^{-1}) using a homemade environmental cell coupled with a controlled humidity N_2 gas generator. Supporting XRD and electron microscopy data are presented.

Unexpectedly, large portions of all expanded halloysites were reproducibly inaccessible to D_2O exchange. The residual material in H-form displayed only the spectrum of inner surface and inner structural OH groups and was insensitive to drying. It was therefore attributed to anhydrous interlayers, probably present as random interstratifications among their expanded counterparts. The exact signature of the OH modes (position, width, relative intensities, fine structure) was sample-dependent and correlated with the cylindrical or polygonal morphology of the samples. The remaining H/D accessible portions exhibited very similar spectra of D_2O and inner-surface structural OD which responded to drying. Inner structural OH groups were not accessible to H/D exchange. Based on these D_2O spectra, the contribution of the so called "hole water" was already detectable in well hydrated halloysite and its spectrum consists of two instead of one stretching mode at ~ 3620 cm^{-1} (masked by the sharp inner OH mode) and 3550 cm^{-1} .

Acknowledgements

Work at NHRF was supported by a) project "Advanced Materials and Devices" (MIS 5002409) of TPCI-NHRF, funded by the Operational Program "Competitiveness, Entrepreneurship and Innovation" and co-financed by Greece and the European Union, and b) the Applied Spectroscopy Lab at TPCI.

SPECTRAL X-RAY COMPUTED MICRO-TOMOGRAPHY: TOWARDS 3-DIMENSIONAL ORE CHARACTERIZATION

Sittner Jonathan¹, Guy Bradley M.², Godinho Jose R. A.¹, Renno Axel D.¹, Cnudde Veerle³, Merkulova Margarita³, Boone Marijn⁴, De Schryver Thomas⁴, Van Loo Denis⁴, Liipo Jussi⁵, Roine Antti⁵

¹Analytics, Helmholtz-Zentrum Dresden-Rossendorf, Helmholtz Institute Freiberg for Resource Technology, Germany, ²Department of Geology, University of Johannesburg, South Africa, ³Geology Department, Ghent University, Belgium, ⁴TESCAN XRE, Belgium, ⁵Metso Outotec, Finland

Most ore characterization studies are based on analytical tools that are limited to a 2-dimensional (2D) surface of a 3-dimensional (3D) sample. This not only limits the number of particles available for analysis but also results in a lack of 3D morphological information. Especially for the characterization of trace phases, 2D analysis is time consuming. X-ray computed micro-tomography (micro-CT) represents an established 3D technique that is used in numerous applications such as medicine, material science, biology, and geoscience. However, a major drawback of micro-CT in the characterization of ores is the absence of chemical information, which makes mineral classification challenging.

Therefore, we present Spectral X-ray computed micro-tomography (Sp-CT). It is an evolving technique in different research fields and is based on a semiconductor detector that provides chemical information of a sample (e.g., CdTe). This detector can be used with a conventional CT scanner (TESCAN CoreTOM in this study) to image a sample and detect its transmitted polychromatic X-ray spectrum. Based on the spectrum, elements in a sample can be identified by an increase in attenuation at specific absorption edge energies. Therefore, chemically different minerals can be distinguished inside a sample from a single CT scan in the micrometer range. The method is able to distinguish elements with absorption edges in the range from 25 to 160 keV, which applies to elements with $Z > 48$. We present the workflow of an ore characterization study using a combination of Sp-CT and high-resolution micro-CT with an example of Au-U ores from the Witwatersrand Supergroup. Different drill core samples from the Kalkoenkrans Reef at the Welkom Gold field were investigated. With the chemical information from the Sp-CT, minerals such as gold, U-phases, and galena can be identified based on their K-edge energies in the spectrum. Several Sp-CT scans were used to train a machine learning segmentation model in the software Dragonfly (version 2021.1) to segment the high-resolution CT data into multiple segments, e.g., gold, U-minerals, sulfide minerals and matrix minerals. The segmented data was then used to extract 3D mineral properties of the segments such as 3D volume or 3D surface area. This new non-destructive approach provides 3D information on distribution of chemically different minerals without any sample preparation. This information can potentially be used for mineral processing simulations but also for genetic mineralogical studies.

DESULFURIZATION OF LIQUID FUELS BY AG MODIFIED FLY ASH DERIVED NA-X ZEOLITE-CARBON COMPOSITE

Skalny Mateusz¹, Bajda Tomasz¹

¹Faculty of Geology, Geophysics and Environmental Protection, AGH University of Science and Technology, Poland

The world's demand for energy is increasing from year to year, and most of it is still covered by fossil fuel combustion, of which petroleum is the most significant one. Crude Oil as a source of petroleum is usually a mixture of hydrocarbons, but also a great amount of heteroatomic organic compounds is inherent. These are mainly sulfur species as thiols, sulfides, and thiophenes. During combustion S compounds are oxidized to harmful SO₂, may corrode refining infrastructure and act like poison for catalyst beds. The most commonly applied technology of fuel desulfurization is hydrodesulfurization (HDS) in which large amounts of H₂, high temperature and pressure is required for obtaining low sulfur fuel. Moreover there is a group of refractory sulfur compounds, which are unreactive to HDS, examples of these are aromatic thiophenes like benzothiophene or dibenzothiophene. That's why there is a need for novel and more efficient methods of sulfur removal, like adsorptive desulfurization. Due to their high porosity, large surface and active sides materials like zeolites, active carbons, metalorganic frameworks or metal oxides may be applied as sorbents for these sulfur compounds and make desulfurization mild conditions process.

In this study fly ash derived zeolite-carbon composite with Faujasite structure were modified with Ag⁺ ions by ion exchange method using AgNO₃ and tested for sorption efficiency of 3-methylthiophene(3MT), benzothiophene (BT) and dibenzothiophene (DBT). Experiments were conducted in static conditions and as matrix for sulfur compounds isoctane was chosen to simulate model fuel. To determine selectivity of sorbents, 1% of toluene was added to mixture. Concentration of thiophenes were measured by gas chromatography coupled with mass spectrometry (GC-MS), phase composition and surface morphology of materials were examined by X-ray diffraction (XRD), and scanning electron microscopy (SEM).

The diffraction patterns of pristine and Ag⁺ modified zeolite-carbon composite show mainly reflections characteristic for NaX zeolite and baseline elevation between 20-30 °2θ typical for amorphous phase, which in this case is carbon. Modified sample exhibit additional reflections connected to Ag species. SEM microphotographs indicate that zeolite crystallized on surface of carbonic matrix and allowed also to get sight of Ag species present on surface of zeolite and carbon. Different size and shape of Ag particles crystallized with no regular layout.

Sorption experiments of thiophene compounds indicate that materials modified with Ag⁺ exhibit higher sorption capacity than pristine zeolite-carbon composite. However in presence of toluene general sorption capacity of both materials decrease. Reason of better sorption properties is the fact, that Ag species present on surface of material are likely to form coordination bonds with lone pairs of electrons of sulfur atoms and π electrons present in aromatic rings.

MINERALOGICAL AND THERMOBAROMETRIC EVIDENCE OF HIGH-PRESSURE OROGENIC LOWER CRUST WITHIN THE THICKENED COLLISIONAL ROOTS (SOUTH MUYA BLOCK, EASTERN SIBERIA)

Skuzovatov Sergei¹, Ragozin Alexey², Sklyarov Eugene³, Iizuka Yoshiyuki⁴, Wang Kuo-Lung⁴

¹Vinogradov Institute of Geochemistry, Russian Academy of Sciences, Siberian Branch, Russian Federation, ²Sobolev Institute of Geology and Mineralogy, Russian Academy of Sciences, Siberian Branch, Russian Federation, ³Institute of Earth's Crust, Russian Academy of Sciences, Siberian Branch, Russian Federation, ⁴Institute of Earth Sciences, Academia Sinica, Taiwan

Within the northern part of the Central Asian Orogenic belt (CAOB), multiple occurrences of high-pressure metamorphic rocks (predominantly blueschist-bearing associations) have been documented, whose N-MORB or E-MORB affinity reflects cold oceanic subduction of the oceanic crust in tectonic settings similar to those of the modern western Pacific. To date, the only example of the subducted continental lithologies was distinguished and described in the Baikal-Muya Foldbelt (BMFB) (North Muya block), where eclogites are closely associated with felsic rocks and metasediments. The rocks with arc and continental affinities record variable P-T paths following both relatively cold (close to that of oceanic subduction) (560°C at 2.5-2.7 GPa) and hotter geotherms (up to 760°C at similar P), which indicate gradual subduction of the crust with different thicknesses. Along with eclogites, high-pressure garnet granulites are deep-seated components of many collisional belts and provide with the valuable evidence of the former convergence-related thickening within continental crust. Here we report the findings of high-pressure mafic (garnet-clinopyroxene) granulites in the South Muya block (SMB), which is interpreted as a fragment of a former Early Neoproterozoic sedimentary basin metamorphosed at deep crustal levels. Though earlier reported regional metamorphic P-T conditions correspond only to slightly elevated pressures (670-750°C at 1.0-1.2 GPa), mafic granulites exhibit clear evidences of higher-pressure origin, such abundant exsolution textures of plagioclase in clinopyroxene along with rarer amphibole + quartz exsolution lamellae in same pyroxene grains. Petrological modeling indicates possible initiation of garnet growth at least at ~740-760°C and 1.6-1.7 GPa and potentially higher peak temperatures (up to 790-800°C) indicated by Zr-rutile-temperatures of inclusions in garnets. Calculated ratios and overall contents of Al^{IV} and Al^{VI} in the rock-forming pyroxenes are typical of pyroxene from granulites. However, reintegration of the original pyroxene composition in exsolved clinopyroxene cores yields up to 30 mol. % of jadeitic mineral and >15 mol. % of chermakite, which strongly supports the origin of the former Al₂O₃-rich pyroxene beyond 15 kbar.

High-pressure, “dry” mafic (garnet-clinopyroxene) granulites originated from melts from the metasomatized subcontinental mantle, which intruded the crustal unit no older than ~740 Ma, have continental geochemical (slightly negative trace-element distribution patterns with Eu anomalies, HFSE and P minima) and isotopic εNd(t) signatures. Mafic granulites do not exhibit any records of the low-pressure subduction history (stressed by rutile inclusions in central parts of both garnet and pyroxene grains and the absence of hydrous phases in garnet porphyroblasts). Thus, the interpreted rock precursors are fractionated mafic melts, which crystallized and stored in the deep lithosphere of SMB (probably near Moho), and were then decompressed to shallower levels during final collision related to the same Late Neoproterozoic orogeny as mentioned above for eclogites, but a bit later on (616±11 Ma, LA-ICP-MS, zircon U-Pb). Strongly deformed nature of the host metasediments implies that the folding and regional compressional deformations might significantly assist the exhumation of HP-HT lower-crustal fragments.

PRESSURE-TEMPERATURE EVOLUTION OF AMPHIBOLITES IN THE STARÉ MĚSTO BELT IN THE SUDETES

Śliwiński Marek¹, Jastrzębski Mirosław¹

¹Institute of Geological Sciences, Polish Academy of Sciences, Poland, marek.sliwinski@twarda.pan.pl, mjast@twarda.pan.pl

The Staré Město Belt (SMB) is a narrow tectonic zone in the Central Sudetes mainly composed of metavolcanic and metasedimentary rocks that are thought to have experienced polyphase metamorphic evolution. We used thermodynamic modeling to reconstruct the metamorphic conditions in the SMB amphibolites for which only conventional thermobarometric methods have been applied thus far. As the SMB is also sometimes considered the Variscan suture zone in which deep-seated thrusts have developed, we also gave special attention to any variations in metamorphic gradients and P-T conditions for different types of amphibolites.

Based on microscopic observations, three types of metabasites were distinguished in the SMB: 1) amphibole schists, 2) banded amphibolites and 3) massive amphibolites. The main metamorphic fabric in all these rock types is defined by the preferential orientation of amphibole grains or alternating plagioclase-rich and amphibole-rich laminae. To determine the temperature and pressure paths of the three samples representative of the three types of amphibolites we used the Theriak-Domino software containing the database devoted for metabasite rocks.

In amphibole schists, the main metamorphic fabric consists of Amp-Pl-Cpx-Qz-Ilm-Ttn. Amphibole and plagioclase grains have a strong zonation. Amphibole cores are actinolite in composition, whereas rims are represented by Mg-hornblende. Plagioclase cores are oligoclase and andesine in composition (An₂₆₋₄₀) while plagioclase rims are mainly andesine and rarely labradorite in compositions (An₂₈₋₆₃). Thermodynamic modeling indicates that mineral assemblages compatible with the main metamorphic fabric are stable within the temperature range of 700–880 °C and pressures of 5–10.5 kbar. Trends of compositional isopleths of amphibole (Si and Mg contents) and plagioclase indicate progressive metamorphism conditions from ~500 °C and 2 kbar to 800 °C and ~8 kbar. Massive amphibolites contain Amp-Pl-Ilm-Ttn-Qz-Chl and Bt. In the sample selected for the microprobe study, amphibole grains revealed no chemical zonation and are represented by Mg-hornblende. Plagioclase grains are either oligoclase (An₂₅₋₃₀) or andesine (An₃₀₋₃₃) which do not reveal a significant zonation from core to rim. The peak mineral assemblage is stable in a wide range of P-T conditions of 500–700 °C and 3–9 kbar. Maximum temperature conditions were calculated using andesine and hornblende isopleths at c. 680 °C and c. 7 kbar. The main metamorphic fabric of banded amphibolites is defined by parallel alignment of Amp (Mg-hornblende and tschermakite) and Pl (An₄₁₋₅₆) with subordinate Qz and Ilm. This assemblage is stable within temperatures of 550–800 °C and pressures up to 8.5 kbar. Compositional isopleths indicate lower temperatures ranging from 520 to 650 °C and pressures from 2.5 to 4.5 kbar.

The results of this study indicate that the metavolcanic rocks in the SMB experienced progressive metamorphism from greenschist- to granulite-facies conditions. All types of amphibolites were metamorphosed along a high temperature – medium pressure metamorphic gradient.

The research was financed from the grant of the National Science Center, Poland No. 2018/29/B/ST10/01120.

CONTROLS ON REE ZONING IN GARNET AND IMPLICATIONS FOR CHRONOLOGY

Smit Matthijs¹, Guilmette Carl², Kielman-Schmitt Melanie³, Kooijman Ellen³, Ratschbacher Lothar⁴, Scherer Erik⁵, Mezger Klaus⁶

¹Earth, Ocean and Atmospheric Sciences, University of British Columbia, Canada, ²Département de Géologie et Génie Géologique, Laval University, Canada, ³Department of Geosciences, Swedish Museum of Natural History, Sweden, ⁴Institute of Geology, TU Bergakademie Freiberg, Germany, ⁵Institut für Mineralogie, Westfälische Wilhelms-Universität, Germany, ⁶Institut für Geologie, Universität Bern, Switzerland

Garnet chronometry provides a powerful means of placing in time the rich petrogenetic record of garnet in rocks ranging from metapelitic to ultramafic. Analytical innovation continues to push the limits, both in terms of sample size requirements in high-precision garnet chronometry, as well as in the precision of new laser-based Lu-Hf chronometry. These advances further necessitate a robust framework for age interpretation, also—or perhaps especially—for high-grade or poly-metamorphosed rocks.

A key issue in this regard is the interpretation of garnet REE zoning. Primary growth features are often difficult to discern from any effects of diffusive re-equilibration, and experimental and empirical observations are discrepant with regards to the possible effects of the latter on age systematics. To address this issue, we investigated the REE composition and zoning of garnet from various modern and ancient (ultra-)high temperature rocks, for which high-precision Lu-Hf ages were obtained previously.

Garnet grains were mapped for trace elements using an ArF excimer laser ablation system, coupled to a sector-field ICP-MS. A small-cell geometry and rectangular-spot ablation capabilities were used to optimize spatial resolution. Most grains show relatively well-developed, commonly step-wise concentric zoning, with large chemical gradients on the scale of micrometers. Oscillatory zoning, locally with a very short (10- μ m) wave length, was also observed. In all cases, REE zoning shows angular geometries that mimic the crystal faces. Cloudy and smooth zoning coexist with sharper features; the general interpretation of such zoning as reflecting diffusive re-equilibration is non-unique. The observations show that the (H)REE systematics of natural garnet are robust to thermal overprinting and support the hypothesis that diffusive transport of REE in natural garnet is limited by the sluggish diffusion kinetics of coupled trivalent cations. The thermal histories that the analyzed garnet grains underwent are extreme. The preservation of prograde features in these grains thus suggests that REE zoning in natural garnet is likely to largely reflect growth zoning, even when it is smooth and seemingly diffuse. The effects of REE volume diffusion on REE zoning and Lu-Hf age systematics of natural garnet thus may be limited, and Lu-Hf ages are likely to reflect growth and/or recrystallization.

BIO-MODIFIED FLY-ASH BASED SYNTHETIC ZEOLITES FOR VOCS REMOVAL

Sobczyk Maciej¹, Muir Barbara¹, Skalny Mateusz¹, Bajda Tomasz¹

¹Mineralogy, Petrography and Geochemistry, AGH University of Science and Technology, Poland

Worldwide industrialization along with rapidly growing urbanization, lead to the overuse of almost all environmental components and increasing presence of various pollutants in air, waters and soils. Water pollution, in particular, is of the greatest concern and further development of methods to effectively neutralize the whole array of chemical species is inevitable.

Sorbents may serve as a prospective path to neutralise water pollutants from which VOCs along with other groups of chemical agents are of an emerging concern.

In this study synthetic zeolites as analogs of natural faujasite (Na-X), Linde-type A (Na-A) and gismondite (Na-P1) were synthesized out of class-f fly-ash using hydrothermal method and applied for VOCs removal from waste waters. For surface functionalisation, betaine-type biosurfactant was used - cocamidopropylbetaine (CAPB), in amount of 1.0 external cation exchange capacity (ECEC) for all zeolites.

Sorption experiments of p-xylene indicate, that bio-modified zeolites produced from fly-ashes are more efficient in terms of their sorption capacity by 20% compared to their unmodified counterparts.

Presented approach of surface functionalization using biosurfactant molecules is in line with circular economy concept as no introduction of any problematic, synthetic chemicals appear. Moreover, research develops a new path to the lab-scale production of bio-mineral sorbents with great application potential in environmental engineering.

CLAY MINERALS FOR REMOVAL OF ORGANIC COMPOUNDS: SORBENTS FEATURES

Solińska Agnieszka¹, Bajda Tomasz¹

¹Department of Mineralogy, Petrography and Geochemistry, AGH University of Science and Technology, Poland

For decades clay minerals have been object of interest the scientific research. Due to their properties such as high surface area, porosity, high ion exchange capacity, hydrophilic properties clay minerals are also found application in industrial technology. They are also used in environmental applications as sorbents for removal contaminants from soils and water including organic compounds. The aim of this study was to characterize the mineralogical and physicochemical features of clay minerals based on halloysite from the Dunino deposit and bentonite from the Jelšovy Potok deposit in terms of sorption properties of clay minerals. The raw sorbents were studied by Fourier-transform infrared spectroscopy (FTIR), thermal analysis (DTA/TG) coupled with the measurement of evolved gases composition by mass spectrometer (QMS). The morphology of raw sorbents was analyzed by scanning electron microscopy (SEM). The cationic exchange capacity (CEC) was also evaluated. Moreover, several batch sorption experiments were performed with used organic compounds dyes and pharmaceuticals. The solids analyses combined with sorption results clearly show that halloysite and bentonite can be used as sorbents for removal organic compounds. The mineralogical and physicochemical features of clay minerals have distinct impact on their sorption behavior. Nevertheless, the improvement of sorption properties of halloysite and bentonite toward removal organic compounds can be simply achieved by mixed with other materials such as lignite and fly ash. It provides the opportunity on design multifunctional composite materials capable of simultaneous removal of different organic contaminations from water.

CRYSTALLOGRAPHIC ORIENTATION RELATIONSHIPS BETWEEN QUARTZ AND FELDSPAR IN MYRMEKITE: A CASE STUDY IN MONZODIORITE FROM MEICHUAN PLUTON, CHINA

Song Yueting¹, Zhao Shanrong¹, Xu Chang¹

¹School of Earth Sciences, China University of Geosciences Wuhan, China

Myrmekites occurring in monzodiorite from Meichuan pluton in the Dabie ultrahigh-pressure metamorphic belt were investigated. The microscopic petrographic evidence demonstrates a metasomatism origin for myrmekite formation in the scale of individual alkali feldspar grains, and that the myrmekitic quartz and plagioclase matrix are generated simultaneously replacing precursor feldspar. Energy-dispersive X-ray spectroscopy and electron microprobe analysis indicate a low anorthite content in the narrow rim of host plagioclase near the myrmekite–alkali-feldspar interface. The Ca²⁺, Na⁺ proportion of hydrothermal fluids replacing precursor alkali feldspar is 1:5.4, calculated by the anorthite content of inner part of the host plagioclase and the neighbouring alkali feldspar. Electron back-scattered diffraction was used to identify the crystallographic orientation of myrmekitic quartz, plagioclase matrix and the precursor alkali feldspar. The crystallographic orientation relationships (110)Kfs//((11-21)Qtz, (20-1)Kfs//((11-2-1)Qtz and [11-23]Qtz//[001]Kfs between myrmekitic quartz and adjacent alkali feldspar were obtained from statistical analysis. No clear crystallographic orientation relationship between quartz and plagioclase was found. The growth of myrmekitic quartz is constrained by the precursor alkali feldspar rather than the simultaneously crystallised plagioclase. This research is helpful for understanding the intergrowth mechanism during metasomatism.

SYNTHESIS AND CHARACTERIZATION OF REE- AND Th-RICH PYROMORPHITE $Pb_5(PO_4)_3Cl$

Sordyl Julia¹, Manecki Maciej¹

¹Faculty of Geology, Geophysics and Environmental Protection, AGH University of Science and Technology, Poland

The presence of rare-earth elements (REE) in calcium apatites has been known and studied for a long time. The occurrence of lead apatites containing REE has also been sporadically described, but these issues have received little attention so far. Therefore, in this study, the incorporation of REE and Th into pyromorphite structure upon precipitation from aqueous solution was analyzed. This allowed for mineralogical characterization of the effect of these substitutions on selected properties of the pyromorphite and evaluation of the extent of maximum REE and Th substitutions.

Synthetic analog of REE-rich pyromorphite was precipitated from aqueous solutions using $Pb(NO_3)_2$, $NaH_2PO_4 \cdot xH_2O$, NaCl and standard solution of a mixture of REE and Th in HNO_3 (VHG, USA). The synthesis was carried out at ambient conditions at pH = 3 (HNO_3 , NaOH). The initial concentration of each REE and Th equaled to 100 mg/L. The precipitate was characterized using scanning electron microscopy with energy dispersive spectroscopy (SEM-EDS), powder X-Ray diffraction (XRD), infrared absorption spectroscopy (FTIR), and Raman microspectroscopy. In addition, the concentration of the REE incorporated into the pyromorphite structure was determined by wet chemical analysis of the product (dissolved in 6M HNO_3) using inductively coupled plasma mass spectrometry (ICP-MS).

The synthesis resulted in a white powder of crystals 1 to 3 μm in size. They formed aggregates of elongated, slightly rounded rods resembling pyromorphite synthesized in the absence of REE. SEM imaging, semi-quantitative EDS analysis and XRD revealed the absence of components other than the intended synthesis product. Unit cell parameters, refined in hexagonal system, were: $a = 9.9996 \text{ \AA}$, $c = 7.3192 \text{ \AA}$, $V = 633.82 \text{ \AA}^3$ which are identical to pure pyromorphite. Wet analysis indicated that the precipitate contained 10 wt.% of all REE and Th combined. Most of the REE were incorporated at the same level (showing little fractionation of light or heavy REE) except for Sc and Th, which were preferentially scavenged from the solution: their content in the pyromorphite was two times higher than that of the other REE.

Pyromorphite may contain more REE and Th than other apatites due to its larger unit cell. This is probably also the reason for a weaker fractionation. Precipitation of pyromorphite from aqueous solution at the presence of REE and Th significantly lowers their concentration in the remaining solution. Due to this very high removal efficiency, pyromorphite can act as a filter for REE and Th.

This research was funded by NCN research grant no. 2019/33/B/ST10/03379

TWO-STAGE DEVELOPMENT OF CORUNDUM-BLUE SAPPHIRE SYENITE PEGMATITES FROM ILMEN MOUNTAINS, SOUTH URALS

Sorokina Elena¹, Botcharnikov Roman¹, Kostitsyn Yuriy², Rösel Delia³, Häger Tobias¹, Rassomakhin Mikhail⁴, Kononkova Natalia², Somsikova Alina², Berndt Jasper⁵, Ludwig Thomas⁶, Medvedeva Elena⁷, Hofmeister Wolfgang¹

¹Institute of Geosciences, Johannes Gutenberg University Mainz, Germany, ²Vernadsky Institute of Geochemistry and Analytical Chemistry RAS, Russian Federation, ³University of Gothenburg, Sweden, ⁴Institute of Mineralogy SU FRC MiG UB RAS, Russian Federation, ⁵Westfälische Wilhelms-Universität Münster, Germany, ⁶Universität Heidelberg, Germany, ⁷Ilmen State Reserve SU FRC MiG UB RAS, Russian Federation

Natural aluminum oxide (α -Al₂O₃), the mineral corundum, is a component of some metamorphosed and igneous rocks and appears in secondary placers as detrital crystal fragments. Rare gem-quality corundum varieties – ruby and sapphire occur only in a few primary rock types (Giuliani et al., 2014; Hughes, 2017). This reflects the scarcity of geological environments and necessary conditions for their formation.

The sapphire mineralization in syenite pegmatites of the Ilmenogorsky complex (Russia) is notable for the presence of unusually large and commonly zoned gem-quality megacrysts. They reach up to 10 cm in length and exhibit brownish cores and blue rims. Despite their discovery in the last century, the genesis of sapphires and the geochemical relationships to the deposit remain enigmatic. Furthermore, the mineralization process, its link to the parental rocks and geodynamic environment are poorly constrained and understood.

Here we demonstrate that:

1. Corundum syenite pegmatites of Ilmenogorsky complex trace its multistage development in the processes of continental collision and post-collision stretching of the Uralian orogeny. The initial formation stage was constrained by in situ LA-ICP-MS U-Pb zircon dating of corundum syenite pegmatites that yields ages at about 275 – 295 Ma for “298” and “349” mines (Sorokina et al. 2021). These ages are associated with a broader process of the continental collision and formation of the Uralian orogeny in Ilmenogorsky complex. The next stage was yielded by Rb-Sr isotopic systematics in corundum syenite pegmatites from “298” mine demonstrating two parallel isochrones with ages at 249 ± 2 Ma and 254±22 Ma (Sorokina et al. 2021). This stage was linked to the limited post-collision stretching during the Uralian orogeny in the area of Ilmenogorsky complex.

2. The pegmatites from mines “299” and “349” were linked to nepheline syenites-miaskite that possessed the mantle isotopic signatures (Rb-Sr isotopic signature). The fluid source for “298” mine pegmatites (with zonal corundum megacrysts) is associated with crustal amphibole- and biotite-bearing syenite host rocks (267±3 Ma). However, corundum megacrysts from this mine revealed mantle isotopic signatures ($\delta^{18}\text{O}$ +3.4 to +4.4‰) as those at mines “299” and “349”, which were formed during the collision time of the Uralian orogeny (275 – 295 Ma). Hence, during the continental-stretching time, “original” (non-altered) pegmatites from “298” mine expressed metamorphic overprint (ca. 250 Ma), which reset the Rb-Sr isotopic system within those pegmatites (Sorokina et al. 2021).

References:

1. Giuliani G. et al (2014). The geology and genesis of gem corundum deposits. In: Groat, L.A. (Ed), *Geology of Gem Deposits*, 2nd ed. Mineralogical Association of Canada, Tucson, pp. 29–112.
2. Hughes R.W. (2017). *Ruby & sapphire: a gemologist's guide*. RWH Publishing/Lotus Publishing, 816 p.
3. Sorokina E.S. et al. (2021). Sapphire-bearing magmatic rocks trace the boundary between paleo-continent: a case study of Ilmenogorsky alkaline complex, Uralian collision zone of Russia. *Gondwana research*, 92, 239 - 252.

USING OXYGEN ISOTOPIC COMPOSITION AS A PROXY IN SEPARATION NATURAL VS. SYNTHETIC CORUNDUM MATERIAL

Sorokina Elena¹, Häger Tobias¹, Ludwig Thomas², Botcharnikov Roman¹

¹Institute of Geosciences, Johannes Gutenberg University Mainz, Germany, ²Universität Heidelberg, Germany

Corundum varieties – rubies and sapphires are second after diamond most valued gemstones from commercial point of view with annual worldwide production exceeding several billion dollars (Graham 2008). Their high demand is linked to the rarity of large-scale deposits available for exploitation. Thus, only about 15 occurrences worldwide produce ruby and sapphire suitable for cutting or even for caboshoning (Hughes 2017). The rarity of ruby and sapphire deposits initiated a development of several methods allowing for the synthesis and treatment of corundum crystals. Nowadays the quality of synthetic materials is so close to that of natural minerals that the separation of synthetic counterparts is often quite challenging.

Secondary ion mass-spectrometry (SIMS) analysis is a micro-destructive method using spot size down to about 5µm on the sample. However, it requires complex sample preparation procedure, which is difficult to apply for the treated jewellery materials. Therefore, once applied to corundum, SIMS was used only in measuring the oxygen isotopic composition ($\delta^{18}\text{O}$) of naturally-occurring ruby and sapphire raw materials formed in different geological environments (Giuliani et al. etc.). Here we present a first attempt to use $\delta^{18}\text{O}$ isotopic composition as a proxy allowing us to distinguish between synthetic and natural corundum materials.

We studied 5 Be-diffused and 16 synthetic gem corundum samples grown by flame-fusion and hydrothermal methods. Be-diffused sapphires showed both positive and negative oxygen isotopic composition: 2 samples yielded the values from $+10.12 \pm 0.1\%$ to $+10.53 \pm 0.1\%$ $\delta^{18}\text{O}$, while, in 3 samples, detected values varied from $-2.08 \pm 0.10\%$ to $-3.55 \pm 0.15\%$ $\delta^{18}\text{O}$. On the other hand, analyses of all studied synthetic stones have shown negative oxygen isotopic composition varying from $-2.08 \pm 0.1\%$ to $-17.05 \pm 0.09\%$ $\delta^{18}\text{O}$. These values are not typical for natural analogs, where $\delta^{18}\text{O}$ varies from ca.+1 to +15 ‰. Only one of the known ruby deposits in Karelian Russia demonstrates the exotic negative oxygen isotopic composition with ca. -29% $\delta^{18}\text{O}$ due to the interaction with meteoric waters. This value is, however, lower than those detected in synthetic stones. Therefore, obtained results indicate that, SIMS oxygen isotopic analysis is a promising method in separation natural from synthetic corundum material.

References:

1. Giuliani G. et al. (2005) Oxygen isotope composition as a tracer for the origins of rubies and sapphires. *Geology* 33, 249–252.
2. Graham I. et al. (2008) Advances in our understanding of the gem corundum deposits of the West Pacific continental margins intraplate basaltic fields. *Ore Geology Reviews* 34, 200–215
3. Hughes R.W. (2017) *Ruby & sapphire: a gemologist's guide*. RWH Publishing/Lotus Publishing, 816 p.

IRONING OUT ISOTOPIC DIFFERENCES AMONG ROCKY BODIES

Sossi Paolo¹, Shahar Anat²

¹Institute of Geochemistry and Petrology, ETH Zurich, Switzerland, ²Carnegie Institution for Science, United States

The stable isotopes of heavy elements in igneous rocks from the Earth and other rocky bodies are a window into the events that lead to their assembly in the inner solar system. Iron is isotopically variable among rocky bodies, attesting to differences in the mechanisms of their formation among one another and in their potential building blocks. The magnitude of the isotopic variation in mantle-derived rocks within a given body is similar to that observed between different planetary bodies. On a planetary scale, the primary mechanisms producing such differences are i) evaporation/condensation, ii) core formation and iii) melting/crystallization. Isotopic signatures arising from these events may be progressively diluted, modified and re-distributed over time according to global recycling processes, such as plate tectonics. Here we assess the relative influence of each of these mechanisms on the iron isotope compositions of igneous rocks, and their implications for the structure and accretion of rocky planets.

QUALITATIVE ANALYSIS AND MONTE CARLO MODELING OF THE ORE-FORMING FLUIDS FROM THE ATTICO-CYCLADIC METALLOGENIC MASSIF, GREECE

Spiliopoulou Aikaterini¹, Kokkalas Sotirios¹, Triantafyllidis Stavros², Tombros Stylianos³, Fitros Michalis⁴, Simos Xenofon¹

¹Geology, University of Patras, Greece, ²School of Mining and Metallurgical Engineering, National Technical University of Athens, Greece, ³Material Sciences, University of Patras, Greece, ⁴Hellenic Survey of Geology and Mineral Exploration, Greece

In the Attico-Cycladic Metallogenic Massif (ACMM) numerous mineralizations of various types are hosted in the marbles and schists of the Cycladic Blueschist unit, genetically related to I- and S-type Miocene granitoids. A total of 10483 fluid inclusion data (e.g., microthermometry, salinity and pressure), gas/liquid chemistry and physicochemical parameters of the ore fluids, ages and orientations of tectonic discontinuities were collected. The dataset includes ore deposits from the central (islands of Syros, Tinos, Mykonos, Antiparos, Naxos), northern (Kallianos Evia, Lavrion, Sifnos) and western part of ACMM (Serifos and Milos) from published data. Data statistics were made using the IBM SPSS Statistics v.26 (2019).

Descriptive statistics suggest that the ACMM deposits are classified as epithermal (~36% of the population) and carbonate-replacement type (~29%), manifest a NW-to-NNW trending structural control (~69%) and ~52% were dated at mean ages of 8.6 Ma (st.d=2.7 Ma). They precipitated from low temperature (~43%), salinity (~42%) and pressure (~76%), H₂O-, and CO₂-rich (~90%), Na-, K-, Mg-, Ca- and chlorine-poor, oxidized to reduced, almost neutral ore-forming fluids. The Pearson's chi-square test (using Monte Carlo accuracy) suggests strong dependence between tectonism and location, age and type of deposits (used as independent variables, $\chi^2=351-1521$, $\Lambda=0.4-0.6$, $\eta^2=0.8$ to 0.9 , $p=0.000$), whereas salinity, temperature, pressure, CO₂, Mg and chlorine contents contribute to a lesser extent. Moreover, strong-to-medium positive correlations are shown for pH and fS₂ and chlorine and CO₂ ($r \geq +0.7$), and negative between fS₂ and fO₂ and temperature and salinity ($r \geq -0.7$).

Varimax rotated factor analysis suggests that three factors account for ~79% of the total variance during ore formation. The first factor (~42%) indicates strong positive interrelations between fS₂, fO₂ and pH ($I \geq 0.8$) depicting the expected physicochemical parameters during ore formation, and negative among temperature and salinity (≥ -0.8) suggesting dilution and mixing as the prominent mechanisms of ore deposition. The second factor (~27%) implies a strong positive link between location and tectonism (≥ 0.9) and negative with age (~-1.0) correlating local geology with the spatial evolution of each deposit. The third factor is associated to pressure (0.8) implying pressure-drop during ore formation. The Monte Carlo method simulates the optimal conditions of ore formation. The results suggest that the predicted pressure and chlorine contents are almost identical with the ones observed. Temperature is predicted to be higher by ~30°C whereas salinity and CO₂ to be lower (~3 wt. % equiv. NaCl, ~2.5 moles %). F-test suggests that for the ore deposits adjoining the North Cycladic Detachment System the main control factors were temperature and salinity, whereas the ones adjacent to the Western Cycladic Detachment System are pressure controlled. The ACMM ore deposits are anticipated to form under hydrostatic pressures along the NW fault trend and major detachments, which are linked to the establishment of an extensional regime mainly active during late Miocene. Structural control was the major factor in shifting the physicochemical conditions and sources of the ACMM ore fluids, thus effectively modifying their flow and reactivity. The latter can be very helpful in future targeting for the ACMM ore deposits.

ENTRAPMENT CONDITIONS OF SUBDUCTION FLUIDS FROM THE CABO ORTEGAL COMPLEX – IMPLICATIONS USING ELASTIC THERMOBAROMETRY

Spránitz Tamás¹, Szabó Csaba¹, Berkesi Márta¹

¹Lithosphere Fluid Research Lab, Department of Petrology and Geochemistry, Eötvös University, Budapest, Hungary

Primary multiphase fluid inclusions (MPI) trapped in garnets from high-pressure metamorphic rocks, such as the Cabo Ortegal Complex (COC, NW-Spain), yield direct information on the chemistry of subduction-zone fluids. These MPI were studied in detail from eclogites and granulites (intermediate and ultramafic) using Raman imaging, SEM-EDS and FIB-SEM analyses combined with thermodynamic modeling. The studied MPI occur in 3D clusters or along a growth-zone in garnet together with quartz and rutile in each rock type, whereas besides them, zircon inclusions are also present in this zone in ultramafic granulites. They are mainly composed of intergrowth of carbonates and sheet silicates, together with a residual fluid phase of $N_2 \pm CH_4 \pm CO_2$, furthermore MPI are interpreted to have trapped a homogeneous COHN fluid, which have interacted with the host garnet after entrapment via carbonation and hydration reactions. Therefore, besides detailed study on fluid chemistry, another key issue is to determine their P-T trapping conditions during subduction-zone metamorphism. Our recent study, applying elastic thermobarometry aims to obtain the entrapment pressure (P) and temperature (T) of the quartz and zircon inclusions in garnet coexisting with the studied primary fluid inclusions in ultramafic granulite. Our preliminary results show that entrapment of quartz and zircon inclusions occurred possibly during prograde-to peak stage is, which is supported by our previous observations, that coexisting primary MPI have been trapped during garnet-growth along prograde metamorphism.

Quartz and zircon inclusions have been selected in garnet with respect to approach the most ideal geometrical conditions (spherical small inclusions with 2.5-8.4 μm radius and isolated from other inclusions, cracks and sample surface). We carried out Raman spectroscopic measurements in order to calculate residual strain from Raman shifts of the inclusions compared to a free quartz and zircon crystal for reference. Our test measurements show that residual pressure has been preserved in both quartz and zircon inclusions. Our first results of calculations using stRAInMAN and EntraPT software imply that quartz and zircon inclusions should have been entrapped at high pressure conditions along prograde-to peak stage, i.e. between around 1.5-2.2 GPa and 650-900 °C, shown by intersection of their isomekes, calculated with garnet of pure almandine endmember composition. Although, garnet compositions are in the range of $Alm_{38-55}Grs_{17-32}Prp_{15-34}And_{2-13}Sps_{1-4}$ in the studied granulite and almandine-pyrope ratio in the host garnet show a significant influence on entrapment temperature and to some extent on entrapment pressure of zircon inclusions. Calculating with pure pyrope endmember composition, a decrease was observed in entrapment T and P with up to ca. 200 °C and 0.2-0.3 GPa, respectively. Considering these effects on residual inclusion pressure, slightly lower entrapment PT conditions can be estimated than calculated with pure almandine endmember chemistry, which corresponds with HP peak conditions (up to 800 °C and 1.5-1.7 GPa) recorded on these granulites of the COC. This study provides a better understanding of the trapping conditions of subduction fluids, and giving a contribution to the knowledge on PT evolution of the investigated metamorphic complex in a subduction environment.

NITROGEN ENRICHMENT DURING EXHUMATION IN SUBDUCTION ZONES: CONSTRAINTS FROM MULTIPHASE INCLUSIONS IN HP METAMORPHIC ROCKS OF THE CABO ORTEGAL COMPLEX (SPAIN)

Spránitz Tamás¹, Padrón-Navarta José Alberto², Szabó Csaba¹, Berkesi Márta¹

¹Lithosphere Fluid Research Lab, Department of Petrology and Geochemistry, Eötvös University, Budapest, Hungary, ²Instituto Andaluz de Ciencias de la Tierra (IACT) (CSIC-Universidad de Granada), Av. Palmeras 4, 18100 Armilla, Granada, Spain; Géosciences Montpellier, Université de Montpellier & CNRS, F-34095 Montpellier cedex 5, France, France

Metamorphic rocks of exhumed high-pressure (HP) terranes, such as the Cabo Ortegal Complex (COC, NW-Spain), preserve direct evidence of fluid-rock interactions during subduction zone processes. Primary fluid inclusions trapped in subducted and exhumed HP metamorphic rocks provide constraints on composition and evolution of fluid regime of subduction-zone environment.

This study presents detailed data on primary multiphase inclusions (MPI) in garnet from eclogites and granulites from the COC. These inclusions are hosted by garnet porphyroblasts and occur in 3D clusters or along a growth zone together with quartz, rutile ± zircon inclusions. MPI have irregular to negative crystal shape and 1-40 µm size. We carried out Raman imaging, SEM-EDS, and FIB-SEM analyses, which confirmed that MPI have a uniform phase assemblage and fairly constant volume proportions dominated by a tight intergrowth of Fe-Mg-Ca-carbonates and phyllosilicates (pyrophyllite, chlorite, and margarite) together with N₂-CH₄-CO₂ fluid among the minerals. Thermodynamic modeling in the CaFMAS-COHN system confirmed that the bulk composition of the MPI in eclogites is highly similar to the host garnet+COHN composition, supporting the step-daughter origin of the minerals listed in the MPI. Most of the MPI should have experienced a partial loss of some H₂O after entrapment by diffusion and/or cracks. This COHN fluid could have interacted with garnet by means of carbonation and hydration reactions leading to the consumption of H₂O and CO₂ in the fluid phase. As a result, residual fluid became highly enriched in N₂, that is, to our best knowledge has not been reported in such detail. The nitrogen content of the originally trapped COHN fluid in eclogites was estimated to have a maximum value of 0.31 mol%, although the observed MPI contain 13-68 mol% in their residual fluid. Pseudosection modeling revealed the production of the observed assemblage in the MPI in a specific low P-T stability field (between 300-400°C, at pressures lower than 1.2 GPa). Our model and the FIB-SEM exposure of the MPI suggest that the formation of the step-daughter minerals is expected to have taken place at the same time due to metastable behavior at elevated pressure and temperature.

This process suggests that in the shallow exhumation zone there might be a horizon of a fluid regime with significantly elevated nitrogen content. This finding indicates that such a process in the exhuming HP units may play an important role in global nitrogen cycling as well as may contribute to nitrogen supply to the subsurface-surface environment during devolatilization in the forearc regions of convergent plate margins.

This research was supported by the NRDIO_FK research fund nr. 132418.

RAMAN INVESTIGATION OF DEFERNITE

Środek Dorota¹, Dulski Mateusz², Galuskin Evgeny¹, Galuskina Irina¹

¹Faculty of Natural Sciences, University of Silesia, Poland, ²Institute of Material Science, University of Silesia, Poland

Defernite, with simplified formula $\text{Ca}_6[(\text{CO}_3)_{2-x}(\text{Si}_2\text{O}_7)_{x/2}](\text{OH})_7[\text{Cl}_{1-x}(\text{H}_2\text{O})_x]$ where $x \approx 0.4$, was found in an altered part of the big carbonate-silicate xenolith within ignimbrite of the Upper Chegem Caldera, Northern Caucasus, Russia. It is the third known location of this mineral. To date, defernite was described only from the Ikizdere area (Turkey) and Kombat mine (Namibia). It forms colorless and white aggregates (up to 150 μm) composed of needle-like crystals. The chemical composition of defernite from the Upper Chegem Caldera and its Raman spectrum confirm the identification of this mineral.

Raman spectra of defernite from different localities were similar. The main bands have corresponded to vibrations of CO_3 groups: 200-212 cm^{-1} ν_2 , 709-717 cm^{-1} ν_4 , 1087-1085 cm^{-1} ν_1 , and 1447- 1560 cm^{-1} ν_3 , and to stretching vibrations of hydroxyl groups in the 3000 - 38000 cm^{-1} region. Also, we conducted the temperature Raman experiments and also measurements using polarization filters. It shows that the character of bands in the 3200 - 3800 cm^{-1} region depends on the orientation of defernite crystal. The spectrum obtained at room temperature on natural (010) cleavage surface of defernite crystal perpendicular to the laser beam [$y(x,x/z)y$] shows a wide band centered at about 3590 cm^{-1} . Crystal rotation about 90° leads to a reduction of intensity of most bands in the spectrum [$y(z,x/z)y$] to one-quarter and an appearance of the broad additional band near 3390 cm^{-1} .

Accordingly to the structural data of defernite, it is assumed that Raman bands at 3590 cm^{-1} are related to vibrations in OH groups with weak hydrogen bonds in channel. The weak broad band about 3390 cm^{-1} in $y(z,x/z)y$ spectra respond to vibrations of H_2O molecules lying at the plane parallel to the channel axis (= z axis). The strong band near 3590 cm^{-1} in the $y(x,x/z)y$ spectrum does not polarize in full at rotation on 90. This fact can point out that directions of O-H bonds in OH groups deflect from the (001) plane, whereas in the structural study of defernite a structural model was accepted, in which all O-H bonds are in the (001) plane.

The temperature experiment shows that water partially substituting for Cl in the channels of defernite structure is unstable above 473 K.

FLUID-INDUCED ALTERATION OF CHEVKINITE-(Ce) AND STRUCTURAL ORIENTATION RELATIONS AT THE PHASE BOUNDARY

Stachowicz Marcin¹, Jokubauskas Petras¹, Harlov Daniel E.², Bagiński Bogusław¹, Matyszcak Witold¹, Kotowski Jakub¹, Macdonald Ray¹

¹Institute of Geochemistry, Mineralogy and Petrology, University of Warsaw, Poland, ²Section 3.6, GeoForschungsZentrum, Germany

During hydrothermal alteration, the REE-bearing minerals of the chevkinite group (CGM) have the potential to release not only REE but also high field-strength elements and the actinides, into the fluid, such they can act as both a storehouse as well as a source of these elements in fluid-altered systems. A commonly observed alteration sequence in natural rocks is chevkinite → titanite plus a REE phase, such as allanite and bastnäsite. To provide quantitative information on such reactions, we have experimentally subjected a natural chevkinite-(Ce) from the Diamer District, Pakistan to fluid-induced alteration involving a Ca(OH)₂-bearing hydrous fluid. The experimental conditions were: temperature 600°C; pressure 400 MPa; duration 21 days. Natural albite and quartz were added to the charge to simulate natural rock-forming conditions more closely.

Significant reaction between the chevkinite-(Ce) and fluid occurred, with the formation of titanite and britholite-(Ce), plus minor hedenbergite. The nature of the reaction zones was very variable. Commonly, the rims of chevkinite-(Ce) were replaced by thin zones comprised first of britholite-(Ce) followed by titanite.

Electron backscatter diffraction (EBSD) within SEM allowed us to observe the crystal structure orientation of individual crystallites, and to distinguish their boundaries within one phase or on interphase border. Mutual orientations on the interfaces between chevkinite-(Ce) and britholite-(Ce), wollastonite and pyroxene; britholite-(Ce) and titanite, wollastonite and plagioclase were determined.

EBSD imaging also confirmed the presence of a rare fluoride, Na(Ca,Ce)(Ce,Ca)F₆. Its counterpart in nature is gagarinite-(Ce), a mineral known from only one locality, the Strange Lake pluton, Canada, where it occurs in a hypersolvus granite, and has never been recorded in association with CGM. Gagarinite-(Ce) was structurally identified using EBSD in order to confirm the WDS quantitative element composition. Sodium devolatilization was found to occur over time during WDS analysis. This caused an artificial increase in the apparent concentrations of the other elements in the gagarinite-(Ce), which resulted in an imbalance in the chemical formula. An alternative approach with multiple EDS measurements was established to correctly determine the gagarinite-(Ce) composition. It consisted of a reduction in the spot exposure to the electron beam by ca. 150 nA·s, and simultaneous analysis of all elements, which gave better counting statistics per element without damaging the sample.

We gratefully acknowledge funding by NCN Harmonia no. 2017/26/M/ST10/00407.

EXPERIMENTAL INVESTIGATION OF THE KINETICS OF BRIDGMANITE POLYMORPHIC BACK-TRANSFORMATION WITH IMPLICATIONS FOR THE ASCENT RATE OF SUPERDEEP DIAMONDS

Stagno Vincenzo¹, Angellotti Antonio¹, Fei Yingwei², Higo Yuji³, Nestola Fabrizio⁴, Wang Yanbin⁵

¹Earth Sciences, Sapienza University of Rome, Italy, ²Earth and Planets Laboratory, Carnegie Institution for Science Washington, United States, ³SPring-8, Japan Synchrotron Radiation Research Institute, Japan, ⁴Geosciences, University of Padua, Italy, ⁵Center for Advanced Radiation Sources, The University of Chicago, United States

Bridgmanite (bgm), the high-pressure polymorph of orthopyroxene (opx) is the dominant mineral of the deep Earth's lower mantle. However, its direct observation is limited to few and uncertain findings of trapped enstatite and SiO₂-rich glasses characterized by low nickel contents in sublithospheric diamonds. The lack of observations of bridgmanite in nature can be either due to the limited number of observations of sublithospheric diamonds (about 6% of the total investigated diamonds), or kinetic reactions that would preclude the stability of this high-pressure mineral during the ascent of diamonds to the Earth's surface. A detailed investigation of the possible amorphization/back-transformation of bridgmanite as function of pressure and temperature is, therefore, necessary to understand the possible mechanisms of structural destabilization. Importantly, the knowledge of the time associated to the bridgmanite-to-enstatite back transformation can be used to model the average ascent rate of diamonds by kimberlitic magmas throughout the Earth's interior. We present preliminary results that are aimed to improve our current knowledge regarding the metastability and the rate of transformation of MgSiO₃ perovskite at pressure and temperature of the Earth's upper mantle.

Polycrystalline bridgmanite samples were, first, synthesized from MgSiO₃ glass at 26 GPa and 2000 kelvin using the multi-anvil. The recovered bridgmanite was checked by both X-ray diffraction (XRD) and scanning electron microscopy (SEM). Then, small cylinders of synthetic bridgmanite were placed in graphite capsules, compressed to the target pressures of 3-10 GPa at room temperature using WC anvils and, then, heated up at 900-1400 °C. These experiments were performed both at the 13ID-D beamline of GSECARS sector (Advanced Photon Source, Argonne) using a 1000-ton press and a T-25 multi-anvil module, and at BL04B1 beamline (SPring-8, Hyogo) with SPEED-1500 multi-anvil press. A mixture of Au and MgO was placed at the top of the sample to serve as pressure markers. Synchrotron X-ray diffraction data were collected in situ every 60 to 300 seconds at constant temperature and pressure at the aim to monitor any polymorphic transformation. Phase identification and textural observations of the run products were, then, investigated by Raman and Scanning Electron Microscopy, respectively. Our preliminary results are discussed in light of previous studies performed at ambient P and allow to calculate the activation energy of back-transformation. Finally, we present a preliminary model of ascent rate of sublithospheric diamonds.

XENOLITHS IN THE DARLING BATHOLITH, WESTERN CAPE, SOUTH AFRICA, DISCLOSE THE DEEP (30KM) CRUSTAL STRUCTURE AND ANATEXIS OF THE MALMESBURY ACCRETIONARY PRISM.

Stevens Gary¹, Kisters Alex¹, Cilliers Kirstin¹

¹Earth Science, Stellenbosch University, South Africa

The fate of fore-arc sediments is either to be subducted and recycled into the mantle, or to be thickened and ultimately caught up in continental collision. The closure of the southern Adamastor ocean resulted in the Neoproterozoic to Cambrian Saldanian orogeny (560-520 Ma) along the western margin of the Kalahari Craton. Crustal convergence produced an accretionary prism of metasedimentary rocks, the top of which is preserved as the lower greenschist-facies Malmesbury Group, recording deposition and deformation continuing until at least ~560 Ma. The predominantly S-type Darling granite batholith intruded the low-grade Malmesbury Group at ~540 Ma and is exposed over ~ 600km² as a NW-SE trending elongate body bounded on its northern edge by the crustal-scale Colenso strike-slip fault. Magmatic fabrics are co-axially overprinted by narrower domains of high- and low temperature solid-state fabrics that testify to the syntectonic emplacement of granite phases related to the Darling batholith along the Colenso Fault. Metapelitic, metapsammitic and rare metamafic xenoliths contain pervasive transposition fabrics. In places, the xenoliths form clusters in low-strain domains of the Darling batholith that may suggest their concentration around the magma conduits that fed the batholith. Peak metamorphic assemblages in the xenoliths are syntectonic and record a wide range of metamorphic conditions, from partial melting and melt loss under granulite facies conditions at approximately 10kbar, to a range of amphibolite facies conditions under approximately mid-crustal pressures (4.5 to 6.5kbar). Additionally, xenoliths sourced from the low-grade country rocks are common and record a low-pressure thermal overprint. Detrital zircon U:Pb ages demonstrate that all varieties of metasedimentary xenoliths represent Malmesbury Group rocks. The granulite-facies xenoliths reflect the source conditions for the higher temperature magmas that produced the batholith. The mid-crustal xenoliths contain some compositions that have not undergone anatexis, whilst other strongly peraluminous examples are free of quartz and almost free of plagioclase and are characterized by the assemblage: Grt + Crd + Sp + Sil + Bt + Pl(minor), with common corundum inclusions in spinel. At low water activities this assemblage spans a wide temperature range, but garnet compositions are consistent with amphibolite-facies temperatures. These highly refractory, foliated rocks formed by melt loss after water- or melt-fluxed melting of metasediments in the middle portions of the imbricated metasedimentary prism. This type of water-saturated low-temperature anatexis was driven by the advection of water and heat by the ascending deeper sourced magmas and preferentially consumes quartz and plagioclase. The resultant peraluminous trondhjemitic magma contributed to the batholith in subordinate amounts relative to the hot, high-K, water undersaturated magmas sourced from near the base of the metasedimentary pile, where fluid-absent anatexis was driven by mantle heat. This study demonstrates that forearc metasedimentary mélanges can attain thicknesses of >30km and that such mélanges can undergo differentiation and stabilization by anatexis within 20Ma of deposition.

HIGH TEMPERATURE X-RAY DIFFRACTION STUDIES OF PEROVSKITE WITH THE CHEMICAL COMPOSITION $\text{CaFe}_x\text{Mn}_y\text{Ti}_{[1-(x+y)]}\text{O}_{3-\delta}$, $x = 1/4$, $3/8 \leq y \leq 1/2$

$(x+y)]\text{O}_{3-\delta}$, $x = 1/4$, $3/8 \leq y \leq 1/2$

Stoeber Stefan¹, Pöllmann Herbert¹

¹Institut fuer Geowissenschaften & Geographie, Martin - Luther - Universität, Germany

The aim of this study was to investigate the temperature driven structural changes in oxygen-deficient $\text{CaFe}_x\text{Mn}_y\text{Ti}_{[1-(x+y)]}\text{O}_{3-\delta}$ perovskites used as possible fuel cell materials.

The phases were synthesized by the Pechini methods, varying the substitution $\text{Mn}^{4+} \leftrightarrow \text{Ti}^{4+}$ in the range $3/8 \leq y \leq 1/2$. The investigated phases were all single-phased, which has been proven by ICP/OES and microprobe analysis. X-ray diffraction (HT-XRD) data were collected at room and non ambient temperatures between 298 to 1273 K (Mo radiation) applying a PANalytical Empyrean diffractometer equipped with an Anton Paar HTK 1200N oven chamber with capillary extension and a GaliPIX3D detector. For the evaluation of the X-ray data TOPAS-Academic (version 6) was used.

Different modifications with space groups Pbnm /1/, Cmcn, I4/mcm and Pm-3m were detected. The stability fields and transformation temperatures were determined. The refinement of structure data yielded temperature dependent alterations in tilting and distortion of B - site octahedra/2/ and differentially coordinated A - site polyhedra. Symmetry-mode Rietveld refinement (Isodistort Version 6.5.0)/3/ was applied and the results are compared with the traditional refinement of atomic xyz coordinates.

/1/ Ross, N. L., J. Zhao, et al. (2004): "High-pressure structural behavior of GdAlO_3 and GdFeO_3 perovskites." *Journal of Solid State Chemistry* 177(10): 3768-3775.

/2/ Glazer, A. (1972): „The classification of tilted octahedra in perovskites.“ *Acta Crystallographica Section B* 28(11): 3384-3392.

/3/ B. J. Campbell, H. T. Stokes, D. E. Tanner, and D. M. Hatch, "ISODISPLACE: An Internet Tool for Exploring Structural Distortions. *J. Appl. Cryst.* 39, 607-614 (2006).

EXPERIMENTAL VISCOSITY MEASUREMENTS OF BASALTIC AND PICRITIC MELTS AT PRESSURES AND TEMPERATURES OF THE EARTH'S UPPER MANTLE

Stopponi Veronica¹, Bonechi Barbara¹, Hrubik Rostislav², Misiti Valeria³, Perinelli Cristina¹, Gaeta Mario¹, Nazzari Manuela³, Scarlato Piergiorgio³, Stagno Vincenzo¹

¹Sapienza University of Rome, Italy, ²High Pressure Collaborative Access Team (HPCAT), X-ray Science Division, Argonne National Laboratory, Argonne, IL, United States, ³Istituto Nazionale di Geofisica e Vulcanologia (INGV), Roma, Italy

Viscosity plays a key role in controlling magma dynamics from the mantle source rock up to volcanic vents. While most of the efforts have been made to determine the viscosity of erupted lavas of active volcanoes, less is known on the viscosity of their parental melts at mantle pressures (P) and temperature (T) conditions, the knowledge of which would allow modeling the mobility and ascent rate through the surrounding rocks.

In this study we investigated the viscosity of both dry and volatile-bearing picritic, Na-rich and K-rich basaltic synthetic melts at P of 0.4-7 GPa and T between 1335 and ~2000 °C using the Paris-Edinburgh press combined with in-situ ultrafast X-ray radiography at 16 BM-B beamline of the Advanced Photon Source (Lemont, Illinois, USA). Viscosity measurements were conducted using the falling-sphere technique with the use of a high-resolution fast camera, which allowed the collection of radiographic images at a rate of 250-500 frames per second.

The obtained results show that the viscosity increases from 0.2 Pa·s to 0.8 Pa·s for picritic melts, from 0.6 to 3.3 Pa·s for Na-rich basaltic melts and from 0.3 Pa·s to 1.9 Pa·s in the case of K-rich basalts within the investigated P-T range. The calculated viscosity values combined with the estimates of density contrast (melt-rock), rock grain size and permeability, resulted in a melt mobility of 2 g·cm⁻³·Pa⁻¹·s⁻¹, for instance, in the case of the picritic liquid, with an ascent rate of ~ 4 km per year.

This study sheds light on the melt infiltration and recharge of deep magmatic chambers through time, and represents a step forward in unraveling pre-eruptive conditions of potentially hazardous active volcanoes.

MOBILITY OF VOLATILE-BEARING MAGMAS IN OXIDISED PLANETESIMALS: IMPLICATIONS FOR CO₂ LOSS AND STORAGE DURING ACCRETION

Stopponi Veronica¹, Stagno Vincenzo¹, Sena Francesco¹, Marras Giulia¹, Codispoti Niccolò¹, Gréaux Steeve²

¹Sapienza University of Rome, Italy, ²Geodynamics Research Center, Ehime University, Matsuyama, Japan

Carbonaceous chondrites represent the most primitive matter of the Solar system and are proved to be the building blocks of planetesimal and proto-planets constituting their major source of volatiles elements. During the early stages of accretion of planetesimals, rocky planetesimals experienced internal melting due to radiogenic heating with consequent mineral segregation, percolation of metallic liquids to form the proto-core, and loss of primordial volatiles such as carbon. While recent studies have explored the ascent rate and mobility of magmas formed in anhydrous planetesimals of O₂-depleted enstatite chondrite composition, the role of volatiles during accretion of oxidized planetesimals is unclear. Indeed, oxidized volatiles-rich planetesimals are proposed to form beyond the Frost Line (2.7 AU) but, however, as suggested by recent computational models, the rapid formation of giant planets (e.g., Jupiter) likely perturbed their orbits with consequent crossing of the proto-Earth region.

This work investigates the role of magma rheology on the amount of carbon either preserved or loss during planetesimal accretion by coupling experimental viscosity and density data of various CO₂-rich melts with experimental work conducted at high pressure and temperature on the carbon-rich, H₂O-bearing Tagish Lake primitive chondrite to determine melting relations and mineral phase equilibria. The hydrostatic melt mobility of CO₂-rich melts was calculated using both viscosities determined experimentally and the density difference between the surrounding solid rock and melt, the former calculated using the pressure- temperature-volume equation of state of mineral assemblages coexisting with a CO₂-rich melt retrieved by quenched experimental runs. The migration rate was modeled for different CO₂-bearing magmas as a function of different planetesimal size, melt fraction, and grain size of the coexisting crystalline matrix.

Taking into account three different radii of planetesimals (50, 250, and 500 km), our preliminary results of CO₂-rich melts transport properties during the growth of oxidized planetary embryos show that planetesimals larger than 250 km are likely to generate high melt fractions and experience a pronounced volatile extraction as compared with smaller accreting planetary bodies. We also present estimates on the effects of the gravitational field in the case of either internal homogeneous and heterogeneous distribution of masses on the melt segregation velocities.

MODIFICATION OF NATURAL ZEOLITES TO REMOVE THE HERBICIDE (2,4-DICHLOROPHENOXY)ACETIC ACID FROM WATER THROUGH THE ADSORPTION PROCESS

Straioto Henrique¹, Viotti Paula¹, Moreira Wardleison¹, Vieira Marcelo¹, Bergamasco Rosangela¹, Calabria Giovanna²

¹Department of Chemical Engineering, State University of Maringá, Brazil, ²Indústrias Celta Brasil LTDA, Brazil

The population growth has resulted in a greater demand for of the agricultural sector and, consequently, greater environmental contamination generated by the increased use of herbicides that end up in water bodies, that are not removed by conventional treatment processes. Several materials have been investigated as adsorbents, such as zeolites. Even though zeolites have a high ion exchange capacity, they lack efficiency for removing organic contaminants. Thus, a modification must be employed in zeolites to improve their performance for removing organic compounds. In this work, natural clinoptilolite zeolites were supplied by Celta Brasil and applied in the removal of 2,4-D ((2,4-dichlorophenoxy)acetic acid) through the adsorption process. Four different modifications were performed: 1) ion exchange to obtain a homoionic zeolite; 2) constant agitation in the presence of a modifying agent; 3) heat treatment in a muffle at 550°; and 4) hydrothermal treatment in a subcritical environment. Several modifying agents were tested (H₂O, HCl, KOH, KCl, KHCO₃, CTAB, among others) in the modification by agitation. In the hydrothermal modifications were carried out in the presence and in the absence of surfactant (CTAB), using NaOH (aq), HCl (aq) and H₂O as solvents. After the modifications, the zeolites were washed several times with distilled water until a constant pH and then, proceeded to drying in an oven at 100°C. BET adsorption and desorption isotherms were performed to verify the textural changes of the adsorbent, zeta potential for surface charge variation, while the zeolite functional groups were analyzed using FTIR spectroscopy. The adsorption tests were carried out in a thermostatic bath (Dubnoff Bath, Quimis) for 24 hours at a temperature of 30°C and 150 rpm by using 300 mg of adsorbent in contact with 20 ml of 2,4-D solution at a concentration of 100 mg/L and natural pH. The 2,4-D concentration after the adsorption was measured in a spectrophotometer (DR 5000 UV/VIS, Hach) at a wavelength of 229 nm. The adsorption results showed that the thermal modification did not improve the zeolite capacity for removing 2,4-D (maximum removal of 5.51%) from wastewater. For the modifications by agitation, it was found that the best results were obtained when HCl and CTAB (adsorption capacity of 0.70 and 1.65 mg/g, respectively) were the modifying agents. The best adsorption results were obtained when the adsorbent was modified in subcritical condition by combining HCl and CTAB, the adsorption capacity increased to 5.46 mg/g, which corresponded to the removal of 91.97% of 2,4-D.

HETEROGENEOUS NUCLEATION AND TRANSFORMATION OF IKAITE (CaCO₃ x 6H₂O) IN THE PRESENCE OF MINERAL SURFACES

Strohm Samuel Benedikt¹, Inckemann Sebastian¹, Gao Kun¹, Schmahl Wolfgang W.¹, Jordan Guntram¹

¹Department für Geo- und Umweltwissenschaften, Ludwig-Maximilians-Universität München, Germany

Ikaite (CaCO₃ x 6H₂O) had been overlooked in nature for very long time. Since its first finding in the Ikka fjord in Greenland by Pauly (1963), however, ikaite was discovered in many other locations. Furthermore, it turned out that many calcite crystals in nature are pseudomorphoses after ikaite. From all these occurrences, it can be inferred that ikaite may be a frequent precursor phase for the formation of anhydrous carbonate minerals especially in cold environments of Earth. However, knowledge about the formation kinetics of ikaite and its transformation rate and mechanism to more stable carbonate minerals such as calcite and vaterite is limited. From previous studies, it is evident that cold temperatures, as well as an increased carbonate alkalinity of the aqueous solution, is prerequisite for ikaite formation and that a competing precipitation of calcite and/or vaterite can be inhibited by dissolved Mg²⁺ and/or phosphate. It is important to note, however, that these studies typically concern homogeneous precipitation. Consequently, knowledge about the heterogeneous nucleation and transformation of ikaite, especially at mineral-fluid interfaces, which are ubiquitous in the natural settings of ikaite formation, is largely missing. This deficiency is serious because knowledge of heterogeneous formation of anhydrous minerals cannot be transferred to ikaite formation due the highly hydrated character of the CaCO₃ x 6H₂O units in the ikaite structure, which, according to Chaka (2018), correspond to the hydrated ion pair complexes existing in aqueous solution.

Insights into the effects of mineral surfaces on the nucleation of ikaite and its subsequent transformation into more stable carbonates can be gained by experiments using cryo-mixed-batch-reactors (CMBR) and in-situ flow-through cryo-atomic-force-microscopy (CAFM). Using CMBR, we investigated the kinetics of ikaite nucleation, its decomposition kinetics and the product phase selectivity with and without added mineral surfaces such as quartz and mica. Phase inventories of the CMBR experiments, ex-situ analyses of solution composition and in-situ monitoring of solution pH and Ca²⁺ revealed the behaviour of ikaite in the presence and absence of added mineral surfaces. These CMBR data were complemented by cryo-atomic-force-microscopy experiments. CAFM allows investigations of the temporal evolution of the reactions on defined mineral substrates in high spatial resolution. The setup of the newly developed CAFM and initial results will be presented.

Mn(II) CARBONATE AUTHIGENESIS MARKS THE BENTHIC SMTZ AND IS FUELED BY Mn-DRIVEN ANAEROBIC OXIDATION OF METHANE: A BLACK SEA EVIDENCE

Sun Tiantian¹, Böttcher Michael E.¹, Kallmeyer Jens², Treude Tina³, Lipka Marko¹, Jørgensen Bo B.⁴, Martinez-Ruiz Francisca⁵, Eckert Sebastian⁶

¹Geochemistry & Isotope Biogeochemistry, Leibniz Institute for Baltic Sea Research (IOW), Germany, ²Geomicrobiology, GFZ Potsdam, Germany, ³Marine Geomicrobiology, University of California, United States, ⁴Biogeochemistry, Max Planck Institute for Marine Microbiology, Germany, ⁵Facultad de Ciencias, Instituto Andaluz de Ciencias de la Tierra (CSIC-UGR), Spain, ⁶Microbiogeochemistry, University of Oldenburg, Germany

In the Black Sea, sediment cores covering the last brackish-limnic transition were recovered and investigated for anaerobic biogeochemical processes controlling sulfur, carbon, and metal cycling. The development of a sulfate-methane transition zone (SMTZ) is nowadays found below the brackish zone in the limnic part of the sediments that limits the upward migration of biogenic methane into surface sediments and the water column. The position of the SMTZ may have changed in the past due to dynamic fluxes of dissolved species in the pore water. Besides dissolved sulfate, metal-bearing minerals have been shown to serve as potential reactants, also converting CH₄ into dissolved inorganic carbon (DIC). The pore water and sediment stable isotope (C, S, O) and geochemical composition were investigated, as well as in-situ microbial rates of sulfate reduction and total anaerobic oxidation of CH₄ (AOM) obtained from sediment incubations for the identification of a potential contribution of manganese-bearing minerals to AOM in the limnic part of the sediments (Mn-AOM). In the limnic Black Sea sediments, Mn-AOM is causing an upward flux of dissolved Mn whereas intense SO₄-AOM located in shallower sediments leads to an increase in pH and a maximum in DIC concentrations in the SMTZ. The resulting change in saturation states leads to the precipitation of mixed MnCa-carbonate solid-solutions ('rhodochroxitization front') and the development of a zone enriched in excess sedimentary Mn(II). We further argue that these authigenic fronts may survive changes in pore water composition and are stable in the anoxic sedimentary record, marking the position of paleo-SMTZs. The persisting formation of this geochemical marker has advantage in application over the transient development of a sulfidization front of metastable mackinawite, that is formed by the reaction of downward migrating sulfide with upward diffusing Fe(II), originating from SO₄-AOM and Fe-AOM, respectively.

THE NEW OCCURRENCE OF BENTONITE IN THE CARPATHIANS FORELAND, POLAND: GEOCHRONOLOGICAL AND MINERALOGICAL EVIDENCE FOR THE MIOCENE SUPERVOLCANO (?)

Szopa Krzysztof¹, Wrona Katarzyna¹, Włodyka Roman¹, Drakou Foteini², Chew David², Krzykawski Tomasz¹, Skreczko Sylwia¹, Janeczek Janusz¹

¹University of Silesia in Katowice, Institute of Earth Sciences, Poland, ²Department of Geology, School of Natural Sciences, Trinity College Dublin, Ireland

The Miocene volcanogenic bentonites form large deposits in central Europe, particularly in Slovakia and Hungary. They are related to intense Middle Miocene explosive volcanism in the area between the Carpathians and Dinarides during the final stage of the Paratethys evolution. Smaller deposits of Miocene bentonites occur in the Czech Republic, Germany, Ukraine, Austria, and Poland. Miocene bentonites occur within the so-called Neogene cover of the Holy Cross Mts. in the Polish Carpathians foreland. Carbonate rocks-hosted bentonite layers are up to tens of centimeters thick. Most of them are Ca-rich because they principally consist of Ca-montmorillonite. During this study, the unusually bentonite-rich layer, < 1 m thick, was found within the lithothamnium limestone in the Drugnia Rządowa (DG) quarry. Calcium montmorillonite is a chief component of the bentonite. The bentonite layer contains numerous minerals of volcanic origin (heavy-mineral fraction > light-mineral fraction) including Qtz, Bt, Zr, Ap, Rt, Tnt/Mt. Volcanic glass and feldspar were not observed, most probably due to their complete argillitization. The U-Pb zircon geochronology provided one concordant age of $\sim 13.8 \pm$ Ma (Middle Serravallian, Upper Badenian, Konkian). That age is supported by the determination of foraminifera species. Previously published data (mostly based on Ar/Ar and K/Ar geochronology) for similar bentonites span a wider age range (~ 20 -12 Ma). There are two populations of quartz (detrital and euhedral) in the DG bentonite likely originated from the large-volume volcanic eruption, possibly supervolcano located some 700 km to the south. We suggest that the precisely dated DR bentonite layer can be used as a correlation strata.

APPLICATION OF NATURAL CLINOPTILOLITE MODIFIED WITH TRANSITION METALS IN SELECTIVE CATALYTIC REDUCTION OF NITROGEN OXIDES WITH AMMONIA

Szymaszek Agnieszka¹, Samojedan Bogdan¹, Motak Monika¹

¹Faculty of Energy and Fuels, AGH University of Science and Technology, Poland

Selective catalytic reduction with ammonia (NH₃-SCR) is one of the most widespread methods of nitrogen oxides (NO_x) emission prevention. Even though the commercial catalyst of the process exhibits satisfactory activity above 300 °C, its performance is much poorer below that temperature. Additionally, the material causes other operating problems, such as the production of SO₃ due to SO₂ oxidation or emission of toxic vanadia which is its component. For that reason, novel and non-toxic catalysts of low-temperature activity are in great demand. Intensive studies carried out over natural zeolites proved that the materials can be used as substitutes for the industrial catalyst of NH₃-SCR. One of the representatives is clinoptilolite, belonging to the heulandite-type framework. The low Si/Al molar ratio and thermal stability of the zeolite make it the especially promising precursor of the new NH₃-SCR catalyst. What is more, it was proved that easy modifications, for instance, treatment of clinoptilolite with low-concentrated mineral acids increase its specific surface area and the number of acid sites. According to the above, in this work natural clinoptilolite was transformed into hydrogen form using HCl, functionalized with iron by two different methods, and promoted with copper or cerium. The results of XRD analysis confirmed that iron was well-dispersed on the zeolite surface, while the outcomes of UV-vis suggested that the majority of the active phase is in a form of isolated species. What is more, the presence of iron was also detected in the raw zeolite. Therefore, the non-modified sample exhibited 58% NO conversion at 450 °C. It was observed that the method of iron deposition significantly influenced the catalytic activity of clinoptilolite above 250 °C and the selectivity in the whole analyzed temperature range. The introduction of copper as a promoter influenced positively the low-temperature activity, regardless of the route of iron deposition. On the other hand, the presence of cerium both lowered NO conversion and increased the amount of undesired N₂O in the flue gas.

CATALYTIC POTENTIAL OF MODIFIED NATURAL CLAYS IN SELECTIVE CATALYTIC REDUCTION OF NITROGEN OXIDES WITH AMMONIA

Szymaszek Agnieszka¹, Samojeden Bogdan¹, Motak Monika¹

¹Faculty of Energy and Fuels, AGH University of Science and Technology, Poland

Natural layered clays are one of the most abundant waste materials from many industrial processes. Despite their non-toxicity, the excessive storage on heaps leads to the occupation of the areas that can be effectively managed differently. One of the effective ways to use layered clays is their transformation into materials exhibiting catalytic properties in the selected processes, for instance, selective catalytic reduction of nitrogen oxides (NO_x) with ammonia (NH₃-SCR). NO_x are emitted due to energy production, industrial processes, and transportation. Their presence in the atmosphere causes significant environmental problems, such as acid rain, ozone layer depletion, or photochemical smog formation. NH₃-SCR is one of the most effective methods of NO_x abatement. However, the industrial catalyst causes some significant operation problems related to its temperature window and toxicity of the active phase consisting of vanadia. The so-far research proved that natural clays could be used as the precursors of substitutive catalysts of the process. The aluminosilicate layered structure build of tetrahedral and octahedral sheets placed alternately between each other is a consequence of the excellent ion-exchange properties of these materials. Even though layered clays do not possess a high specific surface area, it can be very easily increased by the application of acid treatment and so-called pillaring (intercalation). As prepared materials exhibit all of the properties characteristic for the promising catalysts of the NH₃-SCR process. The presented work included modification of natural clays using different mineral acids. The results of XRD analysis proved that the crystallinity of the initial sample was violated by acid treatment and the effect was strongly dependent on the parameters of a modification. Additionally, it was observed that the clay was successively pillared with Al₂O₃. It was observed that the performed modifications had a crucial impact on the catalytic activity of the materials in NH₃-SCR.

TITANITE-FLUID INTERACTIONS - A KEY TO THE RECOGNITION OF THE ORIGIN OF EARLY EARTH'S HYDROTHERMAL SYSTEM

Słaby Ewa¹

¹Institute of Geological Sciences Polish Academy of Sciences, Poland

The aim of the research was to determine the composition and age of high-temperature (HT) hydrothermal fluids in the Closepet Archaean batholith (Dharwar craton, India). The HT fluid system, which has the potential to provide strong support for subsequent studies and has been partially investigated, has never been dated. Fluid-mineral interactions are visible in alkali feldspar, apatite and titanite (Słaby et al. 2012, 2021). The isotope study of alkali feldspars and their recrystallization products reveal their mantle-lower crust origin (Słaby et al. 2012). Fluid chemical analyses were conducted focusing on the pristine and altered feldspar domains. However, feldspar is not a suitable phase for dating. Thus, titanite was chosen to study the pristine and altered domains of the batholith to illustrate both its fluid composition and the timing of its activity. Titanite presents distinct enrichment in non-altered domains and strong depletions in trace elements in patchy, marginal zones. The high total rare earth element (REE) concentrations and the marked negative Eu anomalies in this zone suggest crystallization resulting from a residual melt. The negative Eu anomalies diminish the REE patterns of the altered components and become positive. The observed trace element ratios (Nb/Ta, Y/Ho, and U/Th) indicate the presence of fluid-crystal interactions. Strong U/Th fractionation might be linked to the presence of CO₂ and Cl⁻. Zr-in-titanite thermometry yields a crystallization/recrystallization temperature of ~700°C for both the magmatic and altered domains. The titanite factor $Ti^{+4}/(Al^{+3} + Fe^{+3})$ reveals an affinity towards substantial mantle input into the fluid system. Pristine and altered titanite domains have been dated by laser ablation inductively coupled plasma mass spectrometry (Słaby et al., 2021). Reversely discordant apparent ages suggest previous interaction with fluids. The oldest semiconcordant analyses of titanite cores indicated an age of approximately 2500 Ma, which we interpret as the minimum age of magmatic crystallization. Narrow dark rims of titanite with considerably lower Th/U ratios form a more coherent group of analyses defining an upper concordant intercept age of 2345 Ma, which is considered the best estimate for the time of complete titanite resetting associated with the metasomatic event. The HT fluid system appears to have been active into the Palaeoproterozoic. Confirmation that the fluids belonged to the Archaean hydrothermal system provides us information about this system at the time; however, the data suggest that the system was active at least until the Palaeoproterozoic and offer additional valuable information about the character of the hydrothermal system during the Neoarchaean-Palaeoproterozoic transition. The transition time is considered to have been marked by some substantial geochemical changes in the crust-mantle system. However, we do not have sufficient data regarding the period ranging from 2400 to 2200 Ma related to deep mantle cooling. Such a process would influence an HT fluid system with a mantle-crust origin. Certainly, the Dharwar craton is not the only example of such a fluid origin. To confirm this expectation, parallel research on hydrothermal systems in the transitional period and their ages is needed.

Słaby et al. 2012, *JPetrol* 63, 57-98; 2021, *Lithos* 386-387.

The work was funded by the NCN Project UMO-2018/31/B/ST10/01060.

ZIRCON AND QUARTZ CRYSTAL CARGOS IN RHYOLITIC SYSTEM AS A TOOL TO RECONSTRUCT MAGMA PULSES WITHIN VOLCANIC SYSTEM – INSIGHT FROM THE LANDSBERG LACCOLITH (HALLE)

Słodczyk Elżbieta¹, Pietranik Anna¹, Przybyło Arkadiusz¹

¹Institute of Geological Sciences, University of Wrocław, Poland

Accumulation of viscous, high silica rhyolite is related to the process of interstitial melt segregation from partially-crystallized magma body. Such a scenario is consistent with the growing body of evidence that dangerous and voluminous silicic eruptions are preceded by large-scale melt segregation which can be reflected in either post-eruptive pyroclastic composition or scarce subvolcanic record. To address and better understand the processes of rhyolitic magma extraction we looked into subvolcanic system, the Permo-Carboniferous Halle Volcanic Complex (HVC; Germany) consisting of several laccoliths. The samples are from the 500 m deep drill core from the Landsberg coarse grained unit and our study is focused on zircon and quartz composition, as minerals potentially recording magmatic processes.

Hafnium content has been analyzed in zircon from 29, 155, 281, and 378 m depths. No clear patterns were observed in terms of Zr/Hf ratio, which could be constant, increasing, decreasing, V-shaped or irregular-saw-shape from core to rim. Also zircon is chemically similar between different depths with the exception of 29 m depth that is dominated by grains with increasing Zr/Hf ratio (no irregular or decreasing patterns). The implication is that zircon crystallized for a prolonged time in a larger magma reservoir and different crystals were later incorporated within subvolcanic magma body, specifically the uppermost part of the laccolith represent different part of the magma reservoir or different timing of its evolution. Additional evidence for distinctive magma volumes contributing to the laccolith system comes from concurrent studies on quartz cathodoluminescence (CL) images (thin sections from depths: 16, 128, 258, 328, 400m). CL brightness of quartz crystals is positively correlated with Ti contents, reflecting thermal conditions of the magmatic system. Quartz grains revealed normal (bright-core to dark-rim), reverse, oscillatory or no zoning (plane or mottled) patterns with overlay of distinctive disequilibrium resorption. In detail: (1) strongly vermicular resorption texture (with many deep wormy embayments) may represent a volatile-saturated magma; (2) mottled texture may indicate quartz (re-)crystallization under stable conditions; (3) reverse zoning record recharge and reheating event; (4) glomerocrysts indicate dynamic environment.

Different sets of zircon and quartz populations within and between samples from variable laccolith depths show unsystematic variation that requires compositional evolution of melt. Such variation may be explained by (1) variable magma pulses amalgamated to the system with episodic magma mixing (distinct zircon groups in upper parts of the laccolith) and/ or (2) crystal movement from one magmatic environment (mush pocket) to another. The scenario of several magma pulses and following mixing is supported by increasing number of vermicular quartz with depth. Such increased gas content might have caused decreasing density of the magma with depth, consequently leading to convective instability and mixing between magmatic pulses which had been previously amalgamated within the Landsberg laccolith.

ES, AP, AP acknowledge financial support from the Polish National Science Centre (UMO-2017/25/B/ST10/00180).

PRE-NUCLEATION GEOCHEMICAL HETEROGENEITY WITHIN ANATECTIC GLASSY INCLUSION AND THE ROLE OF WATER IN GLASS PRESERVATION

Tacchetto Tommaso¹, Reddy Steven¹, Bartoli Omar², Rickard William³, Fougere Denis¹, Saxey David³, Quadir Zakaria⁴, Clark Chris¹

¹Applied Geology, Curtin University, Australia, ²Department of Geosciences, University of Padova, Italy, ³Geoscience Atom Probe, Curtin University, Australia, ⁴John de Laeter Centre, Curtin University, Australia

Glassy melt inclusions are unique geological repositories that preserve evidence of the formation and evolution of mantle- and crustal-derived magmas. However, the mechanisms responsible for their preservation in slowly-cooled crustal rocks remain largely debated, in some part due to their small size (< 5µm) and the technical difficulty in quantifying composition and microstructures. In this work, time-of-flight secondary-ion mass spectrometry (ToF-SIMS), transmission electron microscopy (TEM) and atom probe tomography (APT) are used to characterize glassy melt inclusions (GI) found in peritectic garnets of a quartzo-feldspatic mylonitic diatexite from the Ojén unit, Betic Cordillera (southern Spain). GI are distributed in the core of garnet porphyroblasts and have isometric to negative crystal shapes. These GI are often found coexisting with partially and totally crystallized polycrystalline inclusions comprising micrometric aggregates of quartz, K-feldspar, biotite, muscovite and plagioclase (i.e., nanogranitoids). Analyses of the glassy inclusions show heterogeneous distribution of Na and K, with a thin layer present along inclusions walls. Enriched concentrations of Al, Fe, K, Na, Cl and Li are also found adjacent to inclusion edges. The similar distribution of these elements to micas and feldspars preserved at the rims of nanogranitoid inclusions leads us to interpret that the elemental concentrations in the GI represent the nanoscale manifestation of pre-nucleation compositional heterogeneity at the earliest stages of crystallization. These results prove a common origin of GI and nanogranitoids and discard the hypothesis of GI derivation from a subsequent infiltration of externally derived aqueous-siliceous fluids. A comparison between the melt inclusions composition in the available database reveals that preserved glassy inclusions show a mean value of 2.72 wt.% H₂O whereas nanogranitoids generally show higher H₂O contents with an average value of 6.91 wt.%. This suggests the low-H₂O activity representing a further impediment to crystallization, along with the very small volume of these cavities, favoring the coexistence of GI and nanogranitoids. Contrarily, crystallization is enhanced in wetter melts, where H₂O reduces melt viscosity and promotes diffusivity and in turn nucleation.

BARROVIAN METAMORPHISM IN THE LESSER HIMALAYAN SEQUENCE OF CENTRAL NEPAL SEEN THROUGH THE EYES OF ALUMINOUS METAPELITES

Tamang Shashi¹, Groppo Chiara¹, Rolfo Franco¹

¹Department of Earth Sciences, University of Torino, Italy, shashi.tamang@unito.it

The Lesser Himalayan Sequence (LHS) of the Nepal Himalaya is a thick Paleo- to Meso-Proterozoic sedimentary sequence originally deposited on the northern margin of the Indian plate. Although it is well known that, during the Himalayan orogenic cycle, the LHS developed a Barrovian inverted metamorphism, its metamorphic history is still poorly documented and constrained, the general belief being that it experienced a low-grade metamorphism. However, garnet, staurolite and/or kyanite-bearing assemblages are sporadically reported from the upper structural levels of the LHS, which are in contrast with the supposed low metamorphic grade of the LHS. As a contribution towards a more precise understanding of the LHS metamorphic evolution, this study aims at constraining the peak P-T conditions experienced by the upper-LHS in central Nepal. The study focuses on aluminous metapelites, because these lithologies are more prone to the development of low-variant assemblages compared to other LHS lithologies. The detailed microstructural, petrographic and mineralogical investigation of six aluminous metapelites allows recognizing that the most common aluminous minerals (garnet, staurolite and/or kyanite) show variable relationships with the main foliation (i.e., they can be pre-, syn-, or post-kinematic with respect to the main foliation in different samples). Phase diagram modeling succeeded in reproducing the observed blastesis-deformation relationships. Combined with isopleths thermo-barometry, this approach allowed constraining the P-T evolution of the upper-LHS, which is characterized by peak-P conditions of 9-10 kbar, at T = 590-600°C, followed by heating decompression at 620-630°C, 8-9 kbar.

MINERO-GEOCHEMICAL ANALYSES ON BOTTOM ASH PRODUCED BY THE INCINERATION PLANT IN TRIESTE (FRIULI VENEZIA GIULIA-ITALY).

Tattoni Federico¹, De Lorenzi Lorenzo², Gregorio Stefano³, Russo Livio³, Bevilacqua Paolo², Princivalle Francesco¹

¹Matematica e Geoscienze, Università di Trieste, Italy, ²Ingegneria e Architettura, Università di Trieste, Italy, ³HestAmbiente S.r.l., Italy

In the city of Trieste there is an incineration plant to recover energy from the combustion of not-recoverable municipal waste produced by the city and neighboring municipalities. The plant authorized capacity is 197,000 tons per year. The incineration plant is made up of 3 independent lines, each with a theoretical load of 204 t/day. Each line consists of a furnace, a boiler and a flue gas treatment system. The plant has a steam turbine to recovery energy that allows a production of about 100 GWh / year of electricity.

The furnace has a horizontal grate system of combustion and produces a bottom ash that is collected in a water filled discharger at the end of combustion, and fly ash, present in the flue gas: fly ash is collected from flue gas treatment system and then appropriately disposed of.

The present study focused on bottom ash. In the laboratories of the University of Trieste, magnetic and particle size separations were performed on a representative sample of bottom ash. After separating the metal phases (ferrous and non-ferrous metals), the focus was on the fine fractions of the samples, between 2 and 0.5 mm and less than 0.5 mm, carrying out overall elementary chemical analyzes (bulk analysis), with the aid of spectrometry inductively coupled plasma mass and optical emission (ICP-MS / OES), to determine the composition of the slag and X-ray analysis, using a diffractometer (XRPD), to determine the mineral phases present within the slag. The XRPD analysis highlighted the presence in addition to quartz and calcite, which are the most abundant phases, also of hydrocalumite, portlandite, gypsum, anhydrite, bassanite, plagioclase, larnite, magnetite, etc. Among the metallic elements the presence of iron, lead, copper and zinc has been ascertained. The mineralogy and chemistry found are on average among the values found for the bottom ash of other European incineration plants.

The incineration process of municipal solid waste reduces the volume of the waste by about 90% and the mass of waste by about 70%, but a consistent amount of coarse solid waste remains. Pursuing the objective of the circular economy it is important to recover them, giving new life to the waste produced. Metal materials are easily separable and recyclable, the inert fraction (about 20% of incoming waste) can be reused, especially in construction, as an additive in cement or as road substrates. In any case, the content of heavy metals and the possibility of their release following leaching must be checked.

Keynote

CRACKING & DISSOLVING: SOME EXAMPLES OF HOW BRITTLE AND DIFFUSIVE PROCESSES RULE FAULT ZONES

Tesei Telemaco¹

¹University of Padova, Italy

The strength, fluid transport processes and seismic/aseismic behavior of faults is strongly influenced by feedbacks between ambient PT conditions, rock composition deformation and fluid/rock alteration. Diffusive mass transfer in tandem with brittle fracturing, is a fundamental but somehow underappreciated mechanism of fault rock evolution, which leads to formation of new, often mechanically weaker, synkinematic minerals and rock fabrics. I will make a brief overview of the diffusive processes active in fault zones, with examples of fault zones exhumed from different depths in the Earth and involving different lithologies. In particular I will focus on concentration, crystallization and deformation of phyllosilicates and amphiboles in major faults. I will also review some recent data on the brittle strength and behavior of fault rocks formed with the aid of diffusive processes.

The combination of field and laboratory observations indicate that the classical transition from brittle to plastic deformation with depth should be enriched by the inclusion of diffusive processes, which call for a more thorough study of their kinetics and constitutive deformation laws.

COESITE INCLUSIONS IN PRISMATINE FROM WALDHEIM, GERMANY: NEW CONSTRAINTS ON THE PRESSURE-TEMPERATURE EVOLUTION OF THE SAXONY GRANULITE COMPLEX

Thomas Rainer¹, Grew Edward²

¹Helmholtz-Centre Potsdam, German Research Centre for Geoscience - GFZ, Germany, ²School of Earth and Climate Sciences, University of Maine-Orono, United States

Coesite has been found for the first time as an inclusion in prismatic at its type locality in Waldheim, Germany; this is also the first occurrence of coesite in the Saxon granulite complex. Prismatic, $(\square, \text{Mg, Fe})(\text{Al, Mg, Fe})_9(\text{Si, Al, B})_5\text{O}_{21}(\text{OH, F})$, is a borosilicate almost entirely restricted to upper amphibolite- and granulite-facies rocks formed at $T \approx 700\text{-}1000\text{ }^\circ\text{C}$ and $P \approx 4\text{-}13\text{ kbar}$, well outside the stability field for coesite: $P > 27/31\text{ kbar}$ at $700\text{-}1000\text{ }^\circ\text{C}$. The single coesite-bearing inclusion is $50 \times 60\text{ }\mu\text{m}$ across and comprises several rounded coesite grains mostly $20\text{-}25\text{ }\mu\text{m}$ across as well as phlogopite and rutile. A Raman spectrum of the inclusion has the bands characteristic of coesite at $176, 272, 422$ and 528 cm^{-1} , well as bands for quartz at $213, 391$ and 458 cm^{-1} . Other minerals enclosed in prismatic include brookite, anatase and graphite, as well as several phases that most likely result from crystallization of "nano-melts": α - and β -cristobalite, tridymite, kumdykolite and kokchetavite. Stishovite and nanodiamond have been provisionally identified as metastable phases. The presence of coesite requires a reevaluation of the metamorphic evolution of prismatic at Waldheim. Firstly, experimental studies by Krosse in the model $\text{MgO-Al}_2\text{O}_3\text{-B}_2\text{O}_3\text{-SiO}_2\text{-H}_2\text{O}$ system (MABSH) at Bochum in 1995 revealed that the stability of prismatic extended to nearly 40 kbar at $800\text{ }^\circ\text{C}$, resulting in overlap with the coesite stability field at temperatures inferred for peak conditions of metamorphism of the prismatic granulite. Secondly, although quartz is a sparse and late-formed constituent at the type locality, where corundum is a major constituent of the prismatic granulite, quartz is a major constituent and corundum sparse in prismatic granulites at a second occurrence 800 m east of the type locality. Here, prismatic formed with quartz, implying a potential involvement of coesite in forming prismatic at pressures sufficient for coesite stability. Thirdly, although textural relationships suggest that prismatic crystallized mostly in the latter half of the metamorphic evolution of the prismatic granulite, some of these relationships could relate to increase in pressure and temperature during the prograde stage rather than to peak conditions and subsequent decompression, i.e., prismatic began crystallizing relatively early in the metamorphic evolution and continued crystallization during decompression. Krosse's experiments in MABSH gave the reaction magnesio-foitite (tourmaline lacking alkali) + chlorite + corundum \Rightarrow prismatic at $25\text{ kbar}, 653\text{-}677\text{ }^\circ\text{C}$. However, the prismatic granulite contains constituents not present in the MABSH system, notably Fe, K and Na, which would have expanded the stability ranges of garnet, biotite and tourmaline (as the Na-bearing dravite) at the expense of chlorite and prismatic, e.g., experiments show that dravite could be stable to nearly $1000\text{ }^\circ\text{C}$ and 40 kbar in MABSH to which Na_2O has been added. A possible reaction on the prograde path in the natural system is kyanite + garnet + dravite \Rightarrow prismatic + SiO_2 + plagioclase $\pm \text{H}_2\text{O} \pm \text{B}_2\text{O}_3$ at pressures and temperatures straddling the quartz \Leftrightarrow coesite reaction at $\sim 900\text{-}1000\text{ }^\circ\text{C}$, requiring additional burial corresponding to at least 7 kbar more than suggested by the most recently proposed P-T path for the Waldheim prismatic granulite.

HELPING ORTHODONTICS – PRECIPITATION OF “BIO-PYROMORPHITES” WITHIN HUMAN ENAMEL AFFECTED BY INTERPROXIMAL SURFACES REDUCTION AS POST-TREATMENT REMINERALIZATION.

Topolska Justyna¹, Motyl Sylwia², Kozub-Budzyń Gabriela³

¹Mineralogy, Petrography and Geochemistry, AGH University of Science and Technology, Poland, ²Faculty of Medicine, Department of Orthodontics, Jagiellonian University, Poland, ³Department of Geology of Mineral Deposits and Mining Geology, AGH University of Science and Technology, Poland

Artificial abrasion of interproximal surfaces (stripping) is often a part of the orthodontic treatment in which the orthodontist narrows the enamel, thus making the teeth aesthetic, ergonomic and fit into the jaw. Stripping has opponents among some patients and clinicians who prefer permanent reduction of a teeth number in the jaw as an alternative. Reduction of the mesiodistal dimensions of the teeth is a multi-stage procedure that can be performed with a wide range of tools. It is well known that stripping affects the condition of the enamel (morphology) and a discussion among orthodontists about which stages of the procedure and what tools are best for its implementation is ongoing. However, the impact of the particular steps and tools applied during interproximal surfaces abrasion on the post-treatment enamel remineralization process has not been investigated so far in detail. The aim of this study was to investigate the effect of selected stripping steps and tools on the process of assimilation by enamel of elements from the remineralizing solution under thermodynamically favorable conditions. The experiments were designed based on the thermodynamic properties of apatite oriented to the preferential assimilation of Pb and Cl in the structure and formation of minerals from the $X_5(PO_4)_3Y$ series, where $X = Ca$ or Pb and $Y = OH, F$ or Cl . Three pairs of molars were subjected mesiodistally to three different stripping steps: (i) - abrasion with a metal strip, (ii) - (i) + polishing with a mechanical polisher, (iii) - (ii) phosphoric acid etching. A pair of teeth abraded with a mechanical diamond disk was used as a control. At the end of the procedure, one tooth from each pair received a fluorizing foam on the treated surface (30 minutes). The tooth samples were then reacted with the remineralizing fluid for 14 days. After this time, the calcium in the remineralizing solution was changed to lead and a demineralization-remineralization cycle was introduced for the next 21 days. During the experiment, the abraded surfaces of the samples were observed using a Scanning Electron Microscope (SEM), and after its termination, the teeth were polished, revealing their mesiodistal profiles, and analyzed with a use of an Electron Microprobe (EMP). The depth of Pb assimilation as well as the Pb concentrations, spatial distribution and its correlation with the main enamel-building elements were examined in detail on both stripped and intact surfaces of the samples. The most interesting results and conclusions: (i) even after 14 days of remineralization, the abraded enamel surface was evident by SEM and the effect was different depending on the stripping technique used; (ii) Lead was assimilated by the enamel to a depth of several to several dozen micrometers, and the depth and lead concentration depended on the side of the tooth (mesial, distal) and the striping method; (iii) lead has accumulated in the enamel mostly in the form of diffuse elongated nanoprisms, preferentially occupying cavities and irregularities in enamel; (iv) distal sides were particularly prone to assimilate Pb (in depth and concentration), however, mechanical abrader and acid etching diminished this effect; (v) no significant average fluoridation effect was observed, nevertheless single local anomalies of elevated lead concentrations were observed at the site of fluorizing foam application.

The studies were supported with the NSCentre of Poland grant no: 2016/21/D/ST10/00738

TEM AND LA-ICPMS STUDY OF AN ALTERED ZIRCON-XENOTIME INTERGROWTH IN PEGMATITE FROM PIŁAWA GÓRNA (GÓRY SOWIE BLOCK, SW POLAND)

Tramm Fabian¹, Wirth Richard², Budzyń Bartosz¹, Sláma Jiří³, Schreiber Anja²

¹Institute of Geological Sciences, Polish Academy of Sciences, Kraków, Poland, ²GeoForschungsZentrum Potsdam (GFZ), Section 3.5 Interface Geochemistry, Potsdam, Germany, ³The Czech Academy of Sciences, Institute of Geology, Prague, Czech Republic

An intergrowth of significantly altered zircon and xenotime in pegmatite from Piława Górna (Góry Sowie Block, SW Poland) was studied with transmission electron microscopy (TEM) and laser ablation inductively coupled mass spectrometry (LA-ICPMS) regarding alteration processes, element transport and their influence on the disturbance of U-Th-Pb system.

TEM observations revealed a homogeneous microstructure in xenotime, with micro- to nanopores containing secondary phases, predominantly of Fe-silicates, uraninite and coffinite-thorite solid solution, and rarely Pb-phosphates. A highly porous zircon rim has strong variation of micro to nano inclusions, which include Fe-silicates and uraninite with minor thorite, xenotime and monazite. The metamict core of zircon displays patchy zoning in nanoscale and nanoporosity with inclusions of secondary fluorapatite, uraninite and galena. TEM observations displayed a sharp transition between homogeneous xenotime and the patchy zoned zircon at the interface between both minerals. Occasionally, secondary zircon penetrates the surface of xenotime. In summary, TEM observations demonstrated features typical for coupled dissolution-precipitation processes in xenotime and the zircon rim, whereas the zircon metamict core displayed limited element transport with nanoporosity indicative for diffusion-reaction processes. The combined TEM observations and LA-ICPMS trace element measurements revealed how the fluid-mediated alteration affected individual domains of the studied phases, resulting in supply of Al, Ca, Fe and F by an alkaline-bearing fluid into the xenotime and the porous rim of zircon, whereas Ca and F were added to the metamict core of zircon. Fluid-induced transport of U, Th and Pb resulted in disturbance of a geochronological record. This study demonstrates the importance of TEM observations for reliable interpretation of geochemical data derived from microscopic methods of strongly altered geochronometers.

Acknowledgements: This work was supported by the National Science Centre grant no. 2017/27/B/ST10/00813. M. Jastrzębski is acknowledged for providing the pegmatite sample.

EXPERIMENTAL INVESTIGATIONS OF THE FLUID-INDUCED GRANULITE-ECLOGITE TRANSFORMATION USING A NATURAL GRANULITE SAMPLE

Tropper Peter¹, Hinterwirth Simon², Mair Philipp¹

¹Institute of Mineralogy and Petrography, University of Innsbruck, Austria, ²Institute of Geology, University of Innsbruck, Austria

High pressure and high temperature metamorphic rocks are usually found in the deep continental crust and subduction zones. In rare instances such as in the Bergen Arcs, Norway, one can observe the transformation of granulites into eclogites on a millimeter-scale. In this case fluids play a significant role, migrating in shear zones, and thus inducing this transformation in these shear zones. This transformation leads to the formation of microdomains of equilibration. In order to gain a deeper understanding of these fluid-induced lower crustal processes we performed an experimental investigation of the eclogite-granulite transformation using a granulite (grt + opx + pl + Kfs + ilm + qz) sample from the Moldanubian Zone near Wieselburg, Lower Austria. Four experiments were run at 2.5 GPa and temperatures ranging from 650°C to 700°C for a duration of 14 days. The role of fluid during this transformation was investigated and experiments were carried out with two different water contents (3 wt.% and 14 wt%) as well as with two different fluid compositions (pure H₂O and XNaCl = 0.1). Instead of powders we used solid rock pieces in the experiments to retain the textural features associated with this transformation in the samples. All experiments show the eclogite-facies assemblage jadeite/aegirine + zoisite + phengite + quartz ± amphibole ± melt and the formation of textural microdomains (former plagioclase and orthopyroxene domains). Only in the experiment at 700°C large-scale melting occurs in the charge. Using the software THERMOCALC v.3.33 it was possible to calculate the model reactions leading to the formation of the reaction products in the microdomains. The mineral assemblage of the individual orthopyroxene microdomains can differ significantly depending on the fluid content as well as temperature. In the experiment at 650°C and 2.5 GPa and 3 wt.% H₂O as well as in the experiment at 700°C and 2.5 GPa no amphibole grew in the orthopyroxene domain. The formation of Ca-amphibole around orthopyroxene only takes place at higher water contents. The formation of clinopyroxene around orthopyroxene starts with the growth of Fe-rich aegirine, which changes into jadeite. This indicates that orthopyroxene reacts with adjacent plagioclase to form aegirine until the relict orthopyroxene is separated from the matrix. Afterwards jadeite grows around this microdomain, which results from the massive breakdown of adjacent matrix plagioclase. These clinopyroxenes are rimmed with a corona of phengite. In the plagioclase microdomain only jadeite + zoisite + phengite occur which can be explained with the model reactions albite = jadeite + quartz and sanidine + anorthite + H₂O = muscovite + zoisite + quartz. Comparing the experiments to the rocks from the Bergen Arcs shows a great similarity with respect to the formation of microdomains and the observed mineral assemblages. The main differences to the natural samples are the lack of garnet and kyanite formation in the experiments. Latter can be attributed to the relatively high fluid contents in the experiments. The presence of a H₂O-NaCl fluid led to a complete transformation during the experiment and almost no protolith relicts occur anymore. Due to the lack of retrogression these experiments provide a petrological “snapshot” into the mechanisms of these lower crustal processes.

Lu-Hf DATING OF LASER-MILLED GARNET MICRO-DOMAINS REVEAL <1MA OF RAPID, PACED GARNET GROWTH IN BLUESCHISTS FROM SYROS, GREECE.

Tual Lorraine¹, Smit Matthijs², Cutts Jamie², Kooijman Ellen¹, Kielman-Schmitt Melanie¹, Foulds Ian³

¹Department of Geosciences, Swedish Museum of Natural History, Sweden, ²Department of Earth, Ocean, and Atmospheric Sciences, University of British Columbia, Canada, ³School of Engineering, Faculty of Applied Science, University of British Columbia, Canada

Unravelling the timing and rate of subduction-zone metamorphism requires linking the composition of petrogenetic indicator minerals in blueschists and eclogites to time. Garnet is a key mineral in this regard, not in the least because it best records P-T conditions and changes therein and can be dated, using either Lu-Hf or Sm-Nd chronology. Bulk-grain garnet ages are the norm and can provide important and precise time constraints on reactions across both facies. Domain dating (i.e., dating of individual growth zones) moves beyond that in constraining the precise timing of garnet growth reactions; however, it is generally impeded in "common" centimeter-sized garnet grains due to sample size requirements for a precise analysis. We overcame these limitations by combining a low-loss micro-sampling technique in laser cutting with a refined Lu-Hf routine to precisely date multiple growth zones of a sub-cm-sized garnet in a blueschist. The targeted garnet grain from a glaucophane-bearing micaschist from Syros Island, Greece, was chemically characterized by major- and trace-element mapping (EPMA, LA-ICPMS) and five zones were extracted. The three core and inner mantle zones are chemically comparable and yield identical ages (within 0.1 Myr 2SD uncertainty) indicating initial growth at 51.8 ± 0.1 Ma (MSWD = 1.13). The two rim zones are chemically distinct from the three inner zones and yielded resolvably younger ages at 51.3 ± 0.2 Ma (MSWD = 0.67). The timing of these two major garnet-growth episodes, together with the variations in trace-element chemistry, constrain important fluid-release reactions, such as chloritoid-breakdown. The data show that the integral history of garnet growth in subduction zones may be extremely short (<1 Myr), but still, may consist of multiple short pulses. Beyond subduction-zone processes, our new protocol for Lu-Hf domain geochronology of "common-sized" garnet opens possibilities for constraining the causes and rates of garnet growth and the pace of tectonic processes in general.

AUTOMATED MINERALOGY OF MINING- AND SMELTER-DERIVED PARTICLES DEPOSITED NEAR AN OPERATING COPPER SMELTER

Tuhý Marek¹, Ettlér Vojtěch¹, Hrstka Tomáš²

¹Institute of Geochemistry, Mineralogy and Mineral Resources, Faculty of Science, Charles University, Czech Republic, ²Institute of Geology, Academy of Sciences of the Czech Republic, Czech Republic

We investigated particulates deposited in a highly polluted semiarid area near an operating copper smelter and old mine-tailing disposal sites in Tsumeb (northern Namibia). Heavy mineral fractions were studied by XRD and polished sections were analyzed by optical microscopy, SEM/EDS, autoSEM/EDS and FEG-EPMA. The quantitative EPMA data supplemented the database of the TESCAN Integrated Mineral Analyzer (TIMA) autoSEM/EDS, which was then used for the analysis of modal compositions and for the automated search and identification of metal(loid)-bearing phases. Modal and texture analyses were performed using the “dot mapping mode”. Final optimization of the elemental distributions within individual phases was verified by comparisons with the bulk chemical compositions.

The contaminant-bearing particles were mainly represented by spherical grains, which originate from the smelting process and corresponded to quenched droplets of matte (Cu-Fe sulfides) and slag melts (glass, spinels). In addition, angular grains were probably windblown from the ore processing facilities and/or nearby mine-tailing disposal sites. These particles contained gangue minerals (carbonates) and various metal-bearing sulfides, sulfosalts and arsenates. Parallel digestions and bulk chemical analyses were used as an independent control of the autoSEM-calculated concentrations of the key elements. Large TIMA-collected dataset (approximately 60 million spot analyses per sample) helped to quantify the percentage of individual phases and to perform partitioning of the studied contaminants (Pb, Cu, Zn, As, Sb, Cd). We found that As was mainly bound to the apatite group minerals, slag glass and metal arsenates. Copper was predominantly hosted by the sulfides/sulfosalts and the Cu-bearing secondary carbonates. The deportment of Pb is relatively complex: slag glass, Fe and Mn (oxyhydr)oxides, metal arsenates/vanadates and cerussite were the most important carriers for Pb. Zinc is mainly bound to the slag glass, Fe (oxyhydr)oxides, smithsonite and sphalerite. AutoSEM was found to be a useful tool for the determination of the modal phase distribution and element partitioning in the metal(loid)-bearing soil particulates and will definitely find more applications in environmental soil sciences in the future.

This study was supported by the Czech Science Foundation (GAČR 19-18513S) and the institutional funding from the Center for Geosphere Dynamics (UNCE/SCI/006).

THE KEY ROLE OF $\mu\text{H}_2\text{O}$ GRADIENTS IN DECIPHERING MICROSTRUCTURES AND MINERAL ASSEMBLAGES OF DUCTILE SHEAR ZONES: EXAMPLES FROM THE CALABRIA POLYMETAMORPHIC TERRANE

Tursi Fabrizio¹

¹Dipartimento di Scienze della Terra e Geoambientali, University of Bari Aldo Moro, Italy

A careful petrologic analysis of mineral assemblages of mylonites is crucial for a thorough comprehension of the rheologic behavior of ductile shear zones active during an orogenesis. In this view, the knowledge of the way new minerals form in ductilely sheared rocks and why relict porphyroblasts are preserved in zones where mineral reactions are generally supposed to be deformation-assisted, is essential. To this goal, the role of chemical potential gradients, particularly that of the aqueous fluid ($\mu\text{H}_2\text{O}$), was examined here through phase equilibrium modeling of syn-kinematic mineral assemblages developed in three distinct mylonites from the Calabria polymetamorphic terrane. Results revealed that gradients in chemical potentials are recorded in the mineral assemblages of the studied mylonites, and that new syn-kinematic minerals formed within sites where the $\mu\text{H}_2\text{O}$ was higher than in the surroundings. In each case study, the banded fabric of the mylonites resulted from fluids internally generated by the breakdown of OH-bearing minerals. The gradients in $\mu\text{H}_2\text{O}$ favored the origin of bands enriched in hydrated minerals alternated with bands where anhydrous minerals were preserved even during exhumation. Phase equilibrium modeling shows that during the prograde stage of metamorphism, high $\mu\text{H}_2\text{O}$ were necessary to form new minerals while relict porphyroblasts remained stable in condition of low $\mu\text{H}_2\text{O}$ even during exhumation. Hence, the method used in this contribution is an in-depth investigation of the fluid-present/-deficient conditions that affected mylonites during their activity, and provides a more robust interpretation of their microstructures, finally helping to explain the rheologic behavior of ductile shear zones.

TWO-STEP Pb-DISTURBANCE IN MONAZITES FROM ZIRCON POINT, NAPIER COMPLEX (ANTARCTICA) RESOLVED BY ATOM PROBE ANALYSIS

Turuani Marion J.¹, Laurent Antonin T.¹, Seydoux-Guillaume, Anne-Magali¹, Fougereuse Denis², Saxey David³, Reddy Steven², Harley Simon L.⁴

¹Univ Lyon, UJM, UCBL, ENSL, CNRS, LGL-TPE, F-42023, Saint Etienne, France, ²School of Earth and Planetary Sciences, Curtin University, GPO Box U1987, Perth, Australia, ³Geoscience Atom Probe, Advanced Resource Characterisation Facility, John de Laeter Centre, Curtin University, GPO Box U1987, Perth, Australia, ⁴School of Geosciences, University of Edinburgh, James Hutton Road, Edinburgh EH9 3FE, United Kingdom

Monazite (LREEPO₄) is widely used in Earth Sciences as U–Th–Pb geochronometer. Based on the assumption that U, Th and Pb are immobile overtime in the mineral, measured isotopic ratios yield concordant ages corresponding to grain (re)crystallization. However, isotopic disequilibrium may occur in monazite, resulting in discordant dates which can be difficult to interpret. Discordant monazites from the ultrahigh temperature paragneiss from Zircon Point, in the Archean Napier Complex (Antarctica) have been investigated from the micro- to the nano-scale in order to understand the mineralogical nature of isotopic perturbation and its impact on calculated dates. In-situ U–Th–Pb isotopic analyses (LA-ICP-MS, SIMS) at the micro-scale result in discordant dates spreading along a discordia between 2.44 and 1.05 Ga. Observations with Transmission Electron Microscopy (TEM) reveal that the least discordant monazites, hosted in rutilated quartz and garnet, contain a high density of small Pb-bearing nano-minerals ($\varnothing \sim 50$ nm) while the most discordant monazites, located in the quartzo-feldspathic matrix, contain a lower density of Pb-bearing nano-minerals that are bigger in size ($\varnothing \sim 50$ to 500 nm). The degree of the discordance appears thus related to Pb retention in distinct Pb-bearing nano-minerals within monazite grain, some of them being identified as galena (PbS) by coupling TEM and Atom Probe Tomography (APT). The Pb isotopic signature of those galena is variable but imply a radiogenic origin (Pb*) with no participation of common Pb. The isolation age of those Pb* reservoirs from the host monazite may thus be constrained with the ²⁰⁸Pb/²³²Th of the monazite matrix (excluding Pb-bearing nano-minerals) and the ²⁰⁷Pb/²⁰⁶Pb of galena measured with APT. This study suggests that monazite grains crystallized at 2.44 Ga and were subsequently affected by two episodes of Pb* mobility. The first one at ca. 1 Ga is characterized by Pb*-loss at the grain scale and resetting of the monazite matrix along with the crystallization of a first generation of galena. The second episode is characterized by the crystallization of a second galena generation which results from the mixing of two Pb* components, likely around 0.53 Ga. This study demonstrates the importance of a multi-scale characterization, through nano-scale observations and analyses that can allow to improve the understandings of micro-scale observations and inversely.

IN SITU TEM STUDY OF SHEAR-INDUCED AMORPHIZATION AND GRAIN BOUNDARY SLIDING IN OLIVINE

Ul Haq Ihtasham¹, Samae Vahid¹, Idriss Hosni¹, Schryvers Dominique¹

¹EMAT, University of Antwerp, Belgium

Olivine is the most abundant mineral in Earth's upper mantle. Its mechanical properties are of primary importance to model the rheology of the asthenospheric mantle. However, the microphysics of olivine deformation is not fully understood since this orthorhombic mineral does not exhibit enough slip system to achieve a general deformation. Several recent studies have focused on the possible contribution of grain boundaries (GBs) (sliding, migration) to the deformation of olivine aggregates, but so far, the mechanisms at play are not yet clarified. Recently, a high-resolution TEM microstructural investigation of olivine aggregates deformed at ca. 1100°C revealed a ductile behavior involving amorphization of GBs.

Here we use in situ TEM nanomechanical testing on olivine aggregate specimens (without amorphous layer at the GB) to gain information on the underlying mechanisms. We use the PI-95 TEM Pico-indenter holder and the Push-to-Pull (PTP) device (Bruker, Inc) to perform quantitative in situ TEM tensile tests at room temperature. Bi- and tri-crystal olivine samples were prepared by focused ion beam (FIB). We show that the specimens deform exclusively by grain boundary sliding. We observe evidence of stress-induced amorphization in the sliding GBs. The elementary mechanisms involved are discussed and compared to the literature.

BULK MOLYBDENITE AND RELATED LAYERED POLYTYPES: STRUCTURAL, OPTICAL AND DIELECTRIC PROPERTIES BY DENSITY FUNCTIONAL THEORY SIMULATIONS

Uljan Gianfranco¹, Moro Daniele¹, Valdrè Giovanni¹

¹Dipartimento di Scienze Biologiche, Geologiche e Ambientali, University of Bologna, Italy, gianfranco.ulian2@unibo.it, daniele.moro@unibo.it, giovanni.valdre@unibo.it

Molybdenite (MoS₂) is an important mineral that in standard temperature and pressure conditions crystallizes in the 2H polytype (MoS₂-2H, space group P63/mmc), and it is commonly found in high-temperature hydrothermal ore deposits. Very important and interesting, this mineral is characterized by an heterodesmic structure, i.e., it presents strong covalent Mo – S bonds along the a- and b-axes forming layers of S – Mo – S, which are held together by weak long-range interactions along the [001] direction. For this reason, it presents a perfect cleavage on the {001}, a property that is shared with graphite. In addition of being the main source of molybdenum, a peculiar property of molybdenite is the possibility to obtain single layers of MoS₂, which are referred to MoS₂-1H polytype. While both graphite and its single layer graphene present a well-known “metallic-like” behaviour, the MoS₂ polytypes are semiconductors that could be employed in several and manifold applications. Just to cite some examples, molybdenite attracted much attention for optoelectronics, as solid lubricant and as (photo)catalyst for different reactions, for example to remove sulphur compounds from oil.

In the present contribution, we deal with this important mineral phase, investigating the structure of different MoS₂ polytypes. In detail, starting from the molybdenite bulk, we also considered and investigated a single layer and a bi-layered structure. The study was conducted at the Density Functional Theory level, including specific corrections to take into account van der Waals interactions, simulating the proposed models to characterize how their structures change from the bulk to the “surface-like” layers. Furthermore, other properties have been investigated in detail, such as the optical and dielectric properties, which could be very useful for both the characterization and the technological applications of this important geomaterial.

V-ANALOG OF LEVANTITE, $\text{KCa}_3(\text{Si}_3\text{Al}_2)\text{O}_{11}(\text{VO}_4)$ – A POTENTIALLY NEW MINERAL OF THE LATIUMITE GROUP FROM ESSENEITE PARALAVA OF THE HATRURIM COMPLEX, NEGEV, ISRAEL

Vapnik Yevgeny¹

¹Department of Geological and Environmental Sciences, Ben-Gurion University of the Negev, Israel

In gehlenite pyrometamorphic rocks of the Hatrurim Complex in the Negev Desert, Israel a new mineral levanite, $\text{KCa}_3(\text{Si}_3\text{Al}_2)\text{O}_{11}(\text{PO}_4)$, forming a solid solution with latiumite, $\text{KCa}_3(\text{Si}_2\text{Al}_3)\text{O}_{11}(\text{SO}_4)$, was recently discovered. In levanite Ba, Fe^{3+} and V^{5+} impurities, the content of which usually lower than 0.1 apfu, are detected. The last investigations have shown that levanite is a rock-forming mineral in unusual esseneite paralava forming thin veins in gehlenite hornfelses. In paralava, besides esseneite and levanite, wollastonite, rankinite, garnet of the schorlomite-andradite series, gehlenite and V-bearing fluorapatite are rock-forming minerals. In paralava between rock-forming mineral crystals a small up to 0.3 mm fine-grained aggregates composed of perovskite, celsian, paqueite, latiumite, vorlanite, minerals of the dorrite-khesinite series, magnesioferrite, gorerite are noted. In the one of such aggregates, in association with paqueite and V-bearing fluorapatite, grains of V-analog of levanite up to 10 μm in size were found. Its composition is described by the empirical formula:

$(\text{K}_{0.85}\text{Ba}_{0.15})_{\Sigma 1.00}\text{Ca}_3(\text{Si}_{2.65}\text{Al}_{2.25}\text{Fe}^{3+}_{0.10})_{\Sigma 5.00}\text{O}_{11}[(\text{VO}_4)_{0.5}(\text{PO}_4)_{0.3}(\text{SO}_4)_{0.2}]_{\Sigma 1.00}$, which can be simplified to ideal formula $\text{KCa}_3(\text{Si}_3\text{Al}_2)\text{O}_{11}(\text{VO}_4)$. Raman spectrum of V-analog of levanite significantly differs from the Raman spectra of minerals of the levanite-latiumite solid solution, for which the two strong bands are characteristic at 995 cm^{-1} [$\nu_1(\text{SO}_4)^{2-}$] and 945 cm^{-1} [$\nu_1(\text{PO}_4)^{3-}$]. In V-analog of levanite spectrum there are the four strong bands: 987 cm^{-1} [$\nu_1(\text{SO}_4)^{2-}$], 850 cm^{-1} [$\nu_1(\text{VO}_4)^{3-} + \nu_1(\text{SiO}_4)^{4-}$], 734 cm^{-1} [$\nu_1(\text{AlO}_4)^{5-}$] and 369 cm^{-1} [$\nu_4(\text{VO}_4)^{3-}$]. The band near 942 cm^{-1} responded to vibrations of $\nu_1(\text{PO}_4)^{3-}$ has low intensity. V-analog of levanite is a fourth vanadium mineral discovered in rocks of the Hatrurim Complex. Before, gurimite, aradite, and pliniusite were described from high-temperature paralava (~1000-1200°C).

The investigations were supported by the National Science Centre (NCN) of Poland, grant no. 2016/23/B/ST10/00869.

INCREASED TRACE-ELEMENT MIGRATION IN DEFORMED (U)HP/LT RUTILE: DISLOCATIONS IN LOW-ANGLE BOUNDARIES AS HIGH-DIFFUSIVITY PATHWAYS

Verberne Rick¹, Van Schroyen Lantman Hugo², Reddy Steven³, Alvaro Matteo², Wallis David⁴, Fougere Denis³, Langone Antonio⁵, Saxey David³, Rickard William³

¹Center for Star and Planet Formation, Globe Institute, University of Copenhagen, Denmark, ²Department of Earth and Environmental Sciences, University of Pavia, Italy, ³Geoscience Atom Probe, ARCF, John de Laeter Centre, Curtin University, Australia, ⁴Department of Earth Sciences, University of Cambridge, United Kingdom, ⁵Institute of Geosciences and Earth Resources, National Research Council (C.N.R) Pavia, Italy

The trace-element composition of rutile is commonly used to constrain P-T-t paths for a wide range of metamorphic systems. Recent studies have highlighted the importance of micro- and nanostructures in the redistribution of trace elements in rutile via high-diffusivity pathways and dislocation-impurity associations. In this contribution, we investigate the effect of crystal-plastic deformation of rutile on its composition by combining microstructural and petrological analyses with atom probe tomography. The studied sample is from an omphacite vein of the ultrahigh-pressure metamorphic Lago di Cignana unit, Western Alps, Italy. Zr-in-rutile thermometry and inclusions of quartz in rutile and of coesite in omphacite constrain the majority of rutile deformation to around the prograde HP-UHP boundary at 500–550 °C. Crystal-plastic deformation of a large rutile grain resulted in low-angle boundaries that generate a total misorientation of ~25°. Dislocations constituting the low-angle boundary are enriched in common (Fe, Zr) and uncommon trace elements (Ca). The Ca is interpreted to be derived from the grain exterior, suggesting diffusion of trace elements along the dislocation cores. The potential for dislocation microstructures to act as fast diffusion pathways must be evaluated when applying traditional geochemical analyses as compositional disturbances caused by the presence of dislocations might lead to erroneous interpretations.

Acknowledgements: This project has received funding from the European Research Council under the H2020 research and innovation program (N. 714936 TRUE DEPTHS to M. Alvaro)

TEPHRO-, HYGRO-, THERMO-, PETRO-, NANO-: UNIFYING GEO-CHRONOLOGY

Villa Igor Maria¹

¹DISAT, Universita di Milano Bicocca, Italy

Dating geological events requires a clear perception of which, among the many conceivable geological processes has had the greatest influence on the isotopic record of a rock. According to the studied geological problem, geochronometers are labelled in categories pursued by communities that often do not communicate. Tephrochronology, apparently the simplest category, provides tie-points for volcanic chronostratigraphy. In submarine and subaerial environments minerals are exposed to acid interstitial water and weathering, often causing systematic age inaccuracy. Chemical microanalyses reveal that non-ideal preservation conditions can mutate tephrochronometers to hydrochronometers.

Hydrochronology exploits the fact that aqueous fluids promote retrograde reactions. Prominent hydrochronometers are monazite and epidote (U-Pb), K-feldspars and micas (K-Ar and Rb-Sr), and any mineral that records the metasomatic/metamorphic reactions due to aqueous fluid circulation events. Water was also repeatedly demonstrated to distort laboratory diffusion experiments.

Thermochronology models time-temperature histories by assuming that age measurements can be uniquely assigned to a "closure temperature", which in turn is based on the assumption that the only process occurring in rocks is Fick's Law diffusion. A necessary property of a true thermochronometer is a bell-shaped concentration profile. For He atoms in apatite, which can move in mineral structures at much lower temperatures than the PTAX field allowing the formation of the mineral itself, this is observed. However, bell-shaped isotope concentration profiles have never been documented for nearly-immobile radiogenic daughters (Pb, Ar, Sr). Instead, patchy age distributions matching patchy retrograde reaction textures are attested. Heterochemical microstructures are ubiquitously observed by CL (zircon, K-feldspar) and EPMA (monazite, muscovite, biotite), but normally escape visual detection because they are < 5 µm. Their dissolution/precipitation rates are orders of magnitude faster than Fick's Law diffusion.

Petrochronology is based on opposite assumptions. It recognizes that the mobility of major structure-forming cations is higher than that of radiogenic Pb, Ar, and Sr. Thus, whenever the formation conditions of a mineral (given by major cations) occur at a lower T than its "closure temperature" for diffusive loss of radiogenic isotopes, its apparent age dates its formation. Minerals with this property are called petrochronometers (monazite, allanite, micas). Nanochronology is the new frontier of geochronology. Apparently, nm-scale analyses fall outside the Goldilocks zone for dating, as the formation of clusters of radiogenic daughters trapped in different sites from their radioactive parents can give excessively high ages when the resulting heterogeneity is larger than analyzed sample volumes. However, nm-scale analyses provide an essential perspective to understand processes at the atomic scale. All atoms do diffuse, but the diffusion lengths are small and mostly insufficient to account for the observed intra-grain age distributions. An additional, faster process is required: chemically open-system transport of soluble ions in (mostly, but not exclusively) aqueous fluids.

In summary, the key to producing correct 1000-km-sized tectonic models is the realization that minerals consist of atoms, whose behavior can only be firmly constrained by nm-scale analyses.

LATERITE VS NON-LATERITE GARNIERITES: COMPARISON BETWEEN Ni PHYLLOSILICATE MINERALIZATIONS IN FALCONDO (DOMINICAN REPUBLIC) AND IN BOU AZZER (MOROCCO)

Villanova-de-Benavent Cristina¹, Haissen Faouziya², García-Casco Antonio³, Karfal Abdelhak⁴, Proenza Joaquín A.¹

¹Departament de Mineralogia, Petrologia i Geologia Aplicada, Universitat de Barcelona, Spain, ²Department of Earth Sciences, Université Hassan II de Casablanca, Morocco, ³Departamento de Mineralogía y Petrología, Universidad de Granada, Spain, ⁴Managem Group, Morocco

Garnierites, the green, fine-grained Ni-Mg phyllosilicates often occurring as mixtures, have been widely described in Ni-laterite profiles worldwide, like in New Caledonia and the Dominican Republic. They are typically found in the saprolite horizon of Ni-laterite profiles, formed during tropical weathering of ultramafic rocks. However, they may also occur as alteration products of Ni sulfide and sulphosalt mineralizations. One example of this is in the Bou Azzer Ni-Co arsenide mining district, in the central Anti-Atlas domain, Morocco. The available data of non-lateritic garnierites is very limited, so the aim of this contribution is to shed some light on the formation of garnierites in different environments, by comparing the textures and compositions of the Ni-phyllosilicates and the associated assemblages in the Falcondo and the Bou Azzer mining districts.

On one hand, garnierites in the Falcondo Ni-laterite mining district are found as veinlets and coatings on joints mainly in the serpentine-rich saprolite horizon, but they can also be found within the oxide-rich limonite horizon and the partly serpentinized Mesozoic ultramafic protolith. They mostly consist of mixtures at the nanometre scale between Ni-poor serpentine (lizardite lamellae, chrysotile tubes, and polygonal serpentine) and a Ni-rich talc-like mineral phase (kerolite-pimelite). Also, Falcondo is the type locality of the Ni analog of sepiolite, falcondoite, present in lesser amounts. The assemblage coexists with quartz (locally Ni-bearing), Ni-serpentine, Ni-goethite and altered chromite relicts.

On the other hand, previous work in the Bou Azzer mining district has proposed that garnierites have a low temperature hydrothermal origin in the so-named “filon F51” deposit. In this site, the bedrock geology consists of a partially serpentinized ophiolitic complex of Neoproterozoic age where Ni-Co sulphosalt mineralizations occur associated with quartz, calcite and dolomite. Powder XRD results indicate that the garnierite mineralizations consist of serpentine-like and talc-like minerals, as shown by diffraction peaks at ~7 Å and ~10 Å, respectively. The presence of Ni-chlorite cannot be discarded. The garnierite mineralization coexists with hydrated phases like Ni-arsenates (annabergite) and Ni-sulphates, together with quartz, calcite and gypsum.

The data gathered indicate that garnierites can form in non-lateritic environments if there is availability of Ni and Si in percolating/infiltrating H₂O-rich fluids. One of the major differences between the two localities is that the assemblage also contains secondary sulfates and arsenates in non-lateritic mineralizations.

PALLADIUM TELLURIDES - SOLUBILITY OF SELECTED ELEMENTS, AN EXPERIMENTAL APPROACH

Vymazalova Anna¹, Laufek František¹, Tuhý Marek¹, Chareeva Polina², Chareev Dimitry³

¹Czech Geological Survey, Czech Republic, ²IGEM RAS, Russian Federation, ³IEM RAS, Russian Federation

Among the palladium tellurides there are nine binary phases: Pd₁₃Te₃, Pd₂₀Te₇, Pd₇Te₃, Pd₉Te₄, Pd₃Te₂, PdTe, and PdTe₂. Minerals belonging to the Pd-Te system are: kotulskite (PdTe), merenskyite (PdTe₂), telluropalladinite (Pd₉Te₄), and keithconnite (Pd_{3-x}Te), further the phases Pd₁₃Te₃ and Pd₃Te₂ were observed to occur in nature. Kotulskite and merenskyite are the most abundant minerals of the system Pd-Te.

We have experimentally investigated the solubility of Ag, Bi, Hg, Pb, Sn, and Se in palladium tellurides at temperature of 400 °C. The evacuated silica tube method was applied for the purpose of this study. The experimental products were examined with X-ray powder diffraction, and by means of reflected light and electron microscopy (SEM and WDS analyses).

Among palladium tellurides, kotulskite forms an extensive solid solution and may dissolve up to 45 wt.% Pb; up to 50 wt.% Bi; it can also dissolve up to 20 wt.% Sn; up to 8 wt.% Hg and up to 10 wt.% Se. Kotulskite does not dissolve Ag. Keithconnite, that we equate with the synthetic phase Pd₂₀Te₇, dissolves up to 3.5 wt.% Ag; it can also dissolve up to 9 wt.% Pb; and up to 4.6 wt.% Sn and up to 6 wt.% Se. Merenskyite dissolves up to 4 wt.% Sn and up to 17 wt.% Bi. Telluropalladinite dissolves up to 4 wt.% Pb and may dissolve up to 5 wt.% Se. The phase Pd₁₃Te₃ dissolves up to 2 wt.% Ag. Lead, Sn, Bi, Se, Hg is substituted for tellurium in the crystal structure of palladium tellurides, whereas Ag for palladium.

COMPLEX MAGNETITE TEXTURES REVEALED BY BSE AND EBSD: IMPLICATIONS FOR THE GENESIS OF THE ORE DEPOSIT FROM TAKAB (NW IRAN)

Wagner-Raffin Christiane¹, Boudouma Omar¹, Rividi Nicolas², Orberger Beate³, Nabatian Ghasem⁴, Hornarmand Maryam⁵, Youssef Imam⁵

¹ISTeP, Sorbonne Université, France, ²IPGP, Sorbonne Université, France, ³GEOPS, Université Paris Saclay, France, ⁴Geology, Zanzan University, Islamic Republic of Iran, ⁵Institut of Advanced Studies of Basic Sciences, Islamic Republic of Iran,

The late Proterozoic iron ore deposit of Takab (NW Iran) is mainly composed of magnetite and minor hematite intercalated with quartzite and amphibolites. We report microstructural, textural and chemical analyses of magnetite and hematite combining backscattered electron scanning microscopy (BSE-SEM), and electron backscatter diffraction (EBSD).

Magnetite forms a few mm large grains with striking textural features: the grains are mostly composed of an inhomogeneous dark grey magnetite (Mt), surrounded by a light grey more porous magnetite, which invades the dark Mt (BSE images). The dark Mt shows some stretched or needle-like bands of a bright magnetite aligned along micro fracturing planes. In these bands some relict hematite (Hem) is observed. Both dark and light grey Mt zones are characterized by higher and variable Si (1 wt.%), Al and Mg (1500-4000 ppm) and Ca (2100-3300 ppm) than the bright Mt (Si, 1000 ppm; Al and Mg, <1000 ppm; Ca, 400-800 ppm). EBSD disorientation maps show different behaviours: either crystallographic orientations change across sub-grain boundaries, or the changes are gradual and cannot be associated with distinct boundaries.

The following scenario is proposed. A primary magnetite (Mtn-1) has undergone hydraulic micro fracturing allowing modification by an oxidizing fluid, which penetrated the primary sediment piles and formed hematite. Then the composition of the fluid changed and the transformation of Hem to bright Mt probably occurred through non-redox reaction with Fe²⁺-bearing hydrothermal fluid, in agreement with the higher Fe content of the bright Mt than the dark Mt. After sealing of the fractures the depositional environment became more reduced. The dark and light grey Mt may have formed by progressive coupled dissolution-precipitation process (DRP) of the primary Mtn-1. The extensive fluid-rock interactions result in enrichment in pervasive Si, Al, Mg and Ca, as known elsewhere for hydrothermal iron deposits. Magnetite grains have further been subjected to deformation processes resulting in crystallographic misorientations. The dislocations and their migration may have facilitated the migration of element through the crystal structure.

REDOX VARIATIONS DURING MANTLE MELTING REVEALED BY THE PARTITIONING BEHAVIORS OF Fe³⁺ AND Fe²⁺ BETWEEN MANTLE MINERALS AND BASALTIC MELTS

Wang Jintuan¹, Huang Fangfang¹, Xiong Xiaolin¹

¹State Key Laboratory of Isotope Geochemistry, Guangzhou Institute of Geochemistry, Chinese Academy of Sciences, China

Abundant studies reveal that redox state of mantle-derived melts varies with tectonic settings as represented by the melt Fe³⁺/ΣFe ratios (Cottrell et al.; Gaborieau et al., 2020). Specifically speaking, Fe³⁺/ΣFe ratios show a sequence of MORBs (0.10±0.05) < OIBs (0.13±0.05) < ABs (0.25±0.15) (Gaborieau et al., 2020). The oxidized nature of ABs and OIBs relative to MORBs has been interpreted as to reflect the redox state of their mantle sources which are oxidized by the ingress of oxidized components during plate subduction (Brounce et al., 2015; Brounce et al., 2021; Brounce et al., 2014) and the entrainment of recycled materials during mantle plume upwelling (Moussallam et al., 2019; Shorttle et al., 2015), respectively. These interpretations assume that redox states of primitive melts inherit that of the source rock, namely, oxidation state of the mantle remains unchanged during melting. However, whether this underpinning assumption holds remains elusive (Cottrell et al.; Stagno and Fei, 2020).

Iron is the most abundant multivalent element on Earth and thus the distribution of Fe³⁺ and Fe²⁺ amongst different mineral phases dominate oxidation state of the mantle (Ballhaus et al., 1990; McCammon, 2005). Therefore, oxidation state of the mantle will change once the phase assemblage or abundance varies. According to this rationale, the oxidation state of the mantle should change during partial melting due to the formation of melt and the consumption of minerals. Because how the redox state varies during mantle melting depends on the redistribution of Fe³⁺ and Fe²⁺ amongst minerals and melt. Therefore, to thoroughly study the redox variations during mantle melting, we must determine the partition behaviors of Fe³⁺ and Fe²⁺ between mantle minerals and coexisting melts. The partition coefficient of Fe²⁺ (D_{Fe²⁺}) can be determined by performing experiments at reduced condition (e.g. graphite buffered condition) at which Fe exist almost as Fe²⁺. However, determining the partition coefficient of Fe³⁺ (D_{Fe³⁺}) in silicate minerals confronts challenges for the following reasons. Firstly, we can barely reach oxidizing condition where Fe exist exclusive as Fe³⁺ in experiments. Secondly, direct analysis of Fe³⁺ content in minerals remains unsettled especially for anisotropic minerals such as pyroxenes (McCanta et al., 2018). Thirdly, unlike oxides, Fe³⁺ content in silicate minerals can hardly be accurately calculated from their chemical compositions (Canil and O'Neill, 1996). As hampered by the difficulties in determining D_{Fe³⁺}, no systematic D_{Fe³⁺} values are available to elucidate redox variations during mantle melting.

Here we conducted experiments at 1.5–2.5 GPa, 1150–1420 °C and oxidized conditions and determined D_{Fe³⁺} values from the relationship amongst D_{FeT}, D_{Fe²⁺} and Fe³⁺/ΣFe in the melt" [D_{Fe³⁺} = (D_{FeT} - D_{Fe²⁺}) / ((Fe³⁺/FeT) / (Fe³⁺/ΣFe))]. The results show that D_{Fe³⁺} is moderately incompatible in opx and garnet, moderately incompatible to compatible in cpx, compatible in spinel and magnetite. The D_{Fe³⁺}/D_{Fe²⁺} ratio is always <1 in opx, garnet and magnetite, and >1 in cpx and spinel. Partial melting modelings reveal that mantle melting alone can account for the Fe³⁺/ΣFe ratio in MORBs. However, elevated Fe³⁺/ΣFe ratios in ABs and OIBs require Fe³⁺-rich mantle sources which may be caused by the ingress of oxidized components during plate subduction and the entrainment of recycled materials during mantle plume upwelling.

IN-SITU ANALYSIS OF MAGMATIC AND HYDROTHERMAL SCHEELITE TO TRACK ORE-FORMING PROCESSES: A CASE STUDY FROM THE XINGLUOKENG TUNGSTEN DEPOSIT, SOUTHEAST CHINA

Wang Hui¹, Li Rongxi²

¹School of Earth Science and Resources, CHANG AN UNIVERSITY, China, ²CHANG AN UNIVERSITY, China

The scheelite, as the major ore mineral of the tungsten deposit, can provide critical information on the ore-forming magmatic-hydrothermal processes. In this presentation, we show a case study on the Xingluokeng tungsten deposit, which is located in the middle area of the Wuyishan metallogenic belt, southeast China. It is the largest tungsten discovered in the belt by now, with a WO₃ reserve of 304, 300 tonnes (average grade at 0.23 %). We describe the detailed mineral assemblages, from magmatic to hydrothermal stages, and carry on in-situ Nano-SIMS and LA-ICP-MS trace elements and in-situ fs-LA-MC-ICP-MS Sr isotope on multi-generation scheelites, to track magmatic-hydrothermal processes. The orebody mainly occurs in the roof part of an extensively altered granite stock. Multiple mineralized types have been recognized, including disseminated, veinlet-disseminated, stockwork and vein-type mineralization, with scheelite/wolframite ratios at ~1:1, approximately. The ore-forming processes could be divided into three stages: veinlet-disseminated scheelite-molybdenite stage (stage I), K-feldspar-scheelite-wolframite-beryl stage (stage II) and sulfide-wolframite-scheelite-carbonate stage (stage III). Microthermometric analysis of fluid inclusions indicates the ore-forming fluids belong to NaCl-H₂O-CO₂ system, with medium-high temperature and low salinity. H-O and Sr isotopic compositions suggest the ore-forming fluids dominantly originated from magma water, and limited meteoric water involved in late mineralization stage. The magmatic scheelites and scheelites in early stage have higher contents of REE, Mo, Na and Nb, but lower Sr content; whereas REE, Mo, Na and Nb were gradually depleted and Sr was enriched, with the evolution of ore-forming fluids. The scheelites of stage I are characterized by euhedral or subhedral crystals, with dense and homogeneous oscillation zonation. In this type of scheelites, the REE substituted into the Ca site by Na- and Nd-dominated substitution mechanism. Whereas the scheelites in stage II and III, the incorporation of REE into scheelites can be coupled with □Ca (where □Ca is a Ca site vacancy). Together with mineralization and alteration features, we propose that the scheelites in stage I crystallized in a low fluid/rock ratio condition, by way of pervasive replacement of primary magmatic fluids along micro fractures. Whereas the scheelites in stage II and III were precipitated by extensively fluid-rock interaction accompanying by immiscibility of CO₂. Coupled with the geological characteristics of ore deposit, we consider the Xingluokeng deposit as generalized porphyry tungsten deposit. The veinlet-disseminated tungsten mineralization constitutes the metallogenic base, and the superposition of stockwork and vein tungsten mineralization is a key process for the Xingluokeng tungsten deposit.

REDOX EVOLUTION OF THE MAGMA CONTROLS ON THE Cu FERTILITY IN THE PALEO-TETHYAN OROGEN: A CASE STUDY FROM THE SAISHITANG CU DEPOSIT, NW CHINA

Wang Hui¹

¹School of Earth Science and Resources, CHANG AN UNIVERSITY, China

The reason for the sparsity of economic porphyry Cu deposits in Paleo-Tethyan orogenic belt is still poorly understood. It has been suggested that anoxic conditions of the ocean basin might have dominated Paleo-Tethyan subduction systems and thus produced relatively reduced arc magmas, which thus suppressed Cu fertility in Paleo-Tethyan orogen (Richards and Şengör, 2017). In this presentation, we show a case study on ore-related intrusions of the Saishitang porphyry-skarn Cu deposit in the eastern Paleo-Tethyan orogen to further decipher the reason.

The Saishitang porphyry-skarn Cu deposit is situated on the easternmost part of the East Kunlun orogenic belt, northwest China. It is the largest porphyry-skarn Cu deposits in the region, containing 0.4 Mt Cu with an average grade of 1.13%. The ore-related intrusions consist of medium- to fine-grained quartz diorite (QD) and porphyritic granodiorite (PG), intruded by diorite porphyrite (DP). In-situ compositions of hornblende and zircon, obtained by EPMA and LA-ICP-MS, were used to track the oxygen fugacity evolution of the magma. The calculated average ratios of zircon Ce^{4+}/Ce^{3+} of the QD, PG and DP are 12, 30, 38 and ΔNNO values are -3.2, -4.1 and -2.6, respectively, indicating they were formed in the relatively reduced conditions. Moreover, detailed core-rim texture studies show amphiboles in these intrusions were crystallized at least from two stages. The ΔNNO values of the early amphiboles (core) are -0.67~4.15, whereas ΔNNO values of the late amphiboles (rim) are -1.78~0.06, indicating the initial magma is oxidized. While with the magma rising and evolving in the middle and upper crust, the oxygen fugacity decreases constantly. Based on the published Sr-Nd isotopic data, we infer that the assimilation and contamination of reduced surrounding rocks is the main mechanism for the decrease of magmatic oxygen fugacity. The assimilation and contamination maybe also widespread for coeval intrusions in eastern Paleo-Tethyan belts.

The above results indicate the crustal magma evolution processes, rather than the deep subducted or collisional processes, maybe the more critical factors to control the redox states of the magma and decide the Cu fertility, at least for some Cu deposits in eastern Paleo-Tethyan orogen.

COMPLETE RECONSTRUCTION OF THE PROCESS AND CONDITIONS DURING GOLD SMELTING IN THE 15-17TH CENTURY IN ZŁOTY STOK BASED ON METALLURGICAL SLAGS

Warchulski Rafał¹, Kupczak Krzysztof¹, Gawęda Aleksandra¹

¹Faculty of Natural Sciences, University of Silesia, Poland,

Gold is a metal that has played a significant role in the history of humanity for millennia. Its presence contributed to the development and decline of many civilizations. All over the world, mining and metallurgical works have been carried out for millennia to produce this widely desirable metal. The production of gold, like other metals, leaves behind residues in the form of waste from various production stages. One of the possible remnants of historical metallurgy is slag, although slags from the pyrometallurgical processing of gold ores are not as common as those from other metals' production. One of the few places where we can observe the remains of pyrometallurgical gold production is Złoty Stok.

Slags from the Złoty Stok have been used for the complete reconstruction of gold metallurgy, including key parameters of the process (temperature of smelting and solidification, melt viscosity, oxygen fugacity). Investigated slags consist of silicate phases (olivine, pyroxene), sulfides and arsenides (pyrrhotite, Fe₂As), and glass. They are chemically dominated by SiO₂ (up to 56.60wt.%), MgO (up to 18.36wt.%), FeO (up to 15.36wt.%), and CaO (up to 15.19wt.%). The results obtained from four independent methods (furnace experiments, geothermometers, phase diagrams, and the Melts software) indicate that the temperature during the process was at least 1300-1350°C, and the crystallization of the slags took place until they cooled down to <1200°C. The morphology of olivine crystals in the slags indicates a large differentiation of their cooling regime, from 5 to 300 °C/h. Strongly reducing conditions during the metallurgical process (-10.5 to -11.5 log fO₂) was confirmed. Exceptionally low melt viscosity (log η = 0.26 - 0.90 Pa s) facilitated the separation of the sulfide melt rich in gold from the silicate melt being the slag precursor.

The obtained results allowed to reconstruct the smelting furnaces in Złoty Stok and correct the metallurgical process's existing descriptions. The process consisted of the following steps: (i) blending the ore with fluxes (SiO₂, Al₂O₃, and K₂O rich gneisses and schists) and the speiss/matte from the subsequent steps of the process; (2) first smelting process ("raw melting"); (3) the obtained sulfide-arsenide material (speiss/matte) was used in the next furnace ("stone melting") to which metallic lead was dosed to separate Au from speiss/matte in the form of Pb-Au alloy. At this stage, the speiss/matte was repeatedly returned to the furnace to maximize the gold yield, and after that, it was used in the first smelting stage; (4) Au was separated from the Pb-Au alloy during the cupellation process. The broad-spectrum data of high precision on the historical process was obtained in the course of the analysis of by-products (slags), what indicate the great research potential of such studies.

Acknowledgments

This study was supported by NCN grant no. 2016/21/N/ST10/00838 (awarded to RW) and NCN grant no. 2019/35/O/ST10/00313 (awarded to AG).

SOLUBILITY OF CALCINED CLAY MINERALS AND SUITABILITY AS PRECURSORS FOR GEOPOLYMERS

Werling Nadja¹, Krause Felix², Schuhmann Rainer¹, Dehn Frank³, Emmerich Katja¹

¹Competence Center for Material Moisture (IMB-CMM), Karlsruhe Institute of Technology, Germany, ²Institute of Functional Interfaces (IFG), Karlsruhe Institute of Technology, Germany, ³Institute for Concrete Structures and Building Materials (IMB), Karlsruhe Institute of Technology, Germany

Geopolymers (GP) and supplementary cementitious materials (SCM) are potential substitutes for ordinary Portland cement (OPC), which emit up to 40-90% less CO₂ during their manufacturing (Davidovits, 2013; McLellan et al., 2011). In contrast to SCM, which replaces only a certain amount of OPC, GP are OPC free binders. OPC is a hydraulic binder, while GP are low Ca/Ca-free alkaline activated binders (Dehn, Koenig & Hermann, 2017). A GP is a 3-dimensional inorganic polymer, which is formed by the activation of aluminosilicates with a highly alkaline solution (e.g. NaOH or KOH) that results in the hardening of the binder.

Calcined common clays appear to be well suited as raw materials. The properties of the resulting GP are influenced e.g. by the concentration of the alkaline activator, the solid:liquid ratio, the solubility of the precursors and the Si:Al ratio. The cation in the activator (e.g. Na⁺) balances the negative charge resulting from the charge difference of Si⁴⁺ and Al³⁺ in the emerging GP structure. If there is excess of Na⁺ in the added activator, the formation of carbonates with airborne CO₂ can be induced (Werling et al., 2020). The same effect occurs if the calcined clay minerals are not fully dissolved during activation, which leads to unreacted Al. In addition, incongruent solubility leads to Si:Al ratios deviating from stoichiometry. Due to the influence of the solubility of the precursors, calcined model clay minerals have to be investigated before calcined common clays are fully understood.

This study deals with the investigation of the solubility of three different calcined clay minerals in NaOH solutions with varying concentration. The suitability of the calcined clay minerals for the production of GP is derived from these results. A Bavarian kaolin (KBE-1, kaolinite content > 95%), a bentonite (Ceratosil, smectite content > 65%) and an illitic clay (Arginotec NX, illite content > 76%) were investigated. Different calcination temperatures (up to 900 °C) and NaOH concentrations (0.01 N – 10.79 N) were used for the solubility experiments. The solubility was studied with inductively coupled plasma optical emission spectrometry (ICP-OES). The microstructure of the residual solid materials was observed by scanning electron microscopy (SEM). Different formulations for the preparation of GP were tested and the phase content of the hardened binders was investigated by X-ray diffraction (XRD).

Acknowledgement

The project is funded by Deutsche Forschungsgemeinschaft (DFG) under EM79/8-1.

OBSERVATION AND INFERENCE IN THE INTERPRETATION OF ZIRCON AGES OBTAINED FROM A PURPORTED >3.9 GA GNEISS IN THE SAGLEK BLOCK, LABRADOR

Whitehouse Martin J.¹, Kusiak Monika A.², Dunkley Daniel J.², Wilde Simon A.³, Keluskar Tanmay T.²

¹Department of Geosciences, Swedish Museum of Natural History, Sweden, ²Department of Polar and Marine Research, Institute of Geophysics Polish Academy of Sciences, Poland, ³School of Earth and Planetary Sciences, Curtin University, Australia

With due care, all techniques in geochronology can provide precise ages for multiple generations of magmatism and metamorphism in a single complex outcrop. Equally, the same methods can produce spurious interpretations, either through a neglect of statistical reproducibility in age estimates, or through a misunderstanding of the relationships between dated zircon grains and their host rocks. In the Saglek Block of Labrador, NE Canada, a claim for evidence of life in >3.95 Ga supracrustal rocks (Tashiro et al., 2017, Nature) relies on zircon dating and field relationships that are somewhat ambiguous. Conclusions were drawn that contradict evidence from earlier studies (as discussed by Whitehouse et al., 2019, Prec. Res.). This includes ‘cherry-picking’ of >3.9 Ga analyses from an imprecise dataset by Shimojo et al. (2016, Prec. Res.) that contains a more inclusive subset of statistically equivalent data that yield a more robust ‘maximum’ age of ca. 3.87 Ga. A similar age of ca. 3.86 Ga was obtained from a metagranite that Shimojo et al. considered syn-metamorphic, which was therefore used to constrain the time of gneiss formation. This interpretation contradicts the ca. 2.7 Ga granulite-facies metamorphic event recognized across the Saglek Block. Re-analysis of the tonalitic gneiss, and the metagranite that was transposed into the dominant gneissosity, provides ages of emplacement of ca. 3.87 Ga and ca. 2.71 Ga, respectively. Thus, the Eoarchean ages for granitic magmatism and metamorphism estimated by Shimojo et al. actually derive from xenocrystic zircon incorporated into a Neoproterozoic melt and thus cannot be used to constrain pre-Neoproterozoic processes. This case study demonstrates the confusion that can arise when the essential interplay between observation and inference in both field geology and zirconology is overlooked.

This research was funded by NCN grant UMO2019/34/H/ST10/00619 and Alice Wallenberg Foundation grant 2012.0097.

EVALUATING NANOSCALE INCLUSIONS AND CLUSTERS OF RADIOGENIC LEAD IN ZIRCON

Wilde Simon A.¹, Kusiak Monika A.², Dunkley Daniel J.², Whitehouse Martin J.³, Wirth Richard⁴

¹School of Earth and Planetary Sciences, Curtin University, Australia, ²Department of Polar and Marine Research, Institute of Geophysics, Polish Academy of Sciences, Poland, ³Department of Geosciences, Swedish Natural History Museum, Sweden, ⁴Section 3.5 Surface Geochemistry, GeoForschungsZentrum Potsdam, Germany

In zircon affected by high-temperature metamorphism, radiogenic lead can be redistributed into nano-inclusions during annealing of a radiation-damaged host. For geochronologists, the discovery of such inclusions provides some answers to the behavior and preservation of radiogenic lead during metamorphism; however, it raises just as many questions. The discovery explains why some analyses of zircon by microbeam techniques, especially SIMS, have irregular count-rates on radiogenic lead, commonly leading to variable degrees of reverse discordance. Such effects disturb isotope systematics and can lead to spurious ages. However, the formation of such nano-inclusions, concomitantly with annealing and repair of zircon structure, can also aid in the preservation of isotopic signatures, resetting the accumulation of radiation damage in the host zircon and protecting radiogenic lead from mobilization and loss.

How widespread this phenomenon is, how important it is to isotopic preservation, and whether it is present in zircon even without evidence of isotopic disturbance in microbeam studies, are questions that have only just begun to be answered.

In this presentation, a ‘casebook’ of lead nano-inclusions will be opened, with a review of the first discoveries of metallic lead nanospheres by TEM in zircon from Ultra-High Temperature (UHT) granulites of Antarctica and India. These will be compared with recent examples of nanoscale observations of lead atom clustering by Atom Probe Tomography. New examples of nano-inclusions will also be showcased from metamorphic rocks in Antarctica, Labrador and the Ukraine, along with other locales. These examples will be evaluated to demonstrate that this little-studied phenomenon conversely plays a significant role in both the disturbance and preservation of isotopic signatures.

This research was funded by NCN grant UMO2019/34/H/ST10/00619 to MAK.

HEAVY METAL RECOVERABILITY OF MSWI FLY ASHES ALONG THE FLUE GAS COOLING PATH

Wolffers Mirjam¹, Eggenberger Urs¹, Schlumberger Stefan², Churakov Sergey³

¹Institute of Geological Sciences, University of Bern, Switzerland, ²Zentrum für nachhaltige Abfall- und Ressourcennutzung (ZAR), Switzerland, ³Laboratory for Waste Management, Paul Scherrer Institute, Switzerland

Each year, around 75'000t of fly ash from municipal solid waste incineration (MSWI fly ash) are produced and deposited on landfills in Switzerland. MSWI fly ash consists of boiler- and electrostatic precipitator ash and contains significant concentrations of heavy metals (e.g., Zn, Cu, Cd, Pb, Sb). From the year 2026 onwards, it will be mandatory to treat Swiss MSWI fly ashes with acid leaching in order to recover the heavy metals prior to deposition. However, it has not yet been legally determined whether the boiler ash is to be treated as fly ash. It could also be treated and deposited together with the bottom ash. Currently, the data available for boiler ashes are very limited, and their metal recovery potential has not been fully explored. Therefore, detailed chemical and mineralogical characterization was performed on the different MSWI ashes that form along the flue gas path (empty pass-ash (EA), boiler ashes (BOA) and electrostatic precipitator ash (ESPA)). Using a broad combination of methods (XRF, XRD, SEM), the ashes from six Swiss MSWI plants were characterized with respect to the chemical and mineralogical composition of major- and minor phases. Important parameters to estimate the suitability of a treatment are the contents of recoverable heavy metals and the extractability of the ashes. The focus was therefore laid on matrix phases affecting leachability (e.g. alkalinity, oxidation-reduction potential), as well as on the distribution and concentration of recoverable heavy metals and their binding forms. In order to estimate the need for metal recovery before landfilling, the contents of non-mobilizable pollutants such as Sb was also recorded along the flue gas path.

EA and BOA showed comparable bulk chemical and mineralogical composition and are composed of two significantly different materials: the airborne ash particles (quenched melt droplets and refractory particles) and deposits formed on heat exchanger surfaces. It is mainly the deposits that contribute to the elevated heavy metal concentration, explained by the well-developed, large (Na,K)-PbSO₄ crystals and the Zn-bearing matrix sulfates. The variation in the amount and chemical composition of the deposits controls the fluctuations in the bulk composition of EA and BOA. The ESPA shows different chemical and mineralogical characteristics than EA and BOA. The ESPA is enriched in the more volatile metals Zn, Pb, Cu, Cd; which are mainly present as chlorides and sulfates. The high content of salt-bound and thus easily soluble heavy metals together with the lower alkalinity and oxidation-reduction potential indicates, that ESPA has a better leachability compared to EA and BOA. These observations suggest that individual treatment of ESPA has higher potential for heavy metal recovery. Comparing the EA and BOA, however, no significant differences could be found in the parameters affecting extractability.

The obtained results provide important insights into the formation of the different ash fractions and its geochemical characteristics. The data may serve as basis for re-evaluating disposal routes of ash fractions with poor extraction properties.

Keynote

QUANTITATIVE EXPERIMENTAL CHARGE DENSITY STUDIES OF MINERALS

Woźniak Krzysztof¹, Stachowicz Marcin², Gajda Roman¹, Parafiniuk Jan²

¹Chemistry Department, University of Warsaw, Poland, ²Geology Department, University of Warsaw, Poland

This is quite a paradox that more than century after introduction of the Independent Atom Model (IAM - Bragg, 1914) of electron density, ca. 99.7% of all 1.5mln crystal structures have still been refined using this model which has obvious methodological deficiencies. In my lecture, I will introduce quantitative experimental charge density investigations of minerals - a modern approaches to refinement of crystal structures which goes beyond IAM of spherical atoms/ions. I will illustrate my lecture by several examples showing, among others, results of experimental charge density investigations of minerals under pressure including detailed analysis of changes of electron density at atoms/ions in crystals of minerals under pressure and at variable temperature. A century after the Braggs, it is possible to obtain H-atom positions from X-ray diffraction studies which are equally reliable as those from neutron diffraction. It is also possible to get reliable positions of H-atoms in the closest neighborhood of very heavy atoms, to study tiny redistribution of electron density in minerals under pressure even at particular ions/atoms, to get three dimensional shapes of atoms/ions which are far from being spherical (when the shape of valence electron density is accounted for) or even to estimate consequences of relativistic or electron correlation effects using X-ray diffraction data. Modern quantum crystallographic methods allow to go well beyond such cornerstones of mineralogy as close and the closest packing of ions, atomic/ionic radii, Goldsmidt and Pauling rules allowing for mineralogy at the level of tiny changes of electron density distribution. This is giving far deeper inside into subatomic properties of minerals. By combining high pressure studies and experimental electron density investigations one can mimic mineralogical processes in the Earth's mantle inside modern Diamond Anvil Cells and trace them course of interactions and phase transitions at the level of redistribution of electron density. So users of X-ray mineralogy/crystallography can do far better than refining poor IAM model against precise, accurate and very often very dear diffractometer/synchrotron/XFEL X-ray data.

TOPOLOGICAL ANALYSIS OF THE EXPERIMENTALLY ATTAINED ELECTRON DENSITY DISTRIBUTION FOR THE PEROVSKITE MINERAL: SULPHOHALITE – NA₆(SO₄)₂FCL.

Wróbel Agata¹, Gajda Roman¹, Woźniak Krzysztof¹

¹Department of Chemistry, Biological and Chemical Research Centre, University of Warsaw, Poland

A charge density study for the double anti-perovskite mineral – sulphohalite [Na₆(SO₄)₂FCl] – was carried out. The experimental distribution of electron density was modeled based on a high-resolution X-ray diffraction data set collected with AgK α radiation ($\lambda = 0.56087 \text{ \AA}$) at 100K. Atom-centered multipole expansion was implemented through consecutive least-square refinements, according to the Hansen-Coppens formalism[1]. Resulting model was deployed for QTAIM analysis[2]. The identified topological objects – atomic basins and critical points – were discussed, as proposed by Pendás[3], in terms of basins of attraction of a nucleus, basins of repulsion of a cage as well as their interconnection. The number and types of critical points were additionally evaluated – Morse's 'characteristic set' condition was found to be met[4]. Finally, the nature of interatomic interactions was assessed through the dichotomous classification[4]. The S–O contact was acknowledged as a covalent with a shared-shell. The remaining contacts were characterized as non-covalent closed-shell (Cl \cdots Na, Na \cdots O and Na \cdots F) or weak van der Waals closed-shell (Cl \cdots S and F \cdots O).

References:

- [1] Hansen, N. K.; Coppens, P. Testing Aspherical Atom Refinements on Small-Molecule Data Sets. *Acta Crystallographica Section A* 1978, 34 (6), 909–921. <https://doi.org/10.1107/S0567739478001886>.
- [2] Bader, R. *Atoms in Molecules: A Quantum Theory*; Oxford University Press: USA, 1994.
- [3] Martín Pendás, A.; Costales, A.; Luaña, V. Ions in Crystals: The Topology of the Electron Density in Ionic Materials. I. Fundamentals. *Phys. Rev. B* 1997, 55 (7), 4275–4284. <https://doi.org/10.1103/PhysRevB.55.4275>.
- [4] *Chemical Bonding in Crystals: New Directions*. *Zeitschrift für Kristallographie - Crystalline Materials* 2005, 220 (5–6), 399–457. <https://doi.org/doi:10.1524/zkri.220.5.399.65073>.

A FIB-TEM STUDY OF GOLD PARTICLES FROM THE IBERIAN PYRITE BELT

Yesares Lola¹, González-Jiménez José María², Piña Rubén¹, Sáez Reinaldo³, Ruiz de Almodóvar Gabriel³

¹Mineralogía y Petrología, Universidad Complutense de Madrid, Spain, ²Mineralogía y Petrología, Universidad de Granada, Spain, ³Ciencias de la Tierra, Universidad de Huelva, Spain

Pyrite, with variable As contents, from hydrothermal deposits has been regarded to contain gold in solid solution as well as nano-to-micron sized particles. Despite of the efforts made in the last decade, no many works have focussed their study to investigate the mineralogical site of gold in volcanogenic massive sulfides (VMS). The careful inspection of the time-resolved spectra collected during laser ablation ICP-MS of some pyrite grains from VMS deposits from the Iberian Pyrite Belt (IPB) confirms that this metal is effectively sited in pyrite mainly as nano-to-micron-sized nanoparticles. Under Field Emission Scanning Electron Microscopy (FESEM) the Au particles are observed associated preferentially to pores in pyrite. A combined Focused Ion Beam and High-Resolution Transmission Electron Microscopy (FIB/HRTEM) investigation of two gold particles reveals that these grains exhibit idiomorphic and anhedral morphology and sizes < 1µm. The X-ray Energy Dispersive Spectra (EDS) single-spot and maps acquired by means of the HRTEM show that Au is alloyed with Ag but not significant amounts of other elements, such as Bi, Se, or Te identified in similar grains from hydrothermal deposits by means of electron microprobe analyzer (EMPA). The study of the internal structure of the gold grains by means of High Magnification TEM images (HMTEM) and Selected Area Electron Diffraction (SAED) patterns indicates that the gold particles are composed by nano-sized particles aggregated and distinctively oriented to the host pyrite. These observations do not concur with previous observations in literature that As-rich pyrite exsolve Au from its structure upon heating. Rather, the observation of the gold particles along with other mineral inclusions in the pyrite pores, such as chalcopyrite, cobaltite, native Bi, Bi-sulfosalts and Te-sulfides suggest precipitation of those minerals by hydrothermal fluids. We propose a model in which already formed pyrites interacted with fluids at increasing temperature able to dissolve it while precipitating new minerals, including native gold. Our results highlight the powerfulness of nanoscale studies when interpreting the origins of visible gold in pyrites.

This research is a contribution to the projects CGL2016-79204-R, PID2019-111715GB-I00 and RTI2018-099157-A-I00.

CONCENTRATION AND DISTRIBUTION OF REE IN LOWER CRETACEOUS KARST BAUXITES AND LATERITIC CLAYS FROM THE MAESTRAZGO BASIN (SE IBERIAN RANGE, NE SPAIN)

Yuste Alfonso¹, Bauluz Blanca¹, Laita Elisa¹, Mayayo María José¹

¹Ciencias de la Tierra, IUCA - Universidad de Zaragoza, Spain

The Maestrazgo basin (SE Iberian Range, NE Spain) is one of the main karstic bauxite regions of NE Spain. In addition to karst bauxites, lateritic clays are also abundant in the region. Recently, remarkable attention has been paid to this type of materials, originated through intense chemical weathering, as a potential source of REE, among other critical elements to industry. In consequence, recent research has dealt with the processes that control the distribution of these elements.

In this study, we compare the concentration and distribution of REE in a set of materials from different localities within the Maestrazgo basin. They include pisolitic bauxites from two karst bauxite deposits (La Ginebrosa -GB- and Fuentespalda -FB-), ferrallitized clays (FC) associated to the Fuentespalda deposit, and lateritic clays from the Blesa (BC) and the Cantaperdius (CC) Fms. They are all Barremian (Lower Cretaceous) except La Ginebrosa deposit, reported as Albian. Nevertheless, it cannot be ruled out that the genesis of La Ginebrosa bauxite is also related to intense weathering processes during the Barremian.

In general, the REE contents in the bauxites are more homogeneous than those of the clays. In addition, the average REE contents of the bauxites (GB: 130.49 ppm, FB: 106.25 ppm) are lower than those of the ferrallitized and lateritic clays (FC: 352.69 ppm, BC: 352.07 ppm, CC: 415.11 ppm). Among the clays, some samples yield values as high as 815.75 ppm (FC) and even 1174.89 ppm (BC). On the other hand, the REE concentrations normalized to the Upper Continental Crust (UCC) show that the clays are enriched in REE, whereas the bauxites are depleted in LREE and enriched in HREE. In view of these data, it can be pointed out that the more intense chemical weathering associated with bauxitization led to chemical homogenization and depletion of the REE, which is more pronounced for the LREE.

The (La/Sm)_c average values (GB: 3.51, FB: 3.34, FC: 5.91, BC: 4.70, CC: 5.44) and (Gd/Yb)_c average values (GB: 0.83, FB: 0.70, FC: 1.12, BC: 1.55, CC: 1.48), show that the bauxites exhibit lower fractionation than the clays, which could be linked to the concentration and/or formation of certain phases that act as scavengers for the REE as weathering progresses and bauxitization takes place. The above values also show that LREE fractionation is higher than HREE fractionation, indicating that the HREE are less mobile than the LREE during weathering, which could be again attributed to the concentration and/or formation of mineral phases which act as scavenger for HREE. Several accessory minerals have been pointed out as playing an important role in the distribution of REE during weathering and karst bauxites formation, such as fluorocarbonates of the bastnäsite group and P-bearing phases. Related to this, in La Ginebrosa deposit an authigenic Ce-bearing phosphate phase has been observed whose average structural formula calculated after EDS analyses indicates that it belongs to the goyazite-crandallite series. In summary, intense weathering leads to REE leaching, with the HREEs being less mobile than the LREEs. Therefore, the ferrallitized and lateritic clays show a greater potential as source of strategic elements such as REEs. Accessory minerals seem to play a remarkable role in the distribution of the REEs.

NALDRETTITE (Pd₂Sb) FROM LUANGA CHROMITITE, BRAZIL, AND COMPARISON WITH WORLDWIDE OCCURRENCES

Zaccarini Federica¹, Garuti Giorgio¹

¹Department of Applied Geosciences and Geophysics, University of Leoben, Austria

Naldrettite (Pd₂Sb) is a platinum group mineral (PGM) discovered in Mesamax Northwest deposit, Canada. The name honors Professor Anthony J. Naldrett (1933-2020), University of Toronto, Canada, in recognition of his incomparable contribution to the understanding the genesis of platinum-group-element (PGE) deposits on Earth, and the service rendered as President of both the Mineralogical Society of Canada and the International Mineralogical Association.

Before and after its approval, naldrettite was described from several localities worldwide. Most frequently, naldrettite has been documented in magmatic Ni-Cu-PGE sulfide deposits, hydrothermal veins in porphyry coppers of the Cu-Au type, and PGE-deposits of Alaskan-type zoned intrusions. Naldrettite, rarely occurs in metasomatic Sb-As sulfide ore, metamorphic Ni-Oxide ore, and podiform chromitites. In this work we report the first discovery of naldrettite in the stratiform chromitite of the Luanga complex, Pará State (Brazil). Paragenetic association with alteration assemblages (ferrianchromite, Fe-hydroxides, chlorite) suggests crystallization of naldrettite from metamorphic hydrothermal fluids. The average composition of the Luanga sample (Pd_{1.76}Pt_{0.24})Σ_{2.00}(Sb_{0.57}As_{0.43})Σ_{1.00} indicates a major substitution of Pt and As. These elements derived from the alteration of magmatic sperrylite, and were incorporated in naldrettite precipitated by percolating fluids, at low temperature. Overview of documented occurrences shows that naldrettite can be found in a variety of igneous ore associations (ultramafic, mafic, felsic), even involving minimal concentrations of Pd and Sb. Crystallization of naldrettite generally is related to the post-magmatic stage, under the activity of low temperature hydrothermal fluids particularly enriched in volatile species Sb, As, Bi, Te, and in Pd due to its higher mobility compared with the other PGE. The origin of fluids that can be: 1) “residual”, after the main crystallization of the host magma, 2) “metamorphic”, during regional metamorphism or serpentinization, and 3) “metasomatic”, emanating from an exotic magma intrusion. The combination of two or three of these factors is the most likely process observed in the naldrettite bearing complexes. This work is dedicated to the everlasting memory of Antony James Naldrett (Tony): a great mentor, scientist and charming gentleman, but above all, an unforgettable good friend.

EVOLUTION OF PHASE COMPOSITION AND PROPERTIES OF NON-CRYSTALLINE MATRIX DURING THE VITRIFICATION IN DIFFERENT INDUSTRIAL CERAMIC FORMULATIONS.

Zanelli Chiara¹, Conte Sonia¹, Molinari Chiara¹, Guarini Guiai¹, Ardit Matteo², Cruciani Giuseppe², Dondi Michele¹

¹CNR-ISTEC, Faenza (Italy), CNR-ISTEC, Faenza (Italy), Italy, ²Dept. Physics and Earth Sciences, University of Ferrara, Ferrara, Dept. Physics and Earth Sciences, University of Ferrara, Ferrara, Italy

In recent years, the continuous innovation in the manufacturing of ceramic tiles is driving, as never before, increasing interest in the phase composition and the main properties of the non-crystalline matrix, as a relevant parameter to monitor and control the different stages of firing at the industrial scale. The sintering process yields transformations on the phase composition, accompanied by a complex evolution of the chemistry of the intergranular liquid phase, in turn, modulated by the dynamic equilibrium established between residual minerals and new crystalline phases formed during firing. The present contribution aims to provide an overview of the evolution of phase composition and non-crystalline matrix properties during the vitrification path of five representative industrial ceramic formulations (soft porcelain, vitreous china; two different batches of porcelain stoneware, and glass-bearing stoneware). Batches of the formulations were designed and prepared at the laboratory scale, simulating the industrial ceramic making process. The phase evolution at temperatures ranging from the onset of the viscous flow up to the start of the plastic deformation was specifically investigated at different dwell times. The phase composition is assessed by X-ray diffraction and subsequent Rietveld refinement, and the chemical composition of the vitreous phase is obtained by subtracting the contribution of each previously identified mineralogical phase, considering its stoichiometric formula. The properties of the melts are estimated by predictive models based on the chemical composition of the liquid phase. Particular focus is given to the kinetics of feldspar dissolution and related quartz melting, a phenomenon common to the different investigated formulations. The thermal treatment has a different impact on the mullite content depending on the starting formulation. Indeed, mullite increases (soft porcelain), keeps steady (vitreous china), slightly decreases (porcelain stoneware); and disappears (glass stoneware). Different ceramic formulations have different evolution of chemical parameters of the non-crystalline matrix (i.e. opposite between porcelain and porcelain stoneware).

COPPER AND ZINC ISOTOPIC COMPOSITIONS OF MAFIC-DOMINATED VOLCANOGENIC SULFIDE DEPOSITS IN THE TROODOS OPHIOLITE, CYPRUS.

Zaronikola Nina¹, Debaille Vinciane¹, Decrée Sophie², Mathur Ryan³, Hadjigeorgiou Christodoulos⁴

¹Département Géosciences, Environnement et Société (DGES), Laboratoire G-Time, Université Libre de Bruxelles (ULB), Belgium, ²Royal Belgian Institute of Natural Sciences, Belgium, ³Juniata College, United States, ⁴Geological Survey Department, Cyprus

The Cyprus-type volcanogenic massive sulfide (VMS) deposits or ophiolite-hosted VMS systems are mafic-dominated VMS, which are found in at least 25 well-known ophiolites in the world (e.g., Cyprus, Oman, Russia, Norway). They are copper and copper-zinc rich sulfide systems, and one of the most famous examples is the Tethyan Troodos ophiolite in Cyprus [1]. The Troodos ophiolite includes 90 exploited deposits, of which 41 of the Cyprus-Type VMS [2], representing around 20Mt in size [3]. Ore-forming hydrothermal systems are formed in the sea floor, along mid-ocean ridges, by the circulation of seawater-derived hydrothermal fluids in the oceanic crust [4]. The metal enriched fluid ascends to the seafloor and, due to the different physicochemical and local conditions, the primary sulfides are precipitated, where pyrite is the dominant mineral [5]. When the primary sulfide ore is being exposed to weathering agents and meteoric water, a secondary enrichment zone is formed, known as supergene/secondary ore deposit zone [6]. Petrographic analyses are commonly used to determine the primary versus secondary mineralization. Isotopes fractionation (e.g., Cu) could help at identifying more accurately the type of mineralization through different fractionation in high versus low temperature ore minerals [7]. Copper coupled with Zn isotopes were applied in bulk-rock ore samples and in sulfides of Cyprus-type VMS deposits from Skouriotissa and Agrokippa mines (Cyprus). The studied samples present a mineralogical assemblage comprising pyrite, chalcopyrite, covellite, bornite and malachite. Here we present trace elements analysis, as well as Cu and Zn isotopes data of ore samples aiming to separate the primary versus secondary mineralization seen by their isotopic composition and explain the trace elements behavior. We show a comparison between the VMS ore isotopes fractionation with the isotopic composition of their host Pillow Lavas (upper and lower units) and the ultimate step of alteration represented by leached caps (i.e., gossans), defining Cu and Zn behavior in hydrothermal systems.

[1] Yıldırım, N., Dönmez, C., Kang, J., Lee, I., Pirajno, F., Yıldırım, E., Günay, K., Seo, J. H., Farquhar, J., & Chang, S. W. (2016). *Ore Geology Reviews*, 79(May), 425–442.

[2] Adamides, N. (1980). *International ophiolite symposium.*, Nicosia, Cyprus, p. 117-127.

[3] Jowitt, S. M., Jenkin, G. R. T., Coogan, L. A., & Naden, J. (2012). *Journal of Geochemical Exploration*, 118, 47–59.

[4] Spooner, E.T.C. & Bray, C.J. (1977). *Nature* 266, 808-812.

[5] Herzig, P.M., Hannington, M.D. (1995). *Ore Geol. Rev.* 10, 95–115.

[6] Constantinou, G., & Govett, G. J. S. (1973). *Economic Geology*, 68(6), 843–858.

[7] Mathur, R., Titley, S., Barra, F., Brantley, S., Wilson, M., Phillips, A., Munizaga, F., MaksaeV, V., Vervoort, J., & Hart, G. (2009). *Journal of Geochemical Exploration*, 102(1), 1–6.

TRENDS IN COMPOSITION OF Ba-Cl MICAS IN GARNET PYROXENITES IN GRANULITE MASSIFS IN LOWER AUSTRIA (GFÖHL UNIT OF THE MOL DANUBIAN DOMAIN, BOHEMIAN MASSIF)

Zelinková Tereza¹, Racek Martin¹, Abart Rainer²

¹Institute of Petrology and Structural Geology, Charles University, Czech Republic, ²Department of Lithospheric Research, Universität Wien, Austria

In garnet pyroxenites from the St. Leonhard and Dunkelsteiner Wald granulite massifs, an exotic mineral assemblage involving Ba and Cl rich mica and Cl rich apatite was observed either in the form of polyphase inclusions in garnet or in the matrix. The polyphase inclusions involve micas with compositions ranging from Ba-rich phlogopite to kinoshitalite and chlorapatite together with spinel, amphibole, orthopyroxene, magnesite, and dolomite. In addition, margarite, aspidolite, monazite, scheelite, cordierite, scapolite, and norsethite were identified. In several cases, goryainovite (Ca₂PO₄Cl) crystals with up to 2.4 wt. % of SrO were observed, making this the second world occurrence of this mineral and showing for the first time that Ca can be partially replaced by Sr in its crystal lattice. In the matrix, micas corresponding to Ba-rich phlogopite with low Cl content are associated with apatite (mostly hydroxyapatite with low Cl content) and occasionally with celsian.

The large range of mica compositions allows a detailed evaluation of various substitutional trends. The full compositional range can be defined as follows: (in p.f.u.): Ba_{0.09–1.00}, K_{0.00–0.71}, Na_{0.01–0.13}, Mg_{0.18–0.25}, Fe²⁺_{0.16–2.76}, Al_{1.30–1.99}, Ti_{0.00–0.79}, Si_{1.68–2.62}, Cl_{0.02–1.98}, F_{0.00–0.02}, XFe²⁺_{0.07–0.94}. Ba correlates positively with Al and negatively with Si and K, which corresponds to the coupled substitution Ba1Al1K-1Si-1 linking phlogopite and kinoshitalite. The Cl content correlates positively with Ba and with the XFe ratio (Fe/(Fe+Mg)). The combination of these substitutions leads to the formation of mica with composition Ba_{0.95}K_{0.03}Fe_{2.69}Mg_{0.37}Al_{1.91}Si_{2.02}Cl_{1.98}, XFe_{0.88}, which represents the most Cl-rich mica so far described from natural samples. Its composition is closely approaching the theoretical formula BaFe₃Al₂Si₂O₁₀Cl₂ that can be classified as chloroferrokinoshitalite. Another trend can be observed in relation to Ti, which correlates positively with Ba but negatively with Cl, XFe, and with the sum of Mg and Fe. Such a correlation implies that Ti is incorporated into the mica crystal lattice in coordination with O (Ti₁O₂(Mg,Fe²⁺)₁(OH)₂) and the resulting mica corresponds to oxykinoshitalite. It is interesting to note that the incorporation of either Cl or Ti + O correlates with XFe of mica. This indicates that XFe can be the crucial factor controlling the ability of mica to incorporate Cl into its crystal lattice. In a few cases, two micas with distinct compositions demonstrated by different XFe, Ti and Cl content (for example in p.f.u.: XFe_{0.20:0.77}, Ba_{0.48:0.63}, Ti_{0.35:0.02}, Cl_{0.27:1.45}) were observed coexisting in one inclusion. This might imply that an area of immiscibility exists between the compositional trends of chloroferrokinoshitalite and oxykinoshitalite.

The phases rich in Ba, Cl, and K that are exotic to the host ultramafic mantle rock and may be interpreted as a result of a fluid influx from crustal material during subduction or exhumation processes or can be related to previous mantle metasomatism. The presence of almost pure Cl mica and apatite endmembers and goryainovite together with carbonates indicates extremely high activity of Cl and CO₂ in the metasomatizing fluid.

ISOTOPIC EVIDENCE OF CALCIFICATION-DRIVEN CO₂ EMISSIONS IN A CARBONATE SEAGRASS MEADOW

Zeller Mary A.¹, Van Dam Bryce², Lopes Christian³, Smyth Ashley⁴, Osburn Christopher⁵, Zimmermann Tristan⁶, Pröfrock Daniel⁶, Thomas Helmuth², James Fourqurean³, Böttcher Michael E.¹

¹Marine Geology, Leibniz Institute for Baltic Sea Research, Germany, ²Institute of Carbon Cycles, Helmholtz-Zentrum Hereon, Germany, ³Biological Sciences, Florida International University, United States, ⁴Soil and Water Sciences, University of Florida, United States, ⁵Marine, Earth, and Atmospheric Sciences, North Carolina State University, United States, ⁶Helmholtz-Zentrum Hereon, Germany

Seagrasses are often considered “Blue Carbon” habitats for their role in sequestering and protecting sedimentary organic matter. However, in shallow calcifying systems the ultimate status of seagrass meadows as a sink or source of atmospheric CO₂ is complicated by the impact of net ecosystem calcification (the difference between CaCO₃ formation and dissolution) on net alkalinity (AT) inventories. The sedimentary organic matter stored as “Blue Carbon” can also be remineralized, with the ultimate impact on atmospheric CO₂ determined by net AT production during these remineralization processes. Generally, net AT production is balanced, or close to zero, when the biogeochemical processes are also balanced (denitrification with nitrification, sulfate reduction with sulfide oxidation, etc). AT consumption occurs when carbonate calcification outpaces dissolution, and AT production occurs with net denitrification as well as the burial of FeS₂.

Here, we report on an interdisciplinary study of a seagrass meadow in central Florida Bay, USA (carbonate content ~90%). We used Eddy Covariance (EC) to assess the air-sea CO₂ flux, flow through core incubations to probe benthos-water fluxes (net denitrification, oxygen uptake, $\delta^{13}\text{C}$ and AT), as well as varied porewater (major cations, $\delta^{13}\text{C}$, sulfide, $^{34}\text{S}^{18}\text{O}_4$) and solid phase geochemical analyses (major and trace metals, PO^{13}C , $\text{Ca}^{13}\text{C}^{18}\text{O}_3$, AVS: FeS + H₂S, CRS: FeS²⁺ + S₀). Our benthic flux experiments and sediment cores compared high and low density seagrass sediments. We will first highlight the flux results (EC and flow through) before diving into the sediments and their determinative role in the source/sink status of this seagrass meadow.

This seagrass meadow was consistently a source of CO₂ to the atmosphere during our study period, as well as during the preceding year. Measured net denitrification was low, and close to zero. Porewaters were elevated in sulfide, at some depths higher than 2 mM for the high density cores, but sulfate concentrations were relatively constant down core. Dissolved sulfate isotopes indicated significant exchange with molecular oxygen ($\delta^{18}\text{O}$ SO₄ up to 21 ‰). Burial of reduced sulfur in the form of CRS was observed, but not in large quantities (~0.16 % dwt). Thus, remineralization of organic matter did not produce or consume substantial quantities of AT to either explain or offset the CO₂ source status of the seagrass meadow. Instead, we see strong signs of sulfide oxidation contributing to the reworking of carbonates through dissolution and subsequent reprecipitation in the high density cores. This is supported by $\delta^{13}\text{C}$ of DIC as well as the solid carbonates, showing accumulation of light PIC and heavy DIC in the rhizosphere, as well as by changes in Ca/Mg of PIC. Net sedimentation of inorganic carbon, as well as seagrass mediated reworking of carbonate sediments, pushes this seagrass meadow towards its CO₂ source status.

IRON SULFIDE AUTHIGENESIS AS AN INDICATOR FOR ANTHROPOGENIC DISTURBANCE OF SEDIMENTS IN THE SOUTHERN BALTIC SEA

Zeller Mary A.¹, Schönke Mischa¹, Clemens David², Kallmeyer Jens³, Roeser Patricia¹, Schmiedinger Iris¹, Sommer Stefan², Böttcher Michael E.¹

¹Marine Geology, Leibniz Institute for Baltic Sea Research, Germany, ²GEOMAR Helmholtz Centre for Ocean Research Kiel, Germany, ³Geomicrobiology, GFZ German Research Centre for Geosciences, Germany

Commercial fishing activity using bottom contact trawling can disturb the sea floor and have profound impacts on benthic biogeochemical cycles. Bottom contact trawling is a physical disturbance, as it both resuspends the surface sediments and shifts sediments to the sides of the gear, forming furrows and mounds. However, it is also a disturbance for organisms on different spatial and temporal scales, starting with microbial activity up to macrozoobenthos with their living space in surface sediments. The superimposition of biological and physico-chemical activity controls benthic ecosystem services that may be impacted by anthropogenic disturbance. It is the aim of the present study to look for geochemical markers that allow for an evaluation of effects of bottom contact trawling on the biogeochemistry of marine surface sediments. These changes may impact retention capacity for different elements, the fluxes of solutes via the sediment-water interface, and mineral authigenesis. In particular, minerals forming by the interaction of biogenic sulfide with metals in the suboxic/anoxic zone can be altered by the exposure to oxygenated bottom waters, as well as a resuspension induced change in grain size distribution. Here, we report on our first biogeochemical findings from the DAM project “MGF-Ostsee”, where we explored the fishing area of the Fehmarn Belt in the southern Baltic Sea. Sites were chosen based on trawling intensity, with two sites unexposed to trawling due to physical hazards for fishing nets present on the sea floor (shipwreck or large boulders). These results are compared to sites which experienced medium trawling intensity, and sites which experienced high trawling intensity. At each site, multiple sediment cores for porewater analysis (including sulfide, major and trace elements, nutrients, and ¹³C-DIC), sediment analysis (including THg, TIC, CNS, HCl extractable metals, CRS: FeS₂ + S₀, and AVS: FeS + HS), as well as rates of sulfate reduction and selected rates of formation of CRS and AVS were collected. For this discussion, we will focus on the solid phase parameters, and explore their potential as markers for trawling disturbance. We pay particular attention to the relative vertical quantitative distribution and sulfur isotope composition of the AVS and CRS fractions, in comparison to the abundance of Fe and Mn oxo(hydrox)ides, which have different susceptibility to disturbance based on the chemical (redox) and physical (grain size) aspects of trawling disturbance.

DEPLETED AND ENRICHED MANTLE SIGNATURES IN OPHIOLITES FROM XIGAZE (TIBET)

Zhao Lingquan¹, Chakraborty Sumit¹, Schertl Hans-Peter¹

¹Institut für Geologie, Mineralogie und Geophysik, Ruhr-Universität Bochum, Germany

The Xigaze ophiolites (Tibet), located in the central segment of the Yarlung Zangbo Suture Zone, compose a chain of well-preserved ophiolite massifs. We studied one mantle section that consists essentially of fresh as well as serpentinized peridotites in Luqu (12 km south of Xigaze city) ophiolite where the lithological sequence is considered as intact. The mantle section is divided into three groups: (A) Fresh harzburgites and dunites on the top of the section. (B) Harzburgites and dunites that are serpentinized in various extents beneath the group A. (C) highly serpentinized Cpx-harzburgites at the bottom.

The bulk composition of harzburgites in three groups (A, B & C) shows a highly depleted feature in comparison to both the primitive mantle and the depleted mantle with high Mg # (A: 0.905-0.913, B: 0.905-0.913 & C: 0.905-0.928), and low contents of Al₂O₃ (A: 0.16-0.61 wt%, B: 0.28-0.81 wt% & C: 0.92-1.42 wt%). The mineral compositions, such as high olivine Fo (A: 0.901-0.912, B: 0.89-0.916 & C: 0.901-0.913) also conform to a depleted nature, as indicated by the bulk compositions.

Although there are such features of depletion, the trace element compositions carry signatures of enrichment, such as (i) “bowl-shaped” patterns of trace elements and positive anomalies in highly incompatible trace elements (eg., Rb, Th, U and Ta) in silicate-Earth normalized spider diagrams, and (ii) enriched LREEs in the clinopyroxenes from dunites and harzburgites in chondrite normalized patterns. Besides, petrographic studies reveal that harzburgite and dunite contain interstitial polyphase aggregates of Ol + Cpx + Spl + Opx and Ol + Cpx + Spl, respectively. Experimental studies (e.g., Morgan and Liang, 2003) suggest that these aggregates represent frozen melt-rich components, indicating that fertile melt was percolating through the depleted harzburgite – dunite matrix. To test both, features of depletion and enrichment in the samples, bulk rock REE concentrations were modeled using batch melting, fractional melting, and dynamic melting (both modal and non-modal types) under anhydrous and hydrous melt mode settings. REEs of Cpx were also modeled using non-modal batch melting and non-modal fractional melting models as well.

HREEs of bulk rocks can be described well using the fractional and/or dynamic melting models with different degrees of melting. However, LREEs are enriched compared to the modeling results. Combined with bulk rock and Cpx modeling results, non-modal fractional and dynamic melting with 0.1 vol. % porosity at melting degree of ca. 15 % could be appropriated melting models for the harzburgites in group A & B. Harzburgites in group C might be the products of a lower degree (10 - 14%) of melting. No modeling results could match the patterns of dunites indicating that they were not the products of partial melting. The enrichment of LREE could be interpreted by the melt-rock interaction process that adds instantaneous or accumulated melts generated from the 0.1 – 1.0% degree of non-modal dynamic melting into the total residue (depleted harzburgites) from the previous step. Thus, the REE contents of the harzburgites record a history of multiple episodes of melt depletion and enrichment.

MAGMATISM IN THE WERRA-FULDA MINING DISTRICT – WINDOW INTO THE MAGMATIC EVOLUTION OF THE CENTRAL EUROPEAN VOLCANIC PROVINCE AND ITS INTERACTION WITH EVAPORITES

Zirkler Axel¹, Glasmacher Ulrich A.², Krob Florian², Zeibig Silvio¹, Olbert Jochen², Dunkl István³

¹OP-GW, K+S Aktiengesellschaft, Germany, ²Institute of Earth Sciences, Heidelberg University, Germany, ³Geoscience Center, Sedimentology & Environmental Geology, University of Göttingen, Germany

The Werra-Fulda mining district, a world-class, sulfate-bearing potash deposit located in Central Germany, and its subsurface mining galleries offer the unique opportunity to study volcanic rocks of the Rhön mountains combined with and compared to magmatic dykes as well as sill structures frequently observed in the underground mine. It is generally accepted, that local volcanism occurred in Neogene times, penetrating the Permian evaporite sequence and overlying strata, mainly Buntsandstein and Muschelkalk.

In this study, geochemical analyses testing for the major, minor, and trace element composition were performed on volcanic rocks of the surface as well as subsurface mafic dykes. The results allow a classification of the rocks as within plate basanites and nephelinites with minor occurrences of phonolitic dykes. Potassium and sodium concentrations of subsurface samples are interpreted as partly altered indicating the interaction of magma with adjacent potash salts. However, the geochemical data reveal two distinct trends in the magmatic composition indicative for at least two magma-sources in the local area. Furthermore, geochemical results are compared to published data of the region and nearby volcanic complexes in the Rhön, Vogelsberg, Westerwald and Siebengebirge. Additionally, intrusion ages of the alkaline rocks were estimated by applying the fission-track and (U-Th-Sm)/He dating techniques to apatite from more than 100 magmatic rock samples. Two magmatic events at about 21 Ma and 13 Ma are inferred by the preliminary results.

HIGH-RESOLUTION SPATIOTEMPORAL pH MONITORING OF COUPLED CO₂ DEGASSING AND CaCO₃ PRECIPITATION DYNAMICS

Zoegl Iris¹, Grengg Cyrill¹, Mueller Bernhard², Wedenig Michael¹, Goetschl Katja¹, Boch Ronny¹, Dietzel Martin¹, Kluge Tobias³

¹Institute of Applied Geosciences, Graz University of Technology, Austria, ²Institute of Analytical Chemistry and Food Chemistry, Graz University of Technology, Austria, ³Institute of Applied Geoscience, Karlsruhe Institute of Technology, Germany

In situ monitoring of chemical and physical parameters of drip sites in caves (or tunnels) allows for an advanced understanding on the controls of carbonate precipitation dynamics. The pH can be used as key parameter to trace varying CO₂ degassing and saturation degrees with respect to CaCO₃ in aqueous media. Due to fast CO₂ degassing of drip water reaching the cave or tunnel atmospheres, and slow drip rates, pH measurements using conventional methods, can be altered toward higher pH within seconds. Thus, a precise and immediate pH measurement is crucial to determine the prevailing CaCO₃-CO₂-H₂O processes, i.e. reaction kinetics, isotope fractionation, and the occurrence of intermediate phases. Furthermore, it may allow to distinguish between site-specific and more general climate related signals.

In the present study novel optical pH sensors are applied to quantify and image spatial pH distributions of simulated and real-life drip water with high-temporal and spatial resolution. Preliminary results in flow path simulating laboratory experiments applying multiple pH sensors show a standard deviation of only ± 0.1 for pH and therefore a good reproducibility of measurements under restrictive conditions with a water film thickness of ~ 1 mm and slow flow rates of ~ 1.5 cm/s. As the pH sensors are expected to be suitable for even thinner water films of ~ 0.1 mm, their applicability to cave systems are going to be tested via field experiments.

THE SUKARI DEPOSIT, EGYPT: A GIANT OROGENIC GOLD DEPOSIT IN A FORTUITOUS NEOPROTEROZOIC STRUCTURAL-LITHOLOGIC CONJUNCTION

Zoheir Basem¹, Holzheid Astrid¹, Zeh Armin², Schwarz-Schampera Ulrich³, Graupner Torsten³, El-Behairy Mohamed⁴, Turrin Brent⁵, Xiong Fahui⁶

¹Geosciences, Kiel University, Germany, ²Angewandte Geowissenschaften, Karlsruher Institut für Technologie, Germany, ³Bundesanstalt für Geowissenschaften und Rohstoffe, Germany, ⁴Centamin Egypt Ltd, Egypt, ⁵Department of Earth and Planetary Sciences, Rutgers University, United States, ⁶Institute of Geology, Chinese Academy of Geological Sciences, China

The Sukari gold deposit (> 15 Moz Au) in the Eastern Desert of Egypt is related to Au-sulfide quartz veins and low-grade, highly sulfidized rocks of the Sukari trondhjemite stock. The relationship between gold mineralization and the host rocks is poorly understood, and the genesis and geodynamic setting of the Sukari granite remains questionable. New LA-ICPMS zircon U-Pb ages of three samples from the Sukari stock are indistinguishable within error and give the best estimate of the crystallization at $\sim 695 \pm 2$ Ma, which is identical to the age of a nearby gabbro-diorite complex. The $\epsilon_{\text{Hf}}(695)$ values of concordant zircons (11.7 to 13.4), and two-stage Hf model ages ~ 0.8 to 0.9 Ga for the Sukari granite samples are suggestive of magma generation via partial melting of thickened (>40 km) TTGs and/or mafic Neoproterozoic crust.

⁴⁰Ar-³⁹Ar dating of hydrothermal sericite returned a plateau age of ~ 630 Ma, in good agreement with a total fusion/integrated age of ~ 600 Ma. This date overlaps a protracted period of regional transpression, positive flower structures, and thoroughgoing shearing in the region. The intense deformation and slicing of the Sukari trondhjemite body along moderately and steeply E-dipping faults provided dilation loci for gold-bearing quartz veins. Recurring brittle-ductile deformation mobilized refractory “invisible” gold from sulfides and resulted in anomalously high-grade ore shoots (with 100s - 1000s ppm Au). LA-ICP-MS analysis indicates that refractory Au in pyrite is associated with elevated As contents, whereas the free gold inclusions and dispersed blebs are mainly Au-Ag-Sb-Hg alloys. Fine- or coarse-oscillatory and sector zoning patterns, irregular As-rich bands and truncations between the early- and late-genetic pyrites, as observed in the SEM BSE images, reflect fluctuation in the ore fluid composition and/or temperature. Free gold deposition did not start during the onset of pyrite deposition under lithostatic pressure, but was attendant to later syn-deformational precipitation of quartz and a late sulfide assemblage (late pyrite, sphalerite, galena, and chalcopyrite). Thallium versus mercury as associate trace elements in early and late gold indicate that evolution to high temperatures or boiling commenced when the system upheaved to shallower crustal levels by tectonism. Unfailing coupling of Au and some trace elements, i.e., As, Bi, Se and Te in the composition of early and late pyrites imply well-buffered or single-source ore fluids.

Gold-associated pyrite and arsenopyrite gave nearly invariable $\delta^{34}\text{S}$ values of -0.9 ‰ to -1.9 ‰, corresponding to $\delta^{34}\text{SH}_2\text{S} = -1.96$ ‰ to -3.04 ‰ calculated for the ore fluids at temperatures of 280-340°C (arsenopyrite geothermometer). The narrow range and consistently negative values are in accord with either magmatic sulfur or metamorphic sulfur, largely buffered and reduced by graphite schists in the mine area. The newly determined U-Pb and Ar-Ar ages together with inference for metal flux in the course of the hydrothermal system lend clear constraints on orogenic gold formation attendant to widespread synkinematic magmatism and terrane exhumation (630-580 Ma) in the northern part of the Arabian-Nubian Shield.

NYEREREITE: A POSSIBLE MESSENGER FROM THE DEEP EARTH.

Zucchini Azzurra¹, Gavryushkin Pavel N.², Golovin Alexander V.², Bolotina Nadezhda B.³, Stabile Paola⁴, Carroll Michael R.⁴, Comodi Paola¹, Frondini Francesco¹, Morgavi Daniele¹, Perugini Diego¹, Arzilli Fabio⁵, Cherin Marco¹, Kazimoto Emmanuel⁶, Kokh Konstantin², Kuznetsov Artem²

¹Physics and Geology, University of Perugia, Italy, ²Sobolev Institute of Geology and Mineralogy, Siberian Branch of Russian Academy of Sciences, Russian Federation, ³Shubnikov Institute of Crystallography, Federal Scientific Research Centre 'Crystallography and Photonics', Russian Academy of Sciences, Russian Federation, ⁴School of Science and Technology, Geology Division, University of Camerino, Italy, ⁵School of Earth and Environmental Sciences, University of Manchester, United Kingdom, ⁶Department of Geosciences, School of Mines and Geosciences, University of Dar es Salaam, United Republic of Tanzania

Alkaline and earth-alkaline carbonatites in the CaCO_3 - $(\text{Na,K})_2\text{CO}_3$ system are intriguing mineral phases. Their paucity with respect to Ca-Mg carbonates is likely due to the ephemeral behavior, at ambient conditions, that rapidly transforms minerals such as nyerereite [approximate chemical formula $(\text{Na}_{1.64}\text{K}_{0.36})\text{Ca}(\text{CO}_3)_2$] and gregoryite [$(\text{NaCa}_x\text{K})_{2-x}\text{CO}_3$] to the end-members Ca-carbonatite rocks through intermediate stages as, for example, pirssonite-like structures [$\text{Na}_2\text{Ca}(\text{CO}_3)_2 \cdot 2(\text{H}_2\text{O})$].

Nyerereite is one of the most interesting alkaline carbonates and the main rock-forming minerals of natrocarbonatites, together with gregoryite. Besides its occurrence in natrocarbonatite magmas, nyerereite-like carbonates were also identified within primary/secondary melt inclusions in rock-forming minerals of kimberlites as well as in multiphase solid inclusions in diamonds.

The aim of the present work is to study K-free synthetic nyerereite samples by a multimethodological approach coupling scanning electron microscopy, energy dispersive spectroscopy, Raman spectroscopy and single crystal X-ray diffraction.

Different attempts on refining the crystal structure of nyerereite have been made in synthetic hydrothermal K-free samples and it results in a three-component twinned structure where the three-domains are orthorhombic with either P21ca or Pbc_a space groups. The crystal structure of nyerereite was here refined as a three-component twinned structure in the centrosymmetric Pbc_a space group, with the ratio of the three twinning components 0.221(3):0.287(3):0.492(3). Therefore, we could speculate that nyerereite can have different space groups and suggest that twinning at micro- and nano- level can introduce some minor structural deformations that are diriment for the likely occurrence of the inversion center as one of the symmetry elements in nyerereite crystal structure. By a comparison between the centrosymmetric Pbc_a nyerereite structure and that of aragonite (CaCO_3 , Pmcn space group), the presence of polysomatic relations in the high pressure (HP) form of $\text{Na}_2\text{Ca}(\text{CO}_3)_2$ (e.g. interlayering of the high pressure polymorphs Na_2CO_3 in P21/m space group and CaCO_3 in the form of aragonite) is hypothesized. The proposed relation of nyerereite with aragonite at HP heightens the interest in the baric behavior of the nyerereite structure and allows speculating about the possibility for the nyerereite crystal structure to be stable at HP conditions. Nyerereite may be transported within carbonatitic melts from the lower mantle to the surface with important implications for the storage of deep mantle carbon and for the deep carbon cycle associated with carbonatites. Synchrotron single crystal X-ray diffraction experiments at non ambient conditions are in scheduled in order to study the behavior of nyerereite at HP and high to low temperature conditions.



3rd European Mineralogical Conference Cracow Poland

AUTHORS' INDEX

EMC 2020

Abad, Isabel, 15, 196, 197, 260, 261, 284
 Abart, Rainer, 16, 18, 37, 65, 170, 344, 422
 Abu, Alex Tiewin, 17
 Adam, Christian, 157, 342
 Adamczyk, Burkart, 342
 Agakhanov, Atali, 300
 Ageeva, Olga, 18, 65, 344
 Agranier, Arnaud, 105
 Ahven, Marjaana, 176
 Aiglsperger, Thomas, 121, 200
 Akinbodunse, Sileola Joseph, 19
 Aksenov, Sergey M., 20
 Albert, Richard, 269
 Alexander, Denis, 241, 242
 Alfonso, Pura, 21
 Alifirova, Taisia, 170
 Alisi, Chiara, 259
 Allabar, Anja, 22
 Allais, Enrico, 299
 Allar, Christian, 23
 Allard, Thierry, 76
 Altona, Karim, 24
 Alvaro, Matteo, 30, 31, 86, 108, 160, 258, 271, 278, 283, 402
 Amicone, Silvia, 25
 Amthauer, Georg, 26
 Andersson, Stefan S., 27, 187
 Andrea, Luca, 318
 Andreou, Fevronia T., 28
 Andreozzi, Giovanni Battista, 79, 250
 Andrunik, Magdalena, 29
 Angel, Ross J., 30, 31, 160, 258, 278, 283
 Angeli, Celestino, 317
 Angellotti, Antonio, 374
 Angerer, Thomas, 32, 341
 Annen, Catherine, 33
 Antonets, Igor, 165
 Anzellini, Simone, 239
 Apostolikas, Athanasios, 167
 Appelt, Oona, 352
 Aprea, Paolo, 301
 Aquino, Andrea, 34, 295
 Ardit, Matteo, 35, 36, 123
 Argenziano, Monica, 132
 Arletti, Rossella, 103, 132, 311
 Arvanitidis, Nikolaos, 187
 Arvidsson, Ronald, 187
 Arzilli, Fabio, 429
 Asenbaum, Rene, 37
 Aspiotis, Stelios, 38
 Astilleros, José-Manuel, 138, 164
 Atıcı, Gokhan, 146
 Attardi, Antonio, 131
 Aulbach, Sonja, 254
 Aurell, Marcos, 223
 Austrheim, Håkon, 125
 Ayora, Carlos, 233, 285
 Bach, Wolfgang, 128
 Bachmann, Kai, 126
 Bádenas, Beatriz, 223
 Baehre, Oliver, 186
 Bagiński, Bogusław, 198, 373
 Bais, Giorgio, 276
 Bajda, Tomasz, 29, 358, 362, 363
 Bajnóczi, Bernadett, 39, 280
 Baker, Tim, 27
 Bakker, Edine, 27, 187
 Bakker, Eleanor, 40
 Bakker, Ronald, 41
 Balassone, Giuseppina, 42, 85
 Ballèvre, Michel, 240
 Bandura, Lidia, 43, 66, 298
 Baraldi, Cecilia, 132
 Barale, Luca, 303
 Baranyi, Viktória, 188
 Baratelli, Lisa, 267
 Barba-Brioso, Cinta, 127
 Barbaro, Anna, 86
 Barbero, Edoardo, 77
 Barella, Vittorio, 299
 Barenghi, Fabiana, 44, 247
 Bargar, John, 7
 Barker, Abigail, 291
 Barone, Germana, 45, 46, 47, 48
 Barrenechea, Jose F, 49
 Bartoli, Omar, 243, 387
 Bartz, Wojciech, 314
 Basallote, Maria Dolores, 83, 285
 Bassez, Marie-Paule, 50
 Battiston, Tommaso, 51, 52, 293, 294
 Bauer, Christine, 53
 Bauer, Christoph, 190
 Bauluz, Blanca, 76, 223, 224, 284, 418
 Baumgartner, Lukas, 240
 Baxter, Ethan, 269
 Beaudoin, Nicolas E., 90
 Beck, Pierre, 54, 134
 Beckmann, Philipp, 55

Bedidi, Ali, 282
 Beirau, Tobias, 56, 57, 106
 Bekker, Andrey, 350
 Belak, Mirko, 188
 Belfiore, Cristina Maria, 45, 48
 Bellendorf, Paul, 296
 Bellmann, Frank, 169
 Benisek, Artur, 169
 Benna, Piera, 61
 Benning, Liane G., 68, 110
 Bente, Klaus, 57
 Beranoaguirre, Aratz, 58, 269, 349
 Bergamasco, Rosangela, 379
 Berger, Alfons, 304
 Berkesi, Márta, 227, 370, 371
 Berkh, Khulan, 59
 Bernabé, Pierre, 281
 Bernadou, Fabien, 60
 Bernasconi, Davide, 61, 299
 Berndt, Jasper, 366
 Bersani, Danilo, 139
 Berthold, Christoph, 25
 Bertolotto, Solène, 140
 Bertrandsson Erlandsson, Viktor, 62
 Bevilacqua, Paolo, 389
 Bhattacharya, Sourabh, 63, 163
 Biagioni, Cristian, 64, 155
 Białek, Dawid, 217
 Białoszewska, Monika, 66
 Bian, Ge, 18, 65
 Bianchini, Gianluca, 77
 Bindi, Luca, 234
 Birkenstock, Johannes, 24, 147
 Birski, Łukasz, 81
 Bish, David, 35
 Blanchard, Marc, 67
 Blannin, Rosie, 126
 Bleeker, Wouter, 172
 Bloise, Andrea, 323
 Blukis, Roberts, 68, 110
 Błachowski, Artur, 232
 Bobos, Iuliu, 191
 Boch, Ronny, 427
 Boddy, Christopher, 212
 Boettcher, Michael E., 194
 Boiadeiro Ayres Negrão, Leonardo, 69, 70, 106
 Boiocchi, Massimo, 264
 Bolalek, Jerzy, 333
 Bolotina, Nadezhda B., 429
 Bonaccorsi, Elena, 64, 71
 Bonadiman, Costanza, 316, 317
 Bonazzi, Mattia, 72, 229
 Bonazzi, Paola, 234
 Bonechi, Barbara, 377
 Boni, Maria, 334
 Boone, Marijn, 181, 357
 Borgognone, Costanza, 79
 Borrueal-Abadía, Violeta, 49
 Botcharnikov, Roman, 366, 367
 Botta, Serena, 303
 Böttcher, Michael E., 73, 173, 211, 381, 423, 424
 Botteon, Alessandra, 276
 Boudouma, Omar, 406
 Bouzahzah, Hassan, 74
 Brčić, Vlatko, 76
 Brey, Gerhard, 75, 185, 349
 Brlek, Mihovil, 76
 Brocławik, Olga, 333
 Brodecka-Goluch, Aleksandra, 333
 Brombin, Valentina, 77
 Brown Jr, Gordon E, 7
 Brugger, Joël, 272
 Brundu, Antonio, 78
 Brunet, Fabrice, 105, 128
 Bruschini, Enrico, 79, 86
 Büchner, Jörg, 254
 Buczko, Daniel, 80
 Budzyń, Bartosz, 81, 192, 393
 Bulakh, Maria, 300
 Bünning, Jens, 73
 Burchardt, Steffi, 291
 Burianek, Manfred, 147, 214
 Burns, Peter C., 20
 Busqesi-Ahmeti, Durime, 40
 Buszko, Eliza, 251
 Caggiani, Maria Cristina, 46, 47
 Calabria, Giovanna, 379
 Callegari, Ivan, 199
 Callot, Jean-Paul, 90
 Cambi, Costanza, 102
 Cametti, Georgia, 287, 326
 Campomenosi, Nicola, 160, 271
 Canali, Francesco, 119
 Canals, Angels, 320
 Cannaò, Enrico, 82, 279
 Cánovas, Carlos R., 83, 233, 268, 285
 Cantaluppi, Marco, 84, 276
 Cantaro, Carmelo, 323

Capitani, Giancarlo, 249
 Cappelletti, Piergiulio, 42, 85, 109
 Caputo, Domenico, 301
 Caracausi, Antonio, 250
 Carli, Cristian, 79, 86
 Carr, Lynnea, 212
 Carrey, Raúl, 17
 Carrez, Philippe, 118
 Carroll, Michael R., 429
 Carvalho, Bruna B., 87
 Casalini, Martina, 86
 Casetta, Federico, 88
 Castelli, Daniele, 241, 242
 Cavalaglio, Gianluca, 102
 Cavalli, Roberta, 132
 Cavallo, Alessandro, 128
 Cavallo, Giovanni, 89
 Cavazzini, Giancarlo, 257
 Centrella, Stephen, 90
 Cerantola, Valerio, 250
 Cerri, Guido, 78
 Cesare, Bernardo, 108, 160
 Chakraborty, Sumit, 92, 425
 Chamberlain, Kevin, 172
 Chareev, Dimitry, 405
 Chareeva, Polina, 405
 Cheeptham, Naowarat (Ann), 212
 Chen Si, Athena, 93
 Cherin, Marco, 429
 Chew, David, 172, 337, 350, 382
 Chiaradia, Massimo, 310
 Chojnacka, Maria, 94
 Chopin, Christian, 271
 Chryssikos, Georgios D., 28, 356
 Chukanov, Nikita V., 20
 Churakov, Sergey, 326, 414
 Chyla, Julia, 207
 Ciapała, Bartłomiej, 265
 Ciążęła, Jakub, 95, 163, 217, 248, 255, 256, 307
 Ciesielczuk, Justyna, 96, 97
 Ciesielska, Zuzanna, 28, 97
 Cieślík, Błażej, 98
 Cilliers, Kirstin, 375
 Ciobanu, Cristiana, 99, 104
 Cirrincione, Rosolino, 332
 Clark, Chris, 387
 Clemens, David, 424
 Cnudde, Veerle, 181, 357
 Coccato, Alessia, 46, 47
 Cocco, Fabrizio, 131
 Codeço, Marta S., 100
 Codispoti, Niccolò, 378
 Colás, Vanessa, 320
 Colombo, Chiara, 253, 276
 Coltorti, Massimo, 88
 Comboni, Davide, 51, 52, 267, 293, 294
 Comodi, Paola, 101, 102, 134, 429
 Confalonieri, Giorgia, 103
 Connolly, James, 241, 242
 Conrad, Anika C., 173
 Conte, Sonia, 36, 123, 420
 Cook, Nigel, 99, 104
 Cordier, Patrick, 118
 Corre, Marianna, 105
 Cortinhas Alves, Tiago Kalil, 106
 Corvò, Stefania, 107, 228, 229
 Costa, Benedetta, 108
 Costa, Letizia Teresa, 109
 Cotana, Franco, 102
 Couasnon, Thaïs, 68, 110
 Creaser, Robert, 208
 Criniti, Giacomo, 101
 Crow, Carolyn, 111
 Cruciani, Giuseppe, 36, 123, 420
 Cultrone, Giuseppe, 302
 Cuppone, Tiberio, 86
 Curetti, Nadia, 61, 299
 Cuthbert, Simon, 112
 Cutts, Jamie, 395
 Czekay, Laura, 113
 D'Angeli, Ilenia Maria, 221
 D'Acapito, Francesco, 234
 Dacheux, Nicolas, 140
 Dachs, Edgar, 169, 244
 Daczko, Nathan, 305
 D'Andretta, Marilina, 71
 Danišík, Martin, 245
 Darling, Robert, 135
 Day, Axelle, 282
 De Bonis, Alberto, 42
 De Gennaro, Bruno, 301
 De Giudici, Giovanni Battista, 117, 259
 De la Horra, Raúl, 49
 De Lorenzi, Lorenzo, 389
 De Matteis, Chiara, 114, 115
 De Schryver, Thomas, 181, 357
 De Simone, Antonio, 42
 Debaille, Vinciane, 421
 Debret, Baptiste, 116

Decrée, Sophie, 421
 Dehn, Frank, 411
 Deidda, Matteo Luca, 117, 131
 Del Campo, Adolfo, 320
 Delbecq, Valentin, 118
 Delgado, Joaquin, 127
 Della Ventura, Giancarlo, 264
 Delledonne, Chiara, 119
 Dellwig, Olaf, 73
 Derkowska, Katarzyna, 120
 Derkowski, Arkadiusz, 28, 232
 Desmaele, Elsa, 67
 Desmau, Morgane, 110
 Destefanis, Enrico, 299
 Dewaele, Stijn, 181
 Dey, Joyjit, 321
 Di Renzo, Francesco, 103, 132
 Diana, Eliano, 318
 Dias, Maria Isabel, 153
 Dietzel, Martin, 427
 Dinelli, Enrico, 114, 148
 Ding, Hongrui, 235
 Dinh, Hoang Duong, 282
 Dini, Andrea, 243
 Domènech, Cristina, 17
 Domeneghetti, Maria Chiara, 86
 Domínguez-Carretero, Diego, 121
 Dominijanni, Serena, 122
 Dondi, Michele, 36, 123, 420
 Donkor, Kingley, 212
 Dore, Elisabetta, 259
 Dosbaba, Marek, 334
 Dragańska-Deja, Katarzyna, 209
 Drakou, Foteini, 382
 Dufrêche, Jean-François, 140
 Dulski, Mateusz, 220, 372
 Dunkl, István, 426
 Dunkley, Daniel J., 124, 216, 350, 412, 413
 Duretz, Thibault, 240
 Duvail, Magali, 140
 Eckert, Sebastian, 381
 Eggenberger, Urs, 414
 Ehrig, Kathy, 99, 104
 El Korh, Afifé, 310
 El-Behairy, Mohamed, 428
 Ellmies, Rainer, 62
 Emmerich, Katja, 40, 411
 Ende, Martin, 57
 Eng, Peter, 93
 Engvik, Ane Karine, 125
 Ennen, Alexander, 53
 Erambert, Muriel, 125
 Ernst, Richard, 172
 Escher, Peter, 73
 Escobar, Alexandra G., 126
 Escobar, Pablo, 127
 Escutia, Carlota, 284
 Eslami, Alireza, 128
 Etschmann, Barbara, 272
 Ettlér, Vojtěch, 129, 396
 Ewing, Rodney, 56
 Fabbiani, Marco, 132, 311
 Fabiańska, Monika, 96, 97
 Faccincani, Luca, 88
 Faggi, Daniela, 144
 Fajrin, Andi, 175
 Falkenberg, Janina, 130
 Fancello, Dario, 117, 131, 259
 Fantini, Riccardo, 132
 Farina, Federico, 243, 279
 Farina, Simone, 64
 Farré-de-Pablo, Júlia, 133, 200
 Farsang, Stefan, 239
 Fastelli, Maximiliano, 101, 102, 134
 Fazio, Eugenio, 332
 Febrianto, Nugroho Nur, 175
 Fehn, Thomas, 219
 Fei, Yingwei, 374
 Fernández-Díaz, Lurdes, 138, 327
 Fernández-Fernández, Luz Eva, 194
 Ferrando, Simona, 241, 242
 Ferrari, Erika, 132
 Ferrari, Francesco, 348
 Ferrero, Silvio, 135
 Ferri, Fabio, 108
 Fiannacca, Patrizia, 332
 Fiebig, Jens, 173
 Filippaki, Eleni, 286
 Filippov, Lev, 141
 Filippova, Inna, 141
 Finocchiaro, Claudio, 45, 46, 47
 Fiore, Gianluca, 61
 Firsching, Markus, 53
 Fischer, Michael, 19, 136
 Fischer, Reinhard X., 24, 147, 214
 Fischer, Timothy, 93
 Fitros, Michalis, 369
 Foltyn, Krzysztof, 137
 Forjanes, Pablo, 138
 Formia, Alessandra, 348

Fornasini, Laura, 139
 Foucaud, Yann, 140, 141
 Fougerouse, Denis, 387, 398, 402
 Foulds, Ian, 395
 Fourdrin, Chloé, 282
 Franke, Mees, 142
 Franus, Wojciech, 43, 66
 Franza, Annarita, 144, 145
 Frenzel, Max, 126
 Frezzotti, Maria Luce, 241, 242, 250
 Friedrichs, Bjarne, 146
 Frondini, Francesco, 429
 Frost, Daniel, 113, 122
 Fuchs, Andreas, 147
 Fugazzotto, Maura, 46, 47
 Fülöp, Réka, 39
 Fumagalli, Patrizia, 44, 82, 247, 267
 Funari, Valerio, 114, 148
 Funedda, Antonio, 131
 Furi, Evenlyn, 60
 Fusswinkel, Tobias, 149
 Gaeta, Mario, 377
 Gaillard, Fabrice, 60, 275
 Gajda, Roman, 415, 416
 Galdenzi, Federico, 264
 Galimberti, Lucia, 249
 Galuskin, Evgeny, 150, 218, 287, 372
 Galuskina, Irina, 150, 151, 202, 218, 287,
 372
 Galzerano, Barbara, 301
 Gao, Kun, 380
 Garbe-Schönberg, Dieter, 273
 Garbin, Enrico, 302
 García-Casco, Antonio, 121, 133, 320, 404
 García-Piña, Carlos, 53, 281
 García-Rivas, Javier, 153, 154, 277
 García-Romero, Emilia, 11, 152, 154, 238,
 277
 García-Tortosa, Francisco Juan, 197
 Garcia-Valles, Maite, 21
 García-Vicente, Andrea, 152, 238, 277
 Gardner, Robyn, 305
 Garrido, Carlos Jesus, 338
 Garuti, Giorgio, 155, 347, 351, 419
 Gasparatos, Dionisios, 167
 Gatta, G. Diego, 8, 51, 52, 128, 253, 276,
 293, 294
 Gault, Baptiste, 16
 Gautheron, Cécile, 105
 Gautneb, Håvard, 125
 Gavryushkin, Pavel N., 429
 Gawel, Adam, 251, 333
 Gawęda, Aleksandra, 350, 410
 Gaynor, Sean, 76
 Geiger, Charles A., 156
 Gentzmann, Marie, 157
 Georgiou, Lazaros, 187
 Gerdes, Axel, 57, 58, 75, 208, 269, 349
 Gerdjikov, Ianko, 337
 Gerhardt, Sebastian, 158
 Germinario, Chiara, 263
 Germinario, Luigi, 159
 Gervilla, Fernando, 338
 Ghatak, Hindol, 305
 Giacomoni, Pier Paolo, 88
 Gianola, Omar, 108
 Gianolla, Piero, 49
 Gibson, Sally Anne, 179
 Giersz, Miłosz, 207, 353
 Gigli, Lara, 316
 Gil, Grzegorz, 168
 Gilio, Mattia, 30, 108, 160, 161
 Giordana, Alessia, 318
 Giorgetti, Giovanna, 249
 Giorno, Eugenia, 323
 Giralt Susqueda, Alberto, 162
 Glasmacher, Ulrich A., 426
 Glazyrin, Konstantin, 101, 267
 Gleeson, Sarah A., 100
 Glenk, Mischa, 335
 Gmochowska, Wiktoria, 163
 Godelitsas, Athanasios, 164, 167
 Godinho, Jose R. A., 357
 Goetschl, Katja, 427
 Golovin, Alexander V., 429
 Golubev, Yevgeny, 165
 Gonzalez, Joseph P., 166, 283
 González-Jiménez, José María, 121, 133,
 320, 338, 417
 Goutzioupa, Konstantina, 167
 Gozzoli, Vittorio, 103
 Grabarczyk, Anna, 168
 Grammatikopoulos, Tassos, 351
 Grathoff, Georg, 173
 Graupner, Torsten, 428
 Graziano Sossio, Fabio, 42, 109
 Gréaux, Steeve, 378
 Grégoire, Michel, 254
 Gregorio, Stefano, 389
 Greiner, Martina, 138

Grengg, Cyrill, 427
 Grevel, Klaus-Dieter, 169
 Grew, Edward, 391
 Grieco, Giovanni, 82, 128
 Griesshaber, Erika, 138
 Grifa, Celestino, 42, 263
 Griffiths, Thomas, 170
 Grizelj, Anita, 76
 Grobéty, Bernard, 310
 Grönholm, Pentti, 281
 Groppo, Chiara, 171, 241, 242, 388
 Gruner, Matthias, 40
 Grybos, Malgorzata, 315
 Gualtieri, Alessandro F., 139
 Guarini, Guiiai, 420
 Guastoni, Alessandro, 294
 Guilmette, Carl, 361
 Gumsley, Ashley, 172, 337
 Gussone, Nikolaus, 173
 Guy, Bradley M., 357
 Haase, Patrick, 174
 Habler, Gerlinde, 16, 18, 65, 170, 213, 344
 Hadjigeorgiou, Christodoulos, 421
 Hagemann, Steffen G., 32
 Häger, Tobias, 366, 367
 Haissen, Faouziya, 404
 Hakim, Andy Yahya Al, 175
 Häkkänen, Heikki, 325
 Halkoaho, Tapio, 176
 Hanfland, Michael, 267
 Hansen, Thomas C., 316
 Hansson, Alexander, 27, 187
 Haproff, Peter J., 321
 Harley, Simon L., 398
 Harlov, Daniel E., 198, 237, 373
 Härtel, Birk, 177
 Harvey, Jason, 321
 Hatert, Frederic, 178
 Hatzipanagiotou, Konstantinos, 351
 Havisto, Jari, 281
 Heaney, Peter, 93
 Heckel, Catharina, 75, 179, 185, 330, 349
 Heilala, Bryan, 281
 Hentschel, Felix, 201, 203
 Hermann, Jörg, 306
 Hernandez-Puentes, Pilar, 195
 Herrington, Richard, 334
 Herwartz, Daniel, 180, 211
 Herwegh, Marco, 304
 Hezel, Dominik, 349
 Hicks, Matthew, 181
 Hidas, Károly, 182, 338
 Higo, Yuji, 374
 Hildebrand, Jan Sebastian, 183, 184
 Hill, Patrick, 212
 Hillier, Stephen, 356
 Hinterwirth, Simon, 394
 Hirschmann, Marc, 329
 Hoareau, Guilhem, 90
 Hoefler, Heidi, 75, 185, 349
 Hoelzig, Hieronymus, 57, 186
 Hofmann, Martin, 40
 Hofmeister, Wolfgang, 366
 Högdahl, Karin, 27, 187
 Hokka, Janne, 176
 Holl, Kristina, 296
 Holtz, François, 55
 Holzheid, Astrid, 428
 Honarmand, Maryam, 53
 Horn, Ingo, 256
 Hornarmand, Maryam, 406
 Horvat, Marija, 188
 Hrstka, Tomáš, 396
 Hrubciak, Rostislav, 377
 Hsu, Yiu-Kang, 210
 Huang, Fang, 225
 Huang, Fangfang, 407
 Huber, Norbert, 56
 Hughes, Hannah, 189
 Huhma, Hannu, 176
 Hycnar, Elżbieta, 346
 Iacono, Marziano Giada, 275
 Iacumin, Paola, 257
 Idini, Alfredo, 117
 Idriss, Hosni, 399
 Idrus, Arifudin, 190, 347
 Ihanus, Jaakko, 181
 Iizuka, Yoshiyuki, 359
 Ildefonse, Benoit, 273
 Inckemann, Sebastian, 380
 Ínsua-Pereira, Guilherme, 191
 Irifune, Tetsuo, 122
 Iskandar, Irwan, 175
 Izzo, Francesco, 42, 263
 Jahn, Sandro, 343
 James, Fourqurean, 423
 Janeczek, Janusz, 382
 Jaranowski, Maciej, 192
 Jastrzębski, Mirosław, 193, 217, 360
 Jedlicka, Radim, 129

Jenner, Anna-Kathrina, 194
 Jesus, Ana, 248
 Jew, Adam, 7
 Jia, Peng, 236
 Jiang, Runze, 225
 Jiménez, Amalia, 327, 328
 Jiménez-Espinosa, Rosario, 195, 196, 197, 260, 261
 Jiménez-Franco, Abigail, 21, 121
 Jiménez-Millán, Juan, 15, 195, 196, 197, 260, 261
 Joachim-Mrosko, Bastian, 142
 Jokubauskas, Petras, 168, 198, 248, 353, 373
 Jonckheere, Raymond, 177
 Jonsson, Erik, 27, 187
 Jordan, Guntram, 380
 Jorge Pinto, Andre, 199
 Jørgensen, Bo B., 381
 Joseph, Bobby, 267
 Joseph, Fabio, 201
 Junge, Malte, 200, 201, 203
 Jura, Dominik, 96
 Jurasinski, Gerald, 194
 Juroszek, Rafał, 202
 Kalageropoulos, Georgios, 187
 Kalampaliki, Sofia, 27
 Kalil Cortinhas Alves, Tiago, 69
 Kaliwoda, Melanie, 200, 201, 203
 Kallio, Rita, 204
 Kallmeyer, Jens, 381, 424
 Kałaska, Maciej, 207, 353
 Kamenov, George, 207
 Kamo, Sandra, 172
 Kamona, Fred, 129
 Kampf, Anthony, 270
 Kananian, Ali, 128
 Kaneva, Ekaterina, 222
 Kaplan, Ulrich, 130
 Kaproń, Grzegorz, 353
 Kapusta, Czesław, 232
 Karali, Marina, 351
 Karfal, Abdelhak, 404
 Karsdorf, Robert, 205, 219
 Kaski, Saara, 325
 Kaufmann, Andreas Benjamin, 206
 Kaufmann, Felix, 200
 Kazimoto, Emmanuel, 429
 Keluskar, Tanmay T., 412
 Kenny, Gavin G., 213
 Khomenko, Volodymir, 282
 Kiefer, Stefan, 206, 208
 Kielman-Schmitt, Melanie, 361, 395
 Kierczak, Jakub, 98, 120, 319
 Kilian, Ruediger, 312
 Kirnbauer, Thomas, 341
 Kisiel, Marta, 209
 Kisters, Alex, 375
 Klein, Sabine, 210, 341
 Klemd, Reiner, 310
 Klipsch, Swea, 211
 Kloess, Gert, 186
 Klomínský, Josef, 192
 Klonowska, Iwona, 80
 Kluge, Tobias, 427
 Knežević Solberg, Janja, 125
 Koch-Müller, Monika, 352
 Kocjan, Izabela, 337
 Koebsch, Franziska, 194
 Koehn, Daniel, 90
 Koenig, Uwe, 313
 Koepke, Jürgen, 248, 273
 Kohn, Victoria, 170
 Kokh, Konstantin, 429
 Kokkalas, Sotirios, 369
 Kölbl-Ebert, Martina, 354
 Kollias, Konstantinos, 164
 Königer, Franz, 40
 Koning, Keegan, 212
 Kononkova, Natalia, 366
 Kooijman, Ellen, 361, 395
 Koshlyakova Natalia, 300
 Kostitsyn, Yuriy, 366
 Kotowski, Jakub, 168, 353, 373
 Koutsovitis, Petros, 351
 Kovács, István János, 227
 Kovaleva, Elizaveta, 213
 Kozak, Krzysztof, 265
 Kozub-Budzyń, Gabriela, 81, 137, 192, 392
 Kraemer, Dennis, 341
 Krämer, Konrad, 214
 Krause, Felix, 411
 Krcmar, Wolfgang, 23, 183, 184, 205, 219, 290, 335
 Kreher-Hartmann, Birgit, 215
 Kreuzburg, Matthias, 194
 Kribek, Bohdan, 129
 Krivovichev, Sergey V., 9, 20
 Krob, Florian, 426
 Król, Piotr, 216
 Kruszewski, Łukasz, 217

Krzątała, Arkadiusz, 218
 Krzemińska, Ewa, 193
 Krzykowski, Tomasz, 96, 382
 Kugler, Felix, 219
 Kuhn, Thomas, 307
 Kukoč, Duje, 76
 Kuligiewicz, Artur, 209
 Kumar, Naresh, 7
 Kupczak, Krzysztof, 220, 410
 Kusiak, Monika A., 124, 213, 216, 412, 413
 Kuznetsov, Artem, 429
 Kylander-Clark, Andrew, 107
 Lacalamita, Maria, 221, 222
 Laita, Elisa, 76, 223, 224, 418
 Lan, Chunyuan, 225
 Lang, Aleksandra, 226
 Lange, Thomas Pieter, 227
 Langella, Alessio, 42, 85, 263
 Langone, Antonio, 72, 86, 107, 228, 229, 402
 Lanson, Martine, 105
 Lanzafame, Gabriele, 46, 47, 88
 Laufek, František, 155, 405
 Laurent, Antonin T., 398
 Laurent, Oscar, 135
 Lawrence, Sara, 212
 Lazaroiu, Andreea, 230
 Lazarov, Marina, 206, 256
 Lee, Yongjae, 231
 Legros, Helene, 75
 Leitner, Christoph, 58
 Lempart-Drozd, Małgorzata, 232
 Leonelli, Cristina, 348
 León, Rafael, 233, 285
 Lepitkova, Sonja, 77
 Lepore, Giovanni Orazio, 234
 Lesieur, Claire, 33
 Lezzerini, Marco, 34, 295
 Li, Chen, 16
 Li, Rongxi, 408
 Li, Xian-Hua, 355
 Li, Yan, 235
 Li, Yanzhang, 235
 Liipo, Jussi, 181, 226, 357
 Lima da Costa, Marcondes, 70
 Linckens, Jolien, 179
 Lindström, Hannu, 281
 Lipka, Marko, 381
 Lis, Grzegorz, 217
 Liu, Yunxia, 236
 Llovet, Xavier, 133
 Lobanov, Sergey S., 339
 Loisel, Claudine, 282
 Lopes, Christian, 423
 Lorenz, Melanie, 237
 Lorenzo, Adrián, 152, 238, 277
 Lotti, Paolo, 51, 52, 267, 293, 294
 Louvel, Marion, 239
 Lovera, Oscar M., 146
 López-Gómez, José, 49
 López-Quirós, Adrián, 284
 Lu, Anhuai, 235
 Luberda-Durnaś, Katarzyna, 232
 Ludwig, Thomas, 366, 367
 Luisier, Cindy, 240
 Lupi, Stefano, 230
 Luth, Stefan, 27
 Luukkanen, Saija, 204
 Łukawska-Matuszewska, Katarzyna, 333
 Macdonald, Ray, 198, 373
 Macías, Francisco, 83, 233, 268, 285
 Macis, Salvatore, 230
 Mackley, Stephanie A., 20
 Macri, Michele, 230
 Macris, Catherine, 297
 Madej, Jarosław, 298
 Madruga, Maria José, 153
 Maffeis, Andrea, 241, 242
 Magnani, Lorenzo, 243
 Magrini, Claudia, 249
 Magro, Massimiliano, 274
 Maino, Matteo, 107, 228, 229
 Mair, Philipp, 394
 Majka, Jarosław, 80
 Maj-Szeliga, Katarzyna, 209
 Majzlan, Juraj, 169, 174, 206, 208, 244
 Makiel, Magdalena, 209
 Malusà, Marco Giovanni, 245
 Malviyag, Vivek P., 355
 Malvoisin, Benjamin, 128
 Mamtani, Manish A., 332
 Mancinelli, Maria Letizia, 144
 Mancini, Lucia, 88, 253
 Manecki, Maciej, 246, 324, 333, 365
 Mangano, Chiara, 44, 247
 Mantovani, Luciana, 114, 115, 148
 Mapani, Ben, 129
 Maras, Serafim, 167
 Marban, Gregorio, 328
 Marcelli, Augusto, 264
 Marchesi, Claudio, 338

Marciniak, Dariusz, 95, 248
 Marciniak-Maliszewska, Beata, 353
 Marengo, Alessandra, 299
 Marian, Narcisa Mihaela, 249
 Marinoni, Nicoletta, 84, 119, 253, 276
 Maritan, Lara, 257, 302
 Marras, Giulia, 250, 378
 Marras, Pier Andrea, 259
 Marrocchi, Yves, 60
 Marschall, Horst, 75, 269, 349
 Marszałek, Mariola, 251
 Martel, Caroline, 331
 Martinez-Ruiz, Francisca, 381
 Martucci, Annalisa, 316, 317
 Masotta, Matteo, 252
 Massinelli, Giulia, 253
 Mastelloni, Maria Amalia, 48
 Mathian, Maximilien, 76
 Mathur, Ryan, 207, 421
 Mattes, Johannes, 145
 Matusiak-Małek, Magdalena, 80, 254, 255,
 256, 266, 307
 Matyszczyk, Witold, 373
 Maurice, Juliette, 267
 Mauro, Daniela, 155
 Mayayo, María José, 224, 418
 Mayne, Matthew, 243, 292
 Mazurek, Hubert, 95, 255, 256
 Mazzoleni, Paolo, 45, 46, 47, 48
 Mazzoli, Claudio, 257
 Mazzucchelli, Mattia Luca, 166, 258, 271,
 283
 McCammon, Catherine, 113, 122, 310
 McFarlane, Richenda, 212
 Medas, Daniela, 259
 Medina-Ruiz, Antonio, 196, 260, 261
 Medvedeva, Elena, 366
 Meheut, Merlin, 262
 Meima, Jeannet, 281
 Melcher, Frank, 62
 Meng, Birgit, 342
 Menold, Carrie, 297
 Mercurio, Mariano, 42, 85, 263
 Merkulova, Margarita, 357
 Merlini, Marco, 44, 119, 247, 253, 267, 276
 Mesto, Ernesto, 222
 Mezger, Klaus, 361
 Mieszczak, Marcin J., 124
 Migliorini, Alessandra, 86
 Mihailova, Boriana, 38, 264, 278, 283
 Mihaljevic, Martin, 129
 Mikoda, Bartosz, 265
 Mikrut, Jakub, 266
 Milani, Sula, 247, 267
 Milcov, Igor, 77
 Milevski, Ivica, 77
 Millan-Becerro, Ricardo, 268
 Millonig, Leo J., 269
 Mills, Stuart, 270, 272
 Mingardi, Giulia, 271
 Mino, Lorenzo, 132
 Misiti, Valeria, 377
 Missen, Owen, 270, 272
 Mišur, Ivan, 76
 Misz-Kennan, Magdalena, 96, 97
 Miyajima, Nobuyoshi, 113, 122
 Mock, Dominik, 273
 Moggi Cecchi, Vanni, 86
 Molinari, Chiara, 36, 123, 420
 Molinari, Simone, 274
 Mollé, Valentin, 275
 Molnár, Gábor, 227
 Mondillo, Nicola, 334
 Mongelli, Giovanni, 76
 Monsef, Iman, 53
 Morabito, Giulia, 276
 Morales, Juan, 238, 277
 Morana, Marta, 278
 Moreira, Wardleison, 379
 Morelli, Marco, 144
 Moreno, Juan A., 355
 Morgavi, Daniele, 429
 Mørkved, Pål-Tore, 125
 Moro, Daniele, 400
 Moroni, Marilena, 117
 Morra, Vincenzo, 42
 Mosconi, Angelica, 279
 Motak, Monika, 383, 384
 Motte, Geoffrey, 90
 Motyl, Sylwia, 392
 Moyon, Jean-François, 292
 Mozgai, Viktória, 280
 Mueller, Bernhard, 427
 Mueller, Kai, 186
 Mueller, Simon, 281
 Muir, Barbara, 362
 Muller, Camille, 282
 Müller, Katrin, 73
 Müller, Samuel, 273
 Müller, Thomas, 321

Murri, Mara, 86, 283
 Musiyachenko, Kira, 160
 Mutterlose, Joerg, 130
 Nabatian, Ghasem, 53, 406
 Nagel, Thorsten J., 180
 Naitza, Stefano, 117, 131
 Narang, Yerie, 175
 Nazzari, Manuela, 72, 377
 Neave, David Axford, 273
 Nejbort, Krzysztof, 168
 Nestola, Fabrizio, 31, 374
 Nieto, Fernando, 15, 284
 Nieto, José Miguel, 233, 285
 Niinikoski-Fusswinkel, Paula, 149
 Nikolopoulou, Athina, 286
 Nimis, Paolo, 31
 Nix, William, 56
 Nobre, Augusto Gonçalves, 316
 Notosiswoyo, Sudarto, 175
 Nowak, Izabella, 307
 Nowak, Katarzyna, 287
 Nowak, Marcus, 22
 Nowak, Monika, 288
 Ntaflos, Theodoros, 88, 254, 256
 O Driscoll, Brian, 289
 Oberti, Roberta, 264
 O'Brien, Patrick J., 135
 Occhipinti, Roberta, 46, 47
 Oeder, Klaus, 290
 Oelze, Marcus, 352
 Ofierska, Weronika, 291
 Oguchi, Chiaki T., 159
 Ohlwärter, Christian, 205
 Ohtani, Eiji, 10
 Olbert, Jochen, 426
 Olías, Manuel, 233, 285
 Oliveira Toscano, Mafalda, 126
 Oliveira, Elson P., 355
 Oliver, Warren, 56
 Ollie, Risby, 291
 Oman Drilling Project Science Team, 273
 Operetto, Maria Teresa, 42
 Orberger, Beate, 53, 406
 Osburn, Christopher, 423
 Otto, Denise, 194
 Otto, Tahnee, 292
 Özdemir, Erdem, 226
 Ozdín, Daniel, 208
 Pacella, Alessandro, 303
 Pachuta, Karolina, 251
 Pack, Andreas, 180
 Padrón-Navarta, José Alberto, 182, 371
 Paganin, Patrizia, 259
 Pagliaro, Francesco, 51, 52, 293, 294
 Pagnotta, Stefano, 34, 295
 Paiva, Isabel, 153
 Pallas, Leander, 296
 Pálos, Zsófia, 227
 Pan, Ruiguang, 297
 Panek, Rafał, 298
 Pantović, Radoje, 226
 Papadopoulos, Argyrios, 167
 Parafiniuk, Jan, 415
 Parise, Mario, 221
 Pasero, Marco, 64
 Pastero, Linda, 299
 Paul, Andrea, 157
 Paul, Jean-François, 118
 Pavese, Alessandro, 61, 84, 299
 Pearson, Graham, 75
 Pekker, Péter, 227
 Pekov, Igor, 300
 Pellino, Annamaria, 85
 Peltz, Markus, 173
 Peluso, Antonio, 301
 Pereira, Dolores, 323
 Perez, Anne, 282
 Pérez-López, Rafael, 83, 233, 268, 285
 Pérez-Monserrat, Elena Mercedes, 302
 Perinelli, Cristina, 250, 377
 Perugini, Diego, 429
 Petrelli, Maurizio, 167
 Petriglieri, Jasmine Rita, 303
 Petrishcheva, Elena, 16
 Petti, Carmela, 85
 Pettke, Thomas, 304
 Peverelli, Veronica, 304
 Peytcheva, Irena, 76
 Pezzotta, Federico, 243
 Phillips, Brian, 35
 Piana, Fabrizio, 303
 Piazzolo, Sandra, 107, 228, 305, 321
 Piccoli, Francesca, 304, 306
 Pieczonka, Jadwiga, 137
 Piestrzyński, Adam, 137
 Pieterek, Bartosz, 95, 248, 255, 256, 307
 Pietranik, Anna, 98, 308, 319, 386
 Piezzo, Amanda, 42
 Piña, Rubén, 417
 Pinizzotto, Maria Rita, 323

Pinna-Jamme, Rosella, 105
 Pinto de Meireles, Carlos, 191
 Pinto, Alvaro MM, 126
 Piovesan, Rebecca, 257
 Pipolo, Silvio, 118
 Pirard, Eric, 74
 Pisarek, Marcin, 353
 Pisova, Barbora, 309
 Pittarello, Lidia, 145
 Plaisier, Jasper R., 267, 316
 Poch, Olivier, 134
 Pohlner, Johannes, 310
 Pokrovski, Gleb, 67
 Polentarutti, Maurizio, 276
 Poli, Stefano, 119
 Polisi, Michelangelo, 311
 Pollastri, Simone, 115, 317
 Pöllmann, Herbert, 23, 56, 69, 70, 106, 158,
 183, 184, 205, 290, 312, 313, 335, 376
 Pölönen, Ilkka, 325
 Possenti, Elena, 253, 276
 Post, Jeffrey, 93
 Potysz, Anna, 314, 315
 Pósfai, Mihály, 227
 Pracejus, Bernhard, 199
 Prakash, Divya, 355
 Pratesi, Giovanni, 86, 144, 145
 Precisvalle, Nicola, 316, 317
 Prell, Marta, 248
 Prencipe, Mauro, 283
 Princivalle, Francesco, 389
 Priola, Emanuele, 318
 Proenza, Joaquín A., 121, 133, 200, 320, 404
 Pröfrock, Daniel, 423
 Prządka-Giersz, Patrycja, 207, 353
 Przybyło, Arkadiusz, 319, 386
 Pujol-Solà, Núria, 320
 Punturo, Rosalda, 323
 Pushkarev, Evgenii, 41
 Putzolu, Francesco, 334
 Puziewicz, Jacek, 254, 255, 256, 266
 Quadir, Zakaria, 387
 Racek, Martin, 37, 422
 Rach, Benjamin, 194
 Radomskaya, Tatiana, 222
 Ragozin, Alexey, 359
 Raith, Johann G., 62
 Ramírez-Salazar, Anthony, 321
 Rammlmair, Dieter, 59
 Rämö, Osmo Tapani, 176
 Raneri, Simona, 139
 Rassomakhin, Mikhail, 366
 Ratschbacher, Lothar, 177, 361
 Raue, Dietrich, 186
 Realini, Marco, 253, 276
 Rečnik, Aleksander, 65
 Reddy, Steven, 387, 398, 402
 Redhammer, Günther, 264
 Reissner, Michael, 69
 Relvas, Jorge, 100, 126
 Renno, Axel D., 181, 357
 Reolid, Matías, 15, 284
 Reutsky, Vadim, 322
 Ricardo da Assuncao Godinho, Jose, 181
 Ricchiuti, Claudia, 323
 Rickard, William, 387, 402
 Riegler, Thomas, 74
 Rigonat, Nicola, 259
 Rispoli, Concetta, 42, 85, 109
 Ristović, Ivica, 226
 Ristovski, Igor, 77
 Rividi, Nicolas, 406
 Rizzo Andrea, Luca, 88
 Rodriguez, Marco, 200
 Roeser, Patricia, 424
 Rogala, Patrycja, 324
 Roine, Antti, 181, 357
 Rolfo, Franco, 171, 388
 Romppanen, Sari, 325
 Roos, Diana, 326
 Roqué-Rosell, Josep, 320
 Rosa, Angelika, 239
 Rose, Thomas, 210
 Rösel, Delia, 366
 Rossano, Stéphanie, 282
 Rossman, George R., 156
 Roth, Thomas, 23
 Rotiroti, Nicola, 294
 Roush, Ted L., 86
 Roy, Jitendra, 63
 Roza-Llera, Ana, 327, 328
 Rubatto, Daniela, 306
 Rudra, Avishek, 329
 Ruiz de Almodóvar, Gabriel, 417
 Ruiz, Miguel, 21
 Rumsey, Mike, 270
 Ruppel, Anna, 330
 Rusiecka, Monika, 331
 Russo, Damiano, 332
 Russo, Giacomo, 109

Russo, Livio, 389
 Rzepa, Grzegorz, 81, 333
 Saari, Juha, 226
 Saccani, Emilio, 77
 Sáez, Reinaldo, 417
 Sahlström, Fredrik, 27
 Šajn, Robert, 226
 Salje, Ekhard, 56
 Salvini, Riccardo, 249
 Salviulo, Gabriella, 274
 Sałacińska, Anna, 172, 337
 Samae, Vahid, 399
 Samojeden, Bogdan, 383, 384
 Samouhos, Michail, 167
 Sanakis, Yiannis, 167
 Sánchez Migalloón, Juan Morales, 152
 Sánchez-Navas, Antonio, 284, 320
 Sanchez-Pastor, Nuria, 199
 Sanchez-Valle, Carmen, 239
 Sandalov, Fedor, 300
 Sandoval Moreno, Daniel G., 27
 Santana, Carlos, 187
 Santoro, Licia, 334
 Sappa, Daniela, 335
 Sardella, Raffaele, 230
 Sarkar, Binoy, 336
 Sartbaeva, Asel, 293
 Sassi, Raffaele, 257
 Sasso, Corrado, 221
 Saunders, Edward, 338
 Saxey, David, 387, 398, 402
 Scambelluri, Marco, 271
 Scarlato, Piergiorgio, 377
 Schafmeister, Maria-Theresia, 73
 Schaltegger, Urs, 76
 Scharf, Andreas, 199
 Schauble, Edwin, 262
 Scherer, Erik, 361
 Schertl, Hans-Peter, 425
 Schettino, Erwin, 338
 Schifferle, Lukas, 339
 Schindler, Maria, 68
 Schingaro, Emanuela, 221, 222
 Schlumberger, Stefan, 414
 Schlüter, Jochen, 38, 264
 Schmahl, Wolfgang W., 138, 201, 203, 380
 Schmalholz, Stefan, 240
 Schmidt, Burkhard, 173
 Schmiedinger, Iris, 73, 173, 194, 424
 Schmitt, Axel Karl, 146, 172, 340
 Schmitt, Bernard, 134
 Schmitt, Fabian, 340
 Schmitt, Leanne, 341
 Schneider, Hartmut, 24, 147, 214
 Schönke, Mischa, 424
 Schraut, Katharina, 342
 Schreiber, Anja, 81, 213, 393
 Schryvers, Dominique, 399
 Schuhmann, Rainer, 40, 411
 Schulze, Maximilian, 343
 Schuster, Roman, 344
 Schwartz, Stéphane, 105
 Schwarz-Schampera, Ulrich, 428
 Schweinar, Kevin, 16
 Scolari, Marco, 119
 Segui, Carolina, 345
 Seibold, Joshua, 183, 184
 Seitz, Hans-Michael, 179, 330
 Sena, Francesco, 378
 Sendrós, Miquel, 21
 Septiana, Sara, 347
 Septianto, Cipto Purnandi, 175
 Serrano, Juan, 157
 Şek, Magdalena, 346
 Sgarlata, Caterina, 348
 Shahar, Anat, 368
 Shcheglov, Vladimir, 165
 Shchipalkina, Nadezhda, 300
 Shendrik, Roman, 222
 Shu, Qiao, 75, 185, 349
 Shumlansky, Leonid, 350
 Siboulet, Bertrand, 140
 Sideridis, Alkiviadis, 351
 Sidorov, Evgeny, 300
 Sieber, Melanie J., 352
 Sierpień, Paula, 353
 Silva, David, 305
 Simon, Gilla, 354
 Simon, Sebastian, 342
 Simonet-Roda, María, 138
 Simonetti, Matteo, 229
 Simos, Xenofon, 369
 Singh, Pradip K., 355
 Singh, Vinod K., 355
 Sinisi, Rosa, 76
 Siranidi, Eirini, 28, 356
 Sittner, Jonathan, 181, 357
 Siuda, Rafał, 217
 Skala, Roman, 309
 Skalny, Mateusz, 29, 358, 362

Skiba, Michał, 209
 Sklyarov, Eugene, 359
 Skreczko, Sylwia, 382
 Skupiński, Sebastian, 298
 Skuzovatov, Sergei, 359
 Sláma, Jiří, 81, 192, 193, 393
 Slattery, Ashley, 99, 104
 Slodczyk, Aneta, 60
 Słaby, Ewa, 95, 163, 248, 385
 Słodczyk, Elżbieta, 386
 Słowik, Grzegorz, 298
 Smirčić, Duje, 188
 Smit, Matthijs, 361, 395
 Smyth, Ashley, 423
 Sobczyk, Maciej, 362
 Söderlund, Ulf, 172
 Solińska, Agnieszka, 363
 Solomon, Betelehem, 74
 Sommer, Stefan, 424
 Somsikova, Alina, 366
 Song, Yueting, 364
 Sordyl, Julia, 246, 324, 365
 Sorger, Dominik, 321
 Sorokina, Elena, 366, 367
 Sossi, Paolo, 368
 Sparta, Deborah, 267
 Spieß, Iris, 19, 24, 214
 Spiliopoulou, Aikaterini, 369
 Spránitz, Tamás, 370, 371
 Sprocati, Anna Rosa, 259
 Stabile, Paola, 429
 Stachowicz, Marcin, 151, 373, 415
 Stagno, Vincenzo, 122, 230, 250, 374, 377,
 378
 Stamm, Franziska, 262
 Stani, Chiara Maria, 317
 Stanley, Chris, 155
 Starinieri, Silvia, 46, 47
 Staubwasser, Michael, 211
 Stefanescu, Eduard, 40
 Stefani, Stefania, 86
 Stephan, Dietmar, 342
 Stevens, Gary, 292, 375
 Števkó, Martin, 208
 Stępień, Ewa, 324
 Stöber, Stefan, 69
 Stoeber, Stefan, 376
 Stopponi, Veronica, 377, 378
 Straioto, Henrique, 379
 Strauss, Harald, 248
 Strączek, Tomasz, 232
 Strohm, Samuel Benedikt, 380
 Stroschio, Antonio, 46, 47
 Struck, Ulrich, 73
 Stubbs, Joanne, 93
 Suárez, Mercedes, 11, 152, 154, 238, 277
 Šuica, Sanja, 76
 Sun, Beilei, 236
 Sun, Shyong, 165
 Sun, Tiantian, 381
 Susta, Umberto, 102
 Swamidharma, Y.C.A., 190
 Szabó, Csaba, 227, 370, 371
 Szczerba, Marek, 28, 97, 208
 Szenknect, Stéphanie, 140
 Szenthe, Gergely, 39, 280
 Szopa, Krzysztof, 172, 337, 350, 382
 Szram, Ewa, 97
 Szymaszek, Agnieszka, 383, 384
 Śliwiński, Marek, 360
 Środek, Dorota, 220, 372
 Środoń, Jan, 12
 Tacchetto, Tommaso, 387
 Taiwo, Aramide, 212
 Tajcmanova, Lucie, 236
 Tamang, Shashi, 388
 Tangeman, Jean, 244
 Tanskanen, Pekka, 204
 Tao, Renbiao, 225
 Tapster, Simon, 76
 Tarasov, Viktor P., 20
 Tasso, Flavia, 259
 Tattoni, Federico, 389
 Tauler, Esperança, 345
 Tedonkenfack, Sylvain, 255
 Teipel, Ulrich, 219
 Ternes, Bernd, 202
 Tesei, Telemaco, 390
 Thomas, Helmuth, 423
 Thomas, Rainer, 391
 Thorne, Warren, 32
 Tiede, Lisa, 344
 Tiepolo, Massimo, 82, 279
 Tollan, Peter, 291
 Tomatis, Maura, 303
 Tombros, Stylianos, 369
 Topolska, Justyna, 392
 Torres, Harlison, 121
 Tramm, Fabian, 81, 393
 Treude, Tina, 381

Triantafyllidis, Stavros, 369
 Tribaudino, Mario, 114, 115, 148
 Tribus, Martina, 32
 Tribuzio, Riccardo, 307
 Trinajstić, Nina, 76
 Tropper, Peter, 394
 Trumbull, Robert, 100
 Tsakiridis, Petros, 167
 Tsikouras, Basilios, 351
 Tual, Lorraine, 395
 Tuhý, Marek, 396, 405
 Turchkova, Anna, 300
 Turci, Francesco, 303
 Turrin, Brent, 428
 Tursi, Fabrizio, 397
 Turuani, Marion J., 398
 Uenver-Thiele, Laura, 254
 Ul Haq, Ihtasham, 399
 Ulian, Gianfranco, 400
 Uusitalo, Sanna, 281
 Vacca, Salvatore, 259
 Valdrè, Giovanni, 400
 Van Dam, Bryce, 423
 Van Loo, Denis, 181, 357
 Van Schrojenstein Lantman, Hugo, 402
 van Wagoner, Nancy, 212
 Vapnik, Yevgeny, 150, 151, 218, 287, 401
 Vasiliev, Iuliana, 58
 Vasilyev, Prokopi, 185
 Vassura, Ivano, 148
 Vaughan-Hammon, Joshua, 240
 Veksler, Ilya, 100
 Verberne, Rick, 402
 Verde, Maria, 42
 Vergani, Fabrizio, 249
 Verma, Sanjeet K., 355
 Veveakis, Manolis, 345
 Vezzalini, Giovanna, 103, 132, 311
 Vianello, Fabio, 274
 Vieira, Marcelo, 379
 Villa, Igor Maria, 245, 280, 403
 Villanova-de-Benavent, Cristina, 404
 Viotti, Paula, 379
 Vitale Brovarone, Alberto, 306
 Vitale, Enza, 109
 Viti, Cecilia, 249
 Vivani, Riccardo, 102
 Vlasáč, Jozef, 206
 Voigt, Claudia, 211
 Vojtko, Rastislav, 208
 Volkmann, Rebecca, 341
 Vollprecht, Daniel, 13
 von Ahn, Catia M. E., 194
 von Werder, Julia, 342
 Vrhovnik, Petra, 226
 Vuilleumier, Rodolphe, 67
 Vymazalova, Anna, 155, 405
 Wade, Benjamin, 99, 104
 Waesermann, Naemi, 264
 Wagner, Christiane, 53
 Wagner, Rebecca, 53
 Wagner, Thomas, 149
 Wagner-Raffin, Christiane, 406
 Wallis, David, 402
 Wallner, Daniela, 62
 Walters, Jess, 349
 Wang, Changqiu, 235
 Wang, Hui, 408, 409
 Wang, Jintuan, 407
 Wang, Kuo-Lung, 359
 Wang, Yanbin, 374
 Wannhoff, Iris, 135
 Warchoń, Jolanta, 94
 Warchulski, Rafał, 220, 353, 410
 Webb, A. Alexander G., 321
 Wedenig, Michael, 427
 Weis, Philipp, 100
 Wells, Stephen, 293
 Werling, Nadja, 411
 Westner, Katrin J., 210
 Westphal, Julia, 194
 Weyer, Stefan, 206
 Whitehouse, Martin J., 124, 216, 412, 413
 Więclaw, Dariusz, 97
 Wijaya, I.G.N.K., 190
 Wilde, Simon A., 124, 216, 412, 413
 Wilke, Franziska D.H., 352
 Wille, Martin, 304
 Winde, Vera, 73
 Winski, Lucas, 194
 Wirth, Richard, 81, 192, 213, 393, 413
 Wiszniewska, Janina, 168
 Witcher, Taylor, 291
 Włodek, Adam, 112
 Włodyka, Roman, 382
 Wojtulek, Piotr M., 217
 Wolffers, Mirjam, 414
 Woodland, Alan B., 179, 254, 330
 Woźniak, Krzysztof, 151, 415, 416
 Wrona, Katarzyna, 382

Wróbel, Agata, 416
Wudarska, Alicja, 246
Wunder, Bernd, 135
Xiong, Fahui, 428
Xiong, Miner, 44, 247
Xiong, Xiaolin, 407
Xu, Chang, 364
Xu, Wei, 264
Yakymchuk, Chris, 135
Yesares, Lola, 417
Yi, Keewook, 216
Youssef, Imam, 406
Yuste, Alfonso, 76, 223, 224, 418
Zaccarini, Federica, 155, 190, 347, 351, 419
Zack, Thomas, 27
Zambon, Alfonso, 132
Zambrana, Rubén, 21
Zampini, Marco, 249
Zanelli, Chiara, 36, 123, 420
Zannella, Alessandra, 71
Zaronikola, Nina, 421
Zeh, Armin, 428
Zeibig, Silvio, 426
Zelinková, Tereza, 422
Zeller, Mary A., 194, 423, 424
Zeng, Fangui, 236
Zhang, Chao, 55
Zhang, Lifei, 225
Zhao, Lingquan, 425
Zhao, Shanrong, 364
Zieliński, Grzegorz, 151
Ziemniak, Grzegorz, 80
Zimmermann, Tristan, 423
Zirkler, Axel, 426
Zoegl, Iris, 427
Zoheir, Basem, 428
Zoleo, Alfonso, 257
Zorzi, Federico, 257
Zubkova, Natalia, 300
Zucali, Michele, 44, 119
Zucchini, Azzurra, 101, 102, 134, 429
Zuo, Jiawei, 321